

A new cryptic species of terrestrial breeding frog of the *Pristimantis danae* Group (Anura, Strabomantidae) from montane forests in Ayacucho, Peru

Valia Herrera-Alva^{1,2}, Alessandro Catenazzi³, César Aguilar-Puntriano^{1,2}

¹ Departamento de Herpetología, Museo de Historia Natural de la Universidad Nacional Mayor de San Marcos, Lima, Peru

² Laboratorio de Sistemática y Ecología de Vertebrados, Facultad de Ciencias Biológicas, Universidad Nacional Mayor de San Marcos, Lima, Peru

³ Florida International University, Department of Biological Sciences, 11200 SW 8th Street, Miami, FL 33199, USA

Corresponding author: César Aguilar-Puntriano (caguilarp@unmsm.edu.pe)

Abstract

Based on morphological and molecular characters, we describe a new species of terrestrial breeding frog of the *Pristimantis danae* Group from montane forests of La Mar Province, Ayacucho Department in southern Peru, at elevations from 1200 to 2000 m a.s.l. The phylogenetic analysis, based on concatenated sequences of gene fragments of 16S rRNA, RAG1, COI and TYR suggests that the new species is a sister taxon of a clade that includes one undescribed species of *Pristimantis* from Cusco, *Pristimantis pharangobates* and *Pristimantis rhabdolaemus*. The new species is most similar to *P. rhabdolaemus*, which differs by lacking scapular tubercles and by its smaller size (17.0–18.6 mm in males [$n = 5$], 20.8–25.2 mm in females [$n = 5$] in the new species vs. 22.8–26.3 mm in males [$n = 19$], 26.0–31.9 mm in females [$n = 30$] of *P. rhabdolaemus*). Additionally, we report the prevalence of *Batrachochytrium dendrobatidis* (Bd) in this species.

Resumen

Describimos una nueva especie de rana terrestre de desarrollo directo del grupo *Pristimantis danae* de bosques montanos procedentes de la provincia de La Mar, departamento de Ayacucho al sur de Perú con rango de distribución altitudinal entre los 1200–2000 msnm, en base a caracteres morfológicos y moleculares. El análisis filogenético basado en las secuencias concatenadas de los fragmentos de genes ARNr 16S, COI, RAG1 y TYR sugiere que la nueva especie es un taxón hermano del clado que incluye a una especie de *Pristimantis* no descrita de Cusco, *Pristimantis pharangobates* y *Pristimantis rhabdolaemus*. La nueva especie se asemeja más a *P. rhabdolaemus*; de la cual difiere por la ausencia de tubérculos escapulares y su menor tamaño corporal (17.0–18.6 mm en machos [$n=5$], 20.8–25.2 mm en hembras [$n=5$] en la nueva especie vs 22.8–26.3 mm en machos [$n=19$], 26.0–31.9 mm en hembras [$n=30$] de *P. rhabdolaemus*). Adicionalmente, reportamos la prevalencia de *Batrachochytrium dendrobatidis* (Bd) en esta especie de Terrarana.

Key words: Chytridiomycosis, cryptic species, montane forests, morphology, phylogeny

Palabras clave: Bosques montanos, especies crípticas, filogenia, morfología, quitridiomycosis



Academic editor: Angelica Crottini

Received: 4 April 2023

Accepted: 21 August 2023

Published: 20 December 2023

ZooBank: <https://zoobank.org/226A24AB-B4BE-4EFD-BF11-D6CA719AB601>

Citation: Herrera-Alva V, Catenazzi A, Aguilar-Puntriano C (2023) A new cryptic species of terrestrial breeding frog of the *Pristimantis danae* Group (Anura, Strabomantidae) from montane forests in Ayacucho, Peru. ZooKeys 1187: 1–29. <https://doi.org/10.3897/zookeys.1187.104536>

Copyright: © Valia Herrera-Alva et al. This is an open access article distributed under terms of the Creative Commons Attribution License ([Attribution 4.0 International – CC BY 4.0](https://creativecommons.org/licenses/by/4.0/)).

Introduction

Pristimantis (Terrarana, Strabomantidae) is an amphibian genus that comprises more than 600 species and occurs throughout the Americas (Hedges et al. 2008; Padial and De La Riva 2009; Padial et al. 2014; Waddell et al. 2018) from Honduras to Argentina. In Peru, there are 145 *Pristimantis*, which represents more than 20% of its global richness (Frost 2023). Many species of *Pristimantis* are morphologically similar despite belonging to different lineages (Elmer and Cannatella 2008; Padial and De la Riva 2009; Siqueira et al. 2009; Kieswetter and Schneider 2013; Hutter and Guayasamin 2015; Ortega-Andrade et al. 2015). The ubiquity of cryptic species in *Pristimantis* has led to underestimation of the real number of species in the genus (Ortega-Andrade et al. 2015; Guayasamin et al. 2017; Paez and Ron 2019; Carrion-Olmedo and Ron 2021). Nevertheless, the application of molecular techniques in an integrative framework (Dayrat 2005) generated a steady increase in species richness of *Pristimantis* (Köhler et al. 2022; Reyes-Puig and Mancero 2022). Integrative taxonomy uses more than one line of evidence and discipline to infer species limits (Simpson 1961; Wiley 1978; De Queiroz 2005; Schlick-Steiner et al. 2010; Aguilar et al. 2013; Hutter and Guayasamin 2015) and has become a critical tool to identify and delimit species as well as in understanding species formation (Aguilar et al. 2013; Minoli et al. 2014; Rojas et al. 2018; Hillis 2019; Zozaya et al. 2019).

One group with cryptic species includes *Pristimantis rhabdolaemus*. The taxonomic history is complex because Lynch and McDiarmid (1987) synonymised *Pristimantis pharangobates* with *P. rhabdolaemus*, until Lehr (2007) again split these two cryptic species. Incorrect labelling of GenBank sequence EF493706 (uploaded during the period from 1987 to 2007 when synonymy was in place) of *P. pharangobates* as "*P. rhabdolaemus*" (Heinicke et al. 2007; Padial et al. 2014; Lehr et al. 2017a, b; Acevedo et al. 2020) contributed to taxonomic confusion. Furthermore, specimens from Bolivia incorrectly assigned to *P. rhabdolaemus* added more confusion. Despite this history, *P. rhabdolaemus* species limits have not been studied using integrative taxonomy.

Therefore, as part of a study of *Pristimantis rhabdolaemus* species boundaries, we collected direct development frogs from the montane forests of La Mar Province, Ayacucho Department. Molecular and morphological analyses revealed that the collected specimens belong to an undescribed species. Our goals are to describe the new species and infer its relationships with other species of the *Pristimantis danae* species Group, as well as provide information about infection by the fungus *Batrachochytrium dendrobatidis* (Bd).

Materials and methods

Fieldwork and voucher specimens

VHA conducted field research in the montane forest of two small valleys (Fig. 1) in the VRAEM (Spanish acronym for Valley of the Rivers Apurimac, Ene and Mantaro), Ayacucho Department, southern Peru. The fieldwork was organised in two stages. The first occurred from November 2018 to June 2019 in the valley of the Chunchubamba River, which goes from Chiquintirca (2900 m a.s.l.)

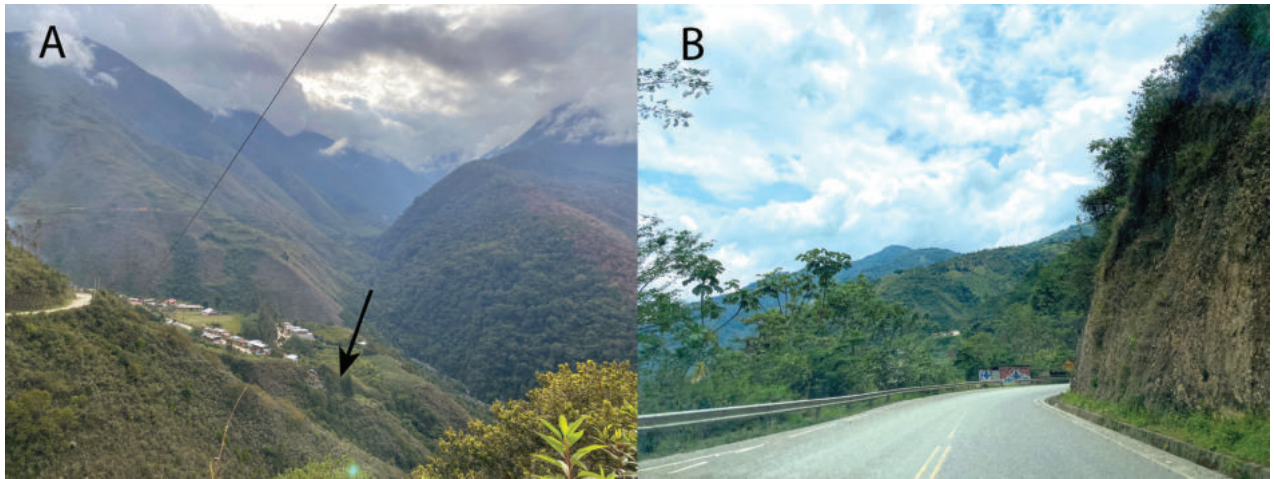


Figure 1. Montane forest of Cajadela (A) and Machente (B), Ayacucho Department. Type locality of *Pristimantis similaris* sp. nov. in Cajadela (A). Note the presence of secondary forest in both localities. Photo A taken on 8 November 2021 and B, on 24 October 2022. Arrow marks the type locality.

to San Antonio (800 m a.s.l.) in the districts of Anco and Anchiuay (both from La Mar Province). The second field-trip was in November 2021 in the valley of the Piene River, which goes from Yanamonte (2900 m a.s.l.) to San Francisco (800 m a.s.l.) in the Districts of Sivia (Huanta Province) and Ayna (La Mar Province), which included the visit to the type locality of *P. rhabdolaemus* in Machente (1650 m a.s.l.), also previously known as Huanhuachayocc, a name no longer recognised by the locals.

We extracted liver tissues by pulling the liver out of a small abdominal incision. We fixed specimens in 10% formaldehyde and stored them in 70% ethanol in the Department of Herpetology of the Museo de Historia Natural Universidad Nacional Mayor de San Marcos (MUSM), Lima, Perú. The Ministry of Agriculture issued research, collecting and genetic resources permits (000063-2018-GRA/GG-GRDE-DRAA-DFFS-D, 029-2016-SERFOR-DGGSPFFS and D000012-2022-MI-DAGRI-SERFOR-DGGSPFFS-DGSPFFS).

Morphology and morphometry

We follow Lynch and Duellman (1997) for the description format, except that we use “vomarine odontophores” instead of “dentigerous processes of vomers” (Duellman et al. 2006) and Duellman and Lehr (2009) for diagnostic characters. We sexed specimens by examining for the presence of vocal slits in mature males and by inspecting gonads in dissected specimens. VHA measured the following distances to the nearest 0.1 mm with digital calipers under a stereomicroscope: 1) snout-vent length (**SVL**), 2) tibia length (**TL**, distance from the knee to the distal end of the tibia), 3) foot length (**FL**, distance from the proximal margin of inner metatarsal tubercle to tip of Toe IV), 4) head length (**HL**, from the angle of the jaw to tip of snout), 5) head width (**HW**, at the level of the angle of the jaw), 6) horizontal eye diameter (**ED**), 7) horizontal tympanum diameter (**TY**), 8) interorbital distance (**IOD**), 9) upper eyelid width (**EW**), 10) internarial distance (**IND**), 11) eye-nostril distance (**EN**, straight line distance between anterior corner of orbit and

posterior margin of external nares) and one extra measurement: 12) Finger IV disc width (**F4**). Fingers and toes are numbered pre-axially to postaxial from I–IV and I–V, respectively. We compared the lengths of toes III and V by addressing both toes against Toe IV; lengths of fingers I and II were compared by addressing the fingers against each other. Vladimir Díaz Vargas photographed live specimens and VHA preserved the specimens. We used photographs for descriptions of skin texture and colouration. Specimens examined are listed in Appendix 1; other collection acronyms are MUSM = Museo de Historia Natural San Marcos (Lima, Peru); KU = University of Kansas, Museum of Natural History (Kansas, USA); LSUZ = Louisiana State University Museum of Zoology (Louisiana, USA).

Molecular phylogenetic analysis

We performed a phylogenetic analysis to infer relationships of the new species with other species of the *Pristimantis danae* Group (Padial et al. 2014). We used fragments of 16S rRNA, COI, RAG1 and TYR genes. We obtained novel sequences by extracting DNA from six specimens of the new species (MUSM 41030, 41031, 41035, 41036, 41037, 41323) with a commercial extraction kit (IBI Scientific, Iowa, USA). We followed Hedges et al. (2008) and von May et al. (2017) for primers and PCR thermocycling conditions. Primers are listed in Table 1. We purified PCR products using Exosap-IT Express (Affymetrix, Santa Clara, CA, USA). MCLAB (San Francisco, CA) performed Sanger sequencing.

We follow Padial et al. (2014) and Pyron and Wiens (2011) for species group assignment within *Pristimantis* and the choice of outgroup taxa. We downloaded from GenBank all available sequences of 16S rRNA, COI, RAG1 and TYR of other species of the *P. danae* Group and some of the outgroup taxa. We used selected species of the *P. conspicillatus* Group (*P. bipunctatus*, *P. iiap* and *P. skydmainos*) and *P. prolatus* as outgroup taxa (Appendix 2).

We used Geneious Prime version 2023.0.1 (Biomatters, <http://www.geneious.com/>) to assemble pair-end reads, generate a consensus sequence for each gene and align our novel and GenBank sequences with MAFFT included in Geneious as a plug-in. Posteriorly, we concatenated the four genes (16S, COI, RAG1 and TYR) using the default settings in Geneious. We trimmed aligned

Table 1. Primers employed in this study for PCR and DNA sequencing. F = forward, R = reverse.

Locus	Primer		Sequence (5' – 3')	Reference
16S	16SAR	F	CGCCTGTTTATCAAAAACAT	Meyer (2003)
	16SBR	R	CCGGTCTGAACCTCAGATCACGT	
COI	dgLC01490	F	GGTCAACAAATCATAAAGAYATYGG	Bossuyt and Milinkovitch (2000)
	dgHC02198	R	TAAACTTCAGGGTGACCAARAAYCA	
RAG1	R182	F	GCCATAACTGCTGGAGCATYAT	Heinicke et al. (2007)
	R270	R	AGYAGATGTTGCCTGGGTCTTC	
TYR	Tyr1C	F	GGCAGAGGAWCRTGCCAAGATGT	Lanfear et al. (2012)
	Tyr1G	R	TGCTGGGCRCTCTCCARTCCCA	

sequences to a length of 591 bp for 16S, 685 bp for COI, 624 bp for RAG1 and 545 bp for TYR (Fasta file included in doi: 10.5281/zenodo.8278333). To obtain the nucleotide substitution model for each gene, we used PartitionFinder with Python v. 2.7 + Anaconda2 (Lanfear et al. 2017). We inferred a Maximum Likelihood phylogenetic tree with IqTree (Nguyen et al. 2015) by using its web server (<http://iqtree.cibiv.univie.ac.at/>) with the following settings: ultrafast bootstrap method, 1000 bootstrap alignments and nucleotide evolution models of GTR+I+G for the gene 16S and for 1st codon position of COI; GTR+G for RAG1, TYR and 3rd codon position of COI; and GTR for 2nd codon positions of COI. Additionally, we generated a tree using Bayesian Inference using the plugin MrBayes for Geneious Prime with 1.1×10^6 generations and sampling every 200 generations from the Markov Chain Monte Carlo (MCMC). We determined stationarity by plotting the log-likelihood scores of sample points against generation time; when the values reached a stable equilibrium and split frequencies fell below 0.01, stationarity was assumed. We discarded 100,000 samples and 10% of the trees as burn-in. We consider Bayesian Posterior Probabilities (BPP) > 95% as evidence of support for a clade (Huelsenbeck and Ronquist 2001; Wilcox et al. 2002; Aguilar et al. 2013). We visualised both trees in FigTree v.1.4.4.

Finally, we compare uncorrected p-distances of 591 bp (including gaps) of 16S mitochondrial rRNA gene of *Pristimantis* included in our analysis (included as a separated file in: doi: 10.5281/zenodo.8278333). To estimate p-uncorrected genetic distances, we used MEGA 11 (Tamura et al. 2021) with a variance estimation method of 1000 bootstrap and rates amongst sites of G+I. We excluded from this analysis species from the sister clade (*P. bounides*, *P. anip-topalmatus*, *P. albertus*, *P. attenboroughi*, *P. humboldti*, *P. danae*, *P. ornatus*, *P. puipui*, *P. reichlei* and *P. sagittulus*, Fig. 2), except from *Pristimantis* sp.3 from Bolivia because these specimens had been identified as *P. rhabdolaemus* on GenBank and *P. scitulus*, because they are novel sequences for this species.

Quantitative PCR assays for fungal infection (Bd)

During fieldwork in 2018, 2019 and 2021, we swabbed live frogs of the new species with a synthetic dry swab (Medical Wire & Equipment #113) to quantify infection by *Batrachochytrium dendrobatidis* (Bd). We stroked swabs across the skin of juveniles and adults a total of 30 times per individual: five strokes on each side of the abdominal mid-line, five strokes on the inner thighs of each hind leg and five strokes on the foot webbing of each hind leg. We used a standard quantitative Polymerase Chain Reaction (qPCR) assay using DNA extracted from swabs to quantify the level of infection (Boyle et al. 2004). Following the protocol of Boyle et al. (2004) and Hyatt et al. (2007), we extracted DNA from swabs using 40 µl of PrepMan Ultra (Applied Biosystems). We analysed each extract once with a QuantStudio 3 qPCR system (ThermoFisher Scientific). We calculated the number of zoospore equivalents (ZE) (i.e. the genomic equivalent for Bd zoospores) by comparing the sample results with a serial dilution of standards (gBlock synthetic standards, IDT DNA, Iowa, USA). We considered any sample with ZE > 1 to be infected or Bd-positive.

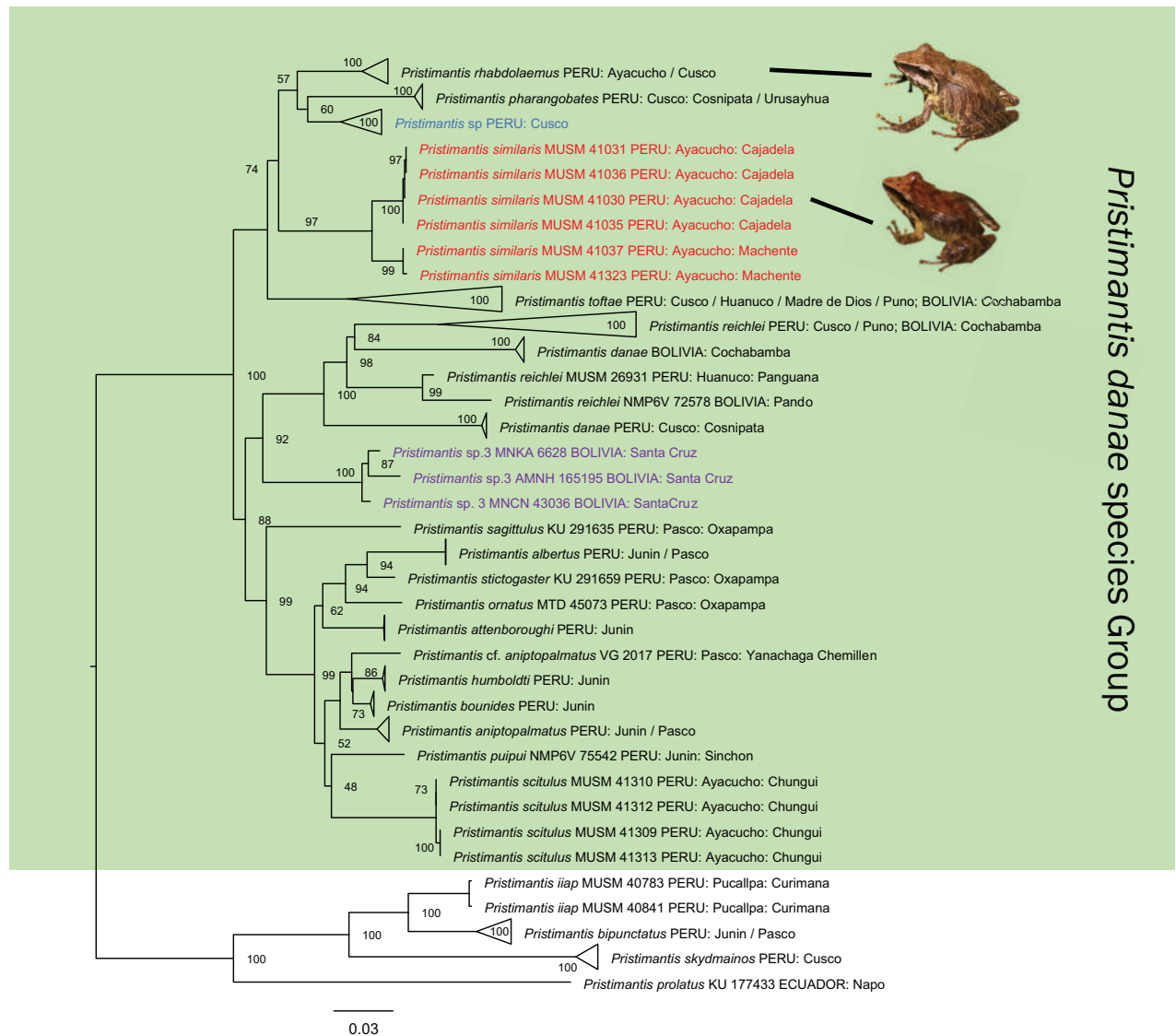


Figure 2. Maximum Likelihood tree of concatenated genes 16S rRNA, COI, RAG1 and TYR taken from GenBank and novel sequences. Numbers on nodes are bootstrap values (see Materials and Methods section for details). Green shadow corresponds to the ingroup. *Pristimantis similaris* sp. nov. in red, *Pristimantis* sp. 3 from Bolivia in purple and *Pristimantis* sp. from Cusco in blue. Maximum Likelihood optimal tree with bootstrap node values from the analysis of a concatenated dataset of 591 bp (16S), 685 bp (COI), 624 bp (RAG1) and 545 bp (TYR) of 128 species aligned by MAFFT and node support assessed using 10,000 replicates in IQTREE.

Nomenclatural acts

The electronic version of this article in Portable Document Format (PDF) will represent a published work according to the International Commission on Zoological Nomenclature (ICZN) and, hence, the new name contained in the electronic version is effectively published under that Code from the electronic edition alone. This published work and its nomenclatural acts have been registered in ZooBank, the online registration system for the ICZN. The ZooBank LSIDs (Life Science Identifiers) can be resolved and the associated information is viewed through any standard web browser by appending the LSID to the prefix <http://zoobank.org/>. The LSID for this publication is urn: urn:lsid:zoobank.org:pub:226A24AB-B4BE-4EFD-BF11-D6CA719AB601.

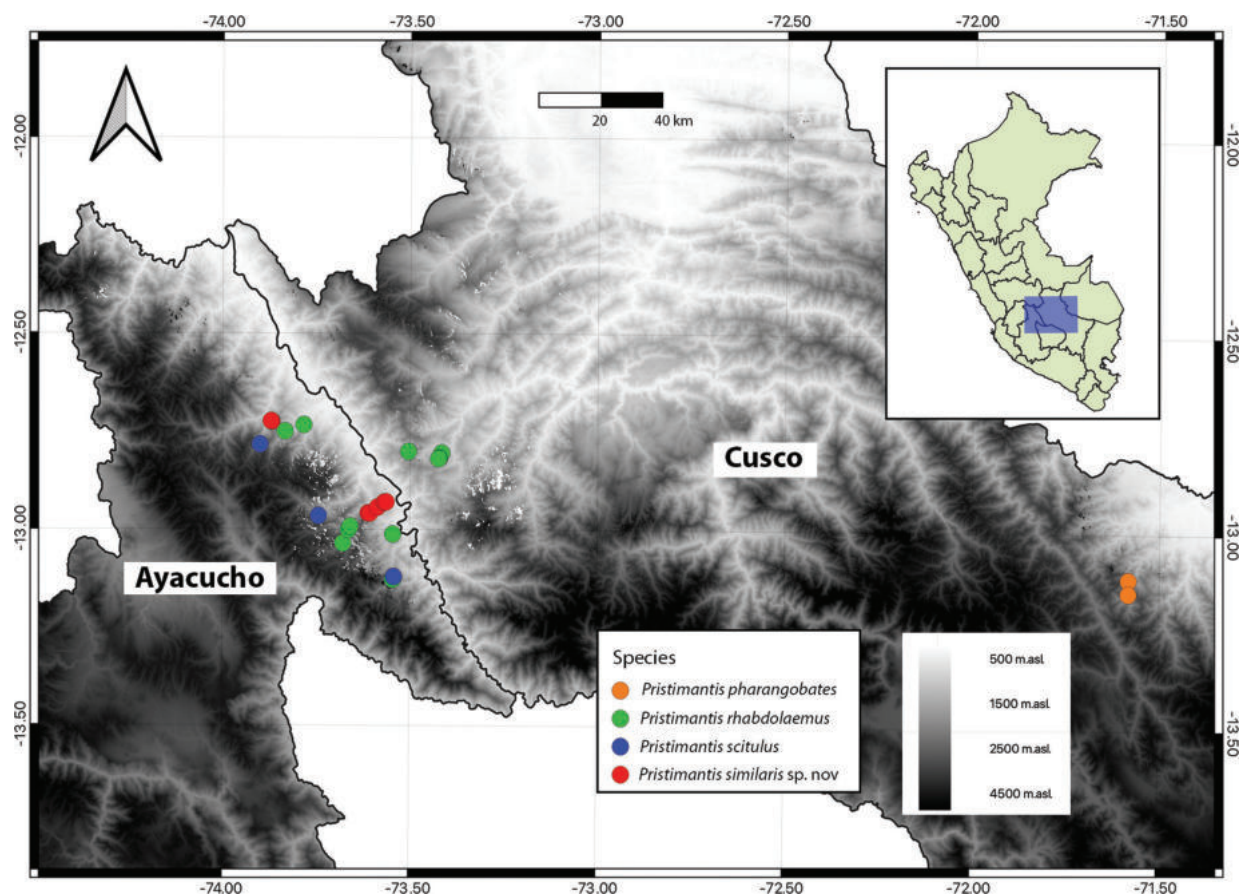


Figure 3. Distribution map of some species of the *Pristimantis danae* species Group in Ayacucho and Cusco Departments. Raster of altitude from 500 to 4500 m. a.s.l. (white to black). Locality of new species in red circles.

Results

Molecular phylogenetic analysis

Our Maximum Likelihood phylogeny, based on four concatenated gene fragments (Fig. 2 and Appendix 3 – expanded ML tree), found the new species (in red) included in a clade with specimens of *Pristimantis rhabdolaemus*, *P. pharangobates* and *P. toftae* from their respective type localities, as well as a candidate species from Cusco (in blue). The results from the Bayesian phylogeny (Appendix 4) are largely congruent with the results from the ML phylogeny.

Pristimantis scitulus is within the *danae* Group and sister to a clade consisting of *P. aniptopalmatus*, *P. humboldti* and *P. bounides*, but with low support. Both our ML and BI phylogenies recover *P. danae* as paraphyletic, with individuals from the type locality in Cosñipata (Cusco, Peru) forming part of a clade that includes *P. danae* specimens from Bolivia and *P. reichlei*, albeit with low support.

Genetic distances (uncorrected p-distances) for the rRNA 16S gene between *P. similaris* sp. nov. and species of the *P. danae* species Group vary from 5.6–6.9% for *P. rhabdolaemus*, 5.9–6.3% for *P. pharangobates*, 6.1–6.7% for *Pristimantis* sp., 6.5–7.5% for *P. scitulus*, 7.3–7.9% for *Pristimantis* sp. 3 and 7.7–9.3% for *P. toftae* (see Suppl. material 1, doi: 10.5281/zenodo.8278333). We also identified two populations within our new species, the first one from the type locality in Cajadela and the second, from Machente. The genetic distances between these populations were 2.7–2.8%.

Fungal infection by *Batrachochytrium dendrobatidis* (Bd)

We found six out of 18 specimens of *P. similaris* (30%) infected by the fungus *Batrachochytrium dendrobatidis* (Bd), with levels of infection varying from 11.5 to 8889.3 zoospore genomic equivalents. Our finding confirms that species of *Pristimantis* can be infected with the fungus (Catenazzi et al. 2011; Warne et al. 2016), despite their life cycle excluding aquatic stages and, thus, limiting the frogs' exposure to the aquatic zoospores of Bd.

Species description

Our phylogenetic tree shows a candidate species from Ayacucho with high support and having high genetic distances with closely-related phylogenetic species (see Fig. 2 and Appendix 3). In addition, after a careful examination of its morphology and pattern of colouration, this candidate species shows differences with other species of the *P. danae* Group. Based on these results, we describe this candidate species from Ayacucho Department as a new species of *Pristimantis*.

***Pristimantis similaris* sp. nov.**

<https://zoobank.org/BC56FD8A-6EBD-43C9-A446-689FC3253576>

Figs 4–6

Common name. English: Similar Rubber Frog. Spanish: Rana cutín similar.

Generic placement. We assign this species to the genus *Pristimantis*, based on morphology and molecular data (Figs 2, 4, 6).

Type material. Holotype. MUSM 41030, adult male (Figs 4, 5) from Comunidad Cajadela (12°57'16.50"S, 73°35'0.70"W, 1460 m a.s.l.), Distrito Anco, Provincia La Mar, Departamento Ayacucho, Peru, collected on 15 November 2018 by V. Herrera-Alva, E. Castillo-Urbina, V. Díaz, M. Fernandez, and J. Gamboa.

Paratypes. Nine specimens. Five adult females (MUSM 41031, 41032, 41035, 41036 and MUSM 41037). Four adult males (MUSM 41029, 41028, 41033 and MUSM 41034). All the specimens were collected at the type locality, except MUSM 41037, which was collected in Comunidad Machente (12°41'31.70"S, 73°51'0.30"W, 1640 m a.s.l.), Distrito Ayna, Provincia La Mar, Departamento Ayacucho, Peru, on 11 November 2021 by V. Herrera-Alva, E. Castillo-Urbina, V. Díaz and K. Ñaccha.

Diagnosis. A new species of *Pristimantis* assigned to the *P. danae* species Group having the following combination of characters: (1) Skin on dorsum shagreen, skin on venter areolate; discoidal and dorsolateral folds present, weak; thoracic fold present; (2) tympanic membrane and tympanic annulus present, distinct, visible externally; (3) snout subaccuminated in dorsal view, round in lateral view; (4) upper eyelid lacking tubercles; EW smaller than IOD; cranial crest absent; two small and flat tubercles above the snout near the eyes; (5) dentigerous processes of vomers low, oblique in five of the paratypes, absent in four paratypes and the holotype; (6) males with vocal slits, subgular vocal sac large extending on to chest and without nuptial pads; (7) Finger I slightly shorter than Finger II; discs of digits expanded, flat and truncated; (8) fingers without lateral fringes; (9) ulnar tubercles present, but diffuse; (10) heel with

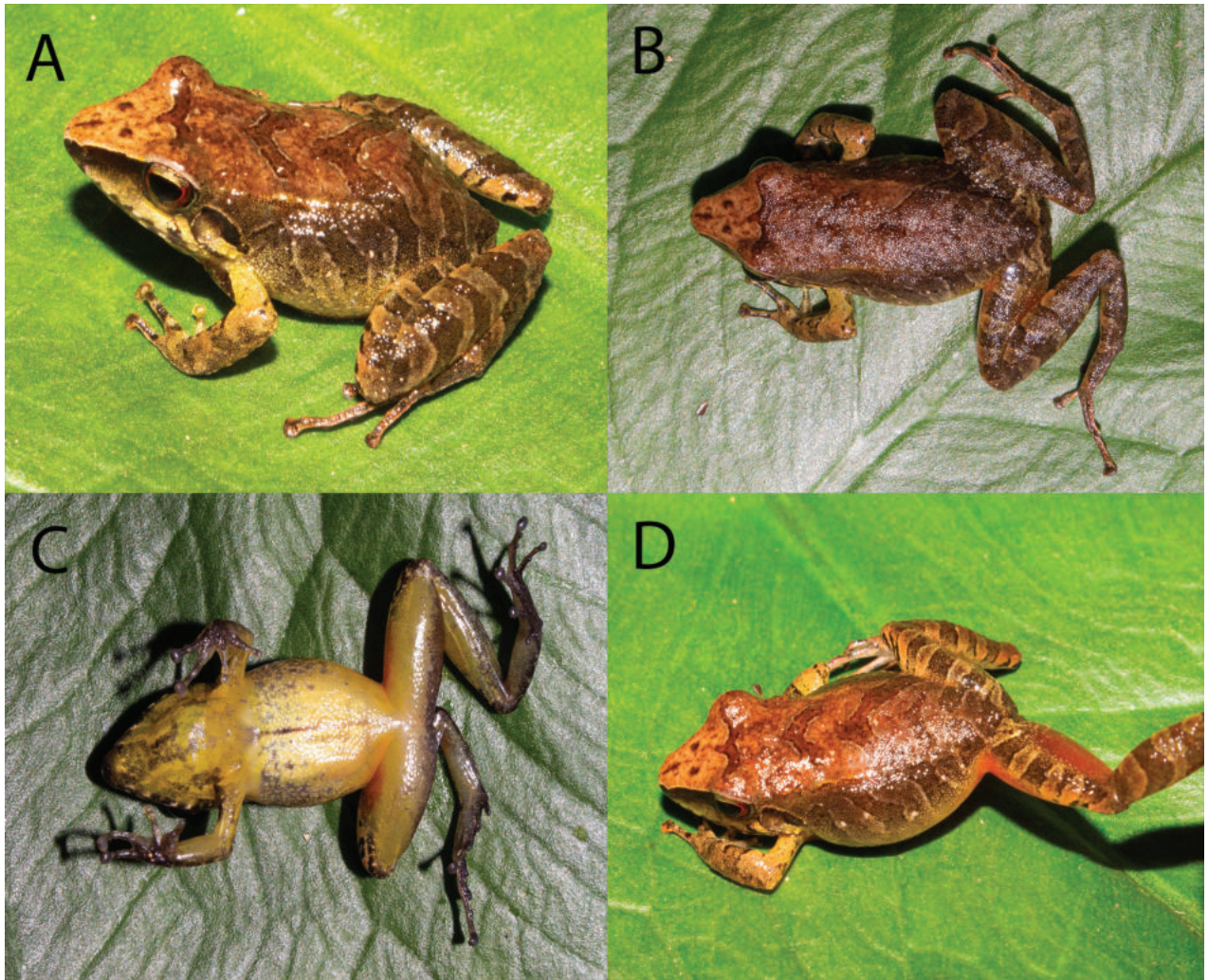


Figure 4. *Pristimantis similaris* sp. nov. (A–D) male. SVL: 17.0 mm. Holotype. MUSM 41030. Photos by Vladimir Diaz-Vargas.

two to three small and flat tubercles; inner tarsal fold present, small; (11) inner metatarsal tubercle ovoid, 2–3 times larger than outer one; outer metatarsal tubercle small, ovoid; numerous and flat supernumerary tubercles; (12) toes without lateral fringes; basal toe webbing absent; toe V is slightly longer than toe III; toe discs about as large as those on fingers; (13) in life, dorsum varies from blackish to dark brown with three conspicuous chevrons (not very visible in some cases) (Fig. 6); in most of the adults, the anterior surfaces of thighs reddish-orange, posterior surfaces of thighs brown; flanks cream without tubercles; groin same pattern as flanks mostly, some specimens with orange-red-dish colouration (Figs 4, 6); venter cream to yellow with black conspicuous reticulations in the throat and black marks in the chest, males present yellow throat with black or white longitudinal reticulations not as conspicuous as in females (Figs 4, 6); iris dark copper-coloured with fine black vermiculations; (14) SVL in adult females 20.8–25.2 mm (mean = 23.4 ± 1.8 SE, $n = 5$), in adult males 17.0–18.6 mm (mean = 18.1 mm ± 0.7 SE, $n = 5$).

Comparisons. *Pristimantis similaris* is distinguished from its congeners in Peru and Bolivia by the following combination of characters: skin on dorsum areolate, tympanum and tympanic annulus distinct, weakly-defined discoidal and dorsolateral folds, two small and flat tubercles above the snout near the

eyes (not conspicuous in preservative), dorsum dark brown with three darker chevrons, anterior surface of thighs usually orange-reddish and posterior surface of thighs dark brown. *Pristimantis similaris* can be distinguished from *P. rhabdolaemus* and *P. pharangobates* by the following characters (characters in parenthesis): smaller SVL of 20.8–25.8 mm in ten females and 15.2–18.9 mm in eight males (*P. pharangobates* 23.1–27.8 mm in females and 15.2–18.2 mm in males; *P. rhabdolaemus* 25.5–31.9 mm in females and 24.1–26.3 mm in males); absence of scapular tubercles (present in both species); presence of conspicuous longitudinal black and white or yellow marks on the throat and chest (less conspicuous in *P. pharangobates* and *P. rhabdolaemus*).

Other species in the *Pristimantis danae* species Group that are similar to *P. similaris* include *P. danae*, *P. reichlei*, *P. scitulus* and *P. toftae*. *Pristimantis danae* and *Pristimantis reichlei* also have brown chevrons in the dorsum and differ from the new species by the combination of the following characters: males nuptial pads absent (present in *P. danae* and *P. reichlei*), dorsolateral folds present (weak in *P. danae* and absent *P. reichlei*), small pale spots in the posterior surfaces of the thighs absent (present in *P. danae* and *P. reichlei*) and smaller size in *P. similaris*. *Pristimantis scitulus* is morphologically similar to *P. similaris* and has a parapatric distribution (Yuraccyacu, in the Piene Valley, Ayacucho Region). *Pristimantis similaris* can be distinguished by lacking a conical tubercle in the upper eyelid and heels (present in *P. scitulus*), mid-ventral line absent (present in *P. scitulus*) and absence of marks in the groin or thighs (conspicuous dark spots in the groin that is continuous as marks on the posterior surfaces of the thighs in *P. scitulus*). *Pristimantis toftae* is a smaller species that is superficially similar to *P. similaris*. The new species can be distinguished by the absence of coloured marks or spots in the groin or other parts of its body (yellow spot in the groins of *P. toftae*), absence of labial bar (presence of a white labial bar in *P. toftae*).

Pristimantis similaris is also similar to some species in the *Pristimantis conspicillatus* species Group, which includes *P. bipunctatus*, *P. skydmainos* and *P. iiap*. The parapatric *Pristimantis bipunctatus* (found in Calicanto at 1940 m. a.s.l. in the Piene Valley, Ayacucho Region), has dorsum and ventral skin shagreen and areolate, snout long, upper eyelids without tubercles similar to *P. similaris*, but the latter differs by having finger I slightly shorter than finger II (finger I and finger II about equal length in *P. bipunctatus*), discs on outer fingers truncated (broadly rounded in *P. bipunctatus*), scapular tubercles absent (present in *P. bipunctatus*) and by its smaller size (22.6–28.8 mm in males and 32.4–41.5 mm in females in *P. bipunctatus*). *P. similaris* can be distinguished from *P. skydmainos* by the absence of a mid-dorsal tubercle (present in *P. skydmainos*), absence of nuptial pads (present in *P. skydmainos*), finger I smaller than finger II (finger I longer than finger II in *P. skydmainos*), absence of spots or marks in the posterior surfaces of the thighs (minute cream flecks on the posterior surfaces of the thighs in *P. skydmainos*) and the absence of W-shaped marks (present in the scapular region in *P. skydmainos*). *Pristimantis similaris* differs from *P. iiap* from the lowland Amazon of the Ucayali Region by lacking large granules on flanks (present in *P. iiap*), lacking granules on the upper eyelids (present in *P. iiap*) and by having finger I shorter than finger II (finger I and II about the same length in *P. iiap*).



Figure 5. *Pristimantis similaris* sp. nov. **A** hand **B** toe. Male. Holotype. MUSM 41030. Photos by VHA.

Another species with some resemblance (mainly on the throat in ventral view) to the new species is *Pristimantis tanyrhynchus*. *Pristimantis similaris* can be distinguished from *P. tanyrhynchus* by the absence of nuptial pads in males (present in *P. tanyrhynchus*) and absence of tubercles on the heel (heel with a conical and large tubercle in *P. tanyrhynchus*).

Description of the holotype. Head longer than wide; head length 43% of SVL; head width 35% of SVL; cranial crests absent; snout subaccuminated in dorsal view and in lateral view (Fig. 4A, B, D); eye-nostril distance same as the eye diameter; nostrils slightly protuberant, directed dorsolaterally; canthus rostralis long, straight in lateral and in dorsal views; loreal region concave; upper eyelid without tubercles, width 90% of IOD (see photo in life Fig. 4); supratympanic fold short and narrow, extending from posterior margin of upper eyelid slightly curved to insertion of arm; tympanic membrane and annulus present; distinct conical postrictal tubercles present bilaterally. Choanae small, ovoid, not concealed by palatal shelf of maxilla; dentigerous processes of vomers absent; vocal slits present; tongue longer than short, oval, about a quarter times as long as wide, notched posteriorly, half of the tongue posteriorly free; one large vocal sac extending on to chest.

Skin on dorsum and flanks shagreen, continuous dorsolateral folds present extending from posterior level of tympanic area to level of hind limb insertion; skin on throat, chest and belly areolate; discoidal fold present; thoracic fold present.

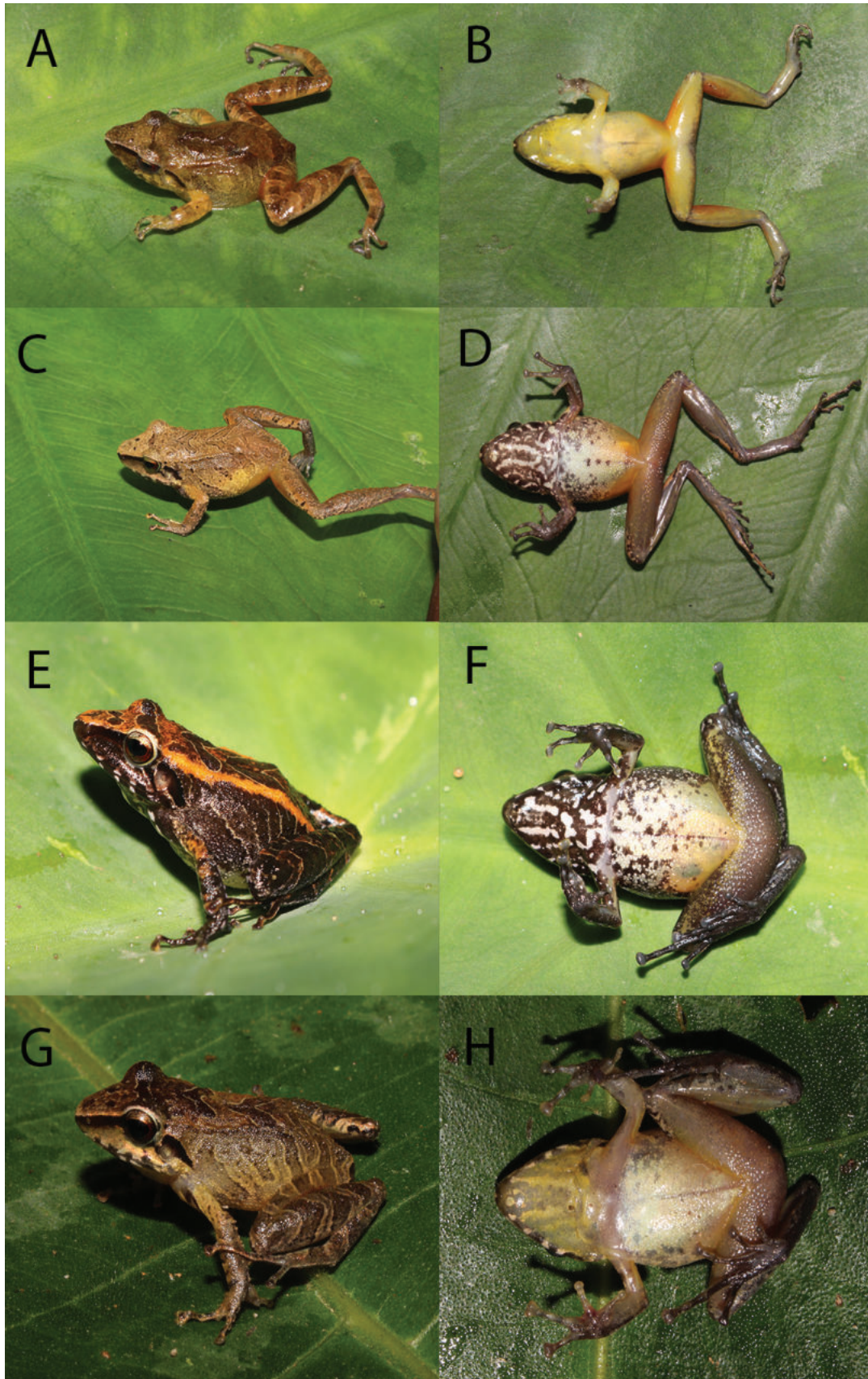


Figure 6. A–H colour and pattern variation of *Pristimantis similaris* sp. nov. Specimen from A–F collected in Cajadela: A, B male MUSM 41029 C, D female MUSM 41031 E, F female MUSM 41032. Specimen G, H male MUSM 41326 collected in Machente. Photos by V. Diaz-Vargas and E. Castillo-Urbina.

Outer ulnar surface without tubercles; palmar tubercle bifid; thenar tubercle ovoid; subarticular tubercles well defined, most prominent on base of fingers, ovoid in ventral view, subconical in lateral view; supernumerary tubercles indistinct; fingers long and thin lacking lateral fringes, Finger I shorter than Finger II; tips of digits of fingers expanded, truncated, with circumferential grooves; nuptial pads absent (Fig. 5A).

Hind limbs long, slender, tibia length 58% of SVL; foot length 49% of SVL; dorsal surfaces of hind limbs tuberculate; inner surface of thighs smooth, posterior surfaces of thighs shagreen, ventral surfaces of thighs smooth; heels each with three small conical tubercles; outer surface of tarsus with one minute low tubercle; inner tarsal fold present; inner metatarsal tubercle ovoid, two times the size of round outer metatarsal tubercle; subarticular tubercles well defined, ovoid in ventral view, subconical in lateral view; few plantar supernumerary tubercles, about one quarter the size of subarticular tubercles; toes without lateral fringes; basal webbing absent; tips of digits expanded, truncated, less expanded than those on fingers, with circumferential grooves; relative length of toes: $1 < 2 < 3 < 5 < 4$; Toe V slightly longer than Toe III (tip of digit of Toe III and Toe V not reaching distal subarticular tubercle on Toe IV; Fig. 5B).

Measurements (in mm) of the holotype. SVL 17.0; tibia length 9.9; foot length 8.4; head length 7.3; head width 5.9; eye diameter 2.3; inter orbital distance 1.9; upper eyelid width 1.7; internarial distance 2.0; eye-nostril distance 2.3; tympanum length 1.0; tympanum height 1.1; forearm length 4.3.

Colouration of the holotype in life (Fig. 4). In life, dorsum dark brown with three conspicuous chevrons; flanks cream without tubercles, groin same pattern as flanks with orange-reddish colouration; anterior surfaces of thighs reddish-orange, posterior surfaces of thighs brown; venter cream to yellow with black conspicuous reticulations in the throat and black marks in the chest; iris dark copper-coloured with fine black vermiculations (Fig. 4).

Colouration of the holotype in preservative. The dorsal ground colouration is pale brown with three browner chevrons; narrow blackish canthal and supratympanic stripes; flanks pale brown with dark brown and cream flecks forming irregularly-shaped diagonal bars; groin and anterior surfaces of thighs brown with dark brown flecks; chest, belly and ventral surfaces of thighs pale cream, throat pale cream and grey-striped; palmar and plantar surfaces and fingers and toes dark brown; iris pale grey.

Variation. All specimens have the same general appearance, with three chevrons on the dorsum. MUSM 41029 is completely yellow and lacks marks on the chest or throat. MUSM 41032 has two brown-yellowish longitudinal bars on the dorsolateral folds. MUSM 41341 is blackish-brown and the three chevrons are not very visible (Fig. 6). Some individuals (MUSM 41030–2, 41036–7) lack the dentigerous processes of vomers. Morphological measurements ranges and proportions of types are included in Tables 2, 3.

Etymology. The specific name corresponds to the Latin word “similar”. This refers to the similarity of the new species and its close phylogenetic relationship with *P. rhabdolaemus* and *P. pharangobates*.

Distribution and natural history. The new species is only known from montane forests of Ayna and Anco in Departamento Ayacucho at elevations from 1200–2000 m a.s.l. in secondary forests (Figs 1, 3). This species was found only at night after 18:00 hours, usually perching on wet leaves 0.5–1.5 m above

Table 2. Morphological measurements (mm) of nine paratype specimens of *Pristimantis similaris* sp. nov. For abbreviations, see Materials and methods.

Character	MUSM 41028	MUSM 41029	MUSM 41031	MUSM 41032	MUSM 41033	MUSM 41034	MUSM 41035	MUSM 41036	MUSM 41037
Sex	Male	Male	Female	Female	Male	Male	Female	Female	Female
SVL	18.1	17.7	25.2	22.7	18.8	18.6	24.7	23.4	20.8
TL	10.3	10.4	14.8	13.5	10.5	10.8	14.0	14.1	12.1
FL	9.0	8.4	12.4	11.3	9.0	9.5	11.6	12.4	9.4
HL	7.2	7.2	9.6	8.9	7.3	7.9	9.8	9.2	8.9
HW	5.9	6.5	8.5	7.5	6.6	6.9	8.2	8.0	7.5
ED	1.9	2.4	2.8	2.5	2.3	2.3	2.9	2.6	2.4
TY	0.9	1.0	1.1	1.1	1.0	1.1	1.3	1.1	1.2
IOD	2.1	2.0	2.4	2.2	2.1	2.0	2.4	2.3	2.2
EW	1.8	1.7	2.3	1.9	1.8	1.8	2.3	2.2	2.1
IND	2.0	2.3	2.9	2.6	2.2	2.2	2.7	2.5	2.5
EN	2.3	2.3	3.1	2.8	2.5	2.6	3.0	2.7	2.8
F4	0.7	0.7	1.0	0.8	0.9	0.7	0.9	1.0	0.8

Table 3. Measurements (in mm) and proportions of adult male and female type specimens of *Pristimantis similaris* sp. nov.; ranges followed by means and one standard deviation in parentheses. For abbreviations, see Materials and methods.

Character	Males (n = 5)	Females (n = 5)
SVL	17.0–18.6 (18.1 ± 0.7)	20.8–25.2 (23.4 ± 1.8)
TL	9.9–10.8 (10.4 ± 0.3)	12.1–14.8 (13.7 ± 1.0)
FL	8.4–9.5 (8.9 ± 0.5)	9.4–12.4 (11.4 ± 1.2)
HL	7.2–7.9 (7.4 ± 0.7)	8.9–9.8 (9.3 ± 0.4)
HW	5.9–6.9 (6.5 ± 1.0)	7.5–8.5 (7.9 ± 0.4)
ED	1.9–2.4 (2.2 ± 0.5)	2.4–2.9 (2.6 ± 0.2)
TY	1.0–1.1 (1.0 ± 0.1)	1.0–1.3 (1.2 ± 0.1)
IOD	1.9–2.1 (2.0 ± 0.1)	2.2–2.4 (2.3 ± 0.1)
EW	1.7–1.8 (1.75 ± 0.05)	1.9–2.3 (2.1 ± 0.2)
IND	2.0–2.3 (2.1 ± 0.1)	2.5–2.9 (2.6 ± 0.2)
EN	2.3–2.6 (2.4 ± 0.3)	2.8–3.1 (2.9 ± 0.2)
F4	0.7–0.9 (0.8 ± 0.1)	0.8–1.0 (0.9 ± 0.1)
TL/SVL	0.56–0.59	0.57–0.60
HL/SVL	0.39–0.43	0.38–0.43
EN/HL	0.32–0.34	0.30–0.33

the ground. Males call rarely and their calls are overshadowed by other male species (*Pristimantis lacrimosus* species Group) calling louder. The species is common and appears to tolerate some human disturbance, because it was found near abandoned farms, less frequented roads and in the surroundings of abandoned houses. Syntopic species included candidate new species in the *Pristimantis lacrimosus* species Group and candidate new species in the *Pristimantis platydactylus* species Group, which were more abundant than the new

species. Sympatric species included frogs and toads *Gastrotheca pacchama-ma*, *Nymphargus pluvialis*, *Boana palaestes*, *Rhinella inca*, *Dendropsophus vraemi* and *Hyalinobatrachium* aff. *bergeri*; lizards *Cercosaura manicata*, *Stenocercus crassicaudatus* and *Potamites montanicola*; and snakes *Dipsas* cf. *peruana*, *Leptodeira annulata* and *Epictia* cf. *peruviana*.

Discussion

We describe *Pristimantis similaris*, a new species morphologically similar and phylogenetically related to *P. rhabdolaemus* and *P. pharangobates*. Despite their confusing taxonomic history (see Introduction), our phylogenetic analyses show that *P. rhabdolaemus* and *P. pharangobates* are distinct evolutionary lineages.

Pristimantis rhabdolaemus was described from mid-altitude montane forests restricted to Ayacucho and Cusco Departments (Duellman 1978). Although we visited the type locality of *P. rhabdolaemus* (Machente, Ayacucho Department) at 1650 m a.s.l., we could not find any specimens from this species. For that reason, we sequenced specimens of *P. rhabdolaemus* from Tocate, Anchihuay district in the Ayacucho Department (~ 38 km straight air line to Machente) because morphological analysis and comparison with the type series confirmed that these specimens corresponded to *P. rhabdolaemus sensu stricto*. Padial et al. (2007) reported *P. rhabdolaemus* from Bolivia on the basis of 16S rRNA of two incorrectly assigned specimens (MNKA 6628 and MNCN 43036), but our concatenated phylogeny suggests that the Bolivian specimens belong to a different and probably undescribed species, *Pristimantis* sp. 3 (in purple, Fig. 2). Likewise, *P. pharangobates* should be restricted to Cusco Department until molecular data become available and support the presence of this species in Puno (south-eastern Peru) and Bolivia.

We also found another candidate species from Cosñipata and Alfamayo in Cusco, morphologically similar and phylogenetically related to *P. pharangobates* and *P. rhabdolaemus* (in blue, Fig. 2). Additional specimens and analyses are needed to assess the taxonomic status of these potential new species.

The taxonomy of other species of the *P. danae* species Group requires further work. For instance, specimens identified as *P. danae* or *P. reichlei* tend to form paraphyletic groups in phylogenies. We suggest that both species might benefit from future studies clarifying the phylogenetic relationships of their assigned populations. Such studies might include the use of genomic data for these species (including *P. toftae*) because the use of four genes (three nuclear) in this study was not sufficiently informative to infer with confidence phylogenetic relationships between the most inclusive clades.

Furthermore, our phylogenies include for the first time sequences of *P. scitulus* from Chungui, Ayacucho previously known only from two type specimens in Yuraccyacu, Ayacucho (at 2600 m a.s.l.) and supports the assignment of this species in the *P. danae* species Group. We also included sequences for the first time of *P. iiap* (outgroup) and it is recovered in the *P. conspicillatus* species Group.

According to Swenson et al. (2012), who discussed the endemism of species (birds, mammals, plants and amphibians) in the eastern Andean slopes from the treeline (~ 3500 m a.s.l.) to the Amazon lowlands, most of the montane forests in the eastern Andean slopes of Peru and Bolivia (fig. 7

in Swenson et al. (2012)) are centres of endemism, specially in areas with little field evaluations due to social problems, such as montane forests in Ayacucho Department.

We would like to highlight the areas surroundings the type locality of *P. similaris* and closely-related species in south-eastern Peru. The Departments of Ayacucho and Cusco have biologically “irreplaceable areas” due to the configuration of the western Andes, the eastern Cordillera de Vilcabamba and the Apurimac River (Swenson et al. 2012). These geographical formations created a deep canyon along the Apurimac River at the border of the Departments of Ayacucho and Cusco (Lehr and Catenazzi 2008; Hazzi et al. 2018; Herrera-Alva et al. 2020), dissecting the Andean cordillera and providing mid-altitude isolated areas. The Apurimac Canyon is an important barrier for the dispersal of amphibians, such as high-altitude species of Terrarana: the Canyon splits the distribution of the genus *Phrynopus* to the northeast part of the Canyon from the distribution of *Bryophryne* southwest of the Canyon (Lehr and Catenazzi 2008, 2009, 2010). We believe that this pattern can be extended to mid-altitude montane forest frogs, such as species in the *P. danae* or *P. lacrimosus* species groups (pers. com. Ernesto Castillo-Urbina) or the distribution of mid-altitude toads, such as *Atelopus moropukaqumir* (northwest of the Apurimac Canyon) and *A. erythropus* (southeast of the Canyon; Herrera-Alva et al. (2020)). Therefore, we hypothesise that the Apurimac Canyon could have promoted vicariant speciation of morphologically-similar *Pristimantis* in these montane forests. For instance, *P. similaris* occurs from 1200 to 2000 m a.s.l. on the northwest of the Apurimac Canyon in Ayacucho Department, while *Pristimantis* sp. occurs from 1200–2000 m a.s.l. in Cusco Department, southeast of the Apurimac Canyon. Nevertheless, the Apurimac Canyon might have not been a geographic barrier to other species, such as *P. rhabdolaemus* which has been found at both sides of the canyon. One population of this species has an altitude range from 2000–2900 m a.s.l. in Ayacucho (eastern part of the Apurimac River) and the other population ranges from 2000–2100 m a.s.l. in Cusco (western part of the Apurimac River) according to available specimens and sequences. The presence of *P. rhabdolaemus* on both sides of the Apurimac River will remain hypothetical until more specimens and tissues from Cusco Department become available and are tested against a hypothesis of two different species following an integrative approach.

We also provide information about infection by the fungus *Batrachochytrium dendrobatidis* (Bd). Chytridiomycosis, caused by the Bd fungus, has negatively affected amphibian communities in the montane forests of Central America and South America (Berger et al. 1998; Lips et al. 2008; Catenazzi et al. 2011; Catenazzi 2015). This pathogen has been associated with amphibian worldwide declines (Berger et al. 1998; Briggs et al. 2005; Lips et al. 2006; Catenazzi et al. 2010; Scheele et al. 2019). Catenazzi et al. (2011) reported a rapid decline in frog species richness and abundance from 1999 to 2008 in the upper Manu National Park (Cusco), which has communities and ecosystems similar to those found in our study area (Ayacucho). The high prevalence of 30% in *P. similaris* suggests that Bd could be threatening amphibians in the area and that Bd transmission (which is typically associated with aquatic species, given that the infective zoospores are aquatic) occurs in terrestrial frogs.

Acknowledgements

Fieldwork was possible by the Vicerrectorado de Investigación y Posgrado de la Universidad Nacional Mayor de San Marcos (award project code B22100451 to CAP and VHA) and Prociencia - Concytec for their financial support under contract PE501081904-2022 to VHA. Furthermore, we thank Ernesto Castillo-Urbina, Vladimir Díaz, Kimberly Ñaccha, Maura Fernandez and Juan Gamboa for their support in the field collecting the specimens; and to Sebastián Riva-Regalado for the final editions in the photos of this manuscript. We thank Anna Motta and Rafe Brown from KU, Pablo Venegas and Juan Carlos Chavez from CORBIDI and Juan Carlos Chaparro and Maria Isabel Diaz from MUBI for their help and guidance in the process of reviewing museum specimens. Finally, we thank Edgar Lehr, Karen Siu Ting and Rudolf von May for their valuable reviews and comments that improved the quality of our manuscript.

Additional information

Conflict of interest

The authors have declared that no competing interests exist.

Ethical statement

No ethical statement was reported.

Funding

Funding from Vicerrectorado de Investigación y Posgrado (UNMSM) B22100451 was provided to CAP and VHA, and Prociencia – Concytec PE501081904-2022 to VHA.

Author contributions

Writing - original draft: VHA. Writing - review and editing: VHA, AC, CAP. Investigation: VHA, AC, CAP. Methodology: VHA, AC, CAP. Funding acquisition: CAP, VHA. Data curation: VHA. Formal analysis: VHA, AC. DNA Sequencing: AC. Thesis advice: CAP, AC.

Author ORCIDs

Valia Herrera-Alva  <https://orcid.org/0000-0001-7858-8279>

Alessandro Catenazzi  <https://orcid.org/0000-0002-3650-4783>

César Aguilar-Puntriano  <https://orcid.org/0000-0001-6372-7926>

Data availability

All of the data that support the findings of this study are available in the main text.

References

- Acevedo AA, Armesto O, Palma E (2020) Two new species of *Pristimantis* (Anura: Craugastoridae) with notes on the distribution of the genus in northeastern Colombia. *Zootaxa* 4750: 499–523. <https://doi.org/10.11646/zootaxa.4750.4.3>
- Aguilar C, Wood Jr PL, Cusi JC, Guzman A, Huari F, Lundberg M, Mortensen E, Ramirez C, Robles D, Suarez J, Ticona A, Vargas VJ, Venegas PJ, Sites Jr JW (2013) Integrative taxonomy and preliminary assessment of species limits in the *Liolaemus walkeri*

- complex (Squamata, Liolaemidae) with descriptions of three new species from Peru. *ZooKeys* 47(364): 47–91. <https://doi.org/10.3897/zookeys.364.6109>
- Berger L, Speare R, Daszak P, Green DE, Cunningham AA, Goggin CL, Scolombe R, Ragan MA, Hyatt AD, McDonald K, Hines HB, Lips KR, Maranteli G, Parkes H (1998) Chytridiomycosis causes amphibian mortality associated with population declines in the rain forests of Australia and Central America. *Proceedings of the National Academy of Sciences of the United States of America* 95(15): 9031–9036. <https://doi.org/10.1073/pnas.95.15.9031>
- Bossuyt F, Milinkovitch MC (2000) Convergent adaptive radiations in Madagascar and Asian ranid frogs reveal covariation between larval and adult traits. *Proceedings of the National Academy of Sciences of the United States of America* 97: 6585–6590. <https://doi.org/10.1073/pnas.97.12.6585>
- Boyle DG, Boyle DB, Olsen V, Morgan JAT, Hyatt AD (2004) Rapid quantitative detection of chytridiomycosis (*Batrachochytrium dendrobatidis*) in amphibian samples using real-time Taqman PCR assay. *Diseases of Aquatic Organisms* 60(2): 141–148. <https://doi.org/10.3354/dao060141>
- Briggs JM, Knapp AK, Blair JM, Heisler JL, Hoch GA, Lett MS, McCarron JK (2005) An ecosystem in transition: Causes and consequences of the conversion of mesic grassland to shrubland. *Bioscience* 55(3): 243–254. [https://doi.org/10.1641/0006-3568\(2005\)055\[0243:AEITCA\]2.0.CO;2](https://doi.org/10.1641/0006-3568(2005)055[0243:AEITCA]2.0.CO;2)
- Carrión-Olmedo JC, Ron SR (2021) A new cryptic species of the *Pristimantis lacrimosus* group (Anura, Strabomantidae) from the eastern slopes of the Ecuadorian Andes. *Evolutionary Systematics* 5: 151–175. <https://doi.org/10.3897/evolsyst.5.62661>
- Catenazzi A (2015) State of the world's amphibians. *Annual Review of Environment and Resources* 40(1): 91–119. <https://doi.org/10.1146/annurev-environ-102014-021358>
- Catenazzi A, Vredenburg VT, Lehr E (2010) *Batrachochytrium dendrobatidis* in the live frog trade of Telmatobius (Anura: Ceratophryidae) in the tropical Andes. *Diseases of Aquatic Organisms* 92(2–3): 187–191. <https://doi.org/10.3354/dao02250>
- Catenazzi A, Lehr E, Rodriguez LO, Vredenburg VT (2011) *Batrachochytrium dendrobatidis* and the collapse of anuran species richness and abundance in the upper Manu National Park, southeastern Peru. *Conservation Biology* 25(2): 382–391. <https://doi.org/10.1111/j.1523-1739.2010.01604.x>
- Dayrat B (2005) Towards integrative taxonomy. *Biological Journal of the Linnean Society, Linnean Society of London* 85(3): 407–417. <https://doi.org/10.1111/j.1095-8312.2005.00503.x>
- De Queiroz K (2005) Ernst Mayr and the modern concept of species. *Proceedings of the National Academy of Sciences* 102(suppl_1): 6600–6607. <https://doi.org/10.1073/pnas.0502030102>
- Duellman WE (1978) Two New Species of *Eleutherodactylus* (Anura: Leptodactylidae) from the Peruvian Andes. *Transactions of the Kansas Academy of Science* (1903) 81(1): 65–71. <https://doi.org/10.2307/3627358>
- Duellman WE, Lehr E (2009) *Terrestrial-breeding frogs (Strabomantidae) in Peru*. Natur und Tier Verlag.
- Duellman WE, Lehr E, Venegas PJ (2006) Two new species of *Eleutherodactylus* (Anura: Leptodactylidae) from the Andes of northern Peru. *Zootaxa* 1285(1): 51–64. <https://doi.org/10.11646/zootaxa.1512.1.3>
- Elmer KR, Cannatella DC (2008) Three new species of leaf litter frogs from the upper Amazon forests: cryptic diversity within *Pristimantis ockendeni* (Anura: Strabomantidae) in Ecuador. *Zootaxa* 1784(1): 11–38. <https://doi.org/10.11646/zootaxa.1784.1.2>

- Faivovich J, Haddad CF, Garcia PC, Frost DR, Campbell JA, Wheeler WC (2005) Systematic review of the frog family Hylidae, with special reference to Hylinae: Phylogenetic analysis and taxonomic revision. *Bulletin of the American Museum of Natural History* 2005(294): 1–240. [https://doi.org/10.1206/0003-0090\(2005\)294\[0001:SR0TFF\]2.0.CO;2](https://doi.org/10.1206/0003-0090(2005)294[0001:SR0TFF]2.0.CO;2)
- Frost DR (2023) Amphibian Species of the World: an Online Reference. Version 6.2 (30 March 2023). Electronic Database accessible at <https://amphibiansoftheworld.amnh.org/index.php>. American Museum of Natural History, New York, USA. <https://doi.org/10.5531/db.vz.0001>
- Guayasamin JM, Hutter CR, Tapia EE, Culebras J, Peñafiel N, Pyron RA, Morochz C, Funk WC, Arteaga A (2017) Diversification of the rainfrog *Pristimantis ornatissimus* in the lowlands and Andean foothills of Ecuador. *PLoS ONE* 12(3): e0172615. <https://doi.org/10.1371/journal.pone.0172615>
- Hazzi NA, Moreno JS, Ortiz-Movliav C, Palacio RD (2018) Biogeographic regions and events of isolation and diversification of the endemic biota of the tropical Andes. *Proceedings of the National Academy of Sciences of the United States of America* 115(31): 7985–7990. <https://doi.org/10.1073/pnas.1803908115>
- Hedges SB, Duellman WE, Heinicke MP (2008) New World direct-developing frogs (Anura: Terrarana): molecular phylogeny, classification, biogeography, and conservation. *Zootaxa* 1737(1): 1–182. <https://doi.org/10.11646/zootaxa.1737.1.1>
- Heinicke MP, Duellman WE, Hedges SB (2007) Major Caribbean and Central American frog faunas originated by ancient oceanic dispersal. *Proceedings of the National Academy of Sciences of the United States of America* 104(24): 10092–10097. <https://doi.org/10.1073/pnas.0611051104>
- Herrera-Alva V, Díaz V, Castillo-Urbina E, Rodolfo C, Catenazzi A (2020) A new species of *Atelopus* (Anura: Bufonidae) from southern Peru. *Zootaxa* 4853(3): 404–420. <https://doi.org/10.11646/zootaxa.4853.3.4>
- Hillis DM (2019) Species delimitation in herpetology. *Journal of Herpetology* 53(1): 3–12. <https://doi.org/10.1670/18-123>
- Huelsenbeck JP, Ronquist F (2001) MRBAYES: Bayesian inference of phylogenetic trees. *Bioinformatics* 17(8): 754–755. <https://doi.org/10.1093/bioinformatics/17.8.754>
- Hutter CR, Guayasamin JM (2015) Cryptic diversity concealed in the Andean cloud forests: Two new species of rainfrogs (*Pristimantis*) uncovered by molecular and bioacoustic data. *Neotropical Biodiversity* 1(1): 36–59. <https://doi.org/10.1080/23766808.2015.1100376>
- Hyatt AD, Boyle DG, Olsen V, Boyle DB, Berger L, Obendorf D, Dalton A, Kriger K, Hero M, Hines H, Phillott R, Campbell R, Marantelli G, Gleason F, Colling A (2007) Diagnostic assays and sampling protocols for the detection of *Batrachochytrium dendrobatidis*. *Diseases of Aquatic Organisms* 73: 175–192. <https://doi.org/10.3354/dao073175>
- Kieswetter CM, Schneider CJ (2013) Phylogeography in the northern Andes: Complex history and cryptic diversity in a cloud forest frog, *Pristimantis w-nigrum* (Craugastoridae). *Molecular Phylogenetics and Evolution* 69(3): 417–429. <https://doi.org/10.1016/j.ympev.2013.08.007>
- Köhler J, Castillo-Urbina E, Aguilar-Puntriano C, Vences M, Glaw F (2022) Rediscovery, redescription and identity of *Pristimantis nebulosus* (Henle, 1992), and description of a new terrestrial-breeding frog from montane rainforests of central Peru (Anura, Strabomantidae). *Zoosystematics and Evolution* 98(2): 213–232. <https://doi.org/10.3897/zse.98.84963>
- Lanfear R, Calcott B, Ho SYW, Guindon S (2012) PartitionFinder: combined selection of partitioning schemes and substitution models for phylogenetic analyses. *Molecular Biology and Evolution* 29: 1695–1701. <https://doi.org/10.1093/molbev/mss020>

- Lanfear R, Frandsen PB, Wright AM, Senfeld T, Calcott B (2017) PartitionFinder 2: New methods for selecting partitioned models of evolution for molecular and morphological phylogenetic analyses. *Molecular Biology and Evolution* 34(3): 772–773. <https://doi.org/10.1093/molbev/msw260>
- Lehr E (2007) New eleutherodactyline frogs (Leptodactylidae: *Pristimantis*, *Phrynobryophryne*) from Peru. *Bulletin of the Museum of Comparative Zoology* 159(2): 145–178. [https://doi.org/10.3099/0027-4100\(2007\)159\[145:NEFLPP\]2.0.CO;2](https://doi.org/10.3099/0027-4100(2007)159[145:NEFLPP]2.0.CO;2)
- Lehr E, Catenazzi A (2008) A new species of *Bryophryne* (Anura: Strabomantidae) from southern Peru. *Zootaxa* 1784(1): 1–10. <https://doi.org/10.11646/zootaxa.1784.1.1>
- Lehr E, Catenazzi A (2009) Three new species of *Bryophryne* (Anura: Strabomantidae) from the region of Cusco, Peru. *South American Journal of Herpetology* 4(2): 125–138. <https://doi.org/10.2994/057.004.0204>
- Lehr E, Catenazzi A (2010) Two new species of *Bryophryne* (Anura: Strabomantidae) from high elevations in southern Peru (Region of Cusco). *Herpetologica* 66(3): 308–319. <https://doi.org/10.1655/09-038.1>
- Lehr E, von May R (2017) A new species of terrestrial-breeding frog (Amphibia, Craugastoridae, *Pristimantis*) from high elevations of the Pui Pui Protected Forest in central Peru. *ZooKeys* 17(660): 17–42. <https://doi.org/10.3897/zookeys.660.11394>
- Lehr E, Moravec J, Cusi JC, Gvoždík V (2017a) A new minute species of *Pristimantis* (Amphibia: Anura: Craugastoridae) with a large head from the Yanachaga-Chemillén National Park in central Peru, with comments on the phylogenetic diversity of *Pristimantis* occurring in the Cordillera Yanachaga. *European Journal of Taxonomy* 325: 1–22. <https://doi.org/10.5852/ejt.2017.325>
- Lehr E, Von May R, Moravec J, Cusi JC (2017b) Three new species of *Pristimantis* (Amphibia, Anura, Craugastoridae) from upper montane forests and high Andean grasslands of the Pui Pui Protected Forest in central Peru. *Zootaxa* 4299(3): 301–336. <https://doi.org/10.11646/zootaxa.4299.3.1>
- Lips KR, Brem F, Brenes R, Reeve JD, Alford RA, Voyles J, Carey C, Livo L, Pessier A, Collins JP (2006) Emerging infectious disease and the loss of biodiversity in a Neotropical amphibian community. *Proceedings of the National Academy of Sciences of the United States of America* 103(9): 3165–3170. <https://doi.org/10.1073/pnas.0506889103>
- Lips KR, Diffendorfer J, Mendelson JR III, Sears MW (2008) Riding the wave: Reconciling the roles of disease and climate change in amphibian declines. *PLoS Biology* 6(3): e72. <https://doi.org/10.1371/journal.pbio.0060072>
- Lynch JD, Duellman WE (1997) Frogs of the genus *Eleutherodactylus* (Leptodactylidae) in western Ecuador: systematic, ecology, and biogeography. Natural History Museum, University of Kansas, 252 pp. <https://doi.org/10.5962/bhl.title.7951>
- Lynch JD, McDiarmid R (1987) Two new species of *Eleutherodactylus* (Amphibia: Anura: Leptodactylidae) for Bolivia. *Proceedings of the Biological Society of Washington* 100: 337–346. <https://doi.org/10.2307/1447850>
- Meyer CP (2003) Molecular systematics of cowries (Gastropoda: Cypraeidae) and diversification patterns in the tropics. *Biological Journal Linnean Society* 79: 401–459. <https://doi.org/10.1046/j.1095-8312.2003.00197.x>
- Minoli I, Morando M, Avila LJ (2014) Integrative taxonomy in the *Liolaemus fitzingerii* complex (Squamata: Liolaemini) based on morphological analyses and niche modeling. *Zootaxa* 3856(4): 501–528. <https://doi.org/10.11646/zootaxa.3856.4.3>
- Nguyen LT, Schmidt HA, Von Haeseler A, Minh BQ (2015) IQ-TREE: A fast and effective stochastic algorithm for estimating maximum-likelihood phylogenies. *Molecular Biology and Evolution* 32(1): 268–274. <https://doi.org/10.1093/molbev/msu300>

- Ortega-Andrade HM, Rojas-Soto OR, Valencia JH, Espinosa de los Monteros A, Morrone JJ, Ron SR, Cannatella DC (2015) Insights from integrative systematics reveal cryptic diversity in *Pristimantis* frogs (Anura: Craugastoridae) from the Upper Amazon Basin. *PLoS ONE* 10(11): e0143392. <https://doi.org/10.1371/journal.pone.0143392>
- Padial JM, De la Riva I (2009) Integrative taxonomy reveals cryptic Amazonian species of *Pristimantis* (Anura: Strabomantidae). *Zoological Journal of the Linnean Society* 155(1): 97–122. <https://doi.org/10.1111/j.1096-3642.2008.00424.x>
- Padial JM, Castroviejo-Fisher S, Köhler J, Domic E, De la Riva I (2007) Systematics of the *Eleutherodactylus fraudator* species group (Anura: Brachycephalidae). *Herpetological Monograph* 21(1): 213–240. <https://doi.org/10.1655/06-007.1>
- Padial JM, Taran G, Frost DR (2014) Molecular systematics of terraranas (Anura: Brachycephaloidea) with an assessment of the effects of alignment and optimality criteria. *Zootaxa* 3825(1): 1–132. <https://doi.org/10.11646/zootaxa.3825.1.1>
- Páez NB, Ron SR (2019) Systematics of Huicundomantis, a new subgenus of *Pristimantis* (Anura, Strabomantidae) with extraordinary cryptic diversity and eleven new species. *ZooKeys* 868: 1–112. <https://doi.org/10.3897/zookeys.868.26766>
- Pinto-Sánchez NR, Ibáñez R, Madriñán S, Sanjurjo OI, Bermingham E, Crawford AJ (2012) The great American biotic interchange in frogs: multiple and early colonization of Central America by the South American genus *Pristimantis* (Anura: Craugastoridae). *Molecular Phylogenetics and Evolution* 62(3): 954–972. <https://doi.org/10.1016/j.ympev.2011.11.022>
- Pyron RA, Wiens JJ (2011) A large-scale phylogeny of Amphibia including over 2800 species, and a revised classification of extant frogs, salamanders, and caecilians. *Molecular Phylogenetics and Evolution* 61(2): 543–583. <https://doi.org/10.1016/j.ympev.2011.06.012>
- Reyes-Puig C, Mancero E (2022) Beyond the species name: An analysis of publication trends and biases in taxonomic descriptions of rainfrogs (Amphibia, Strabomantidae, *Pristimantis*). *ZooKeys* 1134: 73–100. <https://doi.org/10.3897/zookeys.1134.91348>
- Rojas RR, Fouquet A, Ron SR, Hernández-Ruz EJ, Melo-Sampaio PR, Chaparro JC, Vogt RC, Tadeus De Carvalho V, Cardoso Pinheiro L, Avila R, Pires A, Gordo M, Hrbek T (2018) A Pan-Amazonian species delimitation: high species diversity within the genus *Amazophrynella* (Anura: Bufonidae). *PeerJ* 6: e4941. <https://doi.org/10.7717/peerj.4941>
- Scheele BC, Pasmans F, Berger L, Skerratt LF, Martel A, Beukema W, Acevedo AA, Burrowes PA, Carvalho T, Catenazzi A, De la Riva I, Fisher MC, Flechas S, Foster C, Frías-Alvarez P, Garner TWJ, Gratwicke B, Guayasamin JM, Hirschfeld M, Kolby JE, Kosch TA, La Marca E, Lindenmayer DB, Lips KR, Longo AV, Maneyro R, McDonald CA, Mendelson J, Palacios-Rodríguez P, Parra-Olea G, Richards-Zawacki CL, Rödel M, Rovito SM, Soto-Azat C, Toledo LF, Voyles J, Weldon C, Whitfield SM, Wilkinson M, Zamudio KR, Canessa S (2019) The aftermath of an amphibian fungal panzootic reveals unprecedented loss of biodiversity. *Science* 636: 1459–1463. <https://doi.org/10.1126/science.aav0379>
- Schlick-Steiner BC, Steiner FM, Seifert B, Stauffer C, Christian E, Crozier RH (2010) Integrative taxonomy: A multisource approach to exploring biodiversity. *Annual Review of Entomology* 55(1): 421–438. <https://doi.org/10.1146/annurev-ento-112408-085432>
- Simpson GG (1961) Principles of animal taxonomy. In *Principles of Animal Taxonomy*. Columbia University Press, 250 pp. <https://doi.org/10.7312/simp92414>
- Siqueira S, Aguiar Jr O, Souza MB, Lima AP, Recco-Pimentel SM (2009) Unusual intra-individual karyotypical variation and evidence of cryptic species in Amazonian populations of *Pristimantis* (Anura, Terrarana). *Hereditas* 146(4): 141–151. <https://doi.org/10.1111/j.1601-5223.2009.02104.x>

- Swenson JJ, Young BE, Beck S, Comer P, Córdova JH, Dyson J, Embert D, Encarnación F, Ferreira W, Franke I, Grossman D, Hernadez P, Herzog SK, Josse C, Navarro G, Pacheco V, Stein BA, Timaná M, Tovar A, Tovar C, Vargas J, Zambrana-Torrel CM (2012) Plant and animal endemism in the eastern Andean slope: Challenges to conservation. *BMC Ecology* 12(1): 1–19. <https://doi.org/10.1186/1472-6785-12-1>
- Tamura K, Glen S, Sudhir K (2021) MEGA11: Molecular evolutionary genetics analysis version 11. *Molecular Biology and Evolution* 38(7): 3022–3027. <https://doi.org/10.1093/molbev/msab120>
- von May R, Catenazzi A, Corl A, Santa-Cruz R, Carnaval AC, Moritz C (2017) Divergence of thermal physiological traits in terrestrial breeding frogs along a tropical elevational gradient. *Ecology and Evolution* 7(9): 3257–3267. <https://doi.org/10.1002/ece3.2929>
- Waddell EH, Crotti M, Lougheed SC, Cannatella DC, Elmer KR (2018) Hierarchies of evolutionary radiation in the world's most species rich vertebrate group, the Neotropical *Pristimantis* leaf litter frogs. *Systematics and Biodiversity* 16(8): 807–819. <https://doi.org/10.1080/14772000.2018.1503202>
- Warne RW, LaBumbard B, LaGrange S, Vredenburg VT, Catenazzi A (2016) Co-Infection by Chytrid Fungus and Ranaviruses in Wild and Harvested Frogs in the Tropical Andes. *PLoS ONE* 11(1): e0145864. <https://doi.org/10.1371/journal.pone.0145864>
- Wilcox TP, Zwickl DJ, Heath TA, Hillis DM (2002) Phylogenetic relationships of the dwarf boas and a comparison of Bayesian and bootstrap measures of phylogenetic support. *Molecular Phylogenetics and Evolution* 25: 361–371. [https://doi.org/10.1016/S1055-7903\(02\)00244-0](https://doi.org/10.1016/S1055-7903(02)00244-0)
- Wiley EO (1978) The evolutionary species concept reconsidered. *Systematic Zoology* 27(1): 17–26. <https://doi.org/10.2307/2412809>
- Zozaya SM, Higgie M, Moritz C, Hoskin CJ (2019) Are pheromones key to unlocking cryptic lizard diversity? *American Naturalist* 194(2): 168–182. <https://doi.org/10.1086/704059>

Appendix 1

Specimens analysed from museums. See acronyms in Materials and methods. Underlined codes correspond to type material. Coordinates and altitude when available.

Pristimantis pharangobates: AMNH 6099, 153089: Between Abra Accanaco and Pillahuata, Paucartambo, Cusco; KU 173236–173251: Buenos Aires, Cosñipata, Paucartambo, Cusco [-13.15; -71.5833; altitude: 2400 m a.s.l.]; MUBI 4203, 4205, 4209–10, 4212, 4217, 4220, 4222, 4224–4225, 4228, 4390–92, 4395–97, 4399–4400, 4560–61, 4563, 4610: Cosñipata, Paucartambo, Cusco [-13.1153; -71.5833; altitude: 2750 m a.s.l.]; MUBI 11451–52, 11374–87: Trocha Unión, Cosñipata, Paucartambo, Cusco [-13.1061; -71.5897; altitude: 2780 m a.s.l.]; MUSM 27910: Buenos Aires, Cosñipata, Paucartambo, Cusco; MUSM 32932–35, 32952–60: Paucartambo, Cusco.

Pristimantis rhabdolaemus: CORBIDI 10813, 10815–16: Chiquintirca, La Mar, Ayacucho [-13.0350; -73.6786; altitude: 2635 m a.s.l.]; LSUMZ 26150–51, 26153, 26156, 26182, 26251: Huanhuachayocc, Tambo to Apurimac Road [-12.75; -73.7833]; KU 175082–84: Huanhuachayocc, Tambo to Apurimac Road [-12.73; -73.7833]; MUBI 17541–42, 17552, 17555: Aendoshari Community, La Convención, Cusco [-12.8188; -73.4239; altitude: 2350 m a.s.l.];

MUSM 18505-08: Tocate, La Mar, Ayacucho [-12.9950; -73.6685; altitude: 2080 m a.s.l.]; 30206-08: Cielo Punku, Kimbiri, La Convención, Cusco [-12.8008; -73.5042; altitude: 2100 m a.s.l.]; KNC 44-45, 47-48, 106, 116, 118-20, 122, 130: Chaupichaca, Chungui, La Mar, Ayacucho [-13.1219; -73.5439; altitude: 2040-2345 m a.s.l.].

Pristimantis scitulus: KU 175085: Yuraccyacu, Tambo to Apurimac Road; LSUMZ 26097: Yuraccyacu, Tambo to Apurimac Road [-12.7833; -73.9]; MUSM 41309-10, 41312-13: Chaupichaca, Chungui, La Mar, Ayacucho [-13.12; -73.5228; altitude: 2270-2520 m a.s.l.].

***Pristimantis* sp.**: AMNH 153088, 153090: Between Accanaco and Pillahuata, Paucartambo, Cusco; KU 138877: 7 km WSW Santa Isabel, Cosñipata, Paucartambo, Cusco; MUBI 13317, 13323-24, 13333-34: San Pedro, Paucartambo, Cusco; MUSM 21035, 26269-70, 26276, 30418, 30433, 32934: Suecia, Paucartambo, Cusco. KU 175086-88: Huyro, Quillabamba, Echarate, Cusco; MUBI 13612, 13627, 13661: Mesa Pelada, Huayopata, La Convención, Cusco; MUSM 27911-12: Alfamayo, Huayopata, La Convención, Cusco.

***Pristimantis* sp. 4.**: LSUMZ 26147-48, 26154, 26158: Between Pataccocha and San Jose, Santa Rosa, Ayna, Ayacucho.

Appendix 2

Table A1. Sequences used from GenBank and new sequences added in this paper.

N°	Species	Voucher	Group	Locality	Source	16 S	COI	RAG1	TYR
1	<i>Pristimantis albertus</i>	KU 291675	Ingroup	Peru: Pasco, 0.9 km N, 2.1 km E Oxapampa	Hedges et. al (2008)	EU186695	-	-	-
2	<i>Pristimantis albertus</i>	RvM 527	Ingroup	Peru: Junin, Provincia Chanchamayo, Puyu Sacha	Lehr and von May (2017)	KY594751	-	-	-
3	<i>Pristimantis albertus</i>	MUSM 33299	Ingroup	Peru: Junin, Provincia Chanchamayo, Cerro San Pedro	Lehr and von May (2017)	KY594750	-	-	-
4	<i>Pristimantis albertus</i>	MUSM 33298	Ingroup	Peru: Junin, Provincia Chanchamayo, Cerro San Pedro	Lehr and von May (2017)	KY594749	-	-	-
5	<i>Pristimantis aniptopalmatus</i>	KU 261627	Ingroup	Peru: Pasco, 2.9 km N, 5.5 km E Oxapampa	Hedges et. al (2008)	EF493390	-	-	-
6	<i>Pristimantis aniptopalmatus</i>	KU 291666	Ingroup	Peru: Pasco, 2.9 km N, 5.9 km E Oxapampa	Hedges et. al (2008)	EU186694	-	-	-
7	<i>Pristimantis aniptopalmatus</i>	NMP6V 75053	Ingroup	Peru: Junin, Pui Pui	Lehr et. al (2017a)	KY006087	-	-	-
8	<i>Pristimantis aniptopalmatus</i>	NMP6V 75051	Ingroup	Peru: Junin, Pui Pui	Lehr et. al (2017a)	KY006086	-	-	-
9	<i>Pristimantis aniptopalmatus</i>	MUSM 31151	Ingroup	Peru: Pasco, Yanachaga-Chemillen	Lehr et. al (2017a)	KY006085	-	-	-
10	<i>Pristimantis aniptopalmatus</i>	MUSM 31130	Ingroup	Peru: Pasco, Yanachaga-Chemillen	Lehr et. al (2017a)	KY006084	-	-	-
11	<i>Pristimantis aniptopalmatus</i>	MUSM 31128	Ingroup	Peru: Pasco, Yanachaga-Chemillen	Lehr et. al (2017a)	KY006083	-	-	-
12	<i>Pristimantis aniptopalmatus</i>	MUSM 31111	Ingroup	Peru: Pasco, Yanachaga-Chemillen	Lehr et. al (2017a)	KY006082	-	-	-
13	<i>Pristimantis attenboroughi</i>	NMP6V 75529	Ingroup	Peru: Junin, near trail from Tasta to Tarhuish, Polylepis forest patch	Lehr and von May (2017)	KY594757	KY962784	KY962764	-
14	<i>Pristimantis attenboroughi</i>	NMP6V 75528	Ingroup	Peru: Junin, near trail from Tasta to Tarhuish, Polylepis forest patch	Lehr and von May (2017)	KY594756	KY962783	KY962763	-

N°	Species	Voucher	Group	Locality	Source	16 S	COI	RAG1	TYR
15	<i>Pristimantis attenboroughi</i>	NMP6V 75524	Ingroup	Peru: Junin, Upper part of Quebrada Tarhuish, 'Laguna Udrecocha'	Lehr and von May (2017)	KY594754	KY962781	KY962761	–
16	<i>Pristimantis attenboroughi</i>	NMP6V 75522	Ingroup	Peru: Junin, Quebrada Tarhuish, left bank of Antuyo River	Lehr and von May (2017)	KY594753	KY962780	KY962760	–
17	<i>Pristimantis attenboroughi</i>	MUSM 31186	Ingroup	Peru: Junin, Quebrada Tarhuish, left bank of Antuyo River	Lehr and von May (2017)	KY594752	KY962779	KY962759	–
18	<i>Pristimantis attenboroughi</i>	NMP6V 75525	Ingroup	Peru: Junin, Upper part of Quebrada Tarhuish, 'Laguna Udrecocha'	Lehr and von May (2017)	KY594755	KY962782	KY962762	–
19	<i>Pristimantis bounides</i>	NMP6V 75097	Ingroup	Peru: Junin, Quebrada Tasta, "Runda"	Lehr et. al (2017b)	KY962797	KY962790	KY962774	–
20	<i>Pristimantis bounides</i>	NMP6V 75066	Ingroup	"Peru: Junin, Sector Carrizal, Carretera Satipo-Toldopampa, km 134"	Lehr et. al (2017b)	KY962796	–	KY962773	–
21	<i>Pristimantis bounides</i>	NMP6V 75540	Ingroup	"Peru: Junin, Sector Carrizal, Carretera Satipo-Toldopampa, km 134"	Lehr et. al (2017b)	KY962795	–	KY962772	–
22	<i>Pristimantis bounides</i>	MUSM 31198	Ingroup	Peru: Junin, Quebrada Tasta, "Runda"	Lehr et. al (2017b)	KY962794	KY962789	KY962771	–
23	<i>Pristimantis cf aniptopalmtatus</i>	VG-2017	Ingroup	Peru: Pasco, Yanachaga-Chemillen	Lehr et. al (2017a)	KY006088	–	–	–
24	<i>Pristimantis danae</i>	MNCN 44234	Ingroup	Peru: Cusco, Union, Valle de Kosnipata	Padial and De la Riva (2009)	EU192270	–	–	–
25	<i>Pristimantis danae</i>	IDLR 4001	Ingroup	Bolivia: La Paz: Santa Cruz de Valle Ameno	Padial and De la Riva (2009)	EU192260	–	–	–
26	<i>Pristimantis danae</i>	MNK-A 7182	Ingroup	Bolivia: La Paz, Huairuro, senda San Jose - Apolo	Padial and De la Riva (2009)	EU192261	–	–	–
27	<i>Pristimantis danae</i>	MNCN 43062	Ingroup	Bolivia: La Paz, Huairuro, senda San Jose - Apolo	Padial and De la Riva (2009)	EU192262	–	–	–
28	<i>Pristimantis danae</i>	MNCN 43069	Ingroup	Bolivia: La Paz: Arroyo Huacataya. senda San José y Apolo	Padial and De la Riva (2009)	EU192263	–	–	–
29	<i>Pristimantis danae</i>	MNK-A 7190	Ingroup	Bolivia: La Paz: Arroyo Huacataya. senda San José y Apolo	Padial and De la Riva (2009)	EU192264	–	–	–
30	<i>Pristimantis danae</i>	MNK-A 7273	Ingroup	Bolivia: La Paz: Serranía Bella Vista	Padial and De la Riva (2009)	EU192265	–	–	–
31	<i>Pristimantis danae</i>	IDLR 4815	Ingroup	Peru: Cusco: Unión, Valle de Kosñipata	Padial and De la Riva (2009)	EU192266	–	–	–
32	<i>Pristimantis danae</i>	MNCN 44232	Ingroup	Peru: Cusco: Unión, Valle de Kosñipata	Padial and De la Riva (2009)	EU192267	–	–	–
33	<i>Pristimantis danae</i>	MNCN 44233	Ingroup	Peru: Cusco: Unión, Valle de Kosñipata	Padial and De la Riva (2009)	EU192268	–	–	–
34	<i>Pristimantis danae</i>	IDLR 4822	Ingroup	Peru: Cusco: Unión, Valle de Kosñipata	Padial and De la Riva (2009)	EU192269	–	–	–
35	<i>Pristimantis danae</i>	IDLR 4824	Ingroup	Peru: Cusco: Unión, Valle de Kosñipata	Padial and De la Riva (2009)	EU192271	–	–	–
36	<i>Pristimantis danae</i>	IDLR 4825	Ingroup	Peru: Cusco: Unión, Valle de Kosñipata	Padial and De la Riva (2009)	EU192272	–	–	–
37	<i>Pristimantis danae</i>	MVZ 272358	Ingroup	Peru: Cusco: Valle de Kosñipata	von May et. al (2017)	KY652652	KY672984	KY672968	KY681073
38	<i>Pristimantis danae</i>	AC 141.09	Ingroup	Peru: Cusco: Valle de Kosñipata	This paper	OR469891	–	–	OR542804
39	<i>Pristimantis danae</i>	BL 37.13	Ingroup	Peru: Cusco: Valle de Kosñipata	This paper	OR469893	OR478457	OR542831	OR542792

N°	Species	Voucher	Group	Locality	Source	16 S	COI	RAG1	TYR
40	<i>Pristimantis danae</i>	BL 36.13	Ingroup	Peru: Cusco: Valle de Kosñipata	This paper	OR469905	OR478456	OR542830	OR542791
41	<i>Pristimantis humboldti</i>	NMP6V 75538	Ingroup	Peru: Junin, Quebrada Tarhuish, left bank of Antuyo River, Shiusha	Lehr et. al (2017b)	KY962799	KY962792	KY962776	-
42	<i>Pristimantis humboldti</i>	MUSM 31194	Ingroup	Peru: Junin, Quebrada Tarhuish, left bank of Antuyo River, Shiusha	Lehr et. al (2017b)	KY962798	KY962791	KY962775	-
43	<i>Pristimantis ornatus</i>	MTD 45073	Ingroup	Perú: Pasco: Oxapampa: Chinche: Cerca de Aquimarca	Hedges et. al (2008)	EU186660	-	-	-
44	<i>Pristimantis pharangobates</i>	KU 173492	Ingroup	Peru: Cusco: Buenos aires	Heinicke et. al (2007)	EF493706	-	-	-
45	<i>Pristimantis pharangobates</i>	MNCN 9494	Ingroup	Peru: Cusco: Valle de Kosñipata	Padial and De la Riva (2009)	FJ438802	-	-	-
46	<i>Pristimantis pharangobates</i>	MHNC 11451	Ingroup	Peru: Cusco: La Convención: Echarate: Urusayhua	This paper	OR470757	-	-	-
47	<i>Pristimantis pharangobates</i>	MHNC 11452	Ingroup	Peru: Cusco: La Convención: Echarate: Urusayhua	This paper	OR471343	-	-	-
48	<i>Pristimantis pharangobates</i>	AC 96.13	Ingroup	Peru: Cusco: Buenos Aires	This paper	OR471423	OR478463	-	OR542798
49	<i>Pristimantis pharangobates</i>	AC 9.13	Ingroup	Peru: Cusco: Buenos Aires	This paper	-	OR478451	OR542824	OR542787
50	<i>Pristimantis puipui</i>	NMP6V 75542	Ingroup	Peru: Junin, Pui Pui Protected Forest, Laguna Sinchon	von May and Lehr (2017b)	KY962800	-	KY962777	-
51	<i>Pristimantis reichlei</i>	MUSM 9267	Ingroup	Perú	Heinicke et. al (2007)	EF493707	-	EF493436	EF493498
52	<i>Pristimantis reichlei</i>	MNCN 43012	Ingroup	Bolivia: Cochabamba: Los Guácharos	Padial and De la Riva (2009)	EU192287	-	-	-
53	<i>Pristimantis reichlei</i>	MNK-A 6621	Ingroup	Bolivia: Cochabamba: Los Guácharos	Padial and De la Riva (2009)	EU192286	-	-	-
54	<i>Pristimantis reichlei</i>	MNCN 43249	Ingroup	Peru: Cusco: 5 km from San Lorenzo hacia Quince Mil	Padial and De la Riva (2009)	EU192288	-	-	-
55	<i>Pristimantis reichlei</i>	IDLR 4779	Ingroup	Peru: Puno: Entre Puerto Leguía y San Gabán	Padial and De la Riva (2009)	EU192285	-	-	-
56	<i>Pristimantis reichlei</i>	MUSM 26931	Ingroup	Peru: Huanuco: Panguana	Pinto-Sanchez et. al (2012)	JN991461	JN991392	-	-
57	<i>Pristimantis reichlei</i>	CORBIDI 16219	Ingroup	Peru: Cusco: Valle de Kosñipata	von May et. al (2017)	KY652657	KY672989	KY672972	KY681078
58	<i>Pristimantis reichlei</i>	AC 38.15	Ingroup	Peru: Cusco: Valle de Kosñipata	This paper	OR471610	OR478458	OR542832	-
59	<i>Pristimantis reichlei</i>	AC 113.12	Ingroup	Peru: Cusco: Valle de Kosñipata	This paper	OR471611	OR478467	OR542839	OR542801
60	<i>Pristimantis reichlei</i>	AC 20.15	Ingroup	Peru: Cusco: Valle de Kosñipata	This paper	OR471619	OR478454	OR542828	-
61	<i>Pristimantis reichlei</i>	AC 138.17	Ingroup	Peru: Quispicanchi: Soqtapata: Quincemil	This paper	OR471620	OR478469	OR542841	OR542803
62	<i>Pristimantis reichlei</i>	AC 75.17	Ingroup	Peru: Puno: PN Bahuaja-Sonene: Punto 4	This paper	OR471646	OR478460	OR542833	-
63	<i>Pristimantis reichlei</i>	AC 94.17	Ingroup	Peru: Puno: PN Bahuaja-Sonene: Punto 4	This paper	OR471650	OR478462	OR542835	-
64	<i>Pristimantis reichlei</i>	AC 16.17	Ingroup	Peru: Puno, Inambari, Santo Domingo	This paper	OR471653	-	OR542826	-
65	<i>Pristimantis reichlei</i>	AC 33.17	Ingroup	Peru: Puno, Inambari, Santo Domingo	This paper	OR475320	-	OR542829	-
66	<i>Pristimantis reichlei</i>	AC 147.17	Ingroup	Peru: Puno: carretera San Gaban-Ollachea: Casahuirí	This paper	OR471655	OR478472	OR542844	OR542807
67	<i>Pristimantis reichlei</i>	AC 10.14	Ingroup	Peru: Cusco: Pilcopata: Villa Carmen	This paper	OR471656	OR478452	OR542825	-
68	<i>Pristimantis reichlei</i>	AC 106.17	Ingroup	Peru: Puno: Isilluni: Valle Limbani	This paper	OR472333	OR478465	OR542837	OR542799

N°	Species	Voucher	Group	Locality	Source	16 S	COI	RAG1	TYR
69	<i>Pristimantis reichlei</i>	AC 109.17	Ingroup	Peru: Puno: Isilluni: Valle Limbani	This paper	OR472388	-	-	OR542800
70	<i>Pristimantis reichlei</i>	MNCN 4482	Ingroup	Peru: Cusco, Pantiacolla	Padial and De la Riva (2009)	EU712720	-	-	-
71	<i>Pristimantis reichlei</i>	NMP6V 72578	Ingroup	Bolivia: Pando, Bioceanica	Padial and De la Riva (2009)	EU712719	-	-	-
72	<i>Pristimantis rhabdolaemus</i>	FOCAM 34	Ingroup	Peru: Ayacucho: La Mar: Chiquintirca	This paper	OR472495	OR478455	OR478455	OR542790
73	<i>Pristimantis rhabdolaemus</i>	FOCAM 53	Ingroup	Peru: Ayacucho: La Mar: Toccate	This paper	OR472500	-	-	-
74	<i>Pristimantis rhabdolaemus</i>	FOCAM 76	Ingroup	Peru: Ayacucho: La Mar: Toccate	This paper	OR472501	OR478461	OR542834	OR542797
75	<i>Pristimantis rhabdolaemus</i>	FOCAM 145	Ingroup	Peru: Ayacucho: La Mar: Toccate	This paper	OR472507	-	-	-
76	<i>Pristimantis rhabdolaemus</i>	FOCAM 153	Ingroup	Peru: Ayacucho: La Mar: Toccate	This paper	OR472508	-	-	-
77	<i>Pristimantis rhabdolaemus</i>	FOCAM 361	Ingroup	Peru: Ayacucho: La Mar: Toccate	This paper	OR472509	-	OR542849	OR542815
78	<i>Pristimantis rhabdolaemus</i>	KNC 13	Ingroup	Peru: Ayacucho: Chungui: Chaupichaca	This paper	OR472494	-	-	OR542788
79	<i>Pristimantis rhabdolaemus</i>	KNC 47	Ingroup	Peru: Ayacucho: Chungui: Chaupichaca	This paper	OR472498	-	-	OR542795
80	<i>Pristimantis rhabdolaemus</i>	KNC 48	Ingroup	Peru: Ayacucho: Chungui: Chaupichaca	This paper	OR472499	-	-	OR542796
81	<i>Pristimantis rhabdolaemus</i>	KNC 103	Ingroup	Peru: Ayacucho: Chungui: Chaupichaca	This paper	OR472502	OR478464	OR542836	-
82	<i>Pristimantis rhabdolaemus</i>	KNC 106	Ingroup	Peru: Ayacucho: Chungui: Chaupichaca	This paper	OR472503	OR478466	OR542838	-
83	<i>Pristimantis rhabdolaemus</i>	KNC 118	Ingroup	Peru: Ayacucho: Chungui: Chaupichaca	This paper	OR472505	OR478468	OR542840	-
84	<i>Pristimantis rhabdolaemus</i>	KNC 119	Ingroup	Peru: Ayacucho: Chungui: Chaupichaca	This paper	OR472506	-	-	-
85	<i>Pristimantis rhabdolaemus</i>	KNC 116	Ingroup	Peru: Ayacucho: Chungui: Chaupichaca	This paper	OR472504	-	-	OR542802
86	<i>Pristimantis rhabdolaemus</i>	KNC 44	Ingroup	Peru: Ayacucho: Chungui: Chaupichaca	This paper	OR472496	-	-	OR542793
87	<i>Pristimantis rhabdolaemus</i>	KNC 45	Ingroup	Peru: Ayacucho: Chungui: Chaupichaca	This paper	OR472497	-	-	OR542794
88	<i>Pristimantis rhabdolaemus</i>	MHNC 17542	Ingroup	Peru: Cusco: La Convención: Echarate: Aendoshari	This paper	OR472510	OR478479	OR542852	-
89	<i>Pristimantis rhabdolaemus</i>	MUBI 17552	Ingroup	Peru: Cusco: La Convención: Echarate: Aendoshari	This paper	OR472511	-	-	OR542819
90	<i>Pristimantis sagittulus</i>	KU 261635	Ingroup	Peru: Pasco, 0.9 km N, 2.1 km E Oxapampa	Heinicke et. al (2007)	EF493705	-	EF493439	EF493501
91	<i>Pristimantis scitulus</i>	MUSM 41310	Ingroup	Peru: Ayacucho: Chungui: Chaupichaca	This paper	OR469744	-	OR542823	-
92	<i>Pristimantis scitulus</i>	MUSM 41309	Ingroup	Peru: Ayacucho: Chungui: Chaupichaca	This paper	OR469328	-	-	-
93	<i>Pristimantis scitulus</i>	MUSM 41312	Ingroup	Peru: Ayacucho: Chungui: Chaupichaca	This paper	OR469801	-	-	-
94	<i>Pristimantis scitulus</i>	MUSM 41313	Ingroup	Peru: Ayacucho: Chungui: Chaupichaca	This paper	OR469804	-	-	-
95	<i>Pristimantis similaris</i>	MUSM 41031	Ingroup	Peru: Ayacucho: La Mar: Cajadela	This paper	OR478195	OR478473	OR542845	OR542808
96	<i>Pristimantis similaris</i>	MUSM 41030	Ingroup	Peru: Ayacucho: La Mar: Cajadela	This paper	OR478198	OR478475	OR542847	OR542812
97	<i>Pristimantis similaris</i>	MUSM 41035	Ingroup	Peru: Ayacucho: La Mar: Cajadela	This paper	OR478199	OR478476	OR542848	OR542813
98	<i>Pristimantis similaris</i>	MUSM 41036	Ingroup	Peru: Ayacucho: La Mar: Cajadela	This paper	OR478200	-	OR542851	OR542817

N°	Species	Voucher	Group	Locality	Source	16 S	COI	RAG1	TYR
99	<i>Pristimantis similaris</i>	MUSM 41037	Ingroup	Peru: Ayacucho: Ayna: Machente	This paper	OR478196	–	–	OR542810
100	<i>Pristimantis similaris</i>	MUSM 41323	Ingroup	Peru: Ayacucho: Ayna: Machente	This paper	OR478197	–	–	OR542811
101	<i>Pristimantis</i> sp.	MVZ 272360	Ingroup	Peru: Cusco	von May et. al (2017)	KY652655	KY672987	KY681088	KY681076
102	<i>Pristimantis</i> sp.	MUSM 30433	Ingroup	Peru: Cusco	This paper	OR478204	–	OR542855	OR542822
103	<i>Pristimantis</i> sp.	MUSM 30418	Ingroup	Peru: Cusco	This paper	OR478203	–	OR542854	OR542821
104	<i>Pristimantis</i> sp.	AC 179.19	Ingroup	Peru: Cusco	This paper	–	–	OR542846	–
105	<i>Pristimantis</i> sp.	MUSM 27912	Ingroup	Peru: Cusco	This paper	OR478202	–	OR542853	OR542820
106	<i>Pristimantis</i> sp.	AC 365.07	Ingroup	Peru: Cusco	This paper	OR478201	OR478478	OR542850	OR542816
107	<i>Pristimantis</i> sp3	AMNH-A 165195	Ingroup	Bolivia: Santa Cruz: Caballero: Canton San José: Parque Nacional Amboro	Faivovich et. al (2005)	AY843586	–	–	–
108	<i>Pristimantis</i> sp3	MNK-A 6628	Ingroup	Bolivia: Santa Cruz: Serranía de la Siberia	Padial et. al (2007)	EU192258	–	–	–
109	<i>Pristimantis</i> sp3	MNCN 43036	Ingroup	Bolivia: Santa Cruz: La Yunga de Mairana	Padial et. al (2007)	EU192257	–	–	–
110	<i>Pristimantis stictogaster</i>	KU 291659	Ingroup	Peru: Pasco, 2.9 km N, 5.5 km E Oxapampa	Heinicke et. al (2007)	EF493704	–	EF493445	EF493506
111	<i>Pristimantis toftae</i>	KST 208	Ingroup	Peru: Huanuco, Puerto Inca, Panguana, Rio Yuyapichis (AKA Rio Lullapiches) near Rio Pachitea	Pinto-Sanchez et. al (2012)	JN991439	–	–	JN991566
112	<i>Pristimantis toftae</i>	KST 318	Ingroup	Peru: Huanuco, Puerto Inca, Panguana, Rio Yuyapichis (AKA Rio Lullapiches) near Rio Pachitea	This paper	OR538542	–	–	–
113	<i>Pristimantis toftae</i>	KU 215493	Ingroup	Peru: Madre de Dios: Cuzco Amazonico: 15 km E de Puerto Maldonado	Heinicke et. al (2007)	EF493353	–	–	–
114	<i>Pristimantis toftae</i>	MNCN 43025	Ingroup	Bolivia: Cochabamba: Los Guácharos	Padial and De la Riva (2009)	EU192293	–	–	–
115	<i>Pristimantis toftae</i>	MNCN 43246	Ingroup	Peru: Cusco: San Pedro, Valle de Marcapata	Padial and De la Riva (2009)	EU192294	–	–	–
116	<i>Pristimantis toftae</i>	AC 107.07	Ingroup	Peru: Cusco: Valle de Kosñipata	von May et. al (2017)	KY652659	KY672991	KY672974	KY681080
117	<i>Pristimantis toftae</i>	AC 19.15	Ingroup	Peru: Cusco: Valle de Kosñipata	This paper	OR472575	OR478453	OR542827	OR542789
118	<i>Pristimantis toftae</i>	CORBIDI 11889	Ingroup	Peru: Cusco: Valle de Kosñipata	This paper	–	–	–	OR542818
119	<i>Pristimantis toftae</i>	AC 144.16	Ingroup	Peru: Puno: Inambari: Santo Domingo	This paper	OR472576	OR478470	OR542842	OR542805
120	<i>Pristimantis toftae</i>	AC 147.16	Ingroup	Peru: Puno: Inambari: Santo Domingo	This paper	OR472577	OR478471	OR542843	OR542806
121	<i>Pristimantis bipunctatus</i>	MUSM 31120	Outgroup	Peru: Pasco, Yanachaga-Chemillen	Lehr et. al (2017a)	KY006089	–	–	–
122	<i>Pristimantis bipunctatus</i>	MUSM 31179	Outgroup	Peru: Junin, Pui Pui Protected Forest, Hito 3, Entrada del parque	Lehr and von May (2017)	KY594758	KY962785	KY962765	–
123	<i>Pristimantis bipunctatus</i>	KU 291638	Outgroup	Peru: Pasco, 0.7 km S, 4.5 km E Oxapampa	Heinicke et. al (2007)	EF493702	–	EF493430	EF493492
124	<i>Pristimantis iiap</i>	MUSM 40783	Outgroup	Peru: Ucayali: Pucallpa: Curimana	This paper	OR470750	OR478474	–	OR542809
125	<i>Pristimantis iiap</i>	MUSM 40841	Outgroup	Peru: Ucayali: Pucallpa: Curimana	This paper	OR470749	OR478477	–	OR542814
126	<i>Pristimantis prolatus</i>	KU 177433	Outgroup	Ecuador: Napo: Rio Salado	Hedges et. al (2008)	EU186701	–	–	–
127	<i>Pristimantis skydmainos</i>	MUSM 29286	Outgroup	Peru: Cusco: La Convención: Echarate	This paper	OR469849	–	–	–
128	<i>Pristimantis skydmainos</i>	448895	Outgroup	Peru	Heinicke et. al (2007)	EF493393	–	–	–

Appendix 3

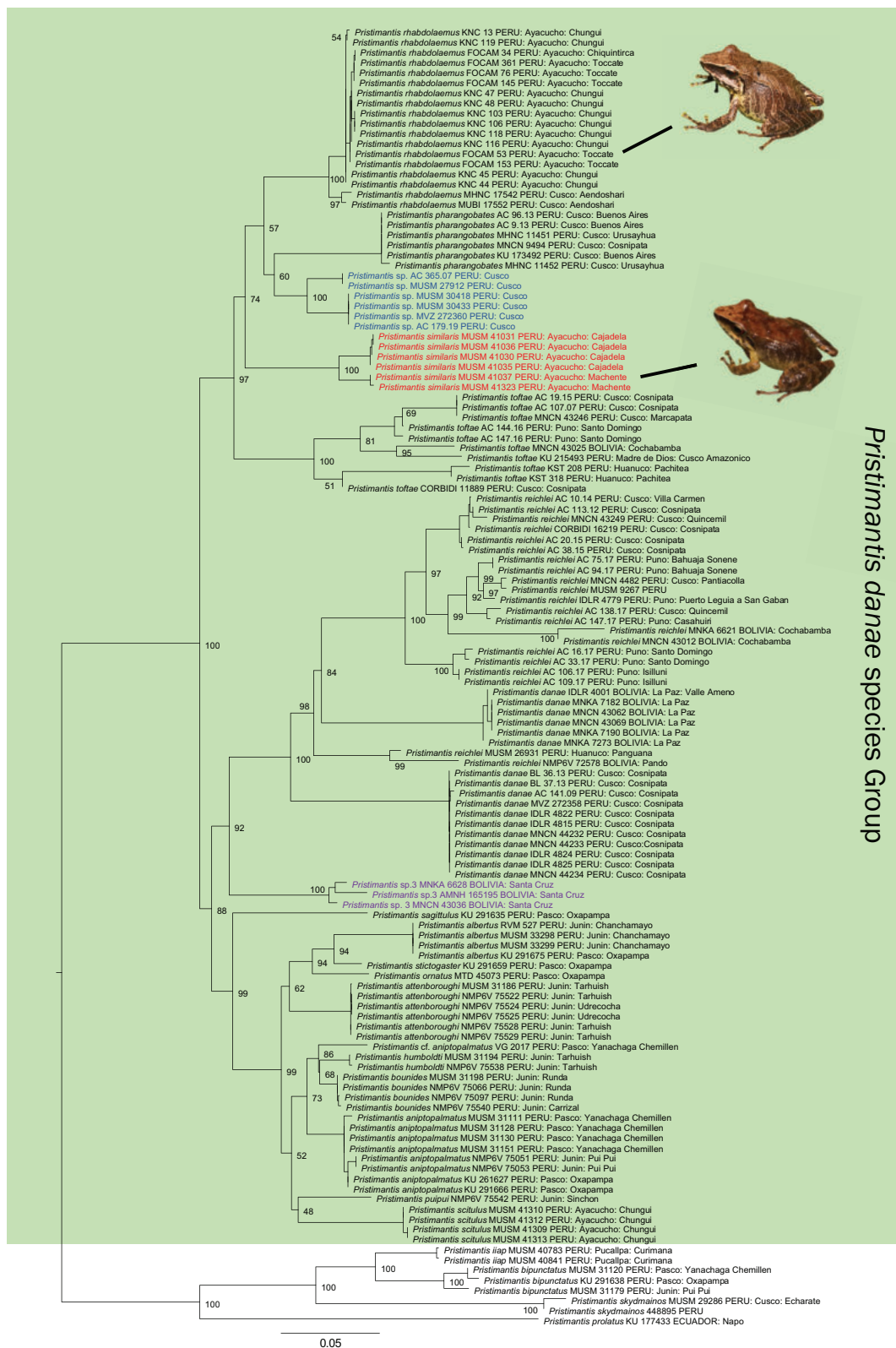


Figure A1. Maximum Likelihood tree non-collapsed of concatenated genes 16S rRNA, COI, RAG1 and TYR taken from GenBank and novel sequences. Numbers on nodes are bootstrap values (see Materials and Methods section for details). Green shadow corresponds to the ingroup. *Pristimantis similaris* sp. nov. in red, *Pristimantis* sp. 3 from Bolivia in purple and *Pristimantis* sp. from Cusco in blue.

Appendix 4

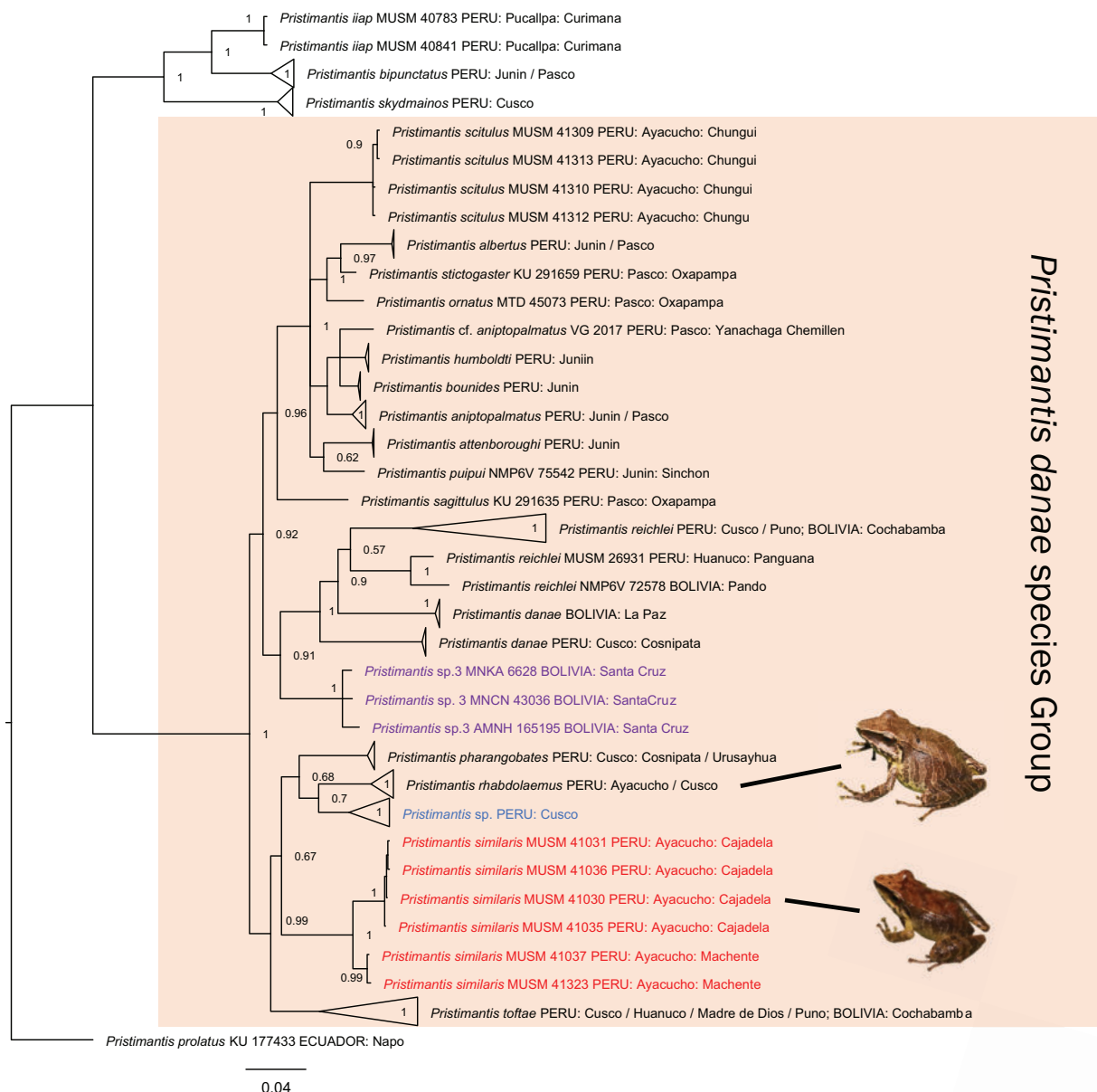


Figure A2. Bayesian Tree phylogeny collapsed of concatenated genes 16S rRNA, COI, RAG1 and TYR. Numbers on nodes are posterior probabilities (see Materials and Methods section for details). Orange shadow corresponds to the ingroup. *Pristimantis similis* sp. nov. in red, *Pristimantis* sp. 3 from Bolivia in purple and *Pristimantis* sp. from Cusco in blue.

Supplementary material 1

p-uncorrected distances of 591 pb including gaps of rRNA 16s gene

Authors: Valia Herrera-Alva, Alessandro Catenazzi, César Aguilar-Puntriano

Data type: xls

Copyright notice: This dataset is made available under the Open Database License (<http://opendatacommons.org/licenses/odbl/1.0/>). The Open Database License (ODbL) is a license agreement intended to allow users to freely share, modify, and use this Dataset while maintaining this same freedom for others, provided that the original source and author(s) are credited.

Link: <https://doi.org/10.3897/zookeys.1187.104536.suppl1>

A new Asian lazy toad of the genus *Scutigera* Theobald, 1868 (Anura, Megophryidae) from southern Tibet, China

Sheng-Chao Shi^{1,2*}, Lu-Lu Sui^{1,2*}, Shun Ma^{1,2}, Fei-Rong Ji^{1,2}, A-Yi Bu-Dian^{1,2}, Jian-Ping Jiang^{1,2,3}

¹ Chengdu Institute of Biology, Chinese Academy of Sciences, Chengdu 610041, China

² University of Chinese Academy of Sciences, Beijing 100049, China

³ Mangkang Biodiversity and Ecological Station, Tibet Ecological Safety Monitor Network, Chengdu 854500, China

Corresponding author: Jian-Ping Jiang (jiangjp@cib.ac.cn)

Abstract

In this study, a new species named *Scutigera luozhaensis* sp. nov. is described from Luozha, southern Tibet, China. Genetic analysis based on two mitochondrial genes 16S rRNA and COI and the nuclear gene RAG1 revealed that the new species belongs to an independent phylogenetic clade close to *S. gongshanensis* and *S. nyingchiensis* and shares no RAG1 haplotype with other species. Morphological comparisons based on examined specimens and literatures indicated that it can be diagnosed from congeners by the following combination of characters: (1) body moderate, male body length 47.0–67.2 mm ($n = 13$), female body length 49.8–66.2 mm ($n = 8$); (2) maxillary teeth and budding absent; (3) numerous tiny dense nuptial spines present on dorsal surface of fingers I, II and inner surface of finger III of males in breeding condition with similar size; (4) spine patches on belly of males in breeding condition absent; (5) spines on inner surface of forearm and upper arm of males in breeding condition absent; (6) small patches of black spines present near armpit of males in breeding condition absent; (7) adult males without vocal sac; (8) some large warts and tubercles on dorsum gathered into short skin ridges with several spines present on top; (9) space between upper eyelids wider than upper eyelids; (10) spots or irregular cross bands on limbs absent; (11) webbing between toes rudimentary; (12) coloration of dorsal body olive brown to bronze.

Key words: Molecular phylogenetic analyses, morphology, *Scutigera*, taxonomy, Tibet Autonomous Region



Academic editor: Bin Wang
Received: 14 June 2023
Accepted: 1 November 2023
Published: 20 December 2023

ZooBank: <https://zoobank.org/9119B60A-7116-4513-A590-471516021060>

Citation: Shi S-C, Sui L-L, Ma S, Ji F-R, Bu-Dian A-Y, Jiang J-P (2023) A new Asian lazy toad of the genus *Scutigera* Theobald, 1868 (Anura, Megophryidae) from southern Tibet, China. ZooKeys 1187: 31–62. <https://doi.org/10.3897/zookeys.1187.107958>

Copyright: © Sheng-Chao Shi et al.
This is an open access article distributed under terms of the Creative Commons Attribution License (Attribution 4.0 International – CC BY 4.0).

Introduction

The Asian lazy toads *Scutigera* Theobald, 1868, is a group of amphibians inhabiting southwestern China, northern Myanmar, Nepal, northern India, and northern Pakistan at altitudes ranging from 1000 to 5300 m (Fei et al. 2009; Fei et al. 2012; Jiang et al. 2020; Frost 2023). Currently, there are 27 valid species in the genus, of which 23 species are distributed in China (Fei et al. 2009; Yang and Huang 2019; Jiang et al. 2020; AmphibiaChina 2023; Frost 2023; Zhou et al. 2023). The species in the genus can be classified into five major clades based

* These authors contributed equally to this work as the first authors.

on phylogenetic analysis (Hofmann et al. 2017; Yang and Huang 2019; Che et al. 2020; Xing et al. 2023; Zhou et al. 2023):

- Clade A (Medog of eastern Himalaya) including *S. wuguanfui* Jiang, Rao, Yuan, Wang, Li, Hou, Che & Che, 2012 from Medog, southeastern Tibet, China;
- Clade B (central Himalayan clade) including *S. nepalensis* Dubois, 1974 and *S. sikimmensis* (Blyth, 1854) from central Himalaya;
- Clade C (Tsinling Mountains-Sichuan Basin clade) including *S. chintingensis* Liu & Hu, 1960, *S. ningshanensis* Fang, 1985, and *S. feiliangi* Zhou, Guan & Shi, 2023;
- Clade D (from eastern Himalaya and Gaoligong Mountains) including species *S. nyingchiensis* Fei, 1977, *S. spinosus* Jiang, Wang, Li & Che, 2016, *S. tengchongensis* Yang & Huang, 2019, and *S. gongshanensis* Yang & Su, 1979;
- Clade E (Tibet & Hengduan Shan region clade) including eight species *S. boulengeri* (Bedriaga, 1898), *S. mammatus* (Günther, 1896), *S. liupanensis* Huang, 1985, *S. tuberculatus* Liu & Fei, 1979, *S. glandulatus* (Liu, 1950), *S. muliensis* Fei & Ye, 1986, *S. jiulongensis* Fei, Ye & Jiang, 1995, and *S. wanglangensis* Ye & Fei, 2007 from Sichuan, China.

Scutigera ghunsa Khatiwada, Shu, Subedi, Wang, Ohler, Cannatella, Xie & Jiang, 2019 was weakly supported in the Himalayan clade (Khatiwada et al. 2019) and *S. occidentalis* Dubois, 1978 has an uncertain phylogenetic position from western Himalaya. However, the phylogenetic relationships of the following eight species remain unresolved: *S. adungensis* Dubois, 1979 from eastern Himalaya; *S. bangdaensis* Rao, Hui, Ma & Zhu, 2022 from eastern Tibet; *S. bhutanensis* Delorme & Dubois, 2001 from Bhutan; *S. biluoensis* Rao, Hui, Zhu & Ma, 2022 from Yunnan, China; *S. maculatus* (Liu, 1950) from northwestern Sichuan and eastern Tibet, China; *S. meiliensis* Rao, Hui, Zhu & Ma, 2022 from northwest Yunnan, China; *S. pingwuensis* Liu & Tian, 1978 from Sichuan and southern Gansu, China.

The Paleo-Tibetan region is believed to be the origin of the genus *Scutigera*, and migration across mountains and drainages along the Himalayas is limited (Hofmann et al. 2017). The deep valleys and high mountains of the Himalayas harbor incredible amphibian species diversity, and many have been described recently (e.g., Che et al. 2020). In July 2021 and August 2022, two field surveys were conducted in southern Tibet, and a series of specimens of the genus *Scutigera* were collected from a southern slope of the Himalayas in Luozha County, Shannan Prefecture, Tibet. Subsequent studies on morphological comparisons and molecular analysis reveal that they represent a species new to science, which is described in this study.

Materials and methods

Sampling

In this study, 34 specimens of *Scutigera* (25 adults, 1 subadult, 2 juveniles, and 6 tadpoles) were collected from Luozha County, Shannan Prefecture, Tibet Autonomous Region, China. The specimens were euthanized and then fixed in

75% ethanol before being deposited in the Herpetology Museum of Chengdu Institute of Biology (CIB), Chinese Academy of Sciences. The sex of specimens was determined by the presence of nuptial spines, chest spines, eggs, or examination of gonads when necessary. Tissue samples were taken from legs and preserved separately in 95% ethanol before fixation.

Molecular phylogenetic analysis

Total genomic DNA was extracted using QIAamp DNA Mini Kit (QIAGEN, Hilden, Germany) following protocol. Fragments of two mitochondrial genes (16S rRNA and COI) and one nuclear gene (RAG1) were amplified and sequenced. The primer sequences for these genes were retrieved from the literature for 16S rRNA (Simon et al. 1994), COI (Che et al. 2012), and RAG1 (Mauro et al. 2004). PCR amplifications for the gene were performed in a 25 µl volume reaction with the following conditions: an initial denaturing step at 95 °C for 4 min; 36 cycles of denaturing at 95 °C for 40 s, annealing at 52 °C (for COI and RAG1) or 54 °C (for 16S rRNA) for 40 s and extending at 72 °C for 40 s, and a final extending step of 72 °C for 10 min. PCR products were sequenced by Beijing Qingke New Industry Biotechnology Co., Ltd., Beijing, China. Sequences were assembled and aligned using BioEdit v. 7.2.5 (Hall 1999) with default settings and were further revised manually when necessary. The COI and RAG1 sequences were translated to amino acid sequences in MEGA X (Kumar et al. 2018), adjusted for open reading frames, and checked to ensure the absence of premature stop codons. All new sequences were deposited in GenBank.

For phylogenetic analysis, corresponding available sequences of *Scutigera* and three outgroups including *Oreolalax omeimontis*, *Leptobranchium boringii*, and *Leptobranchella liui* were obtained from GenBank in accordance with previous studies (Hofmann et al. 2017; Che et al. 2020). A mitochondrial DNA sequence (16S + COI) matrix was generated for the phylogenetic analyses. Phylogenetic analyses were conducted using maximum likelihood (ML) and Bayesian Inference (BI) methods implemented in Phylosuite (Zhang et al. 2020). Each gene was considered as a partition, and the best evolutionary model was chosen for each partition using PartitionFinder2 (Lanfear et al. 2017) based on Bayesian Inference Criteria (BIC). GTR+G and HKY+G were chosen as the best model for the combined mitochondrial DNA sequences and RAG1 respectively. ML phylogenies were inferred using IQ-TREE (Nguyen et al. 2015) under Edge-linked partition model for 10000 ultrafast bootstraps (Minh et al. 2013), as well as the Shimodaira-Hasegawa-like approximate likelihood-ratio test (Guindon et al. 2010). BI phylogenies were inferred using MrBayes 3.2.6 (Ronquist et al. 2012) under partition model (2 parallel runs, 10 million generations), in which the initial 25% of sampled data were discarded as burn-in. Genetic distances between species for each gene were estimated using MEGA X. All sequences used in this study are listed in Table 1.

Morphological analysis

For adults, measurements were taken with a dial caliper to the nearest 0.1 mm. In total, 24 measurements of 21 adults were measured: **SVL** (snout-vent length: distance from the tip of the snout to the posterior edge of the vent), **AG** (trunk

Table 1. Samples and DNA sequences used in this study.

No.	Species	Locality	Voucher no.	GenBank accession No.			Source
				COI	16S	RAG1	
1	<i>Scutigera luozhaensis</i> sp. nov.	Luozha, Tibet, China	CIB QZ2021119	OR141828	OR469879	OR546339	This study
2	<i>S. luozhaensis</i> sp. nov.	Luozha, Tibet, China	CIB QZ2021141	OR141835	OR469884	OR546344	This study
3	<i>S. luozhaensis</i> sp. nov.	Luozha, Tibet, China	CIB QZ2021139	OR141833	OR469882	OR546342	This study
4	<i>S. luozhaensis</i> sp. nov.	Luozha, Tibet, China	CIB 119119	OR141823	OR469858	OR546324	This study
5	<i>S. luozhaensis</i> sp. nov.	Luozha, Tibet, China	CIB 119116	OR141831	OR469855	/	This study
6	<i>S. luozhaensis</i> sp. nov.	Luozha, Tibet, China	CIB QZ2021117	OR141827	OR469878	OR546338	This study
7	<i>S. luozhaensis</i> sp. nov.	Luozha, Tibet, China	CIB QZ2021115	OR141825	/	OR546336	This study
8	<i>S. luozhaensis</i> sp. nov.	Luozha, Tibet, China	CIB CJA 20220066	OR141837	OR469864	/	This study
9	<i>S. luozhaensis</i> sp. nov.	Luozha, Tibet, China	CIB QZ2021090	OR141824	OR469875	OR546335	This study
10	<i>S. luozhaensis</i> sp. nov.	Luozha, Tibet, China	CIB 119117	OR141852	OR469856	OR546322	This study
11	<i>S. luozhaensis</i> sp. nov.	Luozha, Tibet, China	CIB 119118	OR141853	OR469857	OR546323	This study
12	<i>S. luozhaensis</i> sp. nov.	Luozha, Tibet, China	CIB CJA 20220103	OR141841	OR469868	OR546328	This study
13	<i>S. luozhaensis</i> sp. nov.	Luozha, Tibet, China	CIB QZ2021116	OR141826	OR469877	OR546337	This study
14	<i>S. luozhaensis</i> sp. nov.	Luozha, Tibet, China	CIB 119120	OR141836	OR469859	OR546325	This study
15	<i>S. luozhaensis</i> sp. nov.	Luozha, Tibet, China	CIB 119630-2	OR141843	OR469863	OR546327	This study
16	<i>S. luozhaensis</i> sp. nov.	Luozha, Tibet, China	CIB CJA 20220121	OR141849	OR469873	/	This study
17	<i>S. luozhaensis</i> sp. nov.	Luozha, Tibet, China	CIB CJA 20220124	OR141851	OR469874	OR546334	This study
18	<i>S. luozhaensis</i> sp. nov.	Luozha, Tibet, China	CIB 119630-1	OR141842	OR469862	/	This study
19	<i>S. luozhaensis</i> sp. nov.	Luozha, Tibet, China	CIB QZ2021135	OR141830	OR469881	OR546341	This study
20	<i>S. luozhaensis</i> sp. nov.	Luozha, Tibet, China	CIB CJA 20220119	OR141847	OR469872	OR546332	This study
21	<i>S. luozhaensis</i> sp. nov.	Luozha, Tibet, China	CIB QZ2021140	OR141834	OR469883	OR546343	This study
22	<i>S. luozhaensis</i> sp. nov.	Luozha, Tibet, China	CIB QZ2021134	OR141829	OR469880	OR546340	This study
23	<i>S. luozhaensis</i> sp. nov.	Luozha, Tibet, China	CIB CJA 20220117	OR141845	OR469870	OR546330	This study
24	<i>S. luozhaensis</i> sp. nov.	Luozha, Tibet, China	CIB 119115	OR141832	OR469854	OR546320	This study
25	<i>S. luozhaensis</i> sp. nov.	Luozha, Tibet, China	CIB 119122	OR141848	OR469860	/	This study
26	<i>S. luozhaensis</i> sp. nov.	Luozha, Tibet, China	CIB 119123	OR141850	OR469861	OR546326	This study
27	<i>S. luozhaensis</i> sp. nov.	Luozha, Tibet, China	CIB CJA 20220116	OR141844	OR469869	OR546329	This study
28	<i>S. luozhaensis</i> sp. nov.	Luozha, Tibet, China	CIB CJA 20220118	OR141846	OR469871	OR546331	This study
29	<i>S. luozhaensis</i> sp. nov.	Luozha, Tibet, China	CIB CJA 20220074	OR141839	OR469866	/	This study
30	<i>S. luozhaensis</i> sp. nov.	Luozha, Tibet, China	CIB CJA 20220073	OR141838	OR469865	/	This study
31	<i>S. luozhaensis</i> sp. nov.	Luozha, Tibet, China	CIB CJA 20220075	OR141840	OR469867	/	This study
32	<i>S. gongshanensis</i>	Gongshan, Yunnan, China	CIB20070717001	KU243062	/	/	Jiang et al. (2016)
33	<i>S. gongshanensis</i>	Gongshan, Yunnan, China	CIB20070717002	KU243063	/	/	Jiang et al. (2016)
34	<i>S. gongshanensis</i>	—	KIZ020492	/	/	MW111380	Xu et al. (2021)
35	<i>S. gongshanensis</i>	—	CAS 234295	/	/	KX208788	Feng et al. (2017)
36	<i>S. nyingchiensis</i>	Nyingchi, Tibet, China	KIZ017460	KU243057	/	/	Jiang et al. (2016)
37	<i>S. nyingchiensis</i>	Nyingchi, Tibet, China	KIZ017459	KU243056	/	MW111377	Jiang et al. (2016); Xu et al. (2021)
38	<i>S. nyingchiensis</i>	Nyingchi, Tibet, China	CAS_XM1095	KY310877	KY310768	/	Hofmann et al. (2017)
39	<i>S. tengchongensis</i>	Tengchong, Yunnan, China	SYS a005799	MK121783	MK121789	/	Yang and Huang (2019)
40	<i>S. spinosus</i>	Medog, Tibet, China	KIZ011100	KU243054	/	/	Jiang et al. (2016)
41	<i>S. spinosus</i>	Medog, Tibet, China	KIZ012645	KU243055	/	/	Jiang et al. (2016)
42	<i>S. feiliangi</i>	Luoyang, Henan, China	SYAUBAA000040	OR263444	/	/	Zhou et al. (2023)
43	<i>S. feiliangi</i>	Luoyang, Henan, China	SYAUBAA000041	OR263445	/	/	Zhou et al. (2023)
44	<i>S. ningshanensis</i>	Shaanxi, China	-	KX619450	KX619450	/	Song et al. (2017)

No.	Species	Locality	Voucher no.	GenBank accession No.			Source
				COI	16S	RAG1	
45	<i>S. chintingensis</i>	Tianquan, Sichuan, China	LC141	KY310878	KY310769	KY311042	Hofmann et al. (2017)
46	<i>S. cf. boulengeri</i>	Kangding, Sichuan, China	CIB GGS-MGC4-1	MZ342925	/	/	This study
47	<i>S. cf. boulengeri</i>	Ganzi, Sichuan, China	KQ3_2014	KY310861	KY310751	KY311027	Hofmann et al. (2017)
48	<i>S. cf. boulengeri</i>	Ganzi, Sichuan, China	KQ4_2014	KY310862	KY310752	KY311028	Hofmann et al. (2017)
49	<i>S. jiulongensis</i>	Ganzi, Sichuan, China	KIZ045055	KU243066	/	/	Jiang et al. (2016)
50	<i>S. cf. boulengeri</i>	Jone, Gansu, China	jone1	KJ082073	/	/	Hofmann et al. (2017)
51	<i>S. wanglangensis</i>	Mianyang, Sichuan, China	21514N1	OQ361635	/	/	Xing et al. (2023)
52	<i>S. liupanensis</i>	Jingyuan, Ningxia, China	KIZ NX080514	JN700835	/	/	Che et al. (2012)
53	<i>S. liupanensis</i>	/	/	KX352261	KX352261	/	Direct submission
54	<i>S. liupanensis</i>	/	KIZNX080519	/	/	MW111376	Xu et al. (2021)
55	<i>S. mammatus</i>	Kangding, Sichuan, China	CIB GGS-SDX1-1	MZ342926	MZ351374	/	This study
56	<i>S. mammatus</i>	Kangding, Sichuan, China	CIB GGS-PBX4-4	ON422290	ON426806	/	This study
57	<i>S. mammatus</i>	Kangding, Sichuan, China	CIB GGS-PBX4-3	ON422291	ON426807	/	This study
58	<i>S. glandulatus</i>	Ganzi, Sichuan, China	SC1_2014	KY310879	KY310770	KY311044	Hofmann et al. (2017)
59	<i>S. glandulatus</i>	Kangding, Sichuan, China	SH150531	KY310882	KY310773	KY311048	Hofmann et al. (2017)
60	<i>S. glandulatus</i>	Ganzi, Sichuan, China	SC2_2014	KY310880	KY310771	KY311045	Hofmann et al. (2017)
61	<i>S. muliensis</i>	Yanyuan, Sichuan, China	/	MW167047	EF397277	EF397302	Che et al. (2020); Fu et al. (2007)
62	<i>S. tuberculatus</i>	Sichuan, China	/	MW021351	EF397278	EF397299	Che et al. (2020); Fu et al. (2007)
63	<i>S. boulengeri</i>	Tageija, Tibet, China	A1-AL	KY310870	KY310760	KY311036	Hofmann et al. (2017)
64	<i>S. boulengeri</i>	Muktinath, Mustang district, Nepal	JRK2016-215	MK970610	MK950904	/	Khatiwada et al. (2019)
65	<i>S. boulengeri</i>	Damxung, Tibet, China	A3-AL	KY310872	KY310762	KY311038	Hofmann et al. (2017)
66	<i>S. boulengeri</i>	Zhaduo, Qinghai, China	JRK2018-03	MK970611	MK950905	/	Khatiwada et al. (2019)
67	<i>S. boulengeri</i>	Lhasa, Tibet, China	JS1507_C1	KY310875	KY310765	KY311040	Hofmann et al. (2017)
68	<i>S. cf. mammatus</i>	Gongshan, Yunnan, China	Yako01	/	EU180890	/	Rao and Wilkinson (2007)
69	<i>S. sp.</i>	Fugong, Yunnan, China	CAS228188	/	EU180889	/	Rao and Wilkinson (2007)
70	<i>S. ghunsa</i>	Ghunsa, Taplejung district, Nepal	JRK2015-193	MK970591	MK950885	/	Khatiwada et al. (2019)
71	<i>S. occidentalis</i>	Deosai Plateau, Pakistan	MS_PK6	KY310901	KY310796	KY311066	Hofmann et al. (2017)
72	<i>S. nepalensis</i>	Chainpur, Nepal	NME_A2018/13	KY310886	KY310777	KY311052	Hofmann et al. (2017)
73	<i>S. sikimmensis</i>	Kongma Danda, Nepal	JS140524	KY310902	KY310798	KY311068	Hofmann et al. (2017)
74	<i>S. wuguanfui</i>	Medog, Tibet, China	KIZ011101	KU243060	/	/	Jiang et al. (2016)
75	<i>S. wuguanfui</i>	Medog, Tibet, China	KIZ011102	KU243061	/	MW111378	Jiang et al. (2016)
76	<i>Leptobrachium boringii</i>	Mt. Emei, Sichuan, China	Tissue ID: YPX37539	KX812164	KX811930	KX812282	Chen et al. (2017)
77	<i>Oreolalax omeimontis</i>	Mt. Emei, Sichuan, China	CIBEMS18061205	OP247647	MN688660	/	Hou et al. (2020)
78	<i>Leptobrachella liui</i>	Mt. Jinggang, Jiangxi, China	SYSa004045	MH406370	MH406907	MH405153	Liu et al. (2018)

length between axilla and groin: distance between middle point of the two axillae and middle point of groins); **HL** (head length: distance from the rear of the mandible to the tip of the snout); **HW** (head width: distance between the posterior angles of jaw); **HH** (head height: head height at the corner of jaws); **SL** (snout length: distance from tip of snout to anterior border of the orbit); **IND** (internasal distance: distance between inner edge of two nostrils); **IOS** (in-

terorbital space: shortest distance between inner edge of upper eyelids); **UEW** (maximum upper eyelid width); **ACED** (distance between anterior corner of eyes); **PCED** (distance between posterior corner of eyes); **ED** (horizontal eye diameter); **SND** (nostril-snout distance: distance from center of the nostril to tip of the snout); **END** (eye-nostril distance: distance from front of eye to the center of nostril); **LAL** (lower arm length: distance from elbow to wrist); **LAD** (lower arm width: largest diameter of forearm); **HAL** (hand length: distance from wrist to tip of third digit); **HLL** (hindlimb length: distance between vent and tip of fourth toe when leg straightened at right angle to the body); **THL** (thigh length: distance from cloaca to knee); **TL** (tibia length: distance from knee to ankle); **TFL** (tarsal-foot length: length from heel to the tip of the fourth digit); **FL** (foot length: distance from the proximal end of the inner metatarsal tubercle to the tip of the fourth digit); **TW** (tibia width: largest tibia width); **IMTL** (inner metatarsal tubercle length). Morphological terminologies were mostly based on Fei et al. (2009) and webbing formulae are described based on Savage and Heyer (1997). Morphological comparison between the unknown species from Luozha and valid species of genus *Scutigera* were conducted based on data obtained from references (Table 2) and 31 examined specimens of 8 species. For phylogenetical close species, further morphometrics comparison using one-way ANOVA was conducted based on SVL and ratios of another 18 characters to SVL of examined male specimens.

For tadpoles, the stages were identified following Gosner (1960). Thirteen morphometric characters of two tadpoles were measured: **LTRF** (labia tooth row formulae); **TOL** (total length: distance from tip of snout to tip of tail); **BL** (body length: distance from tip of snout to trunk-tail junction); **BH** (maximum body height); **BW** (maximum body width); **SNL** (snout length: distance from tip of snout to anterior border of the orbit); **SSD** (distance from snout to spiraculum: distance from tip of snout to opening of spiraculum); **ODW** (oral disc width: largest width of oral disc); **IOS** (interocular space: minimum distance of eyes); **TMW** (maximum tail muscle width); **TAL** (tail length: distance between posterior side of opening of cloaca to tip of tail); **TMH** (maximum tail muscle height); **HLL** (hindlimb length). Morphological terminologies were based on Fei et al. (2009).

Results

Molecular analysis

The aligned sequence matrices of 16S rRNA, COI, and RAG1 genes contain 532 bps, 622 bps, and 1017 bps, respectively. Mitochondrial phylogenetic analysis indicates that *Scutigera* species can be included in five clades, the topology of phylogenetic tree (Fig. 1) is generally similar to those of previous research (Hofmann et al. 2017; Che et al. 2020). Clade A contains only one species, *S. wuguanfui*. Positions for the four species from central and western Himalaya (*S. ghunsa*, *S. occidentalis*, *S. nepalensis*, *S. sikimmensis*) are uncertain. The clade B are the largest, containing *S. boulengeri* species complex, *S. jiulongensis*, *S. wanglangensis*, *S. liupanensis*, *S. mammatus*, *S. glandulatus*, *S. muliensis*, *S. tuberculatus*, and a lineage including *S. cf. mammatus* and *S. sp.* from Yunnan. The *S. boulengeri* species complex contained three lineages as Lin et

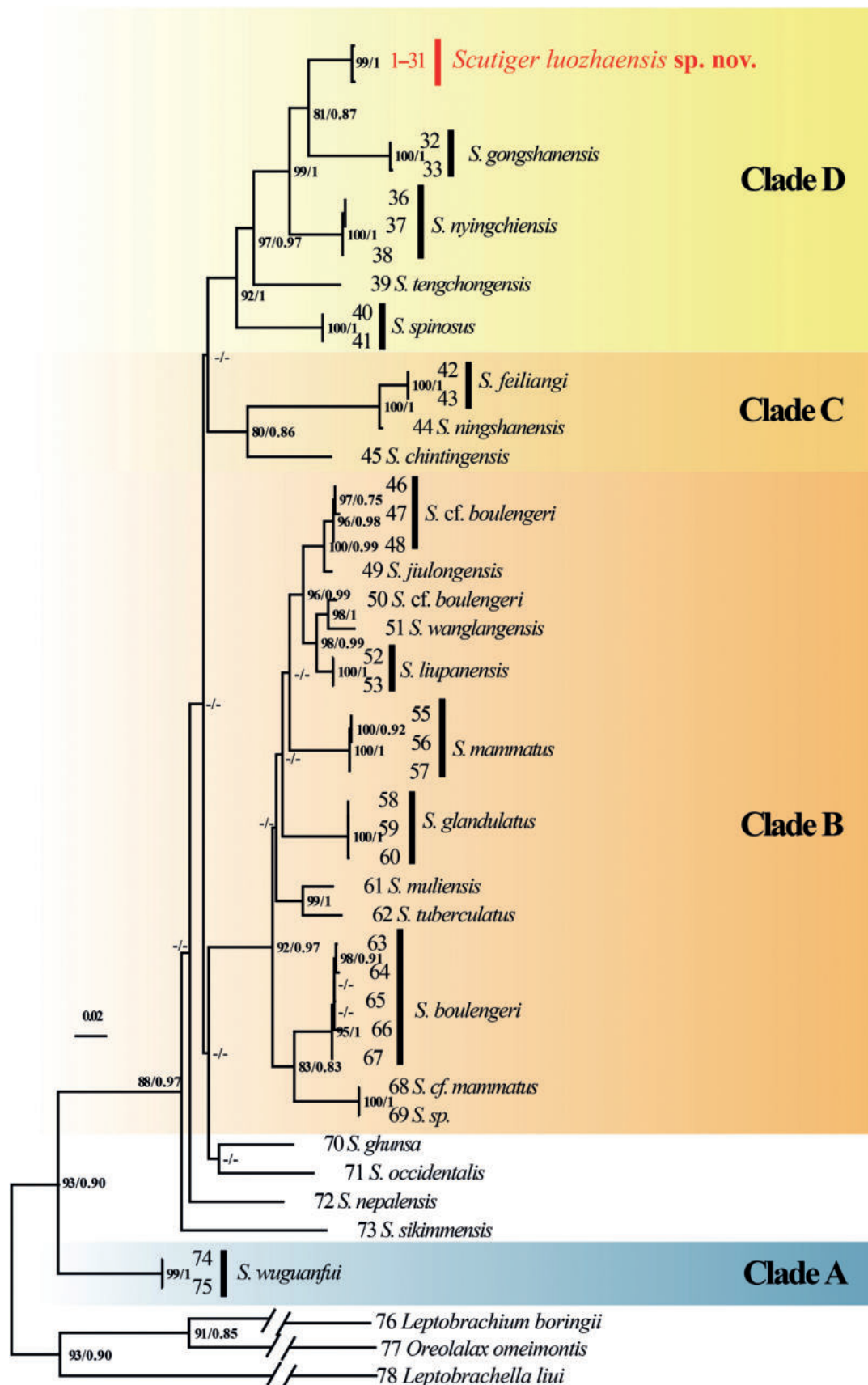


Figure 1. Phylogenetic relationships of *Scutigera* using maximum likelihood (ML) based on the mitochondrial 16S and COI gene sequences. ML bootstrap support/Bayesian posterior probability is denoted beside each node. The symbol “-” represents a value below 70/0.70. For sample numbers refer to Table 1.

al (2023) reported. Clade C contains three species, *S. feiliangi*, *S. ningshanensis* and *S. chintingensis*. The samples collected from Luozha County formed an independent lineage (Luozha lineage) with high bootstrap supports (BS = 99) and Bayesian posterior probabilities (BPP = 1.00). The Luozha lineage further clustered with *S. gongshanensis*, and *S. nyingchiensis* with strong supports (BS = 99, BPP = 1.00). These three species further form clade D with *S. tengchongensis* and *S. spinosus*. Phylogenetic analysis based on RAG1 resulted in a similar topology (Fig. 2). The Luozha lineage is sister to *S. nyingchiensis*.

Genetic distances between species of *Scutigera* are shown in Suppl. materials 1–3 based on 16S rRNA, COI, and RAG1 genes, respectively. The smallest genetic distances between the Luozha lineage and other taxa of *Scutigera* based on 16S rRNA and COI are 0.026–0.030 and 0.064–0.068 respectively (vs *S. nyingchiensis*). These are comparable or larger than multiple known species pair (e.g., *S. glandulatus* vs *S. jiulongensis* 0.066–0.068 for COI; *S. liupanensis* vs *S. mammatus* 0.024 for 16S rRNA, 0.064–0.068 for COI; *S. tengchongensis* vs *S. chintingensis* 0.029 for 16S rRNA, *S. muliensis* vs *S. tuberculatus* 0.008 for 16S rRNA, 0.055 for COI). The genetic distances for nuclear gene RAG1 between the Luozha lineage and other species are much smaller (0.001–0.020); however, three species (*S. occidentalis*, *S. nepalensis*, *S. sikimmensis*) even share the same RAG1 haplotype.

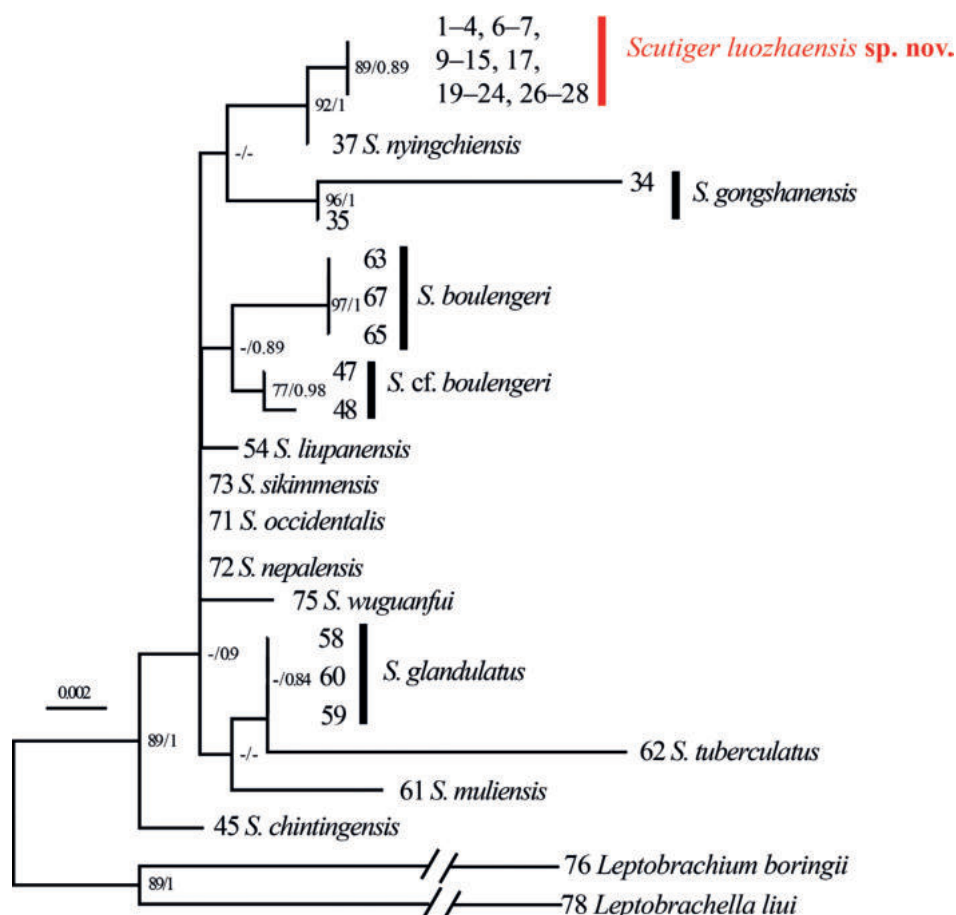


Figure 2. Phylogenetic relationships of *Scutigera* using maximum likelihood (ML) based on RAG1 gene sequences. ML bootstrap support/Bayesian posterior probability is denoted beside each node. The symbol “-” represents a value below 70/0.70. Sample number refer to Table 1.

Morphological results

Comparisons based on ten selected morphological characters for all *Scutigera* species are summarized in Table 2. Images of two phylogenetically close related species to the Luozha lineage (*S. nyingchiensis* and *S. gongshanensis*) were demonstrated in Fig. 3. The Luozha lineage is morphologically distinguished from other known species of *Scutigera* based on a combination of morphological features as follows:

For *S. adungensi*, the Luozha lineage differs by absence of vocal sac for adult males (vs presence); absence of maxillary teeth and budding (vs presence of budding); smaller male body size (SVL 47.0–67.2 mm vs 71–73 mm); presence numerous dense tiny black nuptial spines present on dorsal surface of fingers I, II and inner surface of finger III of males in breeding condition (vs large spines on inner two fingers); two pair of spine patches on chest of breeding male (vs one pair).

For *S. bangdaensis*, the Luozha lineage differs by presence of one to six separated spines on top of each dorsal tubercle of males in breeding condition (vs absence of spines on tubercles); rudimentary webbing between toes (vs developed).

For *S. bhutanensis*, the Luozha lineage differs by numerous dense tiny black nuptial spines present on dorsal surface of fingers I, II and inner surface of finger III of males in breeding condition (vs 16–18 large nuptial spines on each of inner two fingers of males); space between upper eyelids being wider than upper eyelids (vs narrower); forearm being longer than hand (vs equal); relatively larger feet in males (FL/SVL 40.9–50.4% vs 38.5%).

For *S. biluoensis*, the Luozha lineage differs by absence of maxillary teeth (vs presence); presence of nuptial spines on dorsal surface of fingers I, II and inner surface of finger III of males in breeding condition (vs on inner two fingers); smaller male body size (SVL 47.0–67.2 mm vs 73 mm).

For *S. boulengeri*, the Luozha lineage differs by absence of spine patches on belly of males in breeding condition (vs presence); rudimentary webbing between toes (vs well-developed webbing); coloration of dorsal body olive brown to bronze (vs greyish olive).

For *S. chintingensis*, the Luozha lineage differs by absence of spines on inner surface of upper arm and forearm of males in breeding condition (vs presence); rudimentary webbing between toes (vs 1/3 webbing between toes); absence of maxillary teeth (vs developed maxillary teeth); absence of a pair of long glandular skin ridges on shoulder or middle dorsum (vs presence); absence of femoral glands (vs presence).

For *S. feiliangi*, the Luozha lineage differs by presence of one to six separated spines on top of each dorsal tubercle of males in breeding condition (vs a layer of keratinized dense tiny spines on tubercles on dorsum of both gender in breeding); absence of spines on inner surface of forearm of males in breeding condition (vs presence); upper and lower half of iris uniformly bicolored (vs upper half golden, lower half brown).

For *S. ghunsa*, the Luozha lineage differs by pectoral spine patches being slightly larger than the axillary spine patches (vs twice or even larger); larger male body size (SVL 47.0–67.2 mm vs 42.0–47.8 mm); the yellow tubercles scattered around cloaca of males in breeding condition (vs creamy white granules surrounding vent); coloration of dorsal body olive brown to bronze (vs pale

Table 2. Morphological comparison of *Scutigera* species based on ten selected characters. Bold typeface indicates characters different from the new species.

Species	Male SVL	Female SVL	Maxillary teeth or budding	Numbers of fingers with nuptial pads	Spine patches pairs on chest	Size of pectoral spine patches vs axillary spine patches	Spine patches on belly in males	Toe webbing	Tubercles on dorsum with spines	Vocal sac	References
<i>Scutigera luozhaensis</i> sp. nov.	47.0–67.2 (n = 13)	49.8–66.2 (n = 8)	absent	I, II, III	2	slightly larger	absent	rudimentary	yes	absent	This study
<i>S. adungensis</i> *	71–73 (n = 2)	/	budding	I, II	1	/	absent	rudimentary	/	present	Dubois (1979)
<i>S. bangdaensis</i> *	45–50 (n = 2)	48–50 (n = 2)	/	I, II, III	2	larger	absent	developed	no	/	Rao (2022*2020*)
<i>S. bhutanensis</i> *	53.0–64.9 (n = 3)	/	absent	I, II	2	similar	absent	rudimentary	/	absent	Delorme and Dubois (2001); Khatiwada et al. (2019)
<i>S. biluoensis</i> *	73 (n = 1)	53.5 (subadult, n = 1)	teeth	I, II	2	/	absent	rudimentary	/	/	Rao (2022*2020*)
<i>S. boulengeri</i>	44.9–53.7 (n = 20)	40.2–58.2 (n = 8)	absent or only short budding	I, II, III	2	similar	present	well-developed	yes	absent	Fei et al. (2009); Fei et al. (2012)
<i>S. chintingsensis</i>	42.0–50.3 (n = 22)	48.0–52.8 (n = 6)	teeth	I, II, III	2	slightly larger	absent	weak	yes	absent	Fei et al. (2009); Fei et al. (2012)
<i>S. feiliangji</i>	45.7–50.2 (n = 6)	48.9–51.5 (n = 3)	budding	I, II, III	2	slightly larger	absent	rudimentary	yes	absent	Zhou et al. (2023)
<i>S. ghunsa</i>	42.0–47.8 (n = 5)	50.2–53.9 (n = 3)	absent	I, II, III	2	twice or even larger	absent	rudimentary	yes	absent	Khatiwada et al. (2019); This study
<i>S. glandulatus</i>	68.0–90.0 (n = 17)	58.0–83.7 (n = 14)	absent	I, II	2	twice or even larger	absent	developed	no	absent	Fei et al. (2009); Fei et al. (2012)
<i>S. gongshanensis</i>	47.0–57.0 (n = 21)	49.0–60.0 (n = 2)	budding	I, II	1	/	absent	rudimentary	no	present	Fei et al. (2009); Fei et al. (2012); This study
<i>S. jiuolongensis</i>	67.4–81.5 (n = 20)	/	absent	I, II	2	twice or even larger	absent	weak	no	absent	Fei et al. (2009); Fei et al. (2012)
<i>S. jiupanensis</i>	40.6–48.0 (n = 20)	52.0–59.5 (n = 2)	budding	I, II, III	2	similar	present	rudimentary	yes	absent	Fei et al. (2009); Fei et al. (2012)
<i>S. maculatus</i> *	65.4 (n = 1)	69.0 (n = 1)	budding	I, II, III	2	slightly larger	absent	developed	yes	absent	Fei et al. (2009); Fei et al. (2012)
<i>S. mammatus</i>	62.4–80.6 (n = 20)	60.9–77.8 (n = 15)	mostly absent, or with budding	I, II	1	/	absent	well developed	no	absent	Fei et al. (2009); Fei et al. (2012)
<i>S. meiliensis</i> *	70 (n = 1)	65 (n = 1)	teeth	I, II	2	/	absent	rudimentary	/	/	Rao (2022*2020*)
<i>S. mulliensis</i>	68.2–80.0 (n = 11)	60.1–67.5 (n = 10)	absent	I, II	1	/	absent	weak	no	absent	Fei et al. (2009); Fei et al. (2012); This study
<i>S. nepalensis</i>	68.0–76.0 (n = 8)	59.5–66.8 (n = 4)	/	I, II, III	2	similar	absent	rudimentary	/	absent	Dubois (1974); Khatiwada et al. 2019)

Species	Male SVL	Female SVL	Maxillary teeth or budding	Numbers of fingers with nuptial pads	Spine patches pairs on chest	Size of pectoral spine patches vs axillary spine patches	Spine patches on belly in males	Toe webbing	Tubercles on dorsum with spines	Vocal sac	References
<i>S. ningshanensis</i>	51.0 (n = 1)	41.0 (n = 1)	teeth	I, II, III	2	similar	present	rudimentary	yes	absent	Fei et al. (2009); Fei et al. (2012)
<i>S. nyingchiensis</i>	50.9–67.6 (n = 38)	69.6–70.0 (n = 3)	budding	I, II, III	2	slightly larger	absent	1/5 webbing on toe IV	yes	absent	Fei et al. (2009); Jiang et al. (2016); Che et al. (2020); This study
<i>S. occidentalis</i>	51–64 (n = ?)	/	teeth absent	I, II, III	2	slightly larger	absent	clear (weak via fig. S3.3 of Hofmann et al. 2017)	yes	/	Dubois (1978); Hofmann et al. (2017)
<i>S. pingwuensis*</i>	60.7–75.8 (n = 20)	77.5 (n = 1)	absent	I, II, III	2	twice or even larger	present	rudimentary	yes	absent	Fei et al. (2009); Jiang et al. (2012)
<i>S. sikimmensis</i>	46.9–55.3 (n = 28)	50.8–60.5 (n = 7)	budding	I, II, III	2	slightly larger	absent	rudimentary	yes	absent	Fei et al. (2009); Fei et al. (2012); Che et al. (2020); Frost (2023)
<i>S. spinosus</i>	50.5–55.6 (n = 12)	53.8–57.2 (n = 4)	absent	I, II, III	2	twice or even larger	absent	rudimentary	yes	absent	Jiang et al. (2016)
<i>S. tengchongensis</i>	36.0–40.1 (n = 8)	/	absent	I, II, III	2	slightly larger	absent	rudimentary	yes	absent	Yang and Huang (2019)
<i>S. tuberculatus</i>	68.0–76.0 (n = 16)	63.6–79.0 (n = 7)	absent	I, II	2	twice or even larger	absent	rudimentary	no	absent	Fei et al. (2009); Fei et al. (2012)
<i>S. wanglangensis</i>	52.7–58.2 (n = 6)	64.3 (n = 1)	budding	I, II, III	2	twice or even larger	present	1/5 to 1/3 webbing	yes	absent	Fei et al. (2009); Fei et al. (2012)
<i>S. wuguanfui</i>	77.5–83.8 (n = 6)	107.4–116.7 (n = 2)	absent	I, II, III	2	similar	absent	rudimentary	yes	present	Jiang et al. (2012); Jiang et al. (2016); This study

*Species without available gene data in molecular analysis.



Figure 3. Adult male *Scutigiger nyingchiensis* (CIB QX207) from Nyingchi, Tibet, China (**A–D**) and adult male *S. gongshanensis* (KIZ 036221) from Gongshan, Yunnan, China (**E–H**) **A** dorsolateral body **B** ventral body **C** dorsal right hand and **D** ventral foot **E** dorsolateral body **F** ventral body **G** dorsal right hand and **H** ventral foot. Photographed by SCS.

brown); absence of dark brown bands on upper lip (vs present); absence of irregular black spots on limbs (vs present).

For *S. glandulatus*, the Luozha lineage differs by smaller and moderate male body size (SVL 47.0–67.2 mm vs 68.0–90.0 mm, body stout); presence of nuptial spines on dorsal surface of fingers I, II and inner surface of finger III of males in breeding condition (vs on inner two fingers); pectoral spine patches being slightly larger than the axillary spine patches (vs twice or even larger);

rudimentary webbing between toes (vs well-developed webbing); presence of spine on warts and tubercles on dorsum (vs absence).

For *S. gongshanensis*, the Luozha lineage differs by absence of vocal sac for adult males (vs presence); absence of maxillary teeth and budding (vs presence of budding); presence of numerous tiny dense nuptial spines on dorsal surface of fingers I, II, and inner surface of finger III of males in breeding condition (vs large spines on inner two fingers); two pair of spine patches on chest of breeding male (vs one pair); presence of spine on warts and tubercles on dorsum (vs absence); absence of a wide dark strip on dorsum from behind eyes to vent (presence) (Fig. 3).

For *S. jiulongensis*, the Luozha lineage differs by smaller and moderate male body size (SVL 47.0–67.2 mm vs 67.4–81.5 mm, body stout); presence of nuptial spines on dorsal surface of fingers I, II and inner surface of finger III of males in breeding condition (vs on inner two fingers); pectoral spine patches being slightly larger than the axillary spine patches (vs twice or even larger); presence of one to six separated spines on top of each dorsal tubercle of males in breeding condition (vs absence of spines on tubercles).

For *S. liupanensis*, the Luozha lineage differs by absence of maxillary teeth and budding (vs presence of budding); absence of spine patches on belly of males in breeding condition (vs presence); absence of a pair of large tubercles around cloaca (vs presence).

For *S. maculatus* the Luozha lineage differs by absence of maxillary teeth and budding (vs presence of budding); rudimentary webbing between toes (vs well-developed webbing).

For *S. mammatus*, the Luozha lineage differs by moderate body (vs stout body); presence of nuptial spines on dorsal surface of fingers I, II and inner surface of finger III of males in breeding condition (vs on inner two fingers); two pair of spine patches on chest of breeding male (vs one pair); rudimentary webbing between toes (vs well-developed webbing); presence of one to six separated spines on top of each dorsal tubercle of males in breeding condition (vs absence of spines on tubercles).

For *S. meiliensis*, the Luozha lineage differs by absence of maxillary teeth and budding (vs presence of teeth); presence of nuptial spines on dorsal surface of fingers I, II and inner surface of finger III of males in breeding condition (vs on inner two fingers); smaller male body size (SVL 47.0–67.2 mm vs 70 mm).

For *S. muliensis*, the Luozha lineage differs by moderate body and smaller male body size (SVL 47.0–67.2 mm vs stout body, 68.2–80.0 mm); presence of nuptial spines on dorsal surface of fingers I, II and inner surface of finger III of males in breeding condition (vs on inner two fingers); two pair of spine patches on chest of breeding male (vs one pair); presence of spine on warts and tubercles on dorsum (vs absence).

For *S. nepalensis*, the Luozha lineage differs by smaller male body size (SVL 47.0–67.2 mm vs 68.0–76.0 mm); head width being smaller than (males) or subequal to (females) tibia length (vs head width equal or greater than tibia length for males and females of *S. nepalensis* respectively).

For *S. ningshanensis*, by absence of maxillary teeth and budding (vs presence of teeth); absence of spine patches on belly of males in breeding condition (vs presence); dozens of yellow tubercles scattered around cloaca of

males in breeding condition (vs a pair of white glands around vent); absence of a blue spot on tip of snout (vs present).

For *S. nyingchiensis*, the Luozha lineage differs by rudimentary webbing between toes (webbing formula $I\frac{1}{2}-II\frac{1}{2}-2III\frac{1}{2}-2\frac{1}{2}IV\frac{1}{2}-2V$ vs $1/5$ webbing on toe IV, webbing formula $I0-\frac{1}{2}II0-1\frac{1}{2}III1-2IV2-1\frac{1}{2}V$); absence of maxillary teeth and budding (vs presence of budding); coloration of dorsal body olive brown to bronze (vs greyish olive) (Fig. 3).

For *S. occidentalis*, the Luozha lineage differs by coloration of dorsal body olive brown to bronze (vs greyish olive, e.g., fig. S3.2. of Hofmann et al. 2017); rudimentary webbing between toes (vs clear webbing between toes).

For *S. pingwuensis* the Luozha lineage differs by smaller female body size (SVL 49.8–66.2 mm vs 77.5 mm); pectoral spine patches being slightly larger than the axillary spine patches (vs twice or even larger); absence of spine patches on belly of males in breeding condition (vs presence); absence of spines on inner surface of upper arm and forearm of males in breeding condition (vs presence).

For *S. sikimmensis*, the Luozha lineage differs by absence of maxillary teeth and budding (vs presence of budding); presence of numerous tiny dense nuptial spines on dorsal surface of fingers I, II and inner surface of finger III of males in breeding condition (vs large spines on inner two fingers, small spines on inner surface of third finger); absence of distinct irregular cross bands on limbs (vs presence); space between upper eyelids being wider than upper eyelids (vs narrower).

For *S. spinosus*, the Luozha lineage differs by some large warts and tubercles on dorsum gathered into short skin ridges with several spines present on top (vs prominent, conical-shaped tubercles on dorsal and lateral surfaces independent, each tubercle bearing only one black spine); absence of small patches of black spines present near armpit of males in breeding condition (vs presence); pectoral spine patches being slightly larger than the axillary spine patches (vs pectoral twice longer than axillary); absence of cross bands on limbs (vs present).

For *S. tengchongensis*, the Luozha lineage differs by larger male body size (SVL 47.0–67.2 vs 36.0–40.1 mm); absence of small patches of black spines present near armpit of males in breeding condition (vs presence); numerous tiny dense nuptial spines on dorsal surface of fingers I, II and inner surface of finger III of males in breeding condition with similar size (vs black nuptial spines on the first and second fingers being larger than those on the third finger); coloration of dorsal body olive brown to bronze (vs reddish brown).

For *S. tuberculatus*, the Luozha lineage differs by moderate and smaller male body (SVL 47.0–67.2 mm vs stout body 68.0–76.0 mm); numerous tiny dense nuptial spines on dorsal surface of fingers I, II and inner surface of finger III of males in breeding condition (vs large spines on dorsal surface of fingers I, II); pectoral spine patches being slightly larger than the axillary spine patches (vs twice or even larger); presence of spines on tubercles on dorsum (vs absence of spines on large warts on dorsum).

For *S. wanglangensis*, the Luozha lineage differs by absence of maxillary teeth and budding (vs presence of budding); pectoral spine patches being slightly larger than the axillary spine patches (vs twice or even larger); absence of spine patches

on belly of males in breeding condition (vs presence); absence of small patches of black spines present near armpit of males in breeding condition (vs presence); rudimentary webbing between toes (vs 1/5 to 1/3 webbing); coloration of dorsal body olive brown to bronze (vs greyish olive); absence of a longitudinal strip on middle dorsum connecting with brown triangle between eyes (vs presence).

For *S. wuguanfui*, the Luozha lineage differs by moderate and smaller body (SVL 47.0–67.2 mm for male, 49.8–66.2 mm for female vs stout body, 77.5–83.8 mm for male, 107.4–116.7 for female); absence of vocal sac for adult males (vs presence of an internal single subgular vocal sac for males); absence of numerous small black spines on upper chest (vs presence); space between upper eyelids being wider than upper eyelids (vs narrower).

Morphometric comparisons based on 19 characters between the Luozha lineage and two phylogenetically close species *S. gongshanensis* and *S. nyingchiensis* are shown in Table 3 (detailed data provided in Suppl. material 4). The Luozha lineage further differs from *S. gongshanensis* in HL/SVL, LAL/SVL, LAW/SVL, HLL/SVL, THL/SVL, TFL/SVL, FL/SVL, and *S. nyingchiensis* in IND/SVL, LAL/SVL, LAW/SVL.

In conclusion, the unknown *Scutigera* from Luozha presents an independent lineage with interspecific genetic divergence, and it is morphologically distinct from all known species. It is diagnosed as a new species and hence described herein.

Table 3. Morphometric comparisons between Luozha lineage, *S. nyingchiensis*, and *S. gongshanensis*. *P*-values were obtained from the one-way ANOVA for the male group. Significance was set at *P* = 0.05. Bolded numbers indicate significant *P*-values.

Characters	Luozha lineage (A, n = 9)				<i>S. nyingchiensis</i> (B, n = 8)				<i>S. gongshanensis</i> (C, n = 2)				A vs B	A vs C	B vs C
	Min	Max	Average	SD	Min	Max	Average	SD	Min	Max	Average	SD			
SVL	47	57.9	54	3.5	50.9	55.6	53.9	1.6	51	53.2	52.1	1.1	0.962	0.423	0.445
HL/SVL	28.2%	34.3%	30.5%	1.7%	30.0%	34.4%	32.7%	1.4%	31.0%	32.0%	31.5%	0.5%	0.018	0.487	0.377
HW/SVL	30.5%	37.1%	33.8%	2.1%	32.2%	35.2%	33.8%	0.9%	32.2%	34.4%	33.3%	1.1%	0.957	0.707	0.735
SL/SVL	11.4%	14.7%	12.8%	1.0%	12.3%	14.4%	13.4%	0.7%	13.0%	13.5%	13.2%	0.3%	0.186	0.538	0.822
IND/SVL	8.9%	10.3%	9.6%	0.5%	7.9%	10.0%	8.7%	0.6%	8.2%	9.2%	8.7%	0.5%	0.007	0.069	0.985
IOS/SVL	8.0%	10.9%	9.0%	1.0%	7.8%	9.6%	8.6%	0.6%	8.6%	8.8%	8.7%	0.1%	0.307	0.628	0.875
UEW/SVL	5.9%	10.3%	7.6%	1.3%	6.5%	7.9%	7.3%	0.4%	7.3%	7.7%	7.5%	0.2%	0.615	0.909	0.844
ACED/SVL	13.5%	18.8%	16.4%	1.7%	14.8%	17.9%	16.3%	1.0%	15.5%	18.0%	16.8%	1.3%	0.867	0.771	0.697
PCED/SVL	23.9%	31.1%	27.3%	2.3%	6.7%	27.1%	21.4%	8.4%	24.9%	27.6%	26.3%	1.4%	0.069	0.832	0.339
ED/SVL	8.1%	11.3%	9.8%	1.0%	9.4%	10.8%	10.1%	0.5%	10.2%	10.4%	10.3%	0.1%	0.471	0.478	0.794
LAL/SVL	25.1%	32.1%	27.7%	2.1%	23.6%	27.6%	25.8%	1.2%	19.4%	20.4%	19.9%	0.5%	0.040	0.000	0.040
LAW/SVL	9.2%	12.7%	10.4%	1.0%	11.0%	14.1%	12.1%	0.9%	11.5%	13.9%	12.7%	1.2%	0.004	0.014	0.004
HAL/SVL	21.9%	27.9%	25.0%	1.9%	23.1%	26.9%	25.3%	1.3%	22.2%	22.7%	22.5%	0.3%	0.728	0.085	0.059
HLL/SVL	136.2%	164.3%	146.0%	9.6%	143.0%	155.6%	149.2%	3.6%	103.0%	104.9%	104.0%	0.9%	0.390	0.000	0.000
THL/SVL	36.3%	48.9%	41.4%	4.1%	41.1%	44.8%	43.2%	1.1%	33.5%	37.6%	35.6%	2.0%	0.290	0.036	0.010
TL/SVL	36.3%	43.8%	38.4%	2.5%	38.5%	42.5%	40.0%	1.3%	34.1%	36.7%	35.4%	1.3%	0.126	0.087	0.013
TFL/SVL	62.5%	73.6%	66.2%	3.7%	63.4%	69.4%	66.0%	1.9%	52.7%	59.6%	56.2%	3.4%	0.917	0.001	0.002
FL/SVL	42.1%	50.4%	45.8%	2.6%	42.6%	50.3%	45.6%	2.6%	38.3%	38.8%	38.6%	0.2%	0.849	0.003	0.005
IMTL/SVL	4.4%	8.3%	6.6%	1.2%	5.3%	8.5%	6.7%	0.9%	5.9%	6.6%	6.2%	0.3%	0.849	0.672	0.593

Taxonomic account

Scutigera luozhaensis sp. nov.

<https://zoobank.org/4DD29214-7B65-484E-A51F-297C8BF26545>

Figs 4–8; Tables 3–5; Suppl. materials 3, 4

Type material. Holotype: CIB 119115, adult male, collected from Gari Village, Se Town, Luozha County, Tibet, China (28.2413°N, 90.7842°E, 4150 m a.s.l.) by Sheng-Chao Shi, Peng Yan and Shun Ma on August 3rd, 2021. The holotype was found on alpine meadow beside a stream at night.

Paratypes: 8 specimens: CIB 119116, adult male, collected at the same date and location as holotype; CIB 119117–119118, two adult males, and CIB 119122–119123, two adult females collected at Gari village, Se Town (28.2209°N, 90.8290°E, 3970 m a.s.l.); CIB 119119, adult female, collected adjacent to holotype at Gari village, Se Town (28.2216°N, 90.8283°E, 3795 m a.s.l.); CIB 119120, adult female, collected adjacent to holotype at Gari village, Se Town (28.2459°N, 90.7772°E, 4228 m a.s.l.); CIB 119121, adult female, collected at Quzangbu valley, Lakang Town (28.1189°N, 91.1862°E, 3667 m a.s.l.).

Diagnosis. *Scutigera luozhaensis* sp. nov. is assigned to the genus *Scutigera* by the followings: (1) maxillary teeth absent or indistinct; (2) vomerine teeth absent; (3) tympanum and tympanic ring entirely absent; (4) pupil vertical, (5) femoral glands indistinct; (6) pectoral and axillary gland present in males, and covered by black spines in males in breeding condition; (7) inner three fingers with black nuptial spines in males in breeding condition (Fei et al. 2009; Fei and Ye 2016).

Scutigera luozhaensis sp. nov. is diagnosed from its congeners by a combination of the following characters: (1) body moderate, male body length 47.0–67.2 mm ($n = 13$), female body length 49.8–66.2 mm ($n = 8$); (2) maxillary teeth and budding absent; (3) numerous tiny dense nuptial spines present on dorsal surface of fingers I, II and inner surface of finger III of males in breeding condition with similar size; (4) spine patches on belly of males in breeding condition absent; (5) spines on inner surface of forearm and upper arm of males in breeding condition absent; (6) small patches of black spines present near armpit of males in breeding condition absent; (7) adult males without vocal sac; (8) some large warts and tubercles on dorsum gathered into short skin ridges with several spines present on top; (9) space between upper eyelids wider than upper eyelids; (10) spots or irregular cross bands on limbs absent; (11) webbing between toes rudimentary; (12) coloration of dorsal body olive brown to bronze.

Description of holotype. Adult male, body moderate (SVL 56.4, body weight 12.5 g in life, all morphometric measurements in mm).

Head small (HW 17.2, HL 16.6, HH 9.4, ACED 8.0, PCED 13.7), nearly wide as long (HW/HL 1.04), relatively flat (HH/HW 0.55); snout short (SL 6.5), rounded, slightly protruding beyond jaw, rostral appendage absent, canthus rostralis obtuse, loreal region oblique and concave; nostril oval, closer to tip of snout than eyes (SND 3.3, END 4.1); internarial distance larger than distance from anterior margin of eye to nostril (IND/END 1.22); eyes moderate in size (ED 5.9, ED/HL 0.36); pupil narrow and vertical; distance between upper eyelids smaller than distance between nostrils, but larger than upper eyelids width (IOS 4.5, IND 5.0, UEW 3.8), interorbital space flat; tympanum absent; supratympanic ridge thick, from posterior part of upper eyelids to shoulder; pineal ocellus not pres-

ent; maxillary teeth and budding absent; tongue oval, not emarginate behind, without papillae and medial lingual sulcus; choanae oval, located against anterior border of palate, widely separated; vomerine ridges and vomerine teeth absent; choana small and oval, widely apart from each other; vocal sac and openings absent.

Forelimbs long (LAL 14.6, LAW 5.6, HAL 12.6, LAW/LAL 0.38); fingers slender, without web and lateral dermal fringes, relative length of fingers: I<II<IV<III; fingertips rounded, not dilated; subarticular tubercles and supernumerary tubercles below the base of finger absent; inner metacarpal tubercles distinct and flat, positioned at the base of finger I, slightly smaller than outer metacarpal tubercles; nuptial pad present on dorsal surface of finger I, II and inner surface of finger III, nuptial spines on finger I and II numerous dense and tiny, but faded on finger III.

Hindlimbs moderately short (TL 21.0, TL/SVL 0.37); tibiotarsal articulation reaching the shoulder when hindlimbs stretching forward; heels widely separated when hind limbs are flexed and held perpendicular to body; thighs slightly longer to tibia but shorter than feet (THL 21.4, TL 21.0, FL 25.0, TFL 36.0); tibia moderate (TW 5.9, TW/THL 0.28); toes slender, relatively lengths I<II<V<III<IV, rudimentary webbed, webbing formula: I $\frac{1}{2}$ –II $\frac{1}{2}$ –III $\frac{1}{2}$ –II $\frac{1}{2}$ –IV $\frac{1}{2}$ –2V, with narrow lateral fringes, tips rounded and not dilated; subarticular tubercles indistinct; dermal ridges continuous on under toes; inner metatarsal tubercle elliptical and prominent (IMTL 4.1), outer metatarsal tubercle absent; tarsal fold thick.

Skins rather rough on dorsal surface; large warts and tubercles scattered on dorsal body, some arranged in rows, some gathered into short skin ridges; keratinized spines on warts and tubercles not observed, but there are one to six separated pale colored tiny granules on top of each dorsal tubercle (Fig. 4C), presumably to be remains of faded keratinized spines; skins on head between and before eyes relatively smooth; tiny pale-colored granules also present along supratympanic ridge and on upper eyelids; temporal region with several small granules, loreal region relatively smooth; upper and lower lips without spines present but also has tiny pale-colored granules, spines presumably to be faded with the ending of breeding season; skins on dorsal limbs thick, scattered with small granules; skin on dorsal tibiotarsal region with developed dermal glands; dorsolateral skin folds absent; ventral body, flanks and ventral limbs smooth; ventral hands and feet smooth; dozens of fine rounded tubercles scattered around cloaca; a pair of pectoral spine patches faded but with a pair of pectoral skin pads left on chest; axillary glands present and relatively smaller, spines on axillary glands had faded; femoral glands absent.

Coloration. In life (Fig. 4), skin on dorsal surface of body and limbs basically deep olive brown; anterior head pale brown; granules on top of warts and tubercles of dorsal body, limbs, supratympanic ridge and upper eyelids pale yellowish; tubercles around cloaca yellow; ventral surface generally olive grey, more purplish on chest and throat; ventral hands and feet olive yellow; nuptial spines on fingers black; iris basically dark, with numerous bronze pigments and irregular dark gaps; tongue flesh colored. In preservative (Fig. 5), dorsal body mostly black-brown, tubercles on flanks nearly black with yellowish white point, dorsal surface of finger I, II and inner surface of finger III pale yellowish; ventral belly pale grayish brown; ventral limbs, ventral chest and ventral head yellow-



Figure 4. Holotype of *Scutigiger luozhaensis* sp. nov. (CIB 119115) in life **A** dorsolateral body **B** dorsal body **C** short skin ridges and tubercles on dorsal body **D** ventral body **E** lateral head **F** ventral feet **G** ventral hand **H** ventral view of maxillary showing no vomerine or maxillary teeth. Photographed by SCS.

ish brown; granules on lips, metacarpal tubercles, tubercles around cloaca and axillary glands grey; iris dark with uniformly distributed bronze pigments, upper and lower half not bicolored.

Variation. Morphological measurements of the adult type series are summarized in Table 4 (see detailed measurements in Suppl. material 5). The other

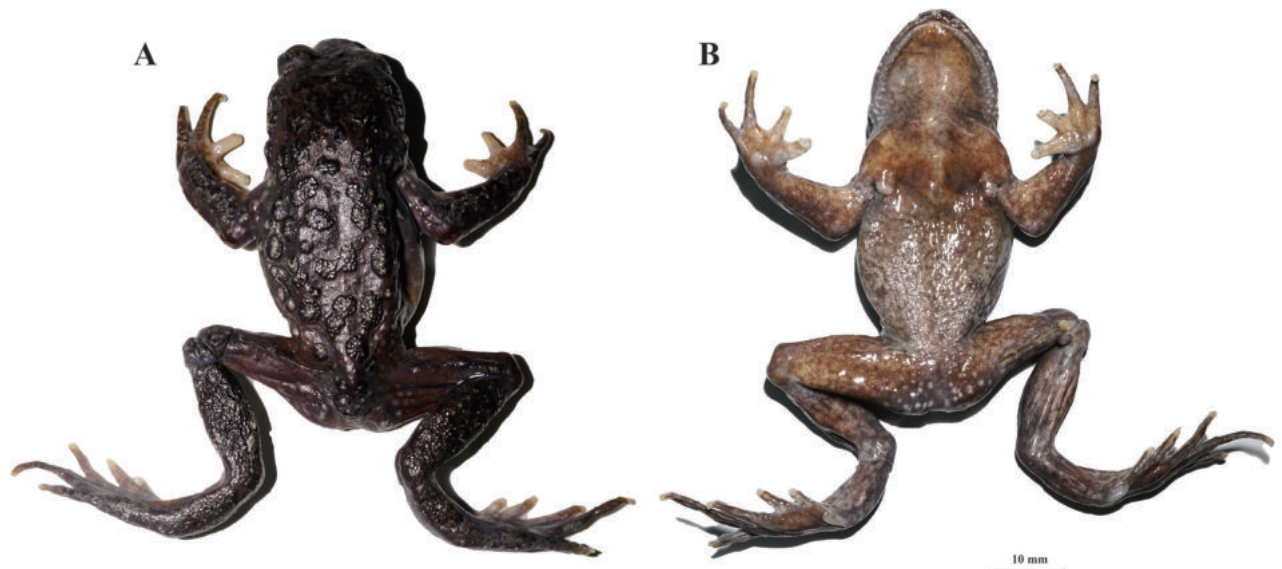


Figure 5. Holotype of *Scutiger luozhaensis* sp. nov. (CIB 119115) in preservative **A** dorsal and **B** ventral body. Photographed by LLS.

Table 4. Morphological measurements (in mm) of adult specimens of *Scutiger luozhaensis* sp. nov.

Characters	Holotype CIB 119115	All males (n = 13)				All females (n = 8)			
		Min	Max	Average	SD	Min	Max	Average	SD
SVL	56.4	47.0	67.2	55.9	4.9	49.8	66.2	59.4	5.5
AG	21.3	17.6	31.7	24.1	3.9	21.4	29.8	27.0	3.5
HL	16.6	15.4	18.6	16.7	0.9	14.4	18.5	17.0	1.5
HW	17.2	16.9	23.1	18.8	1.6	16.4	23.3	20.0	2.6
HH	9.4	6.1	10.3	8.8	1.2	7.3	9.7	8.4	1.0
SL	6.5	6.2	7.9	6.9	0.5	5.8	8.2	7.2	1.0
IND	5.0	4.1	5.7	5.1	0.5	3.8	6.3	5.2	0.8
IOS	4.5	4.1	6.2	4.9	0.5	4.4	7.1	5.2	0.9
UEW	3.8	3.2	5.1	4.0	0.6	3.3	5.3	4.3	0.8
ACED	8.0	6.9	10.5	8.6	0.9	7.0	10.8	9.3	1.4
PCED	13.7	12.5	16.3	14.4	1.1	11.9	17.4	15.4	2.1
ED	5.9	4.4	6.3	5.2	0.6	3.3	6.5	5.4	1.1
SND	3.3	2.6	4.1	3.3	0.5	2.0	4.4	3.3	0.8
END	4.1	2.9	4.3	3.7	0.5	3.3	4.6	4.0	0.5
LAL	14.6	14.1	17.5	15.5	1.2	13.0	16.2	14.8	1.3
LAW	5.6	4.9	6.3	5.6	0.5	3.8	6.6	4.7	0.9
HAL	12.6	12.5	15.1	13.8	1.0	12.9	16.8	14.8	1.3
HLL	78.5	73.3	89.7	80.4	4.5	68.5	84.2	78.0	5.1
THL	21.4	19.7	26.6	22.9	1.8	19.9	25.2	22.3	1.8
TL	21.0	19.6	23.6	21.2	1.2	17.0	21.6	19.8	1.5
TFL	36.0	33.6	39.5	36.3	2.0	31.7	38.4	36.0	2.4
FL	25.0	22.7	27.5	25.4	1.5	22.1	27.9	25.3	2.0
TW	5.9	5.2	6.9	6.0	0.5	4.8	6.4	5.6	0.6
IMTL	4.1	2.4	4.2	3.6	0.7	3.3	5.3	4.1	0.9



Figure 6. Variations of *Scutigiger luozhaensis* sp. nov. **A, B** dorsal and ventral view of an adult male from Lakang Town **C, D** dorsal and ventral view of an adult female from Lakang Town **E** dorsolateral view of an adult female from Lakang Town **F** dorsolateral view of adult female CIB 119120 from Se Town **G, H** dorsolateral and ventral view of juvenile CIB QZ2021115 from Shengge Town. Photographed by SCS.

specimens generally exhibit morphological consistency with the holotype, albeit with some variations. The arrangement and shape of large spiny tubercles on the dorsal surface of body vary among individuals, but all have large longitudinal tubercles; warts and tubercles on dorsum are larger and fewer on some females (Fig. 6C, D), and smaller on juvenile (Fig. 6G). Dorsal coloration varies from olive brown to bronze in adults (Fig. 6A, C, E, F), while darker in some juveniles (Fig. 6G, H). Ventral coloration varies from olive grey to immaculate yellowish (Fig. 6B). Keratinized spines on warts and tubercles did not fade on a male from Lakang Town in early August (Fig. 6A).

Sexual dimorphism. Males are averagely smaller than females, have relatively longer limbs and wider lower arms (Table 4). In adult males, a pair of pectoral glands and a pair of slightly larger axillary glands present on chest, all of them covered by tiny dense black spines in breeding season (Fig. 7). Dorsal surface of first and second fingers, and inner surface of third finger with tiny dense black nuptial spines on adult males in breeding season. Females with a

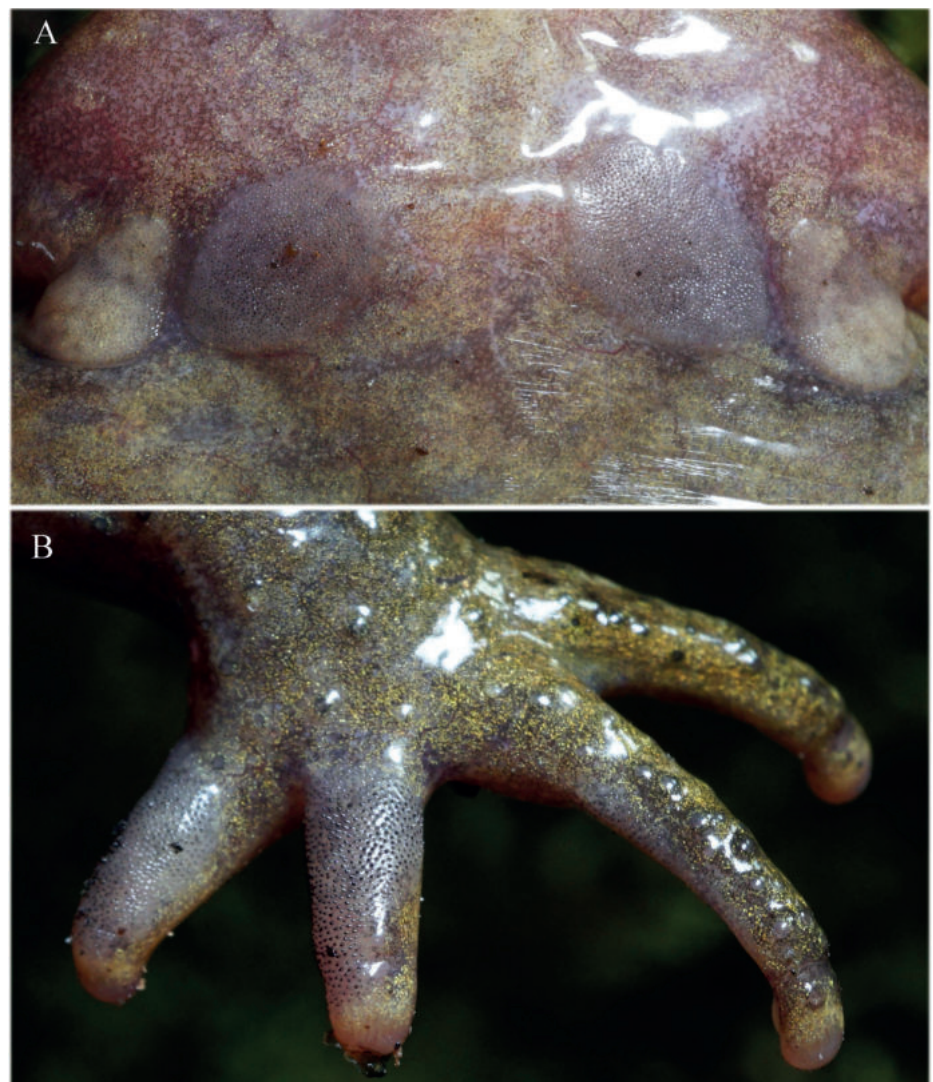


Figure 7. Spine patches and nuptial spines of a male *Scutigera luozhaensis* sp. nov. CIB QZ2021090 from Shengge Town, Luozha County **A** outer smaller axillary spine patches and inner larger pectoral spine patches **B** tiny dense nuptial spines on dorsal surfaces of fingers I, II, and inner surface of finger III. Photographed by SCS.

pair of axillary glands, but no spines covered. No observable lineae masculinae present from ventral view of body in males. Tubercles around cloaca on females (e.g., Fig. 6D) fewer and less distinct compared with those on males. Vocal sac and opening absent in both gender.

Tadpoles. Their description is based on two tadpoles preserved in 75% ethanol at stage 32 (CIB 119630-1) and 29 (CIB 119630-2) from Lakang Town, Luozha County (Fig. 8, Table 5). Identification of the tadpoles was confirmed by DNA analyses. TOL 40.9–50.7 mm, BL 17.7–18.6 mm, tails length average 152% of body; body elliptical in dorsal view, snout rounded; eyes moderate, dorso-laterally positioned; nostril oval, located in the middle of tip of snout and eyes; oral disc ventrally located; papillae on lips well developed, larger on upper labium; tooth row formula I:3+3/3+3:I or I:3+3/2+2:I; spiraculum sinistral, extended as a short tube, spiracular opening oval; tail musculature robust and greatly narrowing to tail tip. Coloration in preservative greyish brown on dorsal view; semitransparent pale grey on ventral view; tail uniformly pale brown without distinct dark spots.

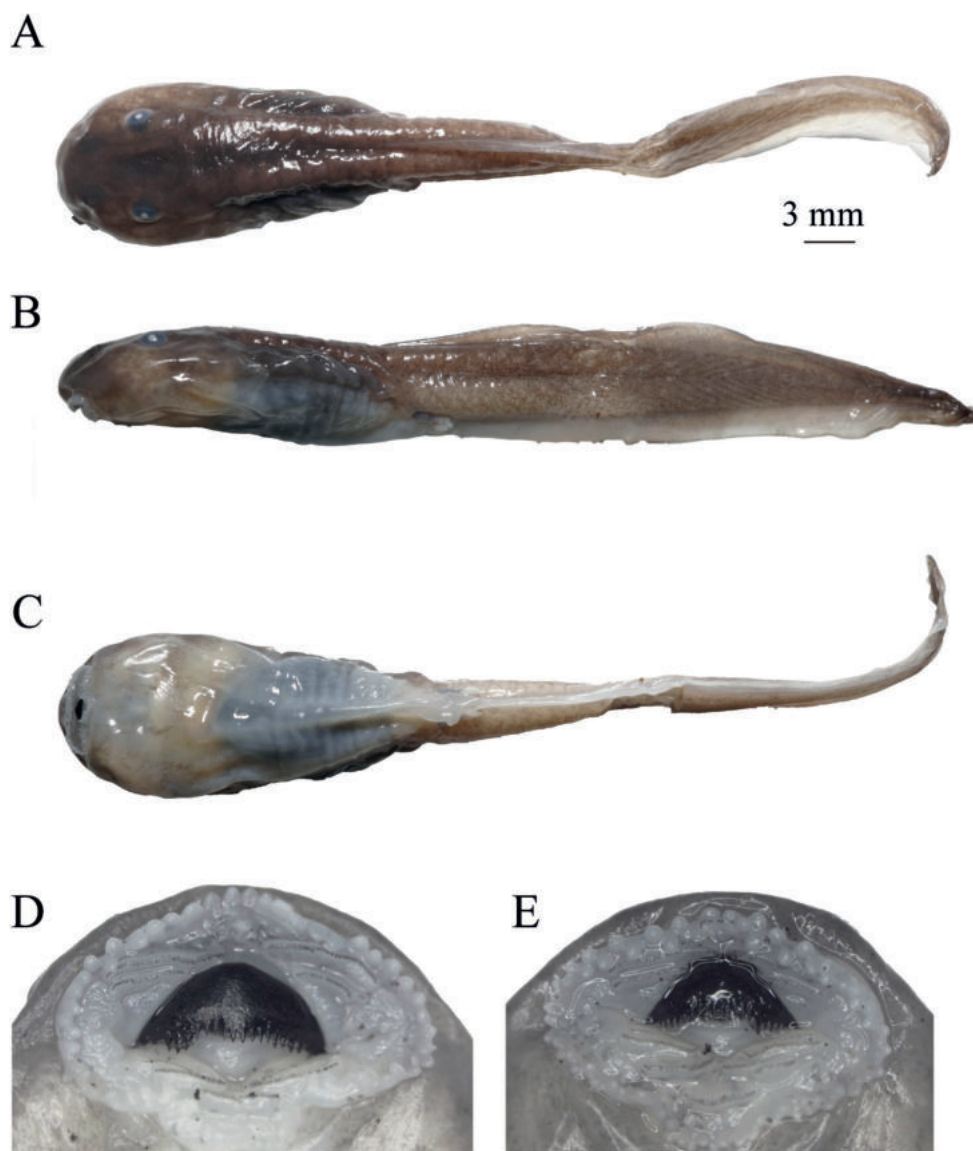


Figure 8. Tadpole of *Scutigera luozhaensis* sp. nov. at Gosner stage 29 from Lakang Town, Luozha County **A** dorsal view **B** lateral view **C** ventral view **D** mouth part of CIB 119630-1 **E** mouth area of CIB 119630-2. Photographed by LLS.

Distribution and ecology. *Scutigera luozhaensis* sp. nov. is currently only known from Luozha county, Shannan Prefecture, Tibet Autonomous Region, China and expected to be found in adjacent areas of Bhutan (Fig. 9). It is a common species in its habitat, which includes mountain streams, moist scrub or forest floors near streams, and ponds of alpine wetlands (Fig. 10). The elevation records of the new species range from 3268 m to 4437 m. Tadpoles at stages 29, 39, and 48 were recorded in a slack head stream from late July to middle August and it is thought that the tadpoles overwinter. No calls were heard in the field from late July to middle August. Spines on nuptial pads and chest of most adult males had faded when found during field work; the breeding season for the species is here recorded to include June. *Nanorana parkeri* (Stejneger, 1927) was found to occur with the new species. Although *S. boulengeri* was also found in Luozha County, it was found near an alpine lake at elevation 4623 m, not sympatrically with *S. luozhaensis* sp. nov., which was found restricted to lower elevation.

Etymology. The specific epithet *luozhaensis* is named after the type locality, Luozha county. We propose the English common name Luozha lazy toad and the Chinese name common name 洛扎齿突蟾 (Luò Zhā chí Tū Chán).

Table 5. Measurements (in mm) of tadpoles of *Scutigera luozhaensis* sp. nov.

Characters	TOL	BL	BH	BW	SNL	SSD	ODW	IOS	TMW	TAL	TMH	HLL
CIB 119630-1	50.70	18.60	5.10	7.80	6.00	9.90	4.50	4.60	3.10	32.10	5.90	2.40
CIB 119630-2	40.90	17.70	4.50	7.00	5.30	8.50	3.90	3.60	3.00	23.30	5.50	1.10
Characters	Stage	LTRF	BW/BH	SSD/BL	TAL/BL	TMW/BH	TMW/TMH	TMW/BW	ODW/BL	ODW/BW		
CIB 119630-1	32	I: 2+2/3+3: I	1.53	0.53	1.73	1.16	1.90	0.40	0.24	0.58		
CIB 119630-2	29	I: 3+3/3+3: I	1.56	0.48	1.32	1.22	1.83	0.43	0.22	0.56		

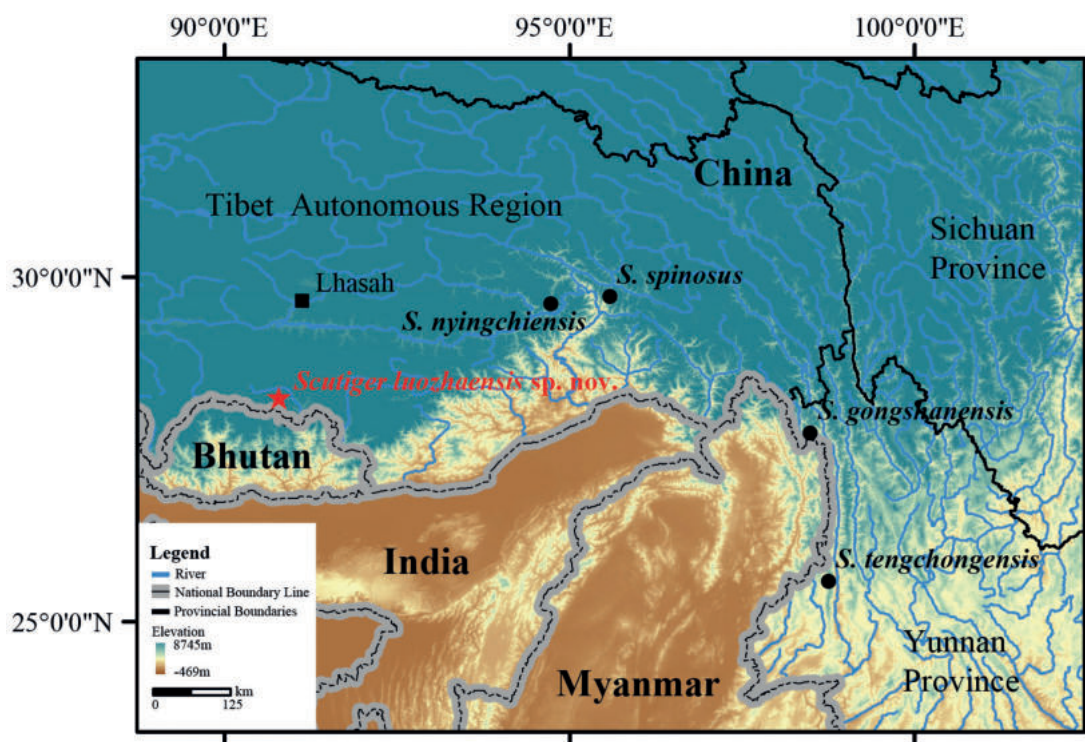


Figure 9. Type localities of *Scutigera luozhaensis* sp. nov. and other species in Clade D.



Figure 10. Habitats of *Scutigera luozhaensis* sp. nov. in Luozha County, Tibet, China **A** Qisehai valley in Lakang Town **B** alpine wetlands in Gari Village, Se Town at elevation 4437 m **C** moist mixed coniferous and broad-leaved in Lajiao Town at elevation 3700 m **D** Pugong stream and the Luozha Canyon in Lakang Town at elevation 3268 m. Photographed by SCS.

Additional specimens examined in this study

Scutigera boulengeri (three adult males): CIB GGS-MGC4-1, CIB GGS-MGC4-9, CIB GGS-MGC4-12 from Kangding, Sichuan, China.

S. ghunsa (two adults): male Holotype NHM-TU-17A-0116 and female paratype NHM-TU-17A-0117 from Ghunsa, Taplejung, Nepal.

S. glandulatus (three adult males): CIB GGS-PBX2-14, CIB GGS-PBX3-1, CIB GGS-GGSX2-1 from Kangding, Sichuan, China.

S. gongshanensis (two adult males): KIZ036221 from Lushui, Nujiang, Yunnan, China; topotype KIZ036222 from Gongshan, Yunnan, China.

- S. mammatus*, (four adult males from near type locality): CIB GGS-SDX1-1, CIB GGS-PBX4-3, CIB GGS-PBX4-4, GGS-PBX4-5 from Kangding, Sichuan, China.
- S. muliensis* (one adult male): topotypic adult male CIB ML20200727-42 from Muli, Sichuan, China.
- S. nyingchiensis* (ten adults): eight males CIB QZ207, CIB QZ398, CIB QZ401, CIB QZ402, CIB QZ403, CIB QZ408, CIB QZ409, CIB QZ410; two females CIB QZ411, CIB QZ407 from Lulang Town, Bayi District, Tibet, China.
- S. wuguanfui* (six adults of type series): five adult males KIZ030101 (holotype), KIZ030103, KIZ030105, KIZ030106, KIZ030104, adult female KIZ030102 from Medog, Tibet, China.

Discussion

Cryptic diversity and puzzles in the genus *Scutigera*

Scutigera species are distributed in high-altitude regions, such as the Tibetan Plateau, the Himalayas, the Tsingling Mountains, and the Hengduan Mountains. The discovery of *Scutigera luozhaensis* sp. nov. provides additional evidence to support the Paleo-Tibetan origin hypothesis by Hofmann et al. (2017). The unique geomorphic features of the Qinghai-Tibetan Plateau, including rapid uplift and mountainous barrier (Ding et al. 2020; Li et al. 2021; Xu et al. 2021; Miao et al. 2022), may have led to high cryptic species diversity of *Scutigera* in the region, multiple species were not discovered until about recent ten years (Jiang et al. 2012; Jiang et al. 2016; Yang and Huang 2019; Rao "2020", 2022). These specific historical processes and genetic patterns have likely contributed to the diverse and intriguing species patterns observed in *Scutigera* (Chen et al. 2009; Che et al. 2020; Lin et al. 2023), necessitating further research. Due to the limited sampling and genetic data, more research is recommended to fully understand the evolutionary history of *Scutigera*. Such as, there are still puzzles about the *S. boulengeri* species complex, which contained three lineages in this research and as Lin et al. (2023) reported. This also raises the problem of the relationship between *S. bangdaensis* and *S. boulengeri*. The former was described based on morphological data of few specimens only, the diagnostic characters were solely based on morphological comparisons with *S. boulengeri* and *S. maculatus* without mention of the localities of specimens of *S. boulengeri* compared (Rao "2020", 2022). However, the samples of *S. boulengeri* from Basu (type locality of *S. bangdaensis*) form part of the W.a clade of Lin et al. (2023) with samples from Zaduo (Upper Yangtze Kiang River, near or at the type locality of *S. boulengeri*, and near Chindu, the locality of neotype *S. boulengeri*) and all other samples from Tibet Autonomous Region (Bedriaga 1898; Fei et al. 2009; Lin et al. 2023). One of the morphological diagnoses "absence of spines on ventral belly" was based on specimens collected in October 2016, those spines might have faded in October after breeding season. Other diagnoses "body length 45–50 mm; head width almost equal head length; large tubercles present on dorsolateral body, light colored, and rounded" could not distinctly differ from those specimens of *S. boulengeri* from Tibet Autonomous Region (Fei et al. 2009; Che et al. 2020; Rao 2022 "2020"). These imply that *S. bangdaensis* is possibly a junior synonym of *S. boulengeri*. Further research based on more specimens and genetical data is recommended to solve the puzzles of *S. boulengeri* species complex.

The invalidity of *Scutigera brevipes* (Liu, 1950)

This species was described based on specimens from Taining Town, Daofu County, Sichuan Province, China (Liu 1950). It was synonymized with *S. glandulatus* (Liu, 1950) by Liu and Hu (1961) for the reason that adults of the former in preservative are difficult to differentiate from those of the latter. However, the name *S. glandulatus* was adopted by some researchers probably because the pages describing *S. brevipes* are anterior to those pages describing *S. glandulatus* (Liu 1950; Ye et al. 1992; Fu et al. 1997; Jiang et al. 2012, 2016; Khatiwada et al. 2019; Yang and Huang 2019; Frost 2023). Fei et al. (2009) discussed that *S. brevipes* should remain as a junior synonym of *S. glandulatus*, because "When the precedence between names or nomenclatural acts cannot be objectively determined, the precedence is fixed by the action of the first author citing in a published work those names or acts and selecting from them..." according to article 24.2.1. of the International Code of Zoological Nomenclature (ICZN 1999). Frost (2023) regards *S. brevipes* as a valid species because Fei et al. (2009) did not address the evidence of Fu et al. (1997). However, Fu et al. (1997) re-analyzed the morphological character data of Ye et al. (1992) but never mentioned the name *S. glandulatus*. Other research treated both *S. glandulatus* and *S. brevipes* as valid species but did not provide evidence supporting both names (Jiang et al. 2012, 2016; Khatiwada et al. 2019; Yang and Huang 2019). Thus, there is no evidence supporting the validity of *S. brevipes*, and *S. brevipes* should be retained as a junior synonym of *S. glandulatus*.

Conservation implications

Although *Scutigera luozhaensis* is a common species in its habitat, its distribution range may be limited to a small area, including the canyon of Luozha County and possibly adjacent Bhutan. The population size and distribution area for the species are still not clear. The conservation status for this species is suggested to be Data Deficient (DD) and further investigations on this species are recommended.

Acknowledgements

Field work was conducted under the permission of the Forestry and Grassland Administration of Tibet Autonomous Region (No. 2021[71]). We thank friends who helped us during field trips in Luozha County during the COVID-19 pandemic, especially Zhen Xiao, Duozha and Mao Weise of the Forestry and Grassland Administration of Luozha County, Zhongchuan Bai of Lakang Town Government and Dazeng Gusang of Lajiao Town. We thank Peng Yan for his help in field work and Ningning Lu and Simeng Du of CIB for help in lab work. We thank Ke Jiang for providing copy of some old references. We especially thank the reviewers and editor who provided careful and helpful suggestions on the manuscript.

Additional information

Conflict of interest

The authors have declared that no competing interests exist.

Ethical statement

No ethical statement was reported.

Funding

This work is funded by the Survey of Wildlife Resources in Key Areas of Tibet (ZL202203601), the Second Tibetan Plateau Scientific Expedition and Research Program (STEP, 2019QZKK05010503), and China Biodiversity Observation Networks (Sino BON-Amphibian & Reptile).

Author contributions

Sheng-Chao Shi: methodology, investigation and resources, data analysis, validation, writing: origination and draft, writing: review and editing; Lu-Lu Sui: laboratory work, methodology, investigation and resources, data analysis, validation, writing: origination and draft, writing: review and editing; Shun Ma: investigation and resources, writing: review and editing; Fei-Rong Ji: investigation and resources, writing: review and editing; A-Yi Bu-Dian: investigation and resources, writing: review and editing; Jian-Ping Jiang: conceptualization, data curation, project administration, resources, supervision, writing: review and editing.

Author ORCIDs

Sheng-Chao Shi  <https://orcid.org/0000-0003-2337-6572>

Lu-Lu Sui  <https://orcid.org/0009-0007-5229-5401>

Shun Ma  <https://orcid.org/0009-0003-8611-4550>

Fei-Rong Ji  <https://orcid.org/0009-0005-6900-0556>

A-Yi Bu-Dian  <https://orcid.org/0009-0004-9375-5724>

Jian-Ping Jiang  <https://orcid.org/0000-0002-1051-7797>

Data availability

All of the data that support the findings of this study are available in the main text or Supplementary Information.

References

- AmphibiaChina (2023) The database of Chinese amphibians. Electronic Database. Kunming Institute of Zoology (CAS), Kunming, Yunnan, China. <http://www.amphibiachina.org> [Accessed on 20 Sept 2023]
- Bedriaga J von (1898) Amphibien und Reptilien. Wissenschaftliche Resultate der von N. M. Przewalski nach Central-Asien unternommenen Reisen, & c./Nauchnuie Rezul'tatui puteshestvii N. M. Przheval'skagho po tzentral'noi Azii, & c. (Vol. 3) Zoologischer Theil, Part 1. Akademie der Wissenschaften, St. Petersburg.
- Che J, Chen HM, Yang JX, Jin JQ, Jiang K, Yuan ZY, Murphy RW, Zhang YP (2012) Universal COI primers for DNA barcoding amphibians. *Molecular Ecology Resources* 12(2): 247–258. <https://doi.org/10.1111/j.1755-0998.2011.03090.x>
- Che J, Jiang K, Yan F, Zhang YP (2020) Amphibians and Reptiles in Tibet: Diversity and Evolution. Science Press, Beijing, 800 pp.
- Chen W, Bi K, Fu JZ (2009) Frequent mitochondrial gene introgression among high elevation Tibetan megophryid frogs revealed by conflicting gene genealogies. *Molecular Ecology* 18(13): 2856–2876. <https://doi.org/10.1111/j.1365-294X.2009.04258.x>
- Chen JM, Zhou WW, Poyarkov Jr NA, Stuart BL, Brown RM, Lathrop A, Wang YY, Yuan ZY, Jiang K, Hou M, Chen HM, Suwannapoom C, Nguyen SN, Duong TV, Papenfuss

- TJ, Murphy RW, Zhang YP, Che J (2017) A novel multilocus phylogenetic estimation reveals unrecognized diversity in Asian horned toads, genus *Megophrys* sensu lato (Anura: Megophryidae). *Molecular Phylogenetics and Evolution* 106: 28–43. <https://doi.org/10.1016/j.ympev.2016.09.004>
- Delorme M, Dubois A (2001) Une nouvelle espèce de *Scutigera* du Bhoutan, et quelques remarques sur la classification subgénérique du genre *Scutigera* (Megophryidae, Lep-tobrachiinae). *Alytes* 19: 141–153.
- Ding WN, Ree RH, Spicer RA, Xing YW (2020) Ancient orogenic and monsoon-driven assembly of the world's richest temperate alpine flora. *Science* 369(6503): 578–581. <https://doi.org/10.1126/science.abb4484>
- Dubois A (1974) Diagnoses de trois espèces nouvelles d'amphibiens du Népal. *Bulletin de la Société Zoologique de France* 98: 495–497.
- Dubois A (1978) Une espèce nouvelle de *Scutigera* Theobald 1868 de l'Himalaya occidental (Anura: Pelobatidae). *Senckenbergiana Biologica* 59: 163–171.
- Dubois A (1979) Une espèce nouvelle de *Scutigera* (Amphibiens, Anoures) du nord de la Birmanie. *Revue Suisse de Zoologie* 86: 631–640. <https://doi.org/10.5962/bhl.part.82326>
- Fei L, Ye CY (2016) *Amphibians of China* (Vol. 1). Science Press, Beijing, 749 pp.
- Fei L, Hu SQ, Ye CY, Huang YZ (2009) *Fauna Sinica. Amphibia* (Vol. 2). Anura. Science Press, Beijing, 957 pp.
- Fei L, Ye CY, Jiang JP (2012) *Colored Atlas of Chinese Amphibians and Their Distributions*. Sichuan Publishing House of Technology and Sciences, Chengdu, 620 pp.
- Feng YJ, Blackburn DC, Liang D, Hillis DM, Wake DB, Cannatella DC, Zhang P (2017) Phylogenomics reveals rapid, simultaneous diversification of three major clades of Gondwanan frogs at the Cretaceous-Paleogene boundary. *Proceedings of the National Academy of Sciences* 114 (29): E5864–E5870. <https://doi.org/10.1073/pnas.1704632114>
- Frost D (2023) *Amphibian species of the world 6.1*, an online reference. American Museum of Natural History, New York. <https://amphibiansoftheworld.amnh.org> [accessed 20 Sept 2023]
- Fu JZ, Lathrop A, Murphy RW (1997) Phylogeny of the genus *Scutigera* (Amphibia: Megophryidae): a re-evaluation. *Asiatic Herpetological Research* 7: 32–37. <https://doi.org/10.5962/bhl.part.18853>
- Fu JZ, Weadick CJ, Bi K (2007) A phylogeny of the high-elevation Tibetan megophryid frogs and evidence for the multiple origins of reversed sexual size dimorphism. *Journal of Zoology* 273: 315–325. <https://doi.org/10.1111/j.1469-7998.2007.00330.x>
- Gosner KL (1960) A simplified table for saging anuran embryos and larvae with notes on identification. *Herpetologica* 16(3): 183–190. <http://www.jstor.org/stable/3890061>
- Guindon S, Dufayard JF, Lefort V, Anisimova M, Hordijk W, Gascuel O (2010) New algorithms and methods to estimate maximum-likelihood phylogenies: Assessing the performance of PhyML 3.0. *Systematic Biology* 59(3): 307–321. <https://doi.org/10.1093/sysbio/syq010>
- Hall TA (1999) Bioedit: A user-friendly biological sequence alignment editor and analysis program for Windows 95/98/ NT. *Nucleic Acids Symposium Series* 41(2): 95–98. <https://doi.org/10.1021/bk-1999-0734.ch008>
- Hofmann S, Stöck M, Zheng YC, Ficetola FG, Li JT, Scheidt U, Schmidt J (2017) Molecular phylogenies indicate a Paleo-Tibetan origin of Himalayan lazy toads (*Scutigera*). *Scientific Reports* 7(1): e3308. <https://doi.org/10.1038/s41598-017-03395-4>
- Hou YM, Shi SC, Hu DM, Deng Y, Jiang JP, Xie F, Wang B (2020) A new species of the toothed toad *Oreolalax* (Anura, Megophryidae) from Sichuan Province, China. *ZooKeys* 929: 93–115. <https://doi.org/10.3897/zookeys.929.49748>

- ICZN (1999) International Code of Zoological Nomenclature. Fourth edition. London. <https://www.iczn.org/the-code/the-code-online/> [accessed 20 Sept 2023]
- Jiang K, Rao DQ, Yuan SQ, Wang JS, Li PP, Hou M, Che MH, Che J (2012) A new species of the genus *Scutigera* (Anura: Megophryidae) from southeastern Tibet, China. *Zootaxa* 3388(1): 29–40. <https://doi.org/10.11646/zootaxa.3388.1.3>
- Jiang K, Wang K, Zou DH, Yan F, Li PP, Che J (2016) A new species of the genus *Scutigera* (Anura: Megophryidae) from Medog of southeastern Tibet, China. *Zoological Research* 37(1): 21–30. <https://doi.org/10.13918/j.issn.2095-8137.2016.1.21>
- Jiang JP, Xie F, Li C, Wang B (2020) Species catalogue of China (Vol. 2). Animals, Vertebrates (IV), Amphibia. Science Press, Beijing, 1052 pp.
- Khatiwada JR, Shu G, Subedi TR, Wang B, Ohler A, Canatella DC, Xie F, Jiang JP (2019) A new species of Megophryid frog of the genus *Scutigera* from Kangchenjunga Conservation Area, Eastern Nepal. *Asian Herpetological Research* 10(3): 139–157. <https://doi.org/10.16373/j.cnki.ahr.180076>
- Kumar S, Stecher G, Li M, Knyaz C, Tamura K (2018) MEGA X: Molecular evolutionary genetics analysis across computing platforms. *Molecular Biology and Evolution* 35(6): 1547–1549. <https://doi.org/10.1093/molbev/msy096>
- Lanfear R, Frandsen PB, Wright AM, Senfeld T, Calcott B (2017) PartitionFinder 2: New methods for selecting partitioned models of evolution for molecular and morphological phylogenetic analyses. *Molecular Biology and Evolution* 34(3): 772–773. <https://doi.org/10.1093/molbev/msw260>
- Li SF, Valdes PJ, Farnsworth A, Davies-Barnard T, Su T, Lunt DJ, Spicer RA, Liu J, Deng WYD, Huang J, Tang H, Ridgwell A, Chen LL, Zhou ZK (2021) Orographic evolution of northern Tibet shaped vegetation and plant diversity in eastern Asia. *Science Advances* 7(5): eabc7741. <https://doi.org/10.1126/sciadv.abc7741>
- Lin XQ, Hou YM, Yang WZ, Shi SC, Zheng PY, Shih CK, Jiang JP, Xie F (2023) A wide hybrid zone mediated by precipitation contributed to confused geographical structure of *Scutigera boulengeri*. *Zoological Research* 44(1): 3–19. <https://doi.org/10.24272/j.issn.2095-8137.2022.108>
- Liu CC (1950) Amphibians of Western China. *Fieldiana: Zoological Memoirs* (Vol. 2). Chicago Natural History Museum, Chicago, 400 pp.
- Liu CC, Hu SQ (1961) The Tailless Amphibians of China. Science Press, Beijing, 364 pp.
- Liu ZY, Chen GL, Zhu TQ, Zeng ZV, Lyu ZT, Wang J, Messenger K, Greenberg AJ, Guo ZX, Yang ZL, Shi SH, Wang YY (2018) Prevalence of cryptic species in morphologically uniform taxa – Fast speciation and evolutionary radiation in Asian frogs. *Molecular Phylogenetics and Evolution* 127: 723–731. <https://doi.org/10.1016/j.ympev.2018.06.020>
- Mauro DS, Gower DJ, Oommen OV, Wilkinson M, Zardoya R (2004) Phylogeny of caecilian amphibians (Gymnophiona) based on complete mitochondrial genomes and nuclear RAG1. *Molecular Phylogenetics and Evolution* 33(2): 413–427. <https://doi.org/10.1016/j.ympev.2004.05.014>
- Miao YF, Fang XM, Sun JM, Xiao WJ, Yang YH, Wang XL, Farnsworth A, Huang KY, Ren YL, Wu FL, Qiao QQ, Zhang WL, Meng QQ, Yan XL, Zheng Z, Song CH, Utescher T (2022) A new biologic paleoaltimetry indicating Late Miocene rapid uplift of northern Tibet Plateau. *Science* 378(6624): 1074–1079. <https://doi.org/10.1126/science.abo2475>
- Minh BQ, Nguyen MAT, Von Haeseler A (2013) Ultrafast approximation for phylogenetic bootstrap. *Molecular Biology and Evolution* 30(5): 1188–1195. <https://doi.org/10.1093/molbev/mst024>

- Nguyen LT, Schmidt HA, Von Haeseler A, Minh BQ (2015) IQ-TREE: A fast and effective stochastic algorithm for estimating maximum-likelihood phylogenies. *Molecular Biology and Evolution* 32(1): 268–274. <https://doi.org/10.1093/molbev/msu300>
- Rao DQ (2022) Atlas of Wildlife in Southwest China: Amphibian. Beijing Publishing Group, Beijing, 443 pp. [Stated as published in 2020 while citing multiple references published in 2021]
- Rao DQ, Wilkinson JA (2007) Phylogenetic relationships of the mustache toads inferred from mtDNA sequences. *Molecular Phylogenetics and Evolution* 46(1): 61–73. <https://doi.org/10.1016/j.ympev.2007.10.005>
- Ronquist F, Teslenko M, Van Der Mark P, Ayres DL, Darling A, Höhna S, Larget B, Liu L, Suchard MA, Huelsenbeck JP (2012) MrBayes 3.2: Efficient Bayesian phylogenetic inference and model choice across a large model space. *Systematic Biology* 61(3): 539–542. <https://doi.org/10.1093/sysbio/sys029>
- Savage JM, Heyer WR (1997) Digital webbing formulae for anurans: A refinement. *Herpetological Review* 28(3): e131.
- Simon C, Frati F, Beckenbach A, Crespi B, Liu H, Flook P (1994) Evolution, weighting, and phylogenetic utility of mitochondrial gene sequences and a compilation of conserved polymerase chain reaction primers. *Annals of the Entomological Society of America* 87(6): 651–701. <https://doi.org/10.1093/aesa/87.6.651>
- Song J, Tian Y, Guan DL (2017) Characterization of the complete mitochondrial genome of an endangered alpine toad, *Scutigera ningshanensis* (Amphibia: Anura: Megophryidae). *Conservation Genetics Resources* 9(1): 35–38. <https://doi.org/10.1007/s12686-016-0611-2>
- Xing C, Lin Y, Zhou Z, Zhao L, Jiang S, Lin Z, Xu J, Zhan X (2023) The establishment of terrestrial vertebrate genetic resource bank and species identification based on DNA barcoding in Wanglang National Nature Reserve. *Biodiversity Science* 31(7): 1–13. <https://doi.org/10.17520/biods.2022661>
- Xu W, Dong WJ, Fu TT, Gao W, Lu CQ, Yan F, Wu YH, Jiang K, Jin JQ, Chen HM, Zhang YP, Hillis DM, Che J (2021) Herpetological phylogeographic analyses support a Miocene focal point of Himalayan uplift and biological diversification. *National Science Review* 8(9): nwaa263. <https://doi.org/10.1093/nsr/nwaa263>
- Yang JH, Huang XY (2019) A new species of *Scutigera* (Anura: Megophryidae) from the Gaoligongshan Mountain Range, China. *Copeia* 107(1): 10–21. <https://doi.org/10.1643/CH-17-661>
- Ye CY, Fei L, Wei G, Xu N (1992) Study on the phylogenetic relationship between species of *Scutigera* genus in Qinghai-Xizang Plateau (Amphibia: Pelobatidae). *Acta Herpetologica Sinica* 1–2: 27–39.
- Zhang D, Gao F, Jakovlić I, Zou H, Zhang J, Li WX, Wang GT (2020) PhyloSuite: An integrated and scalable desktop platform for streamlined molecular sequence data management and evolutionary phylogenetics studies. *Molecular Ecology Resources* 20(1): 348–355. <https://doi.org/10.1111/1755-0998.13096>
- Zhou SB, Guan P, Shi JS (2023) A new species of the genus *Scutigera* from Eastern Qinling Mountains (Anura: Megophryidae). *Dongwuxue Zazhi* 58(5): 641–650. [In Chinese with English abstract]

Supplementary material 1

Pairwise genetic divergence between lineages of *Scutigera* based on 16S rRNA gene

Authors: Sheng-Chao Shi, Lu-Lu Sui, Shun Ma, Fei-Rong Ji, A-Yi Bu-Dian, Jian-Ping Jiang

Data type: xlsx

Copyright notice: This dataset is made available under the Open Database License (<http://opendatacommons.org/licenses/odbl/1.0/>). The Open Database License (ODbL) is a license agreement intended to allow users to freely share, modify, and use this Dataset while maintaining this same freedom for others, provided that the original source and author(s) are credited.

Link: <https://doi.org/10.3897/zookeys.1187.107958.suppl1>

Supplementary material 2

Pairwise genetic divergence between lineages of *Scutigera* based on COI gene

Authors: Sheng-Chao Shi, Lu-Lu Sui, Shun Ma, Fei-Rong Ji, A-Yi Bu-Dian, Jian-Ping Jiang

Data type: xlsx

Copyright notice: This dataset is made available under the Open Database License (<http://opendatacommons.org/licenses/odbl/1.0/>). The Open Database License (ODbL) is a license agreement intended to allow users to freely share, modify, and use this Dataset while maintaining this same freedom for others, provided that the original source and author(s) are credited.

Link: <https://doi.org/10.3897/zookeys.1187.107958.suppl2>

Supplementary material 3

Pairwise genetic divergence between lineages of *Scutigera* based on RAG1 gene

Authors: Sheng-Chao Shi, Lu-Lu Sui, Shun Ma, Fei-Rong Ji, A-Yi Bu-Dian, Jian-Ping Jiang

Data type: xlsx

Copyright notice: This dataset is made available under the Open Database License (<http://opendatacommons.org/licenses/odbl/1.0/>). The Open Database License (ODbL) is a license agreement intended to allow users to freely share, modify, and use this Dataset while maintaining this same freedom for others, provided that the original source and author(s) are credited.

Link: <https://doi.org/10.3897/zookeys.1187.107958.suppl3>

Supplementary material 4

Morphometrics used for one-way ANOVA analysis

Authors: Sheng-Chao Shi, Lu-Lu Sui, Shun Ma, Fei-Rong Ji, A-Yi Bu-Dian, Jian-Ping Jiang

Data type: xlsx

Copyright notice: This dataset is made available under the Open Database License (<http://opendatacommons.org/licenses/odbl/1.0/>). The Open Database License (ODbL) is a license agreement intended to allow users to freely share, modify, and use this Dataset while maintaining this same freedom for others, provided that the original source and author(s) are credited.

Link: <https://doi.org/10.3897/zookeys.1187.107958.suppl4>

Supplementary material 5

Detailed measurements (in mm) for adults of *Scutigera luozhaensis* sp. nov.

Authors: Sheng-Chao Shi, Lu-Lu Sui, Shun Ma, Fei-Rong Ji, A-Yi Bu-Dian, Jian-Ping Jiang

Data type: xlsx

Copyright notice: This dataset is made available under the Open Database License (<http://opendatacommons.org/licenses/odbl/1.0/>). The Open Database License (ODbL) is a license agreement intended to allow users to freely share, modify, and use this Dataset while maintaining this same freedom for others, provided that the original source and author(s) are credited.

Link: <https://doi.org/10.3897/zookeys.1187.107958.suppl5>

Taxonomic review of the *Calotes versicolor* complex (Agamidae, Sauria, Squamata) in China, with description of a new species and subspecies

Yong Huang^{1,5}, Hongyu Li¹, Yilin Wang¹, Maojin Li³, Mian Hou⁴, Bo Cai²

¹ Guangxi University of Chinese Medicine, Nanning 530200, Guangxi, China

² Chengdu Institute of Biology, Chinese Academy of Sciences, Chengdu 610041, Sichuan, China

³ Hainan Forestry Group Co., Ltd, Haikou 570203, Hainan, China

⁴ College of Continuing (Online) Education, Sichuan Normal University, Chengdu 610068, Sichuan, China

⁵ Key Laboratory of Protection and Utilization of Traditional Chinese Medicine and Ethnic Medicine Resources, Education Department of Guangxi Zhuang Autonomous Region, Nanning 530200, Guangxi, China

Corresponding author: Bo Cai (caibo@cib.ac.cn)



Academic editor: Anthony Herrel

Received: 9 August 2023

Accepted: 29 October 2023

Published: 20 December 2023

ZooBank: <https://zoobank.org/398B07C5-375A-4873-B901-A4EB751AF631>

Citation: Huang Y, Li H, Wang Y, Li M, Hou M, Cai B (2023) Taxonomic review of the *Calotes versicolor* complex (Agamidae, Sauria, Squamata) in China, with description of a new species and subspecies. ZooKeys 1187: 63–89. <https://doi.org/10.3897/zookeys.1187.110704>

Copyright: © Yong Huang et al.
This is an open access article distributed under terms of the Creative Commons Attribution License ([Attribution 4.0 International – CC BY 4.0](https://creativecommons.org/licenses/by/4.0/)).

Abstract

Calotes wangi **sp. nov.**, a new species of the agamid genus *Calotes* Cuvier, 1817, from southern China and northern Vietnam, is described. This species can be distinguished from all known congeners by a combination of morphological characteristics and genetic divergence in the mitochondrial tRNA, ND2, and CO1 genes. Molecular phylogenetic analysis revealed that the new species was formed as a monophyletic group and that considerable genetic divergence existed between its congeners (minimum *p*-distance, 4.6%). *Calotes wangi* **sp. nov.** is distinguished by a combination of the following characteristics: average SVL < 90 mm for adult males; 10–14 dorsal eyelid scales; scales on side of neck and adjacent shoulder area pointing obliquely upward; keels on neck scales weakly to strongly developed; fold in front of the shoulder absent; pair of dark triangular patches extending from the front of the shoulder to the jaw angles; and orange coloration of the tongue. *Calotes wangi* **sp. nov.** is similar to *C. irawadi* but differs in having scales between the nasal shield and the orbit and a fourth toe with a claw that can reach between the eyes and tympanum (even to the snout when hind the limbs are adpressed forward). Phylogenetic analyses revealed two well-supported subspecies, Lineages A and B in *C. wangi* **sp. nov.**, with mean uncorrected *p*-distances between them of 2%. We propose that Lineage A, which is mainly from the central and southern Wuzhi Mountains on Hainan Island, is a subspecies, *C. w. hainanensis* **ssp. nov.** Lineage B mainly comprises individuals from other sites on the island plus the adjacent mainland, and is described as subspecies, *C. w. wangi* **ssp. nov.** A diagnostic key to all *Calotes* species of China is also provided.

Key words: *Calotes irawadi*, *Calotes wangi* sp. nov., garden lizard, southern China, taxonomic review

Introduction

The genus *Calotes* Cuvier, 1817, contains at least 29 species throughout the world, but they are distributed primarily in southern and southeastern Asia

(Uetz et al. 2023). Most species of this genus have narrow geographic distributions except *Calotes versicolor* Daudin, 1802, which is mainly found across continental Asia from southeastern Iran in the west to southern China and Indonesia in the east. In China, this species is thought to occur in Yunnan Province, Guangdong Province, Guangxi Zhuang Autonomous Region, Hainan Province, Hunan Province, Fujian Province, Hong Kong, and Macao (Cai et al. 2022a).

Calotes versicolor has a complicated taxonomic history. One of the main causes of this complexity is that the original description was based on coloration data and was not detailed enough to distinguish the species (Daudin 1802). Another complication is that two type specimens of *C. versicolor* in the Muséum National d'Histoire Naturelle, Paris (MNHN) have been lost, leaving this taxon without valid types or a type locality (Wermuth 1967; Amarasinghe et al. 2009; Gowande et al. 2016). Kuhl (1820) claimed Pondicherry as the type locality (*terra typica*) of *C. versicolor*, and this was corroborated by Smith (1935) who stated that it was distributed across the Indian and Indo-Chinese sub-regions including Afghanistan, Ceylon, the Andaman Islands, Pulo Condore (Côn Sơn Island), south China (including Hainan and Hong Kong), and the Malayan peninsula except Sumatra. However, many studies have found that different populations of this species have different morphological characteristics (Smith 1935; Zug et al. 2006; Gowande et al. 2016, 2021), making *C. versicolor* a species complex. It is difficult to study the taxonomy of this species complex in the absence of a valid type specimen and unambiguous type locality.

In 2016, an adult male from Pondicherry was collected and designated as the neotype of *C. versicolor* (NCBS AT102) (Gowande et al. 2016); but it was invalidated by Chaitanya et al. (2017) for several reasons. Gowande et al. (2021) revised *C. versicolor* in the Indian subcontinent, responding to the critique of Chaitanya et al. (2017) and insisting that the neotype of *C. versicolor* and the type locality be restricted to southern and eastern India.

In China, Huang et al. (2013) found that the population of *Calotes versicolor* in south China was different. Liu et al. (2021) reported that the species previously identified as *C. versicolor* from western Yunnan (Dehong Prefecture) was *C. irawadi* Zug, Brown, Schulte & Vindum, 2006. Other populations of *C. versicolor* in China have yet to be clarified.

From 2009 to 2022, we conducted a series of field surveys in south China and collected 323 specimens of this species complex from Fujian Province, Guangdong Province, Guangxi Zhuang Autonomous Region, Hainan Province, Hong Kong, and Yunnan Province in China, and also examined specimens collected from Fujian Province, Guangdong Province, Guangxi Zhuang Autonomous Region, Hainan Province, Hong Kong, and Yunnan Province in China, and from Myanmar and Vietnam. Based on molecular phylogenetic analyses and morphological comparisons, we believe that these specimens include one new undescribed species and two subspecies, which are described herein.

Materials and methods

Sampling

Fieldwork was carried out around Yunnan Province, Guangdong Province, Fujian Province, and Hainan provinces and Guangxi Zhuang Autonomous Region (Fig. 1, Table 1) from 2009 to 2022 by members of our team, and 323 specimens were

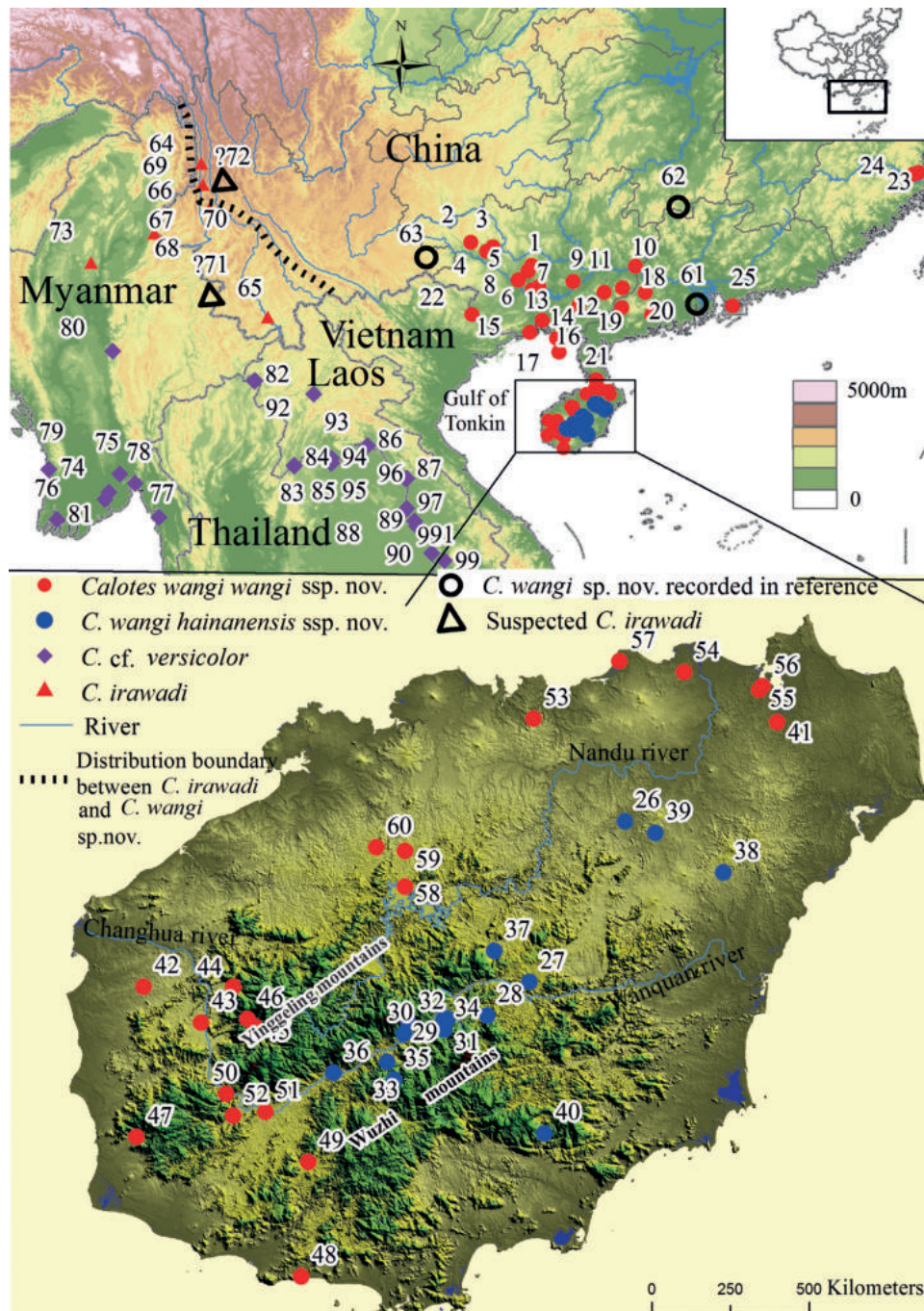


Figure 1. Map [GS(2020)4619] showing representative localities for *Calotes wangi* sp. nov. and morphologically similar species. Color codes: solid red circles *C. w. wangi* ssp. nov., hollow black circles *C. w. wangi*, solid blue circles *C. w. hainanensis* ssp. nov., solid red triangles *C. irawadi*, hollow black triangles suspected *C. irawadi*, solid purple squares *C. cf. versicolor*. Samples are numbered following Table 1 and Suppl. material 1: table S1.

collected. Then we took photographs of live animals and measured them. Muscle tissue samples were taken, fixed, and stored at $-20\text{ }^{\circ}\text{C}$ in absolute ethanol. The type specimens were fixed in 10% formalin, stored in 75% ethanol, and deposited in the herpetological collections of the Chengdu Institute of Biology, Chinese Academy of Sciences (CIB). The specimens were deposited at the CIB, Guangxi University of Chinese Medicine (GXUCM), Kunming Natural History Museum of Zoology, Kunming Institute of Zoology, Chinese Academy of Sciences (KIZ).

Table 1. Voucher specimens and GenBank accession numbers of DNA sequences of *Calotes wangi* sp. nov. used in this study. More species information covered in figure 1 can be found in Suppl. material 1: table S1.

ID	Species	Subspecies	Locality (Abbreviation)	Voucher number	GenBank number	Population number	GPS Coordinates (Latitude, Longitude)	References
1	<i>Calotes wangi</i> sp. nov.	<i>C. w. wangi</i> ssp. nov.	Mt. Daming, Guangxi, China (DM)	2022091533~2022091541	OR828811~OR828819	9	23.548581, 108.353307	This study
2	<i>C. wangi</i> sp. nov.	<i>C. w. wangi</i> ssp. nov.	Taohua, Guangxi, China (TH)	201606139~201606142	OR828796~OR828798	3	24.212539, 106.611948	This study
3	<i>C. wangi</i> sp. nov.	<i>C. w. wangi</i> ssp. nov.	Bama, Guangxi, China (BM)	201606144~201606148	OR828799~OR828803	5	24.09138, 107.250248	This study
4	<i>C. wangi</i> sp. nov.	<i>C. w. wangi</i> ssp. nov.	Naheng, Guangxi, China (NH)	201606143	OR828804	1	23.953857, 107.065068	This study
5	<i>C. wangi</i> sp. nov.	<i>C. w. wangi</i> ssp. nov.	Fucheng, Guangxi, China (FC)	201604082~201604087	OR828805~OR828810	6	23.391183, 108.247992	This study
6	<i>C. wangi</i> sp. nov.	<i>C. w. wangi</i> ssp. nov.	Nanning, Guangxi, China (NN)	HC201002279~HC201002281	KC87576, KC875761, KC875763	3	22.86, 108.37	Huang et al. 2013
7	<i>C. wangi</i> sp. nov.	<i>C. w. wangi</i> ssp. nov.	Wutang, Guangxi, China (WT)	201511048~201511050, 201511052	OR828820~OR828823	4	22.945312, 108.555563	This study
8	<i>C. wangi</i> sp. nov.	<i>C. w. wangi</i> ssp. nov.	Dingdang, Guangxi, China (DD)	201604088~201604102	OR828824~OR828838	15	23.13039, 107.976043	This study
9	<i>C. wangi</i> sp. nov.	<i>C. w. wangi</i> ssp. nov.	Gangbei, Guangxi, China (GB)	201606104~201606108	OR828839~OR828843	5	23.093115, 109.540017	This study
10	<i>C. wangi</i> sp. nov.	<i>C. w. wangi</i> ssp. nov.	Wuzhou, Guangxi, China (WZ)	201606134~201606137	OR828844~OR828847	4	23.526721, 111.329018	This study
11	<i>C. wangi</i> sp. nov.	<i>C. w. wangi</i> ssp. nov.	Cenxi, Guangxi, China (CX)	201606130~201606132	OR828848~OR828850	3	22.914898, 110.958258	This study
12	<i>C. wangi</i> sp. nov.	<i>C. w. wangi</i> ssp. nov.	Rongxi, Guangxi, China (RX)	201606115~201606119	OR828851~OR828855	5	22.784373, 110.43628	This study
13	<i>C. wangi</i> sp. nov.	<i>C. w. wangi</i> ssp. nov.	Qinmanqu, Guangxi, China (QN)	201510030~201510033, 201510035	OR828856~OR828860	5	21.980953, 108.653817	This study
14	<i>C. wangi</i> sp. nov.	<i>C. w. wangi</i> ssp. nov.	Wenming, Guangxi, China (WM)	201512053, 201512056	OR828861~OR828862	2	22.4119, 109.6998	This study
15	<i>C. wangi</i> sp. nov.	<i>C. w. wangi</i> ssp. nov.	Fangchenggang, Guangxi, China (FCG)	201510039~201510044, 201510047	OR828863~OR828869	7	21.635534, 108.301372	This study
16	<i>C. wangi</i> sp. nov.	<i>C. w. wangi</i> ssp. nov.	Yin Haiqu, Guangxi, China (YH)	201509019~201509020, 201509022~201509025	OR828870~OR828875	6	21.468197, 109.078404	This study
17	<i>C. wangi</i> sp. nov.	<i>C. w. wangi</i> ssp. nov.	Weizhou Dao, Guangxi, China (WZD)	201509003~201509007, 201509009, 201509011, 201509012, 201509014~201509017, 201509027, 201509028	OR822208~OR822221	14	21.066718, 109.139317	This study
18	<i>C. wangi</i> sp. nov.	<i>C. w. wangi</i> ssp. nov.	Fuchao, Guangdong, China (FCC)	201606125~201606129	OR828876~OR828879	4	22.781087, 111.608735	This study
19	<i>C. wangi</i> sp. nov.	<i>C. w. wangi</i> ssp. nov.	Xinyi, Guangdong, China (XY)	201606120~201606123	OR828880~OR828883	4	22.339085, 110.937615	This study
20	<i>C. wangi</i> sp. nov.	<i>C. w. wangi</i> ssp. nov.	Yangchun, Guangdong, China (YC)	201606109~201606114	OR828884~OR828889	6	22.141142, 111.78446	This study
21	<i>C. wangi</i> sp. nov.	<i>C. w. wangi</i> ssp. nov.	Haian, Guangdong, China (HA)	HC200908192~HC200908199, HCL200908276	KC875759, KC875749~KC875756	9	20.28, 110.21	Huang et al. 2013
22	<i>C. wangi</i> sp. nov.	<i>C. w. wangi</i> ssp. nov.	Lang Son, Vietnam (LS)	HC201006282~HC201006288	KC875765~KC875777	7	22.15, 106.65	Huang et al. 2013
23	<i>C. wangi</i> sp. nov.	<i>C. w. wangi</i> ssp. nov.	Lianjiang, Fujian, China (LJ)	/	/		26.2189, 119.4314	Hu et al. 2022
24	<i>C. wangi</i> sp. nov.	<i>C. w. wangi</i> ssp. nov.	Jin'an, Fujian, China (JA)	2022091526~2022091527	OR878647~OR878648	2	26.175443, 119.296059	This study
25	<i>C. wangi</i> sp. nov.	<i>C. w. wangi</i> ssp. nov.	Hongkong, China (HK)	HC201006295	KC875772	1	22.4, 114.11	Huang et al. 2013
26	<i>C. wangi</i> sp. nov.	<i>C. w. hainanensis</i> ssp. nov.	Tunchang, Hainan, China (TC)	HCL200907005~HCL200907007	KC875611~KC875613	3	19.58298, 110.17577	Huang et al. 2013
27	<i>C. wangi</i> sp. nov.	<i>C. w. hainanensis</i> ssp. nov.	Wanning, Hainan, China (WL)	HCL200907047~HCL200907052	KC875614~KC875619	6	19.13316, 109.90797	Huang et al. 2013
28	<i>C. wangi</i> sp. nov.	<i>C. w. hainanensis</i> ssp. nov.	Jiachai, Hainan, China (JC)	HCL200907053~HCL200907054	KC875620~KC875621	2	19.04, 109.79	Huang et al. 2013
29	<i>C. wangi</i> sp. nov.	<i>C. w. hainanensis</i> ssp. nov.	Hongmao, Hainan, China (HM)	HCL200907055, HCL200908071	KC875622, KC875638	2	19.03, 109.68	Huang et al. 2013
30	<i>C. wangi</i> sp. nov.	<i>C. w. hainanensis</i> ssp. nov.	Chonggongbao, Hainan, China (CG)	HCL200908056~HCL200908061	KC875623~KC875628	6	18.9886, 109.55716	Huang et al. 2013
31	<i>C. wangi</i> sp. nov.	<i>C. w. hainanensis</i> ssp. nov.	Fanxiang, Hainan, China (FX)	HCL200908062~HCL200908068	KC875629~KC875635	7	19.03, 109.67	Huang et al. 2013

ID	Species	Subspecies	Locality (Abbreviation)	Voucher number	GenBank number	Population number	GPS Coordinates (Latitude, Longitude)	References
32	<i>C. wangi</i> sp. nov.	<i>C. w. hainanensis</i> ssp. nov.	Zayun, Hainan, China (SY)	HCL200908069	KC875636	1	19.02, 109.57	Huang et al. 2013
33	<i>C. wangi</i> sp. nov.	<i>C. w. hainanensis</i> ssp. nov.	Maoyang, Hainan, China (MY)	HCL200908070	KC875637	1	18.91, 109.51	Huang et al. 2013
34	<i>C. wangi</i> sp. nov.	<i>C. w. hainanensis</i> ssp. nov.	Hela, Hainan, China (HL)	HCL200908072~HCL200908075	KC875639~KC875642	4	19, 109.67	Huang et al. 2013
35	<i>C. wangi</i> sp. nov.	<i>C. w. hainanensis</i> ssp. nov.	Hongshan, Hainan, China (HS)	HCL200908076~HCL200908082	KC875643~KC875649	7	18.86, 109.53	Huang et al. 2013
36	<i>C. wangi</i> sp. nov.	<i>C. w. hainanensis</i> ssp. nov.	Fanyang, Hainan, China (FY)	HCL200908083~HCL200908089	KC875650~KC875656	7	18.88, 109.36	Huang et al. 2013
37	<i>C. wangi</i> sp. nov.	<i>C. w. hainanensis</i> ssp. nov.	Limushan, Hainan, China (LMS)	HCL200908168~HCL200908172	KC875731~KC875735	5	19.22, 109.81	Huang et al. 2013
38	<i>C. wangi</i> sp. nov.	<i>C. w. hainanensis</i> ssp. nov.	Huangzhu, Hainan, China (HZ)	HCL200908181~HCL200908184	KC875741~KC875744	4	19.44, 110.45	Huang et al. 2013
39	<i>C. wangi</i> sp. nov.	<i>C. w. hainanensis</i> ssp. nov.	Fuwen, Hainan, China (FW)	CIB091425~CIB091426	KC875778, KC875777	2	19.55, 110.26	Huang et al. 2013
40	<i>C. wangi</i> sp. nov.	<i>C. w. hainanensis</i> ssp. nov.	Lingshui, Hainan, China (LS)	CIB091435~CIB091452	KC875787~KC875804	18	18.71, 109.95	Huang et al. 2013
41	<i>C. wangi</i> sp. nov.	<i>C. w. wangi</i> ssp. nov.	Wenchang, Hainan, China (WC)	HC200907002	KC875610	1	19.86, 110.6	Huang et al. 2013
42	<i>C. wangi</i> sp. nov.	<i>C. w. wangi</i> ssp. nov.	Datian, Hainan, China (DT)	HCL200908091~HCL200908092, HCL200908094~HCL200908098	KC875657~KC875663	7	19.12, 108.83	Huang et al. 2013
43	<i>C. wangi</i> sp. nov.	<i>C. w. wangi</i> ssp. nov.	Donghe, Hainan, China (DH)	HCL200908099~HCL200908104	KC875664~KC875669	6	19.02, 108.99	Huang et al. 2013
44	<i>C. wangi</i> sp. nov.	<i>C. w. wangi</i> ssp. nov.	Wanting, Hainan, China (WT)	HCL200908105~HCL200908109	KC875670~KC875674	5	19.12, 109.08	Huang et al. 2013
45	<i>C. wangi</i> sp. nov.	<i>C. w. wangi</i> ssp. nov.	Sanpai, Hainan, China (SP)	HCL200908110~HCL200908121, HCL200908200, HC200908278	KC875675~KC875760	13	19.01, 109.14	Huang et al. 2013
46	<i>C. wangi</i> sp. nov.	<i>C. w. wangi</i> ssp. nov.	Bawangling, Hainan, China (BWL)	HCL200908122~HCL200908127	KC875687~KC87569	6	19.03, 109.12	Huang et al. 2013
47	<i>C. wangi</i> sp. nov.	<i>C. w. wangi</i> ssp. nov.	Jianfeng, Hainan, China (JF)	HCL200908128~HCL200908134	KC875693~KC875699	7	18.7, 108.81	Huang et al. 2013
48	<i>C. wangi</i> sp. nov.	<i>C. w. wangi</i> ssp. nov.	Tianya, Hainan, China (TY)	HCL200908136~HCL200908139, HCL200908141~HCL200908146, HCL200908275	KC875758, KC875708~KC875709, KC8757095~KC8757097, KC8757092, KC875700~KC875704	11	18.31, 109.27	Huang et al. 2013
49	<i>C. wangi</i> sp. nov.	<i>C. w. wangi</i> ssp. nov.	Zhizhong, Hainan, China (ZZ)	HCL200908147~HCL200908153	KC875710~KC875716	7	18.63, 109.29	Huang et al. 2013
50	<i>C. wangi</i> sp. nov.	<i>C. w. wangi</i> ssp. nov.	Jiangbian, Hainan, China (JB)	HCL200908154~HCL200908155	KC875717~KC875718	2	18.82, 109.06	Huang et al. 2013
51	<i>C. wangi</i> sp. nov.	<i>C. w. wangi</i> ssp. nov.	Yongming, Hainan, China (YM)	HCL200908156~HCL200908159	KC875719~KC875722	4	18.77, 109.17	Huang et al. 2013
52	<i>C. wangi</i> sp. nov.	<i>C. w. wangi</i> ssp. nov.	Zhiwei, Hainan, China (ZW)	HCL200908160~HCL200908167	KC875723~KC875730	8	18.76, 109.08	Huang et al. 2013
53	<i>C. wangi</i> sp. nov.	<i>C. w. wangi</i> ssp. nov.	Fushan, Hainan, China (FS)	HCL200908173~HCL200908178	KC875736~KC875740	5	19.87, 109.92	Huang et al. 2013
54	<i>C. wangi</i> sp. nov.	<i>C. w. wangi</i> ssp. nov.	Haikou, Hainan, China (HK)	HC200907001, HCL200908185~HCL200908191	KC875745~KC875748, KC875609	5	20, 110.34	Huang et al. 2013
55	<i>C. wangi</i> sp. nov.	<i>C. w. wangi</i> ssp. nov.	Yanfeng 1, Hainan, China (YF1)	CIB091420	KC875773	1	19.95, 110.55	Huang et al. 2013
56	<i>C. wangi</i> sp. nov.	<i>C. w. wangi</i> ssp. nov.	Yanfeng 2, Hainan, China (YF2)	CIB091421, CIB091423	KC875774~KC875775	2	19.96, 110.56	Huang et al. 2013
57	<i>C. wangi</i> sp. nov.	<i>C. w. wangi</i> ssp. nov.	Changliu, Hainan, China (CL)	CIB091424	KC875776	1	20.03, 110.16	Huang et al. 2013
58	<i>C. wangi</i> sp. nov.	<i>C. w. wangi</i> ssp. nov.	Nanfeng, Hainan, China (NF)	CIB091427~CIB091433	KC875779~KC875785	7	19.4, 109.56	Huang et al. 2013
59	<i>C. wangi</i> sp. nov.	<i>C. w. wangi</i> ssp. nov.	Nada 1, Hainan, China (ND1)	CIB091434	KC875786	1	19.5, 109.56	Huang et al. 2013
60	<i>C. wangi</i> sp. nov.	<i>C. w. wangi</i> ssp. nov.	Nada 2, Hainan, China (ND2)	CIB091453~CIB091468	KC875805~KC875820	16	19.51, 109.48	Huang et al. 2013
61	<i>C. wangi</i> sp. nov.	<i>C. w. wangi</i> ssp. nov.	Macao, China (MC)	/	/	/	22.158855, 113.577999	This study
62	<i>C. wangi</i> sp. nov.	<i>C. w. wangi</i> ssp. nov.	Yizhang, Hunan, China (YZ)	/	/	/	24.942264, 112.93057	Deng and Ye 1996, 1997
63	<i>C. wangi</i> sp. nov.	<i>C. w. wangi</i> ssp. nov.	Funing, Yunnan, China (FN)	/	/	/	23.484035, 105.793296	Yang and Rao 2008
64	<i>C. irawadi</i>		Mt. Gaoligong, Yunnan, China (GLG)	HC201006290~HC201006291	/	2	26.42, 98.9	Huang et al. 2013
65	<i>C. irawadi</i>		Xishuangbanna, Yunnan, China (XSBN)	HC201006292	/	1	22.01, 100.8	Huang et al. 2013

Morphological characteristics

Measurements were taken as suggested by Zhao et al. (1999) and Zug et al. (2006): head length (**HeadL**) as distance from the posterior edge of the jaw to the tip of the snout; head height (**HeadH**) measured as the dorsoventral distance from the top of the head to the underside of the jaw at the transverse plane intersecting the angle of the jaws; head width (**HeadW**) measured between the widest points of the temporal or jaw muscles without compression of soft tissue; eye-to-ear length (**EyeEar**), the distance from the anterior edge of the tympanum to the posterior part of the orbit (not the pupil opening); eye diameter (**EyeDiam**), measured between the anterior and posterior edges of the orbital bone; naris-to-eye length (**NarEye**), the distance from the anterior edge of the orbit to the posterior edge of the naris; the snout-eye length (**SnEye**), measured between the tip of the snout and the anterior edge of the orbital bone; interorbital width (**Interorb**), the transverse distance between the anterodorsal corners of the left and right orbits; jaw width (**JawW**), the distance from the left to right outer edges of the jaw angles (excluding broadening of the jaw musculature); snout-to-forelimb length (**SnForeL**), the distance from the anterior part of the forelimb, or shoulder, to the tip of the snout; snout-to-vent length (**SVL**), from the tip of the snout to the anterior edge of the cloaca; trunk length (**TrunkL**), the distance between the posterior edge of the forelimb insertion (axilla) to the anterior edge of the hind limb insertion (inguen); tail length (**Tail**), measured from the anterior edge of the cloaca to the tip of tail; forelimb length (**FLL**), the distance between the point of insertion (axilla) to the tip of finger IV (excluding claw), measured with the limb straight; hind limb length (**HLL**), the distance between the point of insertion at the groin to the tip of toe IV (excluding claw), measured with the limb straight; toe IV length (**4ToeLng**), distance from the tip of toe IV to the base between toe III and IV (excluding claw); finger IV length (**4FingLng**), distance from the tip of finger IV to the base between toe III and IV (excluding claw); upper arm length (**UparmL**), distance from the anterior insertion of the forelimb, or shoulder, to the elbow; lower arm length (**LoArmL**), distance from the elbow to the distal end of the wrist, or just before the underside of the fore-foot; upper leg length (**UpLegL**), distance from the anterior edge of the hind limb insertion to the knee; crus length (**CrusL**), length of tibia from knee to heel; and, snout width (**SnW**), transverse distance between left and right nares. All measurements were recorded to the nearest 1 mm using a steel ruler for SVL and tail, and to the nearest 0.1 mm using a digital caliper for shorter measurements.

Definitions of morphological characters and the counting methods also mainly followed Zug et al. (2006), Gowande et al. (2021), and Cai et al. (2022b): supralabial scale count (**Suplab**), number of enlarged, modified labial scales from the rostral area to the corner of the mouth; infralabial scale count (**Inflab**), number of enlarged, modified labial scales from the mental area to the corner of the mouth; nasal-supralabials scale rows (**NSL**), number of horizontal rows of small scales between the first supralabial and the nasal; suborbital scale rows (**SoR**), number of longitudinal rows of scales between supralabials and inferior-most edge of orbit circle, excluding fine ciliary scales in the orbit; ventral scale count (**VN**), number of ventral body scales counted in a straight line along the medial axis between the transverse gular fold and the anterior edge

of cloaca; finger IV subdigital lamellae count (**4FingLm**), number of subdigital lamellar scales from the base between fingers III and IV to the tip of finger IV, excluding the claw; toe IV subdigital lamellae count (**4ToeLm**), number of subdigital lamellar scales from the base between toes III and IV to the tip of toe IV, excluding the claw; post-tympanic scale count (**PtY**), number of enlarged, distinctively-keeled, raised conical, or sub-pyramidal scales posterior to the tympana and superior to the rictus; post-occipital scale count (**PoS**), number of enlarged, distinctively-keeled, raised conical, or sub-pyramidal scales on the occipital region of the head; dorsal scales or spines (**Dorsal**), number of mid-dorsal scales or spines, beginning with the first enlarged spine-like scale on the nape to above the vent; mid-body scale rows (**Mid-bodyS**), number of scale rows around trunk at mid-body; dorsal eyelid scales (**Eyelid**), number of scales along dorsal edge of eyelid; state of scales on side of neck and adjacent shoulder area (**SSneck**), horizontal or pointing obliquely upward; state of keels on scales of the neck and adjacent shoulder area (**Ksneck**), modestly to strongly developed or weakly to strongly developed; nuchal crest state (**NuchalCrest**), nuchal crest scales slightly or significantly larger than dorsal crest scales; trunk scales state (**TrunkSc**), smaller or larger than or equal in size to ventral scales; dorsal crest scales state (**DorsalCrests**), long or short, positioned extending backwards; state of nuchal crest scales (**NuchalCrests**), long or short, compared with the size of the dorsal crest scales; state of supratympanic spines (**SpinesS**), length in proportion to the tympanic chamber diameter; scales between the nasal shield and the orbit (**NarEyeS**), scales of the loreal region in a single row between the nasal shield and the orbit; hind limbs reach the orbit or tympanic membrane when addressed forward (**HAF**); parallel rows of compressed scales above tympanum (**ParallelR**), present or absent; postorbital spine (**PostorbitalS**), present or absent; state of the keels on scales of the lateral trunk (**Kstrunk**), pointing obliquely upward or downward; crescent-shaped patch of granular scales in front of forelimb insertion (**GranularS**), present or absent; gular scale count (**GU**), number of gular scales counted in a straight line along medial axis between and excluding mental and transverse gular fold; gular pouch (**GP**), present or absent; fold in front of shoulder (FS), present or absent; gular fold (**GF**), present or absent.

Coloration descriptions used terminology and codes from RGB (red, green, blue) color scale (Ibraheem et al. 2012; Cai et al. 2022b). Data on coloration and ornamentation were also collected from live specimens, and included the following (Gowande et al. 2021; Cai et al. 2022b): radial stripes below eyes (**RSBE**), present or absent; inner-lip coloration (**ILC**); coloration of the oral cavity (**CO**), defined as the background color of the anterior roof and sides of the mouth, excluding the posterior palate and deep throat; coloration of the tongue (**CTG**), defined as the color of the tongue; dark bands on trunk (**TrnkBand**), number of dark bands (bars) on dorsum of trunk between axilla and inguen, excluding bands over shoulder or pelvis; fore- and hindlimb cross-bands (**LimbBand**); tail cross-bands (**TailBand**); ventral trunk striping (**TrunkSt**), striping ventrally on trunk, none (0), irregular or broken striping (1), or continuous striping (2), excluding midline; dorsal bars mid-dorsal state (**DorsalBar**) broad or narrow, offset on opposite sides of dorsal crest or congruent on opposite sides of dorsal crest; paired nuchal spots (**NucSpot**), shape of paired nuchal spots in front of forelimbs; adult male coloration during breeding season (**Malecolor**).

Since the new species, *Calotes wangi* sp. nov., is geographically and phylogenetically close to *C. irawadi*, enhanced morphometric data of the two species was gathered for statistical analyses. We ln-transformed all trait measurements to normalize and then removed allometric effects of body size for each trait measurement/SVL. Principal component analysis (PCA) was used to distinguish the new species from *C. irawadi* and the dimensionality of morphological characteristics measurements was reduced using SPSS22. Due to sexual dimorphism in *C. versicolor* (Wei et al., 2018), we carried out PCA in both males and females.

DNA extraction and sequencing

DNA was extracted from muscle tissues using a kit (DP304, Tiangen Biotech Co., Ltd). A mitochondrial DNA fragment spanning the tRNA_{Trp}, ND2 (L3705:5'-ATTAGGGTCTGCTACACAAGC AGTTGG-3', H5162:5'-GGTTGARAG-TARTCATCGAGTTAAGAACGAC-3'), and COI (L5037:5'-GAGTAGACCCAGGAAC-CRAAGTTC-3', H6448:5'-GTATACCGGCTAATCCAAGCATGT G-3') was amplified using the primer pairs of Huang et al. (2013).

The polymerase chain reaction (PCR) was carried out in a 25 µL reaction volume containing 1 µL of template DNA (1 ng/µL), 1 µL of each primer (1 µmol each), 2.5 µL of 10×Takara Ex Taq buffer (Mg²⁺Plus), 2 µL dNTPs (2.5 µmol/L each), 0.2 µL of Takara Ex Taq DNA polymerase (5 U/µL), with the volume made up using sterile distilled water. The PCR conditions were initial denaturation step at 95 °C for 4 min, 35 cycles of denaturation at 94 °C for 35 s, annealing at 65 °C for 45 s, extension at 72 °C for 1 min, and final extension at 72 °C for 10 min. PCR products were sequenced using the amplification primers. The sequences were deposited in GenBank (OR822208–OR822221, OR828796–OR828889, OR878647–OR878648). We also obtained sequences of *C. emma* Gray, 1845, *C. liolepis* Boulenger, 1885, and *C. irawadi* from GenBank. We used *Agama agama* (Linnaeus, 1758) as outgroup. Detailed information on these materials is shown in Table 1, Suppl. material 1: table S1, and Fig. 1.

Phylogenetic analyses

The new sequences and all homologous DNA sequences of *Calotes* available in GenBank (Table 1) were aligned by BioEdit 5.0.9 (Hall 1999). We constructed phylogenetic trees using neighbor-joining (NJ), maximum likelihood (ML) and Bayesian inference (BI) methods, respectively. The NJ tree was generated by Mega X (Kumar et al. 2018) with the bootstrap consensus tree inferred from 1000 replicates. Maximum likelihood trees were created using the IQ-TREE web server with 1000 bootstrap alignments (Nguyen et al. 2015; Trifinopoulos et al. 2016). The substitution model was selected using the model selection tool of IQ-TREE. BI was performed using MrBayes 3.2 (Ronquist et al. 2012). We partitioned the data by codon (tRNA, ND2, and COI) and selected the best-fit model of evolution for each partition using the jModelTest (Posada 2008) based on the BI criterion. The best-fitting nucleotide substitution models were HKY+G, TIM2+I+G and TPM3uf+G for tRNA, ND2 and COI, respectively. The random tree used as the starting tree included two independent runs with four Markov chain Monte Carlo simulations (three hot chains and one cold chain), which were repeated for ten million iterations and sampled every 1000 iterations. The initial 25% of

samples were discarded as burn-in to build a consistent tree. An uncorrected *p*-distance was determined in Mega X using the default settings (Kumar et al. 2018). We also constructed phylogenetic trees between new sequences in this study and the sequences of neotypes of *C. versicolor* (Gowande et al. 2021) and other *Calotes* species by the NJ, ML, and BI methods using only the COI gene.

Results

Phylogenetic results

A total of 2663 bp of mitochondrial DNA, spanning tRNA_{Trp}, ND2, and COI was studied. NJ, ML and BI analyses showed essentially similar topologies (Fig. 2). The tree result indicated that populations, which were collected from Fujian Province, Guangdong Province, Hainan Province and Guangxi Zhuang Autonomous Region, China and Lang Son, Vietnam, originally assigned to a potential new species formed a monophyletic group with well-supported values (NJ, ML bootstrap values > 90, BI posterior probabilities > 0.9) and a sister taxon with *Calotes cf. versicolor* as mentioned in Zug et al. (2006). The tree result was also

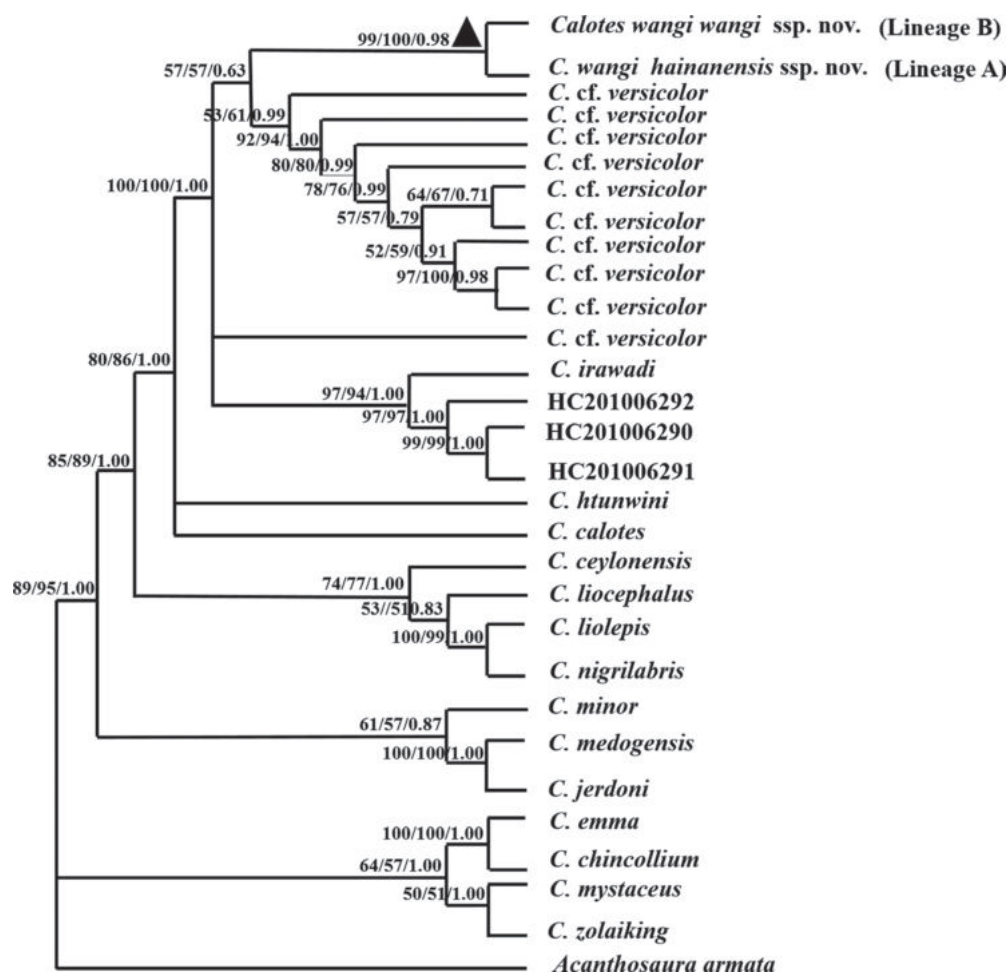


Figure 2. The phylogeny tree of *Calotes wangi* sp. nov. using tRNA_{Trp}, ND2, and COI based on neighbor-joining (NJ), maximum likelihood (ML) and Bayesian inference (BI) methods, respectively. The values displayed above the nodes are the NJ, ML, and BI support rates, respectively. *Calotes cf. versicolor* is from Zug et al. (2006). More structural information of phylogenetic trees can be found in Suppl. material 1: fig. S1.

consistent with the phylogenetic relationship from previous studies with two well separated operational taxonomic units (OTU ; Lineage A and Lineage B) as reported in Huang et al. (2013). Lineage A is represented by specimens from the central and southern Wuzhi Mountains on Hainan Island, while the other OTU (Lineage B) contains all samples from other sites on Hainan Island and the adjacent Chinese mainland, which form two clearly distinct monophyletic lineages and represent subspecies of this potential species (Fig. 2).

Mean uncorrected *p*-distances between and within species of *Calotes* included in this study are given in Table 2. The *p*-distances between the new species *C. wangi* sp. nov. and *C. cf. versicolor*, and 14 of the 22 known *Calotes* species, ranged from 4.6 to 26.8%. The intraspecies genetic distance of *C. wangi* sp. nov. was 1.1%. The *p*-distance between Lineage A and Lineage B was 2%. The intraspecies genetic distance of Lineage A and Lineage B was 0.5% and 0.3%, respectively.

Based on the COI gene (1257 bp) alone, we combined our data and that of Hartmann et al. (2013), Gowande et al. (2021) and Tantrawatpan et al. (2021) to construct a phylogenetic tree by the NJ, ML, and BI methods, respectively. The trees also revealed that our samples of *C. wangi* sp. nov. formed a monophyletic clade with the existence of two deeply divergent OTUs (Lineage A and Lineage B), which were strongly supported (NJ, ML bootstrap values > 90, BI posterior probabilities > 0.9; Fig. 3). The *p*-distances between *C. wangi* sp. nov. and *C. cf. versicolor*, and the other *Calotes* species ranged from 4.4 to 21.5%. The intraspecies genetic distance of *C. wangi* sp. nov. was 1.3%. The *p*-distance between Lineage A and Lineage B was 2% (Table 3), and the intraspecies genetic distance of Lineage A and Lineage B was 0.5% and 0.3%, respectively.

Table 2. Uncorrected *p*-distances of mitochondrial DNA (tRNA_{Trp}, ND2, and COI, 2663 bp) among these new lineages (new species) and other species in the genus *Calotes*.

	<i>C. emma</i>	<i>C. irawadi</i>	<i>C. liolepis</i>	<i>C. minor</i>	<i>C. nigilabris</i>	<i>C. mystaceus</i>	<i>C. cmedogensis</i>	<i>C. liocephalus</i>	<i>C. jerdoni</i>	<i>C. htunwini</i>	<i>C. chincollium</i>	<i>C. ceylonensis</i>	<i>C. calotes</i>	<i>C. zolaiking</i>	<i>C. cf. versicolor</i>	<i>C. wangi</i> sp. nov.
<i>Calotes emma</i>	*															
<i>C. irawadi</i>	0.231	*														
<i>C. liolepis</i>	0.246	0.196	*													
<i>C. minor</i>	0.223	0.186	0.204	*												
<i>C. nigilabris</i>	0.224	0.170	0.118	0.193	*											
<i>C. mystaceus</i>	0.223	0.246	0.226	0.220	0.223	*										
<i>C. cmedogensis</i>	0.235	0.197	0.212	0.185	0.218	0.247	*									
<i>C. liocephalus</i>	0.227	0.185	0.181	0.195	0.163	0.226	0.204	*								
<i>C. jerdoni</i>	0.238	0.194	0.222	0.178	0.218	0.251	0.135	0.196	*							
<i>C. htunwini</i>	0.231	0.164	0.209	0.209	0.179	0.232	0.213	0.188	0.220	*						
<i>C. chincollium</i>	0.022	0.228	0.237	0.220	0.222	0.210	0.236	0.221	0.236	0.227	*					
<i>C. ceylonensis</i>	0.231	0.181	0.190	0.219	0.162	0.244	0.215	0.177	0.207	0.197	0.232	*				
<i>C. calotes</i>	0.224	0.147	0.169	0.183	0.150	0.223	0.195	0.161	0.184	0.148	0.222	0.174	*			
<i>C. zolaiking</i>	0.255	0.261	0.252	0.245	0.259	0.241	0.250	0.249	0.234	0.268	0.250	0.265	0.234	*		
<i>C. cf. versicolor</i>	0.226	0.057	0.193	0.186	0.179	0.242	0.195	0.187	0.190	0.163	0.222	0.184	0.137	0.254	*	
<i>C. wangi</i> sp. nov.	0.228	0.056	0.192	0.185	0.179	0.245	0.203	0.184	0.195	0.164	0.226	0.181	0.142	0.255	0.046	*

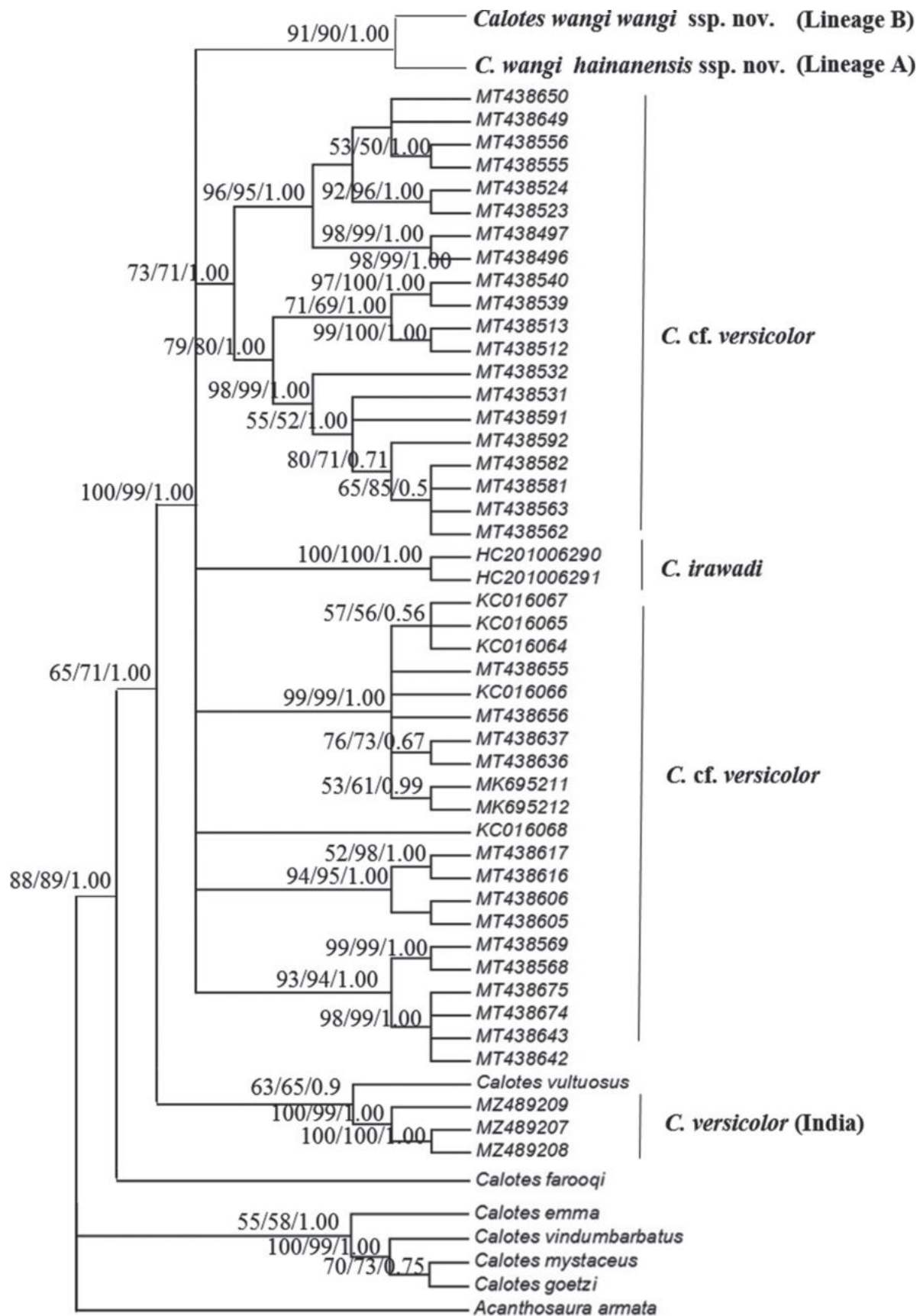


Figure 3. The phylogeny tree of *Calotes wangi* sp. nov. using only COI based on neighbor-joining (NJ), maximum likelihood (ML), and Bayesian inference (BI) methods, respectively. Numbers at the terminals of the branches correspond to the voucher numbers in Table 1. The values displayed above the nodes are the NJ, ML, and BI support rates, respectively.

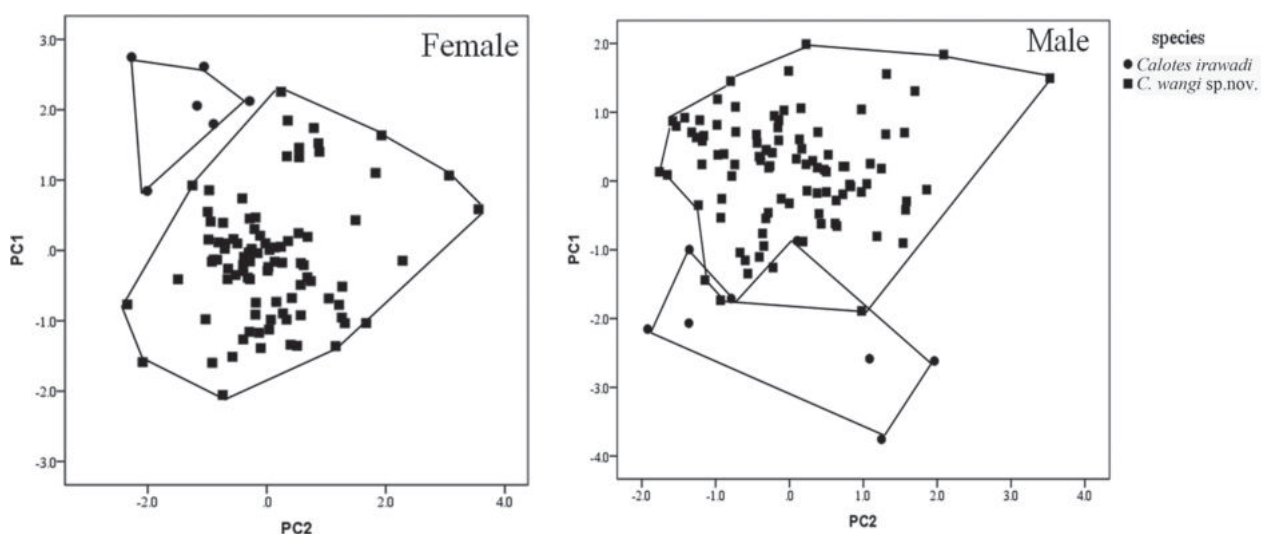
Table 3. Uncorrected *p*-distances of mitochondrial DNA (COI,1257 bp) among these new lineages (new species) and other species in the genus *Calotes*.

	<i>C. emma</i>	<i>C. mystaceus</i>	<i>C. farooqi</i>	<i>C. vindumbarbatus</i>	<i>C. vultuosus</i>	<i>C. goetzi</i>	<i>C. versicolor</i>	<i>C. cf. versicolor</i>
<i>Calotes emma</i>	*							
<i>C. mystaceus</i>	0.154	*						
<i>C. farooqi</i>	0.200	0.179	*					
<i>C. vindumbarbatus</i>	0.165	0.054	0.188	*				
<i>C. vultuosus</i>	0.215	0.192	0.169	0.188	*			
<i>C. goetzi</i>	0.167	0.048	0.179	0.077	0.196	*		
<i>C. versicolor</i>	0.190	0.188	0.171	0.188	0.134	0.189	*	
<i>C. cf. versicolor</i>	0.200	0.181	0.175	0.184	0.152	0.182	0.139	*
<i>C. wangi</i> sp. nov.	0.199	0.177	0.174	0.177	0.151	0.182	0.144	0.044

Morphological results

Based on the morphological data and compared with known species or populations in the *Calotes versicolor* complex, *C. wangi* sp. nov. from southern China (except western Yunnan) distinctly differed from the neotype of *C. versicolor* (India) and other *Calotes* species, showing some unique characteristics. The average adult male had SVL < 90 mm, a smaller HeadH/SVL, a larger HindLimbL/SVL, 4ToeLng/SVL and 4FingLng/SVL, NarEyeS < 6; scales on side of trunk, neck and adjacent shoulder area pointing obliquely upward; paired nuchal spots present and extending below the last infralabial scales; the fourth toe with claw can stretch between the eyes and tympanum, and even to the snout when the hind limbs are adpressed forward. Combined with phylogenetic and morphological differences, we conclude that the specimens from southern China (except for western Yunnan) represent a distinct species and subspecies that are described as follows.

In the PCA results (Fig. 4), the extracted components PC1, PC2, and PC3 accounted for 45.9%, 27.8%, 15.7% for males, and 46.5%, 30.4%, 16.5% for males, respectively. The scatter plots of PC1 and PC2 showed that samples of the new species *C. wangi* sp. nov. and *C. irawadi* were clustered separately and had almost no overlap with each other.

**Figure 4.** Scatter plots of PC1 and PC2 of principal component analysis (PCA) based on morphometric measurements, distinguishing *Calotes wangi* sp. nov. from *C. irawadi*.

Systematics

Calotes wangi sp. nov.

<https://zoobank.org/FE6F8314-08C6-47F5-AA6D-E97E45D0E765>

Figs 5, 6, Table 4

Calotes versicolor: Smith 1935: 189–193 in S. China and Hainan; Zhao and Adler 1993: 189 excluding W. Yunnan; Deng and Ye 1996, 1997; Zhao et al. 1999: 97–110 excluding W. Yunnan; Liu 2000; Cai et al. 2015 excluding W. Yunnan; Ge et al. 2018; Wang et al. 2021 excluding W. Yunnan; Cai et al. 2022a excluding W. Yunnan; Hu et al. 2022.

Type material. Holotype. Adult male, CIB119358 (filed number GXUCM-H202291534). Collected from Daming Montains, Wuming District, Nanning City, Guangxi Zhuang Autonomous Region, China (23.52654°N, 108.342559°E, 326 m a. s. l.) by Yong Huang in September 2022.

Allotype. Adult female, CIB119359 (filed number GXUCM-H202291533), with the same locality and collector information as the holotype.

Paratypes. Adult males (GXUCM-H201604082-4, H201604086-87, GXUCM-H2022091535-36) and adult females (GXUCM-H201604085, H2022091538), with the same locality and collector information as the holotype.

Other examined specimens. CHINA, 1. Guangdong Province, Xuwen (1♂), Yangchun (3♂, 2♀), Luoding (2♂, 3♀), Xinyi (3♂, 2♀). **2.** Guangxi Zhuang Autonomous Region, Bama (3♂, 2♀), Yin Hai (1♂, 2♀), Weizhou island (13♂, 6♀), Cenxi (3♂, 1♀), Gangkou (1♂, 2♀), Shiwandashan (1♂), Guigang (13♂, 6♀), Lingyun (1♂, 3♀), Longzhou (1♀), Longan (3♂, 3♀), Xingning (1♂, 2♀), Pingxiang (1♂), Qinnan (5♂, 5♀), Rong County (3♂, 2♀), Shanglin (3♂), Tiandeng (1♂, 3♀), Tianyang (1♂), Wanxiu- (1♂, 3♀). **3.** Hainan Province, Changjiang (4♂, 11♀), Chengmai (2♂), Ding'an (1♀), Dongfang (7♂, 5♀), Haikou (2♀), Ledong (6♂, 11♀), Sanya (4♂, 4♀), Tunchang (1♂), Qiongzong (8♂, 5♀), Wuzhishan (4♂, 7♀). **4.** Fujian Province, Jin'an (2 subadults). **5.** Hong Kong Special Administrative Region (1 subadult). **VIETNAM:** Lang Son Province (1♂, 1♀).

Description of holotype. Adult male, medium-sized body, SVL 96.40 mm, trunk length 49.82 mm, head length 24.29 mm, head depth 13.18 mm, head width 15.42 mm, interorbital width 9.47 mm, snout width 5.87 mm, eye-ear length 5.97 mm, eye diameter 8.56 mm, naris-eye length 4.58 mm, jaw width 16.14 mm, snout-eye length 8.82 mm, snout-forelimb length 32.65 mm, tail length 256.15 mm, finger IV length 14.10 mm, toe IV length 19.04 mm, upper arm length 15.80 mm, lower arm length 14.34 mm, upper leg length 21.94 mm, crus length 16.87 mm, forelimb length 46.03 mm, hind limb length 73.17 mm, when hind limbs adpressed forward to reach between eyes and tympanum.

Supralabial scale count 10:11, infralabial scale count 10:11, nasal-supralabial scale rows 1:1, suborbital scale rows 3:3, gular scale count 30, ventral scale count 48, finger IV subdigital lamellae count 20:21, toe IV subdigital lamellae count 25:25, post-tympanic scale count 3:3, post-occipital scale count 3:2, vertebral scales 42, mid-body scale rows 42, dorsal eyelid scales 13:13, scales between anterior chin-shield 1, scales between nasal shield and orbit 5:5, state of scales on side of neck and adjacent shoulder area pointing obliquely upward, keels on these scales are weakly to strongly developed, nuchal and dorsal crest



Figure 5. Photographs of live specimens and their habitats **A** holotype of *Calotes wangi* GXUCM-H202291534 **B** holotype of *C. w. hainanensis* CIB095629 **C** allotype of *C. wangi* GXUCM-H202291533 **D** allotype of *C. w. hainanensis* CIB095630 **E, F** habitats **G** oral cavity view.

scales short, nuchal crest scales significantly larger than dorsal crest scales, dorsal crest shortens progressively before mid-body, gular fold and fold in front of the shoulder are absent, moderate to large scales in front of forelimb insertion, postorbital spine absent, scales on side of trunk point obliquely upward.

Under stress, the color is khaki (240,230,140) or dark khaki (189,183,107) with pale gray (105,105,105) markings, three black (0,0,0) transverse stripes on top of head, nine blank radial stripes around eyes, throat coloration burly wood (222,184,135) with blank throat stripes, inner-lip coloration is white-smoke (245,245,245), oral cavity coloration is pale flesh (239, 205, 197), tongue coloration is orange (255,165,0), ventral body coloration tan (210,180,140) with dark stripes, presence of dark line on vent midline from throat to pelvis, seven dark kha-



Figure 6. **A** holotype of *Calotes wangi* GXUCM-H202291534, A1, A2, A3 **B** allotype of *C. wangi* GXUCM-H202291533, B1, B2, B3 **C** holotype of *C. w. hainanensis* CIB095629, C1, C2, C3. 1, dorsal view; 2, ventral view, 3; Dorsolateral view.

ki bands on dorsum of trunk between axilla and inguen, 7–8 dark khaki fore- and hindlimb cross-bands, striping ventrally on trunk continuous striping, 22 tail cross-bands (the front 9 bands are black and the rear 13 bands are brown [165, 42, 42]).

Etymology. The species name *wangi* is named after Prof. Yuezhao Wang, a former director of the Amphibian and Reptile Research Laboratory (CIB, CAS) and Museum of Herpetology (CIB, CAS) for his research on Chinese herpetology and his contributions in leading the Amphibian and Reptile Research Laboratory through many difficulties. We suggest the English common name Wang’s garden lizard and the Chinese name 中国树蜥 (zhōng guó shù xī).

***Calotes wangi hainanensis* ssp. nov.**

<https://zoobank.org/E7BCDAA5-6A38-4DE4-A44F-62406C7F1F91>

Fig. 4, Table 4

Calotes versicolor Shi et al. 2011 in part; Huang et al. 2013 in part.

Type material. Holotype. Adult male, CIB095629 (filed number HCL200908058). Collected from Chonggongbao Village, Zayun Town, Qiongzong County, Hainan Province, China (18.9886°N, 109.55716°E, elevation 439 m) by Yong Huang and Bo Cai in August 2009.

Allotype. Adult female, CIB095630 (filed number HCL200908059), with the same locality and collector information as the holotype.

Other material examined. Hainan Province, CHINA: **1.** Qiongzong, Wanling Town (2♂, 1♀), Hongmao Town (1♂, 1♀), Zayun Town (1♂), Hongmao Town (3♂, 1♀), Limushan Town (1♀). **2.** Wuzhishan, Hongshan Town (3♂, 2♀), Fanyang Town (5♀). **3.** Dingan, Donghong (1♀). **4.** Ledong, Yongming (1♀). **5.** Tunchang, Dalupo (1♀).

Description of holotype. Adult male, medium-sized body, SVL 88.34 mm. Trunk length 43.82 mm, head length 24.47 mm, head depth 14.41 mm, head width 16.08 mm, interorbital width 8.51 mm, snout width 5.29 mm, eye-ear length 6.30 mm, eye diameter 7.66 mm, naris-eye length 4.49 mm, jaw width

Table 4. Morphological data of holotypes and allotypes of *Calotes wangi* sp. nov. Morphometric measurements are in units of mm. For measurement and count methods and abbreviations, see the materials and methods.

Subspecies	<i>Calotes wangi wangi</i> ssp. nov.	<i>C. w. wangi</i> ssp. nov.	<i>C. w. hainanensis</i> ssp. nov.	<i>C. w. hainanensis</i> ssp. nov.
Locality	Mt. Daming, Guangxi, China	Mt. Daming, Guangxi, China	Zayun, Hainan, China	Zayun, Hainan, China
specimen type	holotype	allotype	holotype	allotype
Voucher NO.	H2022091534	H2022091533	CIB095629	CIB095630
Sex	♂	♀	♂	♀
Suplab	10:11	9:9	10:10	10:10
Inflab	10:11	9:9	11:11	11:12
NSL	1:1	1:1	1:1	1:1
SoR	3:3	4:4	3:3	4:4
GU	30	27	21	24
VN	48	49	46	50
4FingLm	20:21	21:22	22:22	20:20
4ToeLm	25:25	25:26	27:27	25:26
PtY	3:3	1:1	1:1	1:1
PoS	3:2	2:1	2:2	2:1
DorsalS	42	44	38	43
MidbodyS	42	43	38	37
Eyelid	13:13	12:12	13:13	14:14
SSneck	obliquely upward	obliquely upward	obliquely upward	obliquely upward
Ksneck	modestly to strongly developed	modestly to strongly developed	modestly to strongly developed	modestly to strongly developed
NuchalCrest	significantly larger	significantly larger	significantly larger	significantly larger
DorsalCrests	short, before midbody	short, before midbody	short, before midbody	short, before midbody
SpinesS	1/2	1/3	1/2	1/3
NarEyeS	5	5	5	5
HAF	between eyes and tympanum	between eyes and tympanum	between eyes and tympanum	between eyes and tympanum
TrunkSc	bigger	bigger	bigger	bigger
ParallelR	absence	absence	absence	absence
PostorbitalS	absence	absence	absence	absence
Kstrunk	obliquely upward	obliquely upward	obliquely upward	obliquely upward
GranularS	absent	absent	absent	absent
GP	absent	absent	absent	absent
FS	absent	absent	absent	absent
GF	absent	absent	week present	absent
RSBE	present	present	present	present
TrnkBand	7	7	6	6
LimbBand	7~8	7~8	6~7	7~8
TailBand	22	25	24	23
TrunkSt	2	2	2	2
DorsalBar	absent	week present	absent	week present
HeadL	24.29	23.93	24.47	23.39
HeadH	13.18	13.52	14.41	12.42
HeadW	15.42	14.78	16.08	14.21
Interorb	9.47	10.24	8.51	12.42
EyeEar	5.97	6.17	6.3	5.06
EyeDiam	8.56	7.88	7.66	5.02
JawW	16.14	16.84	16.06	13.47
NarEye	4.58	4.96	4.49	5.69
SnEye	8.82	7.91	7.85	9
SnForeL	32.65	30.4	30.74	25.99

Subspecies	<i>Calotes wangi wangi</i> ssp. nov.	<i>C. w. wangi</i> ssp. nov.	<i>C. w. hainanensis</i> ssp. nov.	<i>C. w. hainanensis</i> ssp. nov.
SnW	5.87	5.76	5.29	5.33
SVL	96.4	96.5	88.34	82
TrunkL	49.82	47.02	43.82	40.81
Tail	256.15	243.5	283.89	329
FLL	46.03	41.5	44.82	38.26
HLL	73.17	64.63	71.77	57.97
4FingLng	14.1	13.68	13.41	9.82
4ToeLng	19.04	17.97	21.57	15.36
UparmL	15.8	15.35	16.64	16.36
LoArmL	14.34	15.11	13.59	13.6
UpLegL	21.94	20.76	23.01	17.27
CrusL	16.87	18.08	20.26	17.38

16.06 mm, snout-eye length 7.85 mm, snout-forelimb length 30.74 mm, tail length 283.89 mm, toe IV length 21.57 mm, finger IV length 13.41 mm, upper arm length 16.64 mm, lower arm length 13.59 mm, upper leg length 23.01 mm, Crus length 20.26 mm, forelimb length 44.82 mm, hindlimb length 71.77 mm, when hind limbs are addressed forward to reach between eyes and tympanum.

Supralabial scale count 10:10, infralabial scale count 11:11, nasal-supralabial scale rows 1:1, suborbital scale rows 3:3, gular scale count 21, ventral scale count 46, finger IV subdigital lamellae count 22:22, toe IV subdigital lamellae count 27:27, post-tympanic scale count 1:1, post-occipital scale count 2:2, vertebral scales 38, mid-body scale rows 38, dorsal eyelid scales 13:13, no scales between anterior chin-shield, scales between nasal shield and orbit 5:5, state of scales on side of neck and adjacent shoulder area pointing obliquely upward, keels on these scales are weakly to strongly developed, nuchal and dorsal crest scales short, nuchal crest scales significantly larger than dorsal crest scales, dorsal crest shortening progressively before mid-body, gular fold and fold in front of the shoulder absent, no patch of granular scales in front of forelimb insertion, pre-axillary area with moderate to large scales, postorbital spine absent, scales on side of trunk pointing obliquely upward.

In ethanol, color is dark khaki or khaki with black or pale gray (105, 105, 105) markings. Tan and black mixed marking on top of head, nine brown (165, 42, 42) radial stripes around eyes, throat coloration burly wood with blank throat stripes, inner lip, oral cavity and tongue coloration is smoky white, ventral body is tan with dark stripes, presence of blank line on vent midline from throat to pelvis, six dark-khaki bands on dorsum of trunk between axilla and inguen, Seven to eight dark-khaki cross-bands on the fore- and hindlimbs, continuous ventral striping on trunk, and 22 cross-bands on tail (anterior nine bands are black, posterior 13 are brown).

Etymology. The specific epithet of *hainanensis* refers to Hainan Island where the new subspecies was discovered. We suggest the English common name Hainan garden lizard and the Chinese name 中国树蜥雷公马亚种 (*zhōng guó shù xī léi gōng mǎ yà zhǒng*), which comes from a colloquial name for *Calotes wangi hainanensis* in Hainan Province, China, meaning Thor's mount that can predict the weather.

Coloration in life. This species is prone to color changes with different colors during the breeding season and as a result of stress. During the breeding season, adult males are uniformly dark orange (255, 140, 0) to orange on the

front half (except for the fingers), with black patches on each side of the neck, darker longitudinal stripes on the chin and darker radial stripes around the eyes. The hind body and toes are uniformly khaki or dark khaki. The dark patches on the sides of the neck are approximately triangular and do not meet, extending from the front of the shoulder to the jaw angles. In the non-breeding season, animals are dark khaki or khaki with black markings.

The coloration of adult females is a relatively pale, uniform khaki over almost the entire body with dark horizontal stripes on a khaki background, and a pale yellow (255, 255, 224) or yellow (255, 255, 0) continuous or discontinuous longitudinal stripe on each side of the trunk in most individuals. They also have black or dark khaki radial stripes around the eyes and dark longitudinal stripes on the chin. Like the females, juveniles are a uniform khaki color over almost the entire body, with dark horizontal stripes and a pair of pale-yellow dorsolateral stripes. Under stress, the coloration of most individuals quickly changes to dark khaki with pale gray markings.

Variations. The means for the measurements of morphological characters are DorsalS 39–52 (average 44.7), Mid-bodyS 36–46 (average 41.2, 2/167 specimen is 35), Eyelid 10–14 (average 12.4, 1/167 specimen is 9 or 15), Nar-EyeS 4–5 (average 4.9, 6/167 specimen is 6), 4ToeLm 22–27 (average 24.25, 4/167 specimen is 20, 5/167 specimen is 21 and 1/167 specimen is 30), HAF between the eyes and snout (6/167 specimen tympanum), FS absent (5/167 specimen present), SVL 66.14–109.1 mm (average 84.9 mm, 6/187 specimens longer than 100 mm). HAF between the eyes and tympanum (6/167 reaching tympanum, 21/167 reaching eye); FS absent (5/167 present). The ranges for each of these characters are given in Table 5.

Calotes wangi wangi ssp. nov. can be separated from *C. w. hainanensis* ssp. nov. by the following characters: **1.** Eyelid 10–13 (average 12.4, few 9 and 15) vs 13–14 (average 13, few 12). **2.** Tail/SVL 1.59–3.36 (average 2.83) vs 1.77–4.01 (average 3.15). **3.** Male, UpLegL/SVL 0.11–0.26 (average 0.23) vs 0.23–0.32 (average 0.25). **4.** Male, CrusL/SVL 0.09–0.24 (average 0.21) vs 0.21–0.3 (average 0.24).

Diagnosis. *Calotes wangi* sp. nov. can be separated from all other species of *Calotes* by having the following characters: **1.** Medium-sized adult male, SVL < 90 mm (66.86–109.1 mm, average 85.64 mm). **2.** Smaller HeadW in males, 11.64–19.72 (average 14.84). **3.** Larger HindLimbL/SVL 0.64–0.89 (average 0.75). **4.** Larger 4ToeLng/SVL 0.08–0.3 (average 0.21). **5.** Larger 4FingLng/SVL 0.11–0.21 (average 0.14). **6.** Eyelid 10–14 (average 12.4). **7.** NarEyeS 4–5 (average 4.9). **8.** Scales on side of trunk point obliquely upward. **9.** Patch of granular scales in front of forelimb insertion absent. **10.** Scales on side of neck and adjacent shoulder area point obliquely upward; keels on neck scales are weakly to strongly developed. **11.** Paired dark patches are approximately triangular, extending from the front of the shoulder to the jaw angles. **12.** Coloration of tongue is orange. **13.** Nuchal and dorsal crest scales short; dorsal crest shortening progressively before mid-body; nuchal crest distinctly larger than dorsal crest. **14.** Supratympanic spines are short. **15.** Fourth toe with claw can stretch between the eyes and tympanum when hind limbs are adpressed forward. **16.** Fold in front of the shoulder is absent. **17.** During breeding season, males are uniformly dark orange to orange on the front half (except for the fingers) with black patches on both sides of neck and darker radial stripes around eyes; Hind body and toes a uniform khaki or dark khaki.

Table 5. Comparison of morphological characters between *Calotes wangi* sp. nov. and other species in the *C. versicolor* complex. Morphometric measurements are in mm. For measurements, count methods, and abbreviations, see the Materials and methods.

Characters	<i>Calotes versicolor</i>	<i>C. vultuosus</i>	<i>C. farooqi</i>	<i>C. htunwini</i>	<i>C. irawadi</i>	<i>C. wangi</i> sp. nov.
References	Gowande et al. 2021	Gowande et al. 2021	Gowande et al. 2021	Zug et al. 2006	Zug et al. 2006, Liu et al. 2021, this study	this study
Sample Size A	30	20	3	49	16	187
HeadW	0.15~0.28	0.16~0.26	0.19~0.21	/	0.13~0.21(0.18)	0.14~0.21(0.17)
Interorb	0.10~0.14	0.09~0.13	0.12~0.15	/	0.11~0.16(0.14)	0.06~0.17(0.10)
JawW	0.15~0.21	0.17~0.21	0.17~0.20	/	0.14~0.19(0.16)	0.14~0.2(0.17)
HeadH	0.14~0.21	0.16~0.21	0.14~0.16	/	0.13~0.17(0.16)	0.11~0.18(0.15)
SnW	0.05~0.07	0.05~0.08	0.06	/	0.06~0.08(0.06)	0.05~0.08(0.06)
SnEye	0.08~0.11	0.08~0.11	0.09~0.11	/	0.1~0.12(0.11)	0.07~0.14(0.10)
NarEye	0.04~0.07	0.04~0.06	0.04~0.05	/	0.05~0.07(0.06)	0.04~0.1(0.06)
EyeEar	0.06~0.09	0.06~0.09	0.07	/	0.06~0.08(0.07)	0.05~0.1(0.07)
SnForeL	0.34~0.41	0.34~0.45	0.31~0.35	/	0.31~0.39(0.35)	0.25~0.45(0.34)
ForeLimbL	0.48~0.59	0.47~0.59	/	/	0.38~0.7(0.47)	0.41~0.58(0.49)
UparmL	0.14~0.23	0.14~0.23	0.13~0.18	/	0.15~0.21(0.19)	0.13~0.24(0.17)
LoArmL	0.16~0.20	0.16~0.23	0.16~0.17	/	0.14~0.18(0.16)	0.13~0.19(0.16)
HindLimbL	0.69~0.91	0.68~0.85	/	/	0.63~0.8(0.70)	0.64~0.89(0.76)
ForeLimbL/ HindLimbL	0.61~0.73	0.65~0.81	/	/	0.58~0.98(0.67)	0.58~0.83(0.65)
UpLegL	0.17~0.25	0.18~0.29	0.21~0.22	/	0.21~0.27(0.24)	0.11~0.32(0.23)
CrusL	0.19~0.28	0.19~0.25	0.22	/	0.21~0.25(0.22)	0.09~0.3(0.21)
4ToeLng	0.15~0.26	0.15~0.23	0.13~0.20	/	0.17~0.21(0.19)	0.08~0.3(0.21)
4FingLng	0.10~0.18	0.10~0.15	0.12~0.13	/	0.09~0.15(0.12)	0.11~0.21(0.14)
TrunkL	0.38~0.50	0.37~0.50	0.48~0.52	/	0.45~0.61(0.51)	30.44~51.95(44.24)
Sample Size B	30	20	3	49	76	167
SVL (adult means)	>90 mm	>90 mm	>90 mm	<90 mm	<90 mm	<90 mm
TailL (adult means)	268.2	/	/	150.8	240.5	242.4
CanthR	6~9	7~8	8	8	5~7(6.11)	4~5(4.91)
VertS	31~51	35~62	40~44	38~57 (47.3)	36~59 (48.2)	39~52(44.7)
Midbody	36~46	37~45	41~44	39~53 (47.1)	38~51(44.9)	36~46(41.2)
4ToeLm	21~30	23~28	24~25	18~26 (22.7)	22~29(24.6)	19~27(24.2)
Eyelid	10~15(12)	11~14 (12)	9~11 (10)	12~13(11.2)	12~13(12.8)	10~14(12.4)
SSstrunk	obliquely upward	obliquely upward	obliquely upward	obliquely upward	obliquely upward	obliquely upward
SSforelimb	no patch of granular scales	no patch of granular scales	no patch of granular scales	no patch of granular scales	no patch of granular scales	no patch of granular scales
SSneck	obliquely upward	obliquely upward	obliquely upward	horizontal	obliquely upward	obliquely upward
Keels	weakly to strongly developed	weakly to strongly developed	weakly to strongly developed	modestly to strongly developed	weakly to strongly developed	weakly to strongly developed
NucSpot	approximately bean-shaped, not extending to the lower jaw	extending from the front of the shoulder to the ½ jaw	extending from the front of the shoulder to the ¾ jaw	frequently in females, not extended to the jaw	frequently in females, few extended to the jaw	approximately triangular, extending from the front of the shoulder to the jaw angles
CTG	pale flesh color	/	/	/	/	orange
DorsalCrests	long, shortens progressively to the base of the tail	short, shortens progressively to the mid-body;	short, shortens progressively to the mid-body	short, shortens progressively to the mid-body	short, shortens progressively after the mid-body	short, shortens progressively before the mid-body
NuchalCrests	long, distinct larger	short, distinct larger	short, distinct larger	short, slightly larger	short, distinct larger	short, distinct larger
SpinesS	long, > 2/3 tympanum diameter	short, < 1/2 tympanum diameter	short, < 1/2 tympanum diameter	short, < 1/2 tympanum diameter	short, < 1/3 tympanum diameter	short, < 1/2 tympanum diameter
NarEyeS	> 6	> 6	< 6	/	5~7(6)	4~5(4.9)
HAF	/	/	/	/	reaching tympanum	crossing tympanum
FS	absence	absence	absence	absence	absence	absence

Comparisons. *Calotes wangi* sp. nov. was previously recognized as *C. versicolor* by previous authors but it can easily be distinguished from true *C. versicolor* (India) by adult males having shorter average SVL < 90 mm vs > 90 mm in *C. versicolor*; fewer scales between the nasal shield and the orbit 4–5 (average 5), < 6 vs > 6; dark patches on neck extending to jowl vs not extending to jowl; nuchal and dorsal crest scales short and nuchal crest larger vs nuchal and dorsal crest scales well developed and nuchal crest scales only slightly larger than dorsal crest scales; pair of short supratympanic spines on each side of the head vs two well-separated supratympanic spines; coloration of tongue orange vs pale flesh color (239, 205, 197).

This species can be separated from others in the *C. versicolor* complex by the following characters (Zug et al. 2006): 36–46 mid-body scale rows (average 41.2) vs 45–55 in the Nat-Ma-Taung *versicolor* group and 46–53 in the Moy-yingyi *versicolor* group; forearm stripe and paired nuchal spots present in adult vs absent in the Thai-east *versicolor* group.

The new species differs from *Calotes irawadi* by its smaller HeadW in males, 11.64–19.72 vs 13.08–28.3 in *C. irawadi*, shorter Interorb 4.59–12.89 vs 6.9–15.07; longer 4FingLng/SVL 0.11–0.21 vs 0.09–0.15; fewer mid-body scale rows 36–46 (average 41.2) vs 38–51 (average 44.9); fewer scales between the nasal shield and the orbit 4–5 (average 4.9) vs 5–7 (average 6.1); progressively shortened dorsal crest before mid-body vs progressively shortened after mid-body (especially in males), fourth toe with claw reaching between the eyes and tympanum when hind limbs adpressed forward vs reaching tympanum.

The new species can be separated from *Calotes htunwini* Zug & Vindum, 2006 (Gowande et al. 2021) by the scales on the side of the neck and adjacent shoulder area pointing obliquely upward vs horizontally in *C. htunwini*; the keels on these scales weakly to strongly developed vs modestly to strongly developed. The new species can be separated from *C. farooqi* Auffenberg & Rehmann, 1995 by the shorter average adult male SVL, < 90 mm vs > 90 mm in *C. farooqi*; the smaller HeadW/SVL, 0.14–0.21 vs 0.19–0.21; more dorsal eyelid scales, 10–14 (average 12.4) vs 9–11 (average 10) in *C. farooqi*. The new species can be separated from *C. vultuosus* (Harlan, 1825) by shorter average adult male SVL, < 90 mm vs > 90 mm in *C. vultuosus*; smaller HeadW/SVL, 0.14–0.21 vs 0.16–0.2; smaller HeadH/SVL, 0.11–0.18 vs 0.16–0.21; more scales between the nasal shield and the orbit, 4–5 (average 4.9) vs > 6; dark patches on neck not extending to 1/2 jowl vs stretching to 1/2 jowl in *C. vultuosus*.

This species can be separated from other members of *Calotes* by a combination of the following characters: **1.** Crescent-shaped patch of granular scales absent at the forelimb insertion vs present in *C. emma*, *C. grandisquamis* Günther, 1875, *C. jerdoni* Günther, 1870, *C. mystaceus* Duméril & Bibron, 1837, and *C. nemoricola* Jerdon, 1853. **2.** Keeled dorsal scales vs smooth in *C. medogensis* Zhao & Li, 1984. **3.** Mid-body scale rows 36–46 (average 41.2) vs 49–65 in *C. emma*, 27–35 in *C. grandisquamis*, 45–57 in *C. jerdoni*, 58–63 in *C. maria*, 48–60 in *C. minor*, 45–58 in *C. mystaceus*. **4.** Nuchal and dorsal crest scales short, nuchal crest distinctly larger vs nuchal spines much longer, dorsal spines reduced in *C. maria* and *C. nemoricola*. **5.** Pair of short supratympanic spines on each side of the head vs a row of three or four compressed supratympanic spines in *C. grandisquamis* and *C. nemoricola*, eight or nine compressed spines above the tympanum in *C. calotes* (Linnaeus, 1758), two parallel rows of su-

pratympnic scales in *C. jerdoni* and *C. maria* Gray, 1845, and a single well-developed postorbital spine in *C. emma*. **6.** Homogeneous scalation on the dorsal region and a comparatively well-developed dorsal crest vs heterogeneous scalation and an undeveloped dorsal crest in *C. paulus* Smith, 1935 and *C. zolaiking* Giri, Chaitanya, Mahony, Lalronunga, Lakrinchhana, Das, Sarkar, Karanth & Deepak, 2019. **7.** Concave orbital region and absence of row of erect scales on sides of neck vs no concave orbital region and presence of row of erect scales in *C. bhutanensis* Biswas, 1975. **8.** Absence of fold in front of shoulder vs presence of fold in *C. chincolium* Vindum, 2003, *C. nigriplicatus* Hallermann, 2000, *C. bachae* Hartmann, Geissler, Poyarkov, Ihlow, Galoyan, Rödder & Böhme, 2013, *C. geissleri* Wagner, Ihlow, Hartmann, Flecks, Schmitz & Böhme, 2021, *C. goetzi* Wagner, Ihlow, Hartmann, Flecks, Schmitz & Böhme, 2021, *C. mystaceus* and *C. vindumbarbatus* Wagner, Ihlow, Hartmann, Flecks, Schmitz & Böhme, 2021. **9.** Posterodorsal orientation of lateral body scales and absence of shoulder pit vs posteroventral orientation and presence of shoulder pit in *C. ceylonensis* Müller, 1887, *C. desilvai* Bahir & Maduwage, 2005, *C. liocephalus* Günther, 1872, *C. liolepis* Boulenger, 1885, *C. manamendrai* Amarasinghe & Karunaratna, 2014, *C. nigrilabris* Peters, 1860, *C. pethiyagodai* Amarasinghe, Karunaratna & Hallermann, 2014.

Measurements and scale counts of specimens are given in Table 5 and Suppl. material 1: table S2.

Distribution and natural history. *Calotes wangi* sp. nov. is a transboundary species, ranging from southern China (Fujian Province, Guangdong Province, Hainan Province and Guangxi Zhuang Autonomous Region, southern Hunan Province, Macao, and Hong Kong) to northern Vietnam (Lang Son). The eastern Yunnan region in China is also likely to harbor this species (Yang and Rao 2008; Shuo Liu, pers. comm. 17 April 2023). The known altitude range of *C. w. wangi* ssp. nov. is 15~2000 m and *C. w. hainanensis* is 47~1867 m. It is found in subtropical evergreen broad-leaved forests and tropical monsoon forests in southern China and northern Vietnam, mostly in mountainous areas, hills and plains on forest edges, arable land, shrub lands, and even urban green belts. It is active at the edge of the forest, and when it is in danger, it rushes into bushes or climbs tree trunks to hide. It is active from April to October every year, while in the tropics it is active from March to November or even longer. The authors investigated in Hainan and found that *C. wangi* sp. nov. was active from 7:30~11:30 hrs in summer and 15:00~19:00 hrs in the afternoon. Investigations in Guangxi found that the lizards lie on sloping shrub branches at night, sleeping close to the branches.

Both *Calotes wangi* sp. nov. and *C. irawadi* are oviparous. It has been reported that females of *C. wangi* sp. nov. contained 5–12 (17 in one specimen in Mt. Diaoluo, Hainan) mature eggs from late April to September, while females of *C. irawadi* contained 12 mature eggs in June (Zhao et al. 1999). After our dissections, 13 specimens of *C. wangi* sp. nov. from Hainan obtained in August had 5–8 eggs (average 6), and five *C. irawadi* from Lushui, Yunnan obtained in late May were pregnant with 5–15 eggs (average 11).

Calotes wangi sp. nov. eats a variety of insects, spiders, and other arthropods (Zhao et al. 1999).

Specimens examined. *Calotes irawadi* ($n = 18$). **MYANMAR:** Kawnglanghpu (CIB097515). **China:** Yunnan Province, Lushui City (Shangjiang CIB001824-26), Baoshan City (Shangjiang CIB001819-23, CIB001827-28), Dehong Dai and Jing-

po Autonomous Prefecture (Hongbenghe CIB116106 and CIB116212, Tongbiguan KIZ 059191, KIZ NB20180905, KIZ HBH20200913 and KIZ HBH20200914), Xishuangbanna Dai Autonomous Prefecture (CIB001610).

Key to the species of *Calotes* in China

Modified from Zhao et al. (1999), Zug et al. (2006), Gowande et al. (2016), Pal et al. (2018), Giri et al. (2019), Gowande et al. (2021), and Wagner et al. (2021).

- 1 Presence of heterogeneous scales on dorsum, caudal vertebrae with transverse processes 14..... ***Calotes paulus***
- Absence of heterogeneous scales on dorsum..... **2**
- 2 Smooth dorsal scales ***C. medogensis***
- Keeled dorsal scales **3**
- 3 Post orbital spine present..... ***C. emma***
- Post orbital spine absent..... **4**
- 4 Two parallel rows of compressed spines above tympanum, dorsum green ***C. jerdoni***
- No parallel rows of compressed scales above tympanum, dorsum not green **5**
- 5 Presence of fold in front of the shoulder **6**
- Absence of fold in front of the shoulder **7**
- 6 No brownish dorsolateral blotches, whitish stripe from tip of snout continuing to beyond limb insertion..... ***C. vindumbarbatus***
- Prominent dark brown dorsolateral blotches ***C. goetzi***
- 7 Fewer scales (4 or 5, average 4.9) between the nasal shield and the orbit, fourth toe with claw crossing tympanum when hind limbs addressed forward..... **8**
- More scales (5–7, average 6.1) between the nasal shield and the orbit, fourth toe with claw reaching tympanum when hind limbs addressed forward..... ***C. irawadi***
- 8 Fewer eyelid scales (10–13, average 12.4), Tail/SVL (1.59–3.36, average 2.83), male UpLegL/SVL (0.11–0.26, average 0.23), male CrusL/SVL (0.09–0.24, average 0.21)..... ***C. w. wangi* ssp. nov.**
- More eyelid scales (13–14, average 13), Tail/SVL (1.77–4.01, average 3.15), male UpLegL/SVL (0.23–0.32, average 0.25), male CrusL/SVL (0.21–0.3, average 0.24)..... ***C. w. hainanensis* ssp. nov.**

Discussion

Based on extensive spatial sampling across China and comprehensive data on morphology and genetics for species delimitation, we add a new species and more stability to the systematics of *Calotes*. Another interesting finding from this study is the presence of subspecies, which highlights the need for more thorough geographic sampling to uncover cryptic lineages. This study provides additional data to clarify the taxonomic status of the widely distributed *Calotes versicolor* complex. *Calotes wangi* sp. nov. is described as a new species in the Guangdong, Guangxi, Hainan, Hong Kong, and Fujian populations of *C. versicolor* complex in this study.

The Yunnan populations in the *Calotes versicolor* complex were recorded from Wenshan Prefecture (Funing), Dehong Prefecture (Yingjiang and Longchuan), Nujiang Prefecture (Lushui), Baoshan City, Dali Prefecture (Yangbi), Pu'er City (Menglian), and Xishuangbanna Prefecture (Zhao et al. 1999; Yang and Rao 2008). Liu et al. (2021) confirmed that the *C. versicolor* complex in Dehong Prefecture contains *C. irawadi*, but the records from Lushui and Baoshan were confused regarding the specific collection localities. The CIB collection information only covered Lushui, while the old labels on the bottles of Zhao and Yang (1997) indicated that the samples were from Lushui and Baoshan. According to our study, the morphology of that group of specimens was consistent with *C. irawadi*. One sequence we obtained from Lushui and the Baoshan region (Mt. Gaoligong) was in the same clade in the phylogenetic tree as *C. irawadi* from the type locality (Fig. 2); therefore, we conclude that the records from Baoshan and Lushui refer to *C. irawadi*. In the records of Xishuangbanna, Zeng (1994) recorded an individual from the Xishuangbanna Tropical Botanical Garden, in which the morphology was consistent with *C. irawadi*; however, other records were not detailed, such as CIB001610. One sequence we obtained from Xishuangbanna is also in the same clade in the phylogenetic tree as *C. irawadi* from the type locality; therefore, we can also state that the records from Xishuangbanna likely refer to *C. irawadi*. The record of Menglian lacks specimen information. Menglian is close and has an environment like that of the Min-Gon-Taung Wildlife Sanctuary in Myanmar, one of the distribution sites of *C. irawadi* (Zug et al., 2006). Whether this record refers to *C. irawadi* needs further study. The record of Yangbi County in northern Yunnan also lacks specimen information (Yang and Rao 2008). Yangbi is near to and the environment is similar to that of Lushui and Baoshan. Whether this record belongs to *C. irawadi* remains unclear. Funing County is in eastern Yunnan, and its topography and climate are like those in western Guangxi. Liu et al. (2021) found that the populations of *C. versicolor* complex in eastern and western Yunnan contained different species during their surveys. The morphology of the eastern population was similar to that of the Guangdong and Guangxi populations, and it is likely to be *C. wangi* sp. nov. (Shuo Liu, pers. comm. 17 April 2023). Thus, the eastern Yunnan populations of *C. versicolor* complexes consist of *C. irawadi* (the records of Meng Lian and Yangbi need further study), while western Yunnan is most likely to have *C. wangi* sp. nov.

The Hunan population of the *Calotes versicolor* complex was recorded from Yizhang County (Deng and Ye 1996, 1997). After comparing the morphological data with the new species in the article, we conclude that the record in Hunan represents *C. wangi* sp. nov.

The literature pertaining to the *Calotes versicolor* complex in Macau also lacks morphological or molecular information. By referring to the morphology in the photographs provided by Hoi Yan Wong from the Macau population of *C. versicolor*, as well as the distance and climatic environment between Macau and the Hong Kong, Guangdong Province, we consider that the Macau population is also *C. wangi* sp. nov.

Gowande et al. (2021) mentioned a single sequence of *Calotes irawadi* from Huanan Province, China (locality 73). The sequence was HM362986 (Xm 3490), which was uploaded to GenBank by Gu et al. (2011) together with HM362984 and HM362985. The location of these specimens was the Huanan district of China (i.e., southern China), not Huanan Province. After phylogenetic analysis, these three se-

quences were clustered together in the clade of *C. wangi* sp. nov., and the morphological characters of these specimens were also consistent with this species.

To date, there are nine species of tree lizards in China: *Calotes emma*, *C. jerdoni*, *C. medogensis*, *C. paulus* (Cai et al. 2022a), *C. irawadi* (Liu et al. 2021), *C. goetzi* (Wagner et al. 2021), and *C. vindumbarbatus* (Liu et al. 2022) and *C. wangi* sp. nov. (this study). *Calotes versicolor* is not distributed in China. In the field surveys, we found that the populations of *C. wangi* sp. nov. were relatively large, and the species is not threatened at present. However, in some areas, their habitat was being fragmented. In addition, their bodies are used medicinally and the lizards are also eaten. We suggest that the local government strengthen the protection of their ecological environment and pay close attention to the population dynamics.

Acknowledgements

We would like to thank the anonymous reviewers for their valuable comments on the manuscript and our colleagues Ke Lyu and Jiatang Li for their help and advice. We also thank Haitao Shi, Jichao Wang, Yueyun Zhang, Xiaomei Wei, Tongliang Wang, Xiaofei Zhai, Lianhua Su, Xianmei Lin, Jialing Li, Zaiwen Huang, Chengjian Zhao and Yingle Gu for their help. We also thank Shuo Liu from KIZ for supplementing the morphological data of *Calotes irawadi*, and Hoi Yan Wong for photographs of *Calotes* from Macao. We also thank Hainan Tropical Rainforest National Park Management Bureau and Damingshan National Nature Reserve of Guangxi for assistance.

Additional information

Conflict of interest

The authors have declared that no competing interests exist.

Ethical statement

No ethical statement was reported.

Funding

This work was supported by Guangxi Natural Science Foundation (Grant No.2023GXNSF-DA026065,2020GXNSFAA238017, 2017GXNSFDA198001 and 2014GXNSFBA118113), and the National Natural Science Fund (Grant No. 31460559).

Author contributions

Methodology: HL, YW. Resources: MH, ML. Writing – original draft: BC, YH.

Author ORCIDs

Yong Huang  <https://orcid.org/0000-0002-3493-9468>

Bo Cai  <https://orcid.org/0000-0002-4214-9060>

Data availability

All of the data that support the findings of this study are available in the main text or Supplementary Information.

References

- Amarasinghe A, Manthey U, Stockli E, Ineich I, Kullander S, Tiedemann F, McCarthy C, Gabadage DE (2009) The original descriptions and figures of Sri Lankan Agamid lizards (Squamata: Agamidae) of the 18th and 19th Centuries. *Taprobanica* 1(1): 2–15. <https://doi.org/10.47605/tapro.v1i1.2>
- Cai B, Wang YZ, Chen YY, Li JT (2015) A revised taxonomy for Chinese reptiles. *Biodiversity Science* 23(3): 365–382. [In Chinese with English abstract] <https://doi.org/10.17520/biods.2015037>
- Cai B, Ji X, Wang YY, Rao DQ, Huang S, Wang YZ, Song ZB, Guo XG, Jiang JP (2022a) An annotated list of lizards (Sauria: Squamata) recorded from the People's Republic of China. *Asian Herpetological Research* 13(1): 64–74. <https://doi.org/10.16373/j.cnki.ahr.210020>
- Cai B, Zhang MH, Li J, Du SM, Xie F, Hou M, Zhou HM, Jiang JP (2022b) Three new species of *Diploderma* Hallowell, 1861 (Reptilia: Squamata: Agamidae) from the Shaluli Mountains in Western Sichuan, China. *Asian Herpetological Research* 13(4): 205–223. <https://doi.org/10.16373/j.cnki.ahr.220040>
- Chaitanya R, Giri VB, Deepak V (2017) On the recent designation of a neotype for the taxon *Calotes versicolor* (Daudin, 1802) (Reptilia: Agamidae). *Zootaxa* 4317(3): 585–587. <https://doi.org/10.11646/zootaxa.4317.3.10>
- Daudin FM (1802) *Histoire Naturelle, Générale et Particulière des Reptiles, Ouvrage Faisant Suite, à l'histoire Naturelle, Générale et Particulière Composée par Leclerc de Buffon, et Rédigée par C. S. Sonnini* (Vol. 3). F. Dufart, Paris, 452 pp. <https://doi.org/10.5962/bhl.title.60678>
- Deng XJ, Ye YY (1996) Faunal analysis and survey on lizard in Hunan Province. *Sichuan Journal of Zoology* 15(1): 15–20. [In Chinese with English abstract]
- Deng XJ, Ye YY (1997) Eight new records of lizards in Hunan. *Chinese Journal of Zoology* 32(6): 40–42. [In Chinese with English abstract] <https://doi.org/10.13859/j.cjz.1997.06.014>
- Ge Y, Wei YF, Chek SN, Gong SP (2018) Diversity and conservation of amphibians and reptiles in Macau, China. *Chinese Journal of Wildlife* 39(3): 639–645. [In Chinese with English abstract] <https://doi.org/10.19711/j.cnki.issn2310-1490.2018.03.030>
- Giri VB, Chaitanya R, Mahony S, Lalrunga S, Lalrinchhana C, Das A, Sarkar V, Karanth P, Deepak V (2019) On the systematic status of the genus *Oriocalotes* Günther, 1864 (Squamata: Agamidae: Draconinae) with the description of a new species from Mizoram state, Northeast India. *Zootaxa* 4638(4): 451–484. <https://doi.org/10.11646/zootaxa.4638.4.1>
- Gowande G, Mishra A, Mirza ZA (2016) Neotype designation for *Calotes versicolor* Daudin, 1802 (Sauria: Agamidae) with notes on its systematics. *Zootaxa* 4126(2): 271–279. <https://doi.org/10.11646/zootaxa.4126.2.7>
- Gowande G, Pal S, Jablonski D, Masroor R, Phansalkar PU, Dsouza P, Jayarajan A, Shanker K (2021) Molecular phylogenetics and taxonomic reassessment of the widespread agamid lizard *Calotes versicolor* (Daudin, 1802) (Squamata, Agamidae) across South Asia. *Vertebrate Zoology* 71: 669–696. <https://doi.org/10.3897/vz.71.e62787>
- Gu HF, Xia Y, Peng R, Mo BH, Li L, Zeng XM (2011) Authentication of Chinese Crude Drug Gecko by DNA Barcoding. *Natural Product Communications* 6(1): 67–71. <https://doi.org/10.1177/1934578X1100600117>

- Hall TA (1999) BIOEDIT: A user-friendly biological sequence alignment editor and analysis program for Windows 95/98/NT. *Nucleic Acids Symposium Series* 41(41): 95–98. <https://doi.org/10.1021/bk-1999-0734.ch008>
- Hartmann T, Geissler P, Poyarkov Jr N, Ihlow F, Galoyan EA, Rödder D, Böhme W (2013) A new species of the genus *Calotes* Cuvier, 1817 (Squamata: Agamidae) from southern Vietnam. *Zootaxa* 3599(3): 246–260. <https://doi.org/10.11646/zootaxa.3599.3.3>
- Hu ZK, Huang Y, Yao ZY, Cai B (2022) *Tropidophorus sinicus* and *Calotes versicolor* found in Jiangkou County of Guizhou and Lianjiang County of Fujian respectively. *Chinese Journal of Zoology* 57(1): 112–116. [In Chinese with English abstract] <https://doi.org/10.13859/j.cjz.202201011>
- Huang Y, Guo X, Ho SY, Shi H, Li J, Li J, Cai B, Wang Y (2013) Diversification and Demography of the Oriental Garden Lizard (*Calotes versicolor*) on Hainan Island and the Adjacent Mainland. *PLoS ONE* 8(6): e64754. <https://doi.org/10.1371/journal.pone.0064754>
- Ibraheem NA, Hasan MM, Khan RZ, Mishra PK (2012) Understanding color models: A review. *Journal of Science and Technology* 2(3): 265–275.
- Kuhl H (1820) *Beiträge zur Zoologie und Vergleichenden Anatomie, Erste Abtheilung*. Verlag der Hermannschen Buchhandlung, Frankfurt am Main, 152 pp.
- Kumar S, Stecher G, Li M, Knyaz C, Tamura K (2018) MEGA X: Molecular Evolutionary Genetics Analysis across computing platforms. *Molecular Biology and Evolution* 35(6): 1547–1549. <https://doi.org/10.1093/molbev/msy096>
- Liu HN (2000) Biodiversity analysis of amphibians and reptiles of Hong Kong Special Administrative Region. *Sichuan Journal of Zoology* 19(3): 112–115. [In Chinese with English abstract]
- Liu S, Zuo C, Rao DQ (2021) Distribution extension of *Calotes irawadi* Zug, Brown, Schulte & Vindum, 2006, previously confused with *C. versicolor* (Daudin, 1802): First record from China. *Herpetozoa* 34: 83–888. <https://doi.org/10.3897/herpetozoa.34.e62596>
- Liu S, Zuo C, Yin F, Hui H, Rao DQ (2022) First record of *Calotes vindumbarbatus* Wagner, Ihlow, Hartmann, Flecks, Schmitz & Böhme, 2021 (Squamata: Agamidae) from China, with revised diagnosis of this species. *Biodiversity Data Journal* 10: e77963. <https://doi.org/10.3897/BDJ.10.e77963>
- Nguyen L, Schmidt H, von Haeseler A, Minh B (2015) IQ-TREE: A fast and stochastic algorithm for estimating maximum likelihood phylogenies. *Molecular Biology and Evolution* 32: 268–674. <https://doi.org/10.1093/molbev/msu300>
- Pal S, Vijayakumar SP, Shanker K, Jayarajan A, Deepak V (2018) A systematic revision of *Calotes* Cuvier, 1817 (Squamata: Agamidae) from the Western Ghats adds two genera and reveals two new species. *Zootaxa* 4482(3): 401–450. <https://doi.org/10.11646/zootaxa.4482.3.1>
- Posada D (2008) jModelTest: Phylogenetic Model Averaging. *Molecular Biology and Evolution* 25(7): 1253–1256. <https://doi.org/10.1093/molbev/msn083>
- Ronquist F, Teslenko M, Paul VDM, Ayres DL, Darling A, Höhna S, Larget B, Liu L, Suchard MA, Huelsenbeck JP (2012) MrBayes 3.2: Efficient bayesian phylogenetic inference and model choice across a large model space. *Systematic Biology* 61(3): 539–542. <https://doi.org/10.1093/sysbio/sys029>
- Shi HT, Zhao EM, Wang LJ (2011) *Herpetological Fauna of Hainan*. Science Press, Beijing, China. [In Chinese]
- Smith MA (1935) *The Fauna of British India including Ceylon and Burma. Reptilia and Amphibia (Vol. II) Sauria*. Taylor and Francis, London, 440 pp.
- Tantrawatpan C, Thongnetr W, Pilap W, Suksavate W, Agatsuma T, Tawong W, Petney TN, Saijuntha W (2021) Genetic Diversity and Population Structure of the Oriental Garden

- Lizard, *Calotes versicolor* Daudin, 1802 (Squamata: Agamidae) along the Mekong River in Thailand and Lao PD. *Asian Herpetological Research* 12(1): 49–57. <https://doi.org/10.16373/j.cnki.ahr.200046>
- Trifinopoulos J, Nguyen L, Haeseler A, Minh B (2016) W-IQ-TREE: A fast online phylogenetic tool for maximum likelihood analysis. *Nucleic Acids Research* 44(W1): W232–W235. <https://doi.org/10.1093/nar/gkw256>
- Uetz P, Freed P, Aguilar R, Hošek J (2023) The Reptile Database. <http://www.reptile-database.org> [Accessed 31 May 2023]
- Wagner P, Ihlow F, Hartmann T, Flecks M, Schmitz A, Böhme W (2021) Integrative approach to resolve the *Calotes mystaceus* Duméril & Bibron, 1837 species complex (Squamata: Agamidae). *Bonn zoological Bulletin* 70(1): 141–171. <https://doi.org/10.20363/BZB-2021.70.1.141>
- Wang YZ, Cai B, Li JT (2021) China's Red List of Biodiversity: Vertebrates (Vol. III), Reptiles. Science Press, Beijing. [In Chinese]
- Wermuth H (1967) Liste der rezenten Amphibien und Reptilien. Agamidae. *Das Tierreich* 86: 1–127.
- Yang DT, Rao DQ (2008) Amphibia and Reptilia of Yunnan. Yunnan Science and Technology Press, Kunming. [In Chinese]
- Zeng XM (1994) Preliminary karyological study of *Calotes versicolor*. *Acta Herpetologica Sinica* 3: 136–137. [In Chinese]
- Zhao EM, Adler K (1993) Herpetology of China. Society for the Study of Amphibians and Reptiles, Oxford.
- Zhao EM, Yang DT (1997) Amphibian and reptiles in the Hengduan Mountains. Science Press Beijing. [In Chinese]
- Zhao EM, Zhao KT, Zhou KY (1999) Fauna Sinica, Reptilia (Vol. 2): Squamata, Lacertilia. Science Press, Beijing. [In Chinese]
- Zug G, Brown H, Schulte IJ, Vindum J (2006) Systematics of the Garden Lizard, *Calotes versicolor* Group (Reptilia, Squamata, Agamidae), in Myanmar: Central Dry Zone Populations. *Proceedings of the California Academy of Sciences* 57: 35–68.

Supplementary material 1

Supplementary information

Authors: Yong Huang, Hongyu Li, Yilin Wang, Maojin Li, Mian Hou, Bo Cai

Data type: docx

Explanation note: **table S1**. Voucher specimens and GenBank accession numbers of DNA sequences of *Calotes wangi* sp. nov., and other species in the genus *Calotes* used in this study. **table S2**. Comparison of measurement data between different populations of *Calotes wangi* sp. nov. and *C. cf. versicolor* populations. **fig. S1**. Local enlarged phylogenetic tree structure corresponding to *Calotes wangi hainanensis* ssp. nov. (Lineage A) and *C. w. wangi* ssp. nov. (Lineage B), respectively.

Copyright notice: This dataset is made available under the Open Database License (<http://opendatacommons.org/licenses/odbl/1.0/>). The Open Database License (ODbL) is a license agreement intended to allow users to freely share, modify, and use this Dataset while maintaining this same freedom for others, provided that the original source and author(s) are credited.

Link: <https://doi.org/10.3897/zookeys.1187.110704.suppl1>

New genera and new species of Hahniidae (Araneae) from China, Laos, Myanmar, and Vietnam

Chang Chu¹, Yejie Lin¹, Shuqiang Li^{1,2}

¹ Institute of Zoology, Chinese Academy of Sciences, Beijing 100101, China

² University of Chinese Academy of Sciences, Beijing 100101, China

Corresponding author: Shuqiang Li (lisq@ioz.ac.cn)

Abstract

Four new genera and 11 new species of Hahniidae Bertkau, 1878 are described. The new genera are *Goblinia* Lin & Li, **gen. nov.**, with the type species *G. tiane* Lin & Li, **sp. nov.** (♂♀) from Guangxi, China; *Myahnia* Lin & Li, **gen. nov.**, with the type species *M. kanpetlet* Lin & Li, **sp. nov.** (♂♀) from Chin, Myanmar; *Troglohnia* Lin & Li, **gen. nov.**, with the type species *Tr. qiubei* Lin & Li, **sp. nov.** (♂♀) from Yunnan, China and *Typhlohnia* Lin & Li, **gen. nov.**, with the type species *Ty. rongshui* Lin & Li, **sp. nov.** (♂♀) from Guangxi, China. Seven additional new species are described: *Tr. dafang* Lin & Li, **sp. nov.** (♂♀) from Guizhou, China; *Tr. shidian* Lin & Li, **sp. nov.** (♀) from Yunnan, China; *Tr. wuding* Lin & Li, **sp. nov.** (♂♀) from Yunnan, China; *Ty. banlaksao* Lin & Li, **sp. nov.** (♀) from Bolikhamxay, Laos; *Ty. kaiyang* Lin & Li, **sp. nov.** (♀) from Guizhou, China; *Ty. sondoong* Lin & Li, **sp. nov.** (♂♀) from Quang Binh, Vietnam and *Ty. suiayang* Lin & Li, **sp. nov.** (♀) from Guizhou, China.

Key words: Comb-tailed spiders, diagnosis, endemic, Hahniinae, taxonomy



Academic editor: Zhiyuan Yao
Received: 19 September 2023
Accepted: 19 November 2023
Published: 20 December 2023

ZooBank: <https://zoobank.org/A09B6A51-1026-4375-A4EA-0EFC676479F1>

Citation: Chu C, Lin Y, Li S (2023) New genera and new species of Hahniidae (Araneae) from China, Laos, Myanmar, and Vietnam. ZooKeys 1187: 91–134. <https://doi.org/10.3897/zookeys.1187.112936>

Copyright: © Chang Chu et al.
This is an open access article distributed under terms of the Creative Commons Attribution License ([Attribution 4.0 International – CC BY 4.0](https://creativecommons.org/licenses/by/4.0/)).

Introduction

Asian spider taxonomists have published a large number of papers in the 21st Century, but due to the rich biodiversity of the Southeast Asia fauna, there are still many unknown species (Li et al. 2021; Yang et al. 2021; Yao et al. 2021; Liu et al. 2022; Lu et al. 2022; Zhao et al. 2022; Zhang et al. 2023). Currently, 354 species in 23 genera of the spider family Hahniidae Bertkau, 1878, the so-called comb-tailed spiders, are known worldwide (WSC 2023), of which 53 species (45 endemic species) in China, followed by six species (four endemics) in Vietnam and one in Laos (WSC 2023). Hitherto, there have been no records from Myanmar (WSC 2023). In this paper, we report 11 new species and four new genera from China, Laos, Myanmar, and Vietnam.

Material and methods

All specimens were preserved in 80% ethanol. The spermathecae were cleared in trypsin enzyme solution to dissolve non-chitinous tissues. Specimens were examined under a LEICA M205C stereomicroscope. Photomicrographs were taken with an Olympus C7070 zoom digital camera (7.1 megapixels).

Photographs were stacked with Helicon Focus (v. 7.6.1) or Zerene Stacker (v. 1.04) and processed in Adobe Photoshop CC2022.

All measurements are in millimetres (mm) and were obtained with an Olympus SZX16 stereomicroscope with a Zongyuan CCD industrial camera. All measurements of body lengths do not include the chelicerae. Eye sizes are measured as the maximum diameter from either the dorsal or the frontal view. Legs were measured laterally. Leg measurements are given as follows: total length (femur, patella, tibia, metatarsus, tarsus). Four paratype male specimens (*Goblinia tiane* sp. nov., *Myahnia kanpetlet* sp. nov., *Troglohnia qiubei* sp. nov. and *Typhlohnia rongshui* sp. nov.) were used for electron microscopy. They were fragile after electron microscopy, so their variation data was not measured. The terminology used in the text and figures follows Zhang et al. (2011) and Huang et al. (2017).

Types from the current study are deposited in the Institute of Zoology, Chinese Academy of Sciences in Beijing (IZCAS).

Abbreviations used in text: **AER** anterior eye row; **ALE** anterior lateral eye; **AME** anterior median eye; **C** conductor; **CD** copulatory duct; **CF** cymbial furrow; **CO** copulatory opening; **D** depression; **d** dorsal; **dRTA** dorsal retrolateral tibial apophysis; **E** embolus; **ET** embolic tooth; **FD** fertilization duct; **GA** glandular appendage; **H** hood; **MOA** median ocular area; **p** prolateral; **PA** patellar apophysis; **PER** posterior eye row; **PLE** posterior lateral eye; **PME** posterior median eye; **PS** primary spermatheca; **r** retrolateral; **RTA** retrolateral tibial apophysis; **S** spermatheca; **SD** sperm dust; **SS** secondary spermatheca; **v** ventral; **vRTA** ventral retrolateral tibial apophysis.

Taxonomic account

Family Hahniidae Bertkau, 1878

Ono and Ogata (2018) divided this family into two subfamilies: Hahniinae Bertkau, 1878 (type genus: *Hahnia* C. L. Koch, 1841) and Cicurinae F. O. Pickard-Cambridge, 1893 (type genus: *Cicurina* Menge, 1871).

Subfamily Hahniinae Bertkau, 1878

Genus *Goblinia* Lin & Li, gen. nov.

<https://zoobank.org/E1AF935B-398E-4BE9-A7E1-81798965C021>

Type species. *Goblinia tiane* sp. nov. from Guangxi, China.

Diagnosis. *Goblinia* gen. nov. can be distinguished from *Iberina* Simon, 1881 by the spineless male palpal femur (Fig. 6A, B) [vs femur with 3–5 spines (see Růžička 2022: fig. 2O)], embolus shorter than perimeter of bulb (Figs 3A, 4A) [vs almost 2× longer (see Růžička 2022: fig. 4A–E)] and epigyne with one pair of spermathecae (Fig. 5B) [vs two pairs of spermathecae, except for *I. difficilis* (Harm, 1966) and *I. microphthalma* (Snazell & Duffey, 1980) (see Růžička 2022: fig. 5A–E)].

Description. Male. Total length 1.87–2.40 ($n = 5$). Carapace pale yellow, covered with few black setae. PER longer than AER, AER and PER procurved. AME separated by less than their diameter, closer to ALE; PME separated by almost their diameter, approximately as far from ALE; Distance between AME and PME

longer than that between ALE and PLE; ALE and PLE almost touching. Clypeus pale yellow, covered with few setae. Chelicerae pale yellow, with three promarginal and three retromarginal teeth, with granular stridulatory files retrolaterally (Fig. 2A). Endites, labium pale yellow, covered with few black setae. Sternum coloured as endites, covered with brown setae. Legs pale yellow. Opisthosoma oval, white. Spinnerets white, M-shaped in posterior view. Tracheal spiracle long and transverse, distance of spiracle to epigastric furrow as long as to spinnerets.

Palpal femur almost 4× longer than patella, spineless. Patella shorter than tibia. Retrolateral tibial apophysis almost as long as tibia, curved to almost 100° angle. Cymbium egg-shaped, cymbial furrow almost as long as bulb. Bulb discoid round, without conductor. Sperm duct with curved course. Embolus whip-shaped, starting at ca 4:30 o'clock position.

Female. Total length 1.96–2.55 ($n = 5$). Somatic characters as in male but chelicerae with two promarginal and three retromarginal teeth, stridulatory files absent.

Epigynal plate wider than long. Copulatory openings located anteriorly, round, touching each other. Copulatory ducts long and intertwined, beginning laminar. Glandular appendages round, touching each other. Spermathecae oval, located posteriorly, separated by less than radius.

Etymology. The new generic name is a combination of *goblin* (a legendary creature that lives underground) and *Hahnia*. The gender is feminine.

Composition. Currently monotypic: *Goblinia tiane* sp. nov.

Distribution. China (Guangxi) (Fig. 30).

***Goblinia tiane* Lin & Li, sp. nov.**

<https://zoobank.org/D311CBBE-BE0C-4137-A678-8AE138F6B480>

Figs 1A, 2A, 3A, 4A, B, 5A, B, 6A, B, 30

Type material. Holotype: ♂ (IZCAS-Ar44648), CHINA, Guangxi: Hechi City, Tian'e County, Bala Town: No. 8 Cave, 24.9337°N, 107.0421°E, ca 685 m, 04.II.2015, Y. Li and Z. Chen leg. **Paratypes:** 5♂ 5♀ (IZCAS-Ar44649–Ar44658), same data as holotype.

Diagnosis. Same as for genus.

Description. Male (holotype; Figs 4A, B, 6A). Total body length 1.87. Carapace 0.93 long, 0.74 wide; opisthosoma 0.94 long, 0.68 wide. AER and PER procurved slightly. Eye sizes and interdistances: AME 0.05, ALE 0.05, PME 0.05, PLE 0.05; AME–AME 0.01, AME–ALE 0.01, PME–PME 0.07, PME–PLE 0.03, ALE–PLE 0.02. MOA 0.12 long, front width 0.08, back width 0.15. Clypeus 0.14 high. Leg measurements: I 2.94 (0.85, 0.29, 0.64, 0.67, 0.49); II 2.75 (0.81, 0.28, 0.59, 0.60, 0.47); III 2.79 (0.77, 0.28, 0.60, 0.66, 0.48); IV 3.06 (0.93, 0.29, 0.73, 0.65, 0.46). Leg spination: patellae I–IV d1; tibiae I–II d1, III–IV p1 d1 r1; metatarsi III p1 d1 r1, IV p1 r1.

Coloration (Fig. 6A). Carapace yellowish, with light brown radiating marks and indistinct marginal brown band. Fovea longitudinal, reddish-brown. Chelicerae, labium, gnathocoxae, and sternum yellowish. Legs yellowish. Opisthosoma oval, grey with dark pattern, venter grey without pattern. Spinnerets white.

Palp (Fig. 4A, B). Patellar apophysis as long as patella, tip hook-shaped; patellar apophysis almost 1.5× longer than tip. Tibia with black, serrated retrolateral

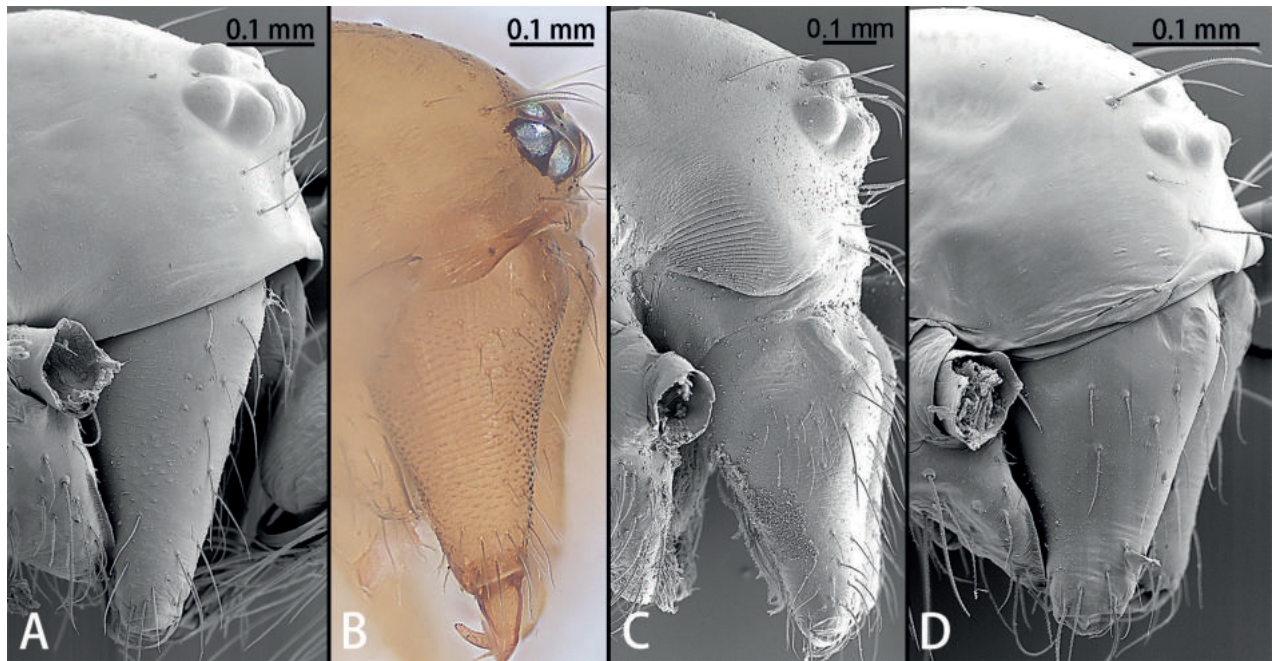


Figure 1. Cephalic region and chelicerae, paratype males, lateral view **A** *Goblinia tiane* sp. nov. **B** *Myahnia kanpetlet* sp. nov. **C** *Troglohnia qiubei* sp. nov. **D** *Typhlohnia rongshui* sp. nov.

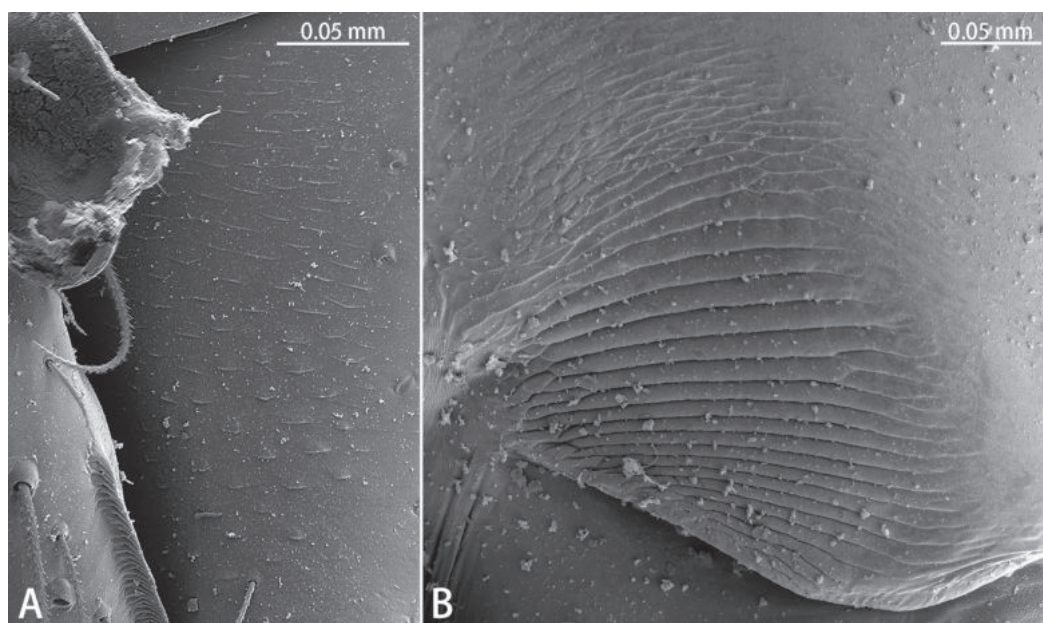


Figure 2. Stridulatory files, paratype males, lateral view **A** *Goblinia tiane* sp. nov. **B** *Troglohnia qiubei* sp. nov.

apophysis, S-shaped in retrolateral view. Cymbium almost egg-shaped, 1.2× longer than wide. Sperm duct long, basal thick part running around of tegulum, forming ~ 270° loop clockwise; middle thin part forming circular anticlockwise, diameter ~ 1/3 of bulb diameter; distal thin part running around of tegulum, forming circular clockwise. Embolus with wide, slightly membranous base and membranous, curved tip; its base arising at 4:30 o'clock position; tip hidden by cymbium in retrolateral view.

Female (paratype IZCAS-Ar44658; Figs 5A, B, 6B). Total body length 2.41. Carapace 0.97 long, 0.76 wide; opisthosoma 1.44 long, 1.09 wide. Eye sizes

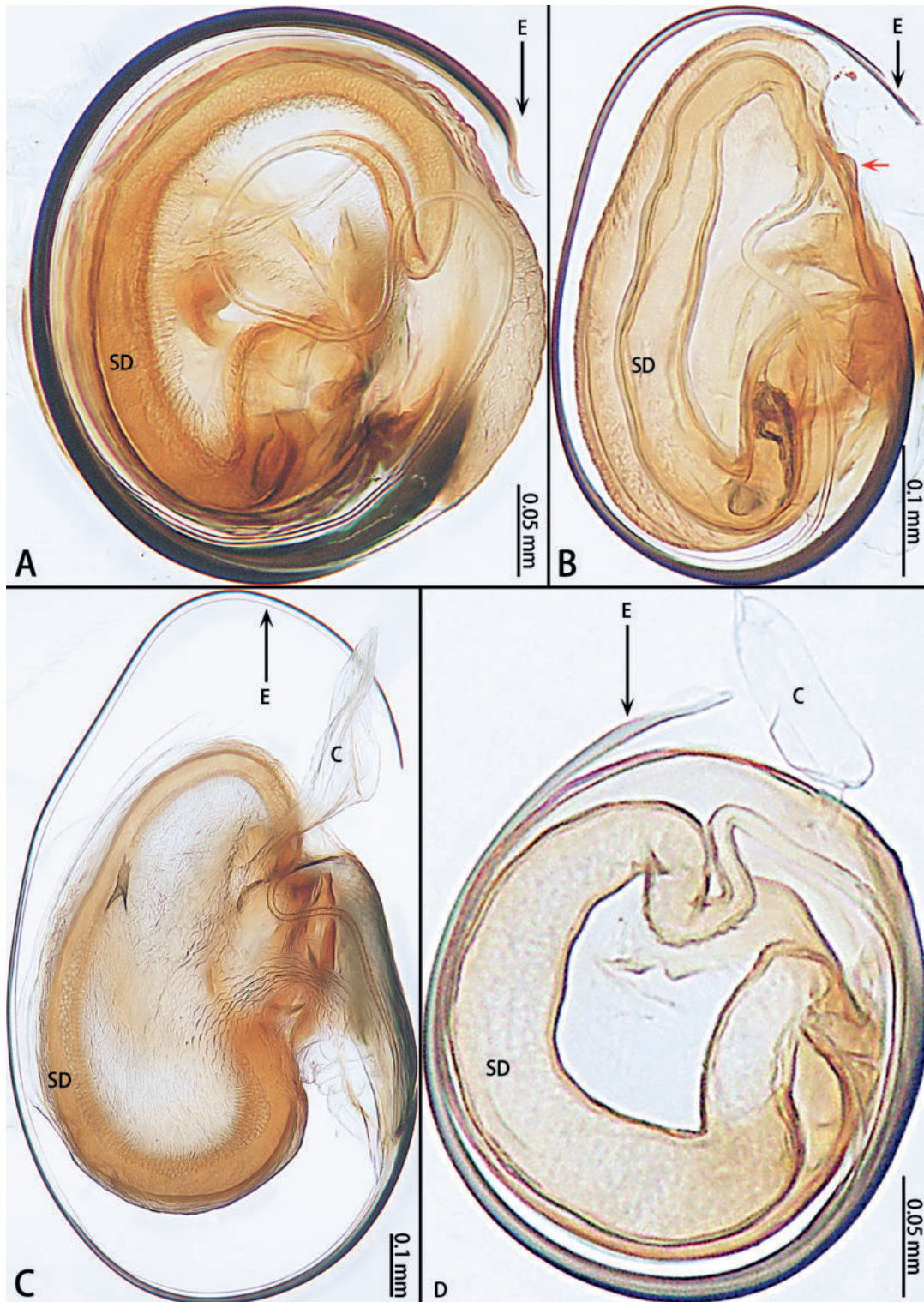


Figure 3. Paratype male bulbs, ventral view **A** *Goblinia tiane* sp. nov. **B** *Myahnia kanpetlet* sp. nov. **C** *Troghlohnia qiubei* sp. nov. **D** *Typhlohnia rongshui* sp. nov. Red arrows show the tegular outgrowth. Abbreviations: C = conductor, E = embolus, SD = sperm duct.

and interdistances: AME 0.04, ALE 0.07, PME 0.06, PLE 0.06; AME–AME 0.03, AME–ALE 0.01, PME–PME 0.07, PME–PLE 0.03, ALE–PLE 0.01. MOA 0.15 long, front width 0.09, back width 0.18. Clypeus 0.11 high. Leg measurements: I 2.42 (0.74, 0.31, 0.50, 0.49, 0.38); II 2.46 (0.73, 0.31, 0.48, 0.51, 0.43); III 2.58

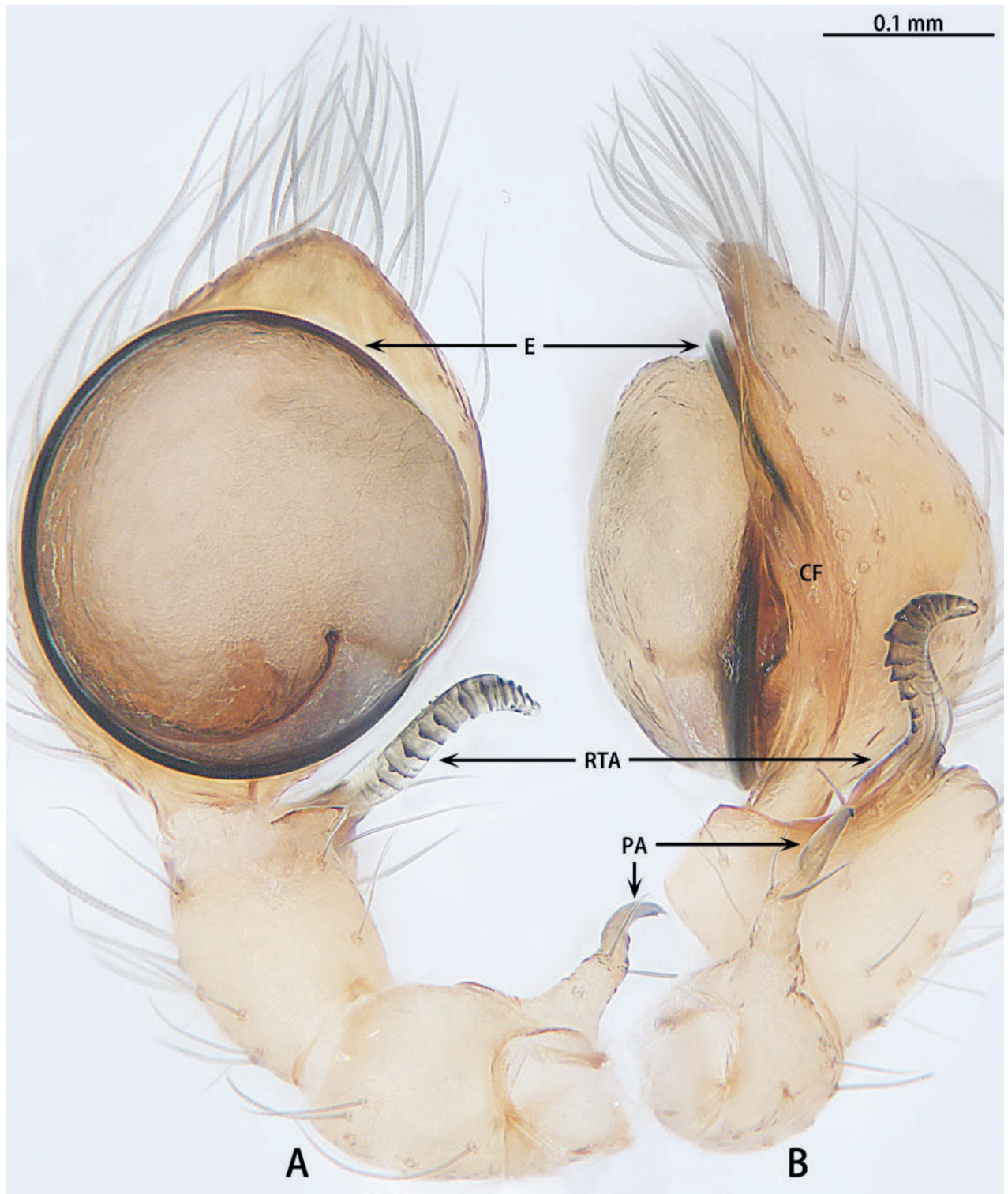


Figure 4. *Goblinia tiane* sp. nov., holotype male **A** ventral view **B** retrolateral view. Abbreviations: CF = cymbial furrow, E = embolus, PA = patellar apophysis, RTA = retrolateral tibial apophysis.

(0.73, 0.31, 0.52, 0.57, 0.45); IV 3.25 (0.88, 0.32, 0.71, 0.76, 0.58). Leg spination: patellae I–IV d1; tibiae I–II d1, III–IV p1 d2 r1; metatarsi III p1 d1 r1, IV p1 r1 v1.

Coloration (Fig. 6B). As in male but opisthosoma without pattern.

Epigyne (Fig. 5A, B). Epigynal plate 1.35× wider than long. Copulatory openings located anteriorly, round, touching each other. Copulatory ducts inter-

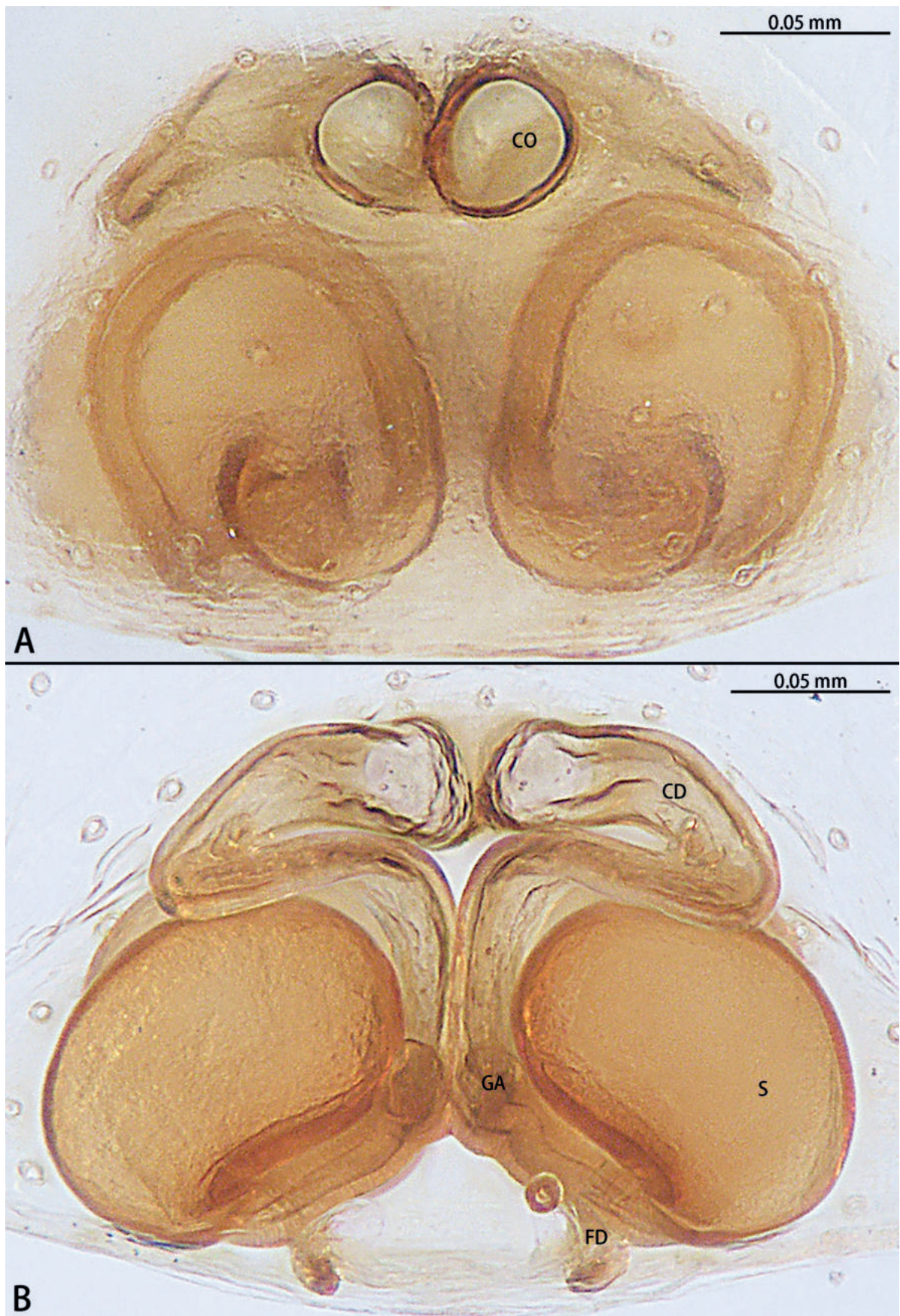


Figure 5. *Goblina tiane* sp. nov., paratype female **A** epigyne, ventral view **B** vulva, dorsal view. Abbreviations: CD = copulatory duct, CO = copulatory opening, FD = fertilization duct, GA = glandular appendage, S = spermatheca.



Figure 6. *Goblinia tiane* sp. nov., habitus, dorsal view **A** male holotype **B** female paratype.

twined, basal part with sharp twist, middle and distal part coiled twice around margin of spermathecae. Glandular appendages round, originating submedially to copulatory ducts, touching each other. Spermathecae oval, 4× wider than copulatory openings. Fertilization ducts directed at 11:00 o'clock position from spermathecae.

Variation. Males ($n = 4$): total body length 1.89–2.40, carapace 0.87–1.09 long, 0.76–0.88 wide, opisthosoma 0.98–1.31 long, 0.71–0.98 wide. Females ($n = 4$): total body length 1.96–2.55, carapace 0.80–0.96 long, 0.63–0.77 wide, opisthosoma 1.09–1.59 long, 0.81–1.18 wide.

Etymology. The specific epithet refers to the type locality; noun in apposition.

Distribution. Known only from the type locality (Fig. 30).

Genus *Myahnia* Lin & Li, gen. nov.

<https://zoobank.org/317A5532-7E8A-4393-9234-A1D857D1BD48>

Type species. *Myahnia kanpetlet* sp. nov. from Chin, Myanmar.

Diagnosis. *Myahnia* gen. nov. can be distinguished from *Hexamatia* Rivera-Quiroz, Petcharad & Miller, 2020 by the larger body size > 1.49 mm (Fig. 9A, B) [vs 1 mm (see Rivera-Quiroz et al. 2020: fig. 2a–c)], chelicerae with stridulatory files (Fig. 1B) (vs without), relatively longer cymbial furrow bend almost 0.5×

length of cymbium (Fig. 7B) [vs almost 0.25× (see Rivera-Quiroz et al. 2020: fig. 3b)], conductor absent (Figs 3B, 7A) [vs present (see Rivera-Quiroz et al. 2020: fig. 3a, b, d, e)], sperm duct with U-shaped curve (Fig. 3B) [vs circular (see Rivera-Quiroz et al. 2020: fig. 3a, c)] and base of copulatory ducts membranous (Fig. 8B) [vs sclerotized (see Zhang et al. 2011: fig. 23E)].

Description. Male. Small size. Carapace yellow, covered with few black setae. Six eyes in two rows; AME absent, PER longer than AER, PER procurved. ALE separated by almost their diameter; PME separated by longer than their diameter; ALE and PLE almost touching. Clypeus yellow, covered with several setae. Chelicerae yellow, with two promarginal and three retromarginal teeth, stridulatory files striped. Endites, labium yellow, covered with few black setae. Sternum coloured as endites, covered with brown setae. Legs yellow. Opisthosoma oval, grey without pattern. Spinnerets grey, straight in posterior view. Tracheal spiracle long and transverse, distance of spiracle to epigastric furrow as long as to spinnerets.

Palpal femur almost 3× longer than patella, spineless. Patella longer than tibia, with retroventral apophysis. Tibia with long, curved serrated retrolateral apophysis. Cymbium 1.7× longer than wide, cymbial furrow almost 0.5× longer than cymbium. Bulb oval, without conductor, with sclerotized apophysis retrolaterally. Embolus whip-shaped, starting at ca 3:00–5:00 o'clock position, curving clockwise along tegular margin.

Female. Total length 1.49–1.76 ($n = 4$). Somatic characters as in male but body pale yellow and stridulatory files absent.

Epigynal plate 2× wider than long. Copulatory openings located posteriorly, unobvious. Copulatory ducts curved, basal part wide and laminar. Vulva with two pairs of spermathecae. Fertilization ducts small, sickle-shaped.

Etymology. The new generic name is a combination of *Myanmar* and *Hahnia*. The gender is feminine.

Composition. Currently monotypic: *Myahnia kanpetlet* sp. nov.

Distribution. Myanmar (Fig. 30).

***Myahnia kanpetlet* Lin & Li, sp. nov.**

<https://zoobank.org/4C1D6538-FBA1-405C-8B59-0D1AF5ACD45F>

Figs 1B, 3B, 7A, B, 8A, B, 9A, B, 30

Type material. Holotype: ♂ (IZCAS-Ar44659), Myanmar, Chin State: Near 16.5 km of the roadside between Kanpetlet to Nat Ma Taung National Park, 21.2199°N, 93.2687°E, ca 2789 m, 30.IV.2017, Y. Li and Z. Chen leg. **Paratypes:** 1♂ 4♀ (IZCAS-Ar44660–Ar44664), same data as holotype.

Diagnosis. Same as for genus.

Description. Male (holotype; Figs 7A, B, 9A). Total body length 2.15. Carapace 1.02 long, 0.77 wide; opisthosoma 1.13 long, 0.81 wide. PER procurved slightly. Eye sizes and interdistances: ALE 0.05, PME 0.04, PLE 0.05; PME–PME 0.06, PME–PLE 0.01, ALE–PLE 0.01. Clypeus 0.03 high. Leg measurements: I 2.75 (0.85, 0.34, 0.69, 0.51, 0.36); II 2.37 (0.75, 0.33, 0.52, 0.44, 0.33); III 1.98 (0.59, 0.28, 0.36, 0.44, 0.31); IV 2.47 (0.77, 0.31, 0.56, 0.45, 0.38). Leg spination: femora I–II d1; patellae I–IV d1; tibiae III p1 d1 r1 v2, IV p1 r2 v2; metatarsi III p1 d1 r1, IV p1 r1.

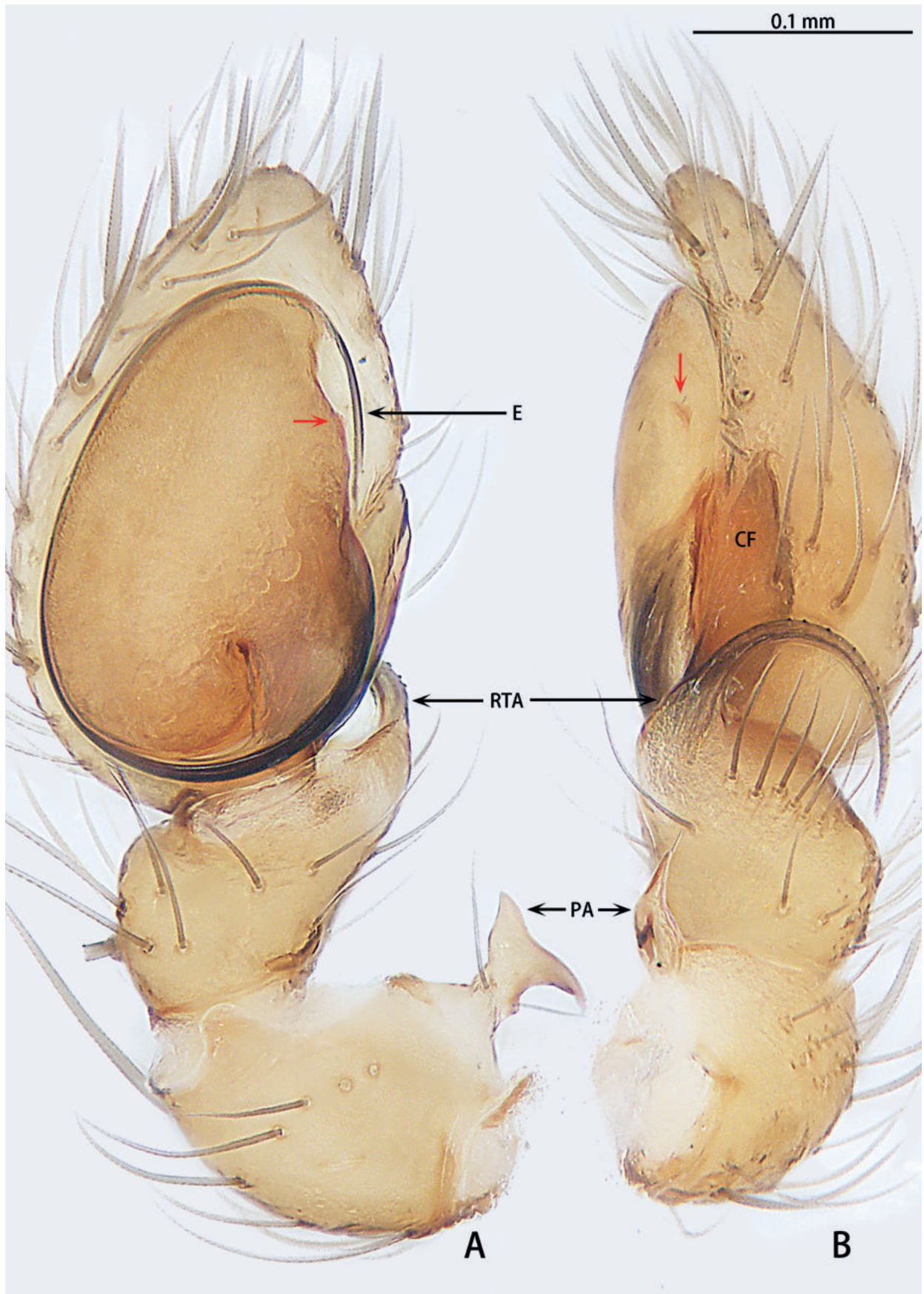


Figure 7. *Myahnia kanpetlet* sp. nov., holotype male **A** ventral view **B** retrolateral view. Red arrows show the tegular outgrowth. Abbreviations: CF = cymbial furrow, E = embolus, PA = patellar apophysis, RTA = retrolateral tibial apophysis.

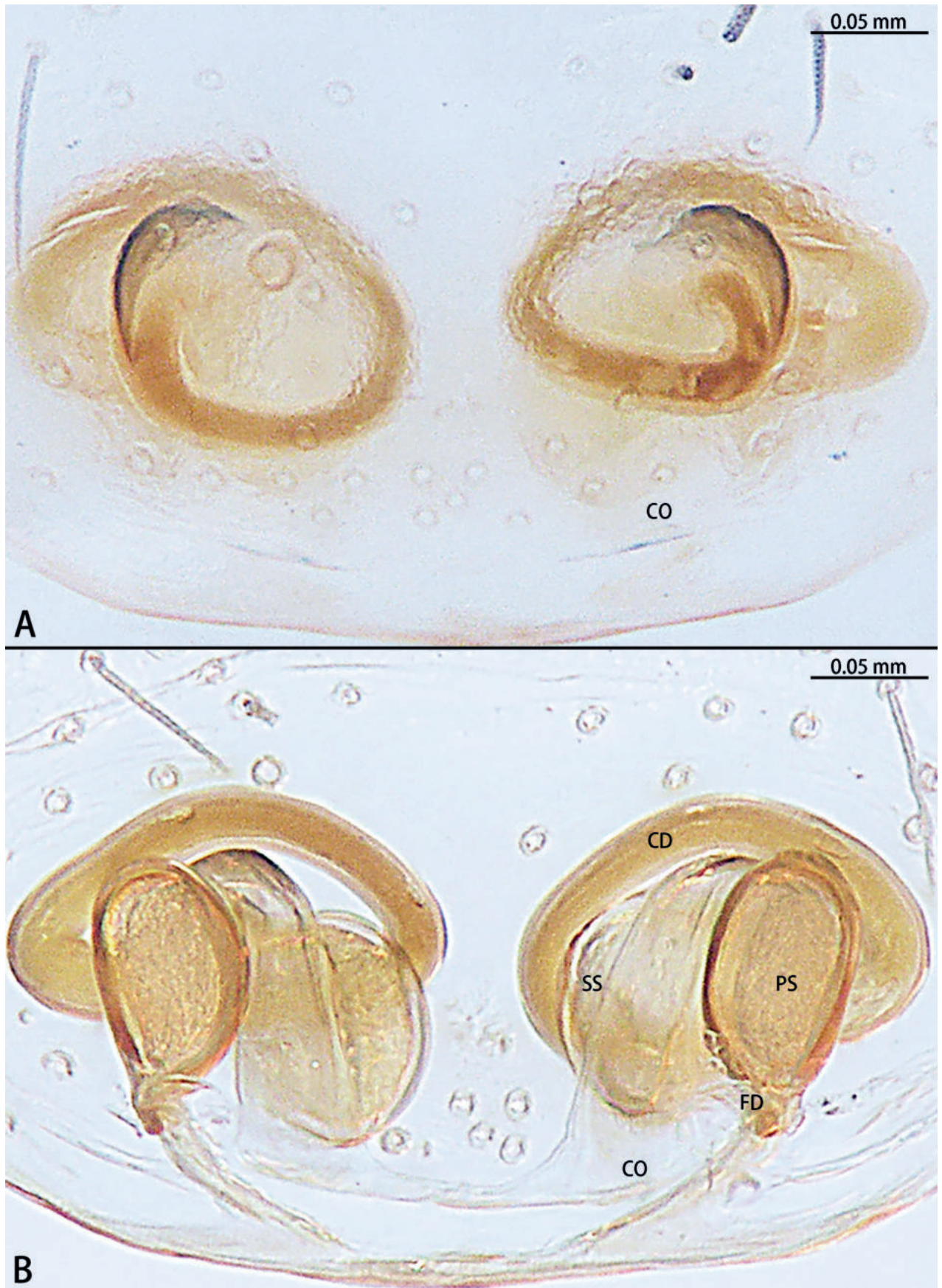


Figure 8. *Myahnia kanpetlet* sp. nov., paratype female **A** epigyne, ventral view **B** vulva, dorsal view. Abbreviations: CD = copulatory duct, CO = copulatory opening, FD = fertilization duct, PS = primary spermatheca, SS = secondary spermatheca.



Figure 9. *Myahnia kanpetlet* sp. nov., habitus, dorsal view **A** male holotype **B** female paratype.

Coloration (Fig. 9A). Carapace yellow, with dark yellow radial grooves. Fovea reddish-brown. Chelicerae, labium and gnathocoxae yellow; sternum yellowish. Sternum without markings. Legs yellow. Opisthosoma oval, grey. Spinnerets grey.

Palp (Fig. 7A, B). Patellar apophysis tip widening; distal part wider than apophysis length. Retrolateral tibial apophysis curved and serrated, almost as long as tibia, C-shaped in retrolateral view. Cymbium elongate egg-shaped, ca 1.7× longer than wide, cymbial furrow almost 2× shorter than cymbium. Bulb oval. Conductor absent, but tegular outgrowth present, sclerotized, located retrolaterally (arrowed in Figs 3B, 7A, B). Middle of sperm duct bent in U-shape. Embolus slender and whip-shaped; base of embolus arising at 3:00–5:00 o'clock position, clockwise, makes ~ 360° loop.

Female (paratype IZCAS-Ar44664; Figs 8A, B, 9B). Total body length 1.76. Carapace 0.69 long, 0.50 wide; opisthosoma 1.07 long, 0.78 wide. Eye sizes and interdistances: ALE 0.03, PME 0.01, PLE 0.02; PME–PME 0.05, PME–PLE 0.01, ALE–PLE 0.02. Clypeus 0.02 high. Leg measurements: I 1.56 (0.48, 0.20, 0.35, 0.28, 0.25); II 1.38 (0.42, 0.19, 0.28, 0.25, 0.24); III 1.24 (0.37, 0.18, 0.22, 0.26, 0.21); IV 1.62 (0.48, 0.20, 0.34, 0.34, 0.26). Leg spination: femora I–III d1; patellae I–IV d1; tibiae III–IV p1 d1 r1 v1; metatarsi III–IV p1 d1 r1.

Coloration (Fig. 9B). As in male but body pale yellow.

Epigyne (Fig. 8A, B). Copulatory openings large, ~ 4× shorter than epigyne width, located on posterior edge. Copulatory ducts intertwined, shorter part with twist, longer part with two twists. Secondary spermathecae oval, almost as long as primary spermatheca. Primary spermathecae elongate. Fertilization ducts directed at 10:00 o'clock position from spermathecae.

Variation. Females ($n = 3$): total body length 1.49–1.76, carapace 0.68–0.71 long, 0.50–0.52 wide, opisthosoma 0.81–1.05 long, 0.60–0.75 wide.

Etymology. The specific epithet refers to the type locality; noun in apposition.

Distribution. Known only from the type locality (Fig. 30).

Genus *Troglohnia* Lin & Li, gen. nov.

<https://zoobank.org/1D333387-6E69-4CCB-862E-256EE2EECB15>

Type species. *Troglohnia qiubei* sp. nov. from Yunnan, China.

Diagnosis. *Troglohnia* gen. nov. can be distinguished from all other genera of Hahniidae by having stridulatory files on sides of pars cephalica (Figs 1C, 2B), strongly modified patella 1.5–2× wider than tibia (Figs 10A, 12A, 15A), retrolateral tibial apophysis with two arms (Figs 10B, 12B, 15B), edge of cymbial furrow S-shaped (Figs 10B, 12B, 15B), base of embolus with tooth and embolus running along tegulum, on some distance, basal part rises from tegular bend at 90° (Figs 10A, 12A, 15A), genital groove with a pair of hoods posteriorly, distance between hoods almost 1.5–2× longer than length of epigynal plate (Fig. 18A–D), and copulatory ducts with a fork at the expanded part of them (Fig. 18A–D).

Description. Male. Total length 2.33–3.21 ($n = 8$). Carapace yellowish, middle region with indistinct brown band, margin with brown pattern, lateral cephalic region with stridulatory files. PER longer than AER, AER straight, PER procurved. AME separated by less than diameter; PME separated by almost diameter, approximately as far from ALE; distance between AME and PME longer than that between ALE and PLE; ALE and PLE almost touching. Clypeus pale yellow, covered with several setae. Chelicerae pale yellow, with two or three promarginal and three or four retromarginal teeth, chelicerae with stridulatory files. Endites, labium pale yellow, covered with few black setae. Sternum brown, covered with brown setae. Legs pale yellow. Opisthosoma grey, middle of anteriorly and laterally with rod-shaped brown patterns, middle of posteriorly with inverted V-shaped brown patterns; venter with brown patterns and brown ring around spinnerets. Spinnerets base brown and tip white, straight in posterior view. Tracheal spiracle long and transverse, located at 3/4 of opisthosoma length.

Palpal femur almost 2× longer than patella, spineless. Patella modified, strongly swollen, longer and > 1.5× wider than tibia. Retrolateral tibial apophysis with 2 sickle-shaped and without serrated arms, basal with an apophysis

with a line of setae. Cymbium kidney-shaped, ~ 1.5× longer than wide. Cymbial furrow S-shaped, almost as long as cymbium. Bulb almost oval, ca 1.23× longer than wide. Sperm duct with U-shaped curve (Fig. 3C). Conductor almost 0.5× longer than bulb, length of stalk almost 1/3–1/2 of total conductor length. Embolic base wide, with embolic tooth. Embolus starting at ca 1:30–4:00 o'clock from tegular, curving clockwise, embolic tip covered by bulb.

Female. Total length 2.25–3.86 ($n = 21$). Somatic characters as in male but chelicerae with three promarginal and three or four retromarginal teeth, stridulatory files absent.

Epigynal plate almost 1.3–1.45× wider than long, genital groove with a pair of posterior hoods. Copulatory openings located medium, arc-shaped. Copulatory ducts long, strongly convoluted, base thick, bifurcate, then become thinner; short one connected to secondary spermathecae, other connected to primary spermathecae. Primary spermathecae oval or bean-shaped, secondary spermathecae globular. Fertilization ducts laminar, sickle-shaped.

Etymology. The new generic name is a combination of *Troglobiont* (refers to the cave habitat) and *Hahnia*. The gender is feminine.

Composition. This new genus includes four species: *Troglohnia dafang* sp. nov. (♂♀), *T. qiubei* sp. nov. (♂♀), *T. shidian* sp. nov. (♀), and *T. wuding* sp. nov. (♂♀).

Distribution. China (Guizhou, Yunnan) (Fig. 30).

***Troglohnia dafang* Lin & Li, sp. nov.**

<https://zoobank.org/5D13FD4B-1068-464F-8E04-6373ACEEB637>

Figs 10A, B, 11A, B, 17A, 18A, 19A, 20A, B, 30

Type material. Holotype: ♂ (IZCAS-Ar44666), CHINA, Guizhou: Dafang County, Sanhe Villiage, Yelaoda Cave, 27.1817°N, 105.4713°E, ca 1438 m, 03.V.2007, Y. Li and J. Liu leg. **Paratypes:** 1♂ 4♀ (IZCAS-Ar44667–Ar44671), same data as holotype.

Diagnosis. *Troglohnia dafang* sp. nov. can be distinguished from *T. qiubei* sp. nov. by the tip of patellar apophysis pointed to 9:30 o'clock position (Fig. 17A) [vs 10:30 o'clock position (Fig. 17B)], ventral retrolateral tibial apophysis almost as long as dorsal retrolateral tibial apophysis (Fig. 10B) [vs 1:2 (Fig. 12B)], conductor stalk makes up 1/3 of total conductor length (Fig. 10A) [vs 1/2 (Fig. 12A)], process on tegulum absent (Fig. 10A) [vs present (arrowed in Fig. 12A)], copulatory openings touching each other (Fig. 11A) [vs facing each other (Fig. 13A)], diameter of primary spermathecae ~ 2× diameters of secondary spermathecae (Fig. 11B) [vs 1.5× (Fig. 13B)], distance between primary spermathecae and secondary spermathecae ~ 2× diameters of secondary spermathecae (Fig. 11B) [vs 1× (Fig. 13B)], secondary spermathecae separated by ~ 4× diameters (Fig. 11B) [vs 1.5× (Fig. 13B)], and fertilization ducts pointing to 9:00 o'clock position (Fig. 11B) [vs 7:30 o'clock position (Fig. 13B)]. Females of *T. dafang* sp. nov. can be distinguished from those of *T. shidian* sp. nov. by the ratio of diameter of secondary spermathecae to length of branched shorter copulatory ducts almost 1:2 (Fig. 11B) [vs 1:1 (Fig. 14B)], primary spermathecae elongate bean-shaped, separated by less than one diameter (Fig. 11B) [vs oval, separated by more than 2× diameters (Fig. 14B)], diameter of primary spermathecae ~ 2× diameters of secondary spermathecae (Fig. 11B) [vs 1.2× (Fig. 14B)], distance between pri-

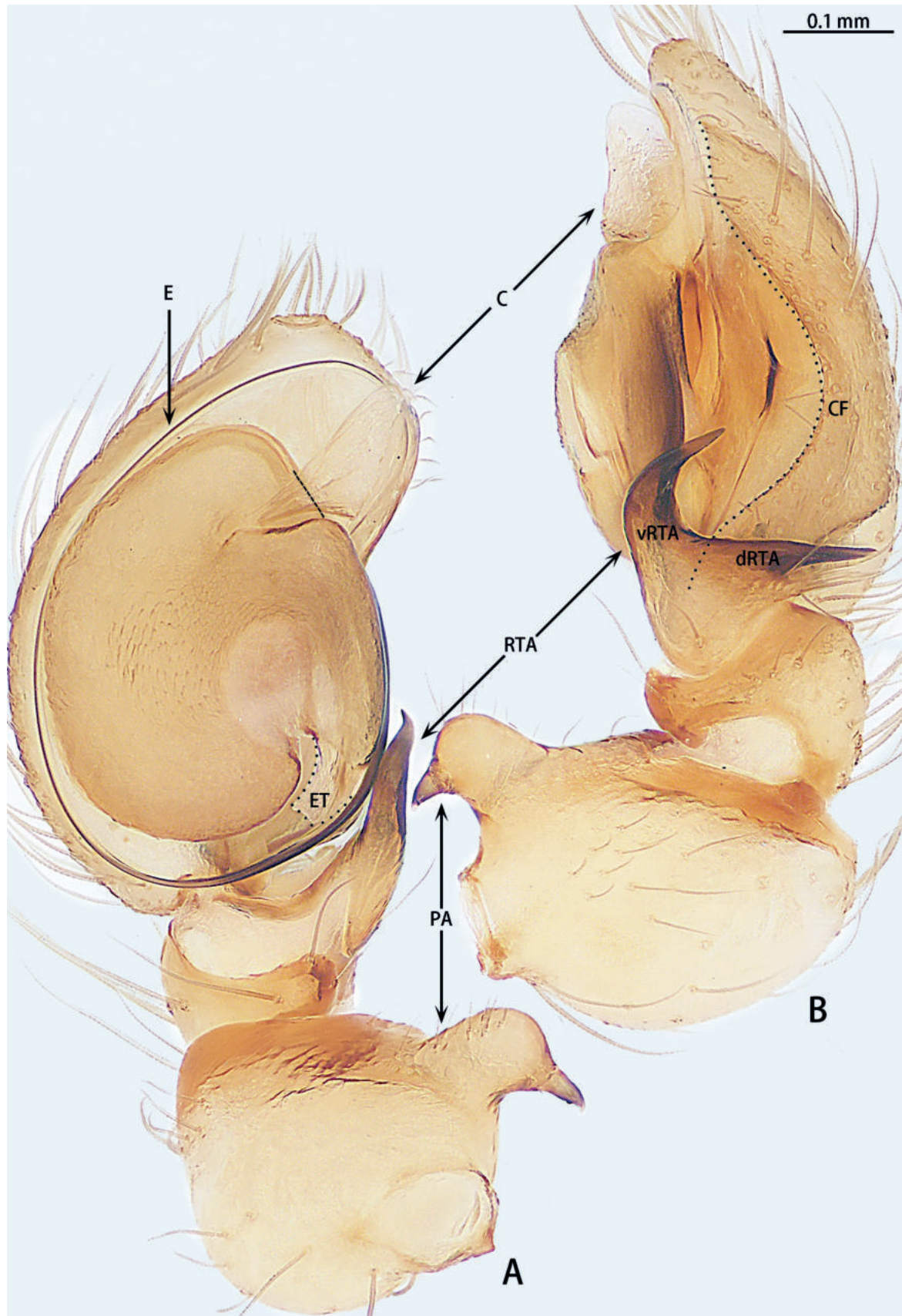


Figure 10. *Troglohnia dafang* sp. nov., holotype male **A** ventral view **B** retrolateral view. Dashed line shows conductor stalk. Abbreviations: C = conductor, CF = cymbial furrow, dRTA = dorsal retrolateral tibial apophysis, E = embolus, ET = embolic tooth, PA = patellar apophysis, RTA = retrolateral tibial apophysis, vRTA = ventral retrolateral tibial apophysis.

primary spermathecae and secondary spermathecae ~ 2× diameters of secondary spermathecae (Fig. 11B) [vs 1× (Fig. 14B)] and secondary spermathecae separated by ~ 4× diameters (Fig. 11B) [vs 3× (Fig. 14B)].

Description. Male (holotype; Figs 10A, B, 17A, 20A). Total body length 2.47. Carapace 1.18 long, 0.97 wide; opisthosoma 1.29 long, 0.94 wide. Eye sizes and interdistances: AME 0.05, ALE 0.08, PME 0.07, PLE 0.06; AME–AME 0.03, AME–ALE 0.02, PME–PME 0.09, PME–PLE 0.04, ALE–PLE 0.03. MOA 0.16 long, front width 0.10, back width 0.19. Clypeus 0.18 high. Chelicerae with three promarginal and four retromarginal teeth. Leg measurements: I 4.09 (1.18, 0.41, 0.96, 0.86, 0.68); II 3.88 (1.11, 0.41, 0.86, 0.83, 0.67); III 3.44 (0.93, 0.33, 0.75, 0.81, 0.62); IV 4.35 (1.15, 0.39, 1.02, 1.08, 0.71). Leg spination: patella III d1; tibiae III p1 d1 v1, IV p1 d1 r1 v1.

Coloration (Fig. 20A). Carapace yellowish, middle region with indistinct brown band, margin with brown pattern. Fovea reddish-brown. Chelicerae, labium, gnathocoxae, and sternum yellowish. Sternum with dark marking. Legs yellowish. Opisthosoma oval, grey, middle of anteriorly and laterally with rod-shaped brown patterns, middle of posteriorly with inverted V-shaped brown patterns; venter with brown patterns and brown ring around spinnerets. Spinnerets base brown and tip white.

Palp (Figs 10A, B, 17A). Patellar apophysis with wide base and narrowed tip, the narrowed tip shorter than the wide base. Ventral retrolateral tibial apophysis curved, almost as long as dorsal retrolateral tibial apophysis, but wider. Cymbium 1.5× longer than wide. Cymbial furrow almost as long as cymbium. Bulb almost oval. Medium of tegulum with globular membranous area. Length of stalk of conductor almost 1/3 of total conductor length. Embolic tooth terminal flat. Embolus slender and whip-shaped.

Female (paratype IZCAS-Ar44671; Figs 11A, B, 18A, 19A, 20B). Total body length 2.41. Carapace 0.92 long, 0.69 wide; opisthosoma 1.50 long, 1.16 wide. Eye sizes and interdistances: AME 0.03, ALE 0.09, PME 0.08, PLE 0.09; AME–AME 0.01, AME–ALE 0.02, PME–PME 0.09, PME–PLE 0.04, ALE–PLE 0.01. MOA 0.18 long, front width 0.10, back width 0.21. Clypeus 0.17 high. Chelicerae with three promarginal and three retromarginal teeth. Leg measurements: I 3.35 (0.99, 0.37, 0.75, 0.70, 0.54); II 3.17 (0.91, 0.36, 0.69, 0.68, 0.53); III 3.04 (0.89, 0.34, 0.63, 0.70, 0.48); IV 3.85 (1.07, 0.37, 0.93, 0.91, 0.57). Leg spination: femora I–III d1; patellae III–IV d1; tibiae III p1 d1 v1, IV p1 d1 r1 v2; metatarsi III d1 v2, IV p1 v2.

Coloration (Fig. 20B). As in male but body yellow.

Epigyne (Figs 11A, B, 18A, 19A). Epigynal plate 1.3× wider than long. Hoods 3× deeper than wide. The posterior edge of copulatory openings touching, slightly curved. The width of thick copulatory ducts base 2× wider than the thinner part. The branched shorter copulatory ducts connected to the secondary spermathecae, the other connected to the primary spermathecae. Primary spermathecae elongate bean-shaped, 2× wider than the secondary spermathecae. Fertilization ducts directed at 9:00 o'clock position from spermathecae.

Variation. Male: total body length 2.33, carapace 1.15 long, 0.93 wide, opisthosoma 1.18 long, 0.92 wide. Females ($n = 3$): total body length 2.25–2.88, carapace 1.00–1.14 long, 0.73–0.88 wide, opisthosoma 1.23–1.74 long, 0.86–1.30 wide.

Etymology. The specific epithet refers to the type locality; noun in apposition.

Distribution. Known only from the type locality (Fig. 30).

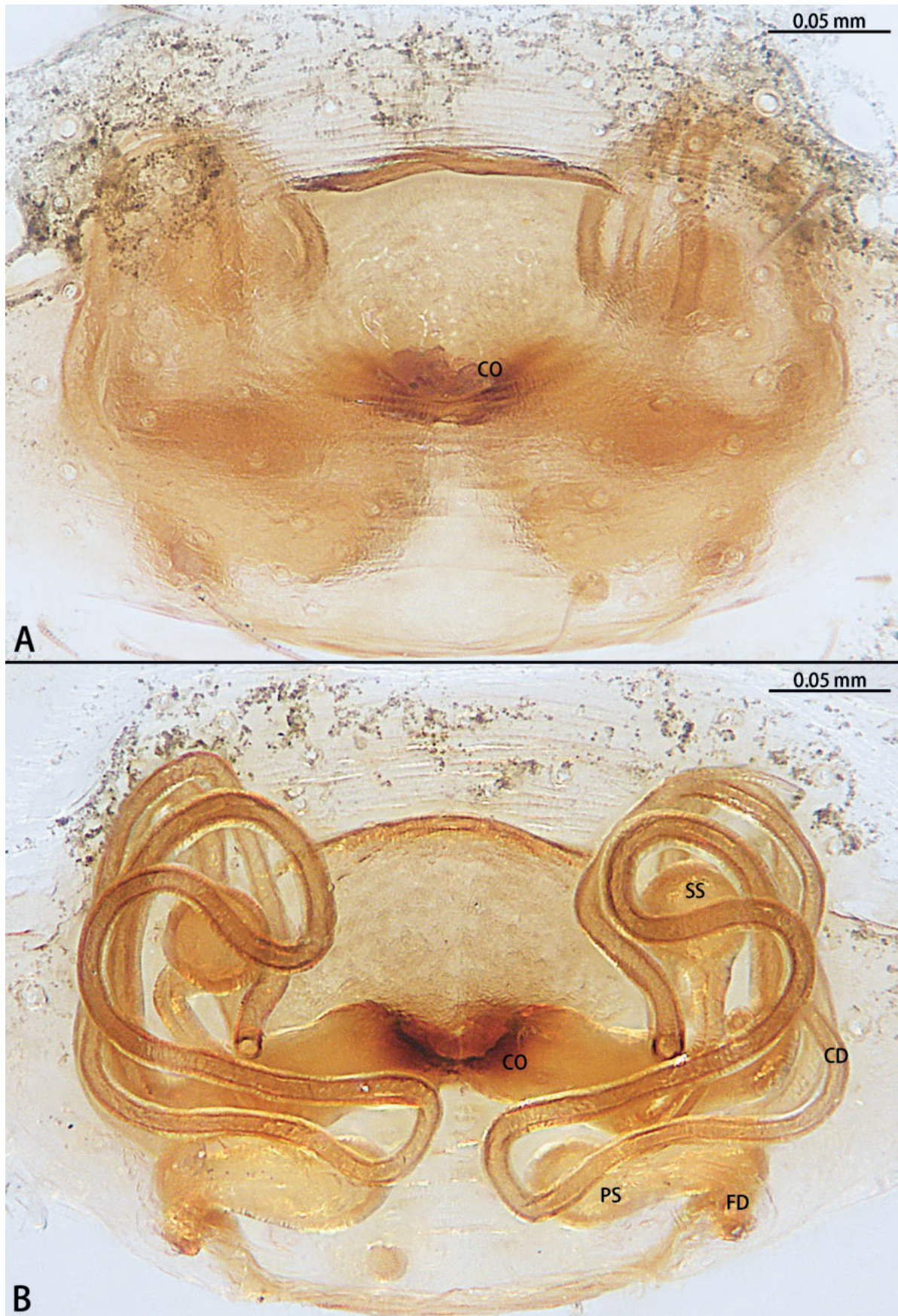


Figure 11. *Troglohnia dafang* sp. nov., paratype female **A** epigyne, ventral view **B** vulva, dorsal view. Abbreviations: CD = copulatory duct, CO = copulatory opening, FD = fertilization duct, PS = primary spermatheca, SS = secondary spermatheca.

***Troglohnia qiubei* Lin & Li, sp. nov.**

<https://zoobank.org/ECD0EC6E-BD4B-41F3-931F-A49F6E2F589F>

Figs 1C, 2B, 3C, 12A, B, 13A, B, 17B, 18B, 19B, 20C, D, 30

Type material. Holotype: ♂ (IZCAS-Ar44672), CHINA, Yunnan: Wenshan Zhuang and Miao Autonomous Pref., Qiubei County, Shuanglongying Town, Puzhehei Villiage, Dongjiadashi Cave, 24.1422°N, 104.0990°E, ca 1455 m, 19.VIII.2010, Z. Yao, X. Wang and C. Wu leg. **Paratypes:** 5♂ 5♀ (IZCAS-Ar44673–Ar44682), same data as holotype.

Diagnosis. *Troglohnia qiubei* sp. nov. can be distinguished from *T. wuding* sp. nov. by the male ventral retrolateral tibial apophysis almost straight and as wide as dorsal retrolateral tibial apophysis (Fig. 12B) [vs strongly curved and wider than dorsal retrolateral tibial apophysis (Fig. 15B)], embolic tooth terminal flat (Fig. 12A) [vs terminal finger-shaped (Fig. 15A)], process on anterior 1/3 of tegulum (arrowed in Fig. 12A) [vs on anterior 3/5 (arrowed in Fig. 15A)] and female can be distinguished by the diameter of secondary spermathecae less than diameter of primary spermathecae (Fig. 13B) [vs almost same diameter (Fig. 16B)], distance between primary spermathecae and secondary spermathecae more than half of diameter of secondary spermathecae (Fig. 13B) [vs less than half of diameter (Fig. 16B)], secondary spermathecae separated by ~ 1.5× diameters (Fig. 13B) [vs 1× (Fig. 16B)] and fertilization ducts pointing to 7:30 o'clock position (Fig. 13B) [vs 9:00 o'clock position (Fig. 16B)]. *T. qiubei* sp. nov. also resembles *T. dafang* sp. nov., but can be distinguished by the tip of patellar apophysis pointed to 10:30 o'clock position (Fig. 17B) [vs 9:30 o'clock position (Fig. 17A)], ventral retrolateral tibial apophysis shorter than dorsal retrolateral tibial apophysis (Fig. 12B) [vs almost as long as dorsal retrolateral tibial apophysis (Fig. 10B)], conductor stalk makes up 1/2 of total conductor length (Fig. 12A) [vs 1/3 (Fig. 10A)], process on tegulum present (Fig. 12A) [vs absent (Fig. 10A)], copulatory openings facing each other (Fig. 13A) [vs touching each other (Fig. 11A)], diameter of primary spermathecae ~ 1.5× diameters of secondary spermathecae (Fig. 13B) [vs 2× (Fig. 11B)], distance between primary spermathecae and secondary spermathecae ~ 1× diameter of secondary spermathecae (Fig. 13B) [vs 2× (Fig. 11B)], secondary spermathecae separated by ~ 1.5× diameters (Fig. 13B) [vs 4× (Fig. 11B)], and fertilization ducts pointing to 7:30 o'clock position (Fig. 13B) [vs 9:00 o'clock position (Fig. 11B)].

Description. Male (holotype; Figs 12A, B, 17B, 20C). Total body length 2.92. Carapace 1.34 long, 1.05 wide; opisthosoma 1.58 long, 1.16 wide. AER straight and PER procurved slightly. Eye sizes and interdistances: AME 0.04, ALE 0.09, PME 0.08, PLE 0.09; AME–AME 0.05, AME–ALE 0.01, PME–PME 0.08, PME–PLE 0.04, ALE–PLE 0.02. MOA 0.20 long, front width 0.11, back width 0.24. Clypeus 0.17 high. Chelicerae with three promarginal and four retromarginal teeth. Leg measurements: I 4.86 (1.39, 0.44, 1.12, 1.05, 0.86); II 4.64 (1.30, 0.45, 1.03, 1.04, 0.82); III 4.29 (1.18, 0.41, 0.95, 1.02, 0.73); IV 5.27 (1.40, 0.44, 1.21, 1.34, 0.88). Leg supination: femora I–III d1; tibiae III v2, IV d1 r1 v1; metatarsi III p1 v2, IV p1 r1 v2.

Coloration (Fig. 20C). Carapace yellowish, with indistinct dark yellow radial grooves, middle region with shield-shaped brown band, margin with brown pattern. Fovea longitudinal, reddish-brown. Ocular area with slight brown band; eight eyes without distinct black rims. Chelicerae, labium, gnathocoxae, and sternum yellowish. Sternum with brown marking and lighter heart region. Legs yellowish.

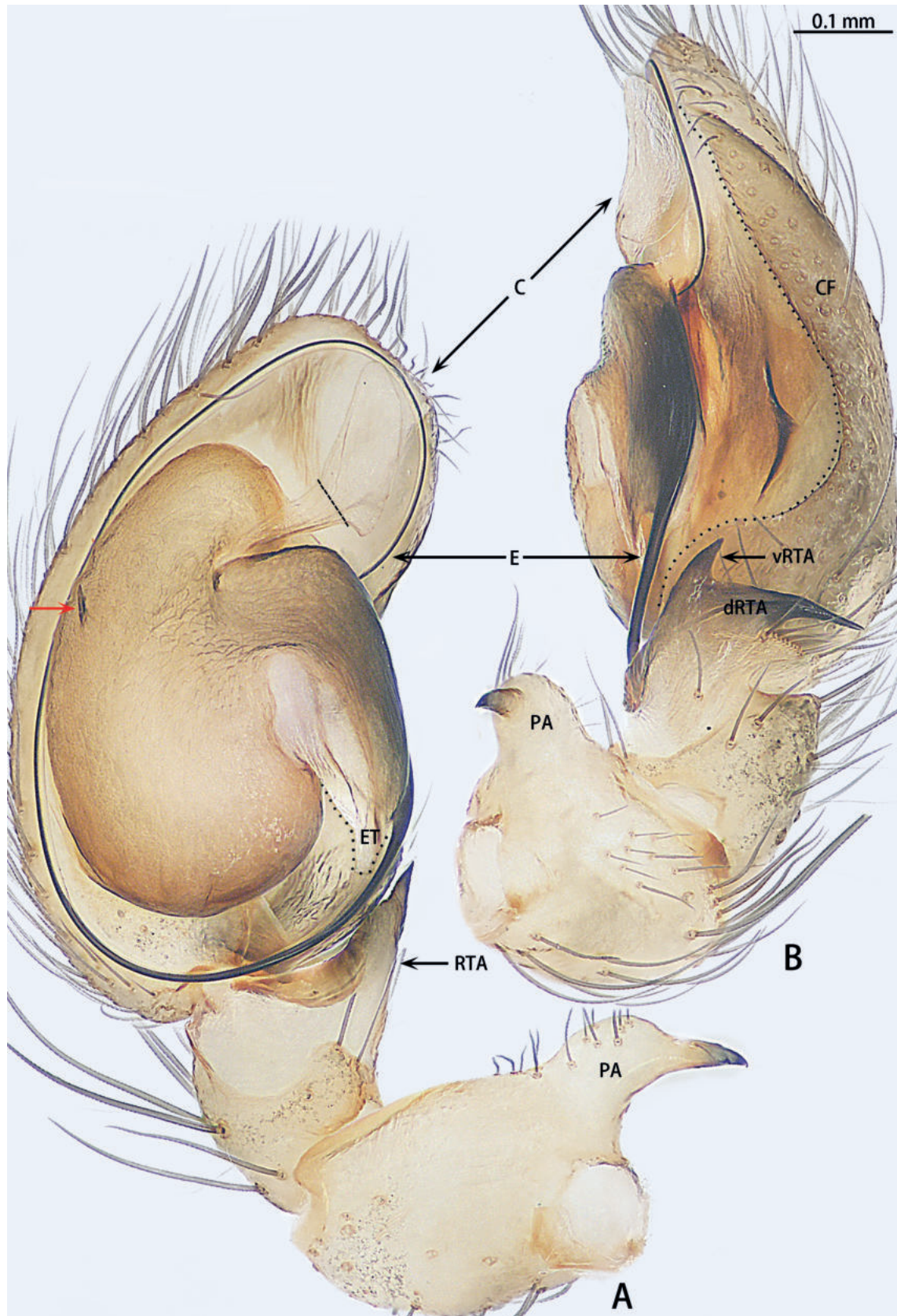


Figure 12. *Troglonnia qiubei* sp. nov., holotype male **A** ventral view **B** retrolateral view. Dashed line shows conductor stalk; red arrow shows the process on tegulum. Abbreviations: C = conductor, CF = cymbial furrow, dRTA = dorsal retrolateral tibial apophysis, E = embolus, ET = embolic tooth, PA = patellar apophysis, RTA = retrolateral tibial apophysis, vRTA = ventral retrolateral tibial apophysis.

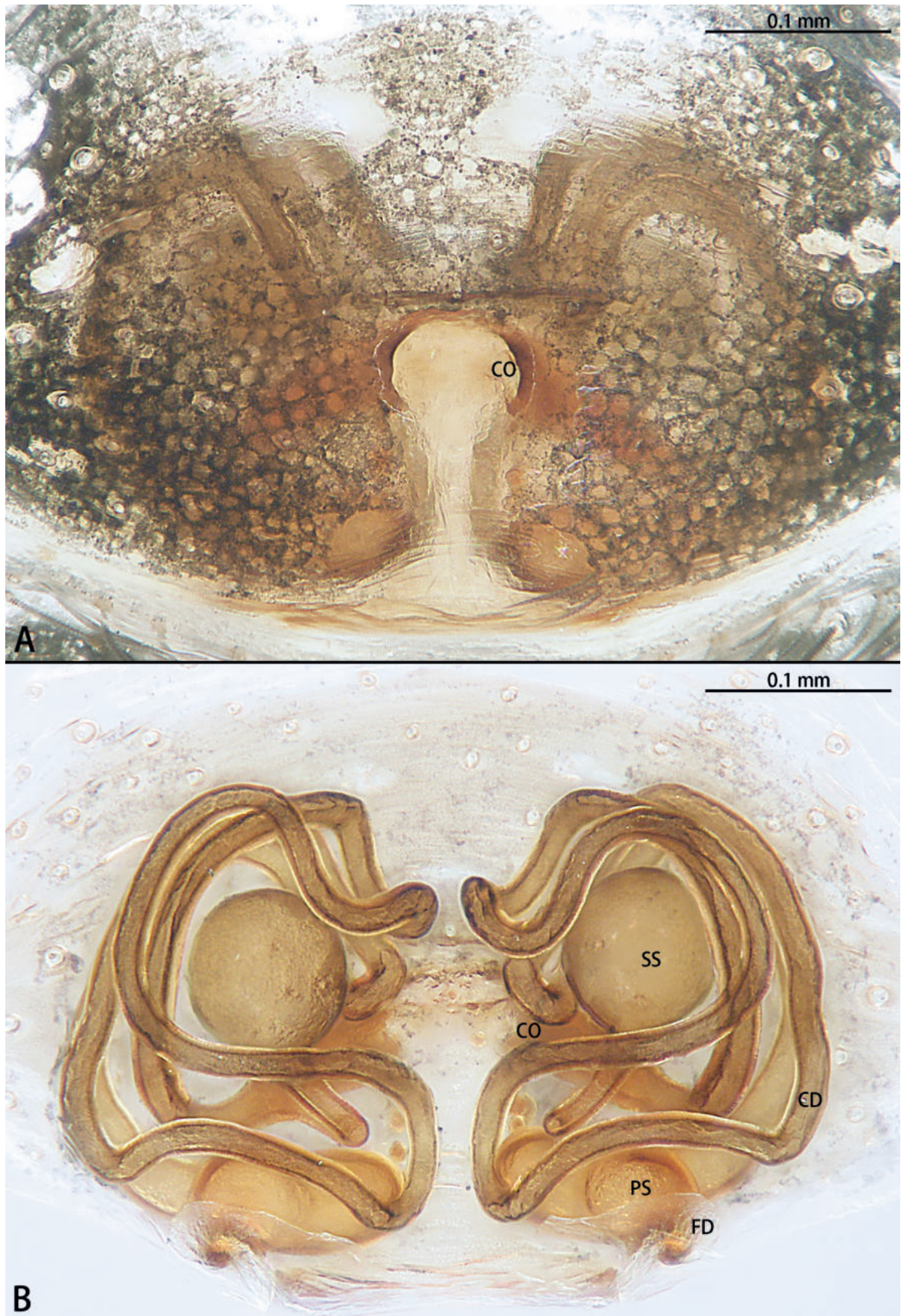


Figure 13. *Troglonnia qiubei* sp. nov., paratype female **A** epigyne, ventral view **B** vulva, dorsal view. Abbreviations: CD = copulatory duct, CO = copulatory opening, FD = fertilization duct, PS = primary spermatheca, SS = secondary spermatheca.

Opisthosoma oval, grey, middle of anteriorly and laterally with rod-shaped dark patterns, middle of posteriorly with inverted dark V-shaped patterns; venter with brown patterns and brown ring around spinnerets. Spinnerets base brown and tip white.

Palp (Figs 12A, B, 17B). Patellar apophysis with wide base and narrowed tip, the narrowed tip as long as the wide base. Ventral retrolateral tibial apophysis almost straight, almost 1/2× longer than dorsal retrolateral tibial apophysis and as wide as dorsal retrolateral tibial apophysis. Cymbium 1.5× longer than wide. Cymbial furrow almost as long as cymbium. Bulb almost oval. A triangle process presents at the prolateral edge of tegulum. Medium of tegulum with oval membranous area. Length of stalk of conductor almost half of total conductor length. Embolic tooth terminal flat. Embolus slender and whip-shaped.

Female (paratype IZCAS-Ar44682; Figs 13A, B, 18B, 19B, 20D). Total body length 3.39. Carapace 1.36 long, 1.04 wide; opisthosoma 2.03 long, 1.44 wide. Eight eyes with distinct black rims. Eye sizes and interdistances: AME 0.04, ALE 0.09, PME 0.08, PLE 0.09; AME–AME 0.03, AME–ALE 0.02, PME–PME 0.09, PME–PLE 0.04, ALE–PLE 0.02. MOA 0.20 long, front width 0.09, back width 0.23. Clypeus 0.17 high. Chelicerae with three promarginal and four retromarginal teeth. Leg measurements: I 4.51 (1.28, 0.46, 1.02, 0.99, 0.76); II 4.43 (1.28, 0.44, 0.98, 0.98, 0.75); III 4.25 (1.20, 0.44, 0.92, 1.03, 0.66); IV 5.37 (1.50, 0.45, 1.25, 1.32, 0.85). Leg supination: femora I–III d1; tibiae I v1, II v2, III p1 d2, r1, v3, IV p1 d2 r1 v2; metatarsi III p1 v2, IV p1 d2 r1 v1.

Coloration (Fig. 20D). As in male but carapace without shield-shaped band.

Epigyne (Figs 13A, B, 18B, 19B). Epigynal plate 1.45× wider than long. Hoods 3× depth than width. Copulatory openings arc-shaped, facing each other, circular. The width of thick copulatory ducts base 2× wider than the thinner part. The branched shorter copulatory ducts connected to the secondary spermathecae, the other connected to the primary spermathecae. Primary spermathecae bean-shaped, longer than the width of the secondary spermathecae. Fertilization ducts directed at 7:30 o'clock position from spermathecae.

Variation. Males ($n = 4$): total body length 2.54–3.21, carapace 1.10–1.47 long, 0.80–1.22 wide, opisthosoma 1.44–1.74 long, 1.09–1.20 wide. Females ($n = 4$): total body length 3.03–3.62, carapace 1.28–1.44 long, 1.08–1.16 wide, opisthosoma 1.68–2.30 long, 1.19–1.48 wide.

Etymology. The specific epithet refers to the type locality; noun in apposition.

Distribution. Known only from the type locality (Fig. 30).

***Troglohnia shidian* Lin & Li, sp. nov.**

<https://zoobank.org/5FBB3B13-DE99-4540-BD18-1EBBA8CCD693>

Figs 14A, B, 18C, 19C, 20E, F, 30

Type material. **Holotype:** ♀ (IZCAS-Ar44683), CHINA, Yunnan: Baoshan City, Shidian County, Bailang Town, Xianren Cave, 24.6536°N, 99.2645°E, ca 1987 m, 29.VII.2010, C. Wang, Q. Zhao and Y. Lin leg. **Paratype:** 1♀ (IZCAS-Ar44684), same data as holotype.

Diagnosis. *Troglohnia shidian* sp. nov. can be distinguished from those of *T. dafang* sp. nov. by the ratio of diameter of secondary spermathecae to length of branched shorter copulatory ducts almost 1:1 (Fig. 14B) [vs 1:2 (Fig. 11B)], primary spermathecae oval, separated by more than 2× diameters (Fig. 14B) [vs elongate

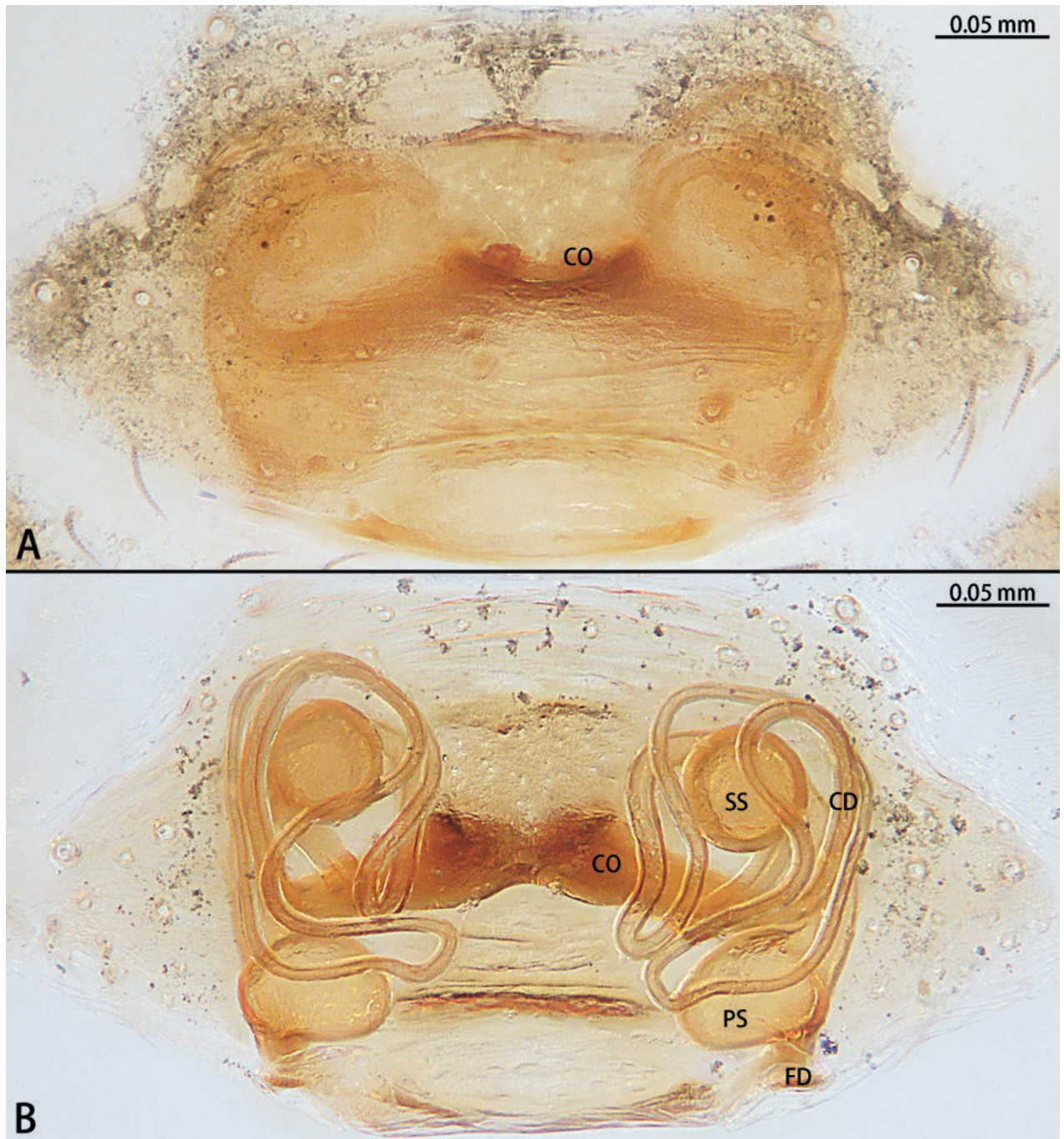


Figure 14. *Troglonnia shidian* sp. nov., holotype female **A** epigyne, ventral view **B** vulva, dorsal view. Abbreviations: CD = copulatory duct, CO = copulatory opening, FD = fertilization duct, PS = primary spermatheca, SS = secondary spermatheca.

bean-shaped, separated by less than one diameter (Fig. 11B)], diameter of primary spermathecae $\sim 1.2\times$ diameters of secondary spermathecae (Fig. 14B) [vs $2\times$ (Fig. 11B)], distance between primary spermathecae and secondary spermathecae $\sim 1\times$ diameter of secondary spermathecae (Fig. 14B) [vs $2\times$ (Fig. 11B)] and secondary spermathecae separated by $\sim 3\times$ diameters (Fig. 14B) [vs $4\times$ (Fig. 11B)].

Description. Female (holotype; Figs 14A, B, 18C, 19C, 20E, F). Total body length 3.75. Carapace 1.74 long, 1.33 wide; opisthosoma 2.01 long, 1.44 wide. AER straight and PER procurved slightly. Eye sizes and interdistances: AME 0.04, ALE 0.08, PME 0.07, PLE 0.09; AME–AME 0.03, AME–ALE 0.03, PME–PME 0.11,

PME–PLE 0.06, ALE–PLE 0.02. MOA 0.17 long, front width 0.10, back width 0.24. Clypeus 0.15 high. Chelicerae with three promarginal and four retromarginal teeth. Leg measurements: I 3.72 (1.08, 0.40, 0.86, 0.78, 0.60); II 3.61 (1.07, 0.38, 0.83, 0.76, 0.57); III 3.39 (0.98, 0.37, 0.71, 0.78, 0.55); IV 4.23 (1.19, 0.40, 1.01, 1.00, 0.63). Leg supination: femora I p1, II–III d1; patellae III–III d1; tibiae I–II p1 d1, III p1 d2 r1 v2, IV p1 d1 r1 v2; metatarsi III p1 d1 v2, IV p1 d2 r1 v2.

Coloration (Fig. 20E, F). Carapace yellow, with indistinct dark yellow radial grooves, middle region with shield-shaped brown band, margin with brown pattern. Fovea longitudinal, reddish-brown. Chelicerae, labium, gnathocoxae, and sternum yellow. Sternum with brown marking. Legs yellow. Opisthosoma oval, grey, middle of anteriorly and laterally with rod-shaped brown patterns, middle of posteriorly with inverted V-shaped brown patterns; venter with brown patterns and brown ring around spinnerets. Spinnerets base brown and tip white.

Epigyne (Figs 14A, B, 18C, 19C). Epigynal plate 1.3× wider than long. Hoods 5× depth than width. The posterior edge of copulatory openings touching, slightly curved. The width of thick copulatory ducts base 3× wider than the thinner part. The branched shorter copulatory ducts connected to secondary spermathecae, the other connected to the primary spermathecae. Primary spermathecae oval, longer than the width of the secondary spermathecae. Fertilization ducts directed at 9:00 o'clock position from spermathecae.

Variation. Second paratype female: total body length 3.47, carapace 1.35 long, 1.01 wide, opisthosoma 2.12 long, 1.42 wide.

Etymology. The specific epithet refers to the type locality; noun in apposition.

Distribution. Known only from the type locality (Fig. 30).

***Troglohnia wuding* Lin & Li, sp. nov.**

<https://zoobank.org/B1F33F50-4AB0-4695-B217-38105B93C644>

Figs 15A, B, 16A, B, 17C, 18D, 19D, 20G, H, 30

Type material. Holotype: ♂ (IZCAS-Ar44685), CHINA, Yunnan: Chuxiong City, Wuding County, Mao Street, Xianren Cave, 25.4655°N, 102.1740°E, ca 2066 m, 18.VI.2010, C. Wang, Q. Zhao and Y. Lin leg. **Paratypes:** 10♀ (IZCAS-Ar44686–Ar44695), same data as holotype.

Diagnosis. *Troglohnia wuding* sp. nov. can be distinguished from *T. qiubei* sp. nov. by the male ventral retrolateral tibial apophysis strongly curved and wider than dorsal retrolateral tibial apophysis (Fig. 15B) [vs almost straight and as wide as dorsal retrolateral tibial apophysis (Fig. 12B)], embolic tooth terminal terminal finger-shaped (Fig. 15A) [vs flat (Fig. 12A)], process on anterior 3/5 of tegulum (arrowed in Fig. 15A) [vs on anterior 1/3 (arrowed in Fig. 12A)] and female can be distinguished by the diameter of secondary spermathecae almost as same as diameter of primary spermathecae (Fig. 16B) [vs less than diameter of primary spermathecae (Fig. 13B)], distance between primary spermathecae and secondary spermathecae less than half of diameter of secondary spermathecae (Fig. 16B) [vs more than half of diameter (Fig. 13B)], secondary spermathecae separated by ~ 1× diameter (Fig. 16B) [vs 1.5× (Fig. 13B)] and fertilization ducts pointing to 9:00 o'clock position (Fig. 16B) [vs 7:30 o'clock position (Fig. 13B)].

Description. Male (holotype; Figs 15A, B, 17C, 20G). Total body length 2.88. Carapace 1.27 long, 1.02 wide; opisthosoma 1.61 long, 1.19 wide. AER straight

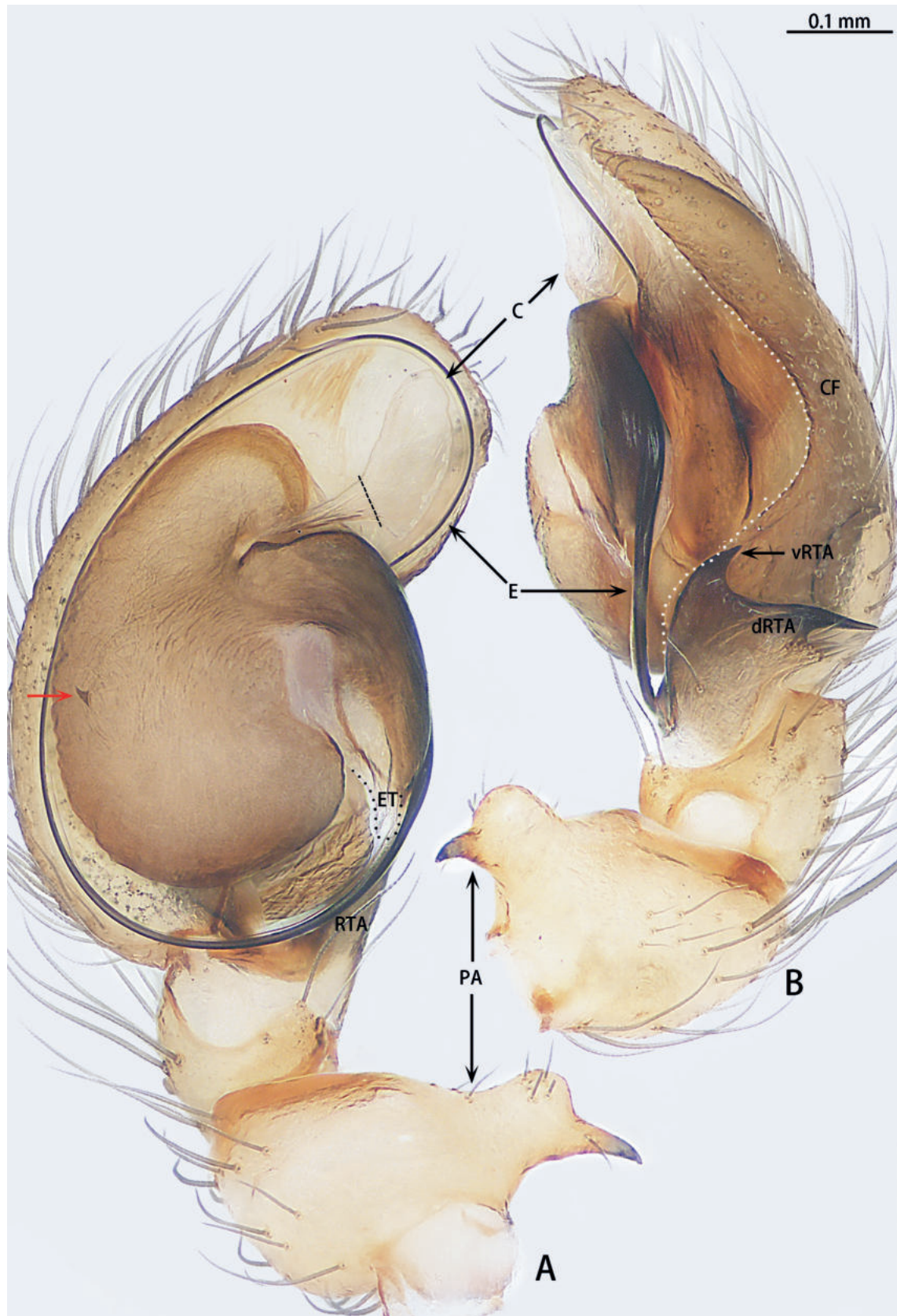


Figure 15. *Troglohnia wuding* sp. nov., holotype male **A** ventral view **B** retrolateral view. Dashed line shows conductor stalk; red arrow shows the process on tegulum. Abbreviations: C = conductor, CF = cymbial furrow, dRTA = dorsal retrolateral tibial apophysis, E = embolus, ET = embolic tooth, PA = patellar apophysis, RTA = retrolateral tibial apophysis, vRTA = ventral retrolateral tibial apophysis.

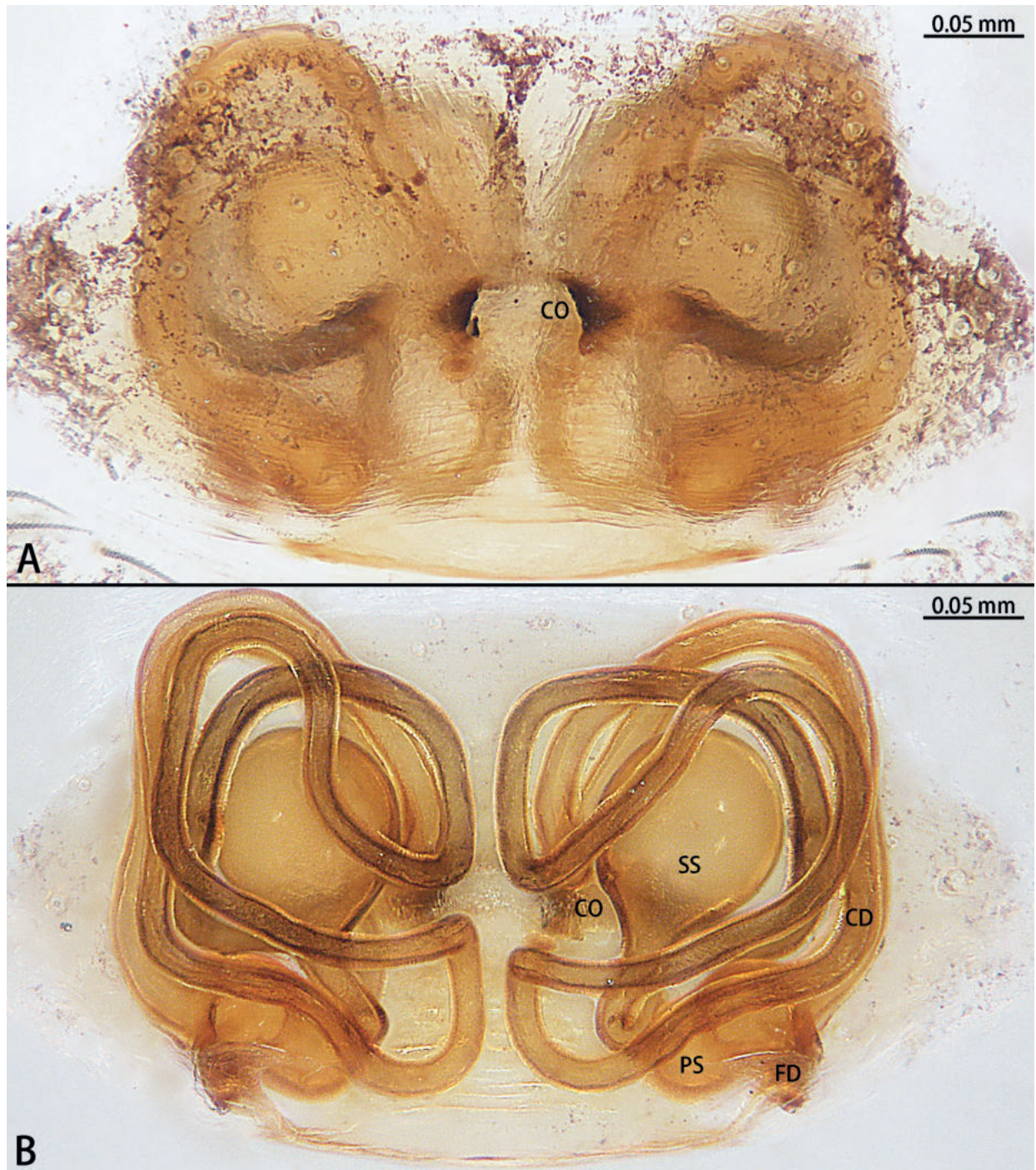


Figure 16. *Troglohnia wuding* sp. nov., paratype female **A** epigyne, ventral view **B** vulva, dorsal view. Abbreviations: CD = copulatory duct, CO = copulatory opening, FD = fertilization duct, PS = primary spermatheca, SS = secondary spermatheca.

and PER procurved in dorsal view. Eye sizes and interdistances: AME 0.05, ALE 0.07, PME 0.05, PLE 0.06; AME–AME 0.01, AME–ALE 0.03, PME–PME 0.08, PME–PLE 0.04, ALE–PLE 0.01. MOA 0.18 long, front width 0.12, back width 0.17. Clypeus 0.16 high. Chelicerae with two promarginal and three retromarginal teeth. Leg measurements: I 4.36 (1.27, 0.43, 1.00, 0.93, 0.73); II 4.19 (1.25, 0.41, 0.94, 0.89, 0.70); III 3.81 (1.11, 0.40, 0.81, 0.86, 0.63); IV 4.73 (1.30, 0.41, 1.14, 1.12, 0.76). Leg spination: femora I–III d1; tibiae I p1 d1, II d2, III p1 d2 r1 v2, IV r1 v2; metatarsi III–IV p1 r1 v2.

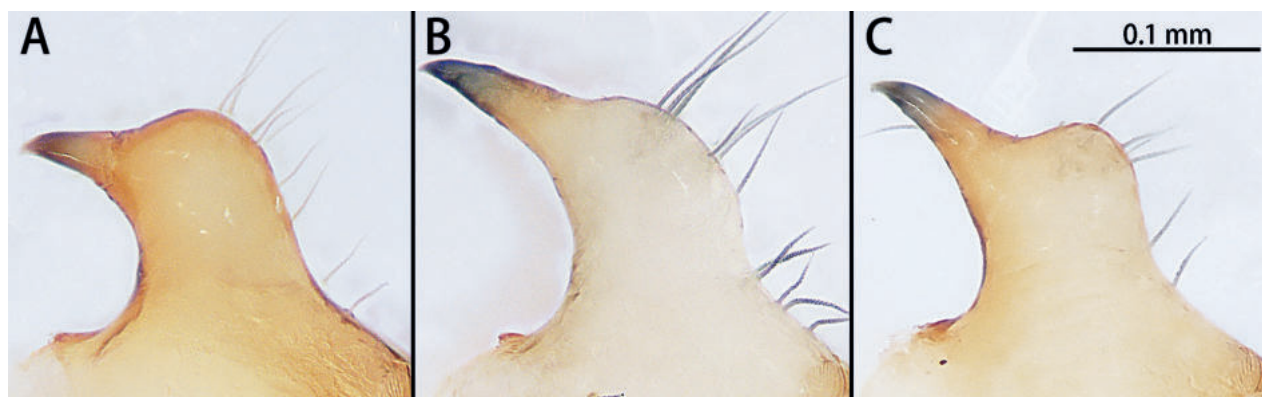


Figure 17. Patella apophyses of *Troglohnia* gen. nov., lateral view **A** *Tr. dafang* sp. nov. **B** *Tr. qiubei* sp. nov. **C** *Tr. wuding* sp. nov.

Coloration (Fig. 20G). Carapace yellowish, middle region with elongated brown band, margin with brown pattern. Fovea longitudinal, reddish-brown. Chelicerae, labium, gnathocoxae, and sternum yellow. Sternum with brown marginal marking. Legs yellow. Dorsal opisthosoma oval, grey, middle of anteriorly and laterally with rod-shaped brown patterns, middle of posteriorly with dotted brown patterns. Ventral opisthosoma grey, anterior and middle part with brown patterns. Spinnerets surrounded by brown rings. Spinnerets base brown and tip white.

Palp (Figs 15A, B, 17C). Patellar apophysis with wide base and narrowed tip, the narrowed tip as long as the wide base. Ventral retrolateral tibial apophysis curved, almost $1/2\times$ longer than dorsal retrolateral tibial apophysis and $2\times$ wider than the dorsal retrolateral tibial apophysis. Cymbium $1.5\times$ longer than wide. Cymbial furrow almost as long as cymbium. Bulb almost oval. A triangle process presents at the prolateral edge of tegulum. Medium of tegulum with oval membranous area. Length of stalk of conductor almost half of total conductor length. Embolic tooth terminal blunt. Embolus slender and whip-shaped.

Female (paratype IZCAS-Ar44695; Figs 16A, B, 18D, 19D, 20H). Total body length 2.26. Carapace 0.93 long, 0.72 wide; opisthosoma 1.33 long, 0.90 wide. Eye sizes and interdistances: AME 0.05, ALE 0.07, PME 0.07, PLE 0.08; AME–AME 0.02, AME–ALE 0.03, PME–PME 0.08, PME–PLE 0.04, ALE–PLE 0.02. MOA 0.18 long, front width 0.07, back width 0.19. Clypeus 0.13 high. Chelicerae with three promarginal and four retromarginal teeth. Leg measurements: I 3.55 (1.03, 0.37, 0.81, 0.77, 0.57); II 3.45 (1.02, 0.36, 0.76, 0.75, 0.56); III 3.15 (0.84, 0.35, 0.70, 0.74, 0.52); IV 4.03 (1.09, 0.39, 0.95, 0.99, 0.61). Leg spination: femora I–III d1; patellae I–IV d1; tibiae I d1, II p1 d2, III–IV p1 d2 r1 v2; metatarsi III–IV p1 r1 v2.

Coloration (Fig. 20H). As in male but carapace with shield-shaped brown band at middle.

Epigyne (Figs 16A, B, 18D, 19D). Epigynal plate $1.35\times$ wider than long. Hoods $3\times$ depth than width. Copulatory openings arc-shaped, facing each other, circular. The width of thick copulatory ducts base $2\times$ wider than the thinner part. The branched shorter copulatory ducts connected to the secondary spermathecae, the other connected to the primary spermathecae. Primary spermathecae bean-shaped, almost as wide as the secondary spermathecae. Fertilization ducts directed at 9:00 o'clock position from spermathecae.

Variation. Females ($n = 9$): total body length 3.06–3.86, carapace 1.26–1.58 long, 1.00–1.23 wide, opisthosoma 1.80–2.33 long, 1.29–1.74 wide.

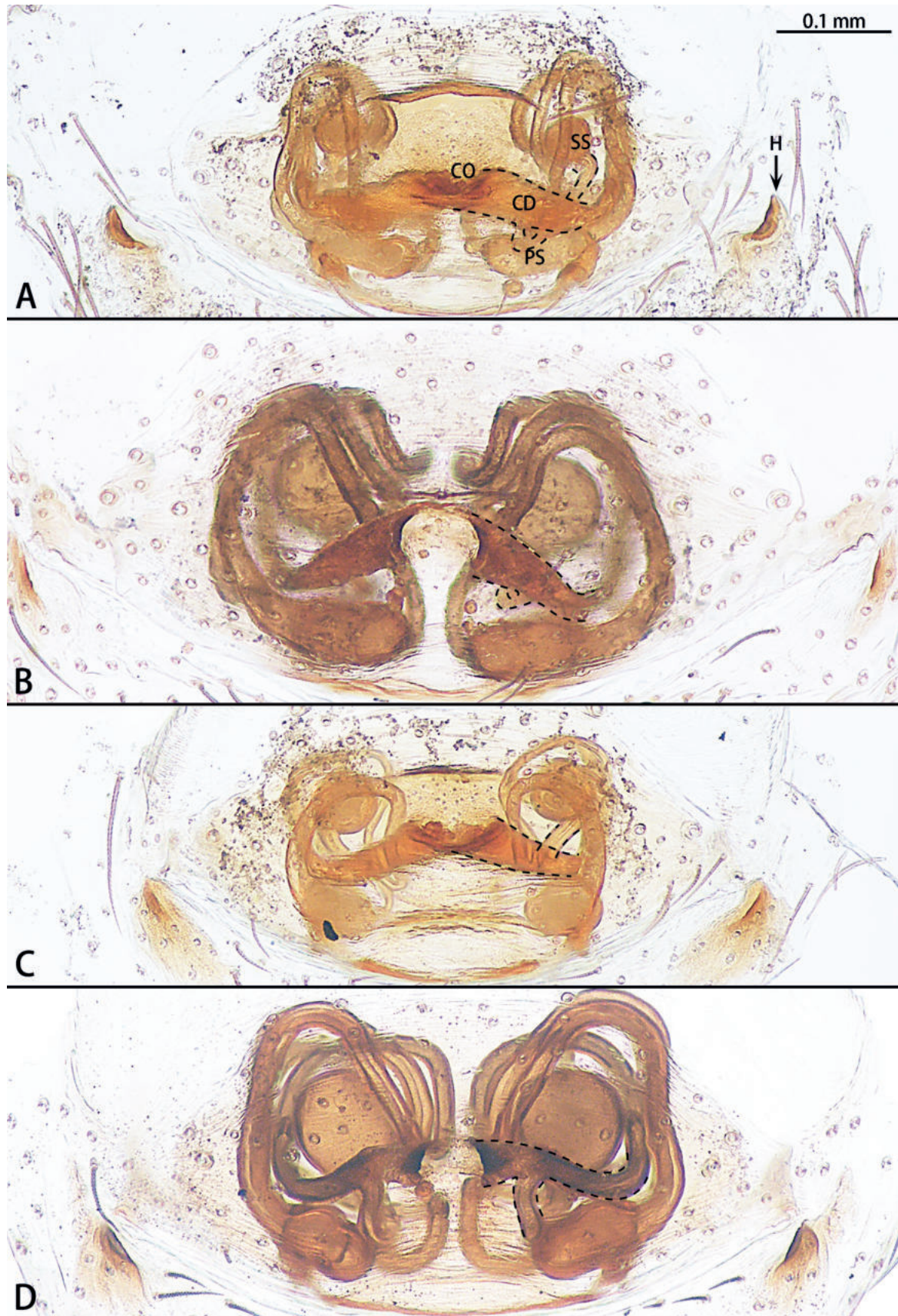


Figure 18. Epigynes of *Troglohnia* gen. nov., ventral view **A** *Tr. dafang* sp. nov. **B** *Tr. qiubei* sp. nov. **C** *Tr. shidian* sp. nov. **D** *Tr. wuding* sp. nov. Abbreviations: CD = copulatory duct, CO = copulatory opening, H = hood, PS = primary spermatheca, SS = secondary spermatheca.

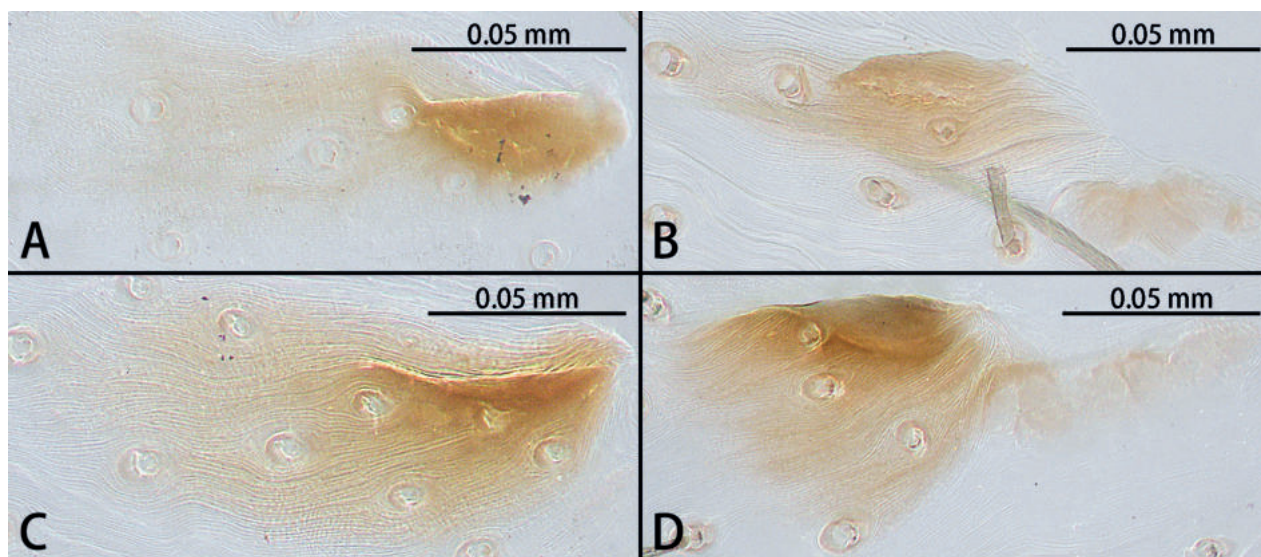


Figure 19. Epigynal hoods of *Troghohnia* gen. nov., ventral view **A** *Tr. dafang* sp. nov. **B** *Tr. qiubei* sp. nov. **C** *Tr. shidian* sp. nov. **D** *Tr. wuding* sp. nov.

Etymology. The specific epithet refers to the type locality; noun in apposition.

Distribution. Known only from the type locality (Fig. 30).

Genus *Typhlohnia* Lin & Li, gen. nov.

<https://zoobank.org/4FDC2FD9-21F4-457C-A0A9-3F2BD5B6AA06>

Type species. *Typhlohnia rongshui* sp. nov. from Guangxi, China.

Diagnosis. *Typhlohnia* gen. nov. can be distinguished from *Asiohahnia* Ovtchinnikov, 1992 by the eyes retrograde (Fig. 28A–G) [vs eyes normal (see Ovtchinnikov 1992: fig. 2.3)], body pale yellow to white (Fig. 29A–G) [vs body with black patterns (see Ovtchinnikov 1992: fig. 2.4)], the length of cymbium almost 3–6× of the length of cymbial furrow (Figs 23B, 25B) [vs 2× (see Ovtchinnikov 1992: figs 2.2, 3.2)], sperm duct with U-shaped curve (Figs 3D, 23A, 25A) [vs without curved (see Ovtchinnikov 1992: figs 2.2, 2.6, 3.2)], copulatory openings anteriorly (Figs 21A, 22A, 24A, 26A, 27A) [vs posteriorly (see Ovtchinnikov 1992: figs 3.3, 3.5, 3.7)] and epigyne with two pairs of spermathecae (Figs 21B, 22B, 24B, 26B, 27B) [vs one pair (see Ovtchinnikov 1992: figs 3.4, 3.6, 3.8)].

Description. Male. Total length 1.38–1.70 ($n = 4$). Carapace pale white to yellowish, without any pattern. 0–6 eyes, white, most species with two eyes. Fovea longitudinal, unobvious. Clypeus pale yellow, covered with several setae. Chelicerae pale yellow, with two or three promarginal and two or three retromarginal teeth, stridulatory files absent. Endites, labium pale yellow, covered with few black setae. Sternum brown, without markings. Legs pale yellow. Opisthosoma oval, pale white to brown. Spinnerets white, straight in posterior view. Tracheal spiracle long and transverse, distance of spiracle to epigastric furrow as long as to spinnerets.

Palpal femur almost 3× longer than patella, spineless. Patella almost as long as tibia, with hook-shaped apophysis. Retrolateral tibial apophysis curved with serrations. Cymbium oval, almost 2× longer than wide, cymbial furrow almost 1/3–1/6× longer than cymbium. Bulb globular to oval. Sperm duct with U-shaped curve. Embolus whip-shaped, curving clockwise along tegular margin.

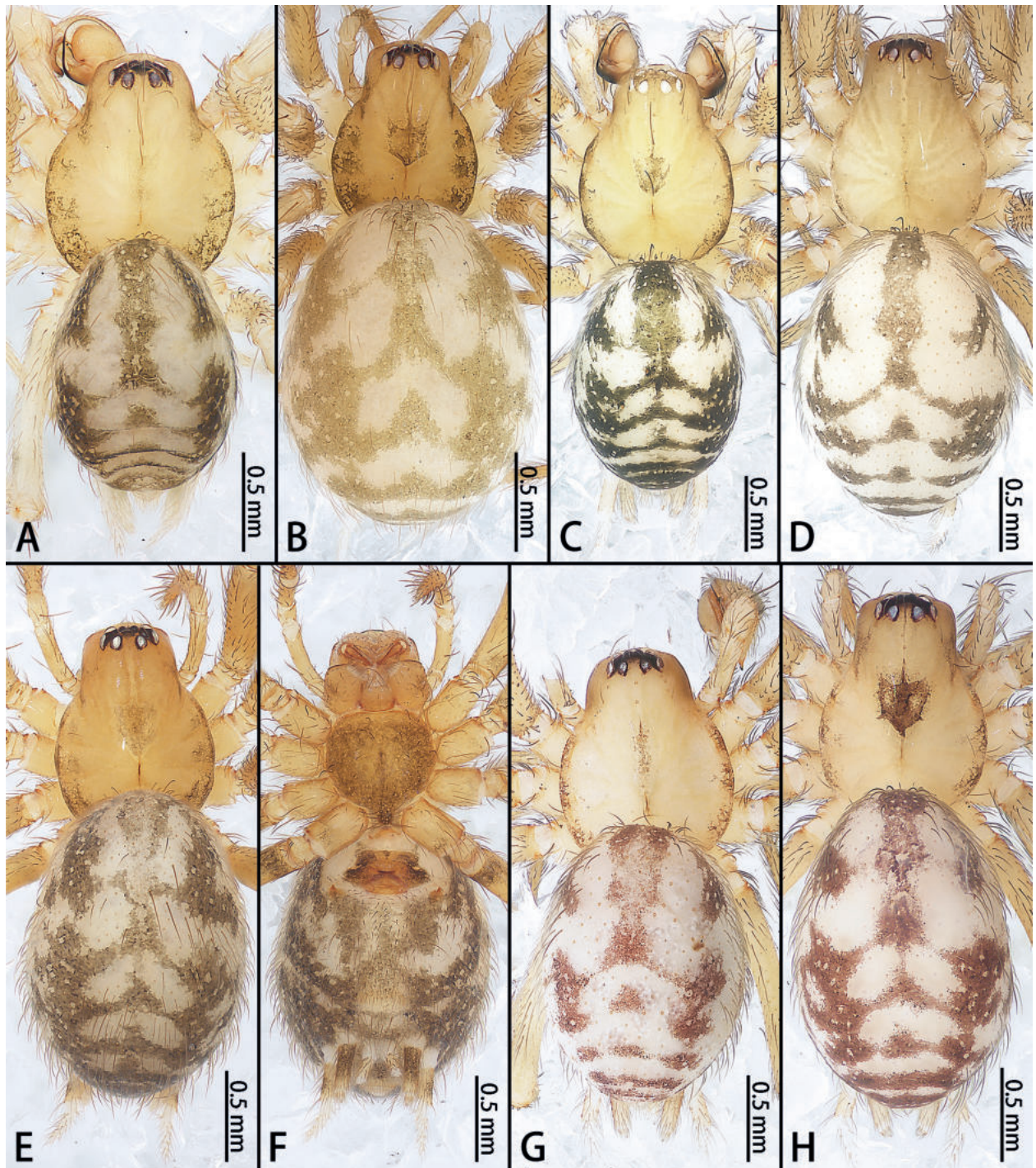


Figure 20. *Troglohnia* gen. nov., habitus, dorsal view (A–E, G, H) and ventral view (F) A *Tr. dafang* sp. nov., holotype male B Same, paratype female C *Tr. qiubei* sp. nov., holotype male D Same, paratype female E *Tr. shidian* sp. nov., holotype female F Same G *Tr. wuding* sp. nov., holotype male H same, paratype female.

Female. Total length 1.30–2.07 ($n = 13$). Somatic characters as in male.

Epigynal plate wider than long, with a depression anteriorly. Copulatory openings located anteriorly, arc-shaped. Copulatory ducts long, in the *rongshui* group strongly convoluted, but in the *sondoong* group simple. The short duct connected to secondary spermathecae, the other connected to primary spermathecae. Primary spermathecae oval to bean-shaped, secondary spermathecae oval to globular. Fertilization ducts laminar, sickle-shaped.

Etymology. The new generic name is a combination of *Typhlo-* (refers to the degenerated eyes) and *Hahnia*. The gender is feminine.

Species groups. Two species groups: the *rongshui* group and the *sondoong* group. These groups can be distinguished by the males embolus originating at 3:00 o'clock position (the *rongshui* group) or 7:30 o'clock position (the *sondoong* group), length of embolus almost 3/4 perimeter of bulb (the *rongshui* group) or half perimeter of bulb (the *sondoong* group) and females have convoluted copulatory ducts (the *rongshui* group) or simple copulatory ducts (the *sondoong* group).

Composition. This new genus includes five species: The *rongshui* group: *Typhlohnia kaiyang* sp. nov. (♀), *T. rongshui* sp. nov. (♂♀) and *T. suiyang* sp. nov. (♀) and the *sondoong* group: *T. banlaksao* sp. nov. (♀) and *T. sondoong* sp. nov. (♂♀).

Distribution. Laos (Bolikhamsay), Vietnam (Quang Binh) and China (Guizhou, Guangxi) (Fig. 30).

***Typhlohnia banlaksao* Lin & Li, sp. nov.**

<https://zoobank.org/977A9612-279D-4DBF-B8D3-26D5CB5F7AC7>

Figs 21A, B, 28A, 29A, 30

Type material. Holotype: ♀ (IZCAS-Ar44696), LAOS, Bolikhamsay: Khamkeut Dist., 17.11 km west of Ban Laksao Town, Tham Mankone, Dragon Cave, 18.2216°N, 104.8127°E, ca 495 m, 27.XI.2012, Z. Yao leg.

Diagnosis. The female of *Typhlohnia banlaksao* sp. nov. can be distinguished from *T. sondoong* sp. nov. by the length of copulatory ducts 4× longer than diameter of primary spermathecae (Fig. 21B) [vs 1.5× (Fig. 26B)], copulatory ducts strongly curved to almost 60° angle (Fig. 21B) [vs 80° (Fig. 26B)] and secondary spermathecae larger than primary spermathecae (Fig. 21B) [vs as wide as primary spermathecae (Fig. 26B)].

Description. Female (holotype; Figs 21A, B, 28A, 29A). Total body length 1.73. Carapace 0.74 long, 0.49 wide; opisthosoma 0.99 long, 0.77 wide. Eye sizes and interdistances: ALE 0.02, PME 0.01, PLE 0.03; PME–PME 0.05, PME–PLE 0.02, ALE–PLE 0.02. Clypeus 0.09 high. Chelicerae with three promarginal and two retromarginal teeth. Leg measurements: I 3.03 (0.84, 0.26, 0.71, 0.67, 0.55); II 2.80 (0.79, 0.26, 0.62, 0.64, 0.49); III 2.58 (0.70, 0.22, 0.57, 0.62, 0.47); IV 3.09 (0.91, 0.26, 0.81, 0.84, 0.57). Leg spination: femur I p1; patellae I–IV d1; tibiae I–II p1 d2, III–IV r1 d1.

Coloration (Figs 28A, 29A). Carapace pale yellow, with a few long brown hairs. Fovea longitudinal, reddish-brown. Six eyes, white. Chelicerae, labium, and gnathocoxae pale yellow, with long brown hairs; sternum yellowish. Legs white with some spines. Opisthosoma oval, grey. Spinnerets white.

Epigyne (Fig. 21A, B). Epigynal plate 1.55× wider than long. Depression obvious, ends with copulatory openings. Copulatory ducts long, almost 4× longer than width of primary spermathecae, strongly curved to almost 60° angle, base bifurcate. The short one connected to secondary spermathecae, the other connected to primary spermathecae. Secondary spermathecae oval, 1.5× wider than primary spermathecae. Fertilization ducts directed at 11:00 o'clock position from spermathecae.

Etymology. The specific epithet refers to the type locality; noun in apposition.

Distribution. Known only from the type locality (Fig. 30).

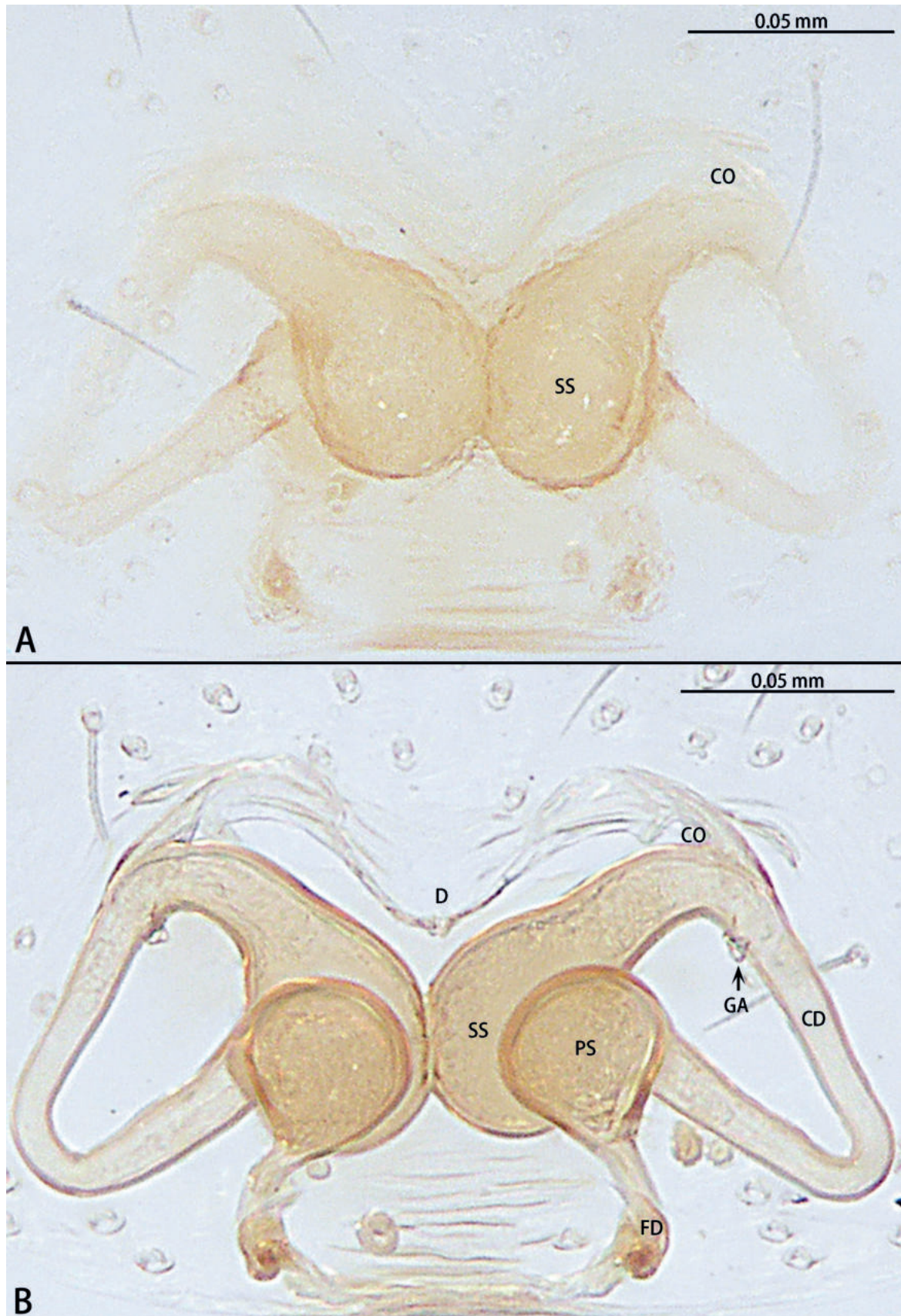


Figure 21. *Typhlohnia banlaksao* sp. nov., holotype female **A** epigyne, ventral view **B** vulva, dorsal view. Abbreviations: CD = copulatory duct, CO = copulatory opening, D = depression, FD = fertilization duct, GA = glandular appendage, PS = primary spermatheca, SS = secondary spermatheca.

***Typhlohnia kaiyang* Lin & Li, sp. nov.**

<https://zoobank.org/865144DC-09CE-4C98-A0F7-C4675AE7BCC3>

Figs 22A, B, 28B, 29B, 30

Type material. Holotype: ♀ (IZCAS-Ar44697), CHINA, Guizhou: Guiyang City, Kaiyang County, Shuangliu Town, Dashan Villiage, Qiaotou Cave, 27.0316°N, 106.8571°E, ca 1380 m, 11.V.2006, Y. Lin and Z. Yang leg.

Diagnosis. The female of *Typhlohnia kaiyang* sp. nov. can be distinguished from all other species in the *rongshui* group by the secondary spermathecae at posterior of primary spermathecae (Fig. 22B).

Description. Female (holotype; Figs 22A, B, 28B, 29B). Total body length 1.53. Carapace 0.66 long, 0.48 wide; opisthosoma 0.87 long, 0.50 wide. Chelicerae with two promarginal and three retromarginal teeth. Leg measurements: I 2.03 (0.58, 0.22, 0.44, 0.40, 0.38); II 1.97 (0.57, 0.21, 0.41, 0.41, 0.37); III 1.80 (0.50, 0.17, 0.39, 0.39, 0.35); IV 2.35 (0.65, 0.22, 0.51, 0.54, 0.43). Leg spination: patellae III–IV d1.

Coloration (Figs 28B, 29B). Carapace pale yellow, with a few long brown hairs. Fovea unobvious. Eyes absent. Chelicerae, labium, and gnathocoxae pale yellow, with long brown hairs. Sternum yellowish. Legs white. Opisthosoma oval, white. Spinnerets white.

Epigyne (Fig. 22A, B). Epigynal plate 1.3× wider than long. Depression unobvious. Copulatory openings arc-shaped. Copulatory ducts long and strongly convoluted, with two turns, medium bifurcate. The short one connected to secondary spermathecae, the other connected to primary spermathecae. Secondary spermathecae oval, as wide as kidney-shaped primary spermathecae. Fertilization ducts directed at 9:00 o'clock position from spermathecae.

Etymology. The specific epithet refers to the type locality; noun in apposition.

Distribution. Known only from the type locality (Fig. 30).

***Typhlohnia rongshui* Lin & Li, sp. nov.**

<https://zoobank.org/E78901D0-F6DA-4033-9D07-5CE389BE5FC3>

Figs 1D, 3D, 23A, B, 24A, B, 28C, D, 29C, D, 30

Type material. Holotype: ♂ (IZCAS-Ar44698), CHINA, Guangxi: Guilin City, Rongshui County, Taoyuan Cave, 25.0579°N, 109.2246°E, ca 131 m, 23.VII.2009, C. Wang leg. **Paratypes:** 3♂ 4♀ (IZCAS-Ar44699–Ar44705), same data as holotype.

Diagnosis. The male of *Typhlohnia rongshui* sp. nov. can be distinguished from *T. sondoong* sp. nov. by the patella with apophysis retrolaterally (Fig. 23B) [vs retrodorsally (Fig. 25B)], retrolateral tibial apophysis point retrolaterally (Fig. 23B) [vs point dorsally (Fig. 25B)], conductor slender and triangle-shaped (Fig. 23A) [vs oval (Fig. 25A)], medium of sperm duct U-shaped (Fig. 23A) [vs upturned U-shaped (Fig. 25A)], embolus originating at 3:00 o'clock position (Fig. 23A) [vs 7:30 o'clock position (Fig. 25A)] and length of embolus almost 3/4 perimeter of bulb (Fig. 23A) [vs half perimeter of bulb (Fig. 25A)]. Females can be distinguished from *T. suiyang* sp. nov. by the unobvious glandular appendages (Fig. 24B) [vs obvious (Fig. 27B)], ratio of length to width of epigynal plate ~ 2:3 (Fig. 24A) [vs 1:1 (Fig. 27A)] and ratio of width between primary spermathecae to secondary spermathecae ~ 1:1 (Fig. 24B) [vs 2:1 (Fig. 27B)].

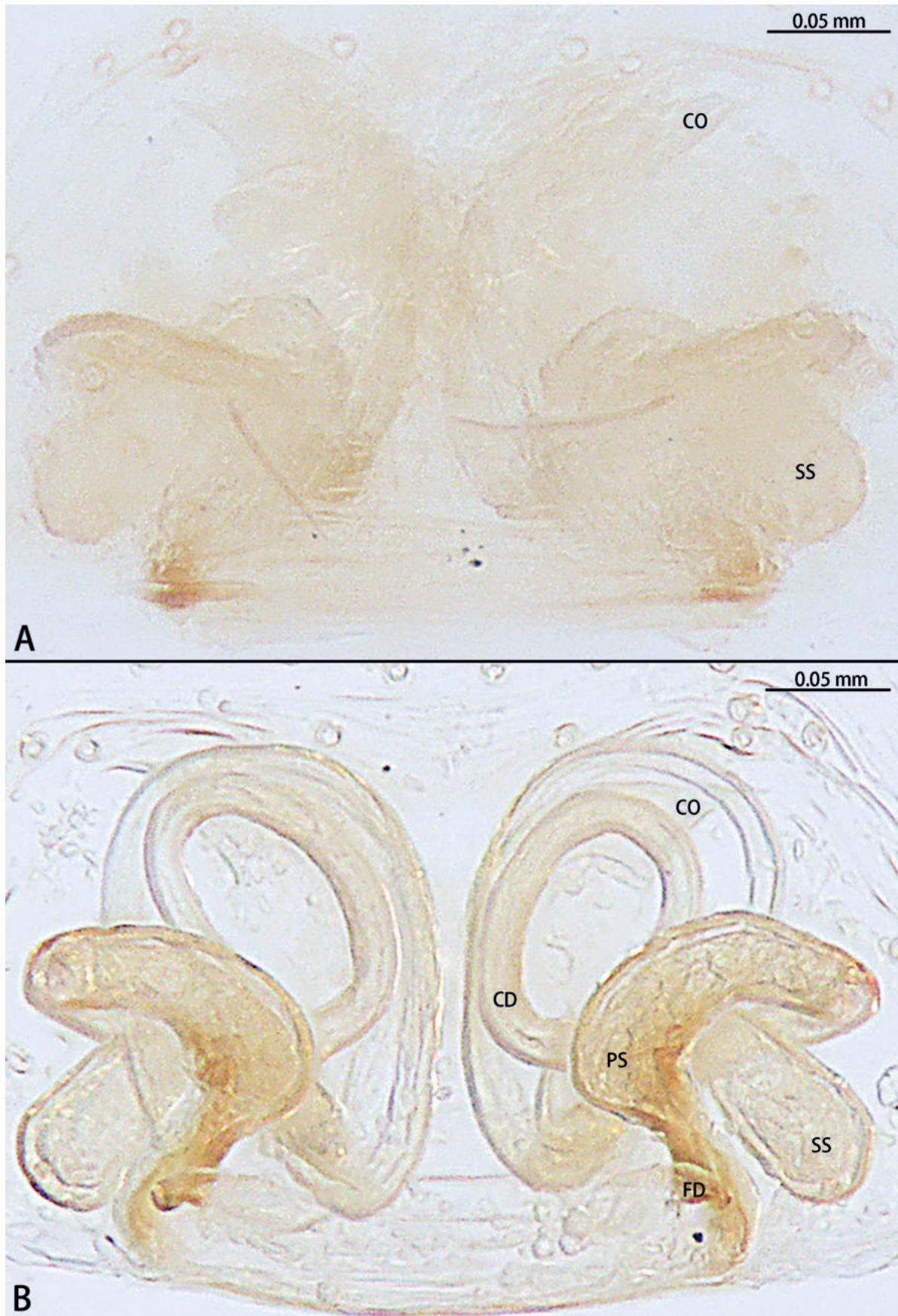


Figure 22. *Typhlohnia kaiyang* sp. nov., holotype female **A** epigyne, ventral view **B** vulva, dorsal view. Abbreviations: CD = copulatory duct, CO = copulatory opening, FD = fertilization duct, PS = primary spermatheca, SS = secondary spermatheca.

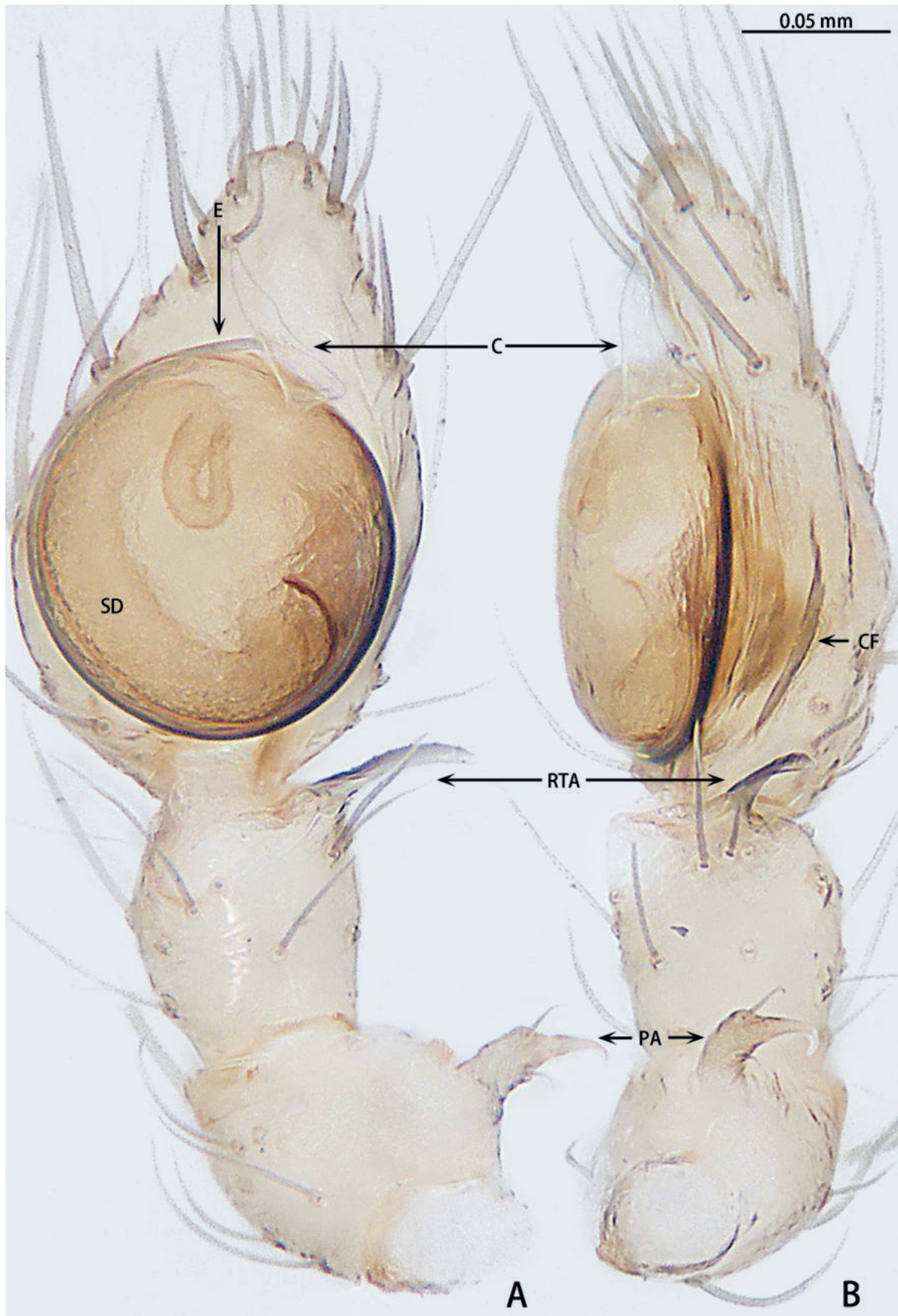


Figure 23. *Typhlohnia rongshui* sp. nov., holotype male **A** ventral view **B** retrolateral view. Abbreviations: C = conductor, CF = cymbial furrow, E = embolus, PA = patellar apophysis, RTA = retrolateral tibial apophysis, SD = sperm duct.

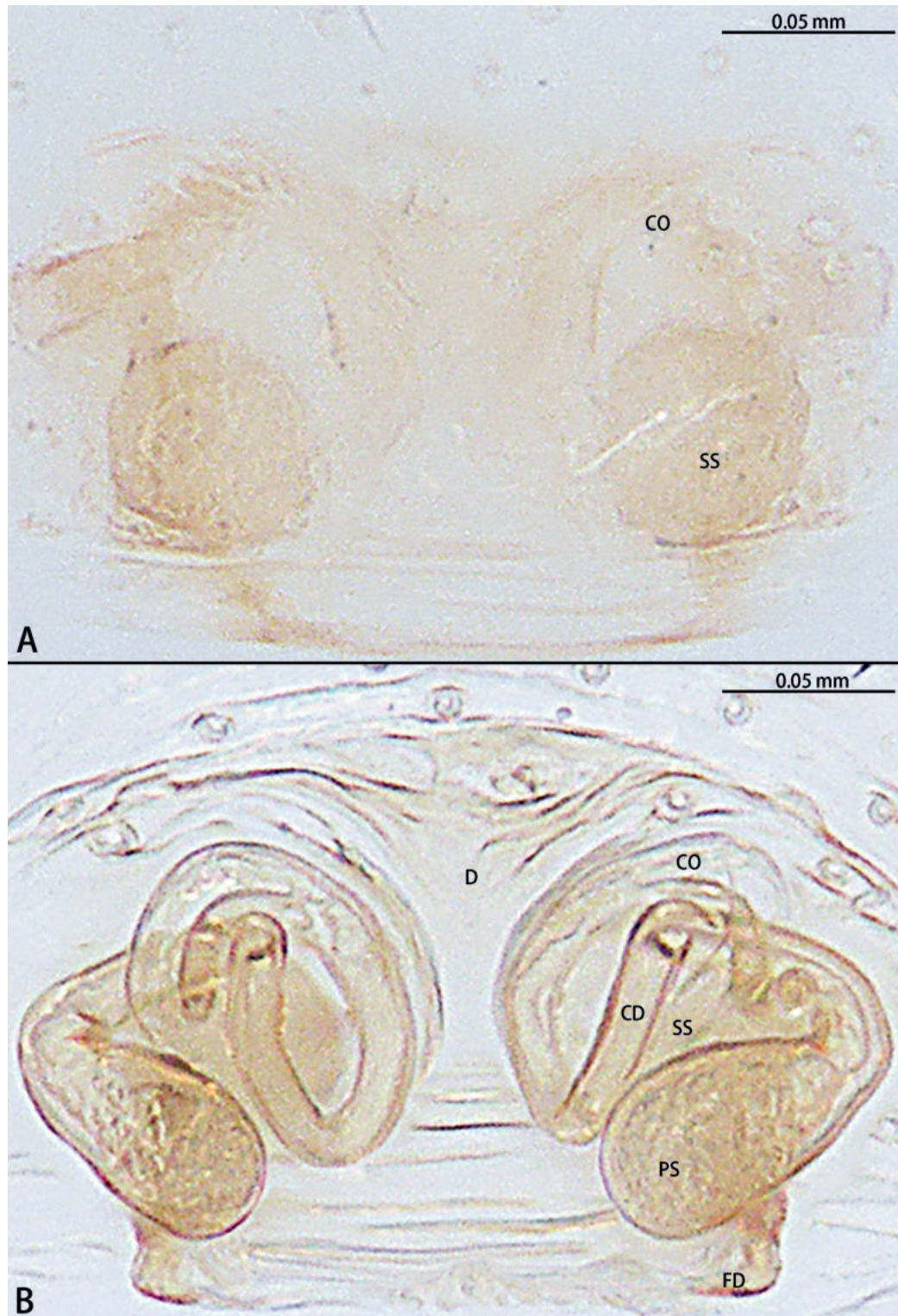


Figure 24. *Typhlohnia rongshui* sp. nov., paratype female **A** epigyne, ventral view **B** vulva, dorsal view. Abbreviations: CD = copulatory duct, CO = copulatory opening, D = depression, FD = fertilization duct, PS = primary spermatheca, SS = secondary spermatheca.

Description. Male (holotype; Figs 23A, B, 28C, 29C). Total body length 1.39. Carapace 0.63 long, 0.48 wide; opisthosoma 0.76 long, 0.56 wide. Eye size and interdistance: PLE 0.03; PLE–PLE 0.11. Clypeus 0.07 high. Chelicerae with two promarginal and three retromarginal teeth. Leg measurements: I 1.98 (0.60,

0.23, 0.45, 0.37, 0.33); II 1.85 (0.56, 0.21, 0.40, 0.35, 0.33); III 1.68 (0.51, 0.18, 0.34, 0.34, 0.31); IV 2.10 (0.61, 0.21, 0.46, 0.45, 0.37). Leg spination: femur I p1; patellae III–IV d1; tibiae III–IV p1 d1; metatarsi III p1 d2, IV d2.

Coloration (Figs 28C, 29C). Carapace pale yellow, with a few long brown hairs. Fovea longitudinal, reddish-brown. Two eyes, white. Chelicerae, labium, and gnathocoxae pale yellow, with long brown hairs; sternum pale yellowish. Legs white. Opisthosoma oval, pale yellow. Spinnerets white.

Palp (Fig. 23A, B). Patella with apophysis retrolaterally, tip hook-shaped. Tibia with black, serrated retrolateral apophysis, little curved, point retrolaterally. Cymbium 1.5× longer than wide, 3× longer than cymbial furrow. Cymbial furrow shallowed. Bulb globular. Conductor sickle-shaped, almost half length of bulb. Middle of sperm duct bent in U-shape. Embolus slender and whip-shaped, almost 3/4 perimeter of bulb. Base of embolus arising at 3:00 o'clock position.

Female (paratype IZCAS-Ar44705; Figs 24A, B, 28D, 29D). Total body length 1.34. Carapace 0.59 long, 0.47 wide; opisthosoma 0.75 long, 0.48 wide. Eye size and interdistance: PLE 0.03; PLE–PLE 0.09. Clypeus 0.06 high. Chelicerae with two promarginal and three retromarginal teeth. Leg measurements: I 1.84 (0.56, 0.20, 0.41, 0.35, 0.32); II 1.76 (0.54, 0.19, 0.38, 0.34, 0.31); III 1.64 (0.49, 0.17, 0.35, 0.33, 0.30); IV 2.07 (0.59, 0.20, 0.46, 0.45, 0.37). Leg spination: patellae III–IV d1; tibiae II–IV r1; metatarsi III–IV p1 d2 r1.

Coloration (Figs 28D, 29D). As in male.

Epigyne (Fig. 24A, B). Epigynal plate 1.5× wider than long. Depression obvious, ends with copulatory openings. Copulatory openings arc-shaped. Copulatory ducts long and strongly convoluted with one turn, medium bifurcate. The short one connected to the secondary spermathecae, the other connected to the primary spermathecae. Secondary spermathecae globular, as wide as bean-shaped primary spermathecae. Fertilization ducts directed at 9:00 o'clock position from spermathecae.

Variation. Males ($n = 2$): total body length 1.38–1.46, carapace 0.68–0.71 long, 0.51–0.59 wide, opisthosoma 0.70–0.75 long, 0.55–0.57 wide. Females ($n = 3$): total body length 1.30–1.40, carapace 0.55–0.61 long, 0.44–0.46 wide, opisthosoma 0.73–0.81 long, 0.50–0.57 wide.

Etymology. The specific epithet refers to the type locality; noun in apposition.

Distribution. Known only from the type locality (Fig. 30).

***Typhlohnia sondoong* Lin & Li, sp. nov.**

<https://zoobank.org/B1DE5788-66C5-4408-9737-9993FB969A70>

Figs 25A, B, 26A, B, 28E, F, 29E, F, 30

Type material. Holotype: ♂ (IZCAS-Ar44706), VIETNAM, Quang Binh: Phong Nha-Ke Bang National Park, Son Doong Cave, 17.4936°N, 106.2942°E, ca 143 m, 25.V.2016, Q. Zhao and Z. Chen leg. **Paratypes:** 6♀ (IZCAS-Ar44707–Ar44712), same data as holotype.

Diagnosis. For males see diagnosis of *Typhlohnia rongshui* sp. nov. and for females see diagnosis of *T. banlaksao* sp. nov.

Description. Male (holotype; Figs 25A, B, 28E, 29E). Total body length 1.70. Carapace 0.83 long, 0.64 wide; opisthosoma 0.87 long, 0.62 wide. Eye sizes and interdistance: ALE 0.03, PLE 0.02; ALE–PLE 0.03. Clypeus 0.12 high. Cheli-

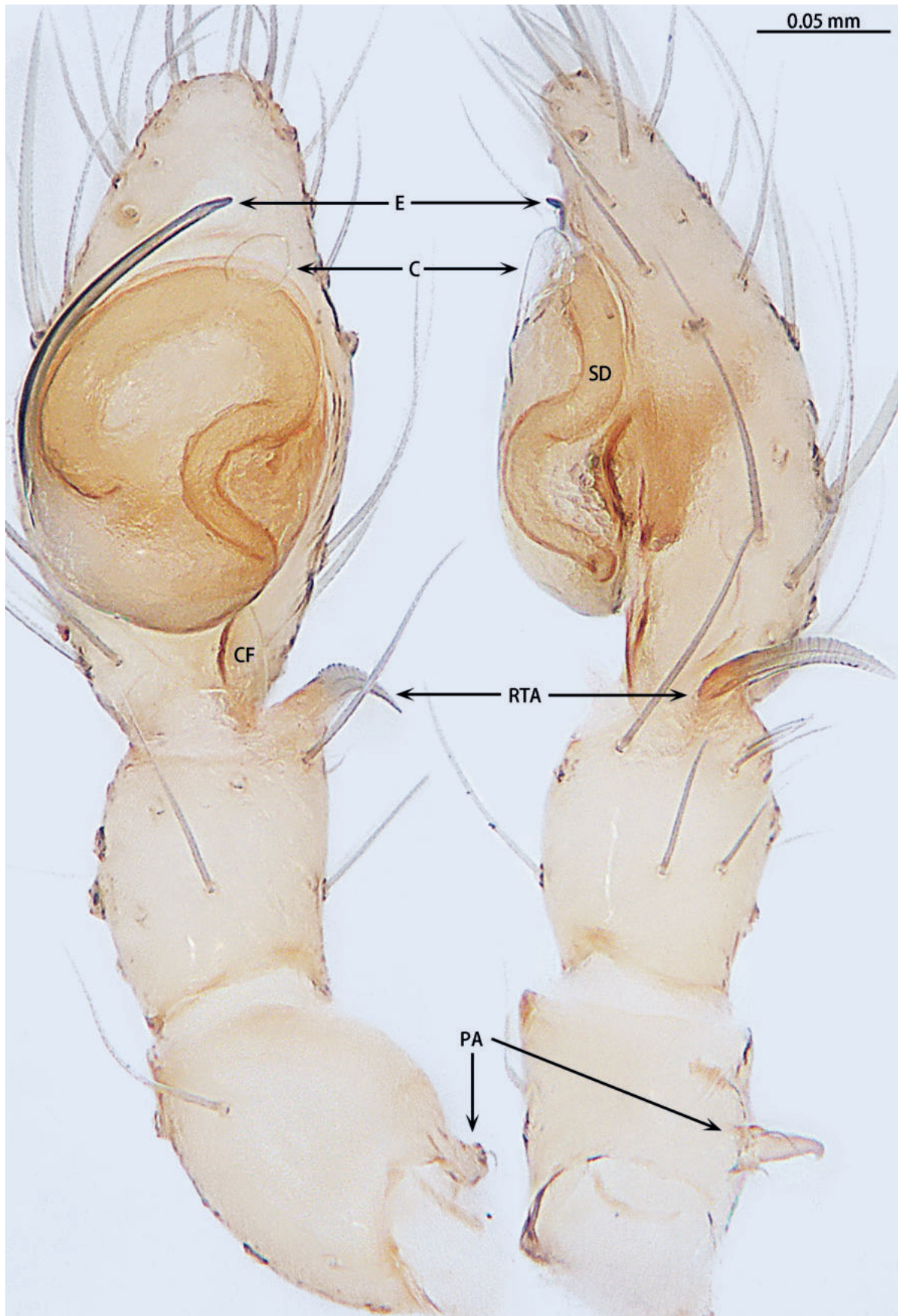


Figure 25. *Typhlohnia sondoong* sp. nov., holotype male **A** ventral view **B** retrolateral view. Abbreviations: C = conductor, CF = cymbial furrow, E = embolus, PA = patellar apophysis, RTA = retrolateral tibial apophysis, SD = sperm duct.

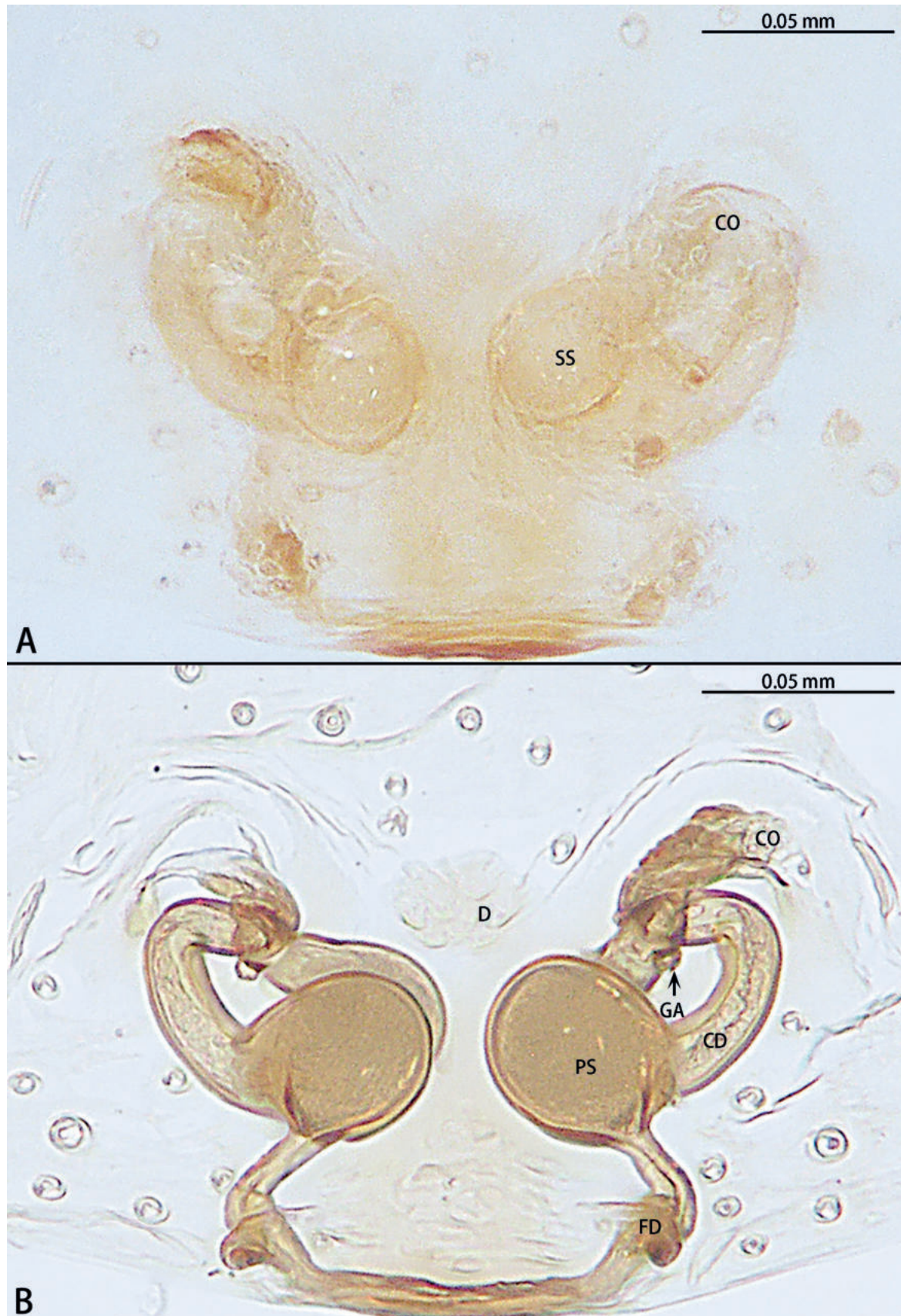


Figure 26. *Typhlohnia sondoong* sp. nov., paratype female **A** epigyne, ventral view **B** vulva, dorsal view. Abbreviations: CD = copulatory duct, CO = copulatory opening, D = depression, FD = fertilization duct, GA = glandular appendage, PS = primary spermatheca, SS = secondary spermatheca.

cerae with three promarginal and two retromarginal teeth. Leg measurements: I 2.84 (0.80, 0.26, 0.68, 0.62, 0.48); II 2.71 (0.77, 0.25, 0.62, 0.61, 0.46); III 2.50 (0.69, 0.24, 0.56, 0.58, 0.43); IV 3.11 (0.85, 0.24, 0.76, 0.74, 0.52). Leg spination: femora I p1 v4, II–IV v4; patellae II–IV d1; tibiae I p1, II p1 d1, III–IV p1 r1; metatarsi III–IV p1 r1 v1.

Coloration (Figs 28E, 29E). Carapace pale yellow, with a few long brown hairs. Fovea longitudinal, reddish-brown. Four eyes, white. Chelicerae, labium, and gnathocoxae pale yellow, with long brown hairs; sternum yellowish. Legs yellow. Opisthosoma oval, pale yellow. Spinnerets white.

Palp (Fig. 25A, B). Patella with apophysis retrodorsally, tip hook-shaped. Tibia with black, serrated retrolateral apophysis, little curved, point dorsally. Cymbium 2× longer than wide, 6× longer than cymbial furrow. Cymbial furrow shallowed, originated on the inside of cymbium. Bulb oval. Conductor oval, almost as wide as middle of sperm duct. Middle of sperm duct bent in upturned U-shape. Embolus slender and whip-shaped, almost half the perimeter of bulb. Base of embolus arising at 7:30 o'clock position.

Female (paratype IZCAS-Ar44712; Figs 26A, B, 28F, 29F). Total body length 1.73. Carapace 0.74 long, 0.55 wide; opisthosoma 0.99 long, 0.76 wide. Eye sizes and interdistance: ALE 0.03, PLE 0.02; ALE–PLE 0.03. Clypeus 0.10 high. Chelicerae with three promarginal and two retromarginal teeth. Leg measurements: I 2.54 (0.74, 0.24, 0.58, 0.54, 0.44); II 2.44 (0.72, 0.23, 0.53, 0.53, 0.43); III 2.30 (0.64, 0.22, 0.52, 0.52, 0.40); IV 2.89 (0.80, 0.25, 0.71, 0.66, 0.47). Leg spination: femora I p1 v4, II–IV v4; tibiae III–IV p1; metatarsi III–IV p1 r1 v1.

Coloration (Figs 28F, 29F). As in male.

Epigyne (Fig. 26A, B). Epigynal plate 1.1× wider than long. Depression obvious, ends with copulatory openings. Copulatory ducts long, almost 1.5× longer than width of primary spermathecae, strongly curved to almost 80° angle, base bifurcate. The short one connected to secondary spermathecae, the other connected to primary spermathecae. Secondary spermathecae oval, as wide as primary spermathecae. Fertilization ducts directed at 9:00 o'clock position from spermathecae.

Variation. Females ($n = 5$): total body length 1.50–2.07, carapace 0.69–0.80 long, 0.51–0.59 wide, opisthosoma 0.75–1.27 long, 0.61–1.02 wide.

Etymology. The specific epithet refers to the type locality; noun in apposition.

Distribution. Known only from the type locality (Fig. 30).

***Typhlohnia suiayang* Lin & Li, sp. nov.**

<https://zoobank.org/0855F4D9-0B3E-407C-85A7-92782883645D>

Figs 27A, B, 28G, 29G, 30

Type material. Holotype: ♀ (IZCAS-Ar44713), CHINA, Guizhou: Suiyang County, Wenquan Town, Guihua Villiage, Mahuang Cave, 28.2437°N, 107.2891°E, ca 730 m, 13.V.2007, Y. Lin and J. Liu leg.

Diagnosis. See diagnosis of *Typhlohnia rongshui* sp. nov.

Description. Female (holotype; Figs 27A, B, 28G, 29G). Total body length 1.31. Carapace 0.61 long, 0.49 wide; opisthosoma 0.70 long, 0.57 wide. Chelicerae with two promarginal and three retromarginal teeth. Leg measurements: I 2.46 (0.72, 0.22, 0.56, 0.51, 0.45); II 2.38 (0.70, 0.21, 0.53, 0.50, 0.44); III 2.27

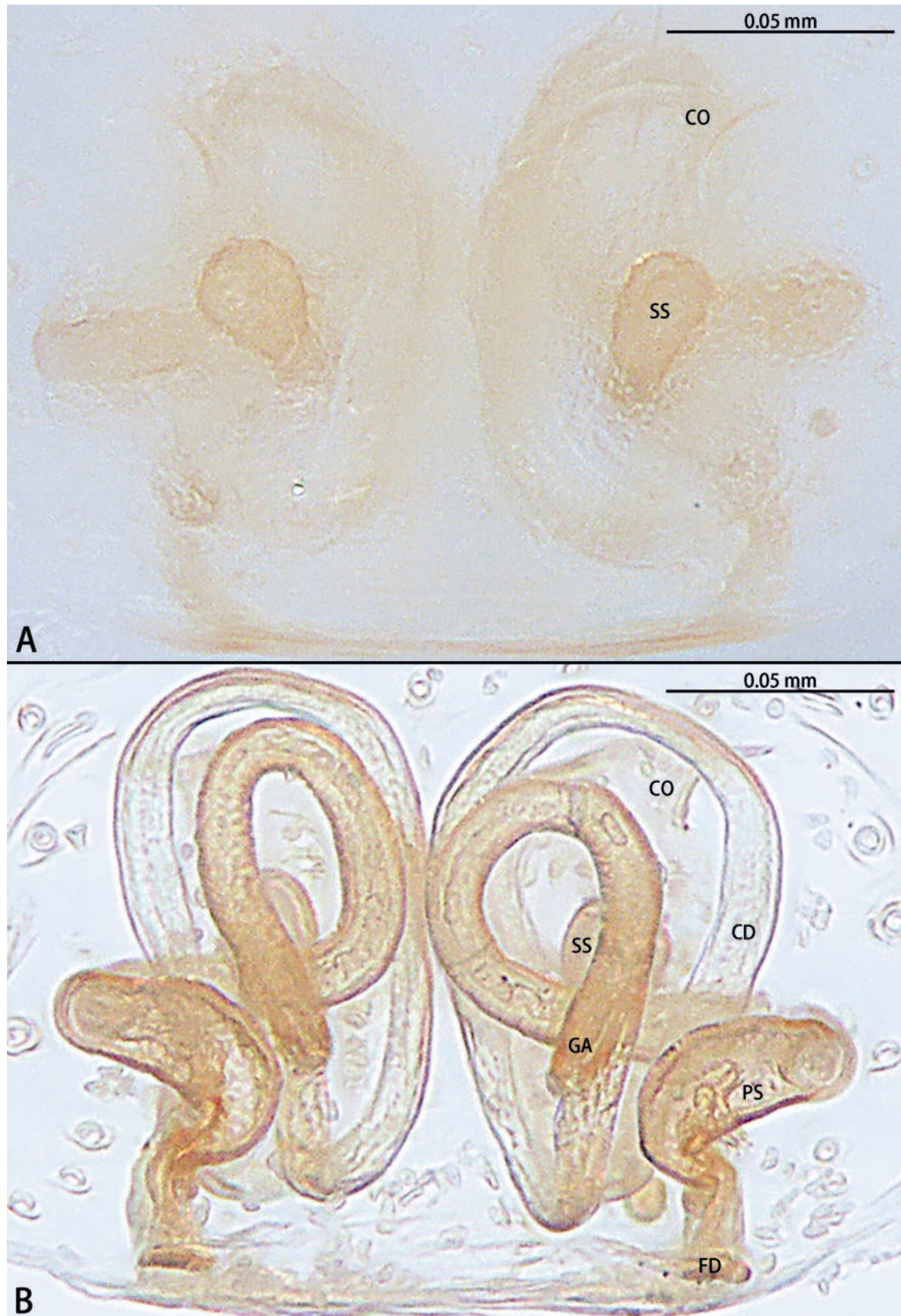


Figure 27. *Typhlohnia suiyang* sp. nov., holotype female **A** epigyne, ventral view **B** vulva, dorsal view. Abbreviations: CD = copulatory duct, CO = copulatory opening, FD = fertilization duct, GA = glandular appendage, PS = primary spermatheca, SS = secondary spermatheca.

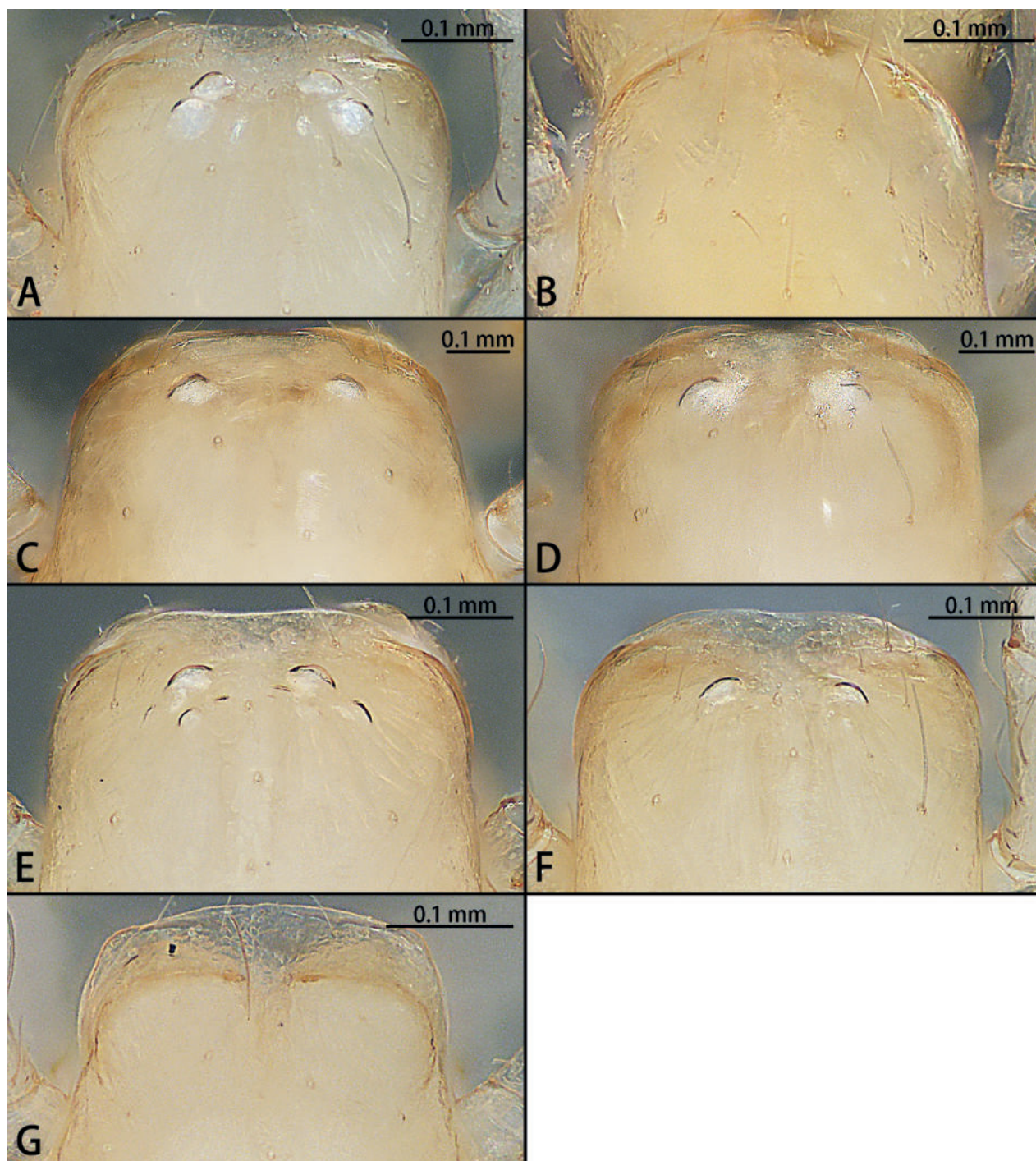


Figure 28. Cephalic regions of *Typhlohnia* gen. nov., dorsal view **A** *Ty. banlaksao* sp. nov., holotype female **B** *Ty. kaiyang* sp. nov., holotype female **C** *Ty. rongshui* sp. nov., holotype male **D** Same, paratype female **E** *Ty. sondoong* sp. nov., holotype male **F** same, paratype female **G** *Ty. suiyang* sp. nov., holotype female.

(0.64, 0.20, 0.50, 0.50, 0.43); IV 2.94 (0.80, 0.23, 0.71, 0.69, 0.51). Leg spination: patella IV p1; tibiae III–IV p1 r1 v1.

Coloration (Figs 28G, 29G). Carapace pale yellow, with a few long brown hairs. Fovea unobvious. Eye absent. Chelicerae, labium, and gnathocoxae pale yellow, with long brown hairs. Sternum yellowish. Legs white. Opisthosoma oval, white. Spinnerets white.

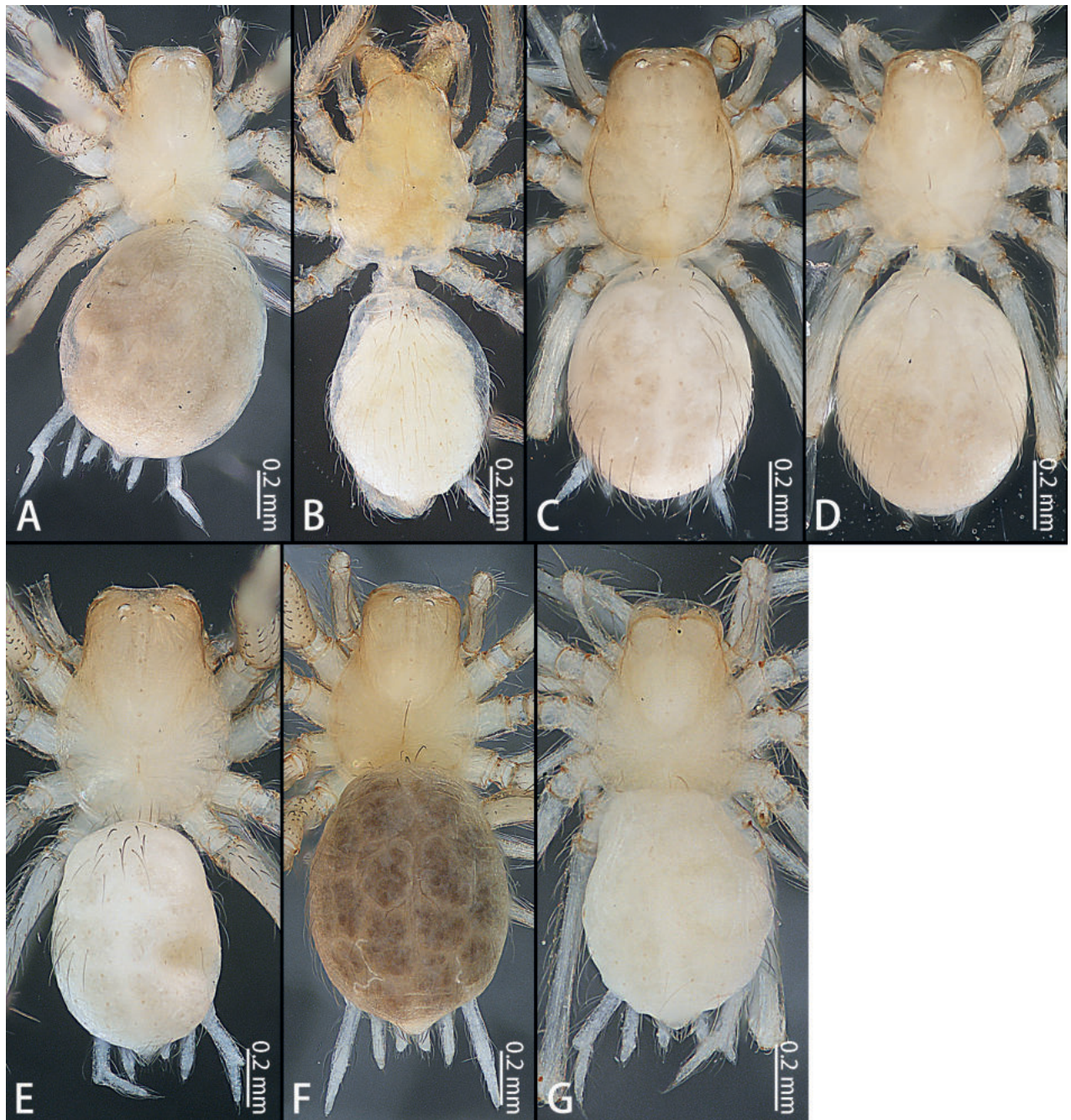


Figure 29. *Typhlohnia* gen. nov., habitus, dorsal view **A** *Ty. banlaksao* sp. nov., holotype female **B** *Ty. kaiyang* sp. nov., holotype female **C** *Ty. rongshui* sp. nov., holotype male **D** Same, paratype female **E** *Ty. sondoong* sp. nov., holotype male **F** same, paratype female **G** *Ty. suiyang* sp. nov., holotype female.

Epigyne (Fig. 27A, B). Epigynal plate as long as wide. Depression unobvious. Copulatory openings arc-shaped. Copulatory ducts long and strongly convoluted, with two turns, medium bifurcate. The short one connected to secondary spermathecae, the other connected to primary spermathecae, medium with glandular appendages. Secondary spermathecae oval, half wide of kidney-shaped primary spermathecae. Fertilization ducts directed at 9:00 o'clock position from spermathecae.

Etymology. The specific epithet refers to the type locality; noun in apposition.

Distribution. Known only from the type locality (Fig. 30).

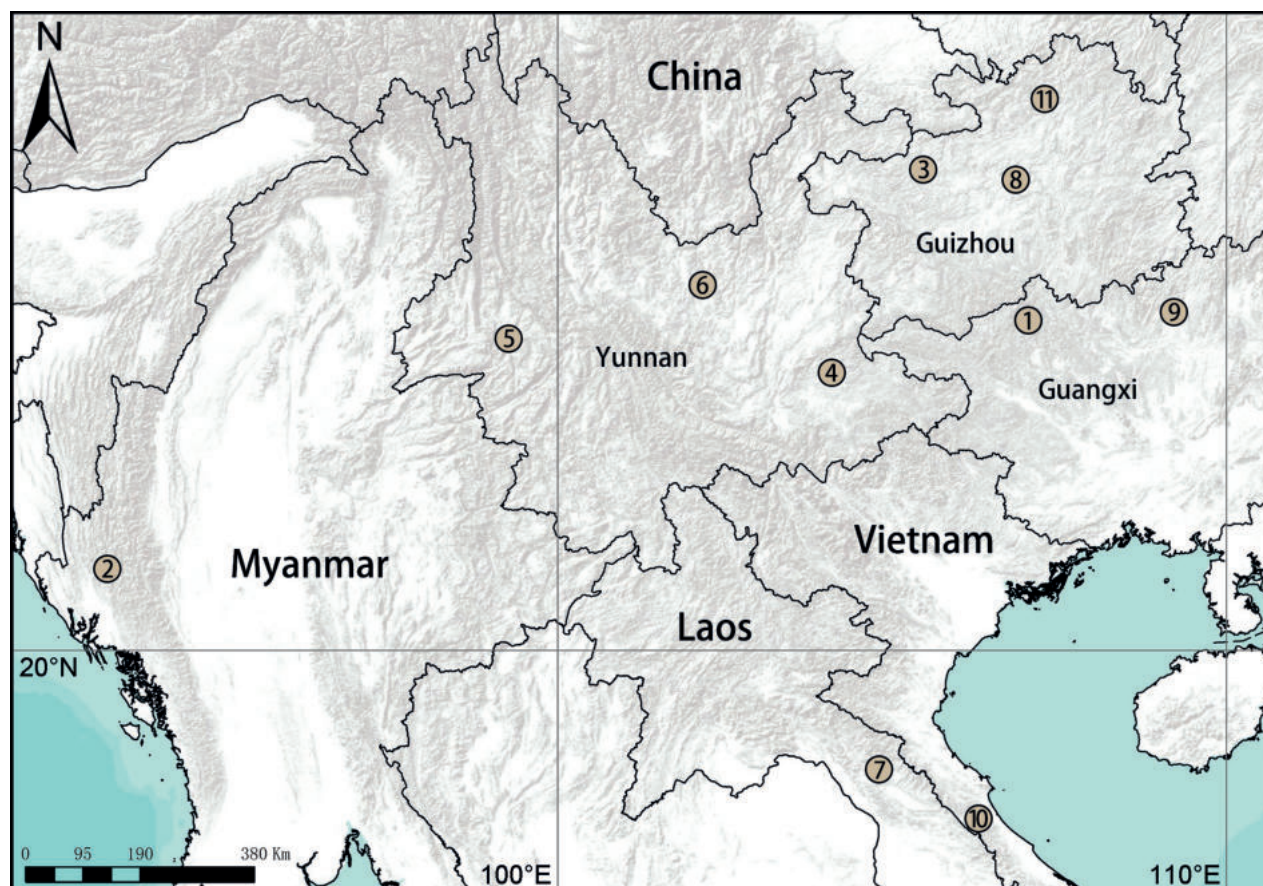


Figure 30. Distribution records of new Hahniidae species in South-east Asia 1 *Goblinia tiane* sp. nov. 2 *Myahnia kanpetlet* sp. nov. 3 *Troglohnia dafang* sp. nov. 4 *Tr. qiubei* sp. nov. 5 *Tr. shidian* sp. nov. 6 *Tr. wuding* sp. nov. 7 *Typhlohnia banlaksao* sp. nov. 8 *Ty. kaiyang* sp. nov. 9 *Ty. rongshui* sp. nov. 10 *Ty. sondoong* sp. nov. 11 *Ty. suiyang* sp. nov.

Acknowledgements

The manuscript benefitted greatly from comments by Zhiyuan Yao (China), Yuri Marusik (Russia), and Mikhail Omelko (Russia). Danni Sherwood (UK) and Nathalie Yonow (UK) checked the English.

Additional information

Conflict of interest

The authors have declared that no competing interests exist.

Ethical statement

No ethical statement was reported.

Funding

No funding was reported.

Author contributions

SL designed the study. YL and SL performed morphological species identification. CC finished the species descriptions and took the photos. CC, YL and SL drafted the manuscript. All authors read and approved the final version of the manuscript.

Author ORCIDs

Chang Chu  <https://orcid.org/0000-0003-3520-5463>

Yejie Lin  <https://orcid.org/0000-0002-6789-2731>

Shuqiang Li  <https://orcid.org/0000-0002-3290-5416>

Data availability

All of the data that support the findings of this study are available in the main text.

References

- Huang G, Zhang Z, Liu Y (2017) Review of the comb-tailed spider genus *Hahnia* C.L. Koch 1841 (Hahniidae) from Gaoligong Mountains in Yunnan, China. *Zootaxa* 4344(3): 444–464. <https://doi.org/10.11646/zootaxa.4344.3.2>
- Li J, Yan X, Lin Y, Li S, Chen H (2021) Challenging Wallacean and Linnean shortfalls: *Ectatosticta* spiders (Araneae, Hypochilidae) from China. *Zoological Research* 42(6): 791–794. <https://doi.org/10.24272/j.issn.2095-8137.2021.212>
- Liu K, Li S, Zhang X, Ying Y, Meng Z, Fei M, Li W, Xiao Y, Xu X (2022) Unknown species from China: The case of phrurolithid spiders (Araneae, Phrurolithidae). *Zoological Research* 43(3): 352–355. <https://doi.org/10.24272/j.issn.2095-8137.2022.055>
- Lu Y, Chu C, Zhang X, Li S, Yao Z (2022) Europe vs China: Spider species richness comparison with *Pholcus* (Araneae, Pholcidae) from Yanshan-Taihang Mountains as evidence. *Zoological Research* 43(4): 532–534. <https://doi.org/10.24272/j.issn.2095-8137.2022.103>
- Ono H, Ogata K (2018) *Spiders of Japan: Their Natural History and Diversity*. Tokai University Press, Kanagawa, 713 pp.
- Ovtchinnikov SV (1992) Description of a new genus *Asiohahnia* gen. n. (Aranei, Hahniidae) with five species from the Tien-Shan. *Zoologicheskii jurnal* 71(5): 28–37.
- Rivera-Quiroz FA, Petcharad B, Miller JA (2020) First records and a new genus of comb-tailed spiders (Araneae: Hahniidae) from Thailand with comments on the six-eyed species of this family. *European Journal of Taxonomy* 724(1): 51–69. <https://doi.org/10.5852/ejt.2020.724.1157>
- Růžička V (2022) A review of the spider genus *Iberina* (Araneae, Hahniidae). *Zootaxa* 5133(4): 555–566. <https://doi.org/10.11646/zootaxa.5133.4.6>
- WSC (2023) World Spider Catalog. Version 24.5. Natural History Museum Bern. <http://wsc.nmbe.ch> [Accessed on 13/09/2023]
- Yang H, Lyu B, Yin H, Li S (2021) Comparative transcriptomics highlights convergent evolution of energy metabolic pathways in group-living spiders. *Zoological Research* 42(2): 195–206. <https://doi.org/10.24272/j.issn.2095-8137.2020.281>
- Yao Z, Wang X, Li S (2021) Tip of the iceberg: Species diversity of *Pholcus* spiders (Araneae, Pholcidae) in Changbai Mountains, Northeast China. *Zoological Research* 42(3): 267–271. <https://doi.org/10.24272/j.issn.2095-8137.2021.037>
- Zhang Z, Li S, Zheng G (2011) Comb-tailed spiders from Xishuangbanna, Yunnan Province, China (Araneae, Hahniidae). *Zootaxa* 2912(1): 1–27. <https://doi.org/10.11646/zootaxa.2912.1.1>
- Zhang Q, Li Y, Lin Y, Li S, Yao Z, Zhang X (2023) Regression of East Tethys resulted in a center of biodiversity: A study of Mysmenidae spiders from the Gaoligong Mountains, China. *Zoological Research* 44(4): 737–738. <https://doi.org/10.24272/j.issn.2095-8137.2023.206>
- Zhao Z, Hou Z, Li S (2022) Cenozoic Tethyan changes dominated Eurasian animal evolution and diversity patterns. *Zoological Research* 43(1): 3–13. <https://doi.org/10.24272/j.issn.2095-8137.2021.322>

Twenty-three new synonyms of the Eastern common groundhopper, *Tetrix japonica* (Bolívar, 1887) (Orthoptera, Tetrigidae)

Ying Long¹, Caili Teng¹, Chaomei Huang¹, Rongjiao Zhang², Weian Deng^{1,2,3,4}, Liliang Lin⁵

1 Key Laboratory of Ecology of Rare and Endangered Species and Environmental Protection (Guangxi Normal University), Ministry of Education, Guilin, Guangxi 541006, China

2 School of Chemistry and Bioengineering, Hechi University, Yizhou, Guangxi 546300, China

3 Guangxi Key Laboratory of Rare and Endangered Animal Ecology, Guangxi Normal University, Guilin, Guangxi 541006, China

4 College of Life Science, Guangxi Normal University, Guilin, Guangxi 541004, China

5 College of Life Sciences, Shaanxi Normal University, Xi'an, Shaanxi 710062, China

Corresponding authors: Rongjiao Zhang (zhangrongjiao0922@163.com); Weian Deng (dengweian5899@163.com)

Abstract

The Eastern common groundhopper, *Tetrix japonica*, is a pygmy grasshopper species widely distributed in the Eastern Palearctic region, and shows a high degree of phenotypic variation. The classification of *Tetrix japonica* is difficult and frequently involved errors. Among the many species of Tetrigidae that have been described in China within the last decades, many synonyms of *Tetrix japonica* were found. The type specimens of many species deposited in the Chinese museums have been re-examined and as a result, *Tetrix japonica* is systematically revised. Based on the results of this review, 23 new synonyms of *Tetrix japonica* are proposed: *Coptotettix circinihumerus* Zheng & Deng, 2004, **syn. nov.**; *Coptotettix emeiensis* Zheng, Lin & Zhang, 2012, **syn. nov.**; *Euparatettix rongshuiensis* Zheng, 2005, **syn. nov.**; *Euparatettix zayuensis* Zheng, Zeng & Ou, 2011, **syn. nov.**; *Macromotettix nigrifubercle* Zheng & Jiang, 2006, **syn. nov.**; *Macromotettix yaoshanensis* Zheng & Jiang, 2000, **syn. nov.**; *Tetrix albistriatus* Yao & Zheng, 2006, **syn. nov.**; *Tetrix albomaculatus* Zheng & Jiang, 2006, **syn. nov.**; *Tetrix albomarginis* Zheng & Nie, 2005, **syn. nov.**; *Tetrix cenwanglaoshana* Zheng, Jiang & Liu, 2005, **syn. nov.**; *Tetrix cliva* Zheng & Deng, 2004, **syn. nov.**; *Tetrix duolunensis* Zheng, 1996, **syn. nov.**; *Tetrix grossovalva* Zheng, 1994, **syn. nov.**; *Tetrix jiuwanshanensis* Zheng, 2005, **syn. nov.**; *Tetrix latipalpa* Cao & Zheng, 2011, **syn. nov.**; *Tetrix liuwanshanensis* Deng, Zheng & Wei, 2007, **syn. nov.**; *Tetrix qinlingensis* Zheng, Huo & Zhang, 2000, **syn. nov.**; *Tetrix rectimargina* Zheng & Jiang, 2004, **syn. nov.**; *Tetrix ruyuanensis* Liang, 1998, **syn. nov.**; *Tetrix xianensis* Zheng, 1996, **syn. nov.**; *Tetrix xinchengensis* Deng, Zheng & Wei, 2007, **syn. nov.**; *Tetrix yunlongensis* Zheng & Mao, 2002, **syn. nov.**; *Tetrix zhoushanensis* Gao, Liu & Yin, 2022, **syn. nov.** It is expected that there will be the discoveries of more synonyms of this and other Tetriginae species from the Eastern Palearctic.

Key words: China, *Coptotettix*, *Euparatettix*, *Macromotettix*, taxonomy, Tetriginae



Academic editor: Zhu-Qing He
Received: 15 August 2023
Accepted: 13 November 2023
Published: 20 December 2023

ZooBank: <https://zoobank.org/BCD4F4C9-1FA2-4368-8DE0-86B79544F060>

Citation: Long Y, Teng C, Huang C, Zhang R, Deng W, Lin L (2023) Twenty-three new synonyms of the Eastern common groundhopper, *Tetrix japonica* (Bolívar, 1887) (Orthoptera, Tetrigidae). ZooKeys 1187: 135–167. <https://doi.org/10.3897/zookeys.1187.110067>

Copyright: © Ying Long et al.
This is an open access article distributed under terms of the Creative Commons Attribution License (Attribution 4.0 International – CC BY 4.0).

Introduction

The Eastern groundhopper, *Tetrix japonica* (Bolívar, 1887), is widely distributed in East Asia (China, Japan, North Korea, and Russia), and may be also present in Mongolia, Myanmar, Laos, and Vietnam. It is a very common species in China. *Tetrix japonica* inhabits many different habitat types, from low grassland areas with moss to higher elevation areas such as hills and mountains. Its main foods are tender mosses and humus. *Tetrix japonica* is a dimorphic species from the standpoint of wings and pronotum length (Deng 2021; Zhang et al. 2022). Within the same population, *T. japonica* can have brachypronotal and brachypterous individuals (Fig. 1A, B), macropronotal, and pauropronotal individuals (Fig. 1C). Brachypronotal and brachypterous individuals are those that have a short pronotum and hind wings. Their pronotum generally does not reach the apex of the hind femur and their hind wings do not reach or only slightly surpass the apex of the hind pronotal process. Macropronotal individuals are these with pronotum longer than the apex of the hind femur, but whose wings do not exceed the tip of the pronotum, while pauropronotal individuals are those with a prolonged pronotum and hind wings. The pronotum reaches the middle of the hind tibia and their hind wings extend beyond the pronotal apex (Devriese et al. 2023) and nearly reach the apex of the hind tibia.

Many new species of Tetrigidae have been described from China in the past (Liang and Zheng 1998; Zheng 2005a; Deng et al. 2007a; Deng 2016; Cigliano et al. 2022); however, many of them are known only from the type material and never recorded again. Tetriginae are an especially complicated subfamily from the standpoint of taxonomy, as its members lack most of clear traits present in other Tetrigidae subfamilies (Skejo and Gupta 2015; Tumbrinck 2019; Kasalo et al. 2023). Revisionary studies have recently discovered that species of some genera were described without clear traits (Adžić et al. 2020; Lu and Zha 2020; Wei and Deng 2023).

Because of the aforementioned, the aim of this study was to revise the type material deposited in the natural history museums of China and find which were *Tetrix japonica* described under different names: we present 23 newly discovered synonyms of this species and analyze the probable causes of the description of so many synonyms. The goals include the determination of species variability and establishment of a good taxonomic practice (Lehmann et al. 2017) in Tetrigidae identification of species found in China.

Materials and methods

Taxonomy, nomenclature, terminology, and measurements

Taxonomy follows Orthoptera Species File [OSF] (Cigliano et al. 2022), a database of Orthoptera taxonomy. Nomenclature is in accordance with the International Code of the Zoological Nomenclature (ICZN 1999). Morphological terminology and landmark-based measurement method followed those used by Zheng (2005a), Deng et al. (2007a), Tumbrinck (2014, 2019), Muhammad et al. (2018), Tan and Artchawakom (2015), Devriese et al. (2023), and Zha et al. (2020). Measurements are given in millimeters (mm).

Photography

Grasshopper specimens were examined using a Motic-SMZ-168 stereo-microscope and photographed using a KEYENCE VHX-600 Digital Microscope. All images were processed with Adobe photoshop CS 11.0.

Type specimen depositories

The specimens examined in this study, including all holotypes and paratypes, have been deposited in the following institutions:

BMSYU	Biology Museum of Sun Yat-sen University, Guangzhou, PR China;
CLSGNU	College of Life Science, Guangxi Normal University, Guilin, China;
EMHU	Entomological Museum of Hechi University, Hechi, China;
IZSNU	Institute of Zoology, Shaanxi Normal University, Xi'an, China;
MHNG	Muséum d'histoire naturelle, Geneve, Switzerland;
MHU	Museum of Hebei University, Baoding, China.

Results

Tetrix japonica (Bolívar, 1887)

Tettix japonicus: Bolívar, 1887: 263 [description] (holotype ♀, Japan, in MHNG).

Acrydium japonicum: Rehn 1902: 629; Kirby 1910: 45.

Tetrix japonica: Bey-Bienko 1934: 9; Bey-Bienko and Mistshenko 1951: 105; Yin 1984: 16; Blackith 1992: 183; Ichikawa 1993: 1; Paris 1993: 241; Storozhenko et al. 1994: 13; Ma and Zheng 1994: 445; Jiang and Zheng 1998: 340; Liang and Zheng 1998: 174; Kim and Kim 2004: 266; Jiang and Liang 2004: 204; Zheng 2005: 334a; Benediktov 2005; Deng et al. 2007a: 302; Tsurui Honma and Nishida 2010: 2; Cao and Zheng 2011: 738; Kim and Puskás 2012: 12; Xiao et al. 2012: 288; Zheng 2014: 56; Storozhenko et al. 2015: 167; Deng 2016: 250.

Previously reported synonyms. *Tettix longulus* Shiraki, 1906, *Tettix sibiricus* Bolívar, 1887, *Tetrix trux* Steinmann, 1964.

Link. <https://orthoptera.speciesfile.org/otus/809028/overview>.

Redescription. Female (Figs 1, 2). Small size and short in brachypronotal and brachypterous individuals, or medium size and long in pauropronotal individuals. Body surface smooth and interspersed with granules.

Head. Head and eyes not exerted above pronotal surface. In dorsal view, fastigium of vertex short; width of vertex between eyes generally wider than width of a compound eye (1.3–1.6 ×), sometimes 1.0 × (such as *T. albistriatus* syn. nov., *T. rectimargina* syn. nov.); anterior margin of fastigium truncated or slightly arcuate and slightly surpassing anterior margin of eye; median carina visible; lateral margins slightly turned backward; depressed on either side of median carina. In lateral view, frontal ridge and vertex forming an obtuse angle; frontal costa slightly straight above antennal groove, protruded anteriorly and broadly rounded between antennal grooves. In frontal view, frontal costa

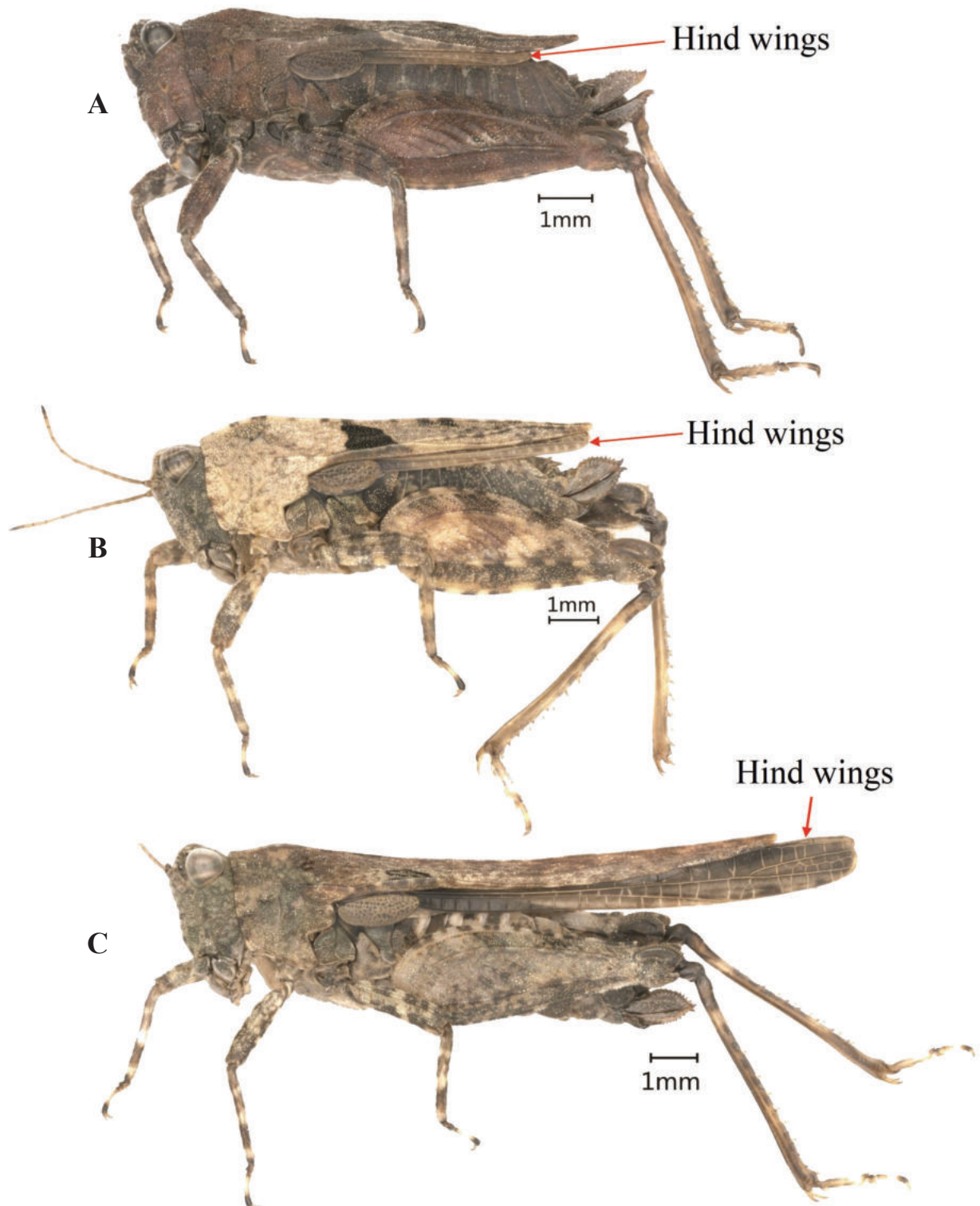


Figure 1. Dimorphism of *Tetrix japonica* (Bolívar, 1887) **A, B** brachypronotal and brachypterous individuals **C** pauropronotal individual.

bifurcated above lateral ocelli, longitudinal furrow divergent between antennae, width of longitudinal furrow of frontal ridge narrower than antennal groove diameter. Antennae short, filiform, antennal grooves inserted between inferior margins of compound eyes, 15-segmented (including scape, pedicel, and a

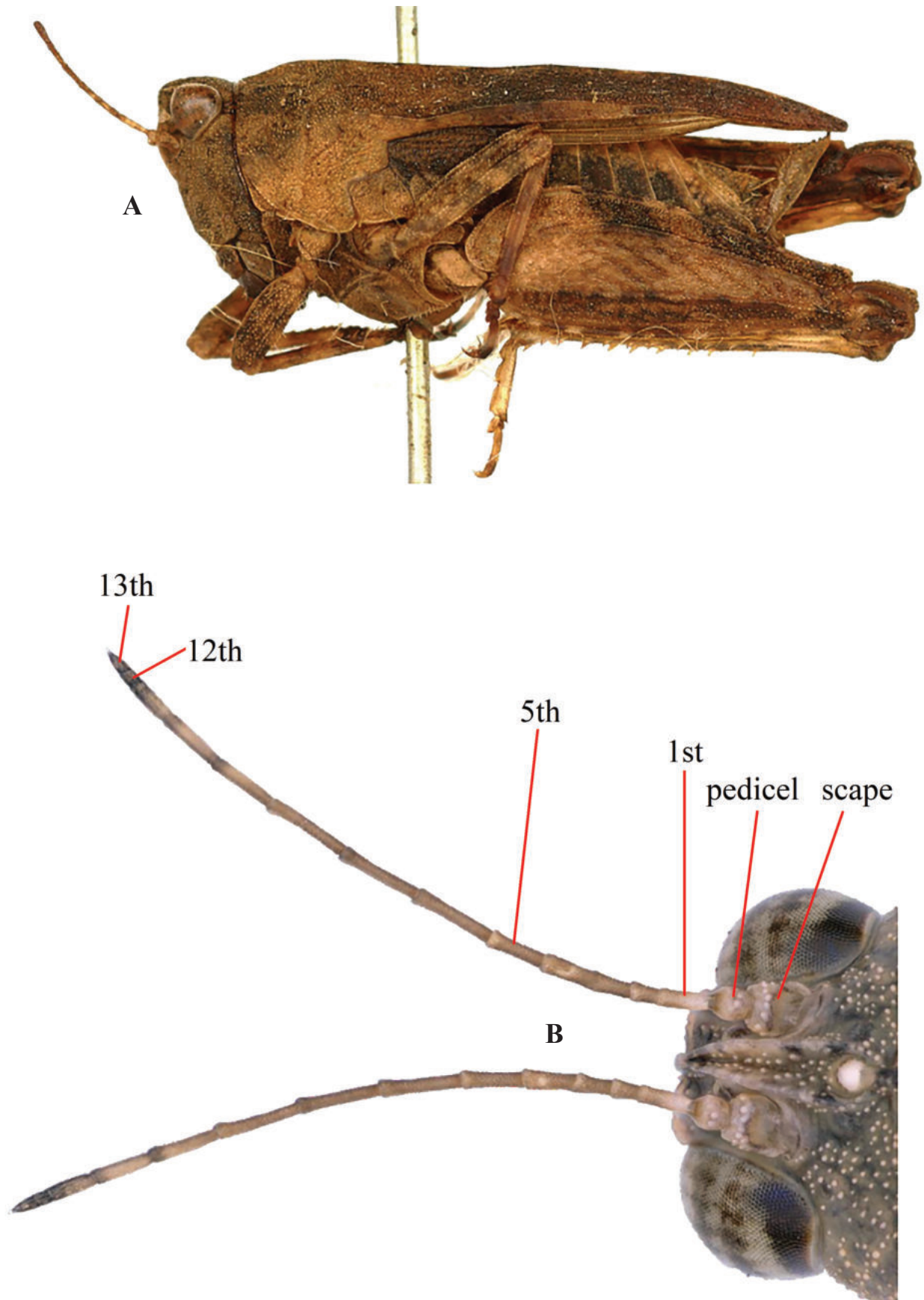


Figure 2. *Tetrax japonica* (Bolívar, 1887) **A** syntype, lateral view (photograph Josef Tumbrinck) **B** antenna, 15-segmented (including scape, pedicel, 13-segmented flagellum).

13-segmented flagellum) (Fig. 2B), the 9th and 10th segment are the longest, ~ 4–5 × longer than its width. Eyes globose, lateral (paired) ocelli located in middle of compound eye height.

Thorax. Pronotum slightly tectiform, its surface smooth and interspersed with dense granules. In dorsal view, anterior margin of pronotum generally truncate, sometimes slightly angular protruding; lateral carinae of prozona generally parallel or sometimes slightly constricted backwards; median carina low and full length entire; humeral angle obtuse; hind pronotal process narrow and long, pronotal apex either generally slightly not reaching or sometimes reaching apex of hind femur in brachypronotal and brachypterous individuals (Fig. 2C) or distinctly surpassing apex of hind femur and reaching approximately the middle of hind tibia in pauropronotal individuals (Fig. 2A, B). In profile, median carina of pronotum slightly straight or slightly arch-like before the shoulders and straight behind the shoulders. Posterior margins of lateral lobes of pronotum with ventral sinus and tegminal sinus. Posterior angles of lateral lobes turned downwards, generally narrow and rounded or sometimes subtruncately at apex. Tegmina long, ovate, apex rounded. Hind wings either slightly not reaching or reaching or slightly surpassing apex of hind pronotal process in brachypronotal and brachypterous individuals (Fig. 2C) or distinctly surpassing apex of hind pronotal process and nearly reaching of apex of hind tibia in pauropronotal individuals (Fig. 2A, B).

Legs. Fore and middle femora slightly compressed and margins finely serrated, ventral margins of middle femora straight or slightly undulated, middle femur slightly narrower than or equal to or slightly wider than visible part of tegmen in width. Hind femora robust and short, 2.8–3.4 × as long as wide; margins finely serrated; antegenicular denticles acute and genicular denticles obtuse. Outer side of hind tibia with seven or eight spines, inner side with six or seven spines. Length of first segment of posterior tarsi longer than third, three pulvilli of first segment of posterior tarsi increased in turn, apices of all pulvilli acute.

Abdomen. Ovipositor narrow and long, length of upper valvulae 3.0 × its width, upper and lower valvulae with slender saw-like teeth. Length of subgenital plate longer than its width, middle of posterior margin of subgenital plate triangularly projecting.

Coloration. Body yellow brown or brown or dark brown; antennae brown; dorsum of pronotum with two black spots behind the shoulders or with two black spots before the shoulders and behind the shoulders respectively or without black spot. Hind femora brown, outer side with two inconspicuous blackish spots in some individuals. Hind tibia yellow brown or brown or dark brown.

Male. Similar to female, but smaller and narrower. Width of vertex between eyes generally 1.2–1.5 × or sometimes equal to width of compound eye; dorsal margins straight and ventral margins of middle femora straight or slightly undulated, middle femur generally wider than or sometimes equal to visible part of tegmen in width. Subgenital plate short, cone-shaped, apex bifurcated.

Measurements (mm). See Table 1. Length of body: ♂ 6.0–10.0 (brachypronotal individuals) or 8.0–10.0 (pauropronotal individuals), ♀ 9.0–12.0 (brachypronotal individuals) or 8.5–11.0 (pauropronotal individuals); length of pronotum: ♂ 6.0–8.5 (brachypronotal individuals) or 6.0–11.0 (pauropronotal individuals), ♀ 7.5–9.0 (brachypronotal individuals) or 7.0–13.0 (pauropronotal individuals); length of hind femur: ♂ 5.0–6.0 (brachypronotal individuals) or 5.0–5.5 (pauropronotal individuals), ♀ 5.0–8.1 (brachypronotal individuals) or 6.0–7.0 (pauropronotal individuals).

Table 1. Measurements for the type specimens of synonyms of *T. japonica*.

Species	V/E		LB (in mm)		LP (in mm)		LF (in mm)		M/T		LH/WH
	female	male	female	male	female	male	female	male	female	male	
<i>C. circinihumerus</i> **	1.6	–	10.3	–	9.2	–	6.0	–	< 1	–	–
<i>C. emeiensis</i> *	1.3	–	10.2	–	8.0	–	8.1	–	< 1	–	–
<i>E. rongshuiensis</i> *	–	1.1	–	8.0	–	6.0	–	5.0	–	> 1	–
<i>E. zayuensis</i> *	1.3	–	10.2	–	8.4	–	6.0	–	> 1	–	–
<i>M. nigrivirus</i> *	1.3	1.3	1.0	8.0	9.0	7.0	5.0	5.0	= 1	> 1	–
<i>M. yaoshanensis</i> *	–	1.0	11.0	8.0	9.0	7.0	6.0	5.5	= 1	> 1	–
<i>T. albistriatus</i> *	1.0	1.0	12.0	10.0	8.5	8.0	7.0	5.0	= 1	= 1	–
<i>T. albomaculatus</i> *	–	1.0	–	9.0	–	8.5	–	5.5	–	= 1	–
<i>T. albomarginis</i> *	–	1.4	–	6.0	–	6.0	–	5.0	–	= 1	–
<i>T. cenwanglaoshana</i> **	1.6	–	9.0	–	10.5	–	6.0	–	< 1	–	–
<i>T. cliva</i> *	–	1.0	–	7.2	–	7.5	–	5.5	–	= 1	3.0
<i>T. duolunensis</i> *	1.6	1.2	9.0	7.0	8.0	6.0	6.0	5.0	= 1	> 1	2.6
<i>T. grossovalva</i> **	1.5	–	11.0	–	13.0	–	7.0	–	–	–	3.5
<i>T. jiuwanshanensis</i> **	1.6	1.5	11.0	8.0	12.0	10.0	6.0	5.0	= 1	> 1	–
<i>T. latipalpa</i> *	1.7	–	10.0	–	7.5	–	7.0	–	= 1	–	–
<i>T. liuwanshanensis</i> *	–	1.1	–	9.5	–	8.0	–	5.5	–	> 1	2.8
<i>T. qinlingensis</i> **	1.6	1.5	11.0	10.0	13.0	11.0	6.5	5.5	< 1	= 1	3.0
<i>T. rectimargina</i> *	1.0	–	11.0	–	8.0	–	7.0	–	> 1	–	3.3
<i>T. ruyuanensis</i> *	1.5	1.5	11.0	9.0	9.0	7.0	7.0	5.0	> 1	> 1	2.8
<i>T. xianensis</i> **	1.1	–	8.5	8.0	7.0	6.0	6.0	5.0	< 1	–	2.5
<i>T. xinchengensis</i> **	–	1.0	11.0	–	9.0	–	7.0	–	–	> 1	3.0
<i>T. yunlongensis</i> *	–	1.4	–	7.5	–	6.0	–	6.0	–	= 1	2.6
<i>T. zhoushanensis</i> *	1.1	1.0	9.9	7.8	8.5	6.3	6.2	6.0	= 1	= 1	3.0

Note: V/E: Vertex wide/eye diameter; LB: Length of body; LP: Length of pronotum; LF: Length of hind femur; M/T: Width of midfemur/width of visible part of tegmina; LH/WH: Length of hind femur/width of hind femur. –: not described or illustrated in the original descriptions of species. *: brachypronotal; **: paupronotal.

Diagnosis. *Tetrix japonica* can be differentiated from all the other Tetrigidae of China, North Korea, and Japan by the following set of the traits: the head not exerted above the upper level of the pronotum (strongly exerted in *Euparatetrix*, *Ergatetrix*, and *Bannatetrix*); in lateral view, frontal ridge and vertex forming an obtuse angle (in lateral view, frontal ridge and vertex forming rounded shape in *Coptotetrix* and *Hedetetrix*); fastigium of vertex in lateral view angulate, not much produced in front of eyes (fastigium of vertex in lateral view oblique, considerably produced in front of eyes in *Clinotetrix*); anterior margin of the vertex truncated, weakly arcuate (strongly angular in *Tetrix bipunctata*, *Tetrix subulate*, *Tetrix similans*); anterior margin of pronotum truncate, weakly angular protruding (strongly angular in *Tetrix tartara*); tegmenula and alae present (absent in *Formosatetrix*, *Aalatetrix*); alae > 2 × longer than tegmenula (short in *Tetrix bipunctata*, *Alulatetrix*).

Tetrix japonica is most similar to *Tetrix tenuicornis* (Sahlberg, 1893) from the Western Palearctic from which it differs in its pronotum slightly tectiform, median carina of pronotum low, not lamellar (vs pronotum distinctly tectiform, median carina of pronotum high, lamellar in *T. tenuicornis*).

A catalog of synonyms. (map of all the type localities of all the synonyms in Fig. 16).

- Coptotettix circinihumerus* Zheng & Deng, 2004a: 79 [description] (holotype ♀, China: Guangxi prov., Nanda County, in IZSNU, examined); Zheng 2005a: 237; Deng Zheng and Wei 2007a: 214; Zheng et al. 2013: 22; Deng 2016: 197. syn. nov. (Fig. 3A–C).
- Coptotettix emeiensis* Zheng, Lin & Zhang, 2012: 2554 [description] (holotype ♀, China: Sichuan prov., Emeishan City, in IZSNU, examined); Zheng et al. 2013: 22; Deng 2016: 197. syn. nov. (Fig. 3D–F).
- Euparatettix rongshuiensis* Zheng, 2005a: 387 [description] (holotype ♂, China: Guangxi prov., Rongshui County, in IZSNU, examined); Zheng 2005b: 99; Deng Zheng and Wei 2007a: 444; Deng 2016: 294. syn. nov. (Fig. 4A–C)
- Euparatettix zayuensis* Zheng, Zeng & Ou, 2011: 387 [description] (holotype ♀, China: Xizang autonomous region, Zayu County, Menkong, in IZSNU, examined); Deng 2016: 293. syn. nov. (Fig. 4D–F).
- Macromotettix nigrifubercle* Zheng & Jiang, 2006: 141 [description] (holotype ♀, China: Guangxi prov., Fusui County, Bapan, in IZSNU, examined); Deng et al. 2007a: 136; Deng 2016: 135; Deng, Xin & Chen, 2018: 423. syn. nov. (Fig. 5A–C).
- Macromotettix yaoshanensis* Zheng & Jiang, 2000: 403 [description] (holotype ♂, China: Guangxi prov., Jinxiu County, Liula, in IZSNU, examined); Zheng 2005a: 143; Deng et al. 2007a: 132; Deng 2016: 130; Deng et al. 2018: 423. syn. nov. (Fig. 5D–F).
- Tetrix albistriatus* Yao & Zheng, 2006: 824 [description] (holotype ♂, China: Yunnan prov., Pingbian County, Daweishan, in IZSNU, examined); Deng 2016: 245. syn. nov. (Fig. 6A–C).
- Tetrix albomaculatus* Zheng & Jiang, 2006: 142 [description] (holotype ♂, China: Guangxi prov., Fusui County, Bapan, in IZSNU, examined); Deng et al. 2007a: 286; Deng 2016: 242. syn. nov. (Fig. 6D–F).
- Tetrix albomarginis* Zheng & Nie, 2005: 582 [description] (holotype ♂, China: Yunnan prov., Dali County, Cangshan, in IZSNU, examined); Deng et al. 2007a: 300; Deng 2016: 245. syn. nov. (Fig. 7A–C).
- Tetrix cenwanglaoshana* Zheng, Jiang & Liu, 2005: 181 [description] (holotype ♀, China: Guangxi prov., Tianlin County, Cenwanglaoshan, in IZSNU, examined). syn. nov. (Fig. 7D–F).
- Tetrix cliva* Zheng & Deng, 2004b: 97 [description] (holotype ♂, China: Guangxi prov., Luocheng County, in IZSNU, examined); Zheng 2005a: 322; Deng et al. 2007a: 291a; Deng 2016: 251 (*Tetrix cliva* Zheng & Deng, 2004 = *Tetrix ruyuanensis* Liang, 1998, proposed in unpublished PhD Dissertation). syn. nov. (Fig. 8A–C).
- Tetrix duolunensis* Zheng, 1996: 178 [description] (holotype ♀, China: Inner Mongolia autonomous region, Duolun County, in IZSNU, examined); Zheng 2005c: 106; Deng 2016: 244. syn. nov. (Fig. 8D–F).
- Tetrix grossovalva* Zheng, 1994: 147 [description] (holotype ♀, China: Jilin prov., Fongman County, Songhuahu, in IZSNU, examined); Liang and Zheng 1998: 148; Zheng 2005c: 99; Deng 2016: 218. syn. nov. (Fig. 9).
- Tetrix jiuwanshanensis* Zheng, 2005a: 274 [description] (holotype ♀, China: Guangxi prov., Rongshui County, in IZSNU, examined); Zheng 2005c: 100; Deng et al. 2007a: 250; Deng 2016: 220. syn. nov. (Fig. 10).

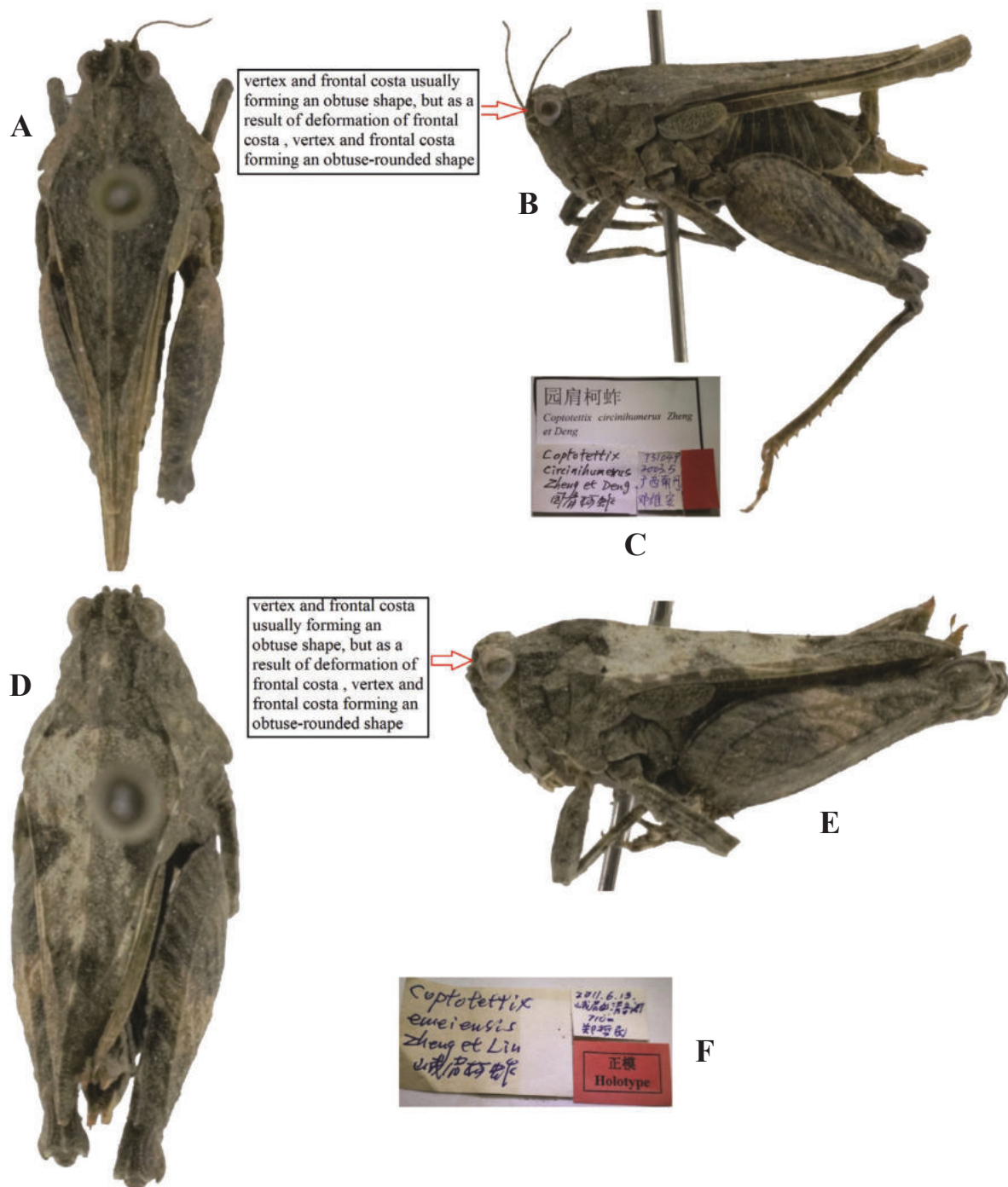


Figure 3. *Tetrix japonica* (Bolívar, 1887) **A–C** holotype of *Coptotettix circinihumerus* Zheng & Deng, 2004, syn. nov. **A** dorsal view **B** lateral view **C** labels **D–F** holotype of *Coptotettix emeiensis* Zheng, Lin & Zhang, 2012, syn. nov. **D** dorsal view **E** lateral view **F** labels.

Tetrix latipalpa Cao & Zheng, 2011: 739 [description] (holotype ♂, China: Sichuan prov., Emeishan County, Mt. Emei, in IZSNU, examined); Deng 2016: 249. syn. nov. (Fig. 11A–C).

Tetrix liuwanshanensis Deng, Zheng & Wei, 2007b: 294 [description] (holotype ♂, China: Guangxi prov., lingshan County, Liuwanda Mountain, in IZSNU, examined); Deng et al. 2007a: 277; Deng 2016: 238. syn. nov. (Fig. 11D–F).

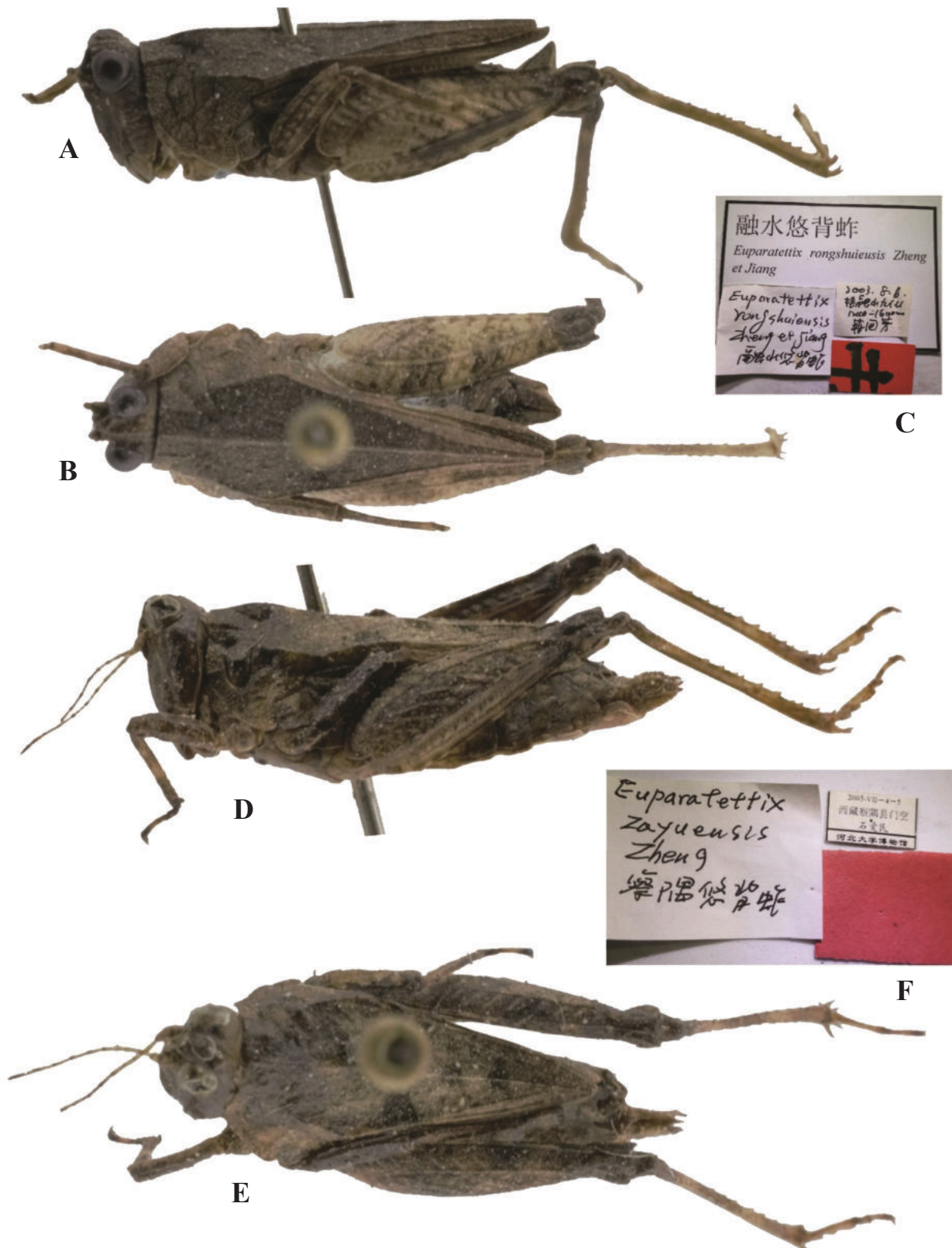


Figure 4. *Tetrix japonica* (Bolívar, 1887) **A–C** holotype of *Euparatettix rongshuiensis* Zheng, 2005, syn. nov. **A** lateral view (The pin passes through the right side of the thorax from the shoulder of pronotum, which tends to push the pronotum down. This elevates the previously non-protruding head) **B** dorsal view **C** labels **D–F** holotype of *Euparatettix zayuensis* Zheng, Zeng & Ou, 2011, syn. nov. **D** lateral view (The pin passes through the right side of the thorax from the shoulder of pronotum, which tends to push the pronotum down. This elevates the previously unprotruding head) **E** dorsal view **F** labels.

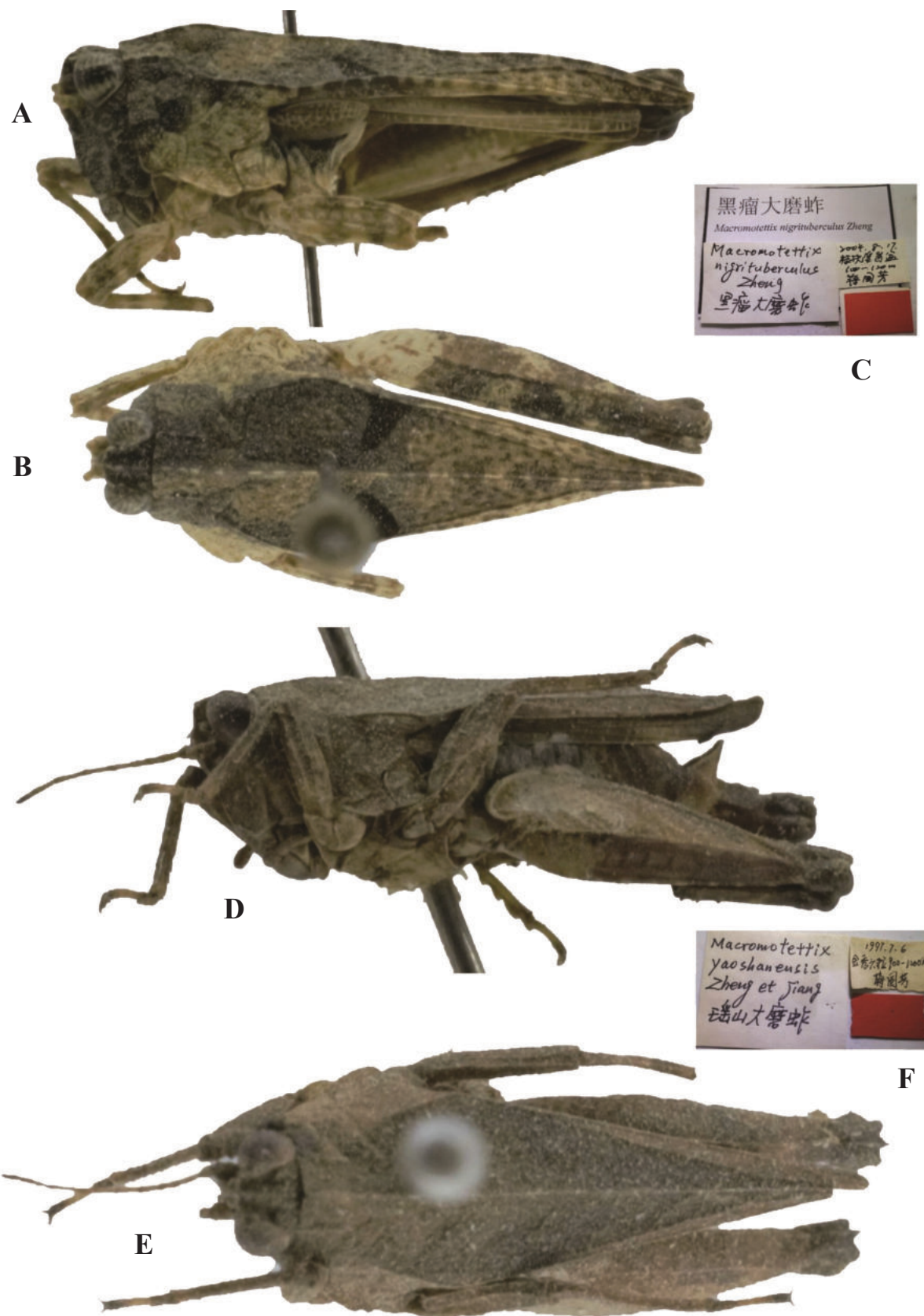


Figure 5. *Tetrix japonica* (Bolívar, 1887) **A–C** holotype of *Macromotettix nigritubercle* Zheng & Jiang, 2006, syn. nov. **A** lateral view **B** dorsal view **C** labels **D–F** holotype of *Macromotettix yaoshanensis* Zheng & Jiang, 2000, syn. nov. **D** lateral view **E** dorsal view **F** labels.

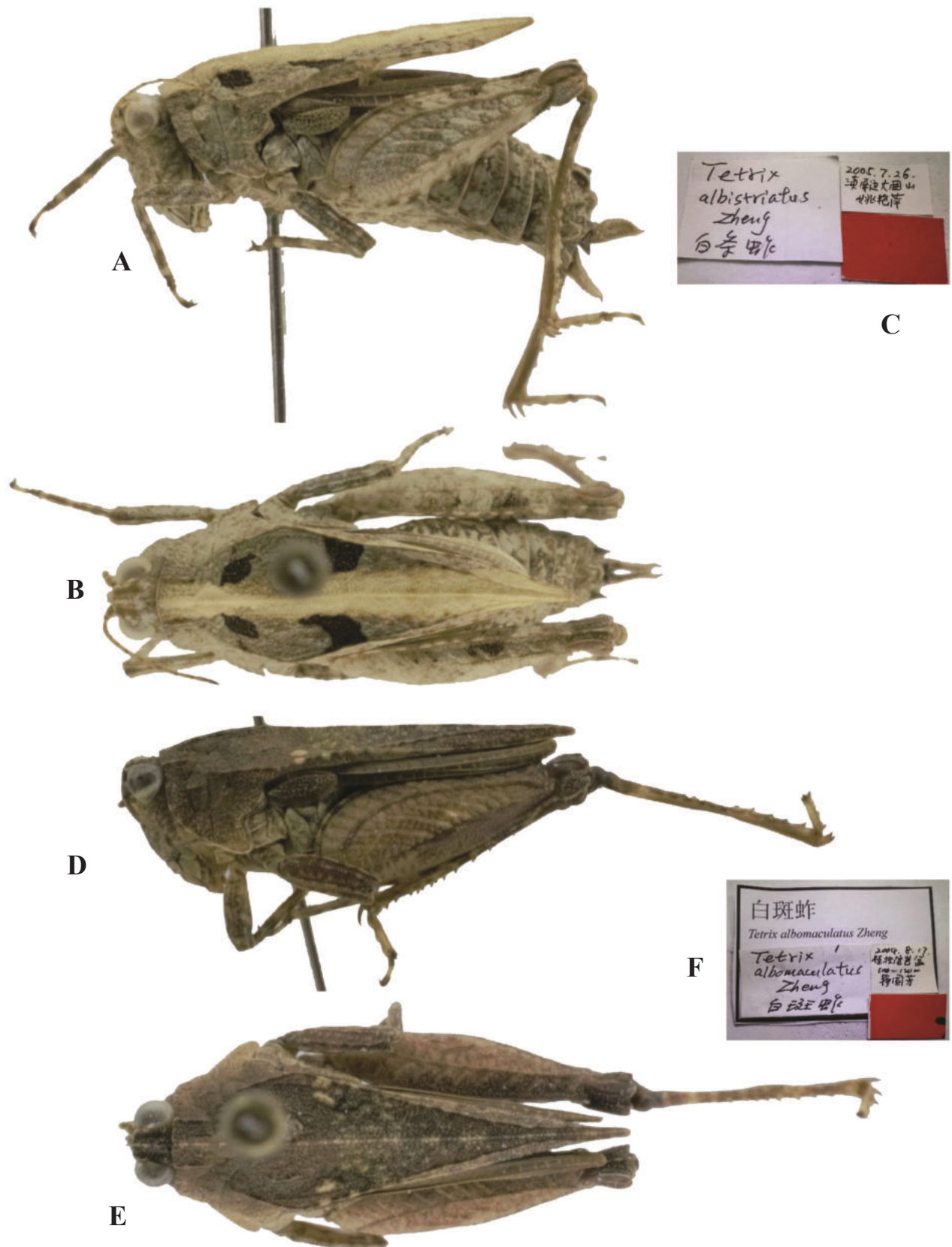


Figure 6. *Tetrix japonica* (Bolivar, 1887) **A–C** holotype of *Tetrix albistriatus* Yao & Zheng, 2006, syn. nov. **A** lateral view **B** dorsal view **C** labels **D–F** holotype of *Tetrix albomaculatus* Zheng & Jiang, 2006, syn. nov. **D** lateral view **E** dorsal view **F** labels.



Figure 7. *Tetrix japonica* (Bolivar, 1887) **A–C** holotype of *Tetrix albomarginis* Zheng & Nie, 2005, syn. nov. **A** dorsal view **B** lateral view **C** labels **D–F** holotype of *Tetrix qinwanglaoshana* Zheng, Jiang & Liu, 2005, syn. nov. **D** lateral view **E** dorsal view **F** labels.

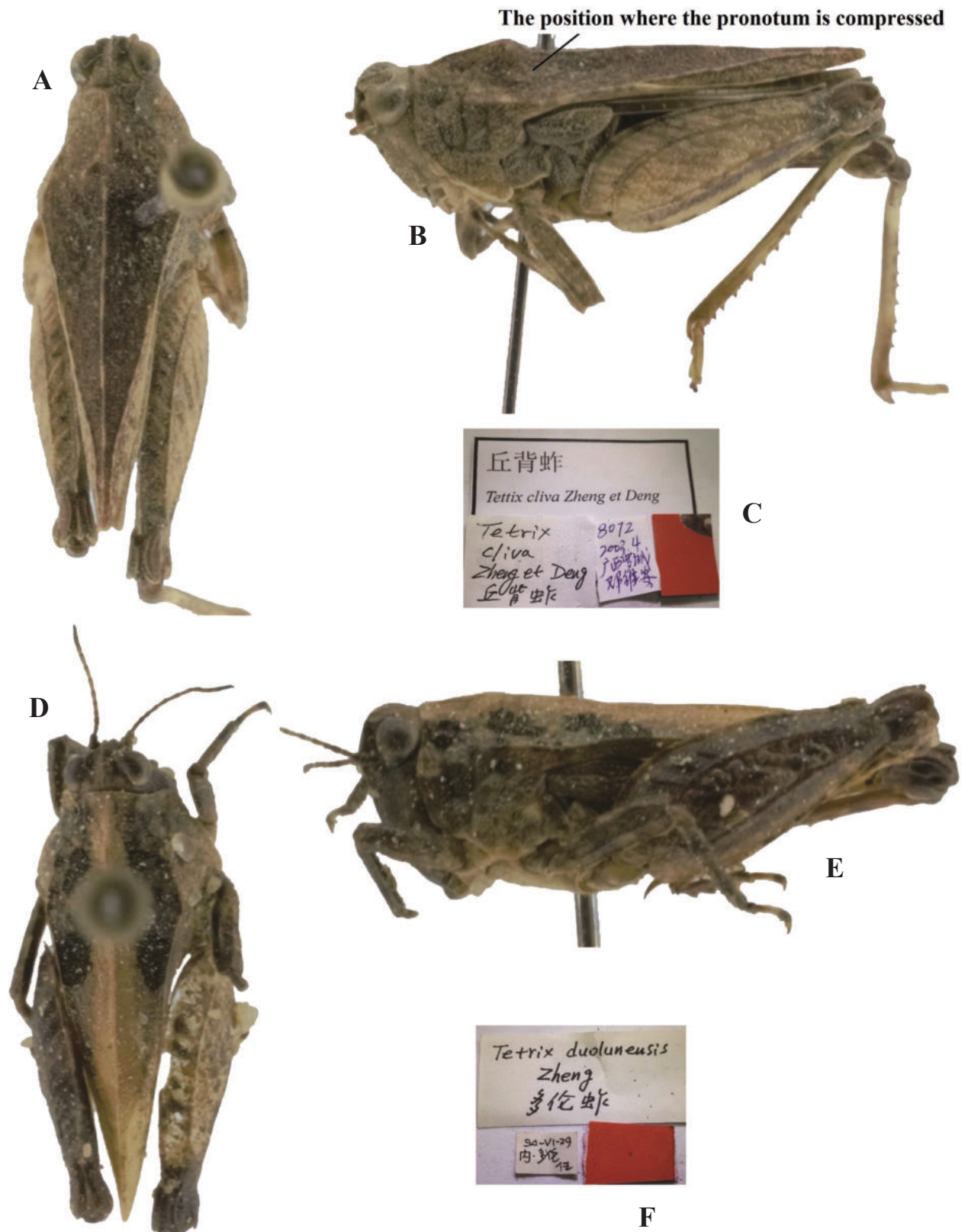


Figure 8. *Tetrax japonica* (Bolívar, 1887) **A–C** holotype of *Tetrax cliva* Zheng & Deng, 2004, syn. nov. **A** dorsal view **B** lateral view **C** labels **D–F** holotype of *Tetrax duolunensis* Zheng, 1996, syn. nov. **D** dorsal view **E** lateral view **F** labels.



Figure 9. *Tetrix japonica* (Bolívar, 1887). Holotype of *Tetrix grossovalva* Zheng, 1994, syn. nov. **A** lateral view **B** dorsal view **C** labels.

- Tetrix qinlingensis* Zheng, Huo & Zhang, 2000: 238 [description] (holotype ♀, China: Shaanxi prov., Foping County, Zhongzui, in IZSNU, examined); Zheng 2005a: 275; Deng et al. 2007a: 251; Deng 2016: 220. syn. nov. (Fig. 12A, B).
- Tetrix rectimargina* Zheng & Jiang, 2004: 3 [description] (holotype ♀, China: Guangxi prov., Tian'e County, Buliu River, in IZSNU, examined); Zheng 2005a: 308; Deng et al. 2007a: 273; Deng 2016: 234. syn. nov. (Fig. 12D–F).
- Tetrix ruyuanensis* Liang, 1998: 174 [description] (holotype ♀, China: Guangdong prov., Ruyuan County, Tianjingshan, in BMSYU, not examined); Zheng 2005a: 307; Deng et al. 2007a: 303; Deng 2016: 251. syn. nov. (Fig. 13A, B).
- Tetrix xianensis* Zheng, 1996: 177 [description] (holotype ♀, China: Shaanxi prov., Xi'an City, Shaanxi Normal University, in IZSNU, examined); Zheng 2005a: 283; Deng 2016: 226. syn. nov. (Fig. 13D–F).
- Tetrix xinchengensis* Deng, Zheng & Wei, 2007a: 289 [description] (holotype ♂, China: Guangxi prov., Xincheng County, in IZSNU, examined); Deng 2016: 242. syn. nov. (Fig. 14A, B).
- Tetrix yunlongensis* Zheng & Mao, 2002: 91 [description] (holotype ♂, China: Yunnan prov., Yunlong County, in IZSNU, examined); Zheng 2005a: 311; Deng et al. 2007a: 275; Deng 2016: 236. syn. nov. (Fig. 14D, F).

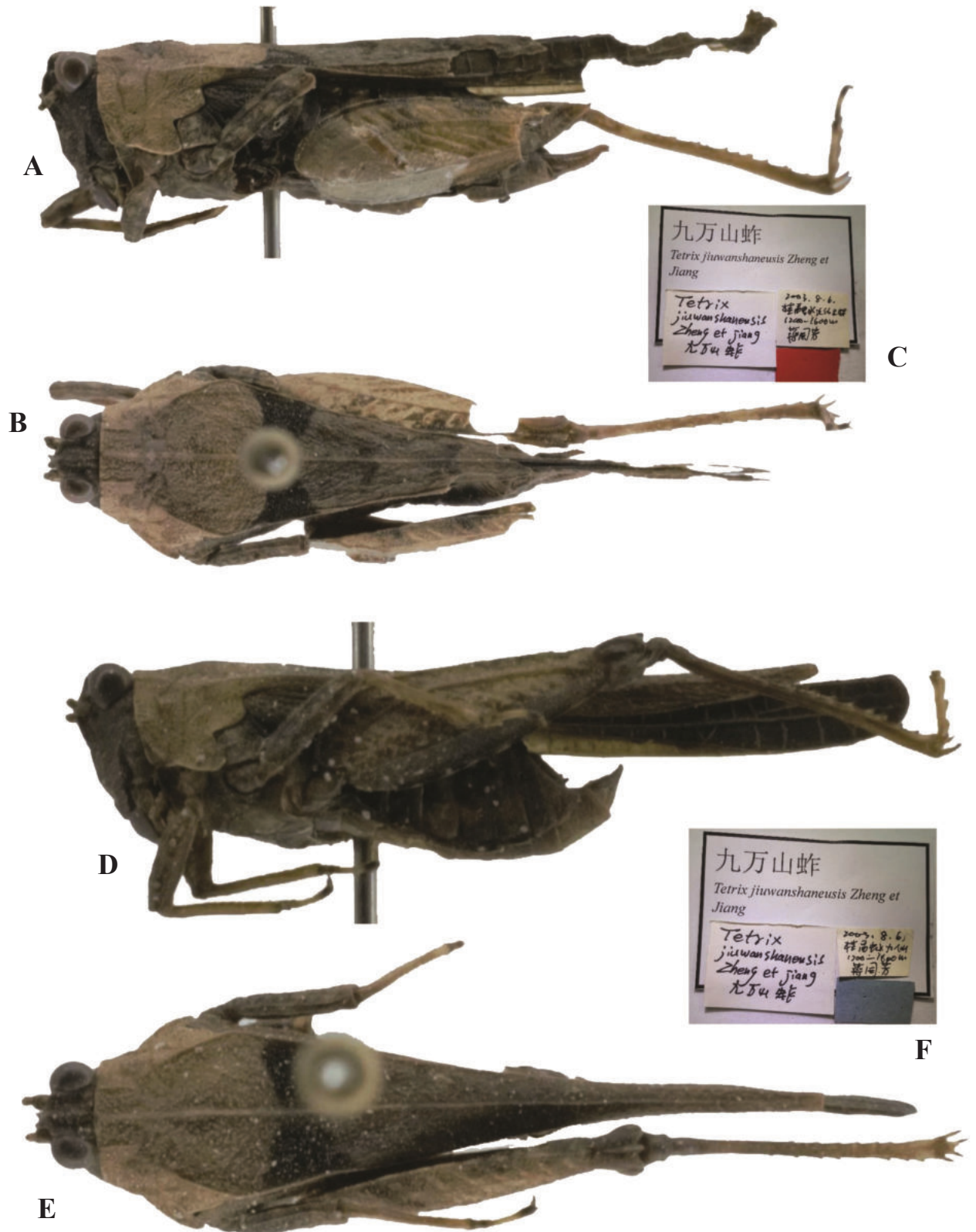


Figure 10. *Tetrax japonica* (Bolívar, 1887). *Tetrax jiuwanshanensis* Zheng, 2005, syn. nov. **A** holotype, lateral view **B** holotype, dorsal view **C**, **F** labels **D** allotype, lateral view **E** allotype, dorsal view.



Figure 11. *Tetrax japonica* (Bolívar, 1887) **A–C** holotype of *Tetrax latipalpa* Cao & Zheng, 2011, syn. nov. **A** dorsal view **B** lateral view **C** labels **D–F** holotype of *Tetrax liuwanshanensis* Deng, Zheng & Wei, 2007, syn. nov. **D** lateral view **E** dorsal view **F** labels.

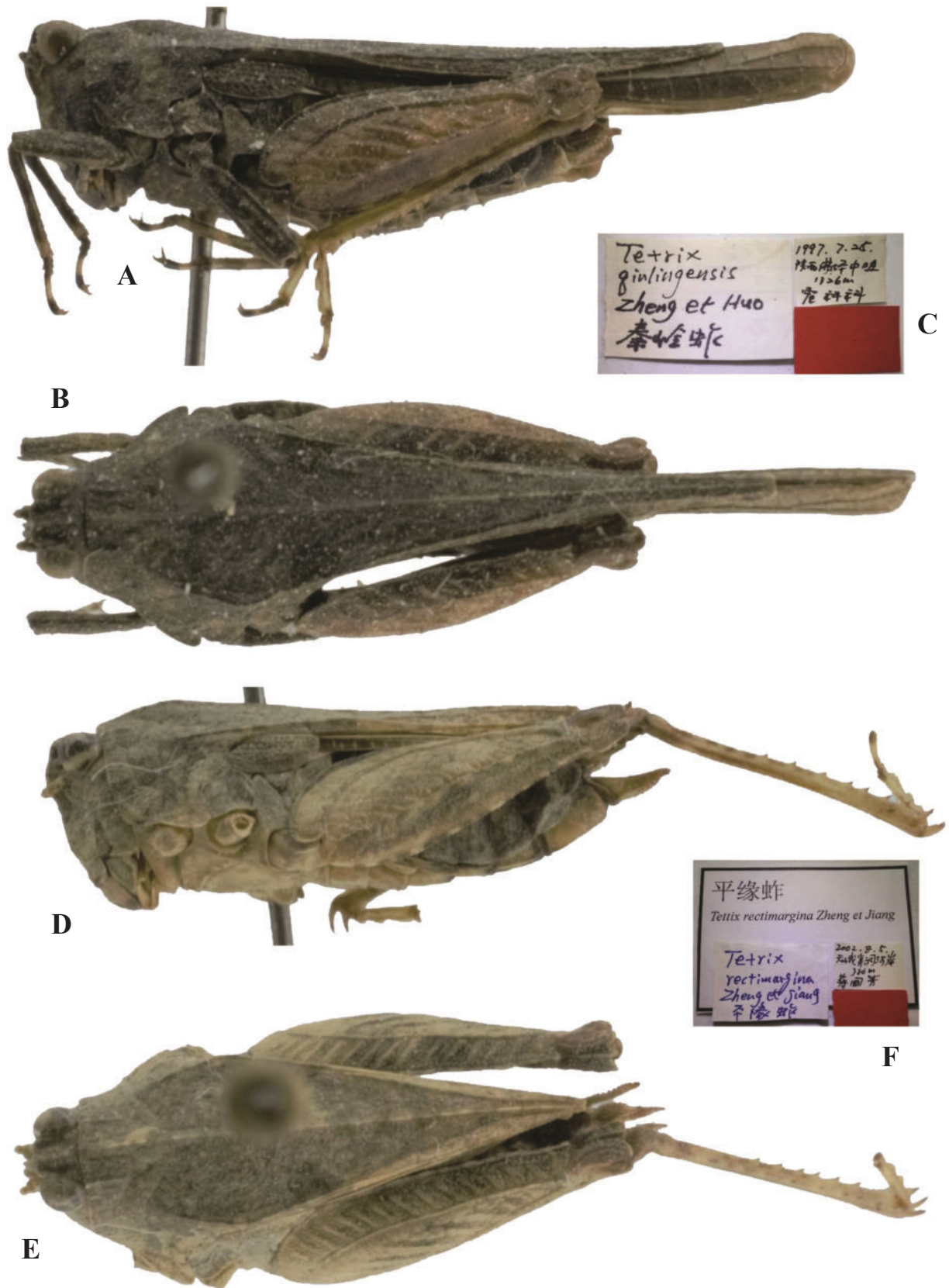


Figure 12. *Tetrix japonica* (Bolivar, 1887) **A–C** holotype of *Tetrix qinlingensis* Zheng, Huo & Zhang, 2000, syn. nov. **A** lateral view **B** dorsal view **C** labels **D–F** holotype of *Tetrix rectimargina* Zheng & Jiang, 2004, syn. nov. **D** lateral view **E** dorsal view **F** labels.

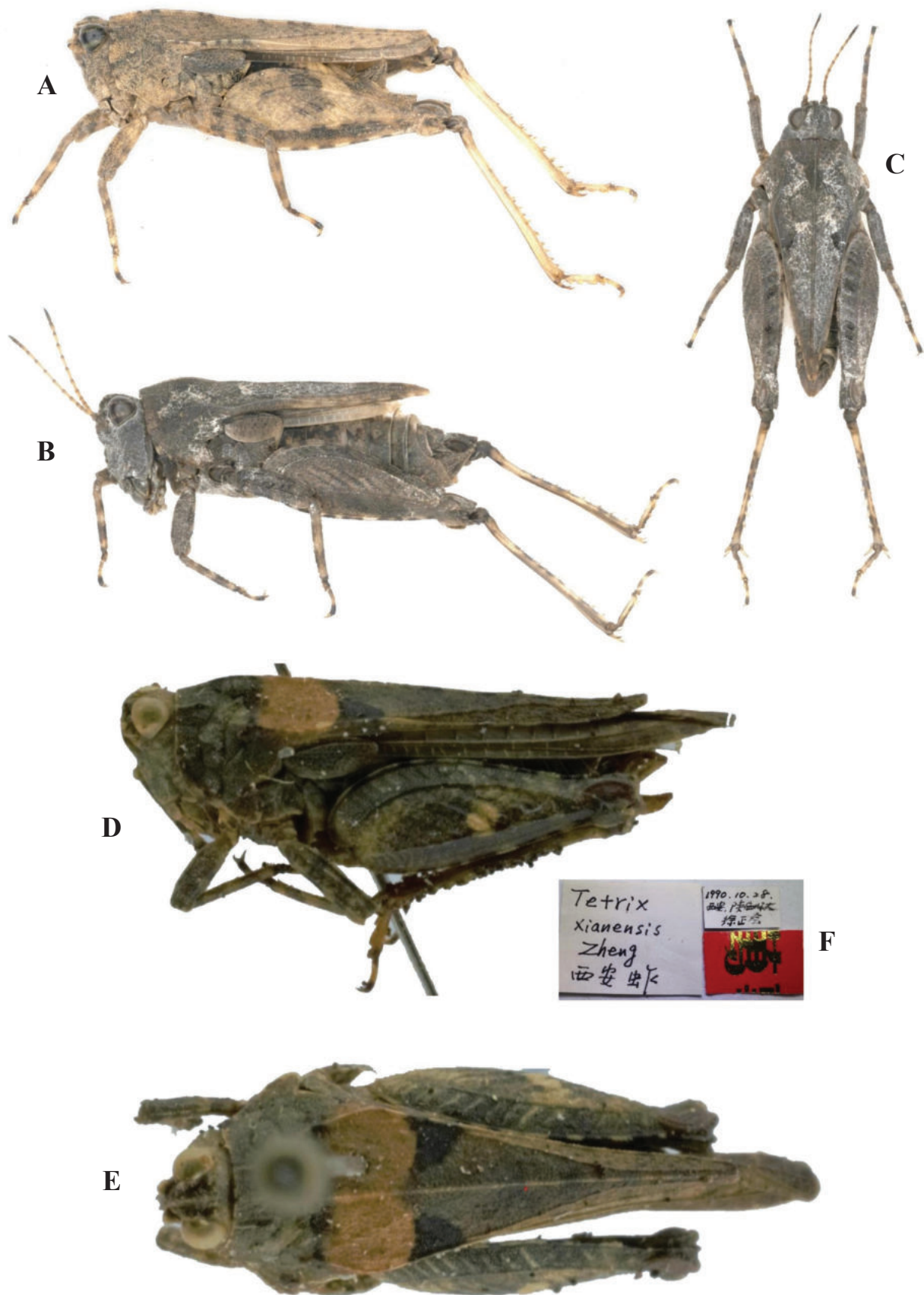


Figure 13. *Tetrrix japonica* (Bolívar, 1887) **A–C** topotype of *Tetrrix ruyuanensis* Liang, 1998, syn. nov. **A** lateral view, pronotum with nearly straight median carina **B** lateral view, pronotum with arcuate median carina before shoulders **C** dorsal view **D–F** holotype of *Tetrrix xianensis* Zheng, 1996, syn. nov. **D** lateral view **E** dorsal view **F** labels.

Tetrix zhoushanensis Gao, Liu & Yin, 2022: 347 [description] (holotype ♂, China: Zhejiang prov., Zhoushan City, in MHU, not examined). syn. nov. (Fig. 15).

Type material examined. Type material of *Tetrix japonica* was examined from the photographs of the syntype (♀, brachypronotal and brachypterous specimen, in MHNG, photographs by Josef Tumbrinck), available online in OSF (Fig. 2A).

Other material of *Tetrix japonica* examined. 11♂23♀, CHINA: Sichuan prov., Emeishan City, 29 July 2018, in EMHU; 17♂13♀, CHINA: Xizang, Zayu County, 25 June 2019, in EMHU; 33♂19♀, CHINA: Guangxi prov., Fusui County, Bapan, 17 August 2014, in EMHU; 24♂23♀, CHINA: Guangxi prov., Jinxiu County, 26 July 2021, in EMHU; 37♂20♀, CHINA: Yunnan prov., Pingbian County, Daweishan, 26 July 2020, in EMHU; 55♂27♀, CHINA: Guangxi prov., Tianlin County, Cenwanglaoshan, 25 May 2018, in EMHU; 52♂38♀, CHINA: Guangxi prov., Longzhou County, nonggang, 18 July 2023, in CLSGNU; 47♂58♀, CHINA: Guangxi prov., Luocheng County, Jiuwanshan, 21 August 2022, in EMHU; 7♂8♀, CHINA: Inner Mongolia autonomous region, Duolun County, 09 August 2019, in EMHU; 27♂32♀, CHINA: Guangxi prov., Rongshui County, 06 August 2003, in EMHU; 17♂21♀, CHINA: Guangxi prov., lingshan County, Liuwanda Mountain, 24 August 2022, in CLSGNU; 20♂8♀, CHINA: Shaanxi prov., Foping County, 28 July 2022, in CLSGNU; 11♂15♀, CHINA: Guangdong prov., Ruyuan County, Tianjingshan, 20 August 2022, in CLSGNU; 17♀10♂, CHINA: Liaoning prov., Benxi County, Tanggou, 27 July 2023 in CLSGNU; 22♀22♂, CHINA: Jilin prov., Changbai County, Changbai, 31 July 2023 in CLSGNU; 14♀23♂, CHINA: Heilongjiang prov., Mudanjiang City, Mudanfen, 3 August 2023 in CLSGNU; 29♀13♂, CHINA: Heilongjiang prov., Yichun City, Jiayin County, 6 August 2023 in CLSGNU; 22♀11♂, CHINA: Heilongjiang prov., Xinlin County, Xinlin, 9 August 2023 in CLSGNU; 26♀43♂, CHINA: Inner Mongolia prov., Tuquan County, Taihe, 12 August 2023 in CLSGNU; 33♀50♂, CHINA: Inner Mongolia prov., Horqin Right Middle Banner, Wutaiyingzi, 13 August 2023 in CLSGNU.

Type material of the synonyms examined.

Coptotettix circinivirus: ♀, holotype (Fig. 3A–C), China: Guangxi prov., Nandan County, Songhuahu, May 2003, in IZSNU.

Coptotettix emeiensis: ♀, holotype (Fig. 3D–F), China: Sichuan prov., Emeishan City, 13 June 2011, in IZSNU.

Euparatettix rongshuiensis: ♂, holotype (Fig. 4A–C), China: Guangxi prov., Rongshui County, 06 August 2003, in IZSNU.

Euparatettix zayuensis: ♀, holotype (Fig. 4D–F), China: Xizang, Zayu County, Menkong, 04–05 July 2005, in IZSNU.

Macromotettix nigrivirus: ♀, holotype (Fig. 5A–C) and 1♂ paratype, China: Guangxi prov., Fusui County, Bapan, 17 August 2004, in IZSNU.

Macromotettix yaoshanensis: ♂, holotype (Fig. 5D–F), China: Guangxi prov., Jinxiu County, Liula, 06 July 1997, in IZSNU.

Tetrix albistriatus: ♀, holotype (Fig. 6A–C) and 1♂3♀ paratypes, China: Yunnan prov., Pingbian County, Daweishan, 26 July 2005, in IZSNU.

Tetrix albomaculatus: ♂, holotype (Fig. 6D–F), China: Guangxi prov., Fusui County, Bapan, 17 August 2004, in IZSNU.

Tetrix albomarginis: ♂, holotype (Fig. 7A–C), China: Yunnan prov., Dali County, Cangshan, 09 August 2004, in IZSNU.

Tetrix cenwanglaoshana: ♀, holotype (Fig. 7D–F), China: Guangxi prov., Tianlin County, Cenwanglaoshan, 31 May 2002, in IZSNU.



Figure 14. *Tetrix japonica* (Bolívar, 1887) **A–C** topotype of *Tetrix xinchengensis* Deng, Zheng & Wei, 2007, syn. nov. **A** lateral view **B** dorsal view **C** labels **D–F** holotype of *Tetrix yunlongensis* Zheng & Mao, 2002, syn. nov. **D** lateral view **E** dorsal view **F** labels.

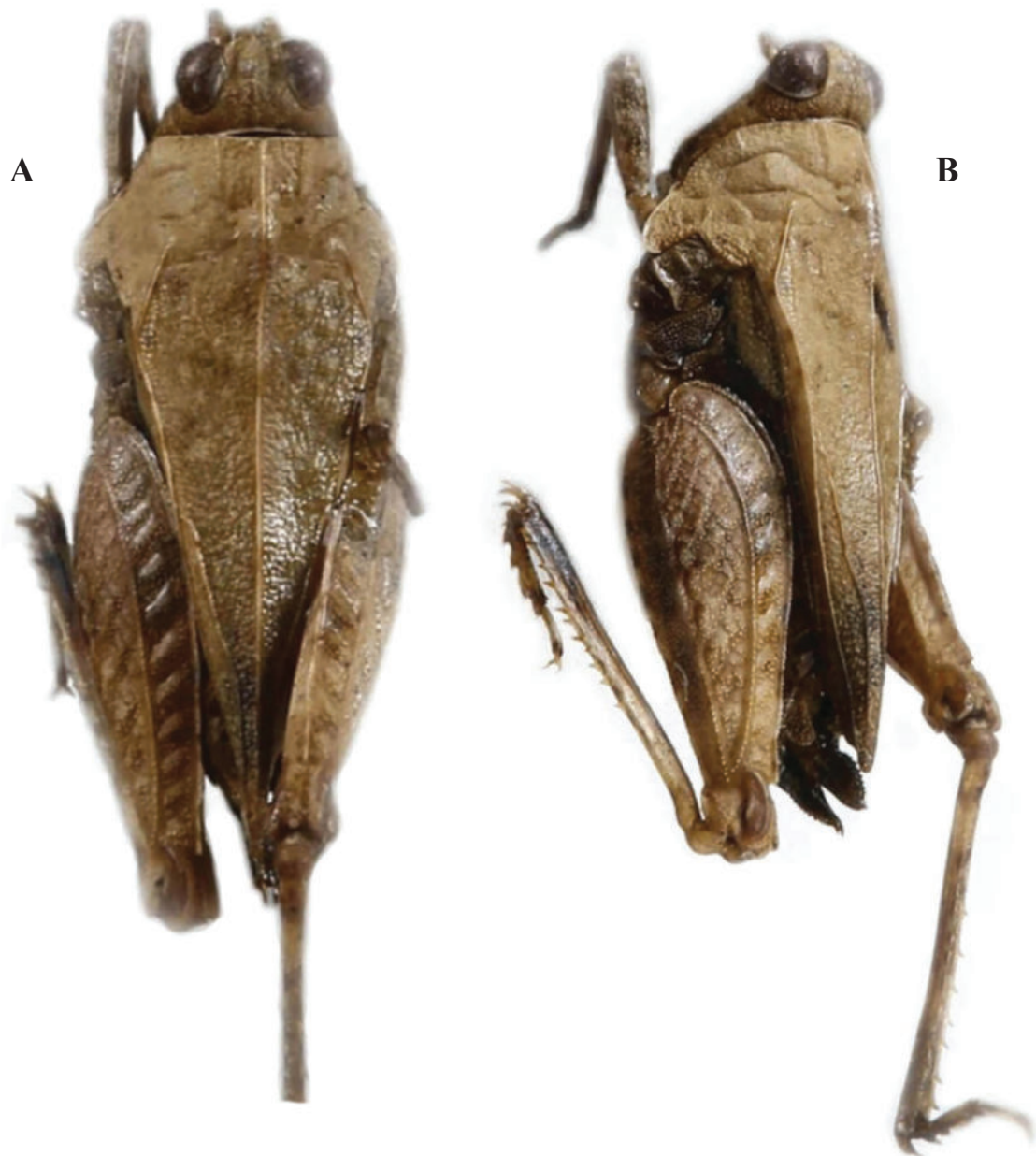


Figure 15. *Tetrix japonica* (Bolívar, 1887). Holotype of *Tetrix zhoushanensis*, Gao, Liu & Yin, 2022, syn. nov. **A** dorsal view **B** lateral view (photo Gao et al.).

Tetrix cliva: ♂, holotype (Fig. 8A–C), China: Guangxi prov., Luocheng County, April 2003, in IZSNU.

Tetrix duolunensis: ♀, holotype (Fig. 8D–F) and 5♂7♀ paratypes, China: Inner Mongolia autonomous region, Duolun County, 29 June 1994, in IZSNU.

Tetrix grossovalva: ♀, holotype (Fig. 9A–C), China: Jilin prov., Fongman County, Songhuahu, 19 July 1990, in IZSNU.

Tetrix jiuwanshanensis: ♀, holotype (Fig. 10) and 1♂ paratype, China: Guangxi prov., Rongshui County, 06 August 2003, in IZSNU.

Tetrix latipalpa: ♂, holotype (Fig. 11A–C), China: Sichuan prov., Emeishan County, Mt. Emei, 16 August 2010, in IZSNU

Tetrix liuwanshanensis: ♂, holotype (Fig. 11D–F) and 1♂ paratype, China: Guangxi prov., lingshan County, Liuwanda Mountain, 24 August 2005, in IZSNU.

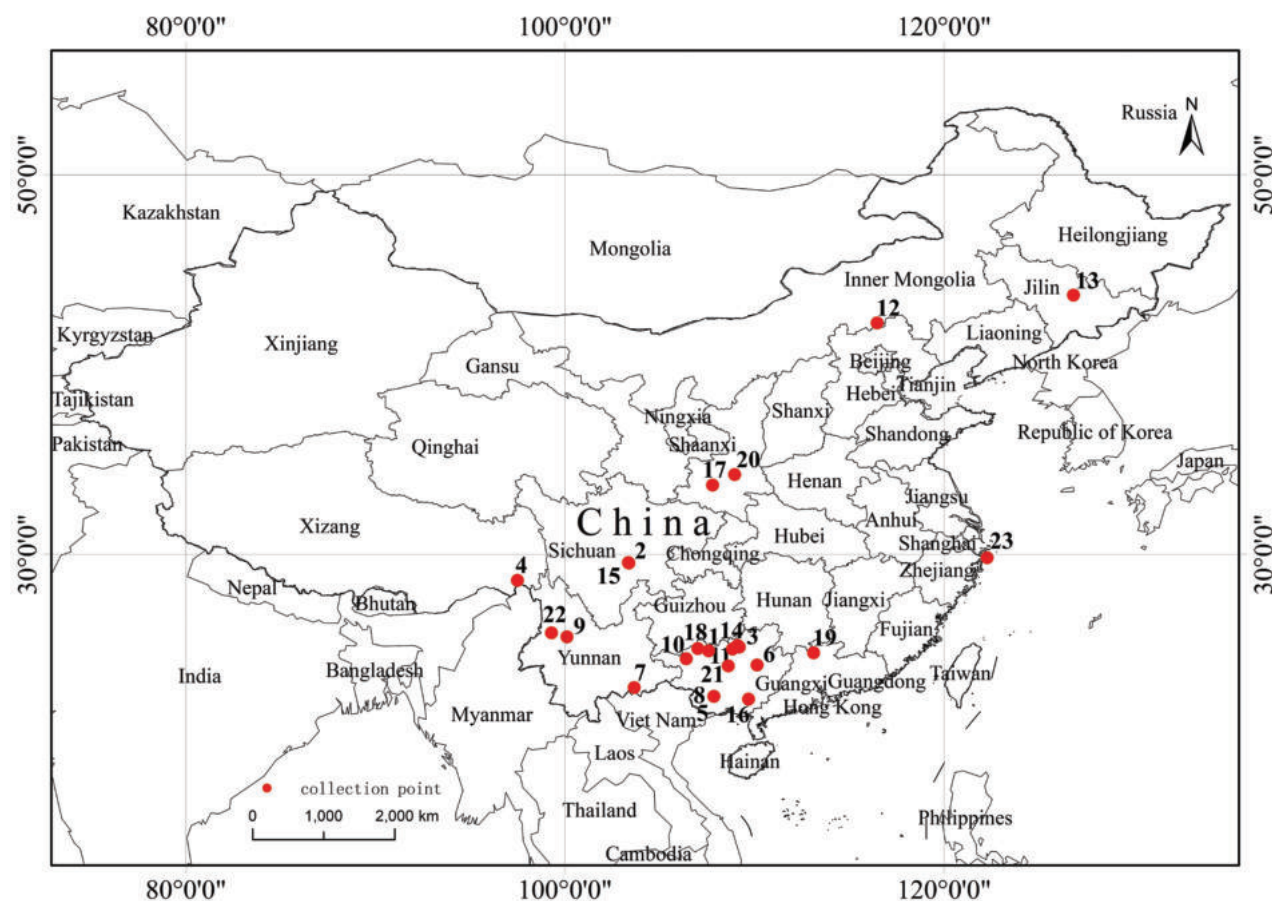


Figure 16. Distribution map of *Tetrix japonica* with all type localities of all the synonyms. 1 *C. circinihumerus*; 2 *C. emeiensis*; 3 *E. rongshuiensis*; 4 *E. zayuensis*; 5 *M. nigrilubercle*; 6 *M. yaoshanensis*; 7 *T. albistriatus*; 8 *T. albomaculatus*; 9 *T. albomarginis*; 10 *T. cenwanglaoshana*; 11 *T. cliva*; 12 *T. duolunensis*; 13 *T. grossovalva*; 14 *T. jiuwanshanensis*; 15 *T. latipalpa*; 16 *T. liuwanshanensis*; 17 *T. qinlingensis*; 18 *T. rectimargina*; 19 *T. ruyuanensis*; 20 *T. xianensis*; 21 *T. xinchengensis*; 22 *T. yunlongensis*; 23 *T. zhoushanensis*.

Tetrix qinlingensis: ♀, holotype (Fig. 12A–C) and 1♂1♀ paratypes, China: Shaanxi prov., Foping County, Zhongzui, 24 July 1997, in IZSNU.

Tetrix rectimargina: ♀, holotype (Fig. 12D–F), China: Guangxi prov., Tian'e County, Buliu River, 05 August 2002, in IZSNU.

Tetrix xianensis: ♀, holotype (Fig. 13C–E), China: Shaanxi prov., Xian City, 28 October 1990, in IZSNU.

Tetrix xinchengensis: ♂, holotype (Fig. 14A–C), China: Guangxi prov., Xincheng County, 14 July 2005, in IZSNU.

Tetrix yunlongensis: ♂, holotype (Fig. 14D–F), China: Yunnan prov., Yunlong County, 03 May 1998, in IZSNU.

Justification of the synonymies. Holotype of *Coptotettix circinihumerus* (Fig. 3A–C) from Guangxi and holotype of *Coptotettix emeiensis* (Fig. 3D–F) from Sichuan have a deformed frontal costa, and vertex and frontal costa forming an obtuse-rounded aspect in profile. These two taxa were misidentified as members of the genus *Coptotettix*: *Coptotettix circinihumerus* has a widened vertex, a low pronotal median carina; antennal grooves inserted between inferior margins of compound eyes; hind wings extending beyond the apex of the pronotum; ventral margins of middle femora are slightly undulated. *Coptotettix emeiensis* is charac-

terized by width of vertex between eyes $1.3 \times$ wider than width of a compound eye; antennal grooves inserted between inferior margins of compound eyes; median carina of pronotum slightly arch-like before the shoulders and straight behind the shoulders in profile; hind wings nearly reach the apex of of the pronotum. *Coptotettix circinivirus* and *Coptotettix emeiensis* are completely consistent with the morphology of brachypronotal and brachypterous individuals of *T. japonica*.

Euparatettix rongshuiensis (Fig. 4A–C) from Guangxi was described on the basis of a single male holotype. The holotype has a deformed head, and the head is slightly exerted above the upper level of the pronotum. However, it is characterized by frontal ridge and vertex forming an obtuse angle; antennal grooves inserted between inferior margins of compound eyes; median carina of pronotum low and full length entire, in profile, slightly straight; ventral margins of middle femora straight; hind wings slightly surpassing apex of hind pronotal process. *Euparatettix zayuensis* (Fig. 4D–F) from Xizang was described based on two female specimens. The holotype has a deformed head, and the head is slightly exerted above the upper level of the pronotum. But it has a widened vertex, a low pronotal median carina, straight and widened middle femora. These two taxa were misidentified as members of the genus *Euparatettix*. *E. rongshuiensis*, and *E. zayuensis* appear to be conspecific with *T. japonica* (brachypronotal and brachypterous individuals).

Macromotettix nigrivirus (Fig. 5A–C) from Guangxi represents a synonym of *T. japonica*. It is the same as *T. japonica* (brachypronotal and brachypterous forms) in all of the characters except for the slightly obliquely truncate posterior angles of the lateral lobes of the pronotum. The slightly truncate posterior angles of lateral lobes of pronotum fit the known variability of *T. japonica*. Examination of *Macromotettix yaoshanensis* (Fig. 5D–F) from Guangxi, shows that this specimen is a brachypronotal and brachypterous *T. japonica*. It is characterized by head and eyes not exerted above pronotal surface; frontal ridge and vertex forming an obtuse angle; antennal grooves inserted between inferior margins of compound eyes; median carina of pronotum low and full length entire; hind wings slightly surpassing apex of hind pronotal process. The specimen also has interhumeral carinae between shoulders, while the interhumeral carinae are inconspicuous and small.

Tetrix albistriatus (Fig. 6A–C) from Yunnan, which completely fits the morphology of brachypronotal and brachypterous individuals of *T. japonica*, also has a white stripe on the median carina of the pronotum. The two taxa are conspecific and characterized by a frontal ridge and vertex forming an obtuse angle; median carina of pronotum nearly straight in profile, slightly arcuate in forepart; lower margins of mid femora slightly straight, width of mid femora equal to width of tegmina in females; hind wings not reaching the apex of the hind pronotal process.

Tetrix albomaculatus (Fig. 6D–F) from Guangxi was described based on a single male holotype. This specimen representing a brachypronotal and brachypterous *T. japonica*, has interhumeral carina between the shoulders and white spots behind the shoulders. It is characterized by head and eyes not exerted above pronotal surface; frontal ridge and vertex forming an obtuse angle; antennal grooves inserted between inferior margins of compound eyes; lower margins of mid femora straight, width of mid femora equal to width of tegmina in females. *Tetrix albomarginis* (Fig. 7A–C) from Yunnan was also described based on a single male holotype. This specimen is similar to the morphology of brachypronotal and brachypterous individuals of *T. japonica*, and has white

pronotal margins and a slightly elevated median carina of the pronotum. But it has a widened vertex, a low pronotal median carina, straight ventral margins of middle femora, as well as shortened pronotum and hind wings.

Tetrix cenwanglaoshana (Fig. 7D–F) from Guangxi was described based on a single female holotype. It is conspecific with *T. japonica* (pauropronotal individuals) and has a widened vertex, frontal ridge and vertex forming an obtuse angle in profile, low and full length entire pronotal median carina, as well as extended hind wings and pronotum.

Tetrix cliva (Fig. 8A–C) from Guangxi was described based on a single male holotype. In the original description, the specific epithet *cliva* refers to the shape of the upper margin of the pronotum, in profile, with a triangular process before the shoulders. Examination of holotype showed that the shoulders of pronotum were compressed and were deformed before the shoulders to create a triangular protuberance. Other important traits are the same as *T. japonica*: it has straight ventral margins of middle femora, as well as shortened pronotum and hind wings; frontal ridge and vertex forming an obtuse angle; antennal grooves inserted between inferior margins of compound eyes. Therefore, *T. cliva* is conspecific with *T. japonica* (brachypronotal and brachypterous individuals).

We examined the type series of *Tetrix duolunensis* (Fig. 8D–F) from Inner Mongolia. The anterior margin of the fastigium of the vertex was slightly arcuate and slightly surpassed the anterior margin of the eye in some individuals. However, most individuals completely fit the morphology of brachypronotal and brachypterous individuals of *T. japonica*. It has a widened vertex, straight frontal costa, low pronotal median carina, and extended hind wings and pronotum. Thus, *T. duolunensis* is considered to be a synonym of *T. japonica*.

Tetrix grossovalva (Fig. 9A–C) from Jilin was described based on a single female holotype that appears to be conspecific with *T. japonica* (pauropronotal individuals). It has a widened vertex, straight frontal costa, low and full length entire pronotal median carina, and extended hind wings and pronotum.

Tetrix jiuwanshanensis (Fig. 10) from Guangxi completely fits the morphology of pauropronotal individuals of *T. japonica*. These two taxa are conspecific and characterized by the frontal ridge and vertex forming an obtuse angle; width of vertex wider than width of an eye, 1.6 ×; median carina of pronotum nearly straight in profile, slightly arcuate in forepart; ventral margins of mid femora slightly undulated, width of mid femora equal to width of tegmina in females.

Tetrix latipalpa (Fig. 11A–C) from Sichuan was described based on a single male holotype. The holotype has a deformed pronotum, and the median carina is slightly elevated and slightly sinuate. It is characterized by the frontal ridge and vertex forming an obtuse angle; width of vertex wider than width of an eye 1.6 ×; ventral margins of mid femora straight, width of mid femora equal to width of tegmina in females; the hind wings distinctly surpass the apex of the hind pronotal process. It is conspecific with brachypronotal and brachypterous *T. japonica*.

Tetrix liuwanshanensis (Fig. 11D–F) from Guangxi completely fits the morphology of brachypronotal and brachypterous individuals of *T. japonica* except for the slightly obtuse anterior margin of the pronotum. The slightly obtuse anterior margin of the pronotum fits the known variability of *T. japonica*. It is characterized by width of vertex between eyes is 1.1 × the width of the compound eye; frontal ridge and vertex forming an obtuse angle; antennal grooves inserted between inferior margins of compound eyes; median carina of pronotum

slightly arcuate in forepart; ventral margins of mid femora straight, width of mid femora wider than width of tegmina.

Tetrix qinlingensis (Fig. 12A–C) from Shaanxi is conspecific with *T. japonica* (pauropronotal individuals). These two taxa are characterized by width of vertex between eyes wider than width of compound eye; frontal ridge and vertex forming an obtuse angle; median carina of pronotum nearly straight in profile, slightly arcuate in forepart; ventral margins of mid femora slightly undulated, width of mid femora slightly narrower than width of tegmina in female; hind pronotal process surpassing apex of hind femur; hind wings surpassing apex of hind pronotal process.

Tetrix rectimargina (Fig. 12D–F) from Guangxi was described based on a single female holotype. *Tetrix rectimargina* represents a synonym of *T. japonica*. It is the same as brachypronotal and brachypterous *T. japonica* in all the characters except for the narrow vertex (width of vertex between eyes is equal to the width of compound eye). The slightly narrow vertex fits the known variability of *T. japonica*.

Tetrix ruyuanensis (Fig. 13A–C) from Guangdong was described based on a single female holotype, according to the description of the species by Liang and Zheng (1998), *T. ruyuanensis* is very similar to brachypronotal and brachypterous individuals of *T. japonica*. The only difference is median carina of pronotum arcuate before shoulders in profile in *T. ruyuanensis* (vs median carina of pronotum nearly straight before shoulders in profile in *T. japonica*). Topotypes of *T. ruyuanensis* were examined, and it was found that some individuals have an arcuate median carina before shoulders (Fig. 13B). However, most individuals have a nearly straight median carina (Fig. 13A). Thus, *T. ruyuanensis* is considered to be a synonym of *T. japonica*.

Tetrix xianensis (Fig. 13D–F) from Shaanxi was described based on a single female holotype, and *T. xianensis* represents a synonym of *T. japonica*. It is the same as brachypronotal and brachypterous *T. japonica* in all the characters except for the slightly arcuate vertex and slightly extended hind wings and pronotum. The slightly arcuate vertex and slightly extended hind wings and pronotum fit the known variability of the species.

Tetrix xinchengensis (Fig. 14A–C) from Guangxi was described based on a single male holotype, and *T. xinchengensis* represents a synonym of *T. japonica*. It is the same as brachypronotal and brachypterous *T. japonica* in all of the characters except for the slightly extended hind wings and pronotum. Extended hind wings and pronotum are consistent with the known variability of *T. japonica*.

Tetrix yunlongensis (Fig. 14D–F) from Yunnan was described based on a single male holotype, and *T. yunlongensis* represents a synonym of *T. japonica*. It is the same as brachypronotal and brachypterous *T. japonica* in all morphological characters except for the slightly obtuse anterior margin of the pronotum. The slightly obtuse anterior margin of the pronotum is consistent with the known variability of *T. japonica*. It is characterized by width of vertex between eyes is $1.4 \times$ the width of the compound eye; frontal ridge and vertex forming an obtuse angle; antennal grooves inserted between inferior margins of compound eyes; median carina of pronotum slightly arcuate in forepart; ventral margins of mid femora straight.

Type material of *Tetrix zhoushanensis* from Zhejiang was not examined, but according to the original description and photographs (Fig. 15) of the type

specimens in Gao et al. (2022), *Tetrix zhoushanensis* is identical to the morphology of brachypronotal and brachypterous individuals of *T. japonica*. *Tetrix zhoushanensis* has a narrower vertex (width of vertex between eyes is 1.1 × the width of the compound eye) than typical *T. japonica*, but this trait should be studied more in future in order to see if it has maybe a subspecies value. It is characterized by antennal grooves inserted between inferior margins of compound eyes; median carina of pronotum slightly arcuate in forepart; ventral margins of mid femora straight.

Discussion

Tetrix japonica is widely distributed in East Asia, and China, where is very common except in Hainan and Xinjiang. The People's Republic of China has a vast and complex ecological environment with an abundance of insect species. It has a huge diversity of Tetrigidae and has the most described species in the world (e.g., Liang and Zheng 1998, Zheng 2005a, Cigliano et al. 2023). However, 23 species are herewith synonymized with *T. japonica* because their descriptions were not based upon valid differences, but a wrongly assessed species variability, often caused by too few specimens being examined. Among the 23 synonyms, 11 synonyms (*E. rongshuiensis*, *T. cliva*, *T. latipalpa*, *T. albomaculatus*, *T. cenwanglaoshana*, *T. grossovalva*, *T. xinchengensis*, *T. rectimargina*, *Tetrix ruyuanensis*, *T. xianensis*, *T. yunlongensis*) were based on single specimens. One should be very careful when describing new Tetriginae species because few individuals can lead to wrong conclusions or a taxonomic inflation.

Additionally, some deformities were observed in the single-specimen species. The main causes of specimen deformities were recorded were two-fold. One was that the body was compressed by external forces during growth (*T. cliva*, *T. latipalpa*, *C. circinihumerus*, *C. emeiensis*). The other is that deformities were caused by humans during specimen preparation. For example, pygmy grasshopper specimens are usually dried and pinned. When inserting a pin into a specimen, the pin typically passes through the right side of the thorax from the shoulder of pronotum, which tends to push the pronotum down. This elevates the previously non-protruding heads such as in *E. rongshuiensis* and *E. zayuensis*.

Some pygmy grasshoppers are highly polymorphic in both colors and markings. *Tetrix japonica*, which occurs in both grass and sand microhabitats, exhibits large variations in body coloration and pronotum markings. Within a single population, the basal body coloration can vary from blackish brown to yellowish brown to pale grey. Some *T. japonica* are bi-colored, with whitish and blackish markings on the dorsal surface of the pronotum. In contrast, some *T. japonica* have no markings, whereas others have spots on the pronotum. The number, shape, and position of spots also varies among the spotted morphs (Tsurui et al. 2010). Therefore, in the classification of Tetrigoidea, and especially in Tetriginae: Tetrigini the spots on the dorsal pronotum are not a reliable taxonomic feature. In Batrachideinae and Metrodorinae, some group coloration is helpful (Tumbrinck and Skejo 2017; Kasalo et al. 2021; Itrac-Bruneau and Doucet 2023), but these groups are exceptions within Tetrigidae, not the rule. In the early classification of Tetrigoidea in China (Liang and Zheng 1998; Zheng 2005a), this character was often used as a taxonomic feature. As a result, *T. albistriatus*, *T. albomaculatus*, and *T. albomarginis* have been synonymized with *T. japonica*.

Dimorphism in wing length is known in many insect species, and in some species of pygmy grasshoppers, both the hind wings and the pronotum can be dimorphic (Deng 2021; Zhang et al. 2022). Because pygmy grasshoppers can vary in pronotum characters and length of the hind wings (Deng 2021; Zhang et al. 2022), the length of the hind wings and the pronotum cannot be used as taxonomic characters for classification of some species. However, in previous classifications of Tetrigoidea in China (e.g., Liang and Zheng 1998; Zheng 2005a; Deng et al. 2007a), these two characters were often used alone as diagnostic features; the dimorphism of these two characters was not considered. Therefore, misidentification of some species of *Tetrix* can readily occur and lead to synonyms, such as *T. cenwanglaoshana*, *T. grossovalva*, *T. jiuwanshanensis*, *T. qinlingensis*, and *T. xinchengensis*, which have all been here synonymized with *T. japonica*.

Similarly, *T. japonica* individuals can also exhibit variability in the shape of posterior angles of lateral lobes of pronotum and fastigium of vertex and anterior margin of pronotum, height median carina of pronotum, width of vertex between eyes, width of the middle femur, length of body, length of pronotum, and length of hind femur (Table 1). Therefore, these features alone cannot be used separately in taxonomic identification. Hence, when *T. japonica* is identified among other *Tetrix* species, we are strongly recommended using a combination of characters: head and eyes not exerted above pronotal surface; width of vertex between eyes generally wider than or sometimes equal to width of a compound eye; anterior margin of fastigium of vertex truncated or slightly arcuate and slightly surpassing anterior margin of eye; frontal ridge and vertex forming an obtuse angle; antennal grooves inserted between inferior margins of compound eyes; anterior margin of pronotum generally truncate; median carina of pronotum low and full length entire, in profile, slightly straight or slightly arch-like before the shoulders and straight behind the shoulders; ventral margins of middle femora straight or slightly undulated; with tegmina and hind wings developed, nearly reach apex of hind process or more.

The problematic taxonomy of *T. japonica* suggests that similar problems will occur in other species of *Tetrix*. This genus requires more research, especially, regarding interspecific and intraspecific variability.

Acknowledgements

We thank LetPub (www.letpub.com) for its linguistic assistance during the preparation of this manuscript.

Additional information

Conflict of interest

The authors have declared that no competing interests exist.

Ethical statement

No ethical statement was reported.

Funding

The project is supported by the National Natural Science Foundation of China (31960111, 31900351, 32360124), Natural Science Foundation of Guangxi (No. 2023GXNSF-

DA026037), High-level Innovation team and Outstanding Scholars Program of Guangxi Colleges and Universities, and Survey and Assessment of priority areas for terrestrial biodiversity conservation in Guangxi (2022–2023).

Author contributions

Funding acquisition: Weian Deng, Rongjiao Zhang. Investigation: Rongjiao Zhang, Ying Long, Caili Teng. Resources: Liliang Lin. Original draft writing: Weian Deng, Ying Long. Illustrations and measurements: Chaomei Huang. Species identification: Weian Deng. Review and editing: Weian Deng, Ying Long.

Author ORCIDs

Ying Long  <https://orcid.org/0009-0003-8226-8958>

Caili Teng  <https://orcid.org/0009-0008-2124-959X>

Chaomei Huang  <https://orcid.org/0000-0003-1046-1348>

Rongjiao Zhang  <https://orcid.org/0000-0001-5545-856X>

Weian Deng  <https://orcid.org/0000-0002-8023-2498>

Liliang Lin  <https://orcid.org/0000-0002-9972-4732>

Data availability

All of the data that support the findings of this study are available in the main text.

References

- Adžić K, Deranja M, Franjević D, Skejo J (2020) Are Scelimeninae (Orthoptera: Tetrigidae) monophyletic and why it remains a question? *Entomological News* 129(2): 128–146. <https://doi.org/10.3157/021.129.0202>
- Benediktov AA (2005) Vibratory signals in the family Tetrigidae (Orthoptera). *Proceedings of the Russian Entomological Society* 76: 131–140.
- Bey-Bienko (1934) Schwedisch-chinesische wissenschaftliche Expedition nach nord-westlichen Provinzen Chinas. Orthoptera, Forficulidae et Tetrigidae. *Arkiv för Zoologi* 25A (20): 1–13.
- Blackith RE (1992) The Tetrigidae (Insecta: Orthoptera) of South-East Asia. 'Rockbottom', Japaga and Ashford Co., Wicklow, 248 pp.
- Bolívar I (1887) Essai sur les Acridiens de la tribu des Tettigidae. *Annales de la Societe entomologique de Belgique* 31: 173–313.
- Cao CQ, Zheng ZM (2011) A survey of Tetrigoidea from Emeishan, Sichuan, China (Orthoptera) with descriptions of two new species. *Dong Wu Fen Lei Xue Bao* 36(3): 737–741.
- Cigliano MM, Braun H, Eades DC, Otte D (2023) Orthoptera Species File Online. Version 5.0/5.0. <http://Orthoptera.SpeciesFile.org> [Accessed 8 November 2022]
- Deng WA (2016) Taxonomic study of Tetrigoidea from China. Huazhong Agricultural University, Ph.D. Dissertation, 341 pp.
- Deng WA (2021) New genus and new species of leaf-mimic pygmy grasshoppers from China (Orthoptera: Tetrigidae: Cladonotinae). *Zootaxa* 4995(3): 573–580. <https://doi.org/10.11646/zootaxa.4995.3.11>
- Deng WA, Zheng ZM, Wei SZ (2007a) Fauna of Tetrigoidea from Yunnan and Guangxi. Science and Technology Press, Nanning, 458 pp.
- Deng WA, Zheng ZM, Wei SZ (2007b) Two new species of the genus *Tetrix* Latreille (Orthoptera, Tetrigoidea, Tetrigidae) from China. *Dong Wu Fen Lei Xue Bao* 32: 293–296.

- Deng WA, Xin L, Wei Q, Chen YZ (2018) Two new species of the genus *Macromotettix* Günther, 1939 (Orthoptera: Tetrigidae, Metrodorinae) from China, with a key to the species of the genus. *Zootaxa* 4370(4): 421–430. <https://doi.org/10.11646/zootaxa.4370.4.7>
- Devriese H, Nguyen E, Husemann M (2023) An identification key to the genera and species of Afrotropical Tetrigini (genera *Paratettix*, *Leptacrydium*, *Hedotettix*, *Rectitettix* nov. gen., and *Alienitettix* nov. gen.) with general remarks on the taxonomy of Tetrigini (Orthoptera, Tetrigidae). *Zootaxa* 5285(3): 511–556. <https://doi.org/10.11646/zootaxa.5285.3.4>
- Gao GZ, Liu PY, Yin Z (2022) Description of a new species of the genus *Tetrix* Latreille (Orthoptera: Tetrigoidea: Tetrigidae) from Zhejiang, China. *Zootaxa* 5138(3): 347–350. <https://doi.org/10.11646/zootaxa.5138.3.8>
- Ichikawa A (1993) Four new species of the genus *Tetrix* (Orthoptera: Tetrigidae) from Japan. *Akitu* 135: 1–8.
- ICZN [International Commission on the Zoological Nomenclature] (1999) International Code of the Zoological Nomenclature, 4th edition. The International Trust for Zoological Nomenclature, London, 306 pp.
- Itrac-Bruneau R, Doucet G (2023) Apport des collections du Muséum national d'Histoire naturelle et de Didier Morin à la connaissance des Batrachideinae et Lophotettiginae (Orthoptera, Tetrigidae) de Guyane. *Zoosystema* 45(20): 601–634. <https://doi.org/10.5252/zoosystema2023v45a20>
- Jiang GF, Liang GQ (2004) Fifty-Three species of Tetrigoidea (Orthoptera) from Cengwang Mountain in the Western Guangxi Zhuang Autonomous Region, China. *Entomological News* 115(4): 201–206.
- Jiang GF, Zheng ZM (1998) Grasshoppers and Locusts from Guangxi. Guangxi Normal University Press, Guilin, 390 pp.
- Kasalo N, Deranja M, Adzic K, Sindaco R, Skejo J (2021) Discovering insect species based on photographs only: The case of a nameless species of the genus *Scaria* (Orthoptera: Tetrigidae). *Journal of Orthoptera Research* 30(2): 173–185. <https://doi.org/10.3897/jor.30.65885>
- Kasalo N, Skejo J, Husemann M (2023) DNA Barcoding of Pygmy Hoppers – The First Comprehensive Overview of the BOLD Systems' Data Shows Promise for Species Identification. *Diversity (Basel)* 15(6): 696. <https://doi.org/10.3390/d15060696>
- Kim TW, Kim JI (2004) A taxonomic study of Korean Tetrigidae (Orthoptera: Caelifera: Tetrigoidea). *Entomological Research* 34(4): 261–267. <https://doi.org/10.1111/j.1748-5967.2004.tb00121.x>
- Kim TW, Puskás G (2012) Check-list of North Korean Orthoptera Based on the Specimens Deposited in the Hungarian Natural History Museum. *Zootaxa* 3202(1): 1–27. <https://doi.org/10.11646/zootaxa.3202.1.1>
- Kirby WF (1910) A synonymic catalogue of Orthoptera. Vol. III. Orthoptera Saltatoria. Part II. (Locustidae vel Acridiidae). The Trustees of the British Museum, London, 674 pp.
- Lehmann AW, Devriese H, Tumbrinck J, Skejo J, Lehmann GU, Hochkirch A (2017) The importance of validated alpha taxonomy for phylogenetic and DNA barcoding studies: A comment on species identification of pygmy grasshoppers (Orthoptera, Tetrigidae). *ZooKeys* 679: 139–144. <https://doi.org/10.3897/zookeys.679.12507>
- Liang GQ, Zheng ZM (1998) Fauna Sinica, Insecta. Volume 12. Orthoptera, Tetrigoidea. Science Press, Beijing, 278 pp.
- Lu YZ, Zha LS (2020) A new species of the genus *Lamellitettigodes* (Orthoptera: Tetrigidae) from PR China, with taxonomic notes on the genus. *Zootaxa* 4851(2): 338–348. <https://doi.org/10.11646/zootaxa.4851.2.7>

- Muhammad AA, Tan MK, Abdullah NA, Azirun MS, Bhaskar D, Skejo J (2018) An annotated catalogue of the pygmy grasshoppers of the tribe Scelimenini Bolívar, 1887 (Orthoptera: Tetrigidae) with two new *Scelimena* species from the Malay Peninsula and Sumatra. *Zootaxa* 4485(1): 1–70. <https://doi.org/10.11646/zootaxa.4485.1.1>
- Paris M (1993) Catalogo de tipos de ortopteroides (Insecta) de Ignacio Bolívar, I: Blatataria, Mantodea, Phasmoptera y Orthoptera (Stenopelmatoidea, Rhaphidophoroidea, Tettigonioidea, Grylloidea, Tetrigoidea). *Eos* (Washington, D.C.) 69: 143–264.
- Rehn JAG (1902) Contribution toward a knowledge of the Orthoptera of Japan and Korea, I. – Acrididae. *Proceedings. Academy of Natural Sciences of Philadelphia* 54: 629–637.
- Sahlberg J (1893) Om de finska arterna af orthopterslägtet *Tetrix* Charp. *Meddelanden af Societas pro Fauna et Flora Fennica* 19: 43–48.
- Shiraki T (1906) Die Tettigiden Japans. *Transactions of the Sapporo Natural History Society* 1(2): 157–167.
- Skejo J, Gupta SK (2015) On the specific status of *Hedotettix cristatus* Karny, 1915 (Tetrigidae: Tetriginae). *Zootaxa* 4018(4): 584–592. <https://doi.org/10.11646/zootaxa.4018.4.7>
- Steinmann H (1964) Some new Tetrigid species and subspecies from Asia (Orthoptera: Tetrigidae). *Acta Zoologica Academiae Scientiarum Hungaricae* 10: 457–468.
- Storozhenko S Y, Ichikawa A, Uchida M (1994) Review of Orthoptera of the Eastern Palearctica: Genus *Tetrix* Latreille (Tetrigidae, Tetriginae). Part 1–3. *New Entomologist* 43–44: (1) 43: 6–19, (2) 43: 43–54, (3) 44: 7–16.
- Storozhenko SY, Kim TW, Jeon MJ (2015) Monograph of Korean Orthoptera. National Institute of Biological Resources, Incheon, 167 pp.
- Tan MK, Artchawakom T (2015) A new species from the genus *Gorochovitettix* (Tetrigidae: Metrodorinae) from Thailand. *Zootaxa* 3990(3): 444–450. <https://doi.org/10.11646/zootaxa.3990.3.9>
- Tsurui K, Honma A, Nishida T (2010) Camouflage effects of various colour-marking morphs against different microhabitat backgrounds in a polymorphic pygmy grasshopper *Tetrix japonica*. *PLoS ONE* 5(7): e11446. <https://doi.org/10.1371/journal.pone.0011446>
- Tumbrinck J (2014) Taxonomic revision of the Cladonotinae (Orthoptera: Tetrigidae) from the islands of South-East Asia and from Australia, with general remarks to the classification and morphology of the Tetrigidae and descriptions of new genera and species from New Guinea and New Caledonia. In: Telnov D (Ed.) *Biodiversity, biogeography and nature conservation in Wallacea and New Guinea. Vol. II. the Entomological Society of Latvia, Riga*, 345–396, pls. 64–91.
- Tumbrinck J (2019) Taxonomic and biogeographic revision of the genus *Lamellitettigodes* (Orthoptera: Tetrigidae) with description of two new species and additional notes on *Lamellitettix*, *Probolotettix*, and *Scelimena*. *Journal of Orthoptera Research* 28(2): 167–180. <https://doi.org/10.3897/jor.28.34605>
- Tumbrinck J, Skejo J (2017) Taxonomic and biogeographic revision of the New Guinean genus *Ophiotettix* Walker, 1871 (Tetrigidae: Metrodorinae: Ophiotettigini trib. nov.), with the descriptions of 33 new species. *Biodiversity, biogeography and nature conservation in Wallacea and New Guinea* 3: 525–580.
- Wei SZ, Deng WA (2023) Two new species of the genus *Macromotettixoides* Zheng, Wei & Jiang (Orthoptera: Tetrigidae: Metrodorinae) from China. *Oriental Insects* 57(2): 626–642. <https://doi.org/10.1080/00305316.2022.2098198>

- Xiao B, Feng X, Miao WJ, Jiang GF (2012) The complete mitochondrial genome of grouse locust *Tetrix japonica* (Insecta: Orthoptera: Tetrigoidea). *Mitochondrial DNA* 23(4): 288–289. <https://doi.org/10.3109/19401736.2012.674123>
- Yao YP, Zheng ZM (2006) A new species of the genus *Tetrix* Latreille from South Eastern Yunnan (Orthoptera, Tetrigidae). *Dong Wu Fen Lei Xue Bao* 31: 824–825.
- Yin XC (1984) Grasshoppers and locusts from Qinghai-Xizang Plateau of China. Science Press, Beijing, 1–287.
- Zha LS, Wu XM, Ding JH (2020) Two new species of the genus *Formosatettix* Tinkham, 1937 (Orthoptera, Tetrigidae) from Guizhou and Chongqing, PR China. *ZooKeys* 936: 61–75. <https://doi.org/10.3897/zookeys.936.49552>
- Zhang RJ, Wang JG, Huang DL, Deng WA (2022) Life cycle and other biological characteristics of *Tetrix japonica*. *Journal of Environmental Entomology*. <https://kns.cnki.net/kcms/detail//44.1640.Q.20221205.1300.003.html>
- Zheng ZM (1994) A new genus and two new species of Tetrigidae from China (Orthoptera: Tetrigoidea). *Sichuan Journal of Zoology* 13(4): 146–149.
- Zheng ZM (1996) Two new species of *Tetrix* Latreille from China (Orthoptera, Tetrigidae). *Journal of Hubei University* 18(2): 177–180. [Natural Science]
- Zheng ZM (2005a) Fauna of the Tetrigoidea from Western China. Science Press, Beijing, 501 pp.
- Zheng ZM (2005b) Revision of Chinese species of genus *Euparatettix* Hancock (Tetrigoidea: Tetrigidae). *Journal of Shaanxi Normal University* 33(2): 98–102. [Natural Science Edition]
- Zheng ZM (2005c) A taxonomic study of *Tetrix* Latreille from China (Tetrigoidea: Tetrigidae). *Journal of Shaanxi Normal University* 33(3): 99–108. [Natural Science Edition]
- Zheng ZM (2014) Survey of Tetrigoidea from Hunan province (Orthoptera). *Journal of Shaanxi Normal University* 42(6): 54–60. [Natural Science Edition]
- Zheng ZM, Deng WA (2004a) Six new species of Tetrigidae from Jincheng River area of Guangxi (Orthoptera: Tetrigoidea). *Journal of Shaanxi Normal University* 32(4): 77–83. [Natural Science Edition]
- Zheng ZM, Deng WA (2004b) Seven New Species of Tetrigoidea (Orthoptera) from Northern Region of Guangxi. *Entomotaxonomia* 26(2): 91–103.
- Zheng ZM, Jiang GF (2000) New genus and new species of Metrodoridae from Guangxi (Orthoptera: Tetrigoidea). *Dong Wu Fen Lei Xue Bao* 25(4): 402–405.
- Zheng ZM, Jiang GF (2004) Four new species of Tetrigoidea (Orthoptera: Tetrigoidea) from Buliu River northwestern Guangxi, China. *Entomological Journal of East China* 13(1): 1–9. <https://doi.org/10.1080/00305316.2005.10417431>
- Zheng ZM, Jiang GF (2006) Four new species of Tetrigoidea from Zuojiang, Guangxi (Orthoptera). *Dong Wu Fen Lei Xue Bao* 31(1): 141–145.
- Zheng ZM, Mao BY (2002) A survey of Tetrigoidea from north western region of Yunnan, China. *Journal of Shaanxi Normal University* 30(1): 89–98. [Natural Science Edition]
- Zheng ZM, Nie XM (2005) Three new species of Tetrigidae from western Yunnan in China (Orthoptera: Tetrigoidea). *Huazhong Nongye Daxue Xuebao* 24(6): 580–584.
- Zheng ZM, Huo K, Zhang HJ (2000) Three new species of Tetrigidae (Orthoptera: Tetrigoidea) from Shaanxi. *Entomotaxonomia* 22(4): 235–241.
- Zheng ZM, Jiang GF, Liu JW (2005) Six new species of Tetrigoidea (Orthoptera) from Guangxi, P. R. China. *Oriental Insects* 39(1): 175–185. <https://doi.org/10.1080/00305316.2005.10417431>

- Zheng ZM, Zeng HH, Ou XH (2011) A review of the genus *Euparatettix* Hancock (Orthoptera, Tetrigidae) from China with descriptions of two new species. *Dong Wu Fen Lei Xue Bao* 36(2): 383–391.
- Zheng ZM, Lin LL, Zhang HL (2012) A taxonomic study of the genus *Coptotettix* Bolívar, 1887 (Orthoptera: Tetrigidae: Tetriginae) from China with description of a new species. *Journal of Natural History* 46(41–42): 2549–2561. <https://doi.org/10.1080/00222933.2012.708448>
- Zheng ZM, Lin LL, Zhang HL (2013) Review of the genus *Coptotettix* Bolívar, 1887 (Orthoptera: Tetrigidae) from China with description of a new species. *Entomotaxonomia* 35(1): 19–28.

Three new species of *Quadrastichus* Girault (Hymenoptera, Eulophidae) from China with a key to Chinese species

Wen-Jian Li¹ , Cheng-De Li¹

¹ Jiangsu Provincial Key Laboratory of Coastal Wetland Bioresources and Environmental Protection, School of Wetland, Yancheng Teachers University, Yancheng, 224007, China

² School of Forestry, Northeast Forestry University, Harbin, 150040, China

Corresponding author: Cheng-De Li (lichengde0608@sina.com)

Abstract

Six species of *Quadrastichus* Girault (Eulophidae: Tetrastichinae) from China are reviewed, including three new species: *Q. longiseta* **sp. nov.**, *Q. flavomaculatus* **sp. nov.**, *Q. longiscapus* **sp. nov.** and one new country record, *Q. vacuna* (Walker, 1839). New distributional data for *Q. anysis* (Walker, 1839) and *Q. sajo*i (Szelényi, 1941), and a key to the Chinese species of *Quadrastichus* based on females, are included.

Key words: Chalcidoidea, Hymenoptera, identification key, parasitoids, taxonomy

Introduction

The genus *Quadrastichus* (Eulophidae: Tetrastichinae) was established by Girault (1913) with *Quadrastichus nigrinotatus* Girault as type species fixed by original designation. *Quadrastichus* Girault is a large genus containing 89 valid species worldwide (Noyes 2019), but only seven species are known from China: *Q. anysis* (Walker, 1839), *Q. pteridis* Graham, 1991, *Q. sajo*i (Szelényi, 1941), *Q. liriomyzae* Hansson & LaSalle, 1996, *Q. citrella* Reina & LaSalle, 2004, *Q. erythrinae* Kim, 2004 and *Q. mendeli* Kim & LaSalle, 2008 (Hansson and LaSalle 1996; Zhu and Huang 2001, 2002; Kim et al. 2004; Reina and LaSalle 2004; Zhang et al. 2007; Feng et al. 2016).

Quadrastichus species are widely distributed and can be recognized by the following combination of characteristics: submarginal vein (SMV) with a single dorsal seta (occasionally two setae in aberrant specimens of *Q. vacuna*); mid lobe of mesoscutum usually with one adnotaular seta (two or three setae in a few species and five adnotaular setae at most in *Q. erythrinae*); scutellum with submedian grooves; propodeal spiracles close to metanotum; ovipositor sheaths not, or slightly, extending beyond tip of gaster (Graham 1991). When distinguishing different genera, *Quadrastichus* is similar to *Oomyzus* in having only one dorsal seta on the SMV, however, *Quadrastichus* species have all funicular segments longer than broad compared to species of *Oomyzus*. Actually, this genus is most similar to *Aprostocetus*, especially the subgenus *Ootetrastichus*, in the reduced number of adnotaular setae and slender body, however, *Quadrastichus* species have only one dorsal seta on



Academic editor: Zachary Lahey
Received: 27 August 2023
Accepted: 20 November 2023
Published: 20 December 2023

ZooBank: <https://zoobank.org/9CDA1DC0-6B91-42C6-89B4-3F45A9CDF2F2>

Citation: Li W-J, Li C-D (2023) Three new species of *Quadrastichus* Girault (Hymenoptera, Eulophidae) from China with a key to Chinese species. ZooKeys 1187: 169–188. <https://doi.org/10.3897/zookeys.1187.111723>

Copyright: © Wen-Jian Li & Cheng-De Li.
This is an open access article distributed under terms of the Creative Commons Attribution License ([Attribution 4.0 International – CC BY 4.0](https://creativecommons.org/licenses/by/4.0/)).

the SMV and are non-metallic or weakly metallic compared to species of the subgenus *Ootetrastichus*.

Species of *Quadrastichus* are parasitoids of Cecidomyiidae (Diptera) and various Coleoptera, although other hosts include Cynipidae, Eulophidae (Kim et al. 2008), and Torymidae (Yegorenkova et al. 2007) (Hymenoptera); Agromyzidae and Tephritidae (Diptera); and Gracillariidae (Lepidoptera). Species of *Quadrastichus* are also associated with galls. Larvae of *Q. sajo* are also predatory within galls of eriophyid mites (Graham 1991; Hansson and LaSalle 1996). *Quadrastichus erythrinae* was reported from galls on *Erythrina variegata* L. (Kim et al. 2004).

In this paper, we add four more species, including three new species and one new country record to the Chinese fauna. Also, a key to Chinese species is given based on females.

Materials and methods

Specimens were collected by sweeping, yellow-pan trapping and were dissected and mounted (dorsal side up) in Canada Balsam following the method described by Noyes (1982) or glued to triangular cards. Photographs were taken with a CCD digital camera attached to an Olympus BX51 compound microscope (slide-mounted specimens) and Leica M205C microscope (card-mounted specimens). Slide-mounted specimen measurements were made using an eye-piece reticle with an Olympus CX21 compound microscope. Card-mounted specimen measurements were taken using an eye-piece reticle with a Motic SMZ168-B dissecting microscope. In the descriptions below, measurements/ratio in brackets after measurement/ratio ranges refer to the holotype. The terminology follows Graham (1987) and Gibson et al. (1997). The following abbreviations are used:

F1–4	flagellomeres 1–4;
POL	minimum distance between lateral ocelli;
OOL	minimum distance between lateral ocellus and eye margin;
OD	largest diameter of a lateral ocellus;
MV	marginal vein;
STV	stigmal vein;
SMV	submarginal vein.

All specimens studied in this paper are deposited in the insect collections of Northeast Forestry University (NEFU) and Yancheng Teachers University (YCTU).

Results

Key to Chinese species of *Quadrastichus* Girault (females)

- 1 Mid lobe of mesoscutum with 2–5 adnotaular setae on each side **2**
- Mid lobe of mesoscutum with 1 adnotaular seta on each side **7**
- 2 Large fovea below eye present; pronotum with 4 coarsely reticulate yellow areas (Fig. 38) ***Q. sajo* (Szelényi)**
- Large fovea below eye absent; pronotum uniformly sculptured **3**

- 3 Antenna with scape distinctly extending above vertex; clava slender, 6.3–7.0× as long as broad, terminal spine as long as C3 (Fig. 20) ***Q. longiscapus* sp. nov.**
- Antenna with scape not extending above vertex; clava shorter, at most 4.0× as long as broad, terminal spine distinctly shorter than C3 **4**
- 4 Body black without yellow markings; propodeum with a distinct median carina **5**
- Body mainly yellow or black with yellow markings; propodeum without a distinct median carina **6**
- 5 Clava 2.7–3.0× as long as broad (Fig. 28); gaster 2.5–4.0× as long as broad (Fig. 32) ***Q. vacuna* (Walker)**
- Clava 3.5–4.0× as long as broad; gaster 2.0–3.0× as long as broad ***Q. pteridis* Graham**
- 6 Mid lobe of mesoscutum with a distinct median line; hypopygium extending 0.3–0.4× the length of gaster (see Kim et al. 2008: fig. 1) ***Q. mendeli* Kim & La Salle**
- Mid lobe of mesoscutum with a very weak median line or without line; hypopygium extending 0.8–0.9× the length of gaster (see Kim et al. 2004: fig. 28) ***Q. erythrinae* Kim**
- 7 Forewing with speculum present and extending below MV; MV 6.2× STV (see Reina and La Salle 2004: fig. 10) ***Q. citrella* Reina & La Salle**
- Forewing with speculum absent or small, not extending below MV; MV at most 4.4× STV **8**
- 8 Antenna with clava more than 4.5× as long as broad **9**
- Antenna with clava shorter than 4.5× as long as broad **10**
- 9 Mid lobe of mesoscutum without median line; propodeum without paraspiracular carinae (Fig. 3); gaster dark brown without a yellow spot at base (Fig. 9) ***Q. longiseta* sp. nov.**
- Mid lobe of mesoscutum with a distinct median line; propodeum with distinct paraspiracular carinae (Fig. 13); gaster dark brown with a yellow spot at base (Fig. 18) ***Q. flavomaculatus* sp. nov.**
- 10 Mid lobe of mesoscutum mainly yellow but with a dark area anteromedially ***Q. liriomyzae* Hansson & LaSalle**
- Mid lobe of mesoscutum completely dark brown to black (Fig. 34) ***Q. anysis* (Walker)**

***Quadrastichus longiseta* sp. nov.**

<https://zoobank.org/FCF285E8-A935-451D-8E2E-B9AB984E6E87>

Figs 1–10

Type material. *Holotype*, female [on card], CHINA, Jiangxi Province, Yichun City, Mt. Guan Shan, 25.VIII.2018, Xiang-Xiang Jin, Wang-Ming Li, by sweeping (deposited in YCTU). *Paratypes*: 3 females, 1 male. [1 female, 1 male on slides], same data as holotype; [1 female on slide, 1 female on card], same locality as holotype, but collected 24.VIII.2018. All paratypes are deposited in NEFU.

Diagnosis. Female. Body mainly dark brown with weak metallic reflections. Antenna with scape just reaching, not extending above vertex, 4.3–4.6× as long as broad; pedicel longer than F1; funicle slender and thickening at base of each

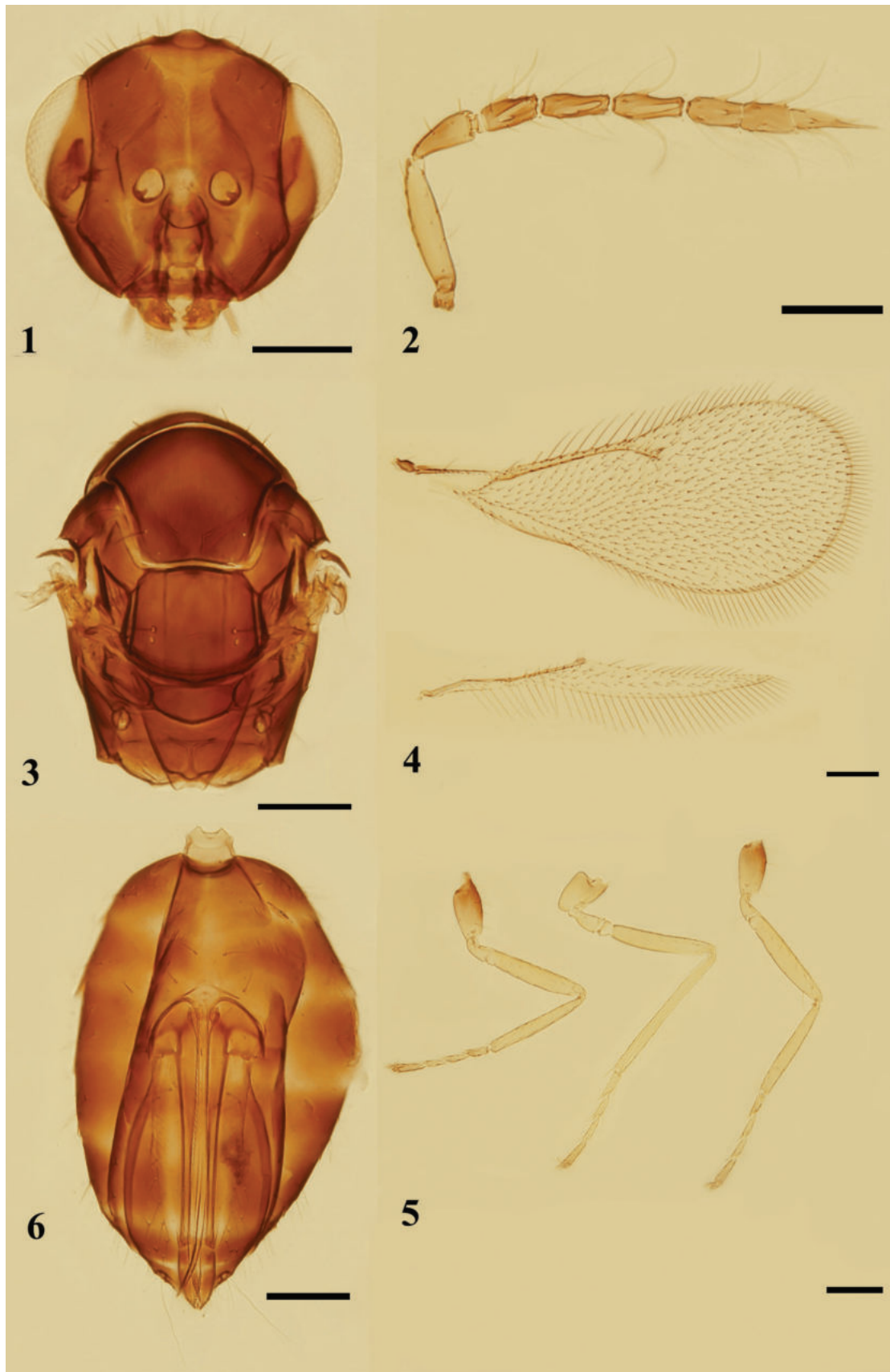
each funicular segment, F1 shortest, F2 shorter than or as long as F3, clava distinctly longer than F2 and F3 combined, 6.0–7.0× as long as broad, terminal spine as long as C3, flagellum with numerous curved long setae on each segment. **Male.** Body black with bluish metallic reflection. Antenna with plaque 0.5× the length of scape, flagellum with numerous whorls of long setae at base of each segment, especially on funicular segments.

Following Graham (1991), *Q. longiseta* should belong in the *anysis*-group as follows: body black with yellow markings; frons with median area but without median carina; malar sulcus curved. This species is similar to *Q. anysis* (Walker), but can be separated from this species by the following combination of characters: pedicel longer than F1 (vs as long as); F1 shortest, F2 shorter than or as long as F3 (vs F1–F3 subequal in length); clava distinctly longer than F2 and F3 combined, 6.0–7.0× as long as broad (vs clava as long as F2+F3, 3.2–3.9× as long as broad).

Description. Female. Body (Figs 9, 10) length 0.9–1.1 mm (1.1 mm). Head dark brown, eyes reddish-white, ocelli white. Antenna with scape yellowish-white; pedicel and flagellum yellowish-brown. Mesosoma dark brown, legs with pro- and metacoxae mainly brown, mesocoxae yellowish with base brown, trochanters, femora, tibiae and basal three tarsomeres yellowish, 4th tarsomere yellowish-brown. Wings hyaline, venation brownish. Gaster dark brown, with 1–3 yellow bands dorsally.

Head (Fig. 1) in dorsal view, slightly broader than mesosoma, 2.2× as broad as long. Vertex and face with numerous erect setae, the longest seta as long as OD. Face depressed; frons with a fine median line; POL 1.5–1.6× (1.5×) OOL, OOL 2× OD. Malar sulcus distinctly curved; malar space 0.6× as long as an eye; mouth opening 1.3–1.4× (1.3×) as wide as malar space. Anterior margin of clypeus weakly bidentate, mandibles tridentate. **Antenna** (Fig. 2) with lower edge of antennal toruli situated above level of lower margin of eyes, scape as long as an eye, just reaching but not extending above vertex, 4.3–4.6× (4.5×) as long as broad; pedicel longer than F1, 2.3× as long as broad; 1 discoid anellus; funicle slender and thickening at base, F1 shortest, F2 shorter than or as long as F3, F1–F3: 1.8–2.0× (2.0×), 2.3–2.6× (2.5×) and 2.3–2.8× (2.5×) as long as broad respectively; clava distinctly longer than F2 and F3 combined, as broad as F3, 6.0–7.0× (6.7×) as long as broad, terminal spine as long as C3, flagellomeres with numerous curved long setae, sensilla few.

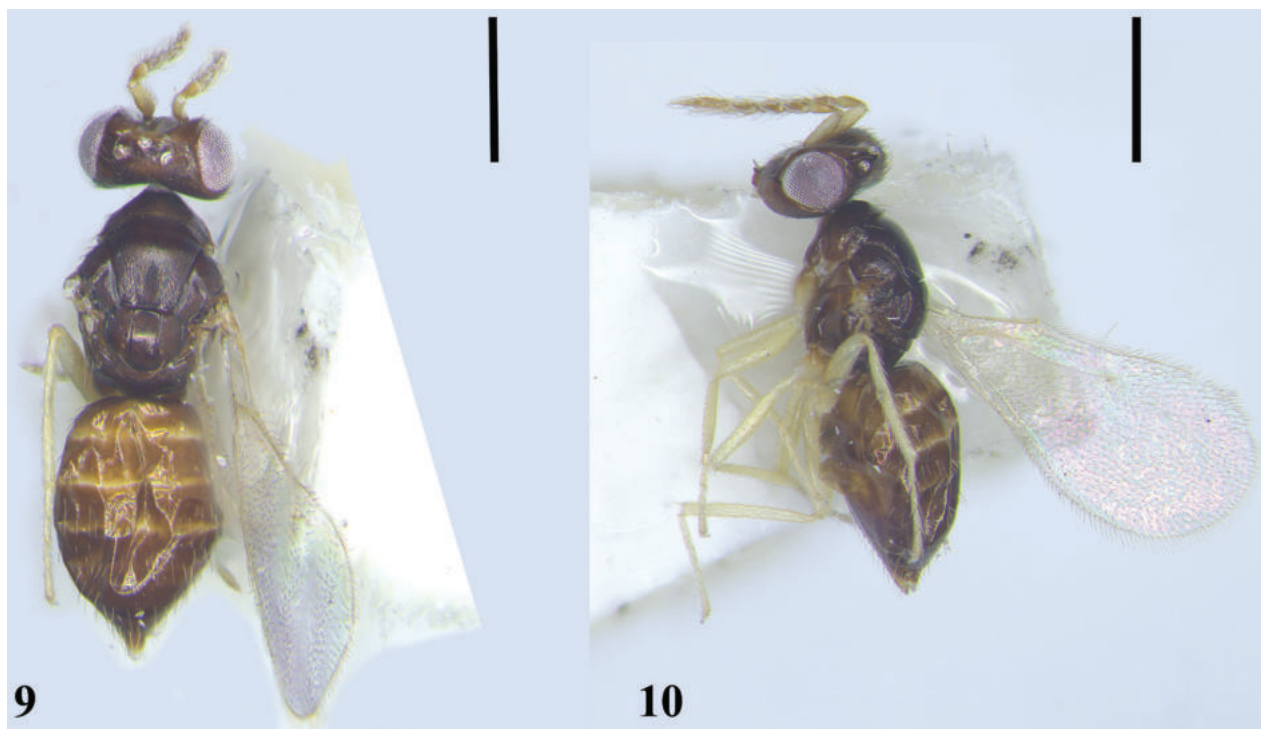
Mesosoma (Figs 3, 9) 1.4–1.5× (1.4×) as long as broad. Pronotum subconical, arched, reticulation fine. Mid lobe of mesoscutum 1.2–1.3× (1.2×) as broad as long, without median line, with 1 adnotaular seta on each side situated in posterior half, reticulation dense and narrow. Scutellum 1.3× as broad as long; anterior pair of setae attached slightly behind the middle, submedian and sublateral grooves distinct, distance between submedian grooves 1.8–2.0× as broad as distance between submedian grooves and sublateral grooves, reticulation dense. Dorsellum about 2.0× as broad as long. Propodeum medially distinctly longer than dorsellum, reticulation extremely fine; median carina weak, only present in posterior half, without paraspiracular carinae; spiracles round, separated from metanotum by less than their own diameter; callus with 2 or 3 setae. **Fore wing** (Fig. 4) 2.2–2.3× (2.3×) as long as broad, costal cell narrow, shorter than MV; MV 3.3–4.0× (3.8×) STV; SMV with 1 dorsal seta; speculum absent; the longest marginal seta slightly longer than STV. **Hind** (Fig. 4) wing pointed, 9.4×



Figures 1–6. *Quadrastichus longiseta* sp. nov., paratype, female 1 head, frontal view 2 antenna, lateral view 3 mesosoma, dorsal view 4 fore and hind wings, dorsal view 5 legs, lateral view, from left to right: fore, mid, and hind legs 6 metasoma, ventral view. Scale bars: 100 μ m.



Figures 7, 8. *Quadrastichus longiseta* sp. nov., paratype, male 7 antenna, lateral view 8 fore and hind wings, dorsal view. Scale bars: 100 μ m.



Figures 9, 10. *Quadrastichus longiseta* sp. nov., holotype, female 9 habitus, dorsal view 10 habitus, lateral view. Scale bars: 300 μ m.

as long as broad. **Legs** (Fig. 5) slender, with meso- and metabasitarsus as long as the corresponding second tarsomere, metafemora 5.1 \times as long as broad.

Gastral petiole (Fig. 6) present and transverse. **Gaster ovate** (Fig. 6), 1.5–1.8 \times (1.5 \times) as long as broad, slightly longer and broader than mesosoma, slightly shorter than head and mesosoma combined; each gastral tergite with long erect setae on dorsal surface; each cercus with 3 setae, the longest seta 2.3 \times as long as the second longest seta; ovipositor 0.7 \times as long as gaster, ovipositor

sheaths extending slightly beyond the tip of gaster; tip of hypopygium situated slightly before middle of gaster.

Male. Body length 0.9 mm. Mostly similar to female. **Antenna** (Fig. 7) with scape robust, shorter than an eye, 2.5× as long as broad; plaque 0.5× as long as scape; pedicel 1.7× as long as broad; F1–F4: 1.3×, 2.4×, 2.8× and 3.5× as long as broad respectively; each flagellomere with numerous whorls of long setae at base, especially on the funicle. **Fore wing** (Fig. 8) with MV 3.5× as long as STV.

Host. Unknown.

Distribution. China (Jiangxi).

Etymology. The epithet *longisetata* refers to the long setae on the antennae in both sexes.

***Quadrastichus flavomaculatus* sp. nov.**

<https://zoobank.org/BF1B3961-2345-4471-AF35-ECBEADD41C43>

Figs 11–18

Type material. **Holotype**, female [on card], CHINA, Shaanxi Province, Ankang City, 5.VIII.2015, Ye Chen, Chao Zhang, by sweeping (deposited in YCTU).

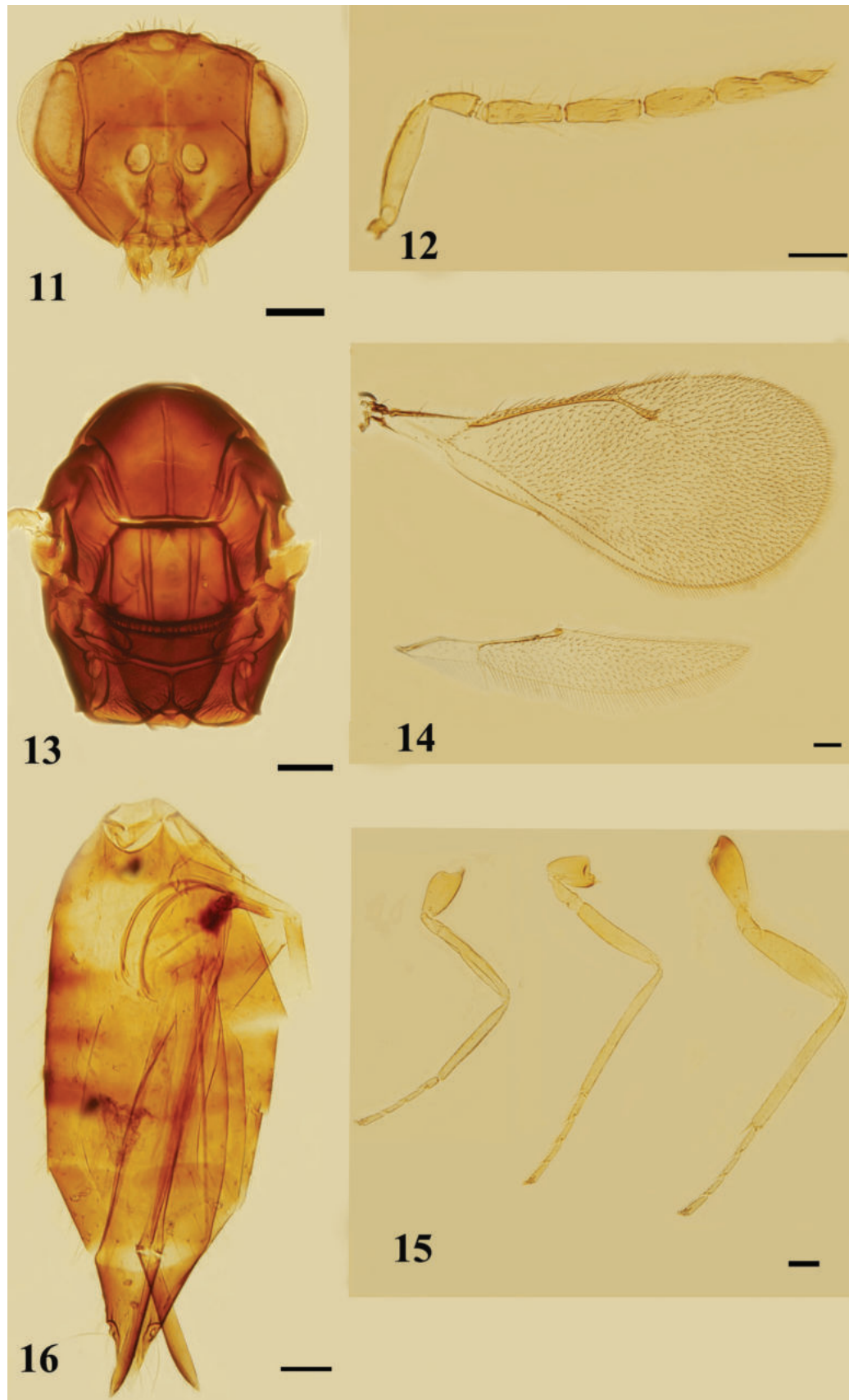
Paratypes: 4 females. [1 female on slide and 1 female on card], same data as holotype; [1 female on slide], CHINA, Liaoning Province, Anshan City, 20.IX.2015, Hui Geng, Yan Gao, Xin-Yu Zhang, by sweeping; [1 female on slide], CHINA, Jilin Province, Mt. Changbai Shan, 6.VII.2012, Si-Zhu Liu, Jiang Liu, by sweeping. All paratypes are deposited in NEFU.

Diagnosis. Female. Gaster with a yellow spot at base dorsally (Figs 17, 18). Frons with a median line. Antenna slender with pedicel distinctly shorter than each funicle segment. Mid lobe of mesoscutum with median line distinct. Propodeum with median carina and paraspiracular carinae distinct. **Male.** Unknown.

Quadrastichus flavomaculatus is similar to *Q. anysis* (Walker), but can be separated from this species by the following combination of characters: pedicel distinctly shorter than F1 (vs as long as); each funicle segment more than 2.5× as long as broad (vs 2.0–2.2×); mid lobe of mesoscutum with a distinct median line (vs weak or absent); gaster 2.7–3.4× as long as broad (vs 1.2–1.8×).

Description. Female. Body (Figs 17, 18) length 1.4–1.8 mm (1.7 mm). Head dark brown, eyes reddish-white, ocelli white. Antenna with scape mainly yellow, dorsal part yellowish-brown, pedicel and flagellum yellowish-brown. Mesosoma dark brown; legs yellow except brown base of metacoxae. Wings hyaline, venation yellow. Metasoma brown with a yellow spot at base of gaster extending from first to third tergite (Fig. 18).

Head (Fig. 11) in dorsal view as broad as mesosoma, 3.2–3.5× (3.2×) as broad as long. Vertex with short setae, the longest seta slightly shorter than OD. Face depressed; frons with a distinct median line; POL 1.8–2.0× (2.0×) OOL, OOL 1.9–2.0× (1.9×) OD. Malar sulcus slightly curved; malar space 0.55× as long as an eye; mouth opening 1.3× as wide as malar space. Anterior margin of clypeus bidentate, mandibles tridentate. Lower edge of antennal toruli situated above level of ventral edge of eyes. **Antenna** (Fig. 12) with scape as long as an eye, reaching but not extending above vertex, 4.0–4.4× (4.2×) as long as broad; 2 anelli; pedicel distinctly shorter than each funicle segment, 2.0–2.2× (2.2×) as long as broad; funicle slender, F1–F3 equal in length, F3 slightly broader



Figures 11–16. *Quadrastichus flavomaculatus* sp. nov., paratype, female 11 head, frontal view 12 antenna, lateral view 13 mesosoma, dorsal view 14 fore and hind wings, dorsal view 15 legs, lateral view, from left to right: fore, mid, and hind legs 16 metasoma, ventral view. Scale bars: 100 μ m.

than F1 and F2, F1–F3: 3.0–3.2× (3.2×), 2.8–3.2× (3.2×) and 2.6–2.8× (2.6×) as long as broad respectively; clava slightly shorter than or as long as F2 and F3 combined, 4.5–5.5× (5.0×) as long as broad, terminal spine shorter than C3, flagellum with numerous short setae.

Mesosoma (Fig. 13) 1.3–1.5× (1.4×) as long as broad. Pronotum short, arched. Mid lobe of mesoscutum 1.2× as broad as long, median line distinct and complete, with 1 adnotaular seta on each side situated in posterior half, reticulation fine. Scutellum 1.4× as broad as long; anterior pair of setae situated a little behind middle; sublateral grooves distinct, submedian grooves narrow posteriorly, distance between submedian grooves 1.2–1.8× as broad as distance between submedian grooves and sublateral grooves, reticulation fine. Dorsellum about 2.6× as broad as long. Propodeum medially slightly longer than dorsellum, reticulation distinct and dense; median carina and paraspiracular carinae distinct; spiracles round, almost touching hind margin of metanotum; callus with 2 setae.

Fore wing (Fig. 14) 2.1–2.2× (2.1×) as long as broad, costal cell narrow, shorter than MV; MV 3.0–3.2× (3.0×) STV; SMV with 1 dorsal seta; speculum present and small, not extending below MV; marginal setae short. Hind wing (Fig. 14) 5.0× as long as broad. **Legs** (Fig. 15) with meso- and metabasitarsus as long as the corresponding second tarsomere, metafemora 4.3–4.6× (4.6×) as long as broad.

Gastral petiole (Fig. 16) transverse. **Gaster** (Fig. 16) lanceolate, 2.5–3.5× (2.5×) as long as broad, distinctly longer than mesosoma, 1.2–1.4× (1.4×) the combined length of head and mesosoma; each tergite with long erect setae on dorsal side; each cercus with 3 setae, the longest seta about 2× as long as next longest seta; ovipositor 0.8× as long as length of gaster, ovipositor sheaths extending slightly beyond the tip of gaster; tip of hypopygium situated at anterior 1/3 of gaster.

Male. Unknown.

Host. Unknown.

Distribution. China (Jilin, Liaoning, Shaanxi).

Etymology. The epithet *flavomaculatus* refers to the yellow spot at the base of the gaster.



Figures 17, 18. *Quadrastichus flavomaculatus* sp. nov., holotype, female 17 habitus, lateral view 18 habitus, dorsallateral view. Scale bars: 500 μ m.

***Quadrastichus longiscapus* sp. nov.**

<https://zoobank.org/93AEE74D-65F1-482B-BC20-C11E5DCDF70C>

Figs 19–26

Type material. *Holotype*, female [on card], CHINA, Jiangxi Province, Yichun City, Mt. Guan Shan, 21.VIII.2018, Xiang-Xiang Jin, Wang-Ming Li, by sweeping (deposited in YCTU). *Paratypes*: 7 females. [4 females on cards], same data as holotype, deposited in YCTU. [2 females on slides, 1 female on card], same locality as holotype, but collected 24.VIII.2018, deposited in NEFU.

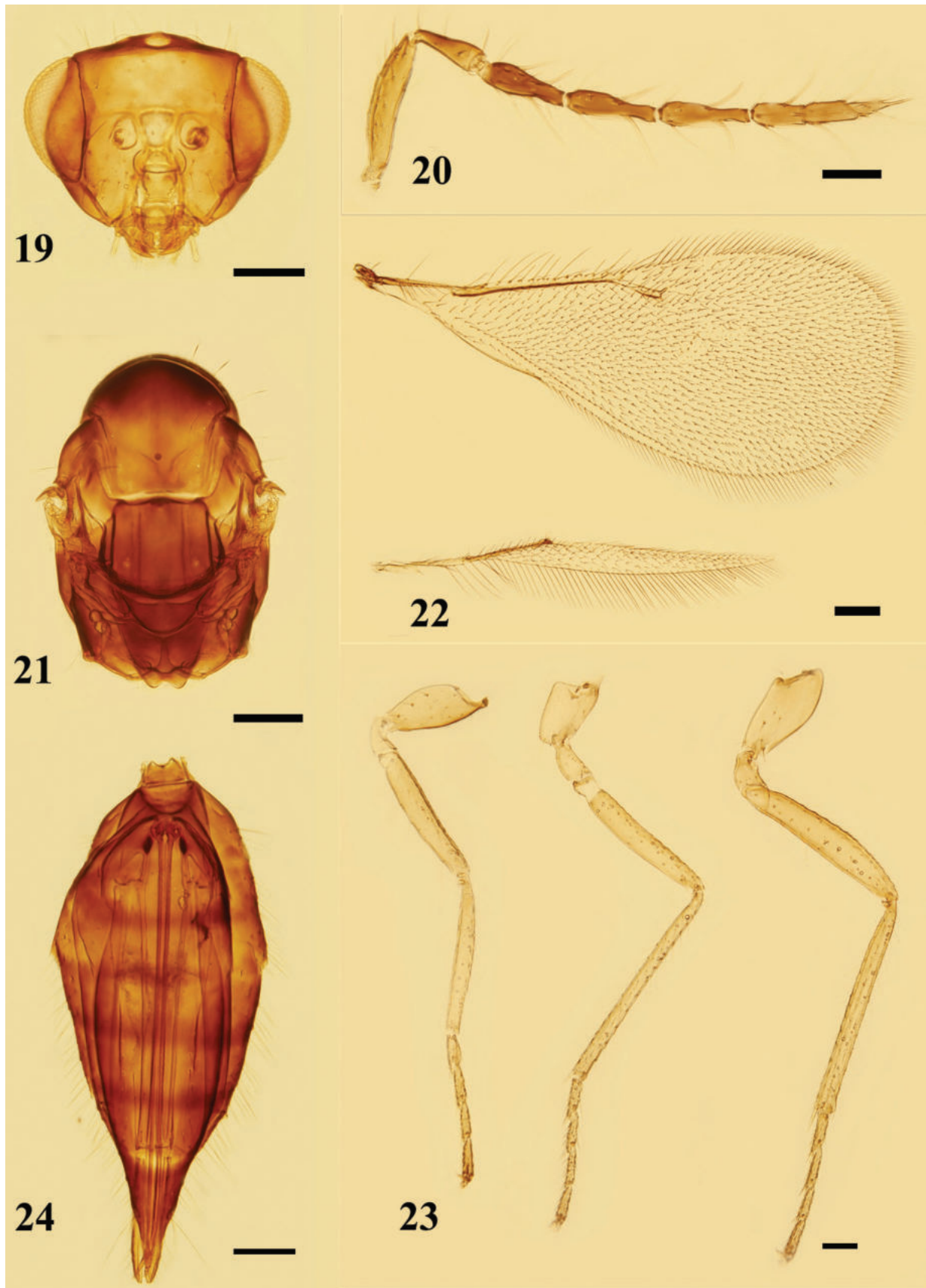
Diagnosis. Female. Mid lobe of mesoscutum and scutellum without reticulation. Antenna with scape distinctly extending above vertex, 4.8–5.0× as long as broad; pedicel shorter than F1, 2.8–3.1× as long as broad; clava distinctly shorter than F2 and F3 combined, as broad as F3, 6.3–7.0× as long as broad, terminal spine as long as C3, flagellomeres with numerous curved long setae.

Quadrastichus longiscapus is similar to *Q. xanthosoma* (Graham), but can be separated from the latter by the following combination of characters: pedicel 2.8–3.1× as long as broad (vs 2.0×); F1 about as long as F2 and F3, 2.8–3.0× (vs F1 longest, 3.0–4.0×); clava 6.3–7.0× as long as broad (vs 3.8–4.0×); body dark brown without yellow markings (vs extensively yellow with blackish markings).

Description. Female. Body (Figs 25, 26) length 1.7–1.8 mm (1.8 mm). Head with vertex dark brown, face yellow, eyes dark red, ocelli brown. Antenna with scape yellow; pedicel and flagellum brown. Mesosoma wholly dark brown or mainly dark brown with mesoscutum, posterior half of sidelobes of mesoscutum and axilla brownish, legs yellow. Wings hyaline, venation brownish. Metasoma dark brown.

Head (Fig. 19) in dorsal view, slightly broader than mesosoma, 2.8× as broad as long. Vertex and face with numerous erect setae, the longest seta slightly longer than OD. Face depressed; frons without a median line; POL 1.4–1.5× (1.4×) OOL, OOL 2× OD. Malar sulcus distinctly curved; malar space 0.5× as long as an eye; mouth opening 1.7–1.8× (1.8×) as wide as malar space. Anterior margin of clypeus weakly bidentate, mandibles tridentate. **Antenna** (Fig. 20) with lower edge of antennal toruli situated above the level of lower margin of eyes, scape as long as an eye, distinctly extending above vertex, 4.8–5.0× (5.0×) as long as broad; pedicel shorter than F1, 2.8–3.1× (3.0×) as long as broad; 1 discoid anellus; funicle slender and thickening at base, F1 about as long as F2 and F3, F1–F3: 2.8–3.0× (3.0×), 3.3–3.8× (3.8×) and 3.2–3.7× (3.7×) as long as broad respectively; clava distinctly shorter than F2 and F3 combined, as broad as F3, 6.3–7.0× (6.8×) as long as broad, terminal spine as long as C3, flagellomeres with numerous curved long setae, sensilla few.

Mesosoma (Fig. 21) 1.4–1.6× (1.4×) as long as broad. Pronotum subconical, arched. Mid lobe of mesoscutum about as broad as long, without median line and reticulation, with 2–3 adnotaular setae on each side. Scutellum 1.3× as broad as long; anterior pair of setae slightly behind middle, submedian and sublateral grooves distinct, distance between submedian grooves 2.0× as broad as distance between submedian grooves and sublateral grooves, without reticulation. Dorsellum long and posterior margin curved down, medially as long as propodeum. Propodeum without reticulation; median carina present and complete, without paraspircular carinae; spiracles round, separated from metanotum by less than their own diameter; callus with 2 or 3 setae. **Fore wing** (Fig. 22) 2.2–2.3× (2.3×) as long as broad, costal cell narrow, shorter than MV;



Figures 19–24. *Quadrastichus longiscapus* sp. nov., paratype, female **19** head, frontal view **20** antenna, lateral view **21** mesosoma, dorsal view **22** fore and hind wings, dorsal view **23** legs, lateral view, from left to right: fore, mid, and hind legs **24** metasoma, ventral view. Scale bars: 100 μ m.



Figures 25, 26. *Quadrastichus longiscapus* sp. nov., holotype, female **25** habitus, dorsal view **26** habitus, lateral view. Scale bars: 500 μ m.

MV 3.1–4.1 \times (3.4 \times) STV; SMV with 1 dorsal seta; speculum absent; the longest marginal seta shorter than STV. **Hind** (Fig. 22) wing pointed, 12–15 \times (14.5 \times) as long as broad. **Legs** (Fig. 23) slender, with metabasitarsus slightly shorter than the second tarsomere, metafemora 5.5 \times as long as broad.

Gastral petiole (Fig. 24) transverse. Gaster lanceolate, 2.1–2.8 \times (2.3 \times) as long as broad, distinctly longer than mesosoma, 1.2 \times as long as head and mesosoma combined; each gastral tergite with numerous long setae on dorsal surface; each cercus with 3 setae, the longest seta 2.0 \times as long as the second longest seta; ovipositor 0.8 \times as long as gaster, ovipositor sheaths extending slightly beyond the tip of gaster; tip of hypopygium situated at anterior 1/3 of gaster.

Male. Unknown.

Host. Unknown.

Distribution. China (Jiangxi).

Etymology. The epithetic *longiscapus* refers to the long scape of the antennae.

***Quadrastichus vacuna* (Walker, 1839)**

Figs 27–33

New record for China

Cirrospilus vacuna Walker, 1839a: 305.

Cirrospilus numeria Walker, 1839a: 321. [Synonymised by Graham 1961b: 43]

Cirrospilus quercens Walker, 1839a: 307. [Synonymised by Graham 1961b: 43]

Cirrospilus alcithoë Walker, 1839b: 416. [Synonymised by Graham 1961b: 43]

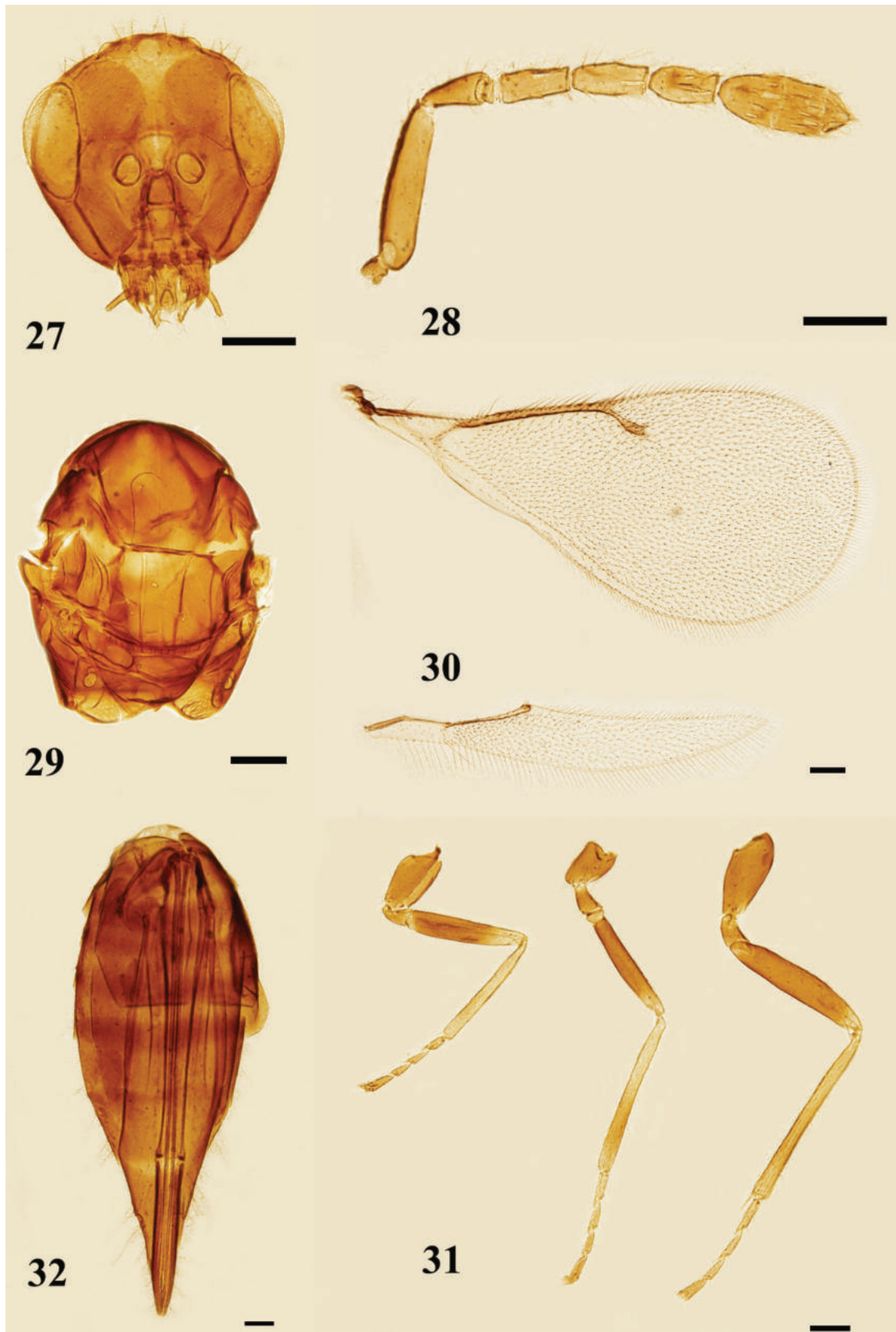
Cirrospilus rhoesus Walker, 1839b: 417. [Synonymised by Graham 1961b: 43]

Cirrospilus sotades Walker, 1839b: 417. [Synonymised by Graham 1961b: 43]

Cirrospilus brunchus Walker, 1840: 236. [Synonymised by Graham 1961b: 43]

Tetrastichus quercens: Walker 1846: 76.

Tetrastichus alcithoe: Walker 1846: 78.



Figures 27–32. *Quadrastichus vacuna* (Walker), female **27** head, frontal view **28** antenna, lateral view **29** mesosoma, dorsal view **30** fore and hind wings, dorsal view **31** legs, lateral view, from left to right: fore, mid, and hind legs **32** metasoma, ventral view. Scale bars: 100 μ m.

Tetrastichus rhoesus: Walker 1846: 78.

Tetrastichus vacuna: Walker 1848: 149.

Tetrastichus numeria: Walker 1848: 150.

Tetrastichus brunchus: Walker 1848: 151.

Tetrastichus migrator Förster, 1861: 38. [Synonymised by Graham 1961b: 43]

Tetrastichus penetrans Förster, 1861: 38. [Synonymised by Graham 1961b: 43]

Tetrastichus compressiventris Thomson, 1878: 286. [Synonymised by Graham 1961b: 43]

Aprostocetus vacuna: Graham 1961: 42.

Quadrastichus vacuna: Graham and LaSalle 1991: 94.

Qudrastichus vacuna: Boyadzhiev 2003: 82. [Misspelling]

Material examined. 5 females: [3 females on cards], China, Shangdong Province, Qindao City, Mt. Lao Shan, 11–13.VII.2014, Guo-Hao Zu, Zhi-Guang Wu, Hai-Feng Bai, by yellow-pan trapping, deposited in YCTU; [1 female on card, 1 female on slide], China, Xizang Province, Linzhi City, Mt. Sejila Shan, 20–24.VIII.2014, Hui-Lin Han, by yellow-pan trapping, deposited in NEFU.

Diagnosis. Female. Body (Fig. 33) black without yellow markings. Antenna (Fig. 28) with scape nearly reaching vertex but not extending beyond it, clava 2.7–3.0× as long as broad. Mid lobe of mesoscutum (Fig. 29) with 2–3 adnotaular setae on each side. Propodeum with median carina and paraspircular carinae. Gaster lanceolate, acuminate, 2.5–4.0× as long as broad, distinctly longer than head and mesosoma combined.

Male. Unknown for Chinese material.

Hosts. Unknown from China. Non-Chinese records include *Dasineura ulmariae* (Graham 1991) and *Leucoptera scitella* (Herting 1975) (Diptera: Cecidomyiidae) and *Heterarthrus vagans* (Askew and Shaw 1974) (Hymenoptera: Tenthredinidae).

Distribution. China (Xizang, Shandong), Russia, Italy, Hungary, Bulgaria (Boyadzhiev 2003), Netherlands (Gijswijt 2003), Romania (Hansson 2016),



Figure 33. *Quadrastichus vacuna* (Walker), female 33 habitus, lateral view. Scale bar: 500 μ m.

Austria, Norway, Poland, Switzerland, Sweden, Czechoslovakia, France, England, Ireland, (Graham 1991).

Comments. Graham (1991) reported that this species occasionally has two dorsal setae on the SMV. However, all specimens we examined only have one dorsal seta on the SMV.

***Quadrastichus anysis* (Walker, 1839)**

Fig. 34

Cirrospilus anysis Walker, 1839c: 203.

Tetrastichus anysis: Walker 1846: 74.

Aprostocetus anysis: Graham 1961b: 42.

Quadrastichus anysis: Graham and LaSalle 1991: 94; Zhu and Huang 2002: 598.

Material examined. 6 females: [2 females on cards], China, Jiangxi Province, Yichun City, Mt. Guan Shan, 21.VIII.2018, Xiang-Xiang Jin, Wang-Ming Li, by sweeping, deposited in YCTU; [1 female on card], China, Heilongjiang Province, Hegang City, Park Beishan, 22.VII.2020, Ming-Rui Li, by sweeping, deposited in YCTU; [2 females on slides], China, Liaoning Province, Anshan City, Mt. Qian Shan, 18.VI.2015, Hui Geng, Yan Gao, by sweeping, deposited in NEFU; [1 female on slide], China, Shaanxi Province, Ankang City, Town Guanghuojie, 3.VIII.2015, Ye Chen, Chao Zhang, by sweeping, deposited in NEFU.

Diagnosis. Female. Face with median area but without median carina. Malar sulcus curved. Antenna with scape reaching vertex, about as long as an eye,



Figure 34. *Quadrastichus anysis* (Walker), female **34** habitus, lateral view. Scale bar: 400 μ m.

pedicel 2.0–2.3× as long as broad; F1–F3 equal in length, each 2.0–2.2× as long as broad; clava 3.0–4.0× as long as broad. Mid lobe of mesoscutum with 1 adnotaular seta on each side situated in posterior half, without median line. Propodeum with median carina. Fore wing 2.0–2.1× as long as broad, costal cell narrow, shorter than MV; MV 3.0–4.0× STV; SMV with 1 dorsal seta; speculum small.

Male. Unknown for Chinese material.

Hosts. Unknown from China. Non-Chinese records include *Monarthropalpus buxi* (Graham 1991) (Diptera: Cecidomyiidae).

Distribution. China (Beijing, Zhejiang (Zhu and Huang 2001), Gansu, Shaanxi, Guangxi (Zhu and Huang 2002), Heilongjiang, Liaoning, Jiangxi [New records]), Romania, Czechoslovakia, France, Hungary, Italy, England, Russia (Graham 1991).

Comments. Graham (1991) reported that this species was variable in color. The colors of the specimens we examined are also not completely consistent, mainly in the yellow area of gaster, extending from the base to basal half.

***Quadrastichus sajo* (Szelényi, 1941)**

Figs 35–41

Myiomisa sajo Szelényi, 1941: 92. [Justified emendation by Graham 1991: 71]

Tetrastichus sajo: Vereshchagina 1961: 31.

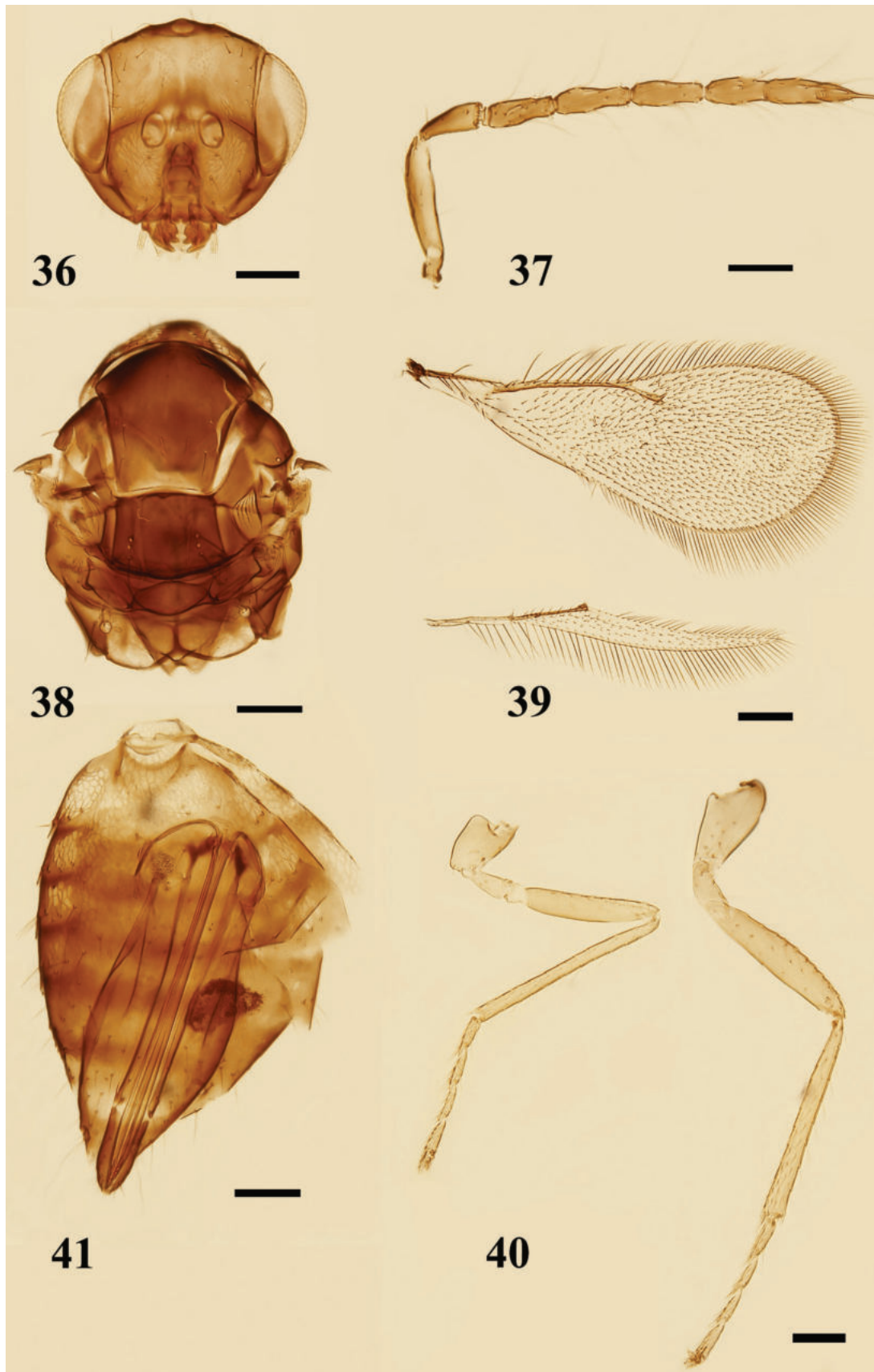
Aprostocetus scabricollis Graham, 1961a: 18. [Synonymised by Graham 1991: 71]

Quadrastichus sajo: Graham 1991: 71; Zhu and Huang 2002: 598.

Cecidotetrastichus sajo: Kostjukov 1997: 800.



Figure 35. *Quadrastichus sajo* (Szelényi), female **35** habitus, lateral view. Scale bar: 500 μ m.



Figures 36–41. *Quadrastichus saji* (Szelényi), female **36** head, frontal view **37** antenna, lateral view **38** mesosoma, dorsal view **39** fore and hind wings, dorsal view **40** legs, lateral view, from left to right: mid and hind legs **41** metasoma, ventral view. Scale bars: 100 μ m.

Material examined. 4 females: [2 females on cards], China, Yunnan Province, Tengchong City, Village Pojiao, 1.V.2013, Xiang-Xiang Jin, Guo-Hao Zu, by sweeping, deposited in YCTU; [1 female on card], China, Jiangxi Province, Yichun City, Mt. Guan Shan, 21.VIII.2018, Xiang-Xiang Jin, Wang-Ming Li, by sweeping, deposited in NEFU; [1 female on slide], China, Jiangxi Province, Yichun City, Mt. Guan Shan, 22.VIII.2018, Xiang-Xiang Jin, Wang-Ming Li, by sweeping, deposited in NEFU.

Diagnosis. Female. Malar sulcus (Fig. 35) distinctly curved, with a large subtriangular fovea below eye. Pronotum (Figs 35, 38) with 4 coarsely reticulate yellowish areas, remaining surface dark. Mid lobe of mesoscutum with 2–3 adnotaular setae on each side. Fore wing (Fig. 39) narrow, 2.2–2.5× as long as broad; MV 3.5–4.0× STV; SMV with 1 dorsal seta; speculum small, marginal setae long.

Male. Unknown for Chinese material.

Hosts. Unknown from China. Non-Chinese records include *Acalitus phloeoptes* (Mezei, 1995) (Acari: Eriophyidae).

Distribution. China (Gansu, Shaanxi, Guangxi (Zhu and Huang 2002), Jiangxi, Yunnan [New records]), Montenegro, Moldova, Serbia, Croatia (Bouček 1977), Syria, Czechoslovakia, Germany, Hungary, Italy, England, Russia (Graham 1991).

Comments. This species can be distinguished from other *Quadrastichus* species by the pronotum with four coarsely reticulate yellowish areas, with the remaining surface dark.

Acknowledgments

We are grateful to Prof Hui-Lin Han, Dr Xiang-Xiang Jin, Dr Guo-Hao Zu, Dr Hui Geng, Dr Ming-Rui Li, Miss Xin-Yu Zhang, Miss Yan Gao, Mr Wang-Ming Li, Mr Zhi-Guang Wu, Mr Jiang Liu and Mr Chao Zhang for specimen collection.

Additional information

Conflict of interest

The authors have declared that no competing interests exist.

Ethical statement

No ethical statement was reported.

Funding

This project was supported by the National Natural Science Foundation of China (grant no. 32000349).

Author contributions

All authors have contributed equally.

Author ORCIDs

Wen-Jian Li  <https://orcid.org/0009-0004-9790-3608>

Data availability

All of the data that support the findings of this study are available in the main text.

References

- Askew RR, Shaw MR (1974) An account of the Chalcidoidea (Hymenoptera) parasitizing leaf-mining insects of deciduous trees in Britain. *Biological Journal of the Linnean Society*. Linnean Society of London 6(4): 289–335. <https://doi.org/10.1111/j.1095-8312.1974.tb00727.x>
- Bouček Z (1977) A faunistic review of the Yugoslavian Chalcidoidea (Parasitic Hymenoptera). *Acta Entomologica Jugoslavica* 13(Supplement): 1–145.
- Boyadzhiev PS (2003) New records to the fauna of Eulophidae in Bulgaria (Hymenoptera, Chalcidoidea) with a checklist of all the Bulgarian species. *Plovdivski Universitet "Paisij Khilendarski"*. *Nauchni Trudove Biologiya Animalia* 39(6): 79–96.
- Feng MX, Cao HX, Hao HH, Wang W, Cheng LS (2016) A New Record Species of *Quadrastichus* (Hymenoptera: Eulophidae) from China. *Chinese Journal of Tropical Crops* 37(3): 582–585. <http://www.rdzwx.com/CN/Y2016/V37/I3/582>
- Förster A (1861) Ein Tag in den Hoch-Alpen. Programm der Realschule zu Aachen 1860–1861: 1–44.
- Gibson GAP, Huber JT, Woolley JB (1997) Annotated keys to the genera of Nearctic Chalcidoidea (Hymenoptera). National Research Council Research Press, Ottawa, 794 pp.
- Gijswijt MJ (2003) Naamlijst van de Nederlandse bronswespen (Hymenoptera: Chalcidoidea). *Nederlandse Faunistische Mededelingen* 18: 17–79.
- Girault AA (1913) Australian Hymenoptera Chalcidoidea – IV. *Memoirs of the Queensland Museum* 2: 140–296. <https://doi.org/10.5962/bhl.title.9562>
- Graham MWR de V (1961a) New species of *Aprostocetus* Westwood (Hym., Eulophidae) from Britain and Sweden. *Opuscula Entomologica*, Lund 26: 4–37.
- Graham MWR de V (1961b) The genus *Aprostocetus* Westwood sensu lato (Hym., Eulophidae) notes on the synonymy of European species. *Entomologist's Monthly Magazine* 97: 34–64.
- Graham MWR de V (1987) A reclassification of the European Tetrastichinae (Hymenoptera: Eulophidae), with a revision of certain genera. *Bulletin of the British Museum (Natural History)*. Historical Series 55(1): 1–392. [Natural History]
- Graham MWR de V (1991) A reclassification of the European Tetrastichinae (Hymenoptera: Eulophidae): revision of the remaining genera. *Memoirs of the American Entomological Institute* 49: 1–322.
- Graham MWR de V, LaSalle J (1991) New synonymy in European Tetrastichinae (Hymenoptera: Eulophidae) including designation of some neotypes, lectotypes and new combinations. *Entomologist's Gazette* 42: 89–96.
- Hansson C (2016) New records of Eulophidae (Hymenoptera: Chalcidoidea) from Romania, including two new species. *Travaux du Muséum d'Histoire Naturelle 'Grigore Antipa', Bucuresti* 59(1): 53–72. <https://doi.org/10.1515/travmu-2016-0017>
- Hansson C, LaSalle J (1996) Two new eulophid parasitoids (Hymenoptera: Chalcidoidea: Eulophidae) of *Liriomyza trifolii* (Burgess) (Diptera: Agromyzidae). *Oriental Insects* 30(1): 193–202. <https://doi.org/10.1080/00305316.1996.10433841>
- Herting B (1975) *Lepidoptera, Part 1 (Microlepidoptera)*. A Catalogue of Parasites and Predators of Terrestrial Arthropods. Section A. Host or Prey/Enemy. Commonwealth Agricultural Bureaux, Slough, 218 pp.
- Kim IK, Delvare G, LaSalle J (2004) A new species of *Quadrastichus* (Hymenoptera: Eulophidae): a gall-inducing pest on *Erythrina* (Fabaceae). *Journal of Hymenoptera Research* 13(2): 243–249.

- Kim IK, Mendel Z, Protasov A, Blumberg D, LaSalle J (2008) Taxonomy, biology, and efficacy of two Australian parasitoids of the eucalyptus gall wasp, *Leptocybe invasa* Fisher & LaSalle (Hymenoptera: Eulophidae: Tetrastichinae). *Zootaxa* 1910(1): 1–20. <https://doi.org/10.11646/zootaxa.1910.1.1>
- Kostjukov VV (1997) Species of the genus *Cecidotetrastichus* (Hymenoptera, Eulophidae) from Khabarovsk and Primorye territories of Russia. *Zoologicheskij Zhurnal* 76(7): 797–805.
- Mezei I (1995) Data on the biology of *Quadrastichus (Myiomisa) sajo*i Szélenyi (Hymenoptera: Chalcidoidea). *Novenyvedelem* 31(5): 211–214.
- Noyes JS (1982) Collecting and preserving chalcid wasps (Hymenoptera: Chalcidoidea). *Journal of Natural History* 16(3): 315–334. <https://doi.org/10.1080/00222938200770261>
- Noyes JS (2019) Universal Chalcidoidea Database. <http://www.nhm.ac.uk/chalcidoids> [Accessed Oct. 2023]
- Reina P, LaSalle J (2004) Two new species of *Quadrastichus* Girault (Hymenoptera: Eulophidae): parasitoids of the leafminers *Phyllocnistis citrella* Stainton (Lepidoptera: Gracillariidae) and *Liriomyza trifolii* (Burgess) (Diptera: Agromyzidae). *Journal of Hymenoptera Research* 13(1): 108–119.
- Szélenyi G (1941) Notes on the *tetrastichine* genus *Myiomisa* Rond. (Hym. Chalc.) with the re-description of the genotype and with description of a new species parasitizing in the galls of *Eriophyes phloeocoptes* Nal. *Jb. amlt. PflGesundh Dienstes Budapest* 1: 89–97.
- Thomson CG (1878) *Hymenoptera Scandinaviae* 5. *Pteromalus* (Svederus) continuatio, Lund, 307 pp.
- Vereshchagina VV (1961) *Tetrastichus (Myiomisa) sajo*i Szélenyi – a predator of the plum shoot mite – *Eriophyes phloeocoptes* Nal. *Trudy Moldavskogo Nauchno-Issledovatel'skogo Instituta Sadovodstva, Vinogradarstva i Vinodeliya*. Kishinev 7: 31–33.
- Walker F (1839a) *Monographia Chalciditum*. London, 333 pp. <https://doi.org/10.5962/bhl.title.67725>
- Walker F (1839b) Descriptions of British Chalcidites. *Annals of Natural History* 3(19): 415–419. <https://doi.org/10.1080/03745483909443254>
- Walker F (1839c) Descriptions of British Chalcidites. *Annals of Natural History* 2(9): 198–205. <https://doi.org/10.1080/00222933809512372>
- Walker F (1840) Descriptions of British Chalcidites. *Annals of Natural History* 4(24): 232–236. <https://doi.org/10.1080/00222933909496690>
- Walker F (1846) List of the specimens of Hymenopterous insects in the collection of the British Museum. Part 1 Chalcidites. E. Newman, London, 100 pp.
- Walker F (1848) List of the specimens of Hymenopterous insects in the collection of the British Museum. Part 2 Chalcidites. E. Newman, London, 99–237 pp.
- Yegorenkova EN, Yefremova ZA, Kostjukov VV (2007) Contributions to the knowledge of tetrastichine wasps (Hymenoptera, Eulophidae, Tetrastichinae) of the middle Volga region. *Entomologicheskoe Obozrenie* 86(4): 781–796. <https://doi.org/10.1134/S0013873807090084>
- Zhang YZ, Ding L, Huang HR, Zhu CD (2007) Eulophidae fauna (Hymenoptera, Chalcidoidea) from south Gansu and Qinling mountain areas, China. *Acta Zootaxonomica Sinica* 32(1): 6–16.
- Zhu CD, Huang DW (2001) A taxonomic study on Eulophidae from Zhejiang, China (Hymenoptera: Chalcidoidea). *Acta Zootaxonomica Sinica* 26(4): 533–547.
- Zhu CD, Huang DW (2002) A taxonomic study on Eulophidae from Guangxi, China (Hymenoptera: Chalcidoidea). *Acta Zootaxonomica Sinica* 27(3): 583–607.

Broadly sympatric occurrence of two thief ant species *Solenopsis fugax* (Latreille, 1798) and *S. juliae* (Arakelian, 1991) in the East European Pontic-Caspian region (Hymenoptera, Formicidae) is disclosed

Sándor Csősz^{1,2}, Bernhard Seifert³, Márk László², Zalimkhan M. Yusupov⁴, Gábor Herczeg^{1,2}

1 HUN-REN-ELTE-MTM Integrative Ecology Research Group, Pázmány Péter ave 1/C, Budapest 1117, Hungary

2 Department of Systematic Zoology and Ecology, Institute of Biology, ELTE-Eötvös Loránd University, Pázmány Péter ave 1/C, Budapest 1117, Hungary

3 Department of Entomology, Senckenberg Museum of Natural History Görlitz, Am Museum 1, 02826 Görlitz, Germany

4 Tembotov Institute of Ecology of Mountain Territories of RAS, Nalchik, 360051, Russia

Corresponding author: Sándor Csősz (csosz.sandor@ttk.elte.hu)



Academic editor: Brian Lee Fisher

Received: 3 May 2023

Accepted: 19 September 2023

Published: 21 December 2023

ZooBank: <https://zoobank.org/78E4BBFE-8A35-4A1D-980E-5D2EE913F6A8>

Citation: Csősz S, Seifert B, László M, Yusupov ZM, Herczeg G (2023) Broadly sympatric occurrence of two thief ant species *Solenopsis fugax* (Latreille, 1798) and *S. juliae* (Arakelian, 1991) in the East European Pontic-Caspian region (Hymenoptera, Formicidae) is disclosed. ZooKeys 1187: 189–222. <https://doi.org/10.3897/zookeys.1187.105866>

Copyright: © Sándor Csősz et al.
This is an open access article distributed under terms of the Creative Commons Attribution License ([Attribution 4.0 International – CC BY 4.0](https://creativecommons.org/licenses/by/4.0/)).

Abstract

This paper presents numeric morphology-based evidence on the broadly overlapping distribution of two thief ant species *Solenopsis fugax* (Latreille, 1798) and *S. juliae* (Arakelian, 1991) in the East European Pontic-Caspian region. The paper integrates two autonomous data collections and independent analyses performed by different researchers, using different equipment, considering different character combinations, and evaluating partially different samples. Five type series, the neotype series of *Solenopsis fugax* (Latreille 1798) and the type series of *S. flavidula* (Nylander, 1849), *S. (Diplorhoptrum) fugax* var. *furtiva* Santschi, 1934, *S. (Diplorhoptrum) fugax* var. *pontica* Santschi, 1934, *S. (Diplorhoptrum) fugax* var. *scytica* Santschi, 1934 were nested in one cluster and we propose the junior synonymy of the latter four taxa names with *S. fugax*. The other cluster contained only one type specimen of *Solenopsis nitida* (Dlussky & Radchenko, 1994) measured from AntWeb images. The naming of this cluster was based on both verbal statements and measurements of gynes given in the original description of *Solenopsis juliae* (Arakelian, 1991), which represents the oldest available name for this cluster. Hence, *S. nitida* is proposed as junior synonym of *S. juliae*. *Solenopsis cypridis* Santschi, 1934 is raised to species rank based on investigation of worker and gyne type specimens.

Key words: Biogeography, cryptic species, dimorphism, exploratory analyses, morphometry, species delimitation

Introduction

The Myrmicine ant genus *Solenopsis* Westwood 1840 is distributed worldwide over the tropical, subtropical, and temperate zones. Approximately 200 species are currently recognized, with 80% of these being distributed in the Neotropical and South Nearctic zone. The catalog of Bolton (2023) lists 24 species plus four subspecies for the West Palaearctic region, mainly described from the African and European parts of the West Mediterranean and temperate France. The

Palaeartic species are essential elements of myrmecocenoses in xerothermous grassland and forest-steppe ecosystems. In oligotrophic xerothermous grasslands of Central Europe, the so-called thief ant *Solenopsis fugax* (Latreille, 1798) may build up maximum densities of 92 nests /100 m² (Seifert 2017) or may constitute up to 20–25% of total ant biomass (Wagner and Wieser 2021). This subterranean species is a true cleptobiont in probably all larger ant species occurring in its habitats. However, it does not depend on this lifestyle as it is necrophagic, strongly trophobiotic, and preys on diverse developmental stages of soil invertebrates. Colonies with strongly cleptobiotic nutrition are apparently selected for uniform smallness of workers, whereas those using diverse food sources usually contain both minor and major workers (Hölldobler 1965). Other researchers have also documented this size dimorphism (e.g., Galkowski et al. 2010; pers. obs.).

The taxonomy of the genus became highly complicated in the West Mediterranean area due to 15 taxa described from France and Corsica. After Latreille (1798) had described *S. fugax*, Santschi (1934) added three taxa, whereas Bernard (1950, 1959, 1978) described as many as 15 taxa, among these 14 from France and four of them from a small area near Banyuls sur Mer. There is little doubt that this inflated list contains many synonyms. Galkowski et al. (2010) attempted to bring some order into this confusing heritage. Fixing a neotype, they redescribed *Solenopsis fugax* and delimited four species groups: the *S. fugax* group, the *S. debilior* group, the *S. lusitanica* group, and the *S. orbula* group. The authors commented, “A largest and most extensive collect will be necessary for a new morphological and molecular approach of the genus and to go further in understanding the *Solenopsis* of France” (Galkowski et al. 2010: 151). We agree, but are unable to give data-based, thoughtful comments on the situation in the Palaeartic west of 8°E; it may be that these species groups represent only a little more than four species. In contrast, the situation farther east is easier to conceive. Therefore, we take the occasion to progress for at least one segment of *Solenopsis* taxonomy for the area of Central Europe, the Balkans, Ukraine, Asia Minor, and the Caucasian region. After Seifert (2018) stated that only a single species occurs north of the Alps, which is by type comparison *Solenopsis fugax*, we became recently aware using morphometric examination that two distinct morphospecies occur in this eastern region in sympatry. One of them is *Solenopsis fugax*, and we provide an argument that the eastern species should be *Solenopsis juliae* (Arakelian 1991). We therefore consider all relevant taxa described from this eastern region or near to it to establish these names.

Morphometric investigation of *Solenopsis* is challenging and requires high-resolution stereo microscopy as the worker thief ants often have a minute size of less than 2 mm in total length. The size dimorphism of workers adds a second complication (e.g., Hölldobler 1965; Galkowski et al. 2010). Gyne dimorphism is also not unusual in *Solenopsis*, confirmed in both *S. geminata* (Fabricius, 1804) and *invicta* Buren, 1972 (McInnes and Tschinkel 1995; Helms and Godfrey 2016), and it also appeared in the two species considered here with the result that microgynes of *S. fugax* have a similar absolute size as do macrogynes of *S. juliae*. This size dimorphism requires corrections for the strong allometric effects to show which morphological differences are “species specific” and to improve the performance of principal component analyses. We follow here the working

rationale of species hypothesis formation by different forms of exploratory data analyses of continuous morphometric data and checking these hypotheses by linear discriminant analysis (Seifert et al. 2014; Csósz and Fisher 2016).

We repeat the parallel data collection procedures of previous papers (Csósz and Seifert 2003; Seifert and Csósz 2015). Both authors had spent a substantial amount of time investigating the *Solenopsis fugax* problem before they realized they were working on the same issue. This led to the recording of different, but partially identical character sets and samples. It is important to note that only 35% of the total 62 worker samples were measured by both SC and BS. We decided to continue with the different approaches, which each followed a robust statistical procedure. Three factors should be noted in this context: (i) this two-dataset setup provides an excellent ground to test whether or not the differently collected morphometric data bias our findings, (ii) a post-hoc synchronization of these different systems was avoided as this would have been overly time-consuming, and (iii) a data synchronization was not performed as this would have implied a loss of information. The disadvantage of the complex presentation is compensated by the pleasant fact that independent approaches led to the same conclusion in the differentiation of cryptic species. Finally, the importance of our research is beyond simply understanding another fragment of European biodiversity; our study also shows that morphometry considering allometry-driven polymorphism is superior in performance compared to subjective evaluation of discrete traits or to presenting a few anecdotal morphometric measurements.

Materials and methods

Material examined

Altogether 63 worker nest samples were investigated, 42 nest series by Seifert (hereafter BS), 52 by Csósz (SC), and 35% of the total were investigated by both observers. In addition, BS measured 26 gyne samples with 41 specimens. We borrowed and investigated all type series of species described from the target region: *S. fugax* neotype series, *S. flavidula* Nylander 1849, *S. fugax furtiva* Santschi, 1934, *S. fugax pontica* Santschi, 1934, *S. fugax scythica* Santschi, 1934, and *S. fugax cypridis* Santschi, 1934. We had to rely upon the morphometric data from images stored in the online virtual collection Antweb.org (AntWeb 2023) in the case of types stored in Kyiv and Moscow due to the Russo-Ukrainian war. Even though we have measured high-resolution AntWeb images with the utmost caution, we carefully concluded that those image-based morphometric data are in accordance with the latest results on applicability of the virtual collection data (Csósz et al. 2023). The full list of examined material is listed in Suppl. material 1 including locality information, number of measured individuals, and the depositories.

Protocol for morphometric character recording

All measurements were made with a cross-scale graticule at μm precision using a pin-holding stage, permitting rotations around X, Y, and Z axes with an Olympus SZX16 stereomicroscope with a 1.6 \times Plan Aplanachromat objective at a

Table 1. Abbreviations for morphometric characters, character definitions and the relevant observers' initials are presented in different columns. SC = Sándor Csósz, BS = Bernhard Seifert. In case the protocol was identical between the observers, initials of both authors are given.

Abbreviation	Character definition	Observer
CL1	Maximum cephalic length from the median point of a reference line connecting the tips of the large clypeal teeth to the hind margin of head; the head must be carefully tilted to the position with the true maximum.	SC
CL2	Maximum cephalic length from anteromedian margin of clypeus to posteromedian margin of head; the head must be carefully tilted to the position with the true maximum.	BS
CLSPD	Distance of tips of the large paramedian clypeal dents	SC, BS
CLSPLM	mean length of the large paramedian clypeal dents measured from bottom of menisci left and right of the spines	BS
CLSPLL	mean length of the more lateral, smaller clypeal dents measured from bottom of menisci left and right of the spines	BS
CW	maximum width of head capsule posterior of the eyes	SC, BS
CS	The arithmetic means of CL2 and CW as less variable indicator of absolute size	BS
EL	longest eye diameter	BS
FL	Maximum distance of frontal carinae; if no maximum is defined by a constriction, set FR equal to FRS	BS
FR	Minimum distance of frontal carinae; if no minimum is defined by a constriction, set FR equal to FRS	BS
FRS	distance of the frontal carinae immediately caudal of the posterior intersection points between frontal carinae and the lamellae dorsal of the torulus. If these dorsal lamellae do not laterally surpass the frontal carinae, the deepest point of scape corner pits may be taken as reference line. These pits take up the inner corner of scape base when the scape is fully switched caudad and produce a dark triangular shadow in the lateral frontal lobes immediately posterior of the dorsal lamellae of scape joint capsule	SC, BS
FULL FACE VIEW	Dorsal aspect of head with both maximum head width and maximum median head length in visual plane	SC, BS
ML	Mesosoma length; anterior measuring point in workers: transition point of the anterior pronotal slope to the anterior pronotal shield; anterior measuring point in gynes: frontalmost point of the pronotal slope; posterior measuring point in both workers and gynes: caudalmost margin of the propodeal lobe.	SC, BS
MPGR	depth of metanotal groove measured down from tangent of mesonotopropodeal profile	BS
MW	mesosoma width; this is in workers maximum pronotal width, in gynes the maximum mesosoma width frontal of the tegulae	SC, BS
NOH	Maximum height of the petiolar node, measured from the uppermost point of the petiolar node perpendicular to a reference line set from the petiolar spiracle to the dorso-caudal corner of caudal cylinder of the petiole	SC
PEH	Petiole height. A straight imagination of ventral petiolar profile at node level is the reference line perpendicular to which the maximum height of petiole node is measured at node level. This is the height of a section line but not height above all.	SC, BS
PEW	maximum width of petiole	SC, BS
PPW	maximum width of postpetiole	SC, BS
PPH	maximum postpetiole height; the lateral suture of dorsal and ventral sclerites is the reference line perpendicular to which the maximum height is measured.	BS
PROC	preocular distance; the shortest distance between the anterior eye margin and the sharp frontal margin of the gena. Caution: do not confuse this with the beaded rim of the mandible that is often very closely appressed to the genal margin.	BS
SL	maximum straight line scape length excluding the articular condyle as arithmetic mean of both scapes	SC, BS
APS	With the swiveling plane of antennal funiculus in visual plane (defined by the swiveling plane of the hinge joint of pedicellus with scape), maximum median length of apical funiculus segment.	SC
SAPS	With the swiveling plane of antennal funiculus in visual plane, maximum median length of sub-apical funiculus segment.	SC

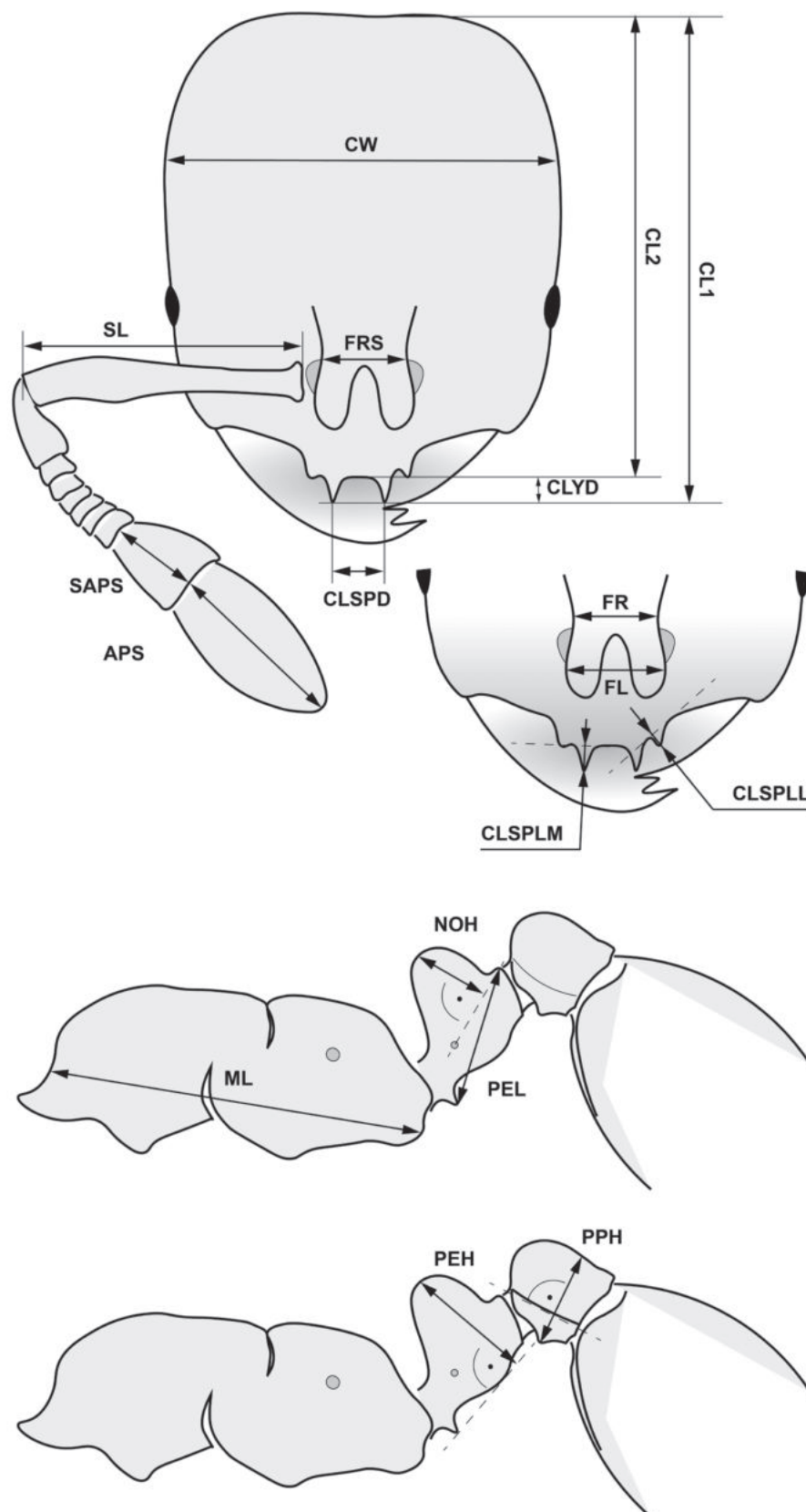


Figure 1. Definition of morphological characters of the *Solenopsis* workers measured in this study. Head in dorsal view with measurement lines for CL1, CL2, CW, FRS, CLSpD, ApS, SApS, and SL; frontal region of the head dorsum with measurement lines for FR, FL, CLSpLL, and CLSpLM; dorsal view of mesosoma with measurement lines for ML, PEH, PEL, NOH, and PPH (for definitions, see Table 1).

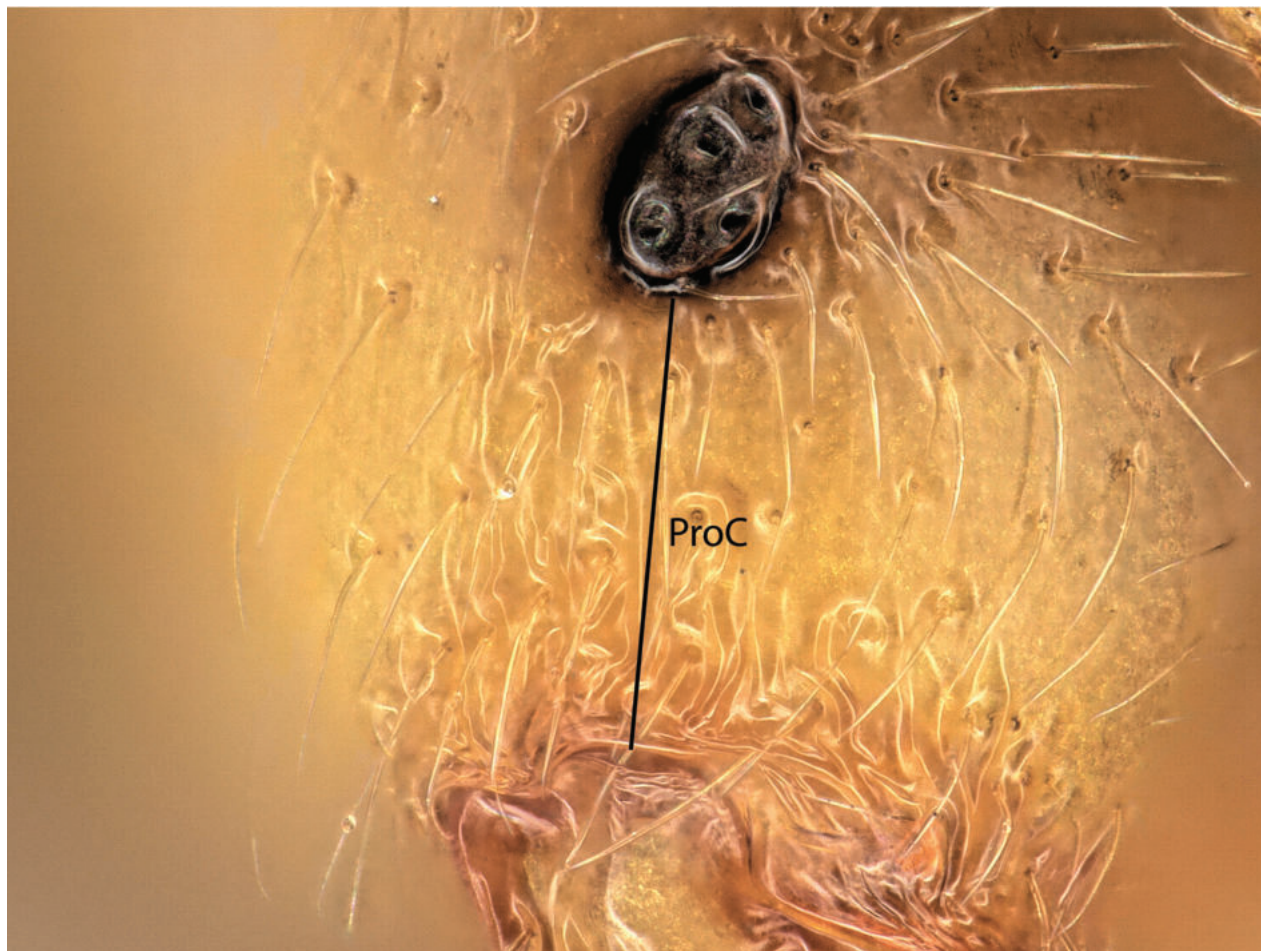


Figure 2. Definition of preocular distance (PROC) of the *Solenopsis* workers measured in this study (for details, see Table 1).

magnification of $\times 240$ for each character (SC); stereomicroscopic and photographic equipment, measurement procedures of BS are as reported in Seifert (2023). Morphometric data are given in μm throughout the paper. Definitions of morphometric characters are listed in Table 1 and are illustrated in Figs 1, 2. Raw data in μm is given in Suppl. materials 1–3.

Data preparation

Allometry is the disproportionate change of body shape and other phenotypic traits with growing body size (Leonart et al. 2000). As body size is in ants strongly dependent on particular environmental conditions during ontogenesis, in particular from larval nutrition (Tschinkel et al. 2003; Molet et al. 2017), removal of allometric variance (RAV) can be considered as approximation of the data to the genetically determined character space. As result, RAV can expose in comparative tables “true” genetically determined interspecific differences and unmask pseudo-differences (Seifert 2008). Furthermore, RAV may increase the performance of some exploratory data analyses – in particular of principle component analyses (PCA; Seifert 2021). If absolute measurements (raw data) are used in a PCA, the first principal component often indicates the size component which is not of interest in separation of cryptic species, and it may blur the analysis. RAV was performed here with two different methods.

Table 2. Removal of allometry via regression model (SC). Residuals for nest samples are calculated via regression analyses for every trait on Cephalic Length (CL1) as the independent variable, coefficients x , and intercept to calculate residuals are provided.

	x(CL1)	(Intercept)
CLYD	0.038	1.555
APS	0.239	74.015
SAPS	0.143	5.354
CWB	1.020	-110.076
FRS	0.219	-10.728
CLYW	0.168	-33.917
SL	0.611	-3.445
MW	0.562	-14.713
PEW	0.321	-14.704
PPW	0.296	5.081
ML	1.183	-60.970
PEL	0.400	-11.529
PEH	0.294	26.156
NOH	0.196	2.364

To remove effects of the disproportionate size dependent trait size changes, SC calculated within-nest sample regression analyses of absolute measurements with cephalic length CL1 (Cephalic Length, see Table 1) as the independent variable. Head size is one of the most popularly used size indicator in ants (see e.g., Tschinkel et al. 2003; Seifert 2008; Molet et al. 2017). Coefficients applied to calculate residuals are given in Table 2. The resulting slope and intercept of the correction functions were then calculated as arithmetic means from the 52 samples' slope and intercept values. RAV was then performed using residuals and with these data an alternative prior species hypothesis was generated via PCA. This procedure does not need a previous formation of species hypotheses but accepts unequal contribution of species to the RAV function finally calculated.

BS performed RAV by following the basic procedure described in Seifert (2008), which uses regression of index values against cephalic size CS as independent variable. The procedure requires a pre-established hypothesis on species identities and results in equal contribution of the considered species to the final RAV function. Slope and intercept were here calculated as the arithmetic mean of the species-specific functions, in this paper of 92 *S. fugax* and 66 *S. juliae* workers. RAV was then performed by calculating the quotient between the real value and the RAV-function value. In order to have a translucent presentation in comparative tables and descriptions, the quotients were then transformed to index values that would be achieved if all worker individuals had the same cephalic size of CS = 480 μm (Table 1). The procedure resulted in a reduction of within-species variance to 29% in CL2/CW, 73% in SL/CS, 76% in CLSPD/CS, and 65% in PEH/CS, but did not show notable effects in the remaining characters. Parameters for RAV in gynes were calculated alone on the basis of data in *S. fugax* as it was the only species with sufficient sample size.

The RAV functions for workers and gynes (sensu BS) are as follows:

$$\begin{aligned}CL2/CW_{480} &= CL2/CW / (-0.5634*CS + 1.4390) * 1.1685 \\SL/CS_{480} &= SL / (-0.1460*CS + 0.7688) * 0.6987 \\FL/CS_{480} &= FL / (0.0036*CS + 0.2223) * 0.2241 \\FR/CS_{480} &= FR / (0.0131*CS + 0.2083) * 0.2146 \\EL/CS_{480} &= EL / (0.0772*CS + 0.0575) * 0.0945 \\PrOc/CS_{480} &= PROC / (-0.0135*CS + 0.1939) * 0.1874 \\CLSPLM/CS_{480} &= CLSPLM / (-0.0388*CS + 0.0750) * 0.0564 \\CLSPLL/CS_{480} &= CLSPLL / (-0.0239*CS + 0.0314) * 0.0199 \\CLSPD/CS_{480} &= CLSPD / (0.1082*CS + 0.0833) * 0.1353 \\ML/CS_{480} &= ML / (-0.0094*CS + 1.1853) * 1.1808 \\MW/CS_{480} &= MW / (-0.0881*CS + 0.6335) * 0.5912 \\MpGr/CS_{480} &= MPGR / (0.0051*CS + 0.0244) * 0.0269 \\PEW/CS_{480} &= Pew / (0.0259*CS + 0.2943) * 0.3068 \\PPW/CS_{480} &= PPw / (-0.0592*CS + 0.3556) * 0.3271 \\PEH/CS_{480} &= PEH / (-0.1487*CS + 0.4487) * 0.3773 \\PPH/CS_{480} &= PPH / (-0.0011*CS + 0.3058) * 0.3006\end{aligned}$$

The RAV functions in gynes are:

$$\begin{aligned}CL2/CW_{850} &= CL2/CW / (-0.2881*CS + 1.1973) * 0.9524 \\SL/CS_{850} &= SL / (-0.2677*CS + 0.8775) * 0.6500 \\FL/CS_{850} &= FL / (-0.1515*CS + 0.3890) * 0.2602 \\FR/CS_{850} &= FR / (-0.1466*CS + 0.3834) * 0.2588 \\EL/CS_{850} &= EL / (-0.1448*CS + 0.4169) * 0.2938 \\PrOc/CS_{850} &= PROC / (0.0899*CS + 0.0388) * 0.1152 \\CLSPLM/CS_{850} &= CLSPLM / (0.0108*CS + 0.0403) * 0.0494 \\CLSPLL/CS_{850} &= CLSPLL / (0.0504*CS - 0.0304) * 0.0125 \\CLSPD/CS_{850} &= CLSPD / (0.0011*CS + 0.1395) * 0.1405 \\ML/CS_{850} &= ML / (0.5567*CS + 1.5727) * 2.0459 \\MW/CS_{850} &= MW / (0.7122*CS + 0.4779) * 1.0833 \\MH/CS_{850} &= MH / (0.6220*CS + 0.7668) * 1.2854 \\PEW/CS_{850} &= Pew / (-0.1511*CS + 0.5986) * 0.4701 \\PPW/CS_{850} &= PPw / (-0.2844*CS + 0.7683) * 0.5265 \\PEH/CS_{850} &= PEH / (0.1010*CS + 0.4025) * 0.4883 \\PPH/CS_{850} &= PPH / (-0.1000*CS + 0.5682) * 0.4832\end{aligned}$$

Statistical framework on morphometric data – hypothesis formation and testing

We use the toolkit of exploratory data analysis of continuous morphometric data (Seifert et al. 2014; Csósz and Fisher 2016) followed by confirmatory data analysis.

Exploratory analyses via NC-PART clustering

The prior species hypothesis was generated based on workers via Nest Centroid clustering (NC clustering; Seifert et al. 2014) in combination with partitioning algorithms PART (Nilsen and Lingjaerde 2013; Csósz and Fisher 2016)

for estimating the number of biologically meaningful clusters. The protocol of this combination was published by Csósz and Fisher (2016), which is now applied with the following specific setups: bootstrap iterations in PART were set to 'b=1000', and the minimum size of clusters were set to 'minSize=5' for both 'hclust' and 'kmeans'. Data input for this analysis was performed as absolute measurements (raw data) in the analysis of SC and as allometrically corrected index data (plus CS as absolute size indicator) in the analysis of BS. The script was written in R and can be found in Suppl. material 4.

Exploratory analyses via PCA using allometrically corrected data

An alternative prior species hypothesis has been generated by SC via the ordinating Principal Component Analysis (PCA) that displays plots in a graphic. Allometries are calculated via regression analyses for every trait on CL1 as the independent variable (see Table 1), and residuals were applied. Coefficients to calculate residuals are provided in Table 2. Shape ratios corrected according to the RAV system of BS were used to demonstrate heterospecificity in a PCA of workers.

Confirmatory data analyses (SC)

The validity of the prior species hypothesis imposed by the exploratory processes was tested via a cross-validated linear discriminant analysis (CV-LDA) using the package MASS (Ripley et al. 2013). Statistical analyses have been done in R (R Core Team 2022). Conventional LDA and backward stepwise method was used to create an easy-to-use numeric key for separating species *via* character reduction. Data input for this analysis was performed as absolute measurements (raw data).

Imaging (BS)

Z.stack images of mounted ants were produced with Keyence a VHX 7000 digital microscope using the multi-lightning mode at magnifications between 80× and 400×.

Results

The two clustering methods 'hclust' and 'kmeans' of PART (SC and BS) and NC-NMDS.kmeans (BS only) in combination with NC-clustering resulted in two clusters. The partitioning methods returned a single alternative assignment out of the total 52 (SC, Fig. 3), and no misplacement was returned in BS' dataset (Fig. 4). The misplaced sample (in SC) was set to wild-card in the confirmatory LDA (Seifert et al. 2014). The syntypes series of *Solenopsis fugax* var. *cypridis* Santschi, 1934 formed an outlier cluster. The PCA after removal of allometric variance (RAV) according to the approach of SC corroborated the pattern returned by the NC-PART-clustering: two clusters are recognized, and the syntype series of *Solenopsis fugax* var. *cypridis* Santschi, 1934 is not nested in either cluster (Fig. 5). The outlying placement of the worker and gyne syntype series of *S. cypridis* is confirmed by the PCA using the character set and the RAV correction according to system of BS (Figs 6, 7).

Classifications of the type materials investigated in workers are as follows (Figs 3–7): Cluster A: *Solenopsis nitida* (Dlussky & Radchenko, 1995) and Cluste B: Neo-

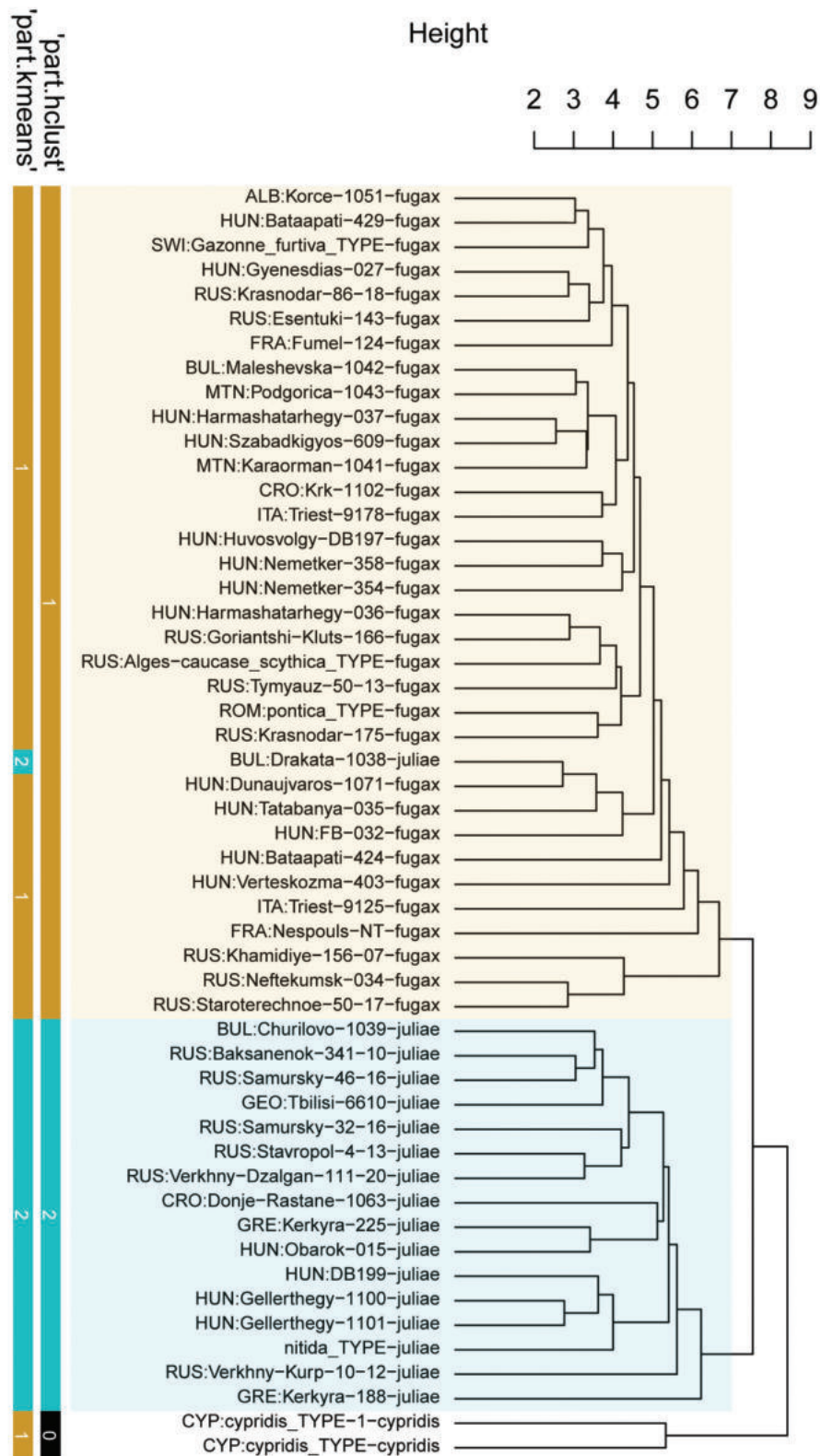


Figure 3. Dendrogram comparing the results of “kmeans”, and “hclust” in NC Clustering using UPGMA distance method of *Solenopsis* workers’ morphometric raw data. Ocher bars: *S. fugax*, blue bars: *S. juliae*. The type material of *S. juliae* was not available for measurements, not shown. Black bar represents the *S. cypridis* samples as outgroup. Data input: raw data within the character system of SC. The *cypridis* cluster (black bars) was assigned as outlier in ‘hclust’ but ‘kmeans’ assigned it in the *fugax* cluster. Note: four workers mounted on different pins (3 and 1 workers respectively) of the *S. cypridis* syntype material appear separately in the tree.

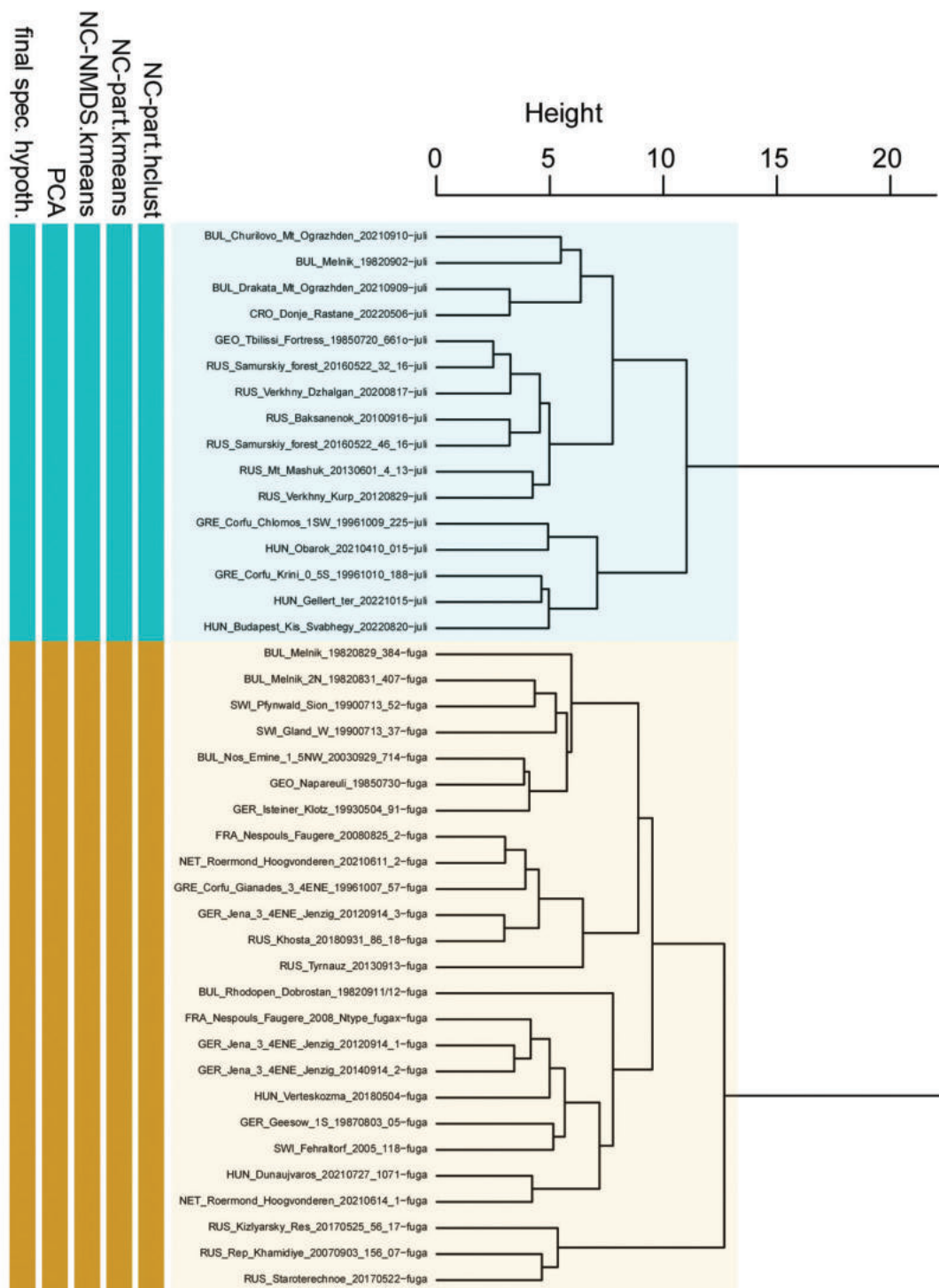


Figure 4. Comparison of five exploratory data analyses with the final species hypothesis. Dendrogram showing NC Clustering using ward distance method. Ocher bars: *Solenopsis fugax*, blue bars: *S. juliae*. Data input: RAV-corrected values of workers in the character system of BS.

type series of *Solenopsis fugax* (Latreille, 1798), *Solenopsis (Diplorhoptrum) fugax* var. *furtiva* Santschi, 1934, *Solenopsis (Diplorhoptrum) fugax* var. *pontica* Santschi, 1934, *Solenopsis (Diplorhoptrum) fugax* var. *scytica* Santschi, 1934.

The cross-validation LDA confirmed this classification on individual level with 98% probability involving all characters (Table 3), and the high divergence

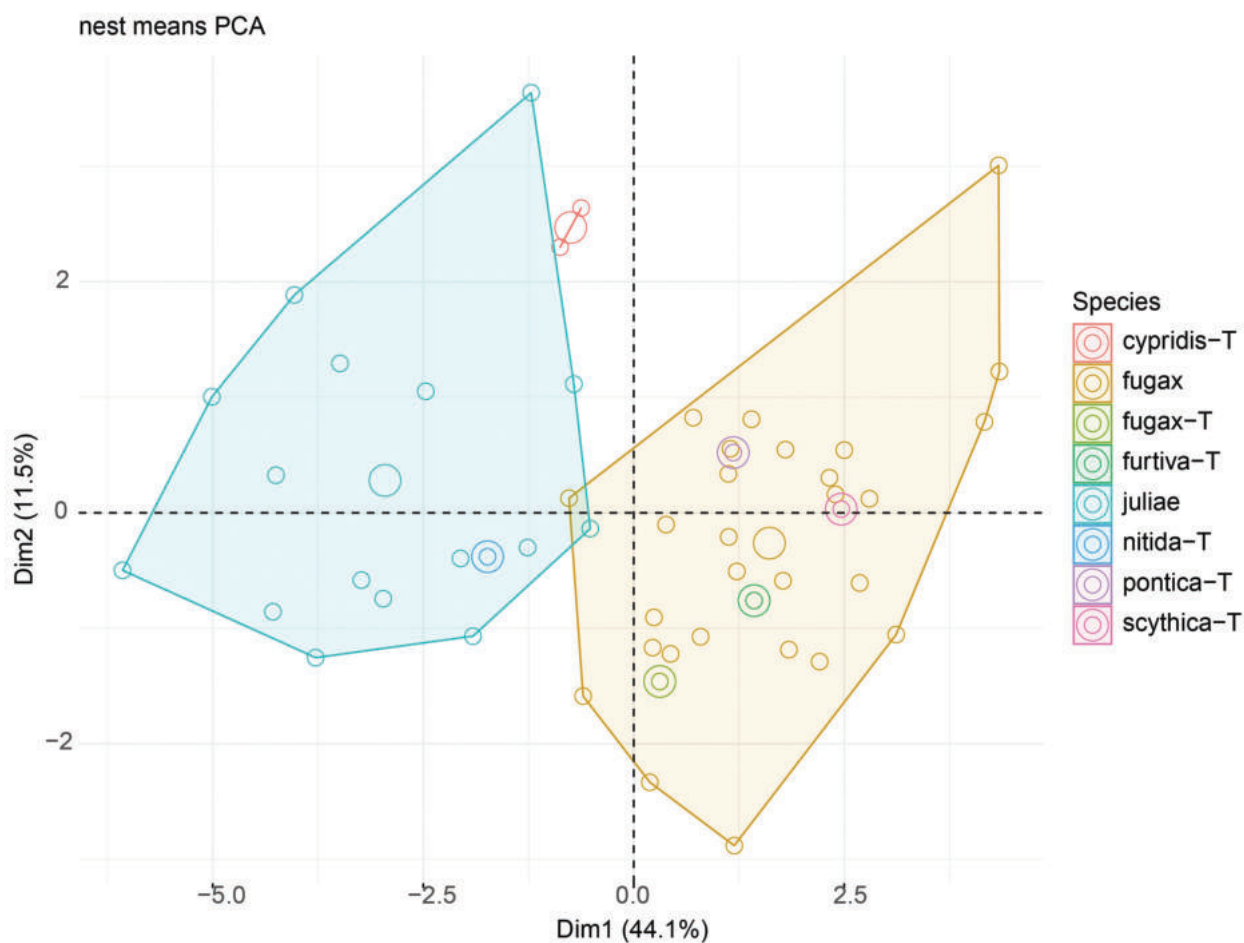


Figure 5. Principal component analyses of residuals of *Solenopsis* worker morphometric data. Each small dot represents a colony sample. Large dots represent centroids. Double rings represent type specimens or type series. Note: four workers mounted on two different pins (3 and 1 workers respectively) of the *S. cypridis* syntype material appear separately in the plot as red circles.

Table 3. Cross-validation table for *S. fugax* and *S. juliae* individuals.

	<i>S. fugax</i>	<i>S. juliae</i>	Percentage correct
<i>S. fugax</i>	134	3	97.8
<i>S. juliae</i>	1	61	98.4

of morphological clusters allows for significant character reduction in creating an easy-to-use numeric key using backward stepwise method in LDA. The three best selected characters returned 96.5% separation between the individuals of the two species, *S. fugax* and *S. juliae*: $D3 = 0.060 \cdot ML - 0.047 \cdot CWb - 0.125 \cdot CLYW - 4.582$, $D3_{fugax} (n = 137) = +1.713 [-1.722, +4.954]$, and $D3_{juliae} (n = 62) = -1.713 [-4.698, +0.454]$

The same function yields non-overlapping range of scores if nest samples are considered:

$D3_{fugax} (n = 33) = +1.776 [+0.931, +3.374]$ and $D3_{juliae} (n = 17) = -1.678 [-3.477, +0.010]$.

Investigation of gynes according to the character system of BS confirmed the results obtained in workers. There is a placement of the two syntype gynes of *S. cypridis* clearly separate from the well-separated clusters of *S. fugax* and *S. juliae* in a PCA (Fig. 7).

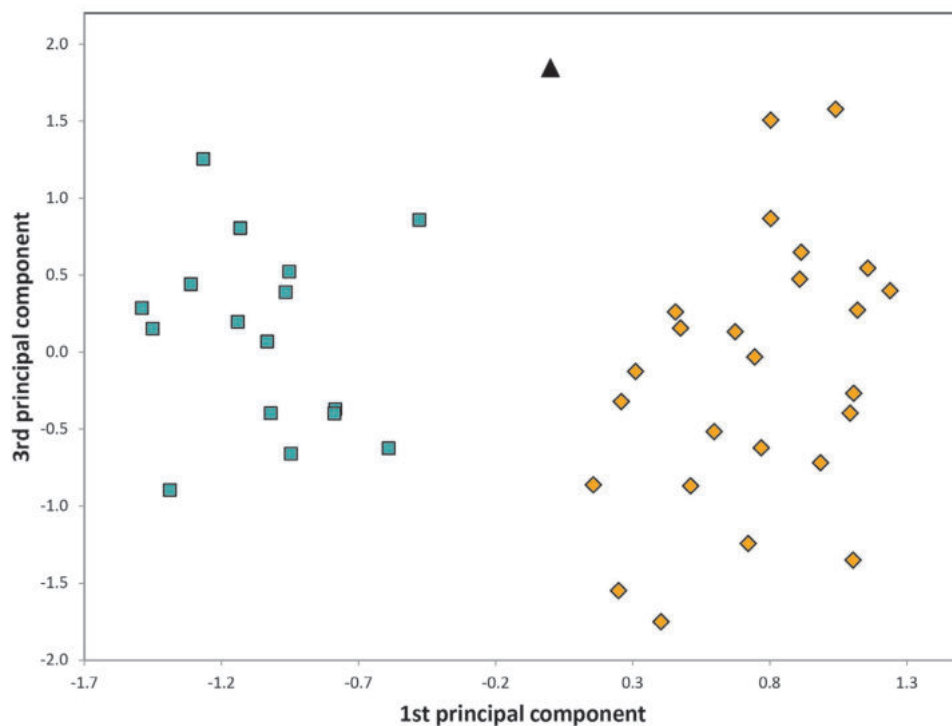


Figure 6. Principal component analyses of RAV data of *Solenopsis* workers. Each dot represents a colony sample. Blue rectangles: *S. juliae*, orange diamonds: *S. fugax*, black triangles: *S. cypridis*.

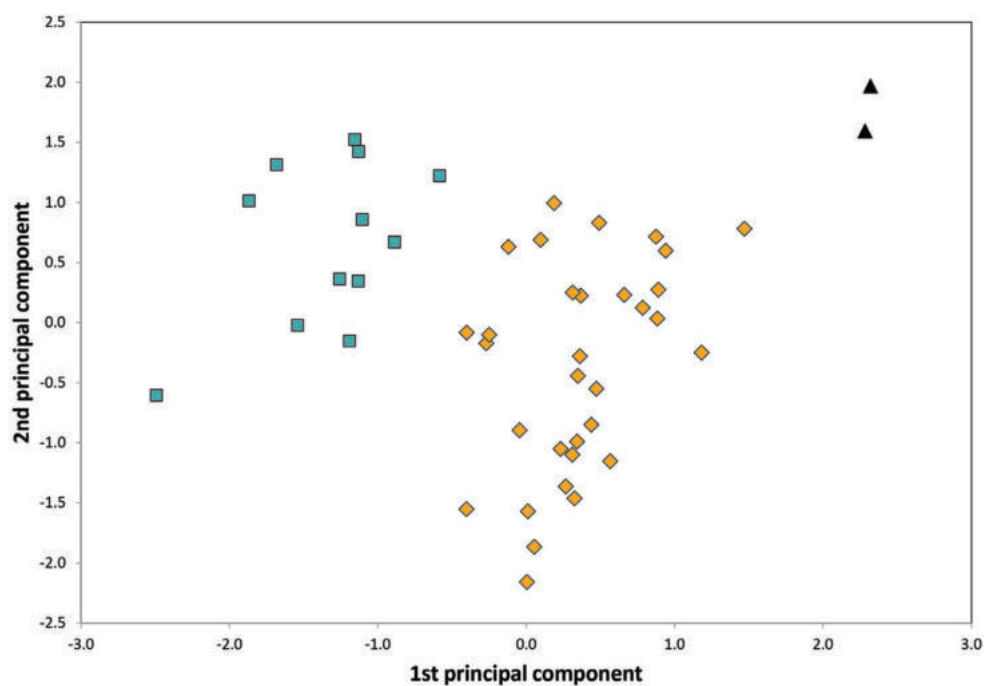


Figure 7. Principal component analyses of RAV data of *Solenopsis* queen individuals. Blue rectangles: *S. juliae*, orange diamonds: *S. fugax*, black triangles: *S. cypridis*.

Taxonomic treatment by species

The main sources for identification of a taxon are given in square brackets after taxonomic name, author and year.

***Solenopsis fugax* (Latreille, 1798)**

Formica fugax Latreille, 1798. [type investigation]

Notes. The species was described from the environs of Brive, France. Five workers and two gynes were investigated from the neotype nest sample, labelled “FRA: 45.0517°N, 1.5372°E, Nespouls-Faugère. 330 m, sous une pierre, leg. Galkowski 25. VIII. 2008 -1”, “Neoparatypes of *Solenopsis fugax* (Latreille, 1798) des. Galkowski, Casewitz-Weulersse et Cagniant 2010”, depository Senckenberg Museum of Natural History Görlitz. The clear placement of the worker and gyne type specimens within the *S. fugax* cluster has been shown in the analyses above.

***Solenopsis flavidula* (Nylander, 1849)**

Myrmica flavidula Nylander, 1849. [type investigation]

Notes. The species was described from the region of the Don river, southern Russia. Seven syntypes from FMNH Helsinki were investigated: two workers on one pin, “Ross. merid.”, “Motchoulsky”, “Coll. Nylandr.”, “Mus. Zool. H: fors Spec. typ. No. 5107 *Myrmica flavidula* Nyl.”; five workers on three pins with the same labels as the previous, but type Nos. 5107, 5108, and 5109. Two type specimens allowed the recording of the full set of 18 characters in the measuring system of BS. The synonymy was confirmed by a wild-card run in a LDA which allocated the two type specimens with $p = 0.9996$ to the *S. fugax* cluster.

***Solenopsis (Diplorhoptrum) fugax* var. *pontica* Santschi, 1934 [type investigation]**

Notes. This taxon was described from Romania. Two syntype workers were investigated labelled “*Solenopsis fugax*. Latr. v. *pontica* Sants” “MOLDAVIE, VALL. DU BERLAD, A. L. Montandon”, “ANTWEB CASENT 0913885”; depository NHM Basel. The placement of the worker type specimens within the *S. fugax* cluster has been shown in the analyses above.

***Solenopsis (Diplorhoptrum) fugax* var. *scythica* Santschi, 1934 [type investigation]**

Notes. This taxon was described from the Great Caucasus. Two syntype workers were investigated labelled “*Solenopsis fugax*. Latr. v. *scythica* Sant”, “Alages Caucase, Mejunoff.”, “ANTWEB CASENT 0913886”; depository NHM Basel. The placement of the worker type specimens within the *S. fugax* cluster has been shown in the analyses above.

***Solenopsis (Diplorhoptrum) fugax* var. *furtiva* Santschi, 1934 [type investigation]**

Notes. This taxon was described from France. Five syntype workers were examined labelled “Hte Garonne, Mt d’Espinasse, Val.Larboust, 1250 m. 03.X.1929”; depository NHM Basel. The placement of the worker type specimens within the *S. fugax* cluster has been shown in the analyses above.

Material examined. Numeric phenotypical data were taken by SC in 35 samples with 137 workers. BS investigated 25 nest samples with 92 workers and 32 gynes, the latter collected either from nests or caught during nuptial flight or in traps. For details see Suppl. materials 2, 3.

Geographic range. According to our data ranging from France over Central Europe, the Balkans, Asia Minor, the Caucasian region, the south Ukrainian and Russian steppes east to the Caspian Sea (Fig. 8). A wider range including Spain and stretching east to east Kazakhstan appears very likely but is not documented so far by examined vouchers.

Diagnoses. Worker (Table 4, Figs 9–12): Small, mean CS 491 μm . All shape ratios given below are mean values allometrically corrected for CS = 480 μm . Head elongated, CL/CW₄₈₀ 1.184. Hind margin of vertex in full face view both in minors and majors straight or very feebly concave. Scape short, SL/CS₄₈₀ 0.705. Frontal carinae short, often slightly diverging frontad, FL/CS₄₈₀ 0.231, FR/CS₄₈₀ 0.221. Preocular distance rather large, PrOc/CS₄₈₀ 0.191. Eye small, EL/CS₄₈₀ 0.091. Inner clypeal dents spiny and moderately long (CLSPLM/CS₄₈₀ 0.058), their tips often slightly incurving and as result more approached (CLSPD/CS₄₈₀ 0.123). Lateral clypeal dents much less developed (CLSPLL/CS₄₈₀ 0.021). Frontal lobes carinulate, whole surface vertex except for numerous foveolae of the seta bases and occasional vestigial microrugulae completely smooth and shiny. Mesosoma long (ML/CS₄₈₀ 1.214), moderately wide (MW/CS₄₈₀ 0.601) and always with a moderately deep metanotal groove (MpGr/CS₄₈₀ 0.028). Whole mesosoma smooth and shiny except for 3–6 longitudinal carinulae on lateral metapleuron. Petiole in lateral view with a relatively short peduncle and a high node with a

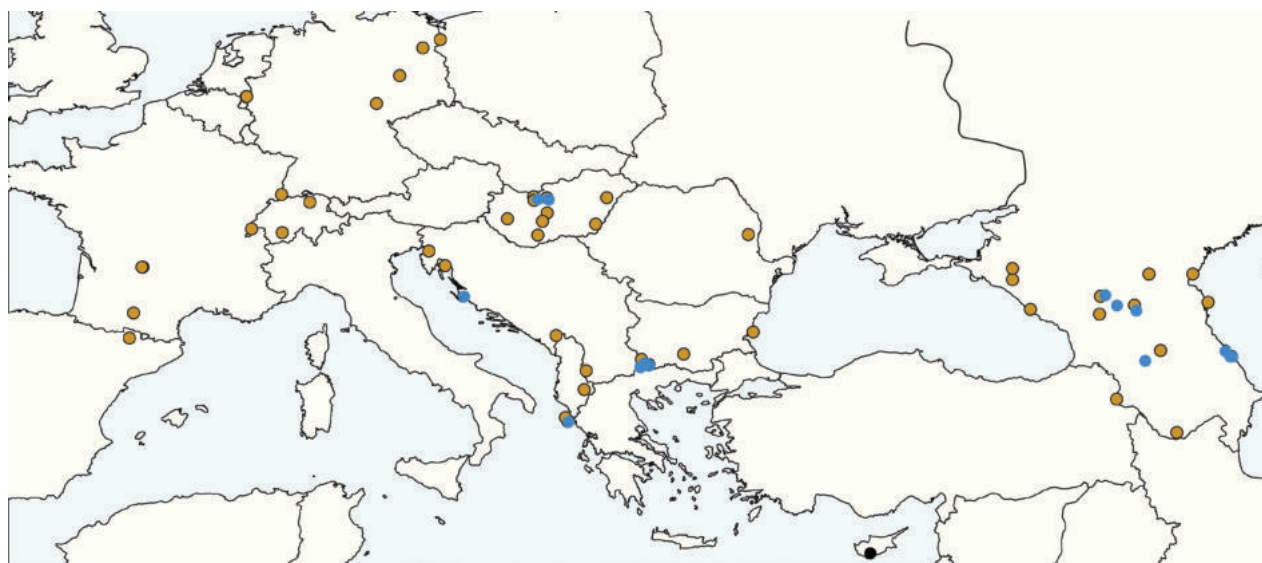


Figure 8. Geographic map shows the distribution of the samples analyzed in this study. Blue dots: *S. juliae*, orange dots: *S. fugax*, black dots: *S. cypridis*.

Table 4. Morphometric data of *Solenopsis* workers in the arrangement of arithmetic mean \pm standard deviation [lower extreme, upper extreme].

Primary indices			Indices after removal of allometric variance, adjusted for CS = 480 μ m				
	<i>S. cypridis</i> (types, n = 4)	<i>S. fugax</i> (n = 92)	<i>S. juliae</i> (n = 66)		<i>S. cypridis</i> (types, n = 4)	<i>S. fugax</i> (n = 92)	<i>S. juliae</i> (n = 66)
CS [μ m]	515 \pm 38 [462, 552]	491 \pm 67 [377, 660]	460 \pm 48 [385, 560]	CS [μ m]	515 \pm 38 [462, 552]	491 \pm 67 [377, 660]	460 \pm 48 [385, 560]
CL/CW	1.143 \pm 0.036 [1.110, 1.182]	1.177 \pm 0.044 [1.068, 1.261]	1.163 \pm 0.034 [1.084, 1.242]	CL/CW ₄₈₀	1.159 \pm 0.028 [1.137, 1.200]	1.184 \pm 0.022 [1.136, 1.238]	1.152 \pm 0.020 [1.102, 1.200]
SL/CS	0.691 \pm 0.010 [0.679, 0.700]	0.703 \pm 0.016 [0.659, 0.738]	0.695 \pm 0.015 [0.652, 0.731]	SL/CS ₄₈₀	0.696 \pm 0.007 [0.688, 0.705]	0.705 \pm 0.014 [0.666, 0.739]	0.692 \pm 0.013 [0.659, 0.717]
FL/CS	0.230 \pm 0.010 [0.219, 0.241]	0.231 \pm 0.010 [0.203, 0.257]	0.218 \pm 0.007 [0.204, 0.237]	FL/CS ₄₈₀	0.230 \pm 0.009 [0.219, 0.241]	0.231 \pm 0.010 [0.203, 0.258]	0.218 \pm 0.007 [0.205, 0.237]
FR/CS	0.230 \pm 0.010 [0.219, 0.241]	0.221 \pm 0.009 [0.198, 0.244]	0.209 \pm 0.008 [0.190, 0.237]	FR/CS ₄₈₀	0.230 \pm 0.009 [0.219, 0.241]	0.221 \pm 0.009 [0.199, 0.242]	0.210 \pm 0.008 [0.189, 0.237]
EL/CS	0.098 \pm 0.014 [0.085, 0.113]	0.092 \pm 0.011 [0.064, 0.124]	0.095 \pm 0.007 [0.082, 0.116]	EL/CS ₄₈₀	0.095 \pm 0.011 [0.082, 0.106]	0.091 \pm 0.010 [0.060, 0.125]	0.096 \pm 0.005 [0.081, 0.109]
PrOc/CS	0.199 \pm 0.013 [0.187, 0.217]	0.191 \pm 0.010 [0.169, 0.214]	0.185 \pm 0.008 [0.168, 0.202]	PrOc/CS ₄₈₀	0.200 \pm 0.012 [0.188, 0.216]	0.191 \pm 0.010 [0.170, 0.214]	0.184 \pm 0.008 [0.168, 0.201]
CLSPLM /CS	0.066 \pm 0.004 [0.059, 0.069]	0.058 \pm 0.006 [0.046, 0.072]	0.055 \pm 0.006 [0.040, 0.070]	CLSPLM /CS ₄₈₀	0.067 \pm 0.005 [0.060, 0.071]	0.058 \pm 0.005 [0.043, 0.073]	0.055 \pm 0.006 [0.040, 0.069]
CLSPLL /CS	0.021 \pm 0.005 [0.016, 0.027]	0.021 \pm 0.006 [0.007, 0.036]	0.019 \pm 0.004 [0.011, 0.028]	CLSPLL /CS ₄₈₀	0.021 \pm 0.005 [0.017, 0.027]	0.021 \pm 0.006 [0.007, 0.041]	0.018 \pm 0.004 [0.011, 0.030]
CLSPD /CS	0.157 \pm 0.015 [0.142, 0.174]	0.124 \pm 0.014 [0.091, 0.154]	0.146 \pm 0.010 [0.120, 0.168]	CLSPD /CS ₄₈₀	0.154 \pm 0.014 [0.137, 0.170]	0.123 \pm 0.012 [0.093, 0.149]	0.148 \pm 0.009 [0.128, 0.164]
ML/CS	1.186 \pm 0.024 [1.164, 1.216]	1.214 \pm 0.029 [1.133, 1.303]	1.155 \pm 0.019 [1.104, 1.186]	ML/CS ₄₈₀	1.186 \pm 0.024 [1.164, 1.216]	1.214 \pm 0.029 [1.133, 1.303]	1.155 \pm 0.019 [1.104, 1.185]
MW/CS	0.596 \pm 0.004 [0.591, 0.600]	0.600 \pm 0.012 [0.577, 0.631]	0.587 \pm 0.012 [0.565, 0.617]	MW/CS ₄₈₀	0.600 \pm 0.005 [0.595, 0.606]	0.601 \pm 0.013 [0.573, 0.637]	0.585 \pm 0.010 [0.565, 0.612]
MpGr /CS	0.034 \pm 0.005 [0.027, 0.038]	0.028 \pm 0.009 [0.009, 0.058]	0.027 \pm 0.005 [0.014, 0.039]	MpGr /CS ₄₈₀	0.035 \pm 0.005 [0.028, 0.040]	0.028 \pm 0.009 [0.009, 0.058]	0.027 \pm 0.005 [0.014, 0.039]
PEW/CS	0.313 \pm 0.009 [0.307, 0.326]	0.321 \pm 0.014 [0.279, 0.356]	0.295 \pm 0.014 [0.269, 0.334]	PEW/CS ₄₈₀	0.311 \pm 0.009 [0.304, 0.324]	0.320 \pm 0.014 [0.281, 0.351]	0.296 \pm 0.014 [0.268, 0.336]
PPW/CS	0.320 \pm 0.009 [0.313, 0.332]	0.333 \pm 0.012 [0.301, 0.373]	0.326 \pm 0.013 [0.289, 0.366]	PPW/CS ₄₈₀	0.322 \pm 0.010 [0.313, 0.335]	0.333 \pm 0.013 [0.306, 0.371]	0.324 \pm 0.012 [0.290, 0.362]
PEH/CS	0.369 \pm 0.016 [0.353, 0.390]	0.386 \pm 0.013 [0.354, 0.418]	0.371 \pm 0.015 [0.343, 0.402]	PEH/CS ₄₈₀	0.375 \pm 0.011 [0.364, 0.387]	0.388 \pm 0.011 [0.361, 0.411]	0.368 \pm 0.012 [0.341, 0.394]
PPH/CS	0.307 \pm 0.015 [0.295, 0.328]	0.307 \pm 0.013 [0.272, 0.369]	0.297 \pm 0.010 [0.270, 0.319]	PPH/CS ₄₈₀	0.307 \pm 0.015 [0.296, 0.328]	0.303 \pm 0.013 [0.268, 0.364]	0.292 \pm 0.010 [0.266, 0.314]

semicircular dorsum, the whole node slightly inclined caudad. Petiole much higher and only slightly narrower than postpetiole (PEH/CS₄₈₀ 0.388, PPH/CS₄₈₀ 0.303, PEW/CS₄₈₀ 0.320, PPW/CS₄₈₀ 0.333). Both waist segments completely smooth and shiny. Head, mesosoma, waist, gaster, femora, tibiae, and scape with very abundant, fine and long setae. Pubescence absent. Whole body and appendages light yellowish, larger major workers often with a brownish color component.

Gyne (Table 5, Figs 13–15): Medium-sized, mean CS 897 μ m. Head clearly shorter than wide, CL/CW 0.939. Inner third of hind margin of vertex in full face view weakly convex or straight. Scape short, SL/CS 0.637. Frontal carinae short, subparallel and moderately distant, FR/CS 0.252. Preocular distance small, PrOc/CS 0.119. Eye moderately large, EL/CS 0.287. Inner clypeal dents spiny and rather long (CLSPLM/CS 0.050), rather approached (CLSPD/CS



Figure 9. Head of major worker of *Solenopsis fugax* in full-face view.

0.141). Lateral clypeal dents much less developed (CLSPLL/CS 0.015). Genae and frontal lobes carinulate, central vertex strongly carinulate-rugulose; these characters are also found in the two microgynes corresponding in size to the *S. juliae* macrogynes. Mesosoma long (ML/CS 2.072) and much higher than wide (MH/CS 1.315, MW/CS 1.117). Dorsal mesonotum and scutum moderately carinulate. Lateral scutum, metapleuron and lower propodeum more strongly carinulate. Petiole in lateral view with a short peduncle, a high node with triangular profile and slightly higher than postpetiole (PEH/CS 0.493, PPH/CS 0.479); dorsal crest of petiole node in dorsal view much wider than long, the petiole slightly narrower than postpetiole (PEW/CS 0.463, PPW/CS 0.513). Postpetiole densely but weakly carinulate. Head, mesosoma, waist, gaster, femora, tibiae, and scape with very abundant, fine and long setae. Pubescence absent. Usually dark to medium brown; legs, antennae and mandibles yellowish.

***Solenopsis juliae* (Arakelian, 1991)**

Diplorhoptum juliae Arakelian, 1991. [description]

Notes. The species was described from Armenia. The type series was collected by G. Arakelian in a clearing of an oak forest at 1750 m near to the



Figure 10. Lateral view of *Solenopsis fugax* major worker.

village Arzakan [40.450°N, 44.608°E], 30 August 1988 (Arakelian 1991). The ongoing Russian-Ukrainian war prevents a direct examination of type specimens deposited in the museums of Erevan, Kiev, and Moscow but the original description allows a fairly good conclusion that *S. juliae* is the oldest available name for our eastern species. This is based on three arguments: (1) using a conversion factor of 1.148 for Arakelian's "head width before eyes" given by him as 0.72 mm, the holotype gyne has a CW of 0.827 mm; (2) the ratio CLSPD/CW in the holotype gyne taken from the drawing is 0.169. This results in a CLSPD of 0.140 mm; (3) Arakelian reported a reduced sculpture: "Body largely smooth and shiny. A weak superficial sculpture is notable on head sides, frontal lobes, around the antennal scrobes, on propodeum and waist". This means the absence of a notable sculpture on central vertex. This is precisely what we found as a character separating it from *S. fugax*. A discriminant $35.24 \cdot CW - 58.91 \cdot CLSPD - 22.59$ provides a full separation of the 12 measured *S. juliae* and 32 measured *S. fugax* gynes with the former species ranging between -2.73 and -0.47 and the latter between +0.47 and +4.32. Run as wild-card, the holotype gyne of *S. juliae* scores -1.69 meaning a posterior probability of 0.9999. A synonymy of *S. juliae* with *S. ilinei* Santschi, 1936 and *S. deserticola* Ruzsky, 1905 is excluded by the much smaller ratio CL/CW.



Figure 11. Head of minor worker of *Solenopsis fugax* in full-face view.

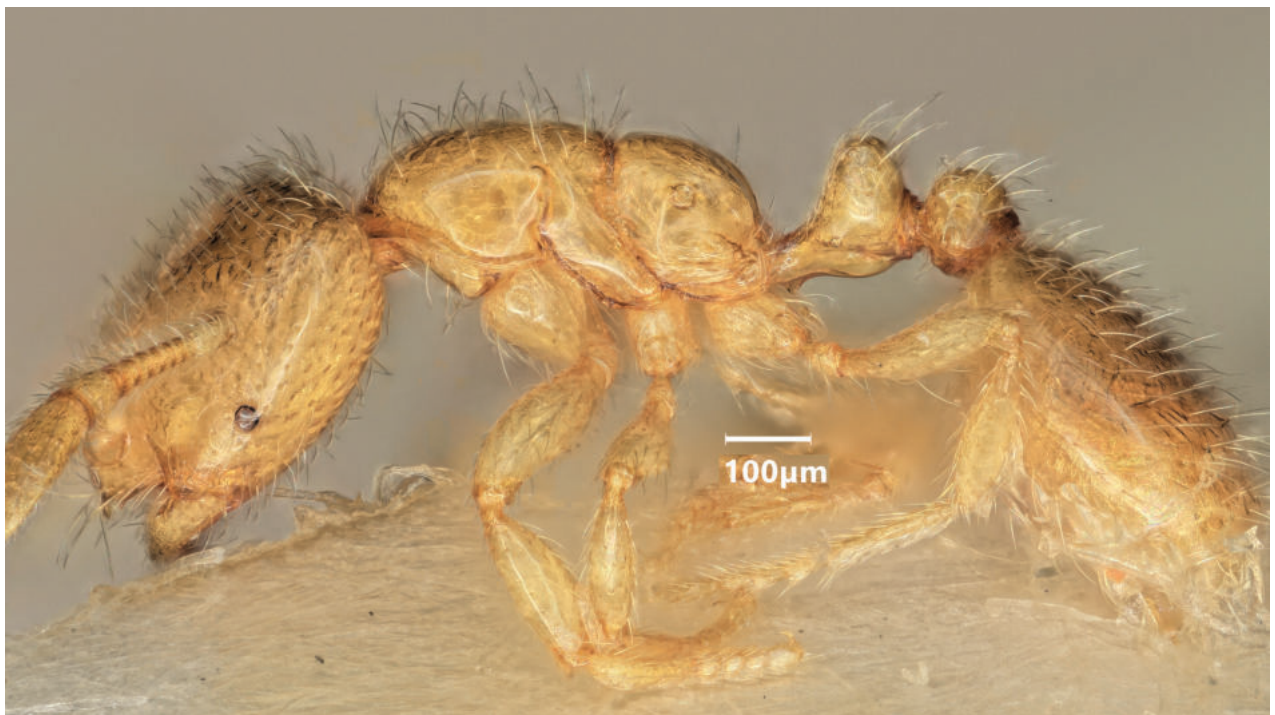


Figure 12. Lateral view of *Solenopsis fugax* minor worker.

Table 5. Morphometric data of *Solenopsis gynes* in the arrangement of arithmetic mean \pm standard deviation [lower extreme, upper extreme].

Primary indices				Indices after removal of allometric variance, adjusted for CS = 850 μm			
	<i>S. cypridis</i> types, n = 2	<i>S. fugax</i> (n = 32)	<i>S. juliae</i> (n = 12)		<i>S. cypridis</i> types, n = 2	<i>S. fugax</i> (n = 32)	<i>S. juliae</i> (n = 12)
CS [μm]	972 \pm 4 [969, 975]	897 \pm 29 [818, 941]	798 \pm 11 [777, 814]	CS [μm]	972 \pm 4 [969, 975]	897 \pm 29 [818, 941]	798 \pm 11 [777, 814]
CL/CW	0.890 \pm 0.008 [0.884, 0.895]	0.939 \pm 0.026 [0.895, 0.988]	0.969 \pm 0.011 [0.953, 0.988]	CL/CW ₈₅₀	0.924 \pm 0.007 [0.919, 0.928]	0.952 \pm 0.024 [0.912, 1.004]	0.953 \pm 0.012 [0.937, 0.975]
SL/CS	0.630 \pm 0.012 [0.622, 0.639]	0.637 \pm 0.015 [0.602, 0.667]	0.657 \pm 0.013 [0.630, 0.678]	SL/CS ₈₅₀	0.664 \pm 0.011 [0.656, 0.672]	0.650 \pm 0.014 [0.620, 0.676]	0.643 \pm 0.013 [0.618, 0.666]
FL/CS	0.281 \pm 0.003 [0.279, 0.283]	0.253 \pm 0.011 [0.233, 0.282]	0.245 \pm 0.010 [0.224, 0.267]	FL/CS ₈₅₀	0.302 \pm 0.002 [0.301, 0.304]	0.260 \pm 0.010 [0.244, 0.291]	0.237 \pm 0.009 [0.218, 0.258]
FR/CS	0.281 \pm 0.003 [0.279, 0.283]	0.252 \pm 0.009 [0.233, 0.264]	0.240 \pm 0.008 [0.221, 0.250]	FR/CS ₈₅₀	0.302 \pm 0.002 [0.300, 0.303]	0.259 \pm 0.008 [0.244, 0.273]	0.233 \pm 0.008 [0.214, 0.243]
EL/CS	0.304 \pm 0.004 [0.301, 0.307]	0.287 \pm 0.010 [0.271, 0.312]	0.295 \pm 0.011 [0.278, 0.312]	EL/CS ₈₅₀	0.324 \pm 0.004 [0.321, 0.326]	0.294 \pm 0.009 [0.276, 0.315]	0.287 \pm 0.010 [0.273, 0.301]
PrOc/CS	0.126 \pm 0.000 [0.126, 0.126]	0.119 \pm 0.008 [0.102, 0.134]	0.125 \pm 0.007 [0.115, 0.138]	PrOc/CS ₈₅₀	0.115 \pm 0.000 [0.115, 0.115]	0.115 \pm 0.008 [0.101, 0.129]	0.131 \pm 0.007 [0.119, 0.144]
CLSPLM /CS	0.055 \pm 0.004 [0.052, 0.058]	0.050 \pm 0.006 [0.037, 0.063]	0.050 \pm 0.006 [0.037, 0.060]	CLSPLM /CS ₈₅₀	0.053 \pm 0.004 [0.050, 0.056]	0.049 \pm 0.006 [0.036, 0.061]	0.050 \pm 0.006 [0.037, 0.061]
CLSPLL /CS	0.014 \pm 0.001 [0.013, 0.014]	0.015 \pm 0.004 [0.007, 0.024]	0.012 \pm 0.003 [0.005, 0.017]	CLSPLL /CS ₈₅₀	0.009 \pm 0.001 [0.009, 0.009]	0.013 \pm 0.003 [0.006, 0.019]	0.016 \pm 0.005 [0.006, 0.023]
CLSPD /CS	0.174 \pm 0.008 [0.168, 0.180]	0.141 \pm 0.008 [0.126, 0.157]	0.162 \pm 0.011 [0.145, 0.185]	CLSPD /CS ₈₅₀	0.174 \pm 0.008 [0.168, 0.179]	0.141 \pm 0.008 [0.126, 0.157]	0.162 \pm 0.011 [0.145, 0.185]
MW/CS	1.154 \pm 0.018 [1.142, 1.167]	1.117 \pm 0.048 [1.043, 1.257]	1.016 \pm 0.030 [0.962, 1.080]	MW/CS ₈₅₀	1.069 \pm 0.013 [1.059, 1.078]	1.083 \pm 0.042 [1.004, 1.189]	1.052 \pm 0.034 [0.994, 1.134]
MH/CS	1.334 \pm 0.055 [1.295, 1.373]	1.315 \pm 0.043 [1.240, 1.397]	1.248 \pm 0.048 [1.175, 1.330]	MH/CS ₈₅₀	1.250 \pm 0.054 [1.212, 1.289]	1.276 \pm 0.038 [1.214, 1.358]	1.270 \pm 0.054 [1.191, 1.357]
ML/CS	2.093 \pm 0.042 [2.064, 2.123]	2.072 \pm 0.050 [1.958, 2.163]	1.991 \pm 0.048 [1.912, 2.085]	ML/CS ₈₅₀	2.026 \pm 0.038 [1.999, 2.053]	2.046 \pm 0.046 [1.929, 2.124]	2.020 \pm 0.053 [1.939, 2.127]
PEW/CS	0.490	0.463 \pm 0.026 [0.401, 0.527]	0.421 \pm 0.017 [0.384, 0.452]	PEW/CS ₈₅₀	0.510	0.470 \pm 0.026 [0.403, 0.534]	0.414 \pm 0.016 [0.378, 0.442]
PPW/CS	0.565	0.513 \pm 0.029 [0.449, 0.565]	0.496 \pm 0.025 [0.440, 0.526]	PPW/CS ₈₅₀	0.604	0.526 \pm 0.029 [0.465, 0.579]	0.482 \pm 0.024 [0.428, 0.510]
PEH/CS	0.494 \pm 0.014 [0.484, 0.503]	0.493 \pm 0.020 [0.451, 0.529]	0.476 \pm 0.018 [0.450, 0.505]	PEH/CS ₈₅₀	0.481 \pm 0.013 [0.472, 0.490]	0.488 \pm 0.019 [0.449, 0.526]	0.482 \pm 0.018 [0.455, 0.512]
PPH/CS	0.515 \pm 0.010 [0.508, 0.522]	0.479 \pm 0.023 [0.417, 0.522]	0.470 \pm 0.020 [0.429, 0.492]	PPH/CS ₈₅₀	0.528 \pm 0.017 [0.516, 0.540]	0.483 \pm 0.023 [0.422, 0.527]	0.465 \pm 0.019 [0.424, 0.484]

***Solenopsis nitida* (Dlussky & Radchenko, 1994)**

Diplorhoptum nitidum Dlussky & Radchenko, 1994. [images of types, description]

Notes. This taxon was described also from Armenia, some 200 km SE of the type locality of *S. juliae*. The type series consists of workers and gynes collected by A. Radchenko from a single nest near to the village Legvaz [38.938°N, 46.216°E], 25 June 1986. Direct examination of type specimens deposited in the museums of Kiev and Moscow was also prevented by the ongoing Russian-Ukrainian war. Instead, we evaluated the images of the holotype gyne and a paratype worker provided by www.antweb.org under the specimen identifiers CASENT 0917366 and CASENT 0917367. The evaluation suggests a synonymy

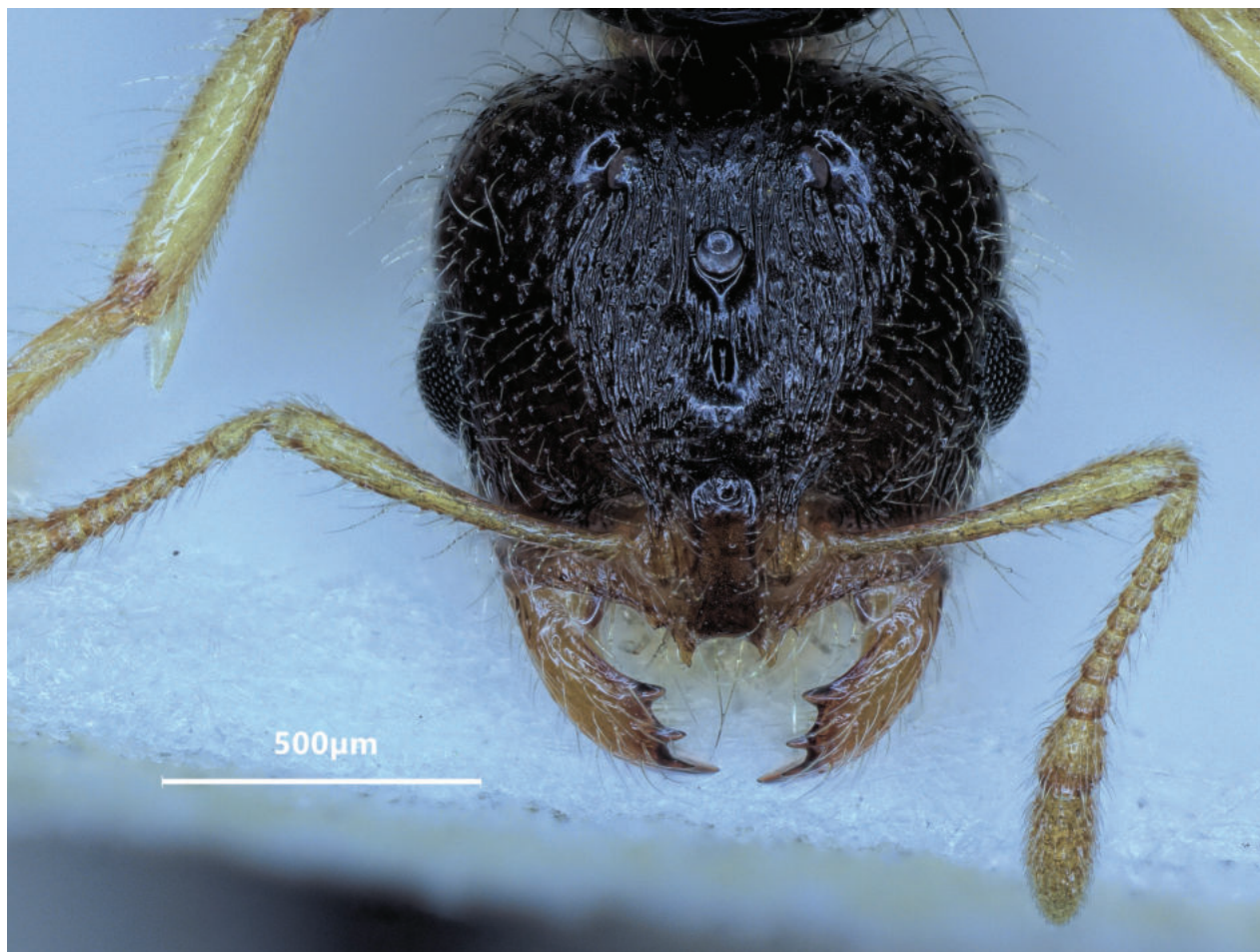


Figure 13. Head of a macrogyne of *Solenopsis fugax* in full-face view.

of *Solenopsis nitida* with *S. juliae* based upon the following arguments. The measurements of the paratype worker derivable with an acceptable error from the images were in μm CL 557, CW 493, FL 99, FR 99, CLSPD 89, PEW 163, PPW 156, MW 293 and ML 609. Running the absolute data as wild-card in a LDA against the data pool of BS, the paratype is allocated with $p = 0.9994$ to the *S. juliae* cluster and it is allocated also to this cluster by the PCA using the data set of SC (Fig. 5). Furthermore, the holotype gyne shows the sculpture reduction characteristic for *S. juliae* but there is one problem: the gyne is, as it is the case in all the paratype gynes, much smaller than average *S. juliae* gynes. As there is no indication for miscalibration of the scale in the images by comparing with measurements given by Dlussky and Radchenko (1994), these small absolute body size values must be considered as real. We derived the following measurements in μm from the images of the holotype gyne: CL 659, CW 668, FL 134, FR 134, CLSPD 100, MW 528, PEH 291, PPH 280, MH 705, and ML 1301. Proposing herewith a synonymy of *S. nitida* with *S. juliae*, we consider the holotype gyne as a microgyne with allometric changes of body shape, but we also encourage a more profound investigation of the problem after extensive collections have been done in the Caucasian region.

Material examined. Numeric phenotypical data were taken by SC in 17 samples (largely nest samples) with 62 workers. BS investigated 16 nest samples



Figure 14. Lateral view of a *Solenopsis fugax* macrogyne.

with 66 workers and 12 gynes, the latter collected either from nests or caught during nuptial flight. For details see Suppl. materials 1, 2.

Geographic range. According to our data including the Pannonian Basin and the complete Balkans and stretching east over Asia Minor (Fig. 8), the whole Caucasian region to the western shores of the Caspian Sea (Yusupov 2014).

Diagnosis. Worker (Table 4, Figs 16–19): Smaller than *fugax*, mean CS 460 μm . All shape ratios given below are mean values allometrically corrected for CS = 480 μm . Head less elongated than in *fugax*, CL/CW_{480} 1.152. Hind margin of vertex in full face view both in minors and majors straight or very feebly concave. Scape slightly shorter than in *fugax*, SL/CS_{480} 0.692. Frontal carinae short, often slightly diverging frontad, FL/CS_{480} 0.218, FR/CS_{480} 0.210. Preocular distance slightly smaller than in *fugax*, $PrOc/CS_{480}$ 0.184. Eye small, EL/CS_{480} 0.096. Inner clypeal dents spiny and moderately long ($CLSPLM/CS_{480}$ 0.055), their tips often diverging and as result more distant than in *fugax* ($CLSPD/CS_{480}$ 0.148). Lateral clypeal dents small ($CLSPLL/CS_{480}$ 0.018). Frontal lobes carinate, whole surface of vertex except for the numerous foveolae of the seta bases completely smooth and shiny. Mesosoma shorter than in *fugax* (ML/CS_{480} 1.155), and less wide (MW/CS_{480} 0.585), always with a moderately deep meta-notal groove ($MpGr/CS_{480}$ 0.027). Whole mesosoma smooth and shiny except for 3–6 longitudinal carinulae on lateral metapleuron. Petiole in lateral view with a relatively short peduncle and a high node with a semicircular dorsum, the whole node slightly inclined caudad. Petiole much higher than postpetiole (PEH/CS_{480} 0.368, PPH/CS_{480} 0.292) but in contrast to *fugax* distinctly narrower than postpetiole (PEW/CS_{480} 0.296, PPW/CS_{480} 0.324). Both waist segments



Figure 15. Head of a microgyne of *Solenopsis fugax* in full-face view.

completely smooth and shiny. Head, mesosoma, waist, gaster, femora, tibiae, and scape with very abundant, fine and long setae. Pubescence absent. Whole body and appendages light yellowish with a brownish color component which is often more expressed than in *fugax*.

Gyne (Table 5, Figs 20, 21): Small, mean CS 798 μm. Head clearly shorter than wide, CL/CW 0.969. Inner third of hind margin of vertex in full face view weakly convex or straight. Scape short, SL/CS 0.657. Frontal carinae short, subparallel and slightly more approached than in *fugax*, FR/CS 0.240. Preocular distance small, PrOc/CS 0.125. Eye moderately large, EL/CS 0.295. Inner clypeal dents spiny and rather long (CLSPLM/CS 0.050), their tips more distant than in *fugax* (CLSPD/CS 0.162) and often slightly diverging. Lateral clypeal dents much less developed than the inner ones (CLSPLL/CS 0.012). Frontal lobes, lateral clypeus and genae carinulate, remaining head surface except for large foveolae of the seta bases completely smooth and shiny, as clearest difference to *fugax* in particular central vertex without any carinulae or rugulae (compare Figs 11, 13, 18). Mesosoma long (ML/CS 1.991) and much higher than wide (MH/CS 1.248, MW/CS 1.016). Whole mesosoma smooth with exception of carinulate lateral scutum and whole metapleuron and anepisternite. Petiole in lateral view with a short peduncle, a high node which is slightly more inclined caudad than in *fugax*; petiole as high as postpetiole (PEH/CS 0.476, PPH/CS 0.470); dorsal crest of petiole node in dorsal view much wider than



Figure 16. Head of major worker of *Solenopsis juliae* in full-face view.

long, the petiole in contrast to *fugax* much narrower than postpetiole (PEW/CS 0.421, PPW/CS 0.496). Dorsum of both waist segments nearly smooth, the lateral surfaces slightly carinulate. Head, mesosoma, waist, gaster, femora, tibiae, and scape with very abundant, fine and long setae. Pubescence absent. Usually dark to medium brown; legs, antennae and mandibles yellowish.

Taxonomic comments

It has been shown that the separation of workers of *S. fugax* and *S. juliae* was very clear in both investigation systems of SC and BS and that gynes were clearly separable with the system of BS. We have also presented an argument that there is most probably no taxon described from Eurasian ranges east of 8°E that could be a senior synonym of *S. juliae*. The exclusion of all 15 taxa described by Bernard (1950, 1959, 1978) from senior synonymy of *S. juliae* is stated here simply for geographic reasons as this species is not known in the western region.

Solenopsi crivellarii Menozzi, 1936, described from Diafani (35.76°N, 27.21°E) on the Aegean island of Karpathos, might possibly represent a senior synonym of



Figure 17. Lateral view of *Solenopsis juliae* major worker.

S. juliae. Because the type is not available, and no images are deposited in www.Antweb.org, we studied the original description. The verbal part does not provide any diagnostic characters. The drawings are without scales but concluded from eye size cited as “eyes barely visible in minor workers and only having four or five ommatidia in major workers” (Menozzi 1936: 284, fig. 10) illustrate a major worker. Images of heads imply the risk that scape lengths are depicted as shorter than actual, but a larger length is not suggested (Menozzi 1936: fig. 10). However, the ratio SL/CS derived from the drawing (Menozzi 1936: fig. 10) is 0.732, which is clearly higher than the range known from *S. juliae* ($= 0.695 [0.652, 0.730]$ ($n = 66$)) (see Fig. 22). The frontal lobe distance FL/CS provides an even stronger indication. The depicted specimen (Menozzi 1936: fig. 10) has FL/CS = 0.195, much lower than in the 66 examined *S. juliae* workers of any body size with $0.218 \pm 0.007 [0.204, 0.237]$. Based on these morphometric arguments and considering the South Aegean insular zoogeography, we conclude that *S. crivellarii* is not a senior synonym of *S. juliae*.

***Solenopsis cypridis* Santschi, 1934**

Solenopsis fugax var. *cypridis* Santschi, 1934. [type investigation]

Notes. This species has been described from Limassol in Cyprus.



Figure 18. Head of minor worker of *Solenopsis juliae* in full-face view.

Four syntype workers and two gynes were investigated from the neotype nest sample, labelled “Chypre 3 Limassol 15. x 30 Mar.....”, “*S. fugax* cypridis Sant” and “ANTWEB CASENT0913887”, depository NHM Basel.

Diagnosis. Worker (Table 4; Figs 23, 24; images CASENT0913887 in www.antweb.org): larger than *fugax*, mean CS = 515 µm. All shape ratios given below are mean values allometrically corrected for CS = 480 µm. Head less elongated than in *fugax*, CL/CW_{480} 1.159. Hind margin of vertex in full face view straight. Scape short, SL/CS_{480} 0.696. Frontal carinae short, parallel, FL/CS_{480} 0.230, FR/CS_{480} 0.230. Preocular distance rather large, $PrOc/CS_{480}$ 0.200. Eye small, EL/CS_{480} 0.095. Inner clypeal dents spiny and moderately long ($CLSPLM/CS_{480}$ 0.067), their tips diverging and as result more distant than in *fugax* ($CLSPD/CS_{480}$ 0.154). Lateral clypeal dents much less developed ($CLSPLL/CS_{480}$ 0.021). Frontal lobes carinulate, whole surface vertex except for numerous foveolae of the seta bases completely smooth and shiny. Mesosoma shorter than in *fugax* (ML/CS_{480} 1.186) but similarly wide (MW/CS_{480} 0.600), always with a moderately deep metanotal groove ($MpGr/CS_{480}$ 0.035). Whole mesosoma smooth and shiny except for 3–6 longitudinal carinulae on lateral metapleuron. Petiole in lateral view with a



Figure 19. Lateral view of *Solenopsis juliae* minor worker.



Figure 20. Head of a macrogyne of *Solenopsis juliae* in full-face view.



Figure 21. Lateral view of a *Solenopsis juliae* macrogyne.

short peduncle and a high node the dorsum of which is broader than in *fugax*; the whole node slightly inclined caudad. Petiole much higher and only slightly narrower than postpetiole (PEH/CS_{480} 0.375, PPH/CS_{480} 0.307, PEW/CS_{480} 0.311, PPW/CS_{480} 0.322). Both waist segments completely smooth and shiny. Head, mesosoma, waist, gaster, femora, tibiae, and scape with very abundant, fine and long setae. Pubescence absent. Head, mesosoma, waist, and gaster dirty brown (i.e., darker than in *fugax*); appendages contrastingly light yellowish.

Gyne (Table 5): Larger than *fugax*, mean $CS = 972 \mu\text{m}$. Head shorter than in *fugax*, CL/CW 0.890, a smaller head length index proves true also after removal of allometric variance. Scape short, SL/CS 0.691. Frontal carinae short, subparallel and much more distant than in *fugax*, FR/CS 0.281, a wider frons also proves true also after removal of allometric variance. Preocular distance small, $PrOc/CS$ 0.126. Eye slightly larger than in *fugax*, EL/CS 0.304; this difference is increased after removal of allometric variance. Inner clypeal dents spiny and rather long ($CLSPLM/CS$ 0.055), their tips much more distant than in *fugax* ($CLSPD/CS$ 0.174). Lateral clypeal dents much less developed than the inner ones ($CLSPLL/CS$ 0.014). Mesosoma long (ML/CS 2.094) and much higher than wide (MH/CS 1.334, MW/CS 1.154).

Differential diagnosis and rank elevation

Based on the following arguments, we consider *Solenopsis cypridis* as a species separate from *S. fugax* – either valid or representing a junior synonym of

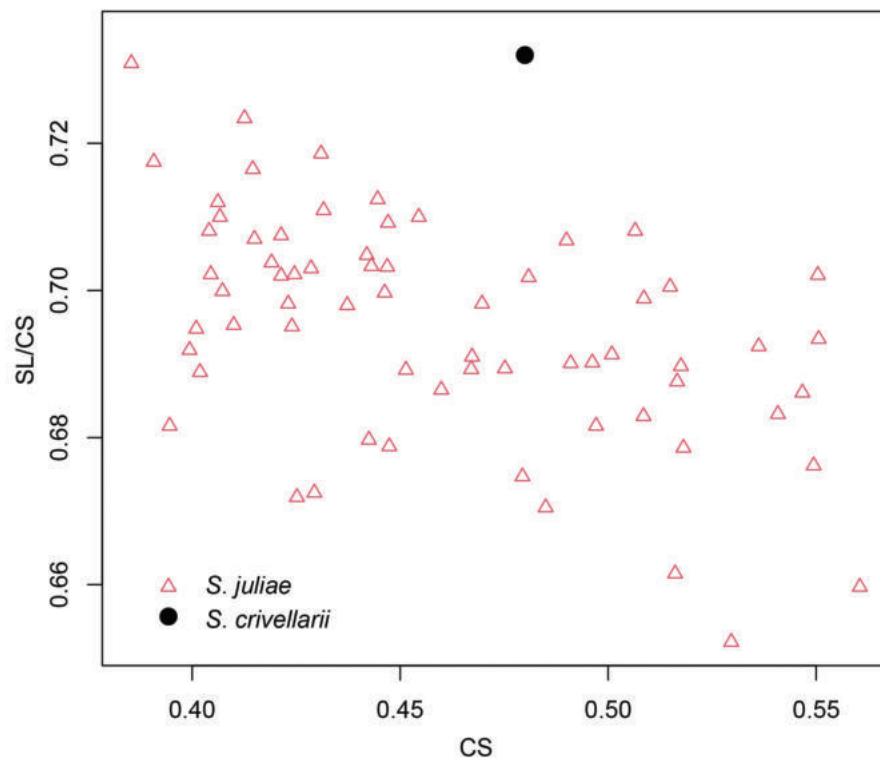


Figure 22. Scatterplot for morphometric ratios of *Solenopsis juliae* workers and *S. crivellarii* type. Red triangles: *S. juliae*; black dot: *S. crivellarii* type (measured from drawings).



Figure 23. Head of worker of *Solenopsis cypridis* in full-face view (CASENT0913887). Photo: AntWeb.org, Photographer: Will Ericson.



Figure 24. Lateral view of *Solenopsis cypridis* worker (CASENT0913887). Photo: AntWeb.org, Photographer: Will Ericson.

another East Mediterranean taxon. Since *Solenopsis cypridis* is not a synonym of *S. fugax* or *S. juliae*, its taxonomic status is beyond the scope of this paper and must be clarified in the future. The gynes differ from *fugax* by larger absolute sizes and larger FR/CS and CLSPD/CS. The differences in the latter indices prove true with removal of allometric variance (Table 5). A principal component analysis considering the characters CS, SL/CS, EL/CS, FL/CS, FR/CS, and CLSPD/CS separates the type gynes from all gynes of *fugax* and *juliae* (Fig. 7). This separation is repeated by the PCA in the workers using RAV-corrected data of CL/CW_{480'}, CLSPD/CS_{480'}, CLSPLM/CS_{480'}, SL/CS_{480'}, FR/CS_{480'}, PEW/CS_{480'}, PEH/CS_{480'} and ML/CS_{480'} (Fig. 6).

Acknowledgements

We wish to thank to Seraine Klopstein and Isabelle Zürcher (Naturhistorisches Museum Basel, Switzerland), Maria Tavano (Museo Civico di Storia Naturale Genova, Italy), and Juho Paukkunen (Finnish Museum of Natural History Helsinki, Finland) for kindly lending indispensable type material, and Tamás Jégh and Albena Lapeva Gjonova for sharing their *Solenopsis* collections.

Additional information

Conflict of interest

The authors have declared that no competing interests exist.

Ethical statement

No ethical statement was reported.

Funding

This project has received funding from the HUN-REN Hungarian Research Network. This research was co-financed by tax money on the basis of the state budget passed by the Sächsischer Landtag according to the Antragsnummer 100590787 of the Sächsische Aufbaubank issued 3 August 2021 (on behalf of BS) and by the Hungarian National Research, Development, and Innovation Fund under Grant No. K 135795 (on behalf of SC).

Author contributions

Conceptualization: SC, BS. Data curation: SC, BS, ML. Formal analysis: SC, BS. Funding acquisition: SC, BS. Investigation: ZMY, SC, BS. Project administration: GH. Resources: GH. Software: ML. Validation: SC, BS. Visualization: SC, BS. Writing – original draft: SC, BS, GH, ZMY, ML. Writing – review and editing: SC, BS.

Author ORCIDs

Sándor Csósz  <https://orcid.org/0000-0002-5422-5120>

Bernhard Seifert  <https://orcid.org/0000-0003-3850-8048>

Zalimkhan M. Yusupov  <https://orcid.org/0000-0002-5149-9679>

Gábor Herczeg  <https://orcid.org/0000-0003-0441-342X>

Data availability

All of the data that support the findings of this study are available in the main text or Supplementary Information.

References

- AntWeb (2023) AntWeb Version 8.91.2. California Academy of Science. <https://www.antweb.org> [Accessed 29 March 2023]
- Arakelian GR (1991) A new ant species of the genus *Diplorhoptrum* Mayr (Hymenoptera, Formicidae) from Armenia. *Doklady Akademii Nauk Armenii* 92: 93–96. [In Russian]
- Bernard F (1950) Notes sur les fourmis de France. II. Peuplement des montagnes méridionales. *Annales de la Société Entomologique de France* 115: 1–36.
- Bernard F (1959) Les fourmis de l'île de Port-Cros. Contribution à l'écologie des anciennes forêts méditerranéennes. *Vie et Milieu* 9: 340–360.
- Bernard F (1978) Révision des *Diplorhoptrum* de France, fourmis plus différenciées par l'écologie que par leurs formes (Hym. Formicidae). *Annales de la Société Entomologique de France* (n.s.) 13: 543–577. <https://doi.org/10.1080/21686351.1977.12278659>
- Bolton B (2023) An online catalog of the ants of the world. <https://www.antcat.org> [Accessed 29 March 2023]
- Csósz S, Fisher BL (2016) Taxonomic revision of the Malagasy members of the *Nesomyrmex angulatus* species group using the automated morphological species delineation protocol NC-PART-clustering. *PeerJ* 4: e1796. <https://doi.org/10.7717/peerj.1796>
- Csósz S, Seifert B (2003) *Ponera testacea* Emery, 1895 stat.nov. – a sister species of *P. coarctata* (Latreille, 1802) (Hymenoptera, Formicidae). *Acta Zoologica Academiae Scientiarum Hungaricae* 49(3): 201–214.

- Csósz S, Báthori F, Rádai Z, Herczeg G, Fisher BL (2023) Comparing ant morphology measurements from microscope and online AntWeb.org 2D z-stacked images. *Ecology and Evolution* 13(3): e9897. <https://doi.org/10.1002/ece3.9897>
- Dlussky GM, Radchenko AG (1994) Ants of the genus *Diplorhoptum* (Hymenoptera, Formicidae) Central Palaearctic. *Zoologicheskij Zhurnal* 73(2): 102–111. [In Russian]
- Galkowski C, Casevitz-Weulersse J, Cagniant H (2010) Redescription de *Solenopsis fugax* (Latreille, 1798) et notes sur les *Solenopsis* de France (Hymenoptera, Formicidae). *Revue Française d'Entomologie* 32(3–4): 151–163. [Nouvelle Série]
- Helms JA, Godfrey A (2016) Dispersal Polymorphisms in Invasive Fire Ants. *PLoS ONE* 11(4): e0153955. <https://doi.org/10.1371/journal.pone.0153955>
- Hölldobler B (1965) Neue Mitteilungen über die Diebsameise (*Solenopsis fugax*), besonders über ihr Verhalten in Formicarien. *Mitteilungen der Schweizerische Entomologische Gesellschaft* 38: 71–79.
- Latreille PA (1798) *Essai sur l'histoire des fourmis de la France*. F. Bourdeaux, Brive, 50 pp.
- Lleonart J, Salat J, Torres GJ (2000) Removing allometric effects of body size in morphological analysis. *Journal of Theoretical Biology* 205(1): 85–93. <https://doi.org/10.1006/jtbi.2000.2043>
- McInnes DA, Tschinkel WR (1995) Queen dimorphism and reproductive strategies in the fire ant *Solenopsis geminata* (Hymenoptera: Formicidae). *Behavioral Ecology and Sociobiology* 36(6): 367–375. <https://doi.org/10.1007/BF00177332>
- Menozi C (1936) Nuovi contributi alla conoscenza della fauna delle Isole italiane dell'Egeo. VI. Hymenoptera – Formicidae. *Bollettino del Laboratorio di Zoologia Generale e Agraria della Reale Scuola Superiore d'Agricoltura*. Portici 29: 262–311.
- Molet M, Péronnet R, Couette S, Canovas C, Doums C (2017) Effect of temperature and social environment on worker size in the ant *Temnothorax nylanderii*. *Journal of Thermal Biology* 67: 22–29. <https://doi.org/10.1016/j.jtherbio.2017.04.013>
- Nilsen G, Lingjaerde OC (2013) clusterGenomics: Identifying clusters in genomics data by recursive partitioning. R package version 1.0. <https://doi.org/10.1515/sagmb-2013-0016> [Retrieved on 10 January 2017]
- R Core Team (2022) R: A language and environment for statistical computing (4.2.2). Computer Software R Foundation for Statistical Computing. <https://www.R-project.org>
- Ripley B, Venables B, Bates DM, Hornik K, Gebhardt A, Firth D, Ripley MB (2013) Package 'mass'. *Cran r* 538: 113–120.
- Santschi F (1934) Contribution aux *Solenopsis* paléarctiques. *Revue Suisse de Zoologie* 41: 565–592. <https://doi.org/10.5962/bhl.part.146021>
- Seifert B (2008) Removal of allometric variance improves species separation in multi-character discriminant functions when species are strongly allometric and exposes diagnostic characters. *Myrmecological News* 11: 91–105.
- Seifert B (2017) The ecology of Central European non-arboreal ants – 37 years of a broad-spectrum analysis under permanent taxonomic control. *Soil Organisms* 89(1): 1–69.
- Seifert B (2018) *The ants of Central and North Europe*. Lutra Verlags- und Vertriebsgesellschaft, Tauer, 425 pp.
- Seifert B (2021) A taxonomic revision of the Palaearctic members of the *Formica rufa* group (Hymenoptera: Formicidae) – the famous mound-building red wood ants. *Myrmecological News* 31: 133–179. https://doi.org/10.25849/myrmecol.news_031:133
- Seifert B (2023) The Ant Genus *Cardiocondyla* (Hymenoptera: Formicidae): the Species Groups with Oriental and Australasian Origin. *Diversity (Basel)* 15(1): 25. <https://doi.org/10.3390/d15010025>

- Seifert B, Csósz S (2015) *Temnothorax crasecundus* sp. n. – a cryptic Eurocaucasian ant species (Hymenoptera, Formicidae) discovered by Nest Centroid Clustering. *ZooKeys* 479: 37–64. <https://doi.org/10.3897/zookeys.479.8510>
- Seifert B, Ritz M, Csósz S (2014) Application of exploratory data analyses opens a new perspective in morphology-based alpha-taxonomy of eusocial organisms. *Myrmecological News* 19: 1–15.
- Tschinkel WR, Mikheyev AS, Storz SR (2003) Allometry of workers of the fire ant, *Solenopsis invicta*. *Journal of Insect Science* 3(2): 1–11. <https://doi.org/10.1673/031.003.0201>
- Wagner HC, Wieser B (2021) Nestdichten, Frischgewicht und Artenreichtum von Ameisen in südoststeirischen Graslandbiotopen (Hymenoptera: Formicidae). *Joannea Zoologie* 19: 115–137.
- Yusupov ZM (2014) Two ant species (Hymenoptera, Formicidae) from the Northern Caucasus, new to the fauna of Russia. *Entomological Review* 94(2): 256–257. <https://doi.org/10.1134/S0013873814020195>

Supplementary material 1

List of morphometrically investigated samples

Authors: Sándor Csósz, Bernhard Seifert, Márk László, Zalimkhan M. Yusupov, Gábor Herczeg

Data type: xls

Explanation note: Unique codes for nest samples, specimens investigated by BS and SC, locality, geographic coordinates (Latitude, Longitude) in decimal format, altitude (Elevation) in meters a.s.l., collector's name, date and depositories are provided. Unique CASENT numbers are given for type specimens.

Copyright notice: This dataset is made available under the Open Database License (<http://opendatacommons.org/licenses/odbl/1.0/>). The Open Database License (ODbL) is a license agreement intended to allow users to freely share, modify, and use this Dataset while maintaining this same freedom for others, provided that the original source and author(s) are credited.

Link: <https://doi.org/10.3897/zookeys.1187.105866.suppl1>

Supplementary material 2

Morphometric data of 15 continuous morphometric traits of 203 individuals collected by SC is given in μm

Authors: Sándor Csósz, Bernhard Seifert, Márk László, Zalimkhan M. Yusupov, Gábor Herczeg

Data type:xlsx

Copyright notice: This dataset is made available under the Open Database License (<http://opendatacommons.org/licenses/odbl/1.0/>). The Open Database License (ODbL) is a license agreement intended to allow users to freely share, modify, and use this Dataset while maintaining this same freedom for others, provided that the original source and author(s) are credited.

Link: <https://doi.org/10.3897/zookeys.1187.105866.suppl2>

Supplementary material 3

Morphometric data of 18 continuous morphometric traits of 171 individuals collected by BS is given in mm

Authors: Sándor Csósz, Bernhard Seifert, Márk László, Zalimkhan M. Yusupov, Gábor Herczeg

Data type: xlsx

Copyright notice: This dataset is made available under the Open Database License (<http://opendatacommons.org/licenses/odbl/1.0/>). The Open Database License (ODbL) is a license agreement intended to allow users to freely share, modify, and use this Dataset while maintaining this same freedom for others, provided that the original source and author(s) are credited.

Link: <https://doi.org/10.3897/zookeys.1187.105866.suppl3>

Supplementary material 4

R script of NC clustering and method PART implementing cluster methods “hclust” and “kmeans”, including “Mark dendrogram” function mapping the results of partitioning algorithm PART on the dendrogram

Authors: Sándor Csósz, Bernhard Seifert, Márk László, Zalimkhan M. Yusupov, Gábor Herczeg

Data type: txt

Copyright notice: This dataset is made available under the Open Database License (<http://opendatacommons.org/licenses/odbl/1.0/>). The Open Database License (ODbL) is a license agreement intended to allow users to freely share, modify, and use this Dataset while maintaining this same freedom for others, provided that the original source and author(s) are credited.

Link: <https://doi.org/10.3897/zookeys.1187.105866.suppl4>

Descriptions of two new species of *Phaecedophora* Walsingham, 1900 (Lepidoptera, Tortricidae, Olethreutinae) from China

Yange Li¹, Wenqing Jing¹, Shulian Hao², Haili Yu^{1,3}

¹ Shaanxi Key Laboratory for Animal Conservation, Northwest University, Xi'an, Shaanxi Province, 710069, China

² Tianjin Natural History Museum, Tianjin, 300201, China

³ Key Laboratory of Resource Biology and Biotechnology in Western China, Northwest University, Ministry of Education, Xi'an, Shaanxi Province, 710069, China

Corresponding author: Haili Yu (yuhaili@nwu.edu.cn)

Abstract

Two new species of the genus *Phaecedophora*, *P. dactylina* **sp. nov.** and *P. vascularis* **sp. nov.**, are described from the southwest China. Photographs of the adults and the genitalia are provided. Keys to the species of the genus based on the male and female genitalia are given.

Key words: Olethreutini, *Phaecedophora dactylina* sp. nov., *Phaecedophora vascularis* sp. nov., taxonomy

Introduction

Phaecedophora was proposed by Walsingham (1900) to accommodate two South and East Asian species, *P. fimbriata* Walsingham from Japan, India and Burma, and *P. acutana* Walsingham from Japan. Later, *P. fimbriata* has been reported from China (Meyrick 1914, 1935; Kawabe et al. 1992; Liu and Li 2002; Li et al. 2020), New Guinea (Diakonoff 1953), Vietnam (Kuznetsov 1997), Russia (Kuznetsov 2001), and Thailand (Pinkaw 2007); *P. acutana* has been found in China (Taiwan) (Diakonoff 1973; Kawabe et al. 1992) and Russia (Far East) (Kuznetsov 2001). To date, these two species are the only known members of the genus (Gilligan et al. 2018). In southern China, *P. fimbriata* is widely distributed in 15 provinces. In this paper, we identify two new species from southwestern China (Tibet and Yunnan), and the purpose of this paper is to describe these two species based on morphological features of adults.

Materials and methods

The materials examined in this study were collected using light traps. Genitalia dissection followed the methods described by Li (2002). Both adults and genitalia were photographed using a digital microscope (VHX-5000). All specimens used in this study are deposited in the Insect Collection of Northwest University, Xi'an, China (NWU).



Academic editor: José Luis Yela

Received: 13 August 2023

Accepted: 23 November 2023

Published: 21 December 2023

ZooBank: <https://zoobank.org/9B1CA3A4-435B-4179-82DE-204771324B1C>

Citation: Li Y, Jing W, Hao S, Yu H (2023) Descriptions of two new species of *Phaecedophora* Walsingham, 1900 (Lepidoptera, Tortricidae, Olethreutinae) from China. ZooKeys 1187: 223–236. <https://doi.org/10.3897/zookeys.1187.111101>

Copyright: © Yange Li et al.

This is an open access article distributed under terms of the Creative Commons Attribution License (Attribution 4.0 International – CC BY 4.0).

Results

Phaecedophora Walsingham, 1900

Phaecedophora Walsingham, 1900: 130. Type species: *Phaecedophora fimbriata* Walsingham, 1900.

Note. Walsingham (1900) defined *Phaecedophora* based on external traits, distinguishing it from *Phaecasiophora* Grote by its narrower forewing, densely scaled hind tibia, and the hindwing featuring a long hair-scaled anal margin in males. In fact, the hind tibiae of males in the *Phaecasiophora* species are frequently broadened by long scales and carry one or two long hair pencils. Diakonoff (1973) and Razowski (1989) redescribed the genus, and both asserted its close relationship to *Temnolopha* Lower and *Saliciphaga* Falkovitsh based on the characteristics of both male and female genitalia. However, they did not provide a specific differential diagnosis for *Phaecedophora*. The two previously known species, in conjunction with the two newly described species in this present investigation, exhibit a conspicuous characteristic in their appearance—fine longitudinal stripes on the forewing. They can be defined by the combination of the following genitalia characters: in males, the tegumen is high and narrow; the uncus is slender, hooked, densely spined, and sometimes shortly furcated apically (*P. dactylina* sp. nov.); the socius is small, oval, and densely spined; the gnathos is a simple band, membranous or weakly sclerotized; the valva is robust and curved, often with a deeply concave area (except *P. vascularis* sp. nov.) that separates the sacculus from the densely bristled cucullus; the basal excavation has a protruding rim above which there is a short, apically spined prominence below the costa (*P. dactylina* sp. nov. and *P. vascularis* sp. nov.); the sacculus is weakly spined, occasionally with a tuft of short spine cluster medially on the ventral margin (*P. fimbriata* and *P. dactylina* sp. nov.); the cucullus bears bristles across its base, enlarged and raised on a ridge (*P. fimbriata* and *P. acutana*), and its ventroproximal base is lightly projecting (*P. acutana* and *P. vascularis* sp. nov.) or produced into a ventral process (*P. fimbriata* and *P. dactylina* sp. nov.), which carries a long spine cluster; the caulis is very short; the anellus is a narrow ring; the phallus is short and the cornuti is present (*P. fimbriata*) or absent. In females, the sterigma is derived from a raised fold encircling the ostium and is aciculate; the colliculum is well developed and normal in shape or expanded caudally (*P. fimbriata* and *P. dactylina* sp. nov.); the signa consist of two double-folded plates, either obviously unequal in size (*P. acutana* and *P. vascularis* sp. nov.) or roughly equal in size (*P. fimbriata* and *P. dactylina* sp. nov.).

Key to species of *Phaecedophora* based on the male genitalia

- 1 Valva with a short prominence above rim of basal excavation below costa **2**
- Valva without prominences below costa **3**
- 2 Valva constricted beyond basal excavation; sacculus with a short spine cluster on ventral edge at midlength, nearly naked apically; cucullus with

- basal 1/3 naked except for a tuft of long strong spines and short spines at basal prominence *P. dactylina* sp. nov.
- Valva not constricted beyond basal excavation; sacculus bearing a round patch of fine spines apically just proximal to cucullus, without spine clusters along ventral edge; whole cucullus with dense spines, and carrying a long spine cluster from outer surface of ventral base *P. vascularis* sp. nov.
- 3 Sacculus with a short spine cluster on midlength of ventral edge; cucullus with ventral base expanded and forming a short blunt prominence, apically bearing a strong thorn and a tuft of long spines, these spines longer than uncus *P. fimbriata*
- Sacculus with weak spines sparsely along ventral edge; cucullus with ventral base not expanded and carrying a tuft of spines, these spines shorter than uncus *P. acutana*

Key to species of *Phaecedophora* based on the female genitalia

- 1 Signa significantly unequal in size 2
- Signa roughly equal in size 3
- 2 Signa oval *P. acutana*
- Signa with the large one somewhat broad rectangular, the small one rounded *P. vascularis* sp. nov.
- 3 Sterigma circular, posterior portions not protruding *P. fimbriata*
- Sterigma narrow, collar-like, with posterior portion on each side protruding and expanded *P. dactylina* sp. nov.

Phaecedophora dactylina Li & Yu, sp. nov.

<https://zoobank.org/5FDA1766-F739-4A04-8E08-F56DCA536F9E>

Figs 1A, B, 2A–D, 3A, 4A–C, 5, 6

Type materials. *Holotype*: ♂, CHINA, Tibet: Motuo County, Beibengxiang, 29°19.00'N, 95°10.80'E, alt. 810 m, 13 Aug. 2017, Mujie Qi and Xiaofei Yang leg., genitalia slide no. YWX18220. *Paratypes*: CHINA, Tibet: 3♂, same data as holotype except 29°14.40'N, 95°19.20'E, alt. 810–990 m, 12–13 Aug. 2017; 1♂, same data as holotype except 29°19.20'N, 95°19.20'E, alt. 1100 m, 10 Aug. 2017; 1♀, Nielamu County, 27°58.80'N, 85°58.20'E, alt. 1960 m, 6 Jul. 2019, Mujie Qi and Jiaqi Deng leg.; Yunnan Prov.: 1♂, 3♀, Tengchong County, Linjiapuzi, 25°17.40'N, 98°42.00'E, alt. 2140 m, 15 Aug. 2014, Kaijian Teng, Shurong Liu and Hua Rong leg.

Diagnosis. The male of *P. dactylina* sp. nov. resembles *P. fimbriata* in appearance in having darker scaling in the forewing pattern, two hair pencils and long scales in the anal roll of hindwing, and the hindleg broadened. Dissection of the genitalia is necessary for identification. Conversely, the female can be readily separated from *P. fimbriata* in having the forewing pale brown suffused with tawny longitudinal markings. More diagnostic characters are found in the male and female genitalia. The male of *P. dactylina* sp. nov. can be distinguished by the apically furcated uncus, the valva adorned with a short finger-like prominence below the costa, a nearly bare basal region of the cucullus, and the absence of cornuti in the phallus. In contrast, *P. fimbriata* presents a hooked uncus,

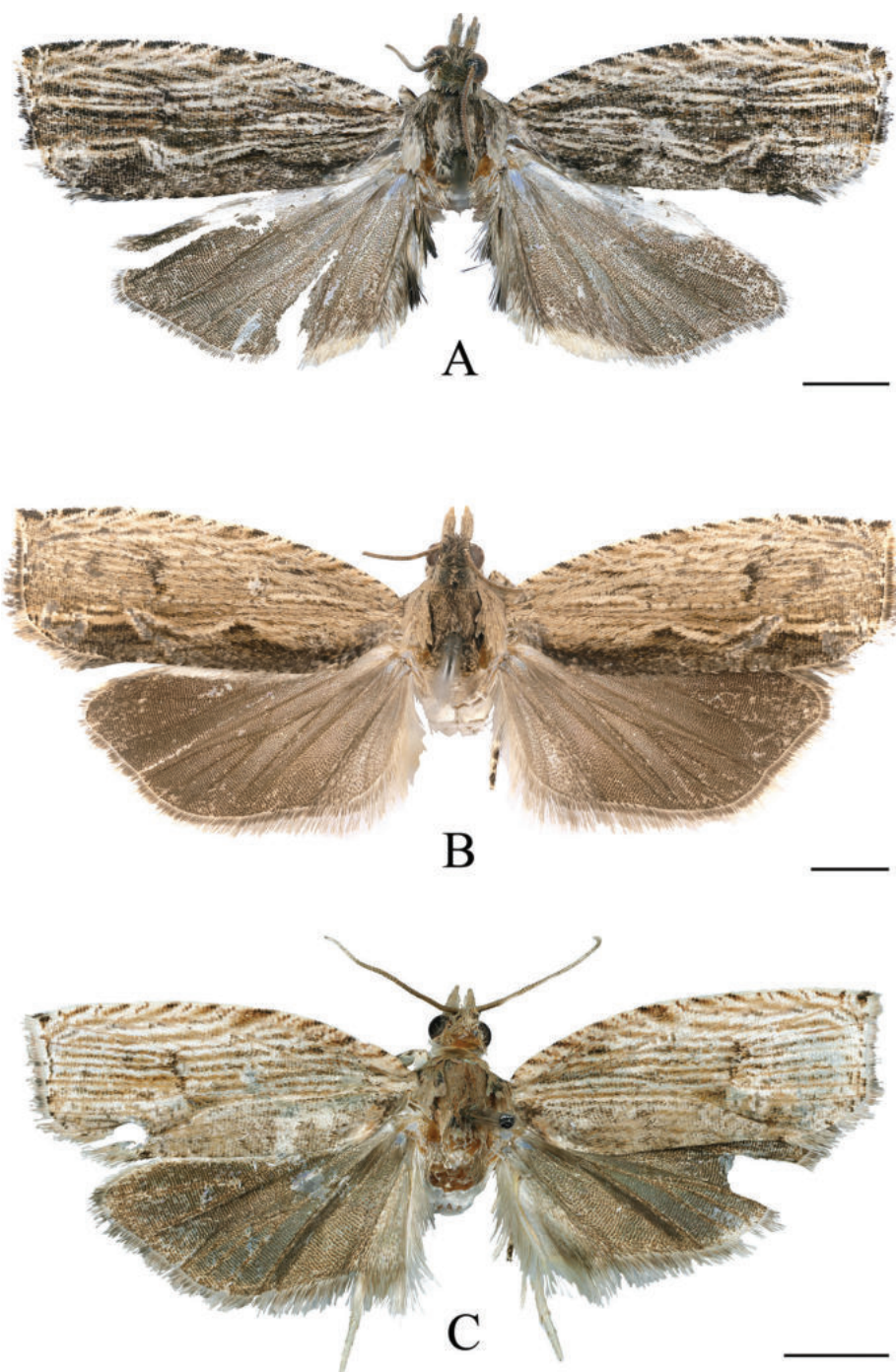


Figure 1. Adults of *Phaecedophora* spp. **A** *P. dactylina* sp. nov. (holotype, male) **B** *P. dactylina* sp. nov. (paratype, female) **C** *P. vascularis* sp. nov. (holotype, male). Scale bars: 2 mm.

the valva devoid of prominences below the costa, and a spined ridge across the base of the cucullus, with the phallus bearing a short spine on the vesica. In the female genitalia, *P. fimbriata* exhibits the sterigma lacking posterior extensions, whereas in *P. dactylina* sp. nov., this structure manifests as two broad plates.

Description. Male (Fig. 1A) with forewing length 8.0–9.0 mm. **Head** (Fig. 2A, B): vertex and upper frons with shaggy, pale gray-tawny scales (shiny gray distally), lower frons with gray-white appressed scales. Antenna gray-tawny, extending to middle of forewing costa. Ocellus well developed; chaetosema present. Labial palpus ascending, basal half white, distal part gray-white, gray-tawny to gray,

medially dusted with a few black scales; median segment broadened distally; terminal segment a little slender, porrect.

Thorax: fuscous basally, suffused with gray-white posteriorly. Hind tibia in male short, distally dilated by dense, long scales, creamy white, with a concolorous hair tuft on apical inner surface (Fig. 3A); tarsus strongly broadened by dense scales dorsally; inner side of first segment forming a short, fuscous suffused with brown, scaled cavity; other tarsal segments creamy. Forewing subrectangular, slightly dilated towards termen, costa curved evenly, apex slightly produced, termen weakly oblique, tornus rounded; upperside fuscous, dusted with brown; pairs of strigulae on costa creamy, well-defined striae from them concolorous, extending longitudinally to termen and occupying halfway across the wing, partly confluent below distal half of costa; a double creamy streaks rising from base of wing, zigzagging between cell and 1A+2A to termen above tornus; cilia pale gray on upper part of termen, fuscous on lower part of termen, gray-white on tornus; underside brown, paler on costa, pairs of strigulae creamy, suffused with pale tawny, area of hindwing overlap white. Hindwing (Fig. 4A) fuscous, paler basally, costal area of forewing overlap white; pecten (Fig. 4B) distinct; with a series of long hair-scales between CuA_1 and distal half of CuA_2 ; anal region triangularly expanded, with pale tawny and fuscous long hair pencils (Fig. 4C) in anal roll; anal roll narrowly folded upward, bearing long hair-scales on margin; cilia gray-white; underside brown.

Female (Fig. 1B) with forewing length 9.0–10.0 mm. **Head** (Fig. 2C, D): vertex and upper frons rough, paler brown; scales shiny gray distally; lower frons with tawny appressed scales. Antenna brown, extending to middle of forewing costa. Ocellus well developed; chaetosema present. Labial palpus ascending, mostly pale brown, paler on inner surface and base; median segment expanded distally, terminal segment porrect, rather slender.

Thorax: brown-fuscous. Legs normal. Forewing subrectangular, slightly dilated towards termen, costa curved evenly, termen straight, tornus rounded; upperside with upper 3/4 longitudinally, finely striped with tawny striae from concolorous pairs of costal strigulae and pale brown broken markings, slightly mottled, except a short streak on outer edge of cell; area below 1A+2A and CuA_1 fuscous, suffused with blackish fuscous, upper edge wavy, produced at middle of fold and base of CuA_1 ; cilia fuscous, suffused with brown; underside tawny, pairs of strigulae on costa tawny, area of hindwing overlap white. Hindwing brown-fuscous; costa area of forewing overlap white; pecten distinct; inner side unmodified; cilia pale brown, with brown-fuscous baseline; underside brown.

Abdomen: male genitalia (Fig. 5A) with tegumen high and narrow. Uncus slender, densely covered with spines; apex bifurcated, with short spines. Socius small, oval, densely covered with spines. Gnathos membranous, forming a broad band. Valva robust, curved, constricted beyond basal excavation, sacculus nearly half length of valva; a short prominence (Fig. 5B) above the rim of basal excavation below costa, about half of uncus in length, finger-like, apex broadened, with short, dense spines; sacculus well defined, weakly spined, with only sparse, fine hairs beyond basal excavation and along ventral edge, and bearing a spine cluster on midlength of ventral edge; cucullus somewhat elongately triangular, basal 1/3 naked except for strongly protruding ventroproximal base which bears dense, short bristles and a tuft of long bristles apically (Fig. 5C), these long bristles longer than uncus; distal 2/3 of cucullus with dense spines. Phallus short, straight, without cornuti. **Female genitalia**



Figure 2. Heads of *Phaecedophora* spp. **A, B** *P. dactylina* sp. nov. (holotype, male) **A** lateral view **B** dorsal view **C, D** *P. dactylina* sp. nov. (paratype, female) **C** lateral view **D** dorsal view **E, F** *P. vascularis* sp. nov. (holotype, male) **E** lateral view **F** dorsal view.

(Fig. 6A) with papillae anales narrow, densely setose. Anterior apophysis a little longer than posterior apophysis. Sterigma (Fig. 6B) derived from a raised spinulose fold encircling ostium, with a dorsal notch and posterior portion on each side produced into a broad plate. Colliculum about 1/3 times of length of ductus bursae, strongly sclerotized, caudally wrench-like, abruptly narrowed below, the rest of ductus bursae membranous, ductus seminalis originating posterior to midlength. Corpus bursae ovoid, granulated; signa (Fig. 6C) two, double-folded, roughly equal in size, generally leaf-like.

Etymology. The specific name is derived from the Latin *dactylinus* (= finger-like), referring to the shape of costal prominence of the valva in the male genitalia.

***Phaecedophora vascularis* Li & Yu, sp. nov.**

<https://zoobank.org/D963BF72-463D-497F-B0FF-E4B3211E6E67>

Figs 1C, 2E, F, 3B, 4D–F, 7, 8

Type materials. Holotype: ♂, CHINA, Yunnan Prov.: Sun River Nature Reserve, 22°36.60'N, 101°06.00'E, alt. 1450 m, 13 May 2014, Zhenguo Zhang leg., genitalia slide no. SXL20569. **Paratypes:** Yunnan Prov.: 1♂, same data as holotype except 11 May 2014; 1♂, Xishuangbanna Reserve, 21°54.60'N, 101°17.40'E, 21 May 2015, Zhenguo Zhang leg.; 1♀, Tengchong County, Mangbang Town, 25°01.80'N, 98°42.00'E, alt. 1330 m, 10 Aug. 2015, Kaili Liu and Hao Wei leg.

Diagnosis. This species shares similar markings on the forewing with *P. fimbriata* and *P. dactylina* sp. nov., yet its scaling is distinctly pale, particularly dorsal area, which is tawny, suffused with pale brown, as opposed to the fuscous to blackish fuscous hue observed in the latter two species. Furthermore, males of *P. vascularis* sp. nov. has no darkened long scales in the anal roll of the hindwing and instead bear a solitary, pale tawny hair pencil. In contrast, males of *P. fimbriata* and *P. dactylina* sp. nov. present two hair pencils alongside dense, darkened long scales in the anal roll of the hindwing—one hair pencil in pale tawny and the other in blackish fuscous. In the male genitalia, *P. vascularis* sp. nov. exhibits similarities to *P. acutana*; however, it is characterized by the valva featuring a short, finger-like prominence below the base of the costa, a tuft of spines proximal to the base of the cucullus, and the cucullus without a densely spiny transversal ridge basally. While in *P. acutana*, the valva lacks a prominence below the costa, the sacculus bears a tuft of spines under the apical margin, and a densely spiny ridge spans across the base of the cucullus. In the female genitalia, *P. vascularis* sp. nov. can be separated from other species within the genus by possessing two unequal signa, one of which is broadly rectangular, as delineated in the key.

Description. Adult (Fig. 1C) with forewing length 8.0–8.5 mm. **Head** (Fig. 2E, F): vertex, antenna and upper frons tawny-cream, paler on lower frons; vertex roughly scaled; antenna extending to middle of forewing costa. Ocellus well developed; chaetosema present. Labial palpus ascending, mostly tawny-cream, paler on inner surface and base, medially dusted with gray scales on outer side; median segment distally expanded, terminal segment porrect, rather slender.

Thorax: pale tawny, without posterior crest. Hind tibia white, simple, not modified in male, without hair pencils (Fig. 3B). Forewing subrectangular, costa curved



Figure 3. Hind tibiae in male of *Phaecedophora* spp. **A** *P. dactylina* sp. nov. (paratype) **B** *P. vascularis* sp. nov. (paratype).

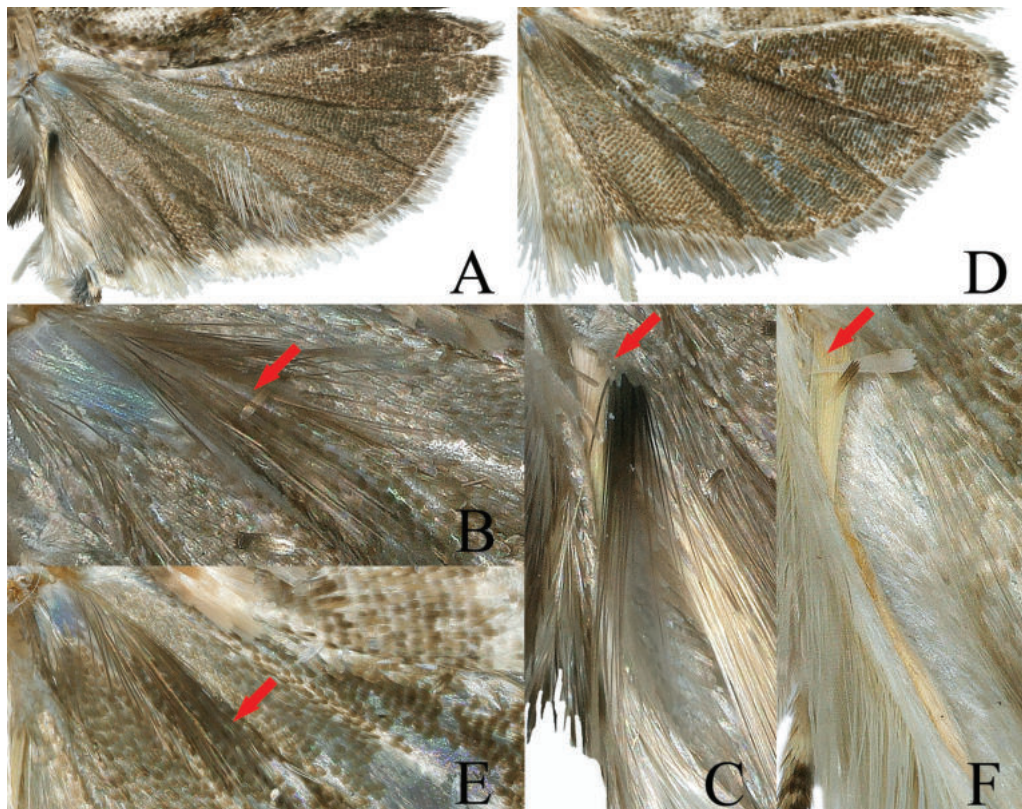


Figure 4. Male hindwings of *Phaecedophora* spp. **A–C** *P. dactylina* sp. nov. (paratype) **A** hindwing **B** cubital pecten **C** axillary hair pencils **D–F** *P. vascularis* sp. nov. (holotype) **D** hindwing **E** cubital pecten **F** axillary hair pencils.

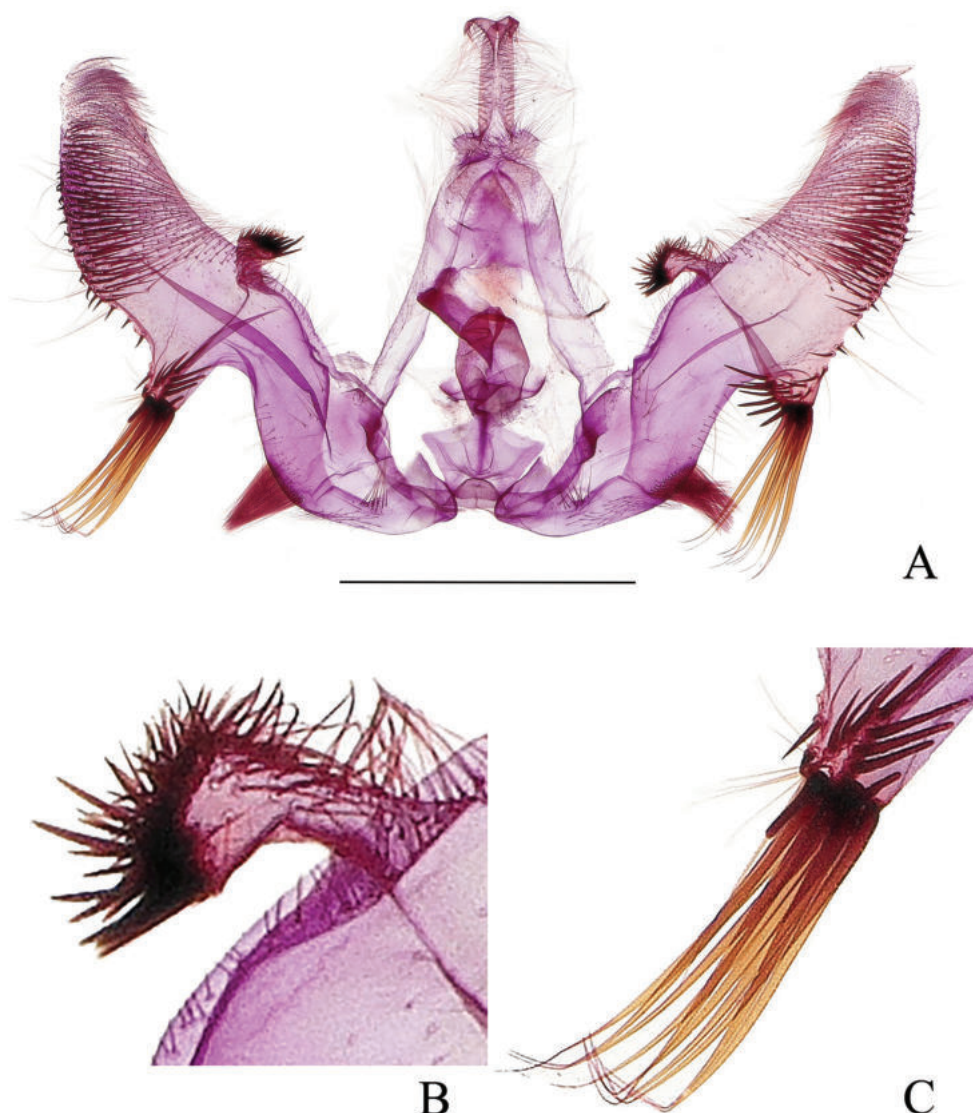


Figure 5. Male genitalia of *Phaecedophora dactylina* sp. nov. (holotype) **A** male genitalia **B** costal prominence of valva **C** ventral prominence of cucullus. Scale bars: 1 mm.

basally and nearly straight distally, termen vertical and straight, tornus rounded; upper side with complex pattern of distinct longitudinal, fine, parallel creamy and pale brown lines, dusted with fuscous rising from base and costa to termen, interrupted by a short, transverse, fuscous marking on outer edge of cell; cilia tawny-white, white on tornus; underside brown, costa pale brown, with pairs of strigulae creamy, area of hindwing overlap white. Hindwing (Fig. 4D) fuscous except costal area of forewing white; cubital pecten (Fig. 4E) present; in male anal region expanded, with anal roll bearing a long pencil (Fig. 4F) of pale tawny hair-scales from base of wing; cilia pale brown basally and pale white apically; underside brown.

Abdomen: male genitalia (Fig. 7A) with tegumen high and narrow, shoulders obvious. Uncus a slender hook, densely spined. Socius small, oval, densely spined. Gnathos membranous. Valva moderate in width, curved, without neck; sacculus about 1/3 times of length of valva, its ventral edge nearly straight; a short finger-like prominence (Fig. 7B) below base of costa and above the protruding rim of basal excavation, with dense, short spines apically; sacculus with sparse spines basally and a rounded tuft of spines proximal to cucullus; cucullus with dense spines and

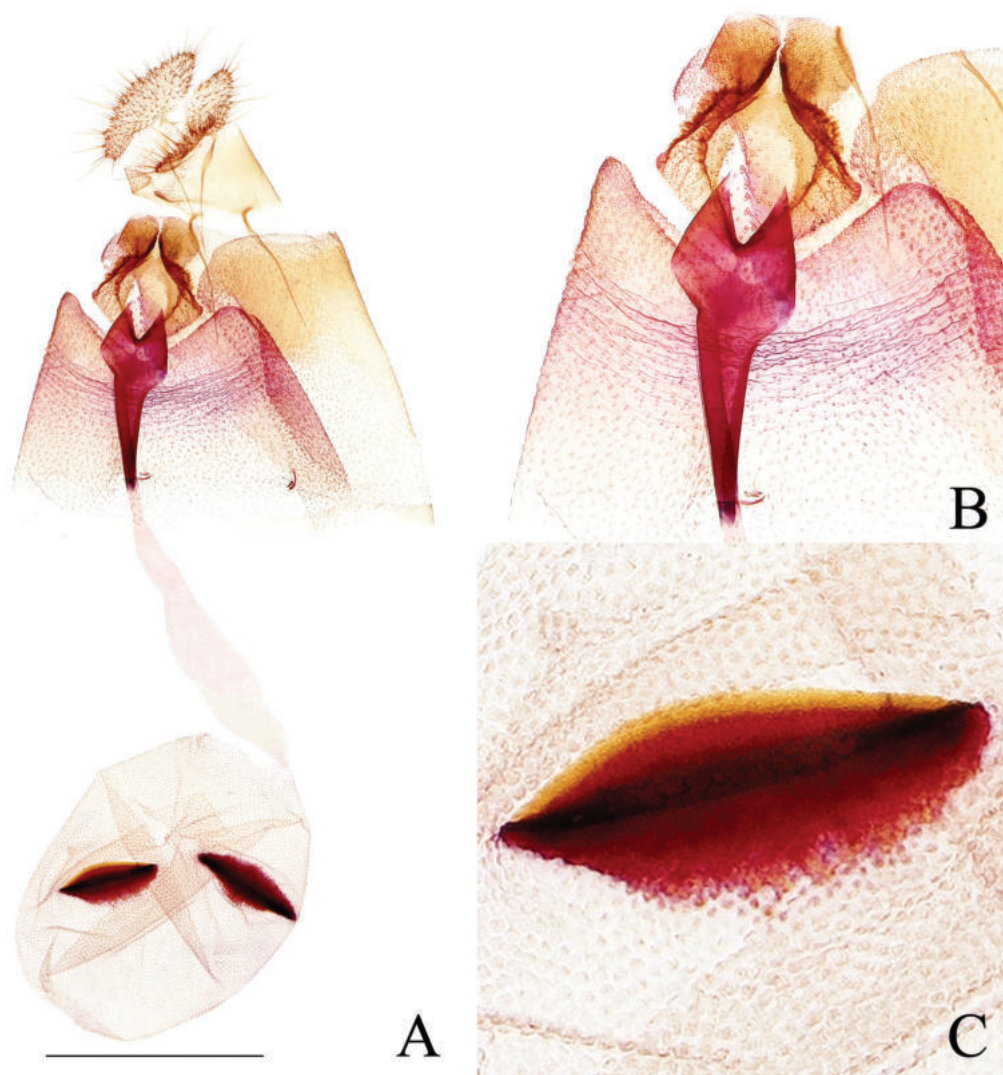


Figure 6. Female genitalia of *Phaecedophora dactylina* sp. nov. (paratype) **A** female genitalia **B** sterigma and colliculum **C** signum. Scale bars: 1 mm.

a slender spine cluster (Fig. 7C) under its ventroproximal base, with these spines shorter than uncus. Phallus short, without cornuti. **Female genitalia** (Fig. 8A) with papillae anales narrow, densely setose. Anterior apophyses a little shorter than posterior apophyses. Sterigma (Fig. 8B) a finely spinulose, inverted, blunt triangular area with a median split containing ostium. Colliculum moderately sclerotized, about 1/4 times of ductus bursae in length, inception of ductus seminalis posterior to midlength. Corpus bursae ovoid, granulated; signa (Fig. 8C) two, double-folded, unequal in size, the large one like a broad and shallow basket, somewhat rectangular, the small one a little oval, about half of the larger one in size.

Etymology. The specific name is derived from the Latin *vascularis* (= veined), referring to the markings of forewing.

Discussion

Diakonoff (1973) classified *Phaecedophora* in the subtribe Neopotamiae based on the shape of signa. Most members of Neopotamiae are characterized by relatively large adults, as does *Phaecedophora*, whose forewing ranges from

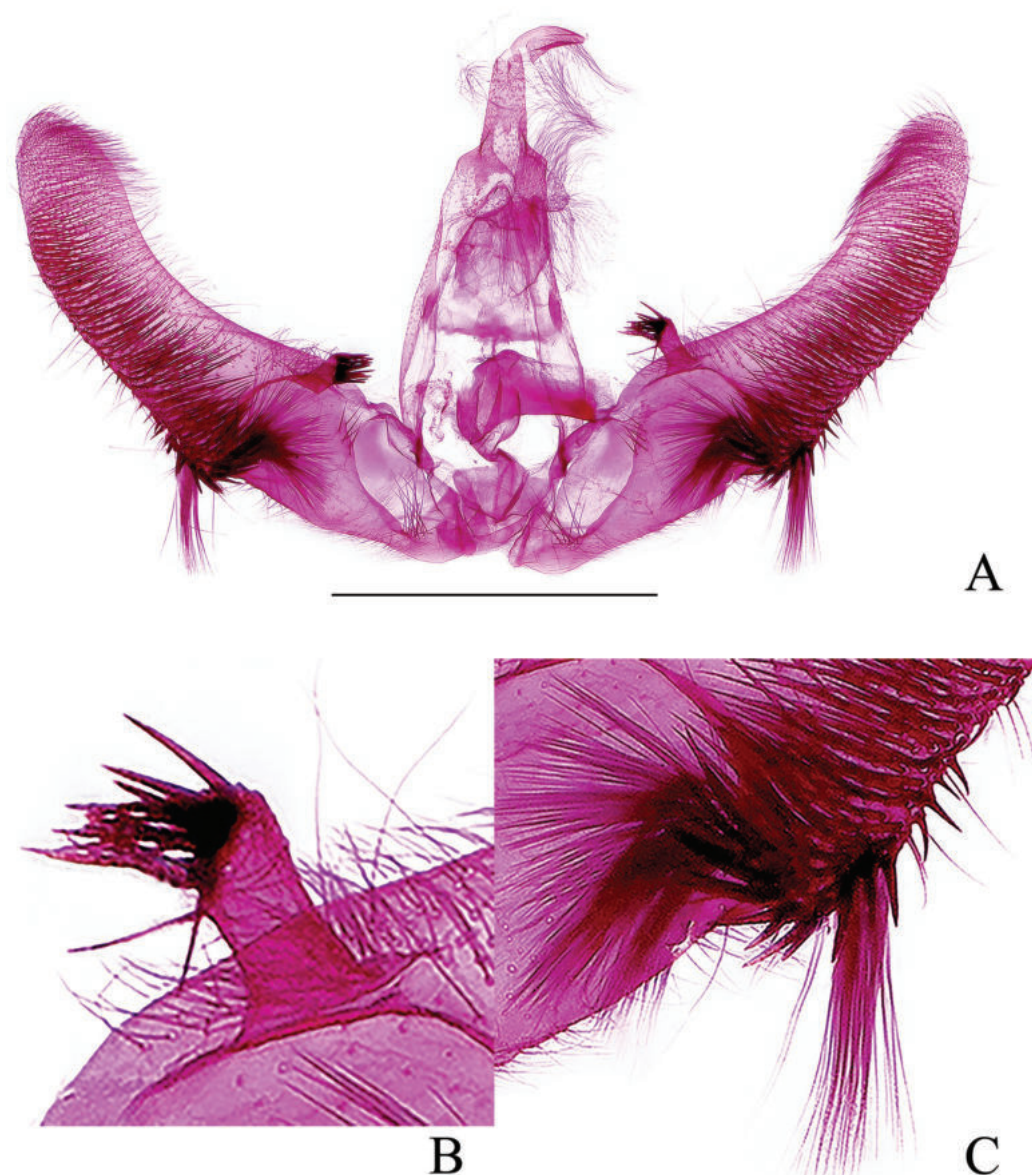


Figure 7. Male genitalia of *Phaecedophora vascularis* sp. nov. (holotype) **A** male genitalia **B** costal prominence of valva **C** ventral base of cucullus. Scale bars: 1 mm.

6.0 mm to 9.5 mm in length. Distinguishing features include the presence of slender longitudinal stripes on the forewing from the base to the termen, setting adults of *Phaecedophora* apart from most genera in Olethreutini, where a common forewing pattern involves several dark, parallel, outwardly oblique, transverse bands—albeit with various developments and modifications. *Phaecedophora* species, especially those discussed here and *P. fimbriata*, share considerable external similarities. However, polymorphism in forewing patterns is frequently observed in adults of *Phaecedophora*. For instance, specimens from Japan exhibit at least five types of forewing patterns in *P. acutana*, (three in females and two in males) (Nasu 2013) and two types in females of *P. fimbriata*. In this study, sexual dimorphism is noted in *P. dactylina* sp. nov. Although the morphological polymorphism of *P. vascularis* sp. nov. remains inconclusive due to a limited sample size (only four specimens were observed and collected in close proximity), it is crucial to exercise caution in drawing conclusions. Specimens

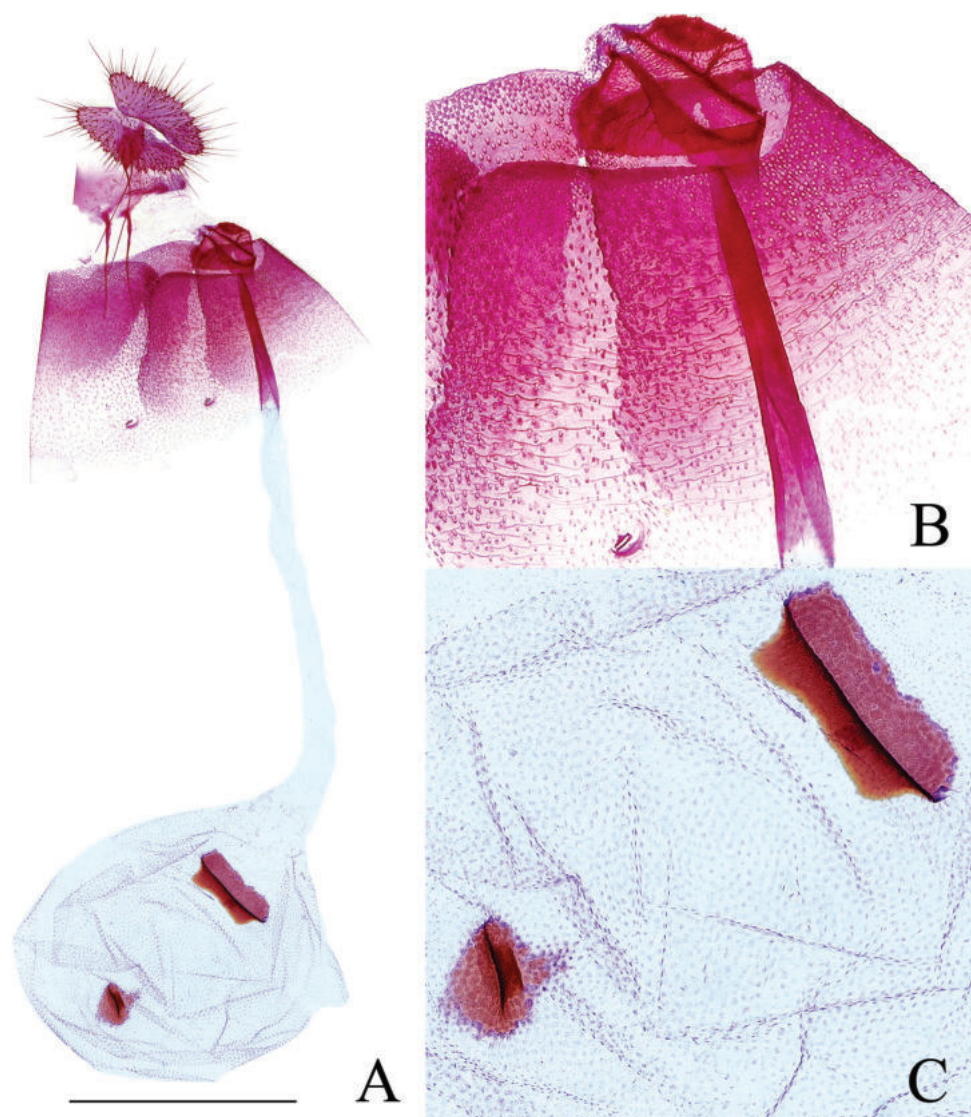


Figure 8. Female genitalia of *Phaecedophora vascularis* sp. nov. (paratype) **A** female genitalia **B** sterigma and colliculum **C** signa. Scale bars: 1 mm.

of *P. fimbriata* from China present a perplexing case, displaying a constant darkened forewing pattern (one of two types in Japanese specimens) across a broad geographical range (between 17–31°N and 97–120°E), without observed dimorphism or polymorphism. Despite marked differences in scent organs among the males of these four species, intriguingly, they exhibit similarities in pairs. Males of *P. fimbriata* and *P. dactylina* sp. nov. demonstrate complex modifications in the hindleg, with the tibia and tarsus strongly broadened, laterally compressed, and forming a cavity (Fig. 3A). They also exhibit modifications in the hindwing, featuring two hair pencils and long scales in the anal roll (Fig. 4C), as well as in the abdomen, with two median tufts of appressed scaling on sternites V–VII. On the other hand, males of *P. acutana* and *P. vascularis* sp. nov. lack modifications in the hindleg (Fig. 3B) and abdomen, carrying only one hair pencil in the anal roll of the hindwing (Fig. 4F). Notably, scent organs prove challenging for classification, as acknowledged by Diakonoff (1981a) and Aarvik (2004). Generally, dissection of the genitalia is necessary for reliable identification. In males, the valva pro-

vides optimal diagnostic characters, while in females, the specific distinction lies in the shapes of the sterigma and signa.

Diakonoff (1973, 1981b), Razowski (1989), and Horak (2006) extensively elucidated the close relationship between *Phaecedophora*, *Saliciphaga*, and *Temnolopha*. In comparison to *Temnolopha*, a suite of genital characteristics in *Phaecedophora* suggests a more intimate connection with *Saliciphaga*. These features include a high, triangular tegumen, a somewhat hooked uncus that is slender, a small oval socius, symmetrical valvae with relatively narrow sacculus, and two large, double-folded signa. While the two previously known species, *P. fimbriata* and *P. acutana*, lack a basal valval prominence in the male genitalia, this structure is well developed in the two species described here, referring the genus to vicinity of *Neopotamia* Diakonoff, 1973. The dorsally split and dorsocaudally enlarged sterigma, along with well-defined signa lacking basal scobination, further supports this association.

Acknowledgements

Our sincere appreciation is extended to Professor Houhun Li of Nankai University, Tianjin, for generously providing a portion of the specimens utilized in this study. We would also like to express our profound gratitude to all those who actively participated in the fieldwork. Special thanks to the editors and two reviewers for their suggestions and revisions to this article.

Additional information

Conflict of interest

The authors have declared that no competing interests exist.

Ethical statement

No ethical statement was reported.

Funding

This research was funded by the Foundation of the Shaanxi Educational Committee of China (grant no. 18JS107) and Fauna Sinica (31093430).

Author contributions

Conceptualization: YL. Data curation: YL. Funding acquisition: HY. Investigation: SH, YL. Methodology: YL. Project administration: YL, HY. Resources: SH. Supervision: HY. Validation: WJ, YL. Visualization: YL. Writing – original draft: YL. Writing – review and editing: YL, HY.

Author ORCIDs

Yange Li  <https://orcid.org/0009-0002-9188-2178>

Wenqing Jing  <https://orcid.org/0009-0007-9306-8854>

Shulian Hao  <https://orcid.org/0009-0005-6556-4151>

Haili Yu  <https://orcid.org/0000-0003-1249-5461>

Data availability

All of the data that support the findings of this study are available in the main text.

References

- Aarvik L (2004) Revision of the subtribe Neopotamiae (Lepidoptera: Tortricidae) in Africa. *Norwegian Journal of Entomology* 51: 71–122.
- Diakonoff A (1953) Microlepidoptera of New Guinea. Results of the third Archbold Expedition (American-Nederlands Indian Expedition 1938–39) Part II. *Verhandelingen der Koninklijke Nederlandse Akademie van Wetenschappen* (2) 49(3): 1–166. <https://doi.org/10.5962/bhl.title.120165>
- Diakonoff A (1973) The south Asiatic Olethreutini (Lepidoptera, Tortricidae). *Zoölogische Monographiën van het Rijksmuseum van Natuurlijke Historie* 1: [i–xxii] 1–700. https://doi.org/10.1163/9789004626645_024
- Diakonoff A (1981a) Tortricidae from Madagascar, Part 2. Olethreutinae, 1. *Annales de la Société Entomologique de France* (N. S.) 17(1): 7–32. <https://doi.org/10.1080/21686351.1981.12278262>
- Diakonoff A (1981b) Three correcting notes on the Tortricidae of New Guinea and South Celebes (Lepidoptera). *Entomologische Berichten* 41: 71–72.
- Gilligan TM, Baixeras J, Brown JW (2018) T@RTS: Online World Catalogue of the Tortricidae. (Ver. 4.0). <http://www.tortricid.net/catalogue.asp> [Accessed 19 July 2023]
- Horak M (2006) Monographs on Australian Lepidoptera (Vol. 10): Olethreutine Moths of Australia (Lepidoptera: Tortricidae). CSIRO Publishing, Collingwood, 528 pp. <https://doi.org/10.1071/9780643094086>
- Kawabe A, Komai F, Razowski J (1992) Tortricodea. In: Heppner JB, Inoue H (Eds) *Lepidoptera of Taiwan* (Vol. 1, part 2): Checklist. Scientific Publishers, Taipei, 103–109.
- Kuznetsov VI (1997) New species of Tortricid moths of the subfamily Olethreutinae (Lepidoptera, Tortricidae) from the South of Vietnam. *Entomologicheskoe Obozrenie* 76(4): 797–812. [In Russian]
- Kuznetsov VI (2001) Tortricidae. In: Ler PA (Ed.) *Key to the insects of Russian Far East* (Vol. V). Trichoptera and Lepidoptera. Pt 3. Dal'nauka, Vladivostok, 11–472. [In Russian]
- Li HH (2002) *The Gelechiidae of China* (I). Nankai University Press, Tianjin, 538 pp. [In Chinese]
- Li HH, Wang SX, Qi MJ (2020) *Fauna of Tianmu Mountain* (Vol. X) Insecta, Lepidoptera, Microlepidoptera. Zhejiang University Press, Hangzhou, 414 pp. [In Chinese]
- Liu YQ, Li GW (2002) *Fauna Sinica Insecta* (Vol. 27) Lepidoptera: Tortricidae. Science Press, Beijing, 463 pp. [In Chinese]
- Meyrick E (1914) H. Sauter's Formosa-Ausbeute. Pterophoridae, Tortricidae, Eucosmidae, Gelechiidae, Oecophoridae, Cosmopterygidae, Hyponomeutidae, Heliodinidae, Sesiadae, Glyphipterygidae, Plutellidae, Tineidae, Adelidae (Lep.). *Supplementa Entomologica* 3: 45–62.
- Meyrick E (1935) In: Caradja A, Meyrick E (Eds) *Materialien zu einer Microlepidopteren Fauna der Chinesischen Provinzen Kiangsu, Chekiang und Hunan*. Friedländer und Sohn, Berlin, 96 pp.
- Nasu Y (2013) Tribe Olethreutini. In: Nasu Y, Hirowatari T, Kishida Y (Eds) *The Standard of Moths in Japan* (Vol. 4). Gakken Education Publishing, Tokyo, 202–224. [In Japanese]
- Pinkaew N (2007) New records and known species of the tribe Olethreutini (Lepidoptera: Tortricidae: Olethreutinae) from Thong Pha Phum National Park, Thailand. *The Thailand Natural History Museum Journal* 2(1): 1–18.
- Razowski J (1989) The genera of Tortricidae (Lepidoptera) Part II: Palaearctic Olethreutinae. *Acta Zoologica Cracoviensia* 32(7): 107–328.
- Walsingham L (1900) Asiatic Tortricidae. *Annals & Magazine of Natural History* 7(6): 121–137. [234–243] <https://doi.org/10.1080/00222930008678346>

Description of three new species of *Callyntrura* (*Japonphysa*) (Collembola, Entomobryidae) from China with the aid of DNA barcoding

Mei-Dong Jing¹, Yin-Huan Ding², Yi-Tong Ma¹

¹ School of Life Sciences, Nantong University, Nantong, Jiangsu 226000, China

² Department of Agronomy and Horticulture, Jiangsu Vocational College of Agriculture and Forestry, Jurong, Jiangsu 212400, China

Corresponding author: Yi-Tong Ma (mayitong@ntu.edu.cn)

Abstract

Callyntrura (*s.l.*) Börner, 1906 is the largest genus of the subfamily Saliniinae and contains 11 subgenera and 98 species from all over the world (mainly Asia), with eight species recorded from China. In the present paper, three new species of *Callyntrura* (*s.l.*) are described from China: *C. (Japonphysa) xinjianensis* **sp. nov.**; *C. (J.) tongguensis* **sp. nov.** and *C. (J.) raoi* **sp. nov.** Their differences in colour pattern, chaetotaxy and other characters are slight, however distances of COI mtDNA support their validation as three new distinct species. A key to the Chinese *Callyntrura* (*s.l.*) is provided.

Key words: Chaetotaxy, DNA sequence, identification key, Saliniinae, subgenus, taxonomy, Yoshii



Academic editor: Louis Deharveng

Received: 15 July 2023

Accepted: 29 November 2023

Published: 21 December 2023

ZooBank: <https://zoobank.org/4C4C934F-4A2F-4493-ABB5-C55604CE4A21>

Citation: Jing M-D, Ding Y-H, Ma Y-T (2023) Description of three new species of *Callyntrura* (*Japonphysa*) (Collembola, Entomobryidae) from China with the aid of DNA barcoding. ZooKeys 1187: 237–260. <https://doi.org/10.3897/zookeys.1187.109608>

Copyright: © Mei-Dong Jing et al.
This is an open access article distributed under terms of the Creative Commons Attribution License ([Attribution 4.0 International – CC BY 4.0](https://creativecommons.org/licenses/by/4.0/)).

Introduction

The genus *Callyntrura* (*s.l.*) Börner, 1906 was previously considered a member of the family Paronellidae, but now belongs to the family Entomobryidae (Godeiro et al. 2022). It is mainly characterized by the smooth dens, fusiform scales on body, the presence of frontal spines on the head and more than three teeth on the mucro. *Callyntrura* was subdivided into 11 subgenera on the base of labral chaetae, antennae, dental spines and other characters (Yoshii 1992). The subgenus *Japonphysa* was established by Yoshii in 1982 and it contains four species. The subgenus can be separated from the other subgenera of *Callyntrura* by the absence of modified labral chaetae and the presence of a blunt basal chaeta on the maxillary outer lobe.

Callyntrura (*s.l.*) specimens are medium-sized and their colour pattern plays a key role in its classification. So far, 97 species of *Callyntrura* have been described from Southeast and South Asia and one species from Africa and the descriptions of most species were quite simple (Bellinger et al. 1996–2023). Prior to this study, eight species belonging to four subgenera were described or reported from China (Ma 2013). Here we describe three new species of *Callyntrura* (*Japonphysa*) from China, based on their morphology and molecular data. A key to Chinese *Callyntrura* (*s.l.*) is also provided.

Materials and methods

Taxon sampling and specimen examinations

Specimens were collected with an aspirator and stored in 99% alcohol. They were mounted on glass slides in Marc André II solution, and were studied with a Leica DM2500 phase contrast microscope. Photographs were taken under a Leica DFC300 FX digital camera which mounted on the microscope and enhanced with Photoshop CS2 (Adobe Inc.). SEM photographs were taken under a ZEISS Gemini SEM 300 after the specimens were coated with a Leica EM ACE600. Type specimens are deposited in School of Life Sciences, Nantong University, Jiangsu, China.

The nomenclature of the dorsal macrochaetotaxy of the head and interocular chaetae are described following Jordana and Baquero (2005) and Mari-Mutt (1986). Labial chaetae are designated following Gisin (1964); labral and tergal chaetae of the body follow Szeptycki (1973, 1979); and teeth of the mucro follow Mitra (1974).

Molecular analysis

DNA was extracted from one specimen per species by using an Ezup Column Animal Genomic DNA Purification Kit (Sangon Biotech, Shanghai, China) following the manufacturer's standard protocols. Amplification of a 658 bp fragment of the mitochondrial COI gene was carried out using a Prime Thermal Cycler (TECHNE, Bibby Scientific Limited, Stone, Staffordshire, UK) in 25 µl volumes using Premix Taq polymerase system (Takara Bio, Otsu, Shiga, Japan). The primers and PCR programs followed Greenslade et al. (2011). All PCR products were checked on a 1% agarose gel electrophoresis. Successful products were purified and sequenced by Majorbio (Shanghai, China) on an ABI 3730XL DNA Analyser (Applied Biosystem, Foster City, CA, USA).

DNA sequences were assembled using Sequencher 4.5 (Gene Codes Corp), and then deposited in GenBank. Sequences were aligned by ClustalW implemented in MEGA 6 (Tamura et al. 2011) with default settings. Pairwise genetic distances were analyzed in MEGA 6 employing the Kimura 2-parameter (K2-P) model (Kimura 1980).

Abbreviations

Ant.	antennal segment(s);
Th.	thoracic segment(s);
Abd.	abdominal segment(s);
mac	macrochaeta(e);
mes	mesochaeta(e);
ms	specialised microchaeta(e);
sens	specialized ordinary chaeta(e).

Results

The distribution in China of the species described in present paper is shown in Fig. 1.

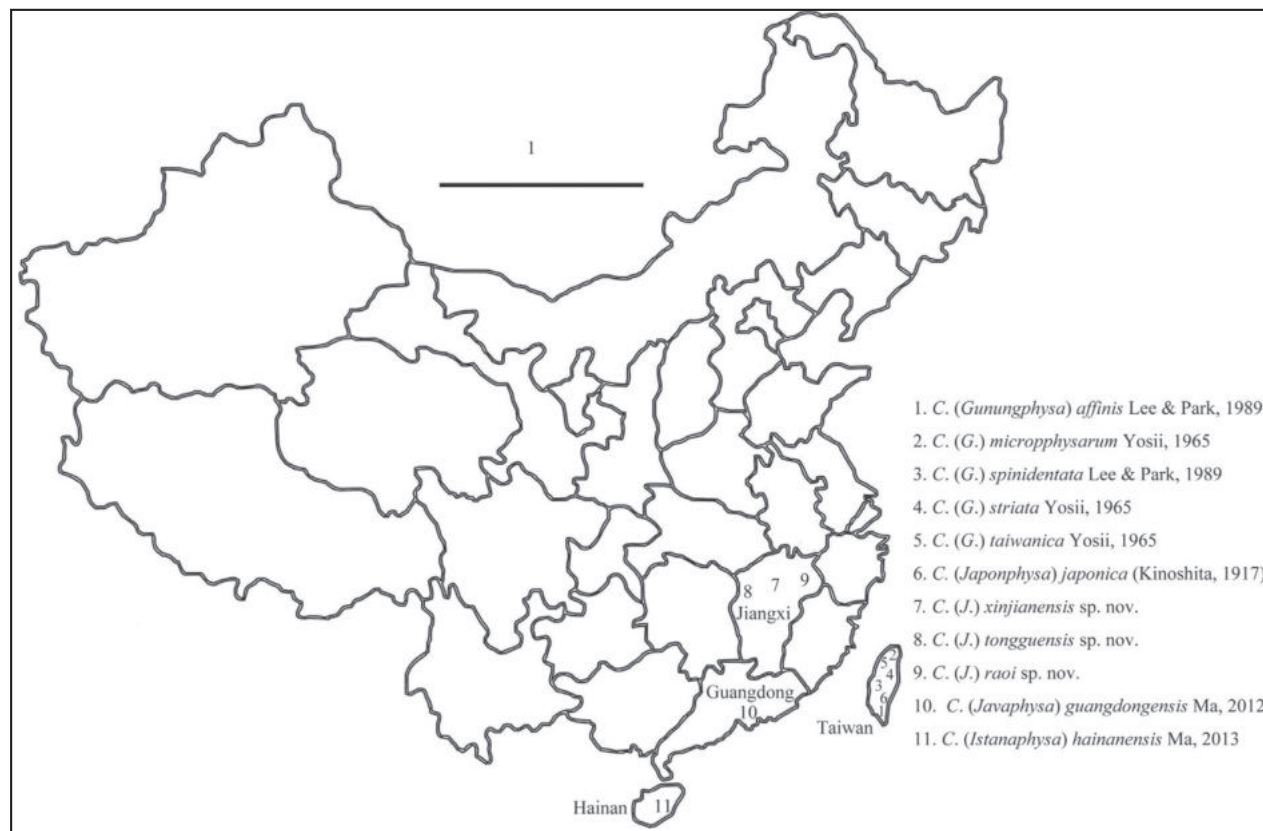


Figure 1. Record locality of all Chinese species of *Callyntrura* (s.l.) in China. Scale bar: 1000 km.

Class Collembola Lubbock, 1873

Order Entomobryomorpha Börner, 1913

Family Entomobryidae Tömösvary, 1882

Genus *Callyntrura* (s.l.) Börner, 1906

Diagnosis. Moderate size, usually 2–3 mm; antennae four segmented and without apical bulb; eyes 8+8; frontal spines on head 4+4; scales present on body; dens smooth; mucro almost square and with more than three teeth.

***Callyntrura (Japonphysa) xinjianensis* sp. nov.**

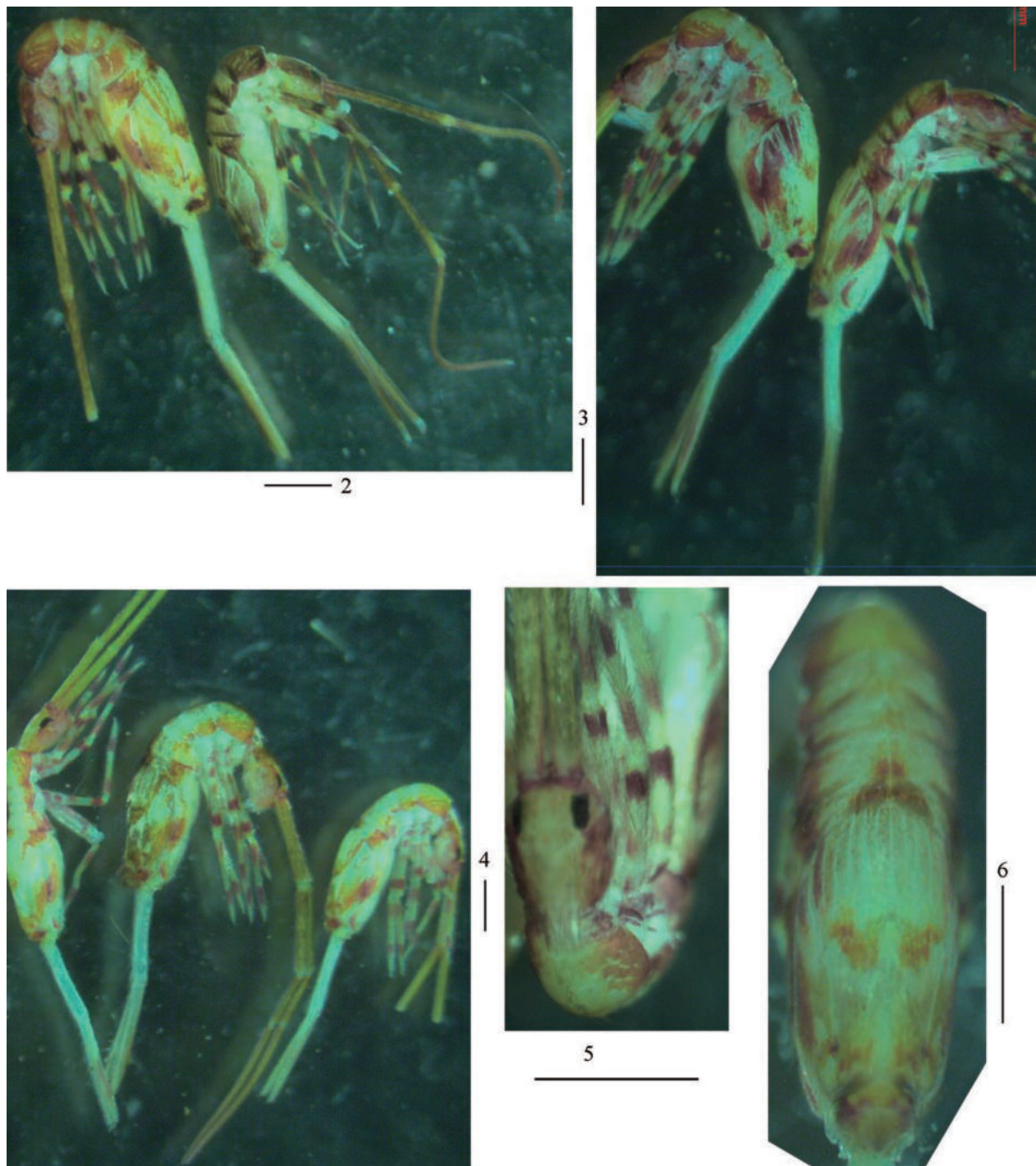
<https://zoobank.org/3984F42A-FBF7-4331-86D1-F2EE71F16DAE>

Figs 2–48, Table 1

Type material. Holotype. ♀ on slide, CHINA, Jiangxi Province, Nanchang City, Xinjian District, Meiling Town, Jiuxi Village, 12-XI-2020, 28°47'56"N, 115°45'11"E, 168 m asl, sample number 1243. **Paratypes.** 3♀♀ on slides, same data as holotype; 6♀♀ on slides, CHINA, Jiangxi Province, Nanchang City, Xinjian District, Meiling Town, Shizifeng Park, 12-XI-2020, 28°49'26"N, 115°43'06"E, 100 m asl, sample number 1242. All collected by Y-T Ma.

Description. Size. Body length up to 2.75 mm.

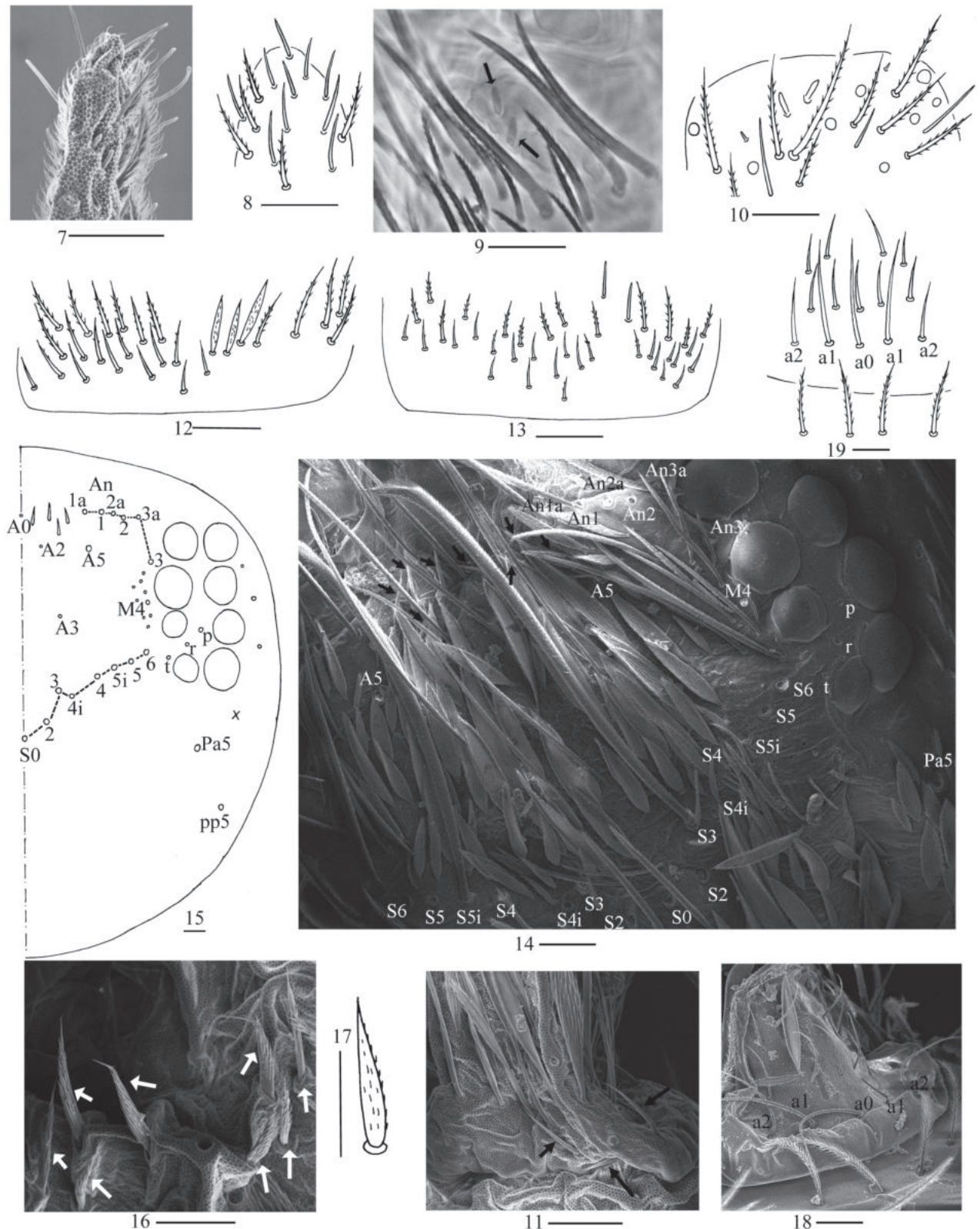
Coloration. Ground colour pale yellow; eye patches dark blue; brown stripe present from head to Abd. III laterally; middle part of Abd. II–III with brown



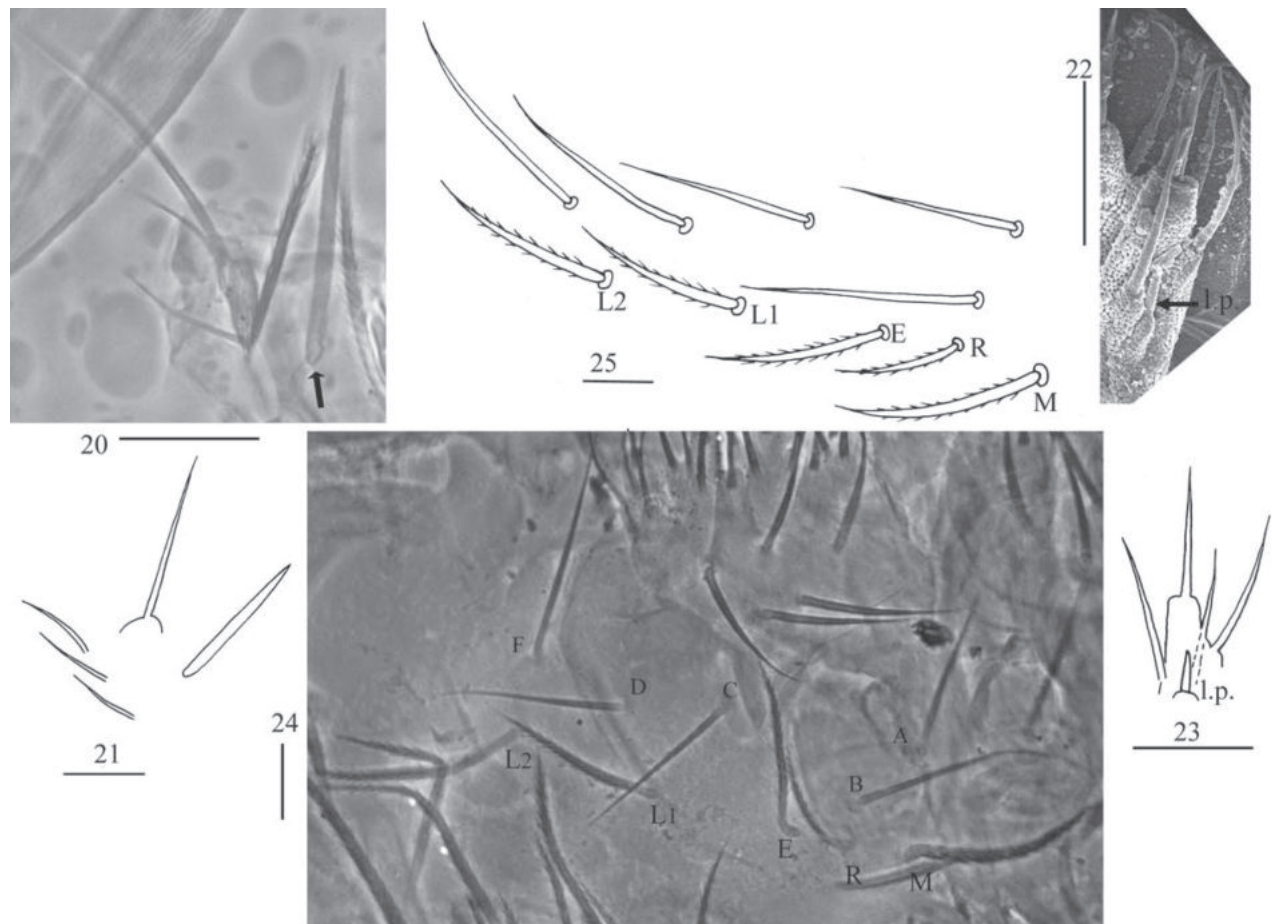
Figures 2–6. Habitus of *Callyntrura xinjianensis* sp. nov. 2–4 lateral view 5 dorsal view of head 6 dorsal view of trunk. Scale bars: 500 μ m.

pigment; medial and posterior margin of Abd. IV with pair of irregular brown patches, respectively; brown pigment scattered on basal Ant. I and distal Ant. IV, legs, anterior part of ventral tube and distal dentes (Figs 2–6).

Head. Antenna not annulated and 1.37–1.57 times length of body. Ratio of Ant. I–IV as 1.00/0.85–1.00/0.49–0.72/1.37–2.00. Distal part of Ant. IV with many sensory chaetae and normal ciliate chaetae, without apical bulb



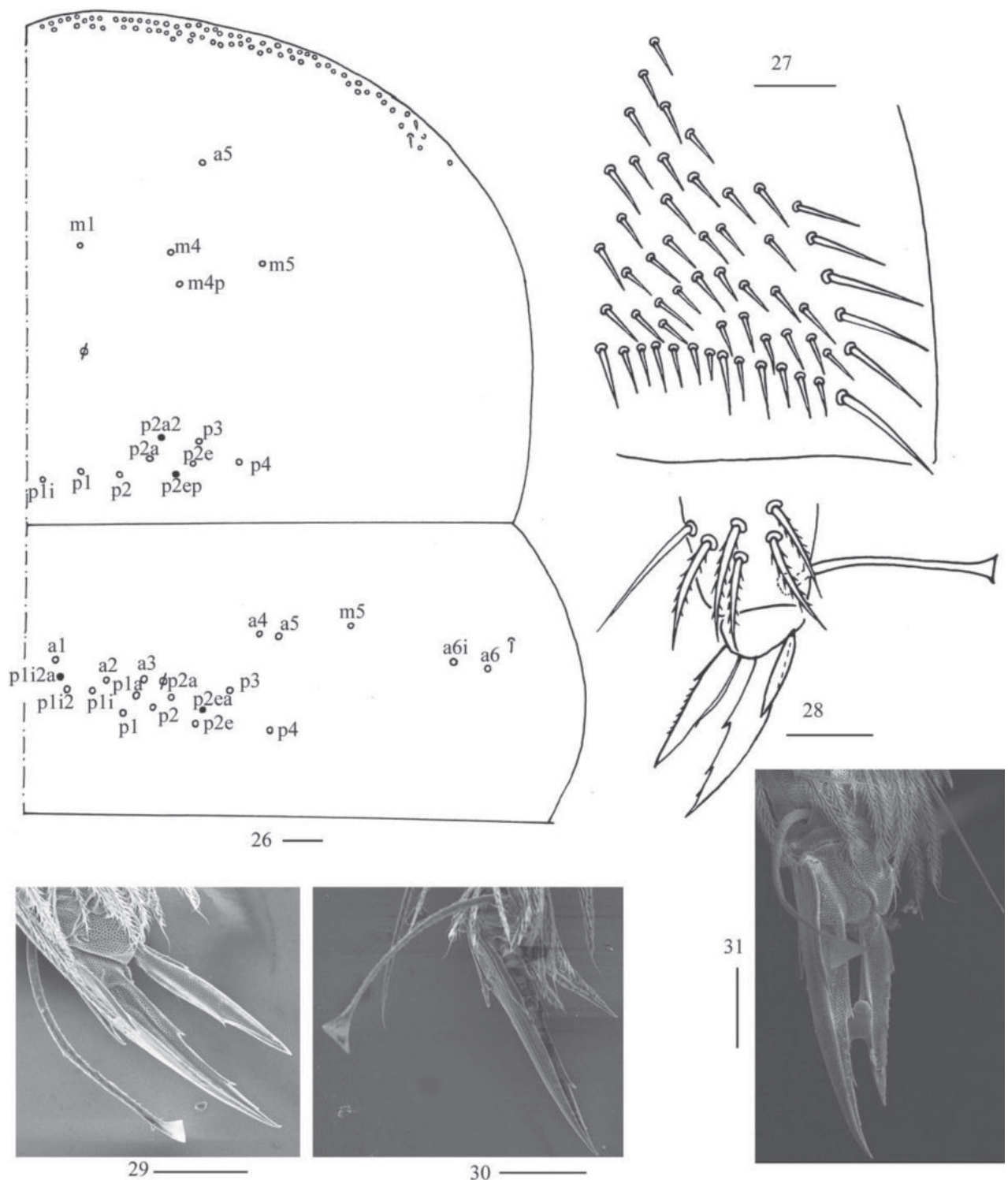
Figures 7–19. *Callyntrura xinjianensis* sp. nov. **7** SEM photomicrograph of apex of Ant. IV **8** apex of Ant. IV (dorsal view) **9** photomicrograph of distal Ant. III (arrow showing rod-like chaeta of Ant. III organ, ventral view) **10** distal Ant. III (ventral view) **11** SEM photomicrograph of basal Ant. I **12** basal Ant. I (dorsal view) **13** basal Ant. I (ventral view) **14** SEM photomicrograph of anterior part of dorsal head **15** dorsal head (right side) **16** SEM photomicrograph of frontal spines of head **17** frontal spine **18** SEM photomicrograph of prelabrum and labrum **19** prelabrum and labrum. Scale bars: 20 μ m.



Figures 20–25. *Callyntrura xinjianensis* sp. nov. **20** photomicrograph of maxillary palp and outer lobe (arrow showing basal chaeta, right side) **21** maxillary palp and outer lobe (right side) **22** SEM photomicrograph of labial palp E (right side) **23** labial palp E (right side) **24** photomicrograph of labial base (left side) **25** labial base (left side). Scale bars: 20 μ m.

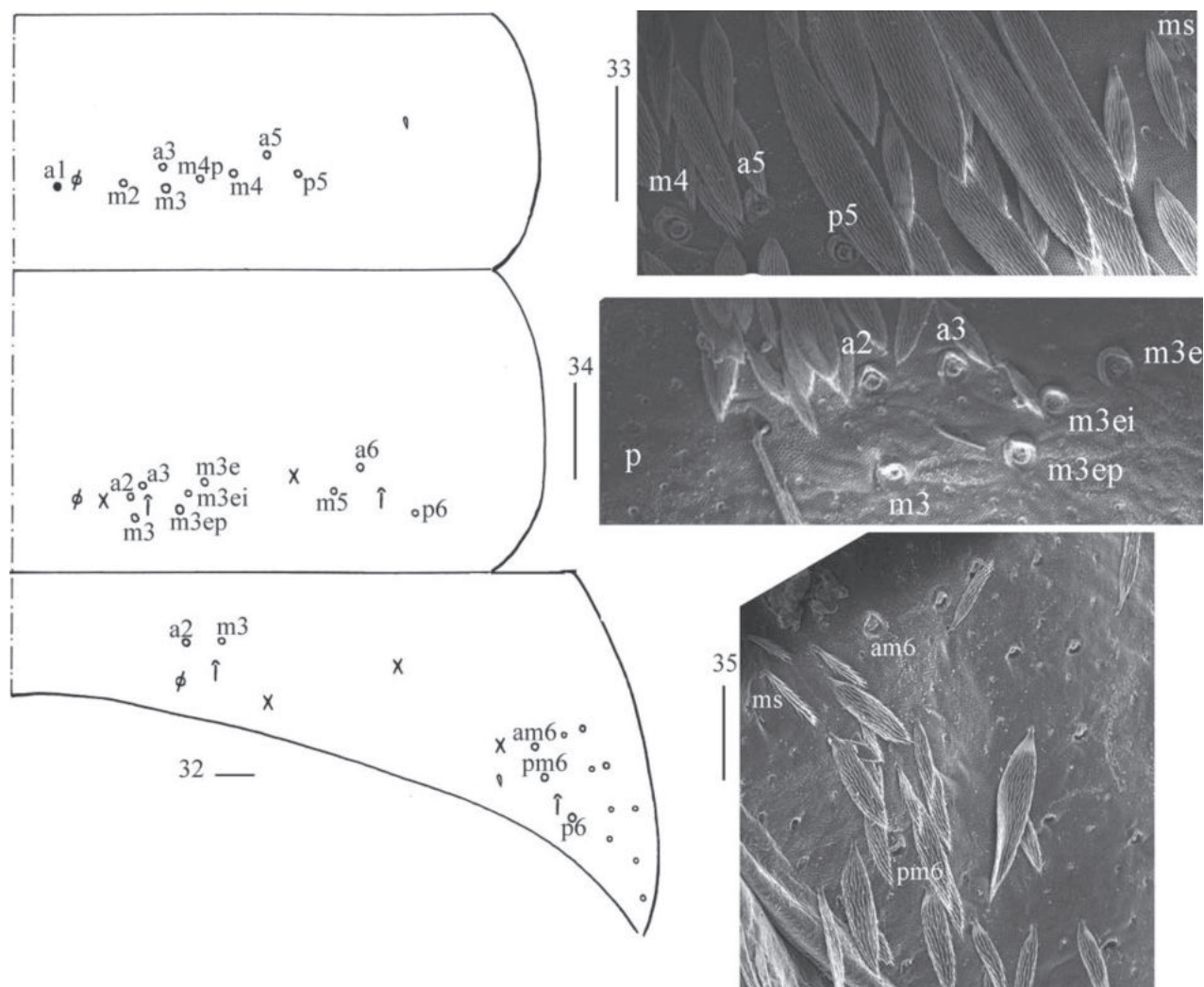
(Figs 7, 8). Ant. III organ with two rod-like chaetae (Figs 9, 10). Basal Ant. I with smooth chaetae (Figs 11–13). Dorsal chaetotaxy of head as in Figs 14, 15. An series with six mac, A with four mac or mes, S with eight mac, P with two mac. Eyes 8+8, G & H smaller than others; interocular chaetae as p, r, t; frontal spines 4+4, all serrate (Figs 16, 17). Prelabral chaetae four, ciliate; labral chaetae 5, 5, 4, smooth and pointed, a0, a1 longer than a2; labral papillae absent (Figs 18, 19). Basal chaeta on maxillary outer lobe thick and blunt; sublobal plate with three smooth chaetae-like processes (Figs 20, 21). Lateral process (l. p.) of labial palp E differentiated, as thick as normal chaeta, with tip not reaching apex of papilla E (Figs 22, 23). Labial base with MREL₁L₂, all ciliate and R 0.51–0.77 length of M (Figs 24, 25).

Thorax. Tergal ms formula on Th. II–Abd. V as 1, 0/1, 0, 1, 0, 0, sens as 1, 1/0, 2, 2, 31–44, 3 (Figs 26, 32, 36, 38). Th. II with medial five (m1, m4, m4p, a5, m5) mac, usually posterior nine (p1i, p1, p2, p2a, p2e, p3, p4 always present, p2a2 or p2ep rarely absent) mac, one ms and one sens. Th. III with anterior-lateral five (a4, a5, m5, a6i, a6), usually posterior 12–14 (p1i2a and p2ea sometimes absent) mac, one sens (Fig. 26). Trochanteral organ with 55–64 chaetae (Fig. 27). Tenent hair clavate and slightly ciliate, 1.00–1.20 as



Figures 26–31. *Callyntrura xinjianensis* sp. nov. **26** chaetotaxy of Th. II–III (right side, solid black dot meaning absence) **27** trochanteral organ **28** hind foot complex (lateral view) **29** SEM photomicrograph of fore foot complex (lateral view) **30** SEM photomicrograph of middle foot complex (lateral view) **31** SEM photomicrograph of hind foot complex (lateral view). Scale bars: 20 μ m.

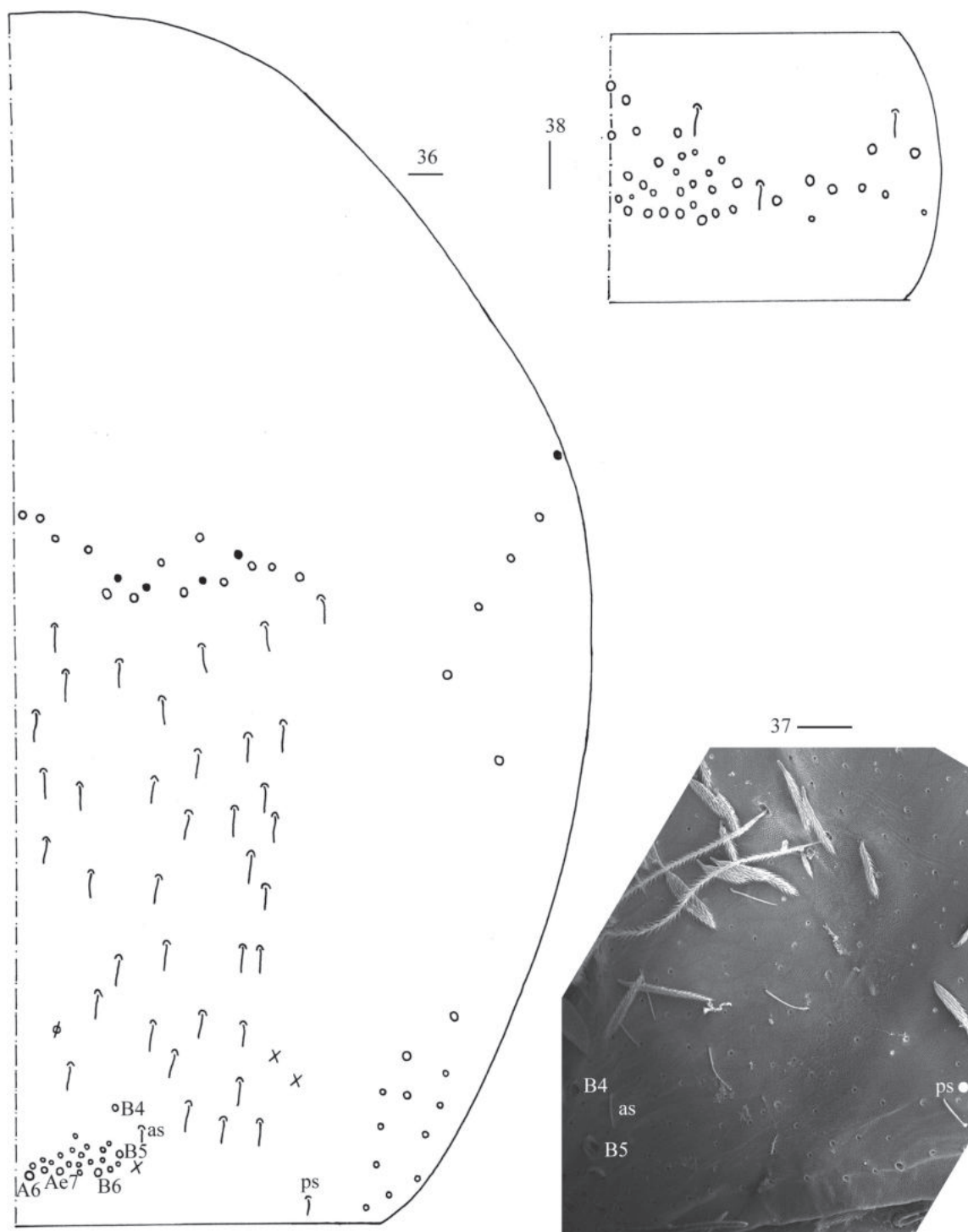
long as inner edge of unguis; unguis with four inner teeth, most distal tooth very faint, basal pair located at 0.30–0.42 distance from base of inner edge of unguis, unpaired teeth at 0.65–0.70 and 0.82–0.90 distance from base,



Figures 32–35. *Callyntrura xinjianensis* sp. nov. **32** chaetotaxy of Abd. I–III (right side, solid black dot meaning absence) **33** SEM photomicrograph of lateral Abd. I (right side) **34** SEM photomicrograph of central Abd. II (right side) **35** SEM photomicrograph of lateral Abd. III (right side). Scale bar: 20 μ m.

respectively; unguiculus lanceolate, with one median inner tooth and outer edge slightly serrate (Figs 28–31).

Abdomen. Range of Abd. IV length as 6.71–13.75 times as dorsal axial length of Abd. III. Abd. I usually with seven (a3, a5, m2, m3, m4, m4i, p5, a1 rarely present) mac and one ms (Figs 32, 33). Abd. II with central six (a2, a3, m3, m3e, m3ei, m3ep), lateral three (m5, a6, p6) mac and two sens (Figs 32, 34). Abd. III with central two (a2, m3), lateral three (am6, pm6, p6) mac and 7–11 mes, one ms and two sens (Figs 32, 35). Abd. IV with 29–42 elongate and two (as, ps) normal sens, medial 15–17 and posterior 13–24 mac or mes, lateral 8–9 mac (Figs 36, 37). Abd. V with three sens (Fig. 38). Ventral tube with 18–22 (rarely 37) ciliate chaetae on each side anteriorly (Fig. 39); numerous ciliate chaetae and two apical smooth chaetae posteriorly (Fig. 40); 14–26 smooth and 5–36 ciliate chaetae on each lateral flap (Fig. 41). Manubrial plaque with four ciliate mac and one pseudopore (Fig. 42). Dens without spines. Mucro with six (v1, v2, v3, d1, d2, i.l.) teeth (Figs 43–45).

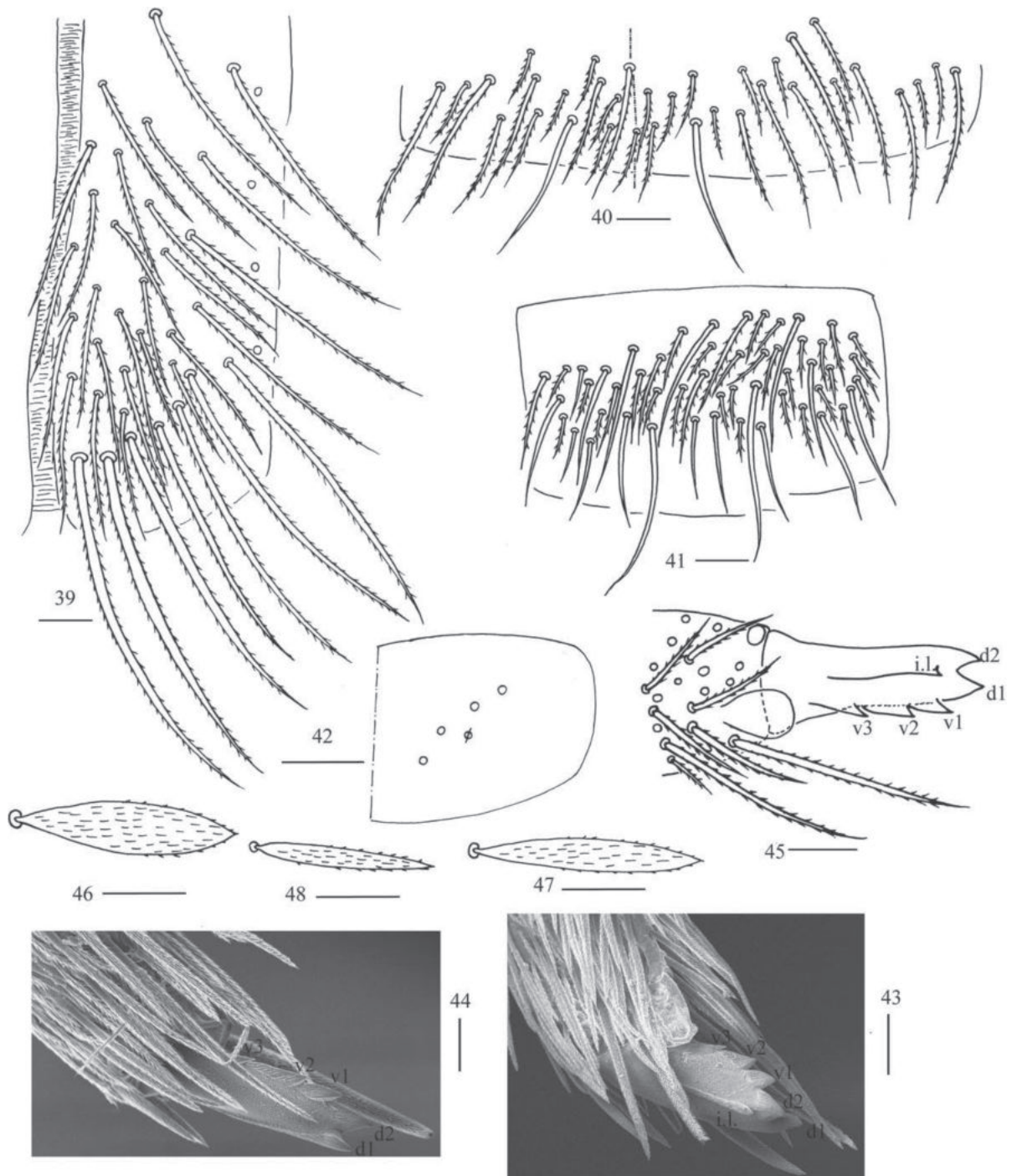


Figures 36–38. *Callyntrura xinjianensis* sp. nov. **36** chaetotaxy of Abd. IV (right side, solid black dot meaning absence) **37** photomicrograph of posterior-lateral Abd. IV (right side) **38** chaetotaxy of Abd. V (right side). Scale bars: 20 μ m.

Scales. Scales present on head, body, legs (Figs 46, 47); Ant. I–III and ventral side of manubrium and dens with narrower scales (Fig. 48). Ant. IV, ventral tube and tenaculum without scales.

Etymology. Named after its locality: Xinjian District.

Ecology. Found in the leaf litter, mainly composed of bamboo.



Figures 39–48. *Callyntrura xinjianensis* sp. nov. **39** anterior face of ventral tube **40** posterior face of ventral tube apically **41** lateral flap of ventral tube **42** manubrial plaque (dorsal view) **43** SEM photomicrographs of mucro (lateral view from internal side) **44** SEM photomicrographs of mucro (lateral view from external side) **45** mucro (upper view) **46, 47** scales on body **48** scale on antenna and furcula. Scale bars: 20 µm.

***Callyntrura (Japonphysa) tongguensis* sp. nov.**

<https://zoobank.org/E6007F8F-1468-44D3-B5F1-E209ED68279A>

Figs 49–70, Table 1

Type material. Holotype. ♀ on slide, CHINA, Jiangxi Province, Yichun City, Tonggu County, Tonggu Park, 9-XI-2020, 31°54'50"N, 114°22'36"E, 239 m asl, sample

number 1235. **Paratypes.** 2 ♀♀ on slides, same data as holotype. All collected by Y-T Ma.

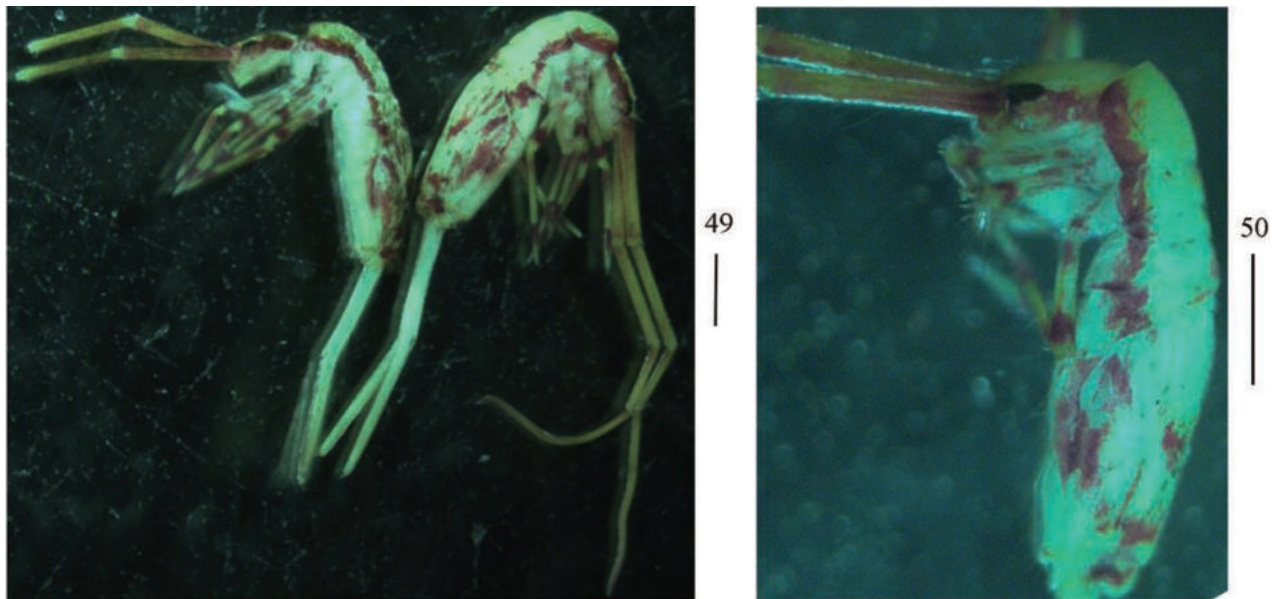
Description. Size. Body length up to 2.23 mm.

Coloration. Ground colour pale yellow; antennae with scattered brown pigment; eye patches dark blue; brown stripe present from head to Abd. III laterally; middle part of Abd. II–III with brown pigment; medial and posterior margin of Abd. IV with pair of irregular brown patches, respectively; brown pigment scattered on antennae and legs (Figs 49, 50).

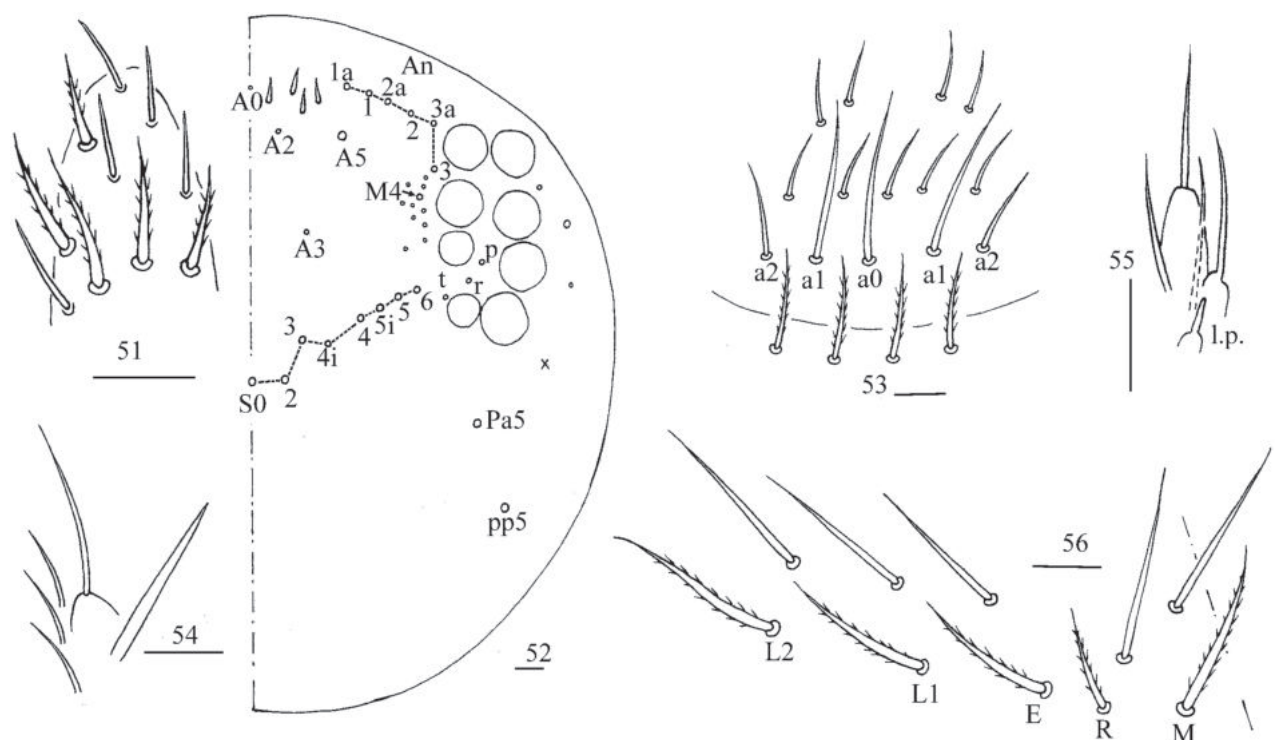
Head. Antenna not annulated and 1.45–1.49 times length of body. Ratio of Ant. I–IV as 1.00/0.90–0.98/0.58–0.63/1.50–1.54. Distal part of Ant. IV with many sensory chaetae and normal ciliate chaetae, without apical bulb (Fig. 51). Ant. III organ not clearly seen. Dorsal chaetotaxy of head as in Fig. 52, An series with six mac, A with four mac or mes, S with eight mac, P with two mac. Eyes 8+8, G & H smaller than others; interocular chaetae as p, r, t; frontal spines 4+4, all serrate. Prelabral chaetae four, ciliate; labral chaetae 5, 5, 4, smooth and pointed, a0, a1 longer than a2; labral papillae absent (Fig. 53). Basal chaeta on maxillary outer lobe thick and blunt; sublobal plate with three smooth chaetae-like processes (Fig. 54). Lateral process (l. p.) of labial palp E differentiated, as thick as normal chaeta, with tip not reaching apex of papilla E (Fig. 55). Labial base with MREL₁L₂, all ciliate and R 0.53–0.68 length of M (Fig. 56).

Table 1. Variation of tergal chaetotaxy of the new species (?, chaetotaxy not seen clearly).

Species	Specimen number	Th. II	Th. III	Abd. I	Abd. III	Abd. IV	
		posterior	posterior		lateral	medial	posterior
<i>Callyntrura xinjianensis</i> sp. nov.	1242-2A	9+?	12+13	7+7	?+?	16+17	23+24
	1242-2B	8+8	14+14	7+7	12+12	16+17	23+24
	1242-2C	8+8	12+13	7+7	13+13	16+17	17+17
	1242-3A	9+9	12+13	7+7	12+14	17+?	18+21
	1242-3B	9+9	13+13	7+7	11+13	15+16	17+17
	1242-3C	9+9	14+14	8+8	11+11	16+16	23+24
	1243-3A	9+9	13+13	7+7	12+?	15+?	14+18
	1243-3B	9+?	14+14	7+8	10+12	16+16	16+19
	1243-3C	9+9	12+13	8+8	14+?	?+?	18+23
	1243-3D	8+9	13+14	7+7	11+?	15+16	13+14
<i>C. tongguensis</i> sp. nov.	1235-3A	10+10	15+15	11+11	16+16	15+15	19+22
	1235-3B	10+10	14+15	11+11	14+14	17+17	20+23
	1235-3C	10+10	15+15	10+11	16+?	17+18	18+19
<i>C. raoi</i> sp. nov.	1244-1A	10+10	14+14	8+9	10+?	17+17	10+11
	1244-1B	10+10	14+14	?+?	15+15	15+15	14+18
	1244-1C	10+10	14+14	9+?	14+18	18+18	19+27
	1244-3A	9+9	14+14	9+9	14+?	15+15	22+24
	1244-3B	10+10	14+14	8+8	12+13	15+15	17+19
	1244-3C	10+10	14+14	8+8	12+?	13+14	10+11
	1244-4A	9+10	14+14	9+9	13+?	12+16	15+16
	1244-4C	9+9	14+14	9+9	17+?	13+14	12+12
	1244-4D	10+10	14+15	9+9	15+?	15+15	14+16

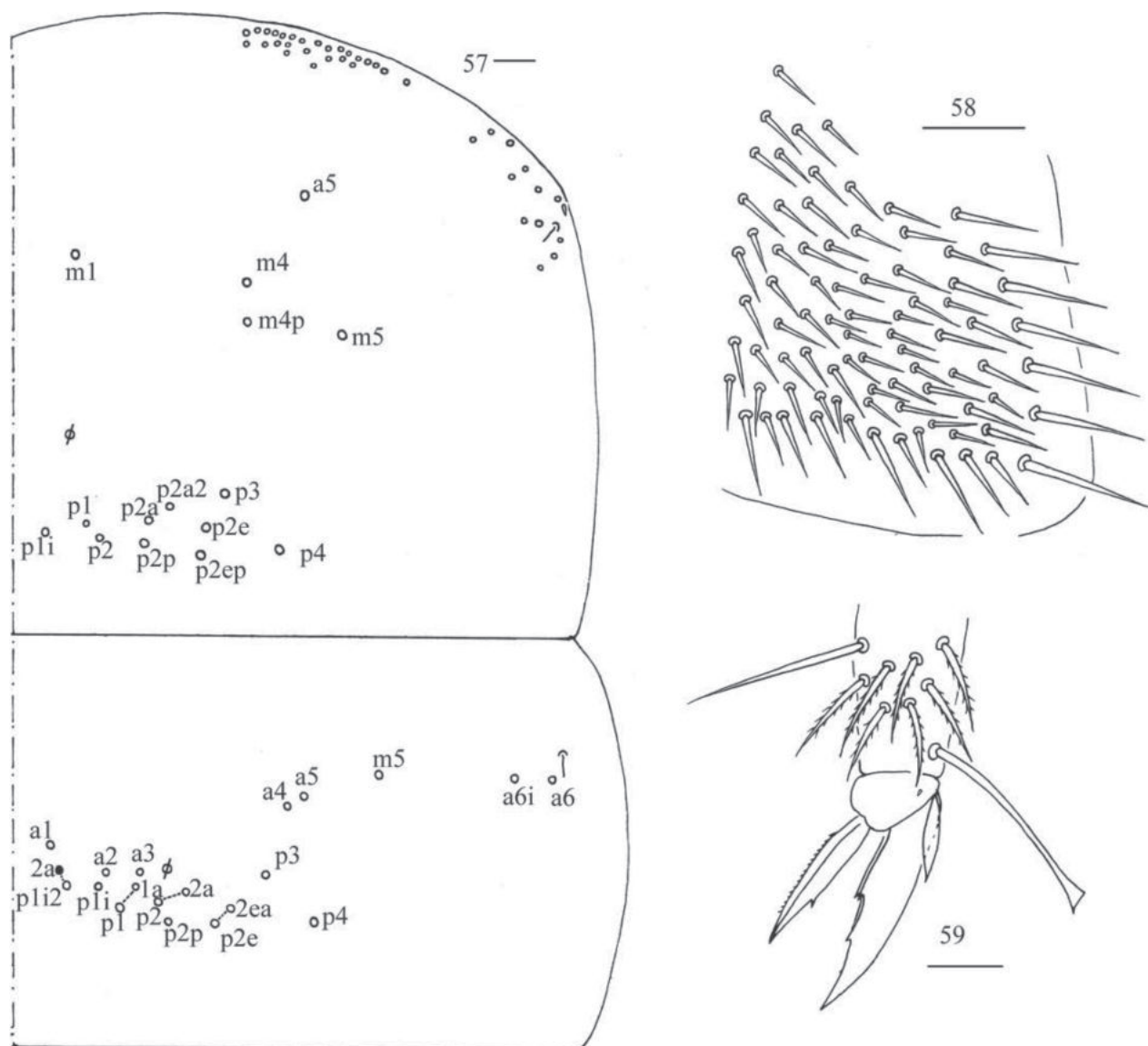


Figures 49, 50. Habitus of *Callyntrura tongguensis* sp. nov. (lateral view). Scale bars: 50 μ m.



Figures 51–56. *Callyntrura tongguensis* sp. nov. **51** apex of Ant. IV (dorsal view) **52** dorsal head (right side) **53** prelabrum and labrum **54** maxillary palp and outer lobe (right side) **55** labial palp E (right side) **56** labial base (left side). Scale bars: 20 μ m.

Thorax. Tergal ms formula on Th. II–Abd. V as 1, 0/1, 0, 1, 0, 0, sens as 1, 1/0, 2, 2, 37–41, 3 (Figs 57, 60–62). Th. II with medial five (m1, m4, m4p, a5, m5) mac, posterior ten (p1i, p1, p2, p2a, p2a2, p2p, p2e, p2ep, p3, p4) mac, one ms and one sens. Th. III with anterior-lateral five (a4, a5, m5, a6i, a6), usually posterior 15 (p1i2a rarely absent) mac, one sens (Fig. 57). Trochanteral organ with 63–81 chaetae (Fig. 58). Tenent hair clavate, 1.10–1.15 as long as inner edge of unguis; unguis with four inner teeth, most distal tooth very faint, basal



Figures 57–59. *Callyntrura tongguensis* sp. nov. **57** chaetotaxy of Th. II–III (right side, solid black dot meaning absence) **58** trochanteral organ **59** hind foot complex (lateral view). Scale bars: 20 μ m.

pair located at 0.37–0.41 distance from base of inner edge of unguis, unpaired teeth at 0.58–0.61 and 0.70–0.78 distance from base, respectively; unguiculus lanceolate, with one inner tooth and outer edge slightly serrate (Fig. 59).

Abdomen. Range of Abd. IV length as 10.00–12.00 times as dorsal axial length of Abd. III. Abd. I usually with 11 (a1–3, a5i, a5, a5p, m2–4, m4i, p5 rarely absent) mac and one ms. Abd. II with central six (a2, a3, m3, m3e, m3ei, m3ep), lateral three (m5, a6, p6) mac. Abd. III with central two (a2, m3), lateral three (am6, pm6, p6) mac and 10–14 mes (Fig. 60). Abd. IV with 35–39 elongate and two (as, ps) normal sens, medial 15–18 and posterior 18–23 mac or mes, lateral 8–9 mac (Fig. 61). Abd. V with three sens (Fig. 62). Ventral tube with 25–29 ciliate chaetae on each side anteriorly (Fig. 63); numerous ciliate chaetae and 2–3 apical smooth chaetae posteriorly (Fig. 64); 17–24 smooth and 10–17 ciliate chaetae on each lateral flap (Fig. 65). Manubrial plaque with four ciliate mac and one pseudopore (Fig. 66). Dens without spines. Mucro with six (v1, v2, v3, d1, d2, i.l.) teeth (Fig. 67).

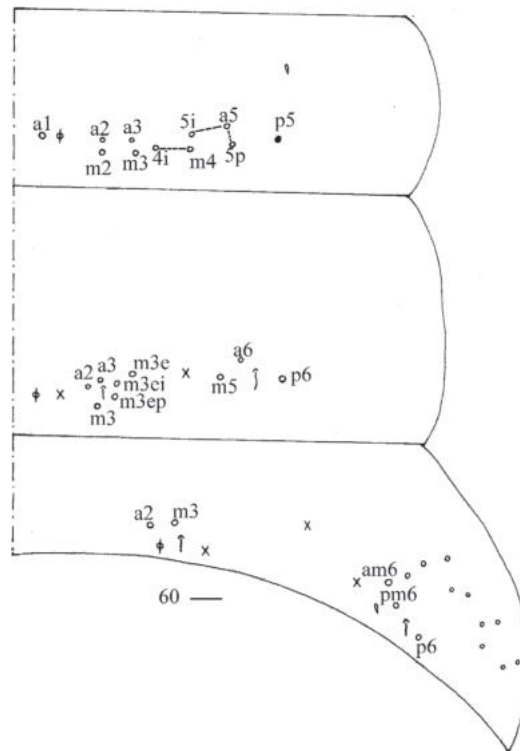
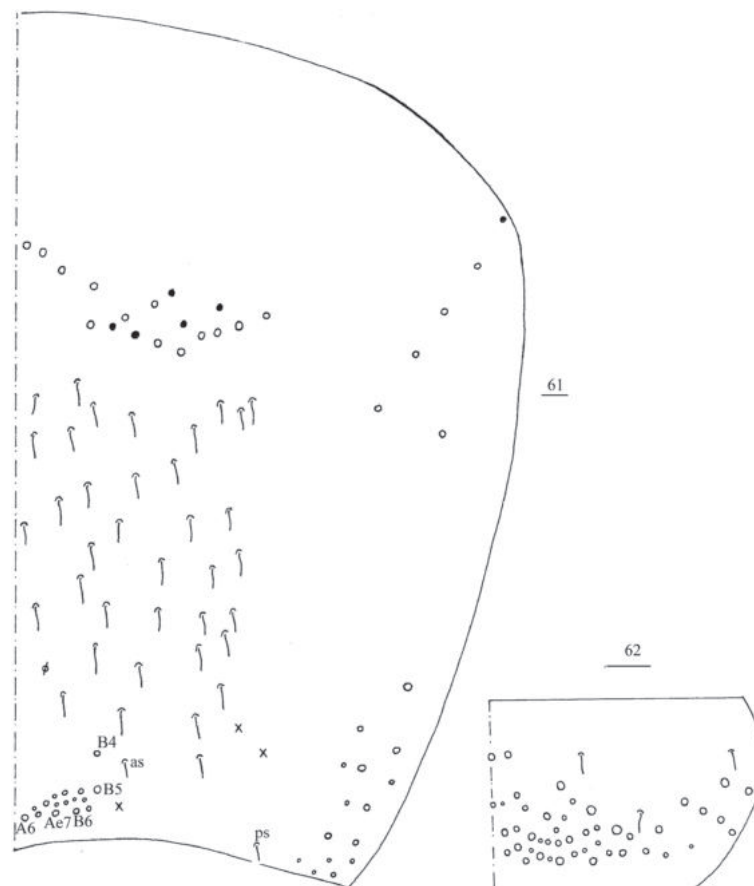
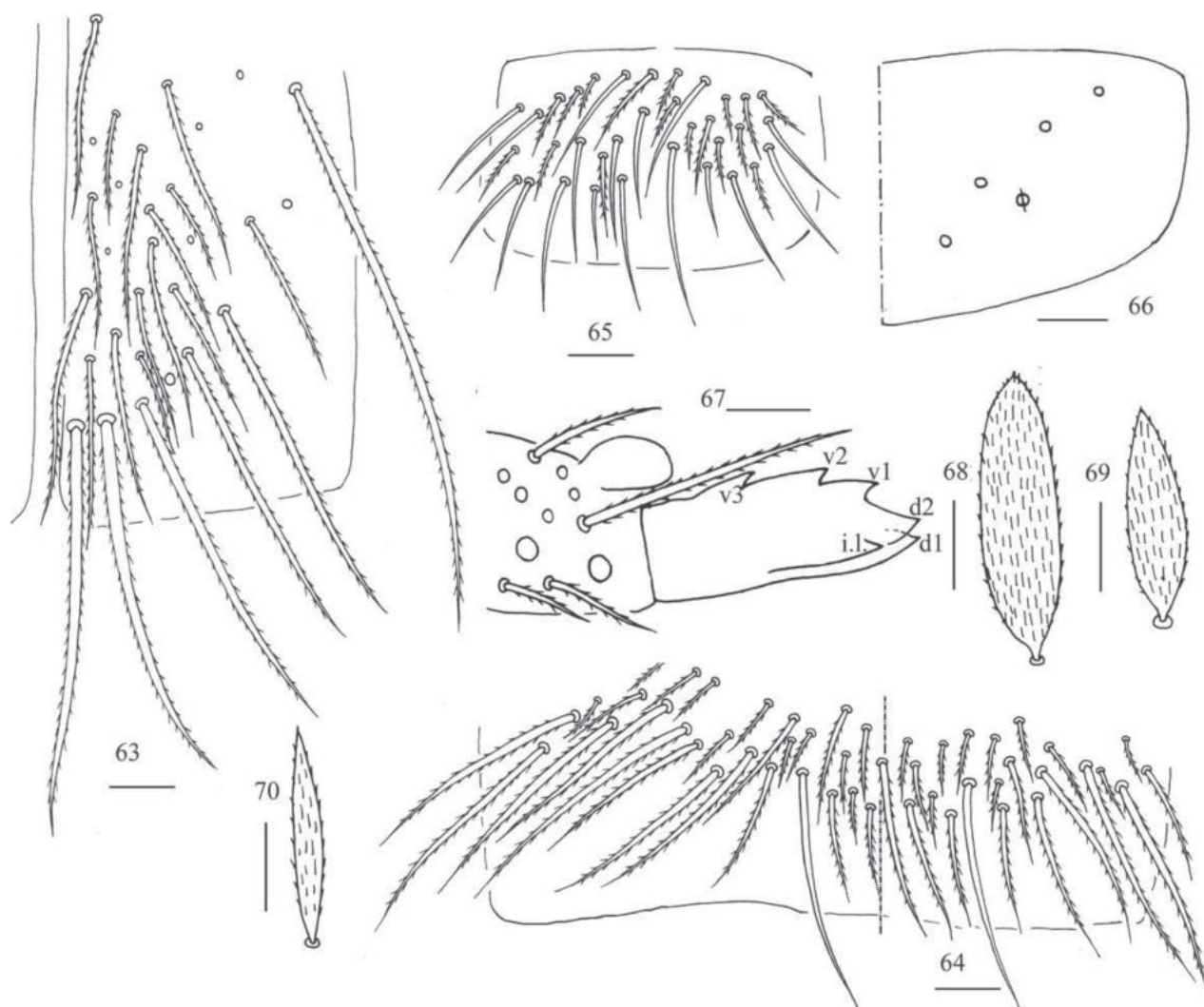


Figure 60. Chaetotaxy of Abd. I–III of *Callyntrura tongguensis* sp. nov. (right side, solid black dot meaning absence). Scale bar: 20 μ m.



Figures 61, 62. *Callyntrura tongguensis* sp. nov. **61** chaetotaxy of Abd. IV (right side, solid black dot meaning absence) **62** chaetotaxy of Abd. V (right side). Scale bars: 20 μ m.



Figures 63–70. *Callyntrura tongguensis* sp. nov. **63** anterior face of ventral tube **64** posterior face of ventral tube apically **65** lateral flap of ventral tube **66** manubrial plaque (dorsal view) **67** mucro (lateral view from internal side) **68**, **69** scales on body **70** scale on antenna and furcula. Scale bars: 20 μ m.

Scales. Scales present on head, body, legs (Figs 68, 69); Ant. I–III and ventral side of manubrium and dens with narrower scales (Fig. 70). Ant. IV, ventral tube and tenaculum without scales.

Etymology. Named after its locality: Tonggu County.

Ecology. Found in the leaf litter.

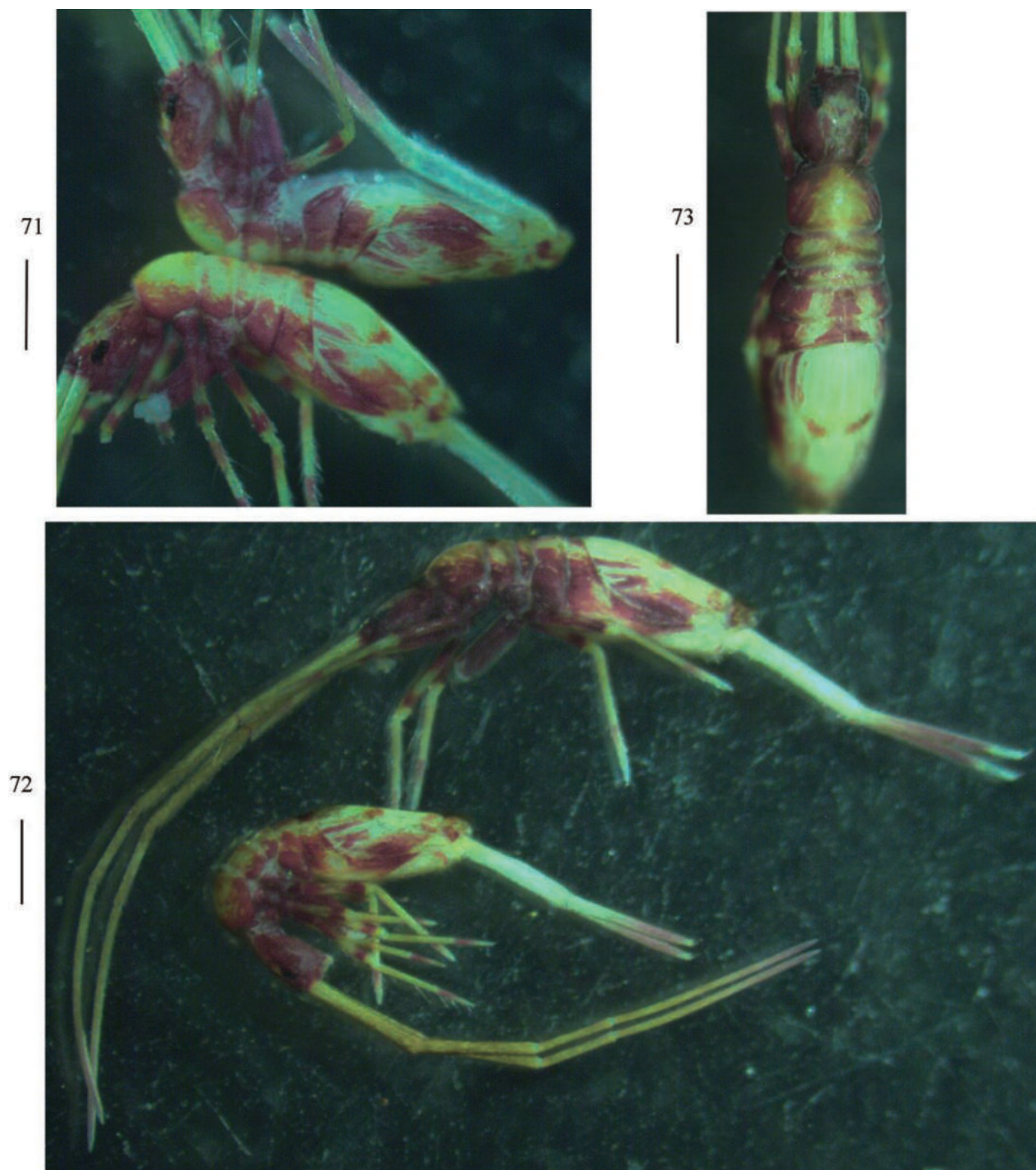
***Callyntrura (Japonphysa) raoi* sp. nov.**

<https://zoobank.org/D2240BC8-FC64-4525-B39B-8AC1E7C68077>

Figs 71–95, Table 1

Type material. Holotype. 1 ♀ on slide, CHINA, Jiangxi Province, Shangrao City, Dexing City, Raoshoukun Memorial Park, 13-XI-2020, 28°57'20"N, 117°34'08"E, 88 m asl, sample number 1244. **Paratypes.** 8 ♀♀ on slides, same data as holotype. All collected by Y-T Ma.

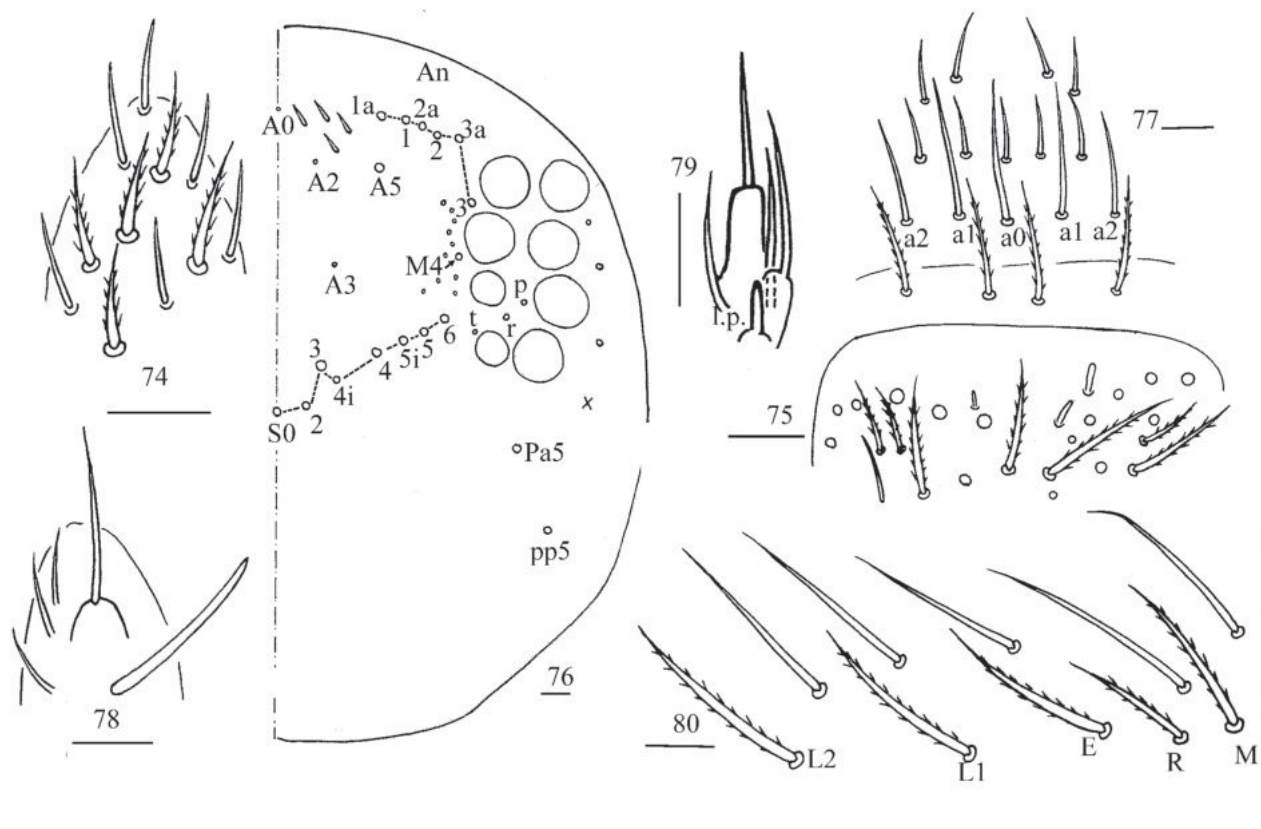
Description. Size. Body length up to 2.45 mm.



Figures 71–73. Habitus of *Callyntrura raoi* sp. nov. 71, 72 lateral view 73 dorsal view. Scale bars: 500 μ m.

Coloration. Ground colour pale yellow; eye patches dark blue; head almost brown entirely; brown stripe present from Th. II to Abd. III laterally; ventral tube, middle part of Abd. II–III brown pigmented; medial and posterior margin of Abd. IV with pair of irregular brown patches, respectively; brown pigment present also on legs, distal Ant. IV and distal dentes (Figs 71–73).

Head. Antenna not annulated and 1.32–1.53 times length of body. Ratio of Ant. I–IV as 1.00/0.92–1.00/0.60–0.75/1.60–2.04. Distal part of Ant. IV with many sensory chaetae and normal ciliate chaetae, without apical bulb (Fig. 74).

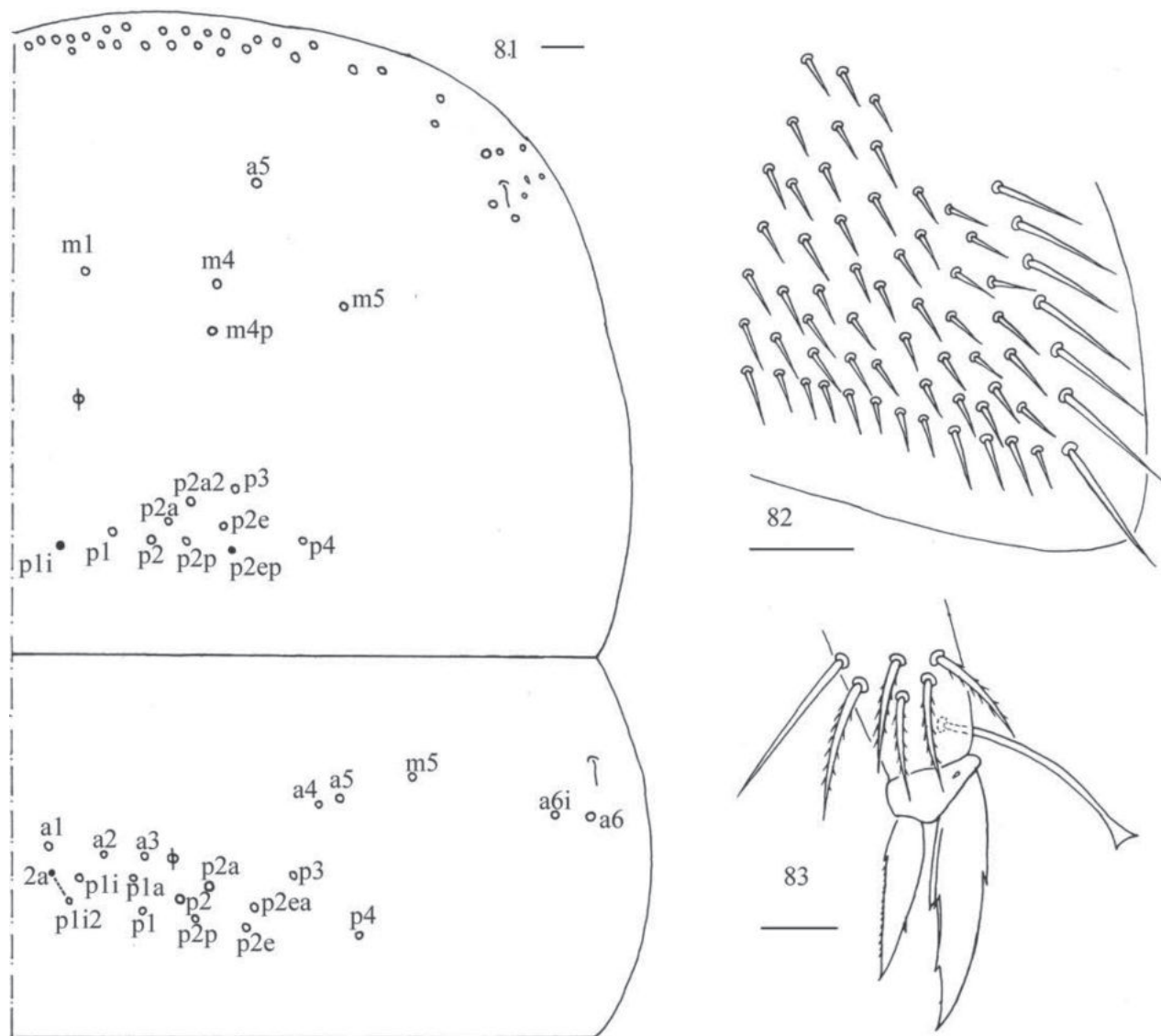


Figures 74–80. *Callyntrura raoi* sp. nov. **74** apex of Ant. IV (dorsal view) **75** distal Ant. III (ventral view) **76** dorsal head **77** prelabrum and labrum **78** maxillary palp and outer lobe (right side) **79** labial palp E (right side) **80** labial base (left side). Scale bars: 20 μ m.

Ant III organ with two rod-like chaetae (Fig. 75). Dorsal chaetotaxy of head as in Fig. 76, An series with six mac, A with four mac or mes, S with eight mac, P with two mac. Eyes 8+8, G & H smaller than others; interocular chaetae as p, r, t; frontal spines 4+4, all serrate. Prelabral chaetae four, ciliate; labral chaetae 5, 5, 4, smooth and pointed, a0, a1 longer than a2; labral papillae absent (Fig. 77). Basal chaeta on maxillary outer lobe thick and blunt; sublobal plate with three smooth chaetae-like processes (Fig. 78). Lateral process (l. p.) of labial palp E differentiated, as thick as normal chaeta, with tip not reaching apex of papilla E (Fig. 79). Labial base with MREL₁L₂, all ciliate and R 0.51–0.77 length of M (Fig. 80).

Thorax. Tergal ms formula on Th. II–Abd. V as 1, 0/1, 0, 1, 0, 0, sens as 1, 1/0, 2, 2, 29–42, 3 (Figs 81, 84–86). Th. II with medial five mac, usually posterior 10 (p1i, p1, p2, p2a, p2a2, p2p, p2e, p2ep, p3, p4, p1i or p2ep rarely absent) mac, one ms and one sens. Th. III with anterior-lateral five (a4, a5, m5, a6i, a6), usually posterior 14 mac (p2a rarely present), one sens (Fig. 81). Trochanteral organ with 63–64 chaetae (Fig. 82). Tenent hair clavate, 1.06–1.20 as long as inner edge of unguis; unguis with four inner teeth, most distal tooth very faint, basal pair located at 0.31–0.42 distance from base of inner edge of unguis, unpaired teeth at 0.66–0.68 and 0.82–0.89 distance from base, respectively; unguiculus lanceolate, with one inner tooth and outer edge slightly serrate (Fig. 83).

Abdomen. Range of Abd. IV length as 7.02–10.67 times as dorsal axial length of Abd. III. Abd. I with 8–9 (a3, a5, a5p, m2–4, m4 always present, a1, a2 or a5i sometimes absent) mac and one ms. Abd. II with central six (a2, a3, m3, m3e, m3ei,



Figures 81–83. *Callyntrura raoi* sp. nov. **81** chaetotaxy of Th. II–III (right side, solid black dot meaning absence) **82** trochanteral organ **83** hind foot complex (lateral view). Scale bars: 20 μm.

m3ep), lateral three (m5, a6, p6) mac. Abd. III with central two (a2, m3), lateral three (am6, pm6, p6) mac and 8–13 mes (Fig. 84). Abd. IV with 27–40 elongate and two (as, ps) normal sens, medial 14–18 and posterior 10–27 mac or mes, lateral 8–9 mac (Fig. 85). Abd. V with three sens (Fig. 86). Ventral tube with 17 ciliate chaetae on each side anteriorly (Fig. 87); numerous ciliate chaetae and two apical smooth chaetae posteriorly (Fig. 88); 14–21 smooth and 6–19 ciliate chaetae on lateral flap (Fig. 89). Manubrial plaque with four ciliate mac and one pseudopore (Fig. 90). Dens without spines. Mucro with six (v1, v2, v3, d1, d2, i.l.) teeth (Figs 91, 92).

Scales. Scales present on head, body, legs (Figs 93, 94); Ant. I–III and ventral side of manubrium and dens with narrower scales (Fig. 95). Ant. IV, ventral tube and tenaculum without scales.

Etymology. “*raoi*” (in apposition) refers to Lieutenant General Shoukun Rao, who made immortal achievements in the Chinese People’s War of Resistance against Japanese Aggression and the War of Liberation.

Ecology. Found in the leaf litter.

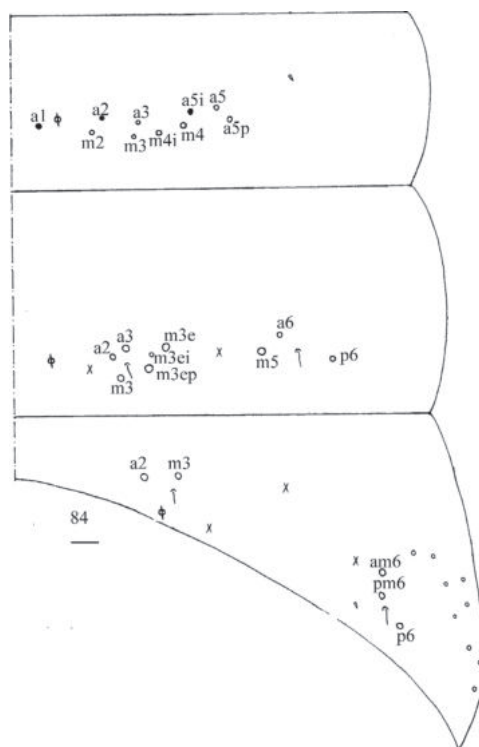
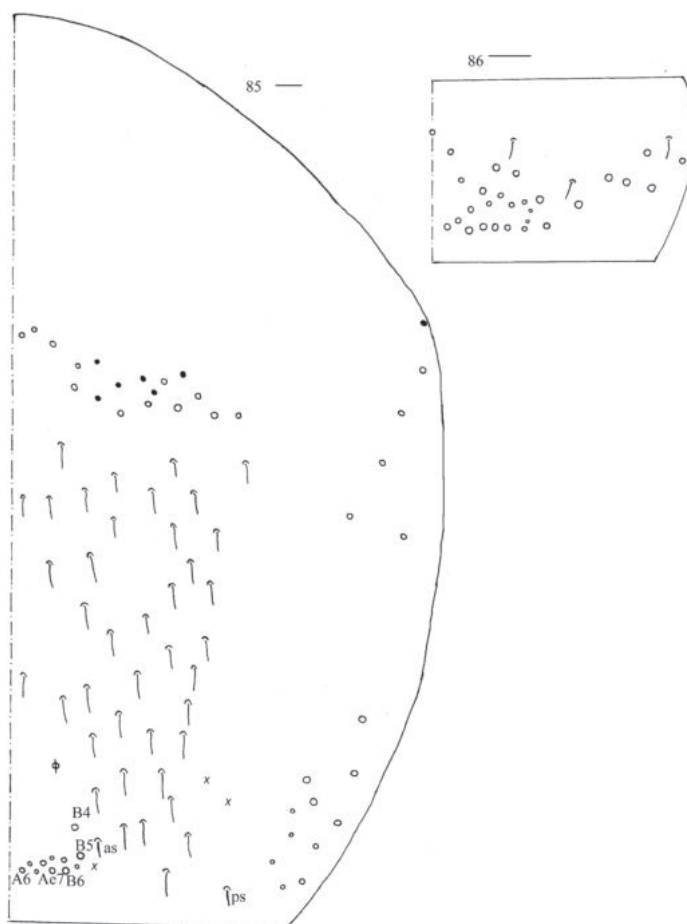
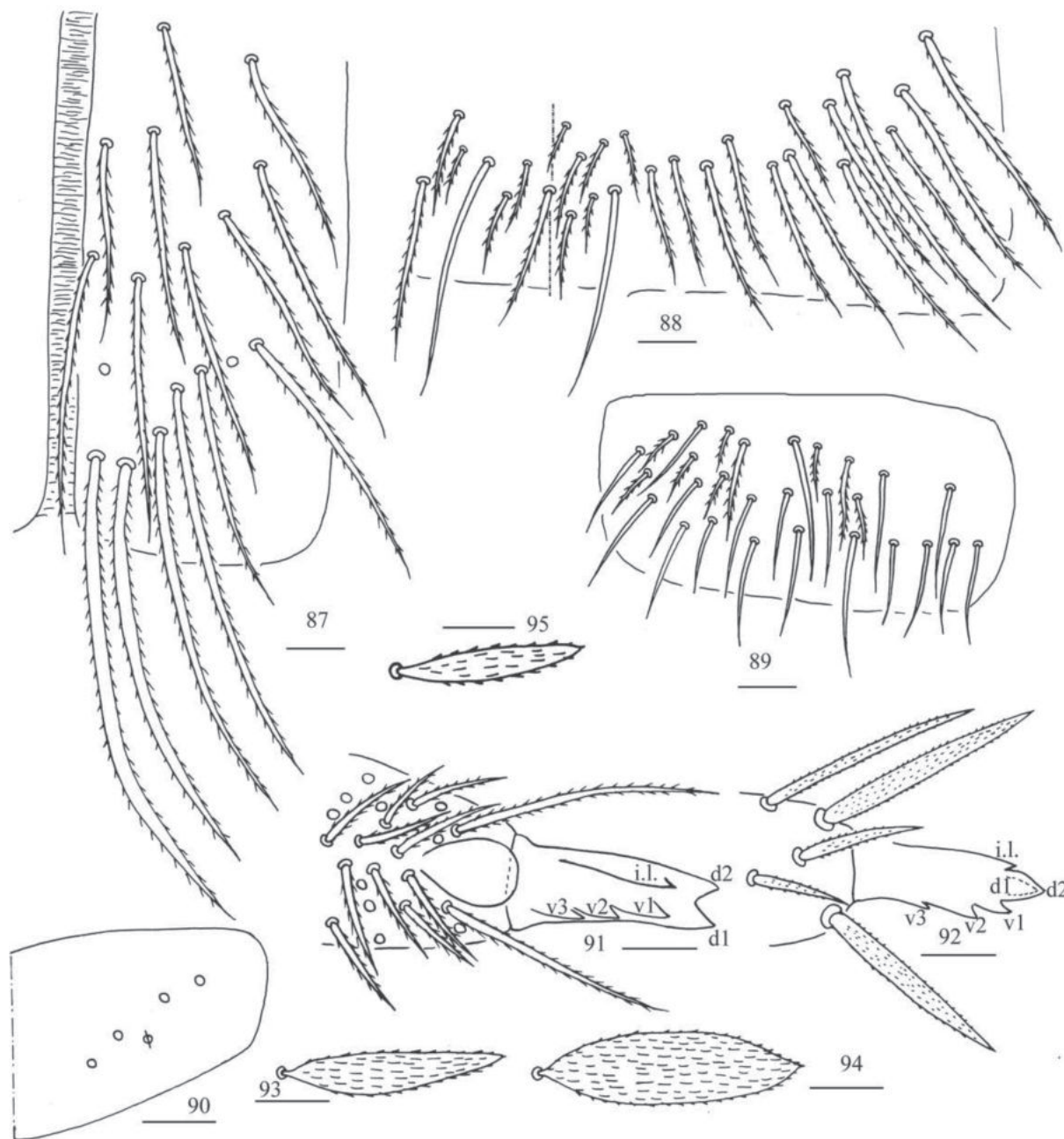


Figure 84. Chaetotaxy of Abd. I–III of *Callyntrura raoi* sp. nov. (right side, solid black dot meaning absence). Scale bar: 20 μ m.



Figures 85, 86. *Callyntrura raoi* sp. nov. **85** chaetotaxy of Abd. IV (right side, solid black dot meaning absence) **86** chaetotaxy of Abd. V (right side). Scale bars: 20 μ m.



Figures 87–95. *Callyntrura raoi* sp. nov. **87** anterior face of ventral tube **88** posterior face of ventral tube apically (partially) **89** lateral flap of ventral tube **90** manubrial plaque (dorsal view) **91** mucro (upper view) **92** mucro (ventral view) **93, 94** scales on body **95** scale on antenna and furcula. Scale bars: 20 μ m.

Remarks. The three new species are very similar in overall chaetotaxy, colour pattern and other characters. The chaetotaxy of each studied specimen is listed in Table 1, and the differences between these three species are slight. One main difference in chaetotaxy is that Abd. I has 7(8), 11, 8–9 mac in *C. (J.) xinjianensis* sp. nov., *C. (J.) tongguensis* sp. nov. and *C. (J.) raoi* sp. nov., respectively. Another difference is p2p mac on Th. II is absent in *C. (J.) xinjianensis* sp. nov., but present in the latter two new species. One main difference in colour pattern between them is that only the lateral side of the head is brown pigmented in *C. (J.) xinjianensis* sp. nov., and *C. (J.) tongguensis* sp. nov., but almost the entire head is brown in *C. (J.) raoi* sp. nov. The brown pigment on the ventral tube is

present anteriorly in *C. (J.) xinjianensis* sp. nov., absent in *C. (J.) tongguensis* sp. nov. and present almost entirely in *C. (J.) raoi* sp. nov.

The subgenus *Japonphysa* contains four species at present: *C. (J.) japonica* (Kinoshita, 1917), *C. (J.) oligosetosa* Kim, Rojanavongse & Lee, 1999, *C. (J.) semilineata* Yosii, 1961 and *C. (J.) unilineata* Yosii, 1961. The differences between the three new species and the four known species are great, especially in chaetotaxy of body (Table 2).

Molecular results

Sequenced individuals in the present study had a mean K2-P distance of COI sequences between 0.190–0.197 (about 19%). The shortest interspecific distance was 0.190 between *C. tongguensis* sp. nov. and *C. raoi* sp. nov. and the longest was 0.197 between *C. tongguensis* sp. nov. and *C. xinjianensis* sp. nov. (Table 3). Therefore, the interspecific distances of COI between the three new species were more than the accepted barcoding gap recently reported for the species of Entomobryidae (Zhang et al. 2018b) and Tomoceridae (Yu et al. 2018). The molecular distances coincided with the morphological divergences, thus further supporting the distinction of the three species.

Table 2. Comparison between the new species and all known species of *Callyntrura (Japonphysa)*.

Characters	<i>C. (J.) xinjianensis</i> sp. nov.	<i>C. (J.) tongguensis</i> sp. nov.	<i>C. (J.) raoi</i> sp. nov.	<i>C. (J.) japonica</i>	<i>C. (J.) oligosetosa</i>	<i>C. (J.) semilineata</i>	<i>C. (J.) unilineata</i>
Brown pigment on head	laterally	laterally	almost entirely	entirely	laterally	laterally	laterally
Brown pigment on ventral tube	anteriorly	absent	almost entirely	entirely	absent	absent	absent
Chaetae on labial base	MREL ₁ L ₂	MREL ₁ L ₂	MREL ₁ L ₂	MREL ₁ L ₂ *	not known	not known	MREL ₁ L ₂
Posterior mac on Th. II	8–9 (p2p absent)	10 (p2p present)	9–10 (p2p present)	7*	0	4	4
Posterior mac on Th. III	12–14	15	14	10*	0	9	7
Mac on Abd. I	7 (rarely 8)	11 (rarely 10)	8–9	6*	7	7	7
Central mac on Abd. II	6	6	6	5*	4	5	5
Central mac on Abd. III	2	2	2	2*	1	2	2
Inner teeth on unguis	4	4	4	3*	4	3	3–4
Anterior chaetae on ventral tube	18–22	25–29	17	not known	7	not known	not known

* based on Yoshii's description (Yoshii 1982).

Table 3. Genetic distances (mean K2-P divergence) of the COI sequences between the new described species.

Species	<i>C. (J.) tongguensis</i> sp. nov.	<i>C. (J.) raoi</i> sp. nov.	<i>C. (J.) xinjianensis</i> sp. nov.	GenBank Accession Numbers
<i>C. (J.) tongguensis</i> sp. nov.				OQ940723
<i>C. (J.) raoi</i> sp. nov.	0.190			OQ940724
<i>C. (J.) xinjianensis</i> sp. nov.	0.197	0.196		OQ940725

Discussion

Colour pattern usually plays a very important role in the classification of Collembola and many species were described based on it previously. Although colour pattern is a good character and intraspecific variability is low in *Callyntrura* taxa, it is sometimes very difficult for taxonomists to distinguish those different species who share similar colouration. DNA barcoding is a good tool to separate species

with a similar colour pattern and well used in classification in some genera of Collembola, such as *Coecobrya* (Nilsai et al. 2017; Zhang et al. 2018a), *Dicranocentrus* (Zhang et al. 2018b) and *Tomocerus* (Yu et al. 2016, 2017; Gong et al. 2018).

Key to the Chinese species of *Callyntrura* (s.l.)

- 1 No labral chaetae modified (subgenus *Japonphysa*) 2
- Part or all chaetae on the first row of labrum modified 5
- 2 Pigment present on Th. II–Abd. III entirely
..... ***C. (Japonphysa) japonica* (Kinoshita, 1917)**
- Pigment mainly present on Th. II–Abd. III laterally 3
- 3 Pigment present on head entirely, Abd. I with 8–9 mac ***C. (J.) raoi* sp. nov.**
- Pigment present on head only laterally, Abd. I usually with 7 or 11 mac... 4
- 4 Abd. I usually with 7 mac, p2p mac absent ***C. (J.) xinjianensis* sp. nov.**
- Abd. I usually with 11 mac, p2p mac present ***C. (J.) tongguensis* sp. nov.**
- 5 Three median chaetae on the first row of labrum modified 6
- All chaetae on the first row of labrum modified (subgenus *Gunungphysa*).... 7
- 6 Abd. III with 1 dorsal mac ***C. (Javaphysa) guangdongensis* Ma, 2012**
- Abd. III with 2 dorsal mac ***C. (Istanaphysa) hainanensis* Ma, 2013**
- 7 Dens with spines ***C. (Gunungphysa) spinidentata* Lee & Park, 1989**
- Dens without spines..... 8
- 8 Abd. I with 3 mac..... ***C. (G.) taiwanica* Yosii, 1965**
- Abd. I with more than 3 mac..... 9
- 9 Abd. I with 5 mac..... 10
- Abd. I with 9 mac..... ***C. (G.) affinis* Lee & Park, 1989**
- 10 A longitudinal stripe present from Th. II to Abd. III laterally
..... ***C. (G.) striata* Yosii, 1965**
- Pigment diffused on body..... ***C. (G.) microphysarum* Yosii, 1965**

Additional information

Conflict of interest

The authors have declared that no competing interests exist.

Ethical statement

No ethical statement was reported.

Funding

This research was funded by the Second Tibetan Plateau Scientific Expedition and Research Program (2019QZKK05010303).

Author contributions

Mei-Dong Jing: Sorting of specimens and writing of manuscript. Yin-Huan Ding: Molecular analysis. Yi-Tong Ma: Observing of specimens under microscope.

Author ORCIDs

Mei-Dong Jing  <http://orcid.org/0000-0002-8498-9498>

Yin-Huan Ding  <https://orcid.org/0000-0002-8002-7056>

Yi-Tong Ma  <http://orcid.org/0000-0002-8660-0503>

Data availability

All of the data that support the findings of this study are available in the main text.

References

- Bellinger PF, Christiansen KA, Janssens F (1996–2023) Checklist of the Collembola of the World. <http://www.collembola.org> [Accessed 24 March 2023]
- Börner C (1906) Das System der Collembolen-nebst Beschreibung neuer Collembolen des Hamburger Naturhistorischen Museums. *Mitteilungen Naturhistorische Museum Hamburg* 23: 147–187.
- Börner C (1913) Die Familien der Collembolen. *Zoologischer Anzeiger* 41: 315–322.
- Gisin H (1964) European Collembola. VII. *Revue Suisse de Zoologie* 71(4): 649–678. <https://doi.org/10.5962/bhl.part.75615>
- Godeiro NN, Ding YH, Cipola NG, Jantarit S, Bellini BC, Zhang F (2022) Phylogenomics and systematics of Entomobryoidea (Collembola): marker design, phylogeny and classification. *Cladistics*: 1–15. <https://doi.org/10.1111/cla.12521>
- Gong X, Qin CY, Yu DY (2018) Two new species of *Tomocerus ocreatus* group with a single large distal dental spine (Collembola, Tomoceridae). *Zootaxa* 4514(2): 273–282. <https://doi.org/10.11646/zootaxa.4514.2.10>
- Greenslade P, Stevens ML, Torricelli G, D’Haese CA (2011) An ancient Antarctic endemic genus restored: morphological and molecular support for *Gomphiocephalus hodgsoni* (Collembola: Hypogastruridae). *Systematic Entomology* 36(2): 223–240. <https://doi.org/10.1111/j.1365-3113.2010.00553.x>
- Jordana R, Baquero E (2005) A proposal of characters for taxonomic identification of Entomobrya species (Collembola, Entomobryomorpha), with description of a new species. *Abhandlungen und Berichte des Naturkundemuseums Goerlitz* 76(2): 117–134.
- Kim JT, Rojanavongse V, Lee BH (1999) Systematic study on Collembola (Insect) from Thailand II. Nine species of *Callyntrura* (Paronellidae). *Korean Journal of Entomology* 29(1): 37–51.
- Kimura M (1980) A sample method for estimating evolutionary rates of base substitution through comparative studies of nucleotide-sequences. *Journal of Molecular Evolution* 16(2): 111–120. <https://doi.org/10.1007/BF01731581>
- Kinoshita S (1917) Honposan Tobimushirui no ni Shinshu. *Zoological Magazine* 29: 40–46.
- Lee BH, Park KH (1989) Systematic studies on Chinese Collembola (Insecta), 1. Four new species and three new records of Entomobryidae from Taiwan. *Chinese Journal of Entomology* 9(2): 263–282.
- Lubbock J (1873) *Monograph of the Collembola and Thysanura*. Ray Society, London, 276 pp. <https://doi.org/10.5962/bhl.title.11583>
- Ma YT (2012) A new species of *Callyntrura* (Collembola: Paronellidae) from Guangdong Province, China. *Entomotaxonomia* 34(2): 103–108. <https://doi.org/10.11646/zootaxa.3389.1.4>
- Ma YT (2013) A new species and a newly recorded species of Paronellinae (Collembola: Paronellidae) from China. *Entomotaxonomia* 35(1): 1–5. <https://doi.org/10.11646/zootaxa.3389.1.4>
- Mari-Mutt JA (1986) Puerto Rican species of *Lepidocyrtus* and *Pseudosinella* (Collembola: Entomobryidae). *Caribbean Journal of Science* 22(1–2): 1–48. <https://doi.org/10.11646/zootaxa.4995.1.11>

- Mitra SK (1974) A critical study on some species of *Callyntrura* Börner, 1906 (Collembola, Entomobryidae, Paronellinae) from India. *Revue d'Écologie et de Biologie du Sol* 11(3): 397–438.
- Nilsai A, Jantarit S, Satasook C, Zhang F (2017) Three new species of *Coecobrya* (Collembola: Entomobryidae) from caves in the Thai Peninsula. *Zootaxa* 4286(2): 187–202. <https://doi.org/10.11646/zootaxa.4286.2.3>
- Szeptycki A (1973) North Korean Collembola. I. The genus *Homidia* Börner 1906 (Entomobryidae). *Acta Zoologica Cracoviensia* 31: 23–40.
- Szeptycki A (1979) Morpho-systematic studies on Collembola. IV. Chaetotaxy of the Entomobryidae and its phylogenetical significance. *Polska Akademia Nauk, Kraków*, 219 pp.
- Tamura K, Peterson D, Peterson N, Stecher G, Nei M, Kumar S (2011) MEGA5: Molecular evolutionary genetics analysis using maximum likelihood, evolutionary distance, and maximum parsimony methods. *Molecular Biology and Evolution* 28(10): 2731–2739. <https://doi.org/10.1093/molbev/msr121>
- Tömösvary O (1882) Adatok Hazánk Thysanure-Faunájához. *A Matematikai és Természettudományi Osztályok Közlönye* 18: 119–130.
- Yoshii R (1982) Studies on the Collembolan genus *Callyntrura* and *Dicranocentroides*. *Japan International Cooperation Agency* 6: 1–38.
- Yoshii R (1992) Paronellid Collembola collected by the Krakatau Expedition, 1984. *Memoirs of the Museum of Victoria* 53(1): 129–133. <https://doi.org/10.24199/jmmv.1992.53.07>
- Yosii R (1961) On some Collembola from Thailand. *Nature and Life in Southeast Asia* 1: 171–201.
- Yosii R (1965) On some Collembola of Japan and adjacent countries. *Contributions from the Biological Laboratory Kyoto University* 19: 1–71.
- Yu DY, Yao J, Hu F (2016) Two new species of *Tomocerus ocreatus* (Collembola, Tomoceridae) from Nanjing, China. *Zootaxa* 4084(1): 125–134. <https://doi.org/10.11646/zootaxa.4084.1.6>
- Yu DY, Ding YH, Ma YT (2017) Revision of *Tomocerus similis* Chen & Ma, with discussion of the *kinoshitai* complex and the distal tibiotarsal chaetae in Tomocerinae (Collembola, Tomoceridae). *Zootaxa* 4268(3): 395–410. <https://doi.org/10.11646/zootaxa.4268.3.5>
- Yu DY, Qin CY, Ding YH, Hu F, Zhang F, Liu MQ (2018) Revealing species diversity of *Tomocerus ocreatus* complex (Collembola: Tomoceridae): integrative species delimitation and evaluation of taxonomic characters. *Arthropod Systematics & Phylogeny* 76(1): 147–172. <https://doi.org/10.3897/asp.76.e31949>
- Zhang F, Jantarit S, Nilsai A, Stevens MI, Ding YH, Satasook C (2018a) Species delimitation in the morphologically conserved *Coecobrya* (Collembola: Entomobryidae): A case study integrating morphology and molecular traits to advance current taxonomy. *Zoologica Scripta* 47(3): 342–356. <https://doi.org/10.1111/zsc.12279>
- Zhang F, Yu DY, Stevens MI, Ding YH (2018b) Colouration, chaetotaxy and molecular data provide species-level resolution in a species complex of *Dicranocentrus* (Collembola: Entomobryidae). *Invertebrate Systematics* 32(6): 1298–1315. <https://doi.org/10.1071/IS18019>

A conspectus of Australian *Apotropina* (Diptera, Chloropidae) with the description of two new species

Yuchen Ang¹, James Lumbers^{2,3}, Paula R. Riccardi⁴

1 Lee Kong Chian Natural History Museum, National University of Singapore, 2 Conservatory Dr., 117377 Singapore, Singapore

2 Australian National Insect Collection (ANIC), CSIRO Black Mountain, 1 Clunies Ross St, Acton Black Mountain, Canberra, ACT 2601, Australia

3 Research School of Biology, Australian National University, Canberra, ACT 2601, Australia

4 Center for Integrative Biodiversity Discovery, Museum für Naturkunde, Leibniz-Institute for Evolution and Biodiversity Science, Invalidenstr. 43, 10115 Berlin, Germany

Corresponding authors: Yuchen Ang (nhmay@nus.edu.sg); Paula R. Riccardi (paularriccardi@gmail.com)

Abstract

The genus *Apotropina* (Diptera, Chloropidae) has a global distribution with more than 80 valid described species, of which 22 are known to occur in Australia. The Australian *Apotropina* fauna is poorly studied, with many species known from single type specimens, more with the morphology of the other sex unknown, and there have been no new species descriptions since 1959. Here, we describe two new species from Australia, *A. maculigena* Riccardi, **sp. nov.** and *A. popeye* Ang, **sp. nov.**, and provide an updated illustrated key. We also provide a conspectus of the known Australian *Apotropina* with images of types and collate all original descriptions and subsequent taxonomic notes of relevance as supplementary information. Finally, we discuss the validity of two known syntype specimens of *A. bispinosa* due to incongruencies with the species description.

Key words: *Apotropina*, Australia, Chloropidae, Diptera, key, Sexual Dimorphism, taxonomy



Academic editor: Owen Lonsdale

Received: 26 June 2023

Accepted: 6 November 2023

Published: 21 December 2023

ZooBank: <https://zoobank.org/919C320F-AA72-4F1D-9028-1ECB12948B8D>

Citation: Ang Y, Lumbers J, Riccardi PR (2023) A conspectus of Australian *Apotropina* (Diptera, Chloropidae) with the description of two new species. ZooKeys 1187: 261–299. <https://doi.org/10.3897/zookeys.1187.108497>

Copyright: © Yuchen Ang et al.

This is an open access article distributed under terms of the Creative Commons Attribution License ([Attribution 4.0 International – CC BY 4.0](https://creativecommons.org/licenses/by/4.0/)).

Introduction

The genus *Apotropina* Hendel (Diptera, Chloropidae) has a worldwide distribution, being the most speciose member of the subfamily Siphonellopsinae Duda with more than 80 described species, largely concentrated in the Southern Hemisphere (Ismay et al. 2021). Thirty-seven species of *Apotropina* are described from the Australasian-Oceanian region, with 22 species known to occur in Australia (Sabrosky 1989).

Apotropina are small (1.5–5.0 mm), dark to yellowish flies, sometimes with distinct tomentosity on their bodies, and with hyaline or patterned wings. *Apotropina* are associated with water bodies, sandy river margins and sea-shores; some adults form congregations in rock shelters (Ismay et al. 2021). While little else is known about their biology, and a majority of chloropids are recorded to be saprophages and phytophages. Evidence of saprophagy in *Apotropina* is inferred from various life-history records: specimens are observed with the infestation of fungi Laboulbeniales (Ascomycota: Laboulbeniomycetes) (primarily on antennae, mouth parts, and female ovipositor) and mites

(likely Pyemotidae [Acari: Acariformes]) (usually found on neck, coxae and posterior margin of tergites) – two parasitic groups which are largely associated with flies that visit decaying matter (M.V. Tschirnhaus, pers. comm. 2023). A more direct observation is the unidentified species shown in Fig. 1 visiting a dead snail shell (S. Grove, pers. comm. 2023). Additionally, some chloropids specialize as predators of other invertebrate eggs or larvae [see Ismay and Ang (2019) for a review]. Indeed, two Australian species *A. proxima* (Rayment, 1959) and *A. raymenti* (Curran, 1930) are known to prey on the immature stages of hymenopterans (Rayment 1935, 1959), and it is likely that there are other predatory species in the genus.

There is also known sexual dimorphism in the genus, largely in differences on the wing venation and coloration between males and females [e.g., *A. anomala* (Malloch, 1925) and *A. maculigena* Riccardi sp. nov.] and antennal modifications in *A. australis* (Malloch). Given that most Australian species are only known from a single sex, it is likely that there are more species with undocumented sexual dimorphism: for example, Fig. 1 shows a species observation [likely of *A. ornatipennis* (Malloch, 1923) or similar, see species remarks] from iNaturalist (Grove 2019) where there are distinct differences in wing color patterning between males and females.

Australian *Apotropina* are poorly studied, with at least ten described species known solely from their type specimen, and thus the morphology for the other sex unknown. The type species for *Apotropina* is *A. viduata* (Schiner, 1868), an Australian species originally described under *Ectropa* Schiner as a member of the family Ephydriidae Zetterstedt. However, *Ectropa* was already preoccupied by the lepidopteran genus *Ectropa* Wallengren, and was renamed *Apotropina* Hendel (1907). Most Australian *Apotropina* were described (predominantly by Malloch) under *Parahippelates* Becker and *Lasiopleura* Becker, with the former synonymized to the latter by Malloch (1936); a few other species were also described under *Ephydroscinis* Malloch. Sabrosky (1980) was able to examine the type specimen for *A. viduata* and transferred *Apotropina* to Chloropidae; he further synonymized *P. fuscipes* Malloch, 1924 with *A. viduata*, effectively synonymizing *Lasiopleura* under *Apotropina*. *Ephydroscinis* was also synonymized under *Apotropina* (Sabrosky 1989). No new Australian species in this genus have been described since 1959 (Sabrosky 1989), and it is likely that many more species remain undescribed.

Here we describe two new species of *Apotropina* to Australia: *A. maculigena* Riccardi, sp. nov. and *A. popeye* Ang, sp. nov.; we also provide an updated illustrated key to the Australian *Apotropina* species, and a conspectus of the known species with images of type specimens for most of these species. Original descriptions and subsequent taxonomic notes of relevance are also collated in a supplementary file. Finally, we propose disregarding the current type specimens [specimen no. 547474 (5c8582 and 5c85bb)] for *Apotropina bispinosa* (Becker, 1911) due to their incongruence with the species descriptions.

Materials and methods

The type series for the two new species are deposited in the following collections: the Australian Museum Research Institute, Sydney, Australia (AMRI),



Figure 1. In situ photo of *Apotropina* sp. showing sexual dimorphism. iNaturalist observation (Grove 2019) of two individuals (likely of *A. ornatipennis* (Malloch) or similar where ♂ wings (bottom left) have color pattern extending to wing apices (blue arrow), while the ♀ color pattern (top right) does not (red arrow).

the Queensland Museum, Brisbane, Australia (**QM**), the Museu de Zoologia da Universidade de São Paulo, São Paulo, Brazil (**MZUSP**), the Museum für Naturkunde, Berlin, Germany (**MfN**) and the Zoological Reference Collection, Lee Kong Chian Natural History Museum, Singapore (**ZRC**). Images of type material were also obtained for 20 *Apotropina* species deposited in the South Australian Museum, Adelaide, Australia (**SAMA**), the Naturhistorisches Museum Wien, Vienna, Austria (**NHMW**), the California Academy of Sciences San Francisco, California, USA (**CAS**), the AMRI, and the MfN. The protocol for preparing wing and terminalia follows Riccardi et al. (2018). Images at different depths of field were taken with either a Leica M205 C or M205 A trinocular stereomicroscope coupled to the software LasX and focus-stacked in either Helicon Focus 6 or Zerene Stacker v. 1.04. Scanning electron micrographs (SEM) were obtained using a JEOL JCM-6000plus high vacuum equipment. Illustrations were treated with Illustrator CS6 and images were further processed and plated in Photoshop CS6. The morphological nomenclature follows primarily Ismay et al. (2021) and also Andersson (1977) (specifically, scapular setae). Three 312-bp COI DNA barcodes for the two new species were also generated: DNA extraction and sequencing procedures followed protocols as described in Mortelmans et al. (2022); the DNA barcodes were then uploaded to GenBank.

Results

Genus diagnosis for *Apotropina* Hendel

Apotropina species are predominantly dark to yellowish species, with various patterns of pruinosity. For chaetotaxy they have three to four long fronto-orbital proclinate setae but with at least (usually the most posterior) one latero-clinate; long, proclinate and divergent ocellar setae; two postpronotal setae with the inner one inclinate and the outer one reclinate; notopleural setae 1+1; a row of dorsocentrals rarely reduced to the posterior pair. Fore femur or tibia not enlarged; hind tibia usually with tibial organ and tibial spur present. Wing vein C extends to M_1 ; M_4 usually with basal sinuosity as a kink (as a plesiomorphy for Chloropidae). Male with postabdomen asymmetrical sclerites; epandrium usually large and with lateral extensions (but minute epandria can also occur; von Tschirnhaus, pers. comm. 2023); hypandrial complex developed.

Illustrated key to the Australian species of *Apotropina* (with parts adapted from Malloch 1924, 1940; Rayment 1959)

- 1 Dark body largely pruinose; pleuron with 2 longitudinal strips on scutum, gena, occiput and abdomen with fine white setulae, femora additionally with longer white setae; frons dark but yellowish near anterior half; 2 short proclinate interfrontal setae; arista almost bare, only the posterior pair of dorsocentrals developed; katapisternal setae distinct; hind tibial spur indistinct, pale and short; wing hyaline, with bm+dm cell wide and dm-m vein approximately perpendicular (Fig. 11)
***A. dasypleura* (Malloch, 1928)**
 - Other combination of characters **2**
- 2 Gena patterned with dark macula medially below eye; male wings with an elongate dark spot across in the middle of cells r_1 and r_{2+3} but never beyond R_{2+3} (Fig. 2C) and veins light brown basally but darkening towards apex; female wings may be hyaline.....**3**
 - Gena without dark macula below eye; wings not as above..... **4**
- 3 Gena yellow with black setae only; genal macula reaches or nears ventral margin of gena; proboscis yellowish brown; ocellar triangle reaching $\sim\frac{1}{2}$ length of head dorsally; frons yellowish except for light brown posterior region; 2 vibrissae; 2 decussate interfrontal setae; 1 postpronotal seta; femora yellow to light brown (Fig. 2)***A. maculigena* Riccardi, sp. nov.**
 - Gena whitish with white and black setae; genal macula does not end near ventral margin of gena; proboscis dark; ocellar triangle reaching at least length of head dorsally; 3 vibrissae; 3 strong decussate interfrontal setae; femora whitish yellow but slightly infuscate near apices (Fig. 10)
.....***A. costumaculata* (Malloch, 1924)**
- 4 At least medial region of wing with distinct black/dark brown marking(s) in radial and medial sectors that extend from costa to beyond R_{2+3} ; may extend to apex of wing; alula usually whitish **5**
 - Wing without well-defined dark area, at most with a linear brownish costal suffusion **8**

- 5 Proboscis long and geniculate; scutum with silvery green metallic pattern divided by three longitudinal black lines; only 2 distal segments of tarsi dark (Fig. 25E, F).....**A. proxima (Rayment, 1959)**
- Proboscis short and capitate; scutum not as above; ≥2 distal tarsal segments dark.....**6**
- 6 Scutal color pattern with paired white lateral vittae on postscutum and none on prescutum; arista completely brown; 1 vibrissa; 2 to 3 weak proclinate interfrontal setae; pleuron completely white (Fig. 20)**A. raymenti (Curran, 1930)**
- Scutal color pattern with white patterning predominantly on prescutum and sometimes reaching towards postscutum; arista brown on basal bulge and apical half but yellow medially; pleuron not completely white; 1 vibrissa; 2 largely proclinate interfrontal setae**7**
- 7 Wing veins lighter basally, darker brown near apex; katapisternum usually completely white; femora dark but broadly yellow at least quarter to apices (Fig. 16)**A. ornatipennis (Malloch, 1923)**
- Wing veins dark brown throughout; katapisternum usually white with dark patches; femora dark with extreme apices yellow (Fig. 13)**A. exquisita (Malloch, 1940)**
- 8 Costal margin of the wing browned from apex of R₁ to M₁; body and legs largely fulvous-yellow with tarsi darker near apex, thorax shiny with a very faint dusting; postpedicel largely brown; arista with short pilosity; proboscis geniculate; 1 vibrissa; 3 or 4 pairs proclinate interfrontal setae; scutellum with 1 discal setula (Fig. 8)**A. brunneicosta (Malloch, 1923)**
- Wing hyaline or with a faint yellowish marking; other combination of characters**9**
- 9 Arista white with dense whitish pilosity; postpedicel yellowish but brown at base of arista; gena yellow, approx. as high as postpedicel; 2 vibrissae; 2 strong decussate interfrontal setae; large geniculate proboscis dark; femora and tibiae largely or entirely brown; halter brown; wing hyaline; thorax dark fulvous with distinct but not dense pruinosity; scutellum with 1 discal setula (Fig. 5).....**A. albiseta (Malloch, 1924)**
- Arista and its pilosity not white; other combination of characters**10**
- 10 Arista plumose, with basal pilosity distinctly long (almost the length of the postpedicel), shorter apically; 2 vibrissae; 3 or 4 proclinate interfrontal setae; body entirely brown and pruinose; legs and gena yellow; hind tibial spur longer than width of tibia, curved (Fig. 21).....**A. rufescens (Duda, 1934)**
- Arista with short pubescence or bare; other combination of characters **11**
- 11 Arista pubescent, with at least the basal pilosity 2× basal width of the arista **12**
- Arista almost bare, or with pilosity approx. as long as the basal width of the arista (Fig. 25C)..... **15**
- 12 Thorax almost uniformly fulvous, entirely pruinose with microtrichia, additionally with distinct grey-dusted central stripe extending beyond dorso-central row; scutellum yellowish on margin; abdomen much uniformly darker than thorax; 1 katapisternal seta; legs yellow with last 2 tarsal segments dark; hind tibial organ distinctly darkened; hind tibial spur curved,

- not longer than width of tibia; antenna entirely pale yellow; M_4 reaches wing margin (Fig. 14) **A. griseovitta (Malloch, 1936) ♂ [part]**
- Other combination of characters **13**
- 13 Body largely covered in distinct white setulae; ventral part of katepisternum, most of scutum and discal region of scutellum black, with margins of scutum and scutellum, and rest of pleuron reddish yellow; in male hypopygium glossy black; gena deeper than half of eye; short geniculate proboscis dark; postpedicel yellow but darker at base of arista; arista densely pilose and dark; 2 vibrissae; 3 inclinate interfrontal setae; scutellum with 2 discal setulae; 1 katepisternal seta; dm-m almost 2× its own length from apex of M_4 ; hind tibial spur \leq width of tibia (Fig. 12) **A. duplicata (Malloch, 1923)**
- Body not covered in distinct white setulae; other combination of characters **14**
- 14 Head, thorax and legs almost entirely reddish yellow without distinct markings, tarsi apices slightly darker, abdomen entirely brown; postpedicel brownish; gena shallower than half of eye; short geniculate proboscis dark; 2 vibrissae; 3 or 4 inclinate interfrontal setae; 1 katepisternal seta; mid coxa with 1 row of long setae; hind tibial spur longer than width of tibia (Fig. 15)..... **A. nigripila (Duda, 1934)**
- Thorax dorsum dusted brown grey with 2 closely associated narrow grey stripes; thorax pleuron completely grey pruinose; abdomen dark with distinct whitish posterior margins; legs brownish with darkened femora and hind legs, hind tibial spur distinctly large and curved; frons dark red-brown that becomes red anteriorly; frontal triangle dull, reaches middle of head; 2 vibrissae; 1 decussate interfrontal seta (Figs 4, 25A, B) **A. aequalis (Becker, 1911)**
- 15 Gena very deep, subequal in height to eye; frons strongly projected anteriorly; parafacial as wide as the postpedicel; bright orangish to yellow species but with darker abdomen; vibrissa very short/missing; 3 decussate interfrontal setae; hind tibial spur shorter than tibia diameter, but strong and curved; proboscis geniculate, longer than head when extended (Fig. 9) **A. conopsea (Duda, 1934)**
- Parafacial $\leq \frac{1}{2}$ as wide as the postpedicel; proboscis not longer than head when extended **16**
- 16 Body largely reddish yellow, legs paler yellow; gena deep, subequal in height to eye; 1 vibrissa; 2 inclinate interfrontal setae; 1 katepisternal seta; tibial spur short and slightly curved, slightly longer than width of tibia; males with hind tibia grossly enlarged, bearing a large and oval tibial organ (Fig. 3)..... **A. popeye Ang, sp. nov.**
- Hind tibia not enlarged; body not largely reddish yellow; other combination of characters..... **17**
- 17 Hind tibial spur almost indistinct and not nearly $\frac{1}{2}$ as long as the tibial diameter; all presutural acrostical setulae minute **18**
- Hind tibial spur curved and stout, usually at least as long as the tibial diameter; presutural acrostical setae distinct **20**
- 18 Frons strongly projected anteriorly; postpedicel dark; males with long, light-colored geniculate arista, females with normal bare arista; no vibrissae; 5 or 6 proclinate interfrontal setae; thorax with dorsum dark and traces of blackish lines and laterals yellow pruinose; scutellum black on the

- disc and grey laterally; a pair of grey spots on the apex of the abdominal syntergite 1+2; male mid tarsi with the 3 apical segments slightly broadened (Fig. 7)..... **A. australis (Malloch, 1924)**
- Male arista and mid tarsi with no modifications; other combination of characters **19**
- 19 Legs at least with hind femur and tibia largely fuscous; thorax with dorsum glossy black; tergites dark but with silver pruinosity along posterior margins; male wings with R_{2+3} curved anteriorly and R_{4+5} curved posteriorly creating a much wider r_{2+3} cell, but parallel in female; presutural setae absent; face dark yellow with a silvery pruinosity, $<2\times$ longer than wide; gena as deep as postpedicel length; parafacial not visible in profile; 1 white vibrissa; 3 proclinate interfrontal setae (Fig. 6).....
- **A. anomala (Malloch, 1925)**
 - Legs pale yellow, the 2 apical tarsomeres of mid and hind legs slightly darkened; thorax with dorsum evenly and densely covered with grey pruinosity; last abdominal segment and male terminalia of male yellow; thorax with dorsum covered with grey pruinosity; anterior half of head yellow, face $2\times$ longer than wide; gena not as deep as postpedicel length; parafacial visible in profile; proboscis capitate; 1 vibrissa; 1 proclinate interfrontal seta (Fig. 19)..... **A. pruinosa (Thomson, 1869)**
- 20 Scutum reddish to dark brown, with a broad grey-dusted stripe extending beyond dorsocentral row; 1 katepisternal seta; scutellum grey-dusted on disc; hind tibial spur approx. as long as diameter of tibia; antenna pale yellow; M_4 reaches wing margin (Fig. 14).....
- **A. griseovitta (Malloch, 1936) ♂ [part]**
 - Scutum without a grey-dusted vitta covering the dorsocentral area; another combination of characters **21**
- 21 Scutum with the anterior acrostichals very short and fine, biseriate but not decussate; most of thorax and head except ventral half of katepisternum and frons heavily pruinose with white microtrichia; 3 vibrissae; 2 or 3 proclinate interfrontal setae; thorax uniformly dark, abdomen dark basally and lighter towards apex; legs uniformly yellow except for brown terminal 2 segments of tarsi; M_4 ends well before wing margin (Fig. 22).....
- **A. taylori (Malloch, 1940)**
 - Scutum with at least some anterior acrostichals $\sim\frac{1}{2}$ as long as the anterior dorsocentrals, decussate; hind tibial spur longer than the tibial width, other combination **22**
- 22 Gena at most as deep as $\frac{1}{2}$ of eye height; hind tibial spur similar to or shorter than width of tibia..... **23**
- Gena almost as high as the eye; arista with short pubescence thorax entirely shiny black with grey or brownish pruinosity; hind tibial spur much longer than width of tibia (Fig. 25D)..... **25**
- 23 Thorax brownish yellow, shiny; 1 katepisternal seta; scutum with 2 grey-dusted lines along the dorsocentrals; postpedicel largely fuscous; M_4 reaches wing margin (Fig. 14)..... **A. griseovitta (Malloch, 1936) ♀ [part]**
- Thorax shiny black or dark brown; stripes on the scutum, if present, almost indistinct; other combination; 2 vibrissae; 3 proclinate interfrontal setae; scutellum without discal setulae; katepisternal setae missing/indistinct **24**

- 24 Legs entirely yellow; postpedicel yellow to light brown; ocellar triangle and gena with distinctly pruinose with white microtrichia; M_4 ends well before wing margin (Fig. 17) ***A. pallipes* (Malloch, 1940)**
- Legs dark yellow to brown, all femora darkened medially; postpedicel dark brown dark; ocellar triangle and gena pruinose but not distinctly white; M_4 ends at or close to wing margin (Fig. 18) ***A. parva* (Malloch, 1928)**
- 25 Legs entirely orangish yellow; scutum pruinose grey with a central faint dark stripe that becomes more distinct towards the posterior; acrostichal row with ≥ 4 strong setae; scutellum not very convex (Fig. 25C, D) ***A. nudiseta* (Becker, 1911)**
- Legs dark yellow but femora largely dark; scutum with brownish pruinosity and 3 brownish stripes; scutellum convex; 3 vibrissae, 3 proclinate interfrontal setae, katepisternal seta white, indistinct (Fig. 23)..... ***A. viduata* (Schiner, 1868)**

***Apotropina maculigena* Riccardi, sp. nov.**

<https://zoobank.org/16906BC7-91B7-48D9-8BEC-6874EA51D48F>

Fig. 2A–H

Type locality and distribution. AUSTRALIA: New South Wales (Taree).

Material examined. Holotype ♂ AUSTRALIA: New South Wales, Taree, Lorien Wildlife Refuge, 3km N Landsdowne; sclerophyle forest, Dec.14–31.2011, Malaise trap; 31°45'04"S, 152°32'03"E; E.G. & B. Williams leg; [AMRI TYPE CODE]. Deposited in the AMRI.

Paratypes ♂♂♀♀ 34 same data as holotype; Deposited in the AMRI (20♂, 5♀), MfN (3♂, 1♀), MZUSP (3♂), ZRC (1♂, 1♀, same as specimens with submitted Genbank barcodes).

GenBank barcodes. Specimen no. ZRCENT0021054: OR136427; specimen no. ZRCENT0021055: OR136428.

Diagnosis. Gena yellow with a dark median macula that reaches ventral margin; frons dark yellow; ocellar triangle with silvery pruinosity; male terminalia with anal area bearing a pair of conical membranous extensions.

Description. Male (Fig. 2A, C–G). Body length, 2.4–2.7 mm. Wing length, 2.28–2.45 mm. **Head** (Fig. 2A, B). Broader than long dorsally and deeper than long in profile, dark yellow except for black ocellar tubercle and a dark occiput. Head and thoracic setae black. Ocellar seta strongly developed, as long as inner and outer vertical setae. Postocellar cruciate, $\sim 2/3$ of ocellars length. Three fronto-orbital setae developed, $\sim 1/3$ of the ocellars; the two anterior proclinate and the posterior latero-clinate. Inner vertical seta inclinate and outer vertical seta latero-clinate. Two pairs of interfrontal setae distinct; as long as fronto-orbitals; proclinate and slightly convergent. Frons as long as broad, lateral margins slightly convergent, front margin straight. Ocellar triangle with a silvery pruinosity, extending to half of frons length, posterior margin two thirds width of frons, lateral margins straight. Eye oval, long axis slightly oblique with short, very sparse pubescence. Face deeper than broad; carina knife-like, restricted to the upper half of frons; antennae dark yellow, postpedicel reniform, as deep as long, mostly yellow; arista blackish, with short sparse pubescence, $\sim 3\times$ as long as postpedicel; gena as wide as the length of postpedicel, with

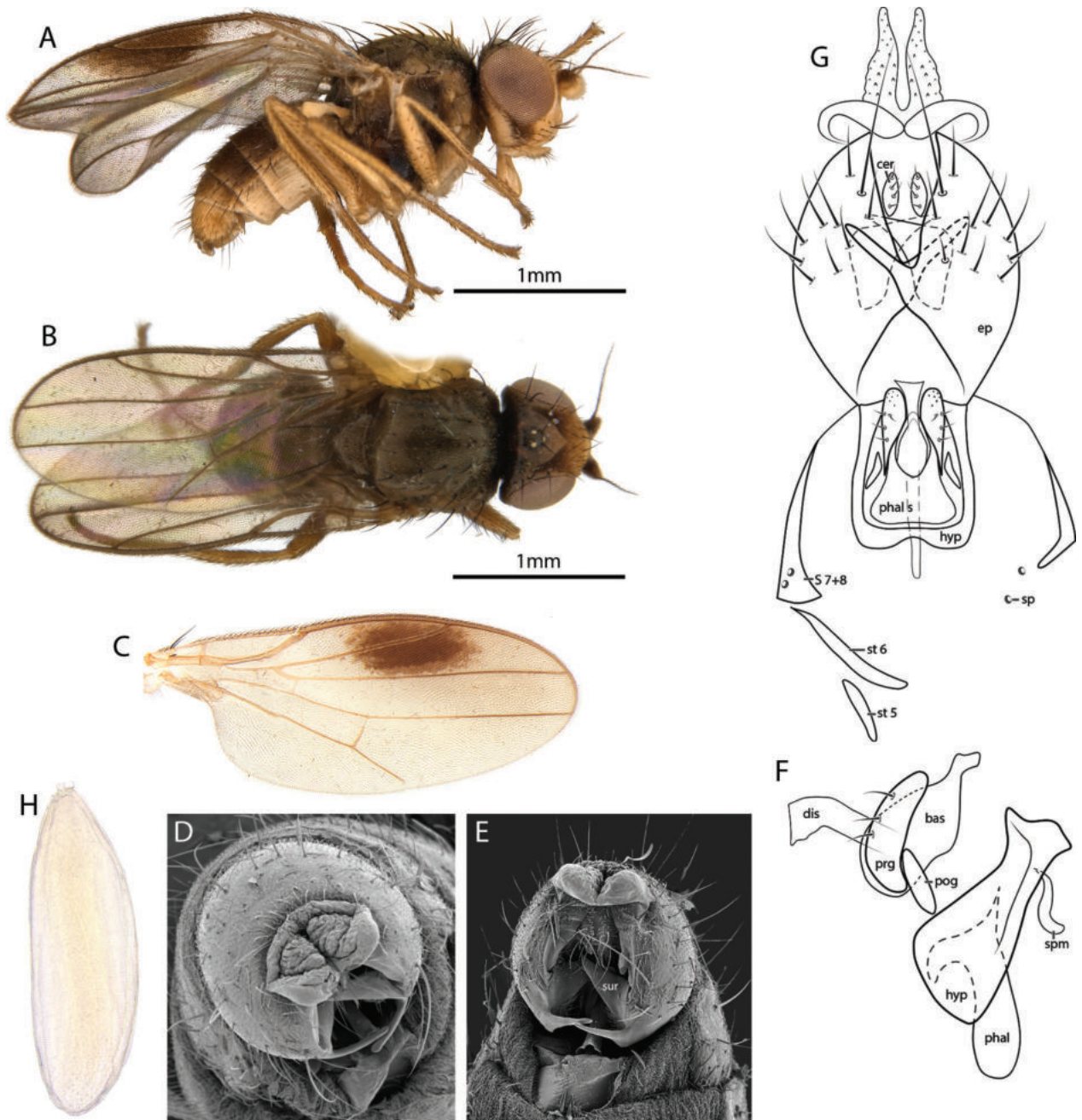


Figure 2. *Apotropina maculigena* Riccardi, sp. nov. ♂♀ **A** ♂ habitus, lateral view **B** ♀ habitus, dorsal view **C** ♂ wing **D** ♂ terminalia, terminal view **E** ♂ terminalia, ventral view **F** hypandrium and phallic complex, lateral view **G** ♂ postabdomen, ventral view **H** egg. Abbreviations: bas, basiphallus; cer, cercus; dis, distiphallus; ep, epandrium; hyp, hypandrium; phal, phallopodeme; phal s, phallopodemic sclerite; pog, postgonite; prg, pregonite; S, sytergosternite; sp, spiracle; spm, sperm pump; st, sternite; sur, surstylus.

~ 2 unordered rows of setulae and two vibrissae; occiput blackish; proboscis short yellow; palpus yellow, small, equal in length to postpedicel, with brown setulae; mouth edge not protruding; clypeus dark brown. **Thorax** (Fig. 2A, B). Scutum approx. as long as broad, dark brown, entirely pruinose; one row of decussate acrostichal setulae and one pair of prescutellar acrostichal seta; four dorsocentral setae developed, the posterior one longer than the remaining three and as long as the ocellar seta; postpronotal lobe concolorous with scutum; one long basal postpronotal seta, equal to notopleurals; anterior post-

pronotal seta short and reclinate; one presutural intra-alar seta developed; notopleuron with 1+1 setae; one long presutural and three short postsutural supra-alar setae; postalar seta as long as ocellar seta. Pleuron dark brown, pruinose, katapisternum with a dorsal long seta. Scutellum concolorous with scutum, pruinose, broader than long, rounded apically with one pair of setulae on the disc; apical scutellar setae with separation greater to that of posterior ocelli and as long as half the scutal length; one pair of lateral scutellar setae inserted on the disc, as long as the prescutellar dorsocentrals; post-scutellum blackish. Halter pale yellow. **Wing** (Fig. 2A, C). Translucent with a large dark spot more than half of second sector, light brown veins covered in sparse brown microtrichia; costal ratios measured from h: R_1 : R_{2+3} : R_{4+5} is 6: 7.5: 7: 2; veins R_{4+5} and M_1 subparallel; distance between r-m and dm-m six times length of r-m. **Legs** (Fig. 2A). Brownish yellow, dark pilosity organized in rows; posterior tibial organ well developed, occupying one third of tibia, narrow, yellow; hind tibial spur subapical, as long as the width of the tibia apex. **Abdomen** (Fig. 2A). Tergites brown. **Terminalia** (Fig. 2D–G). Postabdomen sclerites asymmetric as in generic diagnosis. Epandrium well developed, with a laterobasal projection; surstylus conical, directed inwards; cerci not fused to each other, oval; anal lobe membranous, with a long bifid projection. Hypandrium with arms open; basiphallus oval; distiphallus cylindrical and membranous; pregonite with four setulae and sensorial pores on the apex; postgonite minute, elongated; phallopodeme short, not bifid basally; sperm pump present. **Female** (Fig. 2B). Same as male, except wing completely hyaline; abdominal segments 6–8 narrow; epiproct with one pair of setae; hypoproct pilose; cerci dark yellow, long, and narrow, with short setae at base.

Egg (Fig. 2H). Length 0.43 mm, width 0.14 mm, matt, milky white, elongated, slightly rounded at both ends; one apical pole with four to five spine-like structures. Chorionic surface with poorly visible pattern of small rounded microsculptures.

Etymology. The specific epithet *maculigena* is feminine derived from Latin, meaning gena with macula.

Remarks. The wings of *Apotropina maculigena* sp. nov. males are similar to *A. costomaculata*. However, a yellow gena with a distinct mesal dark spot and postgena yellow are considered distinctive features of *A. maculigena* sp. nov., while *A. costomaculata* has a whitish gena with an indistinct dark marking and dark postgena. Furthermore, the yellow mouthparts and male epandrium of *Apotropina maculigena* sp. nov. differ from the brown coloration of the same structures in *A. costomaculata*.

***Apotropina popeye* Ang, sp. nov.**

<https://zoobank.org/24E61305-A1A4-4C38-A2B3-F547213D2931>

Fig. 3A–H

Type locality and distribution. AUSTRALIA: Queensland (Dinden National Park).

Type material. Holotype ♂ Label transcription: “QLD Dinden NP, 20k EbS Ma-reeba, 17.034°S, 145.6064°E, 9 Nov 2017, Kahlpahlim Rock trail, J A & J G Lumbers”; 710 m a.s.l.; a single male specimen was collected via sweep-netting at the edge of a forest clearing. ZRC issued specimen code ZRCENT0021052. Deposited in the QM.

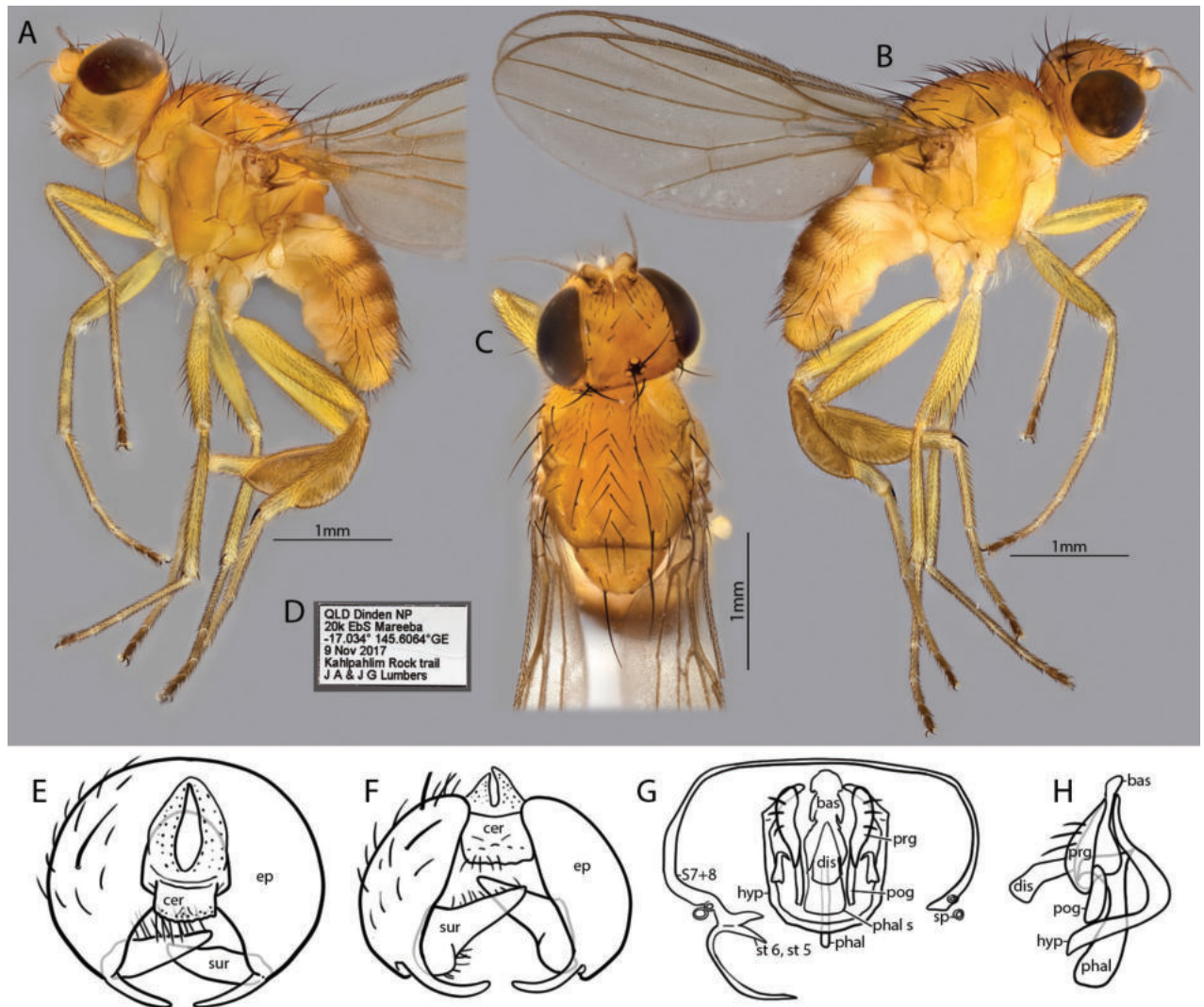


Figure 3. *Apotropina popeye* Ang, sp. nov. Holotype ♂ **A** habitus, left lateral view (wings truncated) **B** habitus, right lateral view **C** head & thorax, dorsal view **D** collection label **E** eandrium, terminal view **F** eandrium, ventral view **G** syntergosternite complex, hypandrium and phallic complex, ventral view **H** hypandrium and phallic complex, lateral view. Abbreviations: bas, basiphallus; cer, cercus; dis, distiphallus; ep, eandrium; hyp, hypandrium; phal, phallopodeme; phal s, phallopodemic sclerite; pog, postgonite; prg, pregonite; S, syntergosternite; sp, spiracle; st, sternite; sur, surstylus.

GenBank barcode. Holotype specimen (ZRCENT0021052): OR136429.

Diagnosis. Body largely yellowish orange except for blackened ocellar tubercle, light brown arista, brown dorsal regions on tergites and light yellow legs with darkened tarsal segments 4 and 5; gena deep, arista fulvous pectinate; wings hyaline with brown veins; hind tibial spur robust but short, male distinctive with extremely large, flattened oval hind tibial organ.

Description. Male. Body length, 4 mm. Wing length, 3.5 mm. **Head** (Fig. 3A–C). Broader than long dorsally, with deep gena in profile, light yellow except for black ocellar tubercle. Head setae black. Ocellar seta strongly developed, as long as inner and outer vertical setae. Postocellars cruciate, slightly shorter than ocellars. Three fronto-orbital setae developed, ~ 1/2 of ocellars; the two anterior proclinate and the posterior latero-clinate. Inner vertical seta latero-clinate and outer vertical seta inclinate. Three pairs of

interfrontal setae distinct; anterior two as long as fronto-orbitals, posterior half-length; all proclinate and slightly convergent. Frons as long as broad, lateral margins slightly convergent, front margin straight. Ocellar triangle with slight pruinosity, extending to half of frons length, posterior margin two thirds width of frons, lateral margins straight. Eye oval, long axis slightly oblique with short, very sparse pubescence. Face deeper than broad; antennae yellow except for brown base of arista, postpedicel reniform, as deep as long, arista with short pubescence, $\sim 3\times$ as long as postpedicel; gena $\sim 1/3$ as deep as eye height, with ~ 2 unordered rows of setulae and two vibrissae; genal dilation distinct. One row of postocular setae. Proboscis short yellow; palpus whitish, small, equal in length to postpedicel, with black setulae; mouth edge not protruding; clypeus light brown. **Thorax** (Fig. 3A–C). Entirely yellow, scutum slightly longer than broad, entirely pruinose; one row of latero-clinate acrostichal setae and one pair of parallel prescutellar acrostichal seta; five dorsocentral setae developed, the posterior one larger than the remaining four and as long as the ocellar seta; postpronotal lobe slightly lighter yellow than scutum; two long postpronotal seta, both similar length to notopleurals; prescutum with a pair of scapular seta (see Andersson 1977) on each side interior to postpronotal lobe at anterior margin; presutural intra-alar seta developed; notopleuron with 1+1 setae; one long presutural and two shorter postsutural supra-alar setae; postalar seta as long as ocellar seta. Pleuron dark brown, pruinose, katepisternum with one black seta on dorsal margin and populated with long white setulae on anterior half. Scutellum concolor, pruinose, broader than long, rounded apically with one pair of setulae on the disc; apical scutellar seta with separation greater to that of posterior ocelli and as long as half scutum; one pair of equally long lateral scutellar setae; postscutellum light brown. Halter pale yellow. **Wing** (Fig. 3B). Hyaline, covered in brown microtrichia; veins brown; costal ratios measured from h: R_1 : R_{2+3} : R_{4+5} : M_1 is 5: 7: 4.5: 1.5; veins R_{4+5} and M_1 subparallel; distance between r-m and dm-m five times length of r-m. **Legs** (Fig. 3A, B). Mostly light yellow except for dark brown on all tarsomeres 4 and 5, and light brown hind tibia, mid-coxal prong black. With dark pilosity organized in rows; posterior tibial organ extremely developed, occupying two-thirds of tibia basally and expanding it into a large, flattened tibial dilation; hind tibial spur subapical, as long as the width of the tibia apex. **Abdomen** (Fig. 3A, B). Tergites yellow with medial region light brown in dorsal view, with dark pilosity. Sternites weakly sclerotized, with white pilosity. **Male terminalia** (Fig. 3E–H). Postabdomen segments asymmetric as in generic diagnosis; sternites 5, 6 and syntergosternite 7+8 fused, spiracle 8 within sclerites on both sides. Epandrium well developed, with a laterobasal projection; surstylus conical, directed inwards; cerci fused, flattened; anal lobe membranous, short. Hypandrium with arms open; basiphallus oval; distiphallus short, cylindrical, and membranous; pregonite with three setulae; postgonite minute, elongate; phallapodeme short, not bifid basally.

Female. Unknown.

Etymology. The specific epithet *popeye* refers to the comically enlarged hind tibia, which in combination with the comparatively thin femur, resembles the distinctive arms and legs of the spinach-powered cartoon character “Popeye the Sailor”. It is a noun in the nominative singular standing in apposition.

***Apotropina aequalis* (Becker, 1911)**

Figs 4A–D, 25A, B

Parahippelates aequalis Becker, 1911: 111; Malloch 1924: 331.

Lasiopleura (*Lasiopleura*) *aequalis*: Malloch 1936: 23; 1940: 271.

Parahippelates variabilis Curran, 1936: 50 (synonymy: Sabrosky 1989: 651).

Type locality. PAPUA NEW-GUINEA: Stephansort, Astrolabe Bay (coll. Biró).

Distribution. AUSTRALIA: Australian Capital Territory (“Blundell’s, Molongo R.”; Canberra), New South Wales (Como; “Coramba-Dorrigo Rd”); PAPUA NEW-GUINEA: Bismarck Archipelago; SOLOMON ISLANDS: (Guadalcanar Is.; Santa Ana Is.; Matema Is.).

Examined material. *Allotype* [= *paratype*] ♀ Label transcription: “Guadalcanar Island, V-20-33; Kau Kau Plantation; Solomon Islands; M Willows Jr., Collector; Templeton Crocker Exped. 1933; *Parahippelates variabilis* Curran Allotype ♀; Collection of the California Academy Of Sciences, San Francisco, California”. Deposited in the CAS.

Taxonomic notes. This species was originally described from Papua New-Guinea based on a single specimen (sex not indicated); some Australian specimens were subsequently determined to the species (Malloch 1924, 1940). Note that Malloch (1940) erroneously stated that the type as “[o]riginally described from Sydney”. Type is indicated to be in the same collection as *A. nudiseta* Becker, apparently deposited in the Hungarian Natural History Museum, Hungary; however, the authors were not able to examine this material for this study, but were able to obtain an allotype of *Parahippelates variabilis* Curran (Fig. 4A–D), with the following chaetotaxy observed: 2 vibrissae; 1 weak decussate interfrontal setae; 2 postpronotal setae; 2 scapular setae; 1+1 notopleural setae; strong biseriate divergent acrostichal row; 1+3 dorsocentral setae; postalar and intrapostalar setae present; 1 weak acrostichal prescutellar setae; 2 setulae on scutellum; katapisternal seta weak. Becker (1911) did include a drawing of the head in lateral view (Fig. 25A) and Malloch (1940) illustrated the hind tibial spur (Fig. 25B). This species does not have any immediately distinctive diagnosable character sets based on existing descriptions. As such, study with more identified material from recorded localities would be useful for determining the limits of this apparently widespread species. Note that the images provided in Fig. 4A–D are of the *P. variabilis* allotype specimen. Original description and subsequent taxonomic notes in Suppl. material 1.

***Apotropina albiseta* (Malloch, 1924)**

Fig. 5A–E

Parahippelates albiseta Malloch, 1924: 330.

Type locality and distribution. AUSTRALIA: Queensland (Eidsvold; Draper).

Examined material. *Holotype* ♂ Label transcription: “Australian Museum, K 584429; Bancroft, Eidsvold Q., 19.8’23; K50096; *Parahippelates albiseta* Type, Det. J R Malloch”; 25°22’14”S, 151°7’21”E. Deposited in the AMRI.

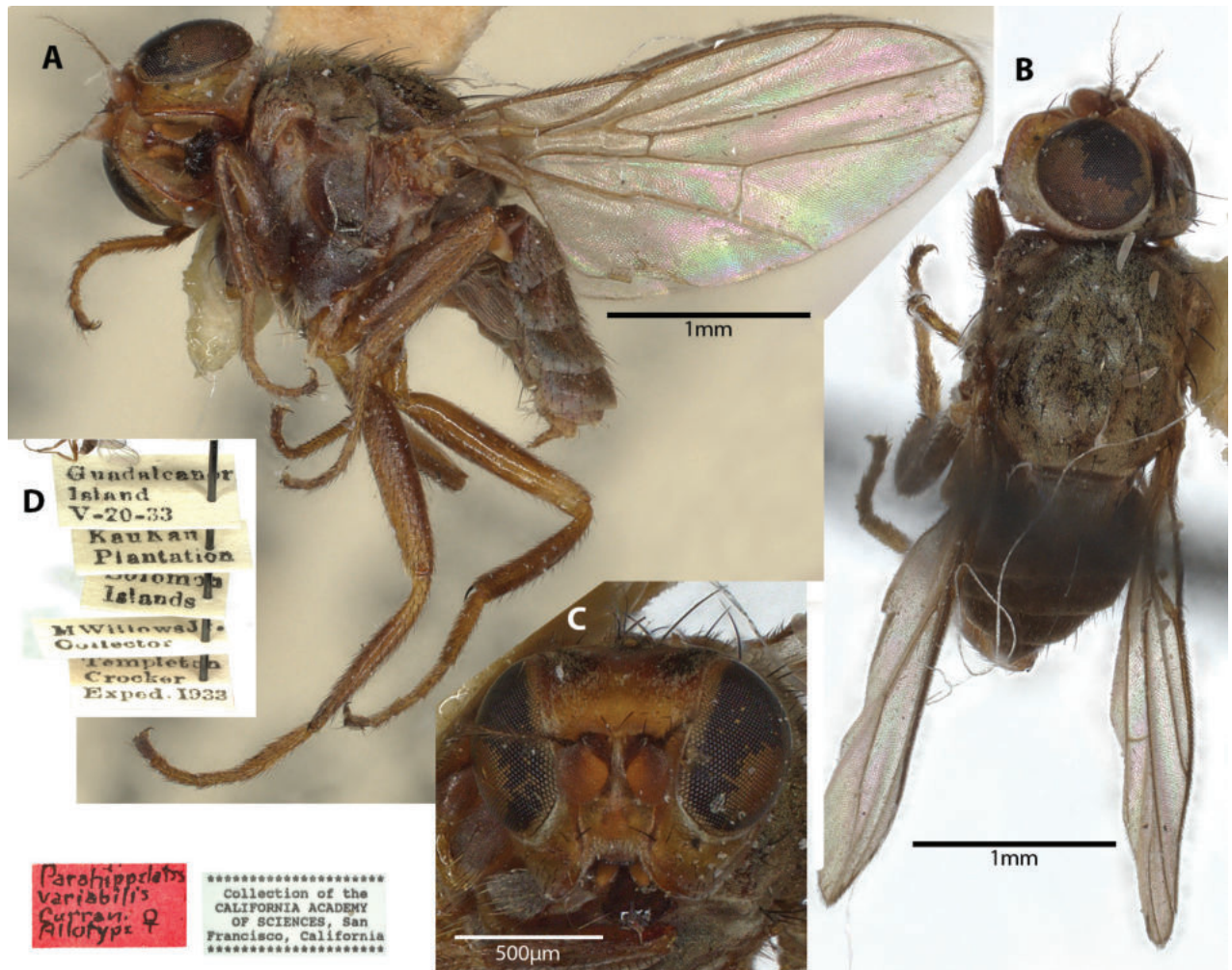


Figure 4. *Parahippelates variabilis* Curran Allotype ♀, (synonym of *Apotropina aequalis*) **A** habitus, lateral view **B** habitus, dorsal view **C** head, anterior view **D** specimen labels.

Taxonomic notes. This is a testaceous species with distinctive white pubescent arista (Fig. 5C). It was described based on a syntype series in AMRI of four specimens with accession code K50096. The specimens are now separated, and we designate one male holotype (K 584429, imaged), and three paratypes (K 584430, male; K 584431, female; K 584432, female). An iNaturalist observation (Sarna 2020) further shows a female specimen in situ from Draper, Queensland (Fig. 5E). Chaetotaxy as observed: 2 vibrissae; 3 strong inclinate interfrontal setae; 2 postpronotal setae; 2 scapular setae; 1+1 notopleural setae; strong biseriate divergent acrostichal row; 1+3 dorsocentral setae; 1+2 supra-alar setae; postalar and intrapostalar setae present; katepisternal seta missing/indistinct. Original description and images of all type specimen labels in Suppl. material 1.

***Apotropina anomala* (Malloch, 1925)**

Fig. 6A–D

Parahippelates anomala Malloch, 1925: 96.

Lasiopleura (Lasiopleura) anomala: Malloch 1940: 273.

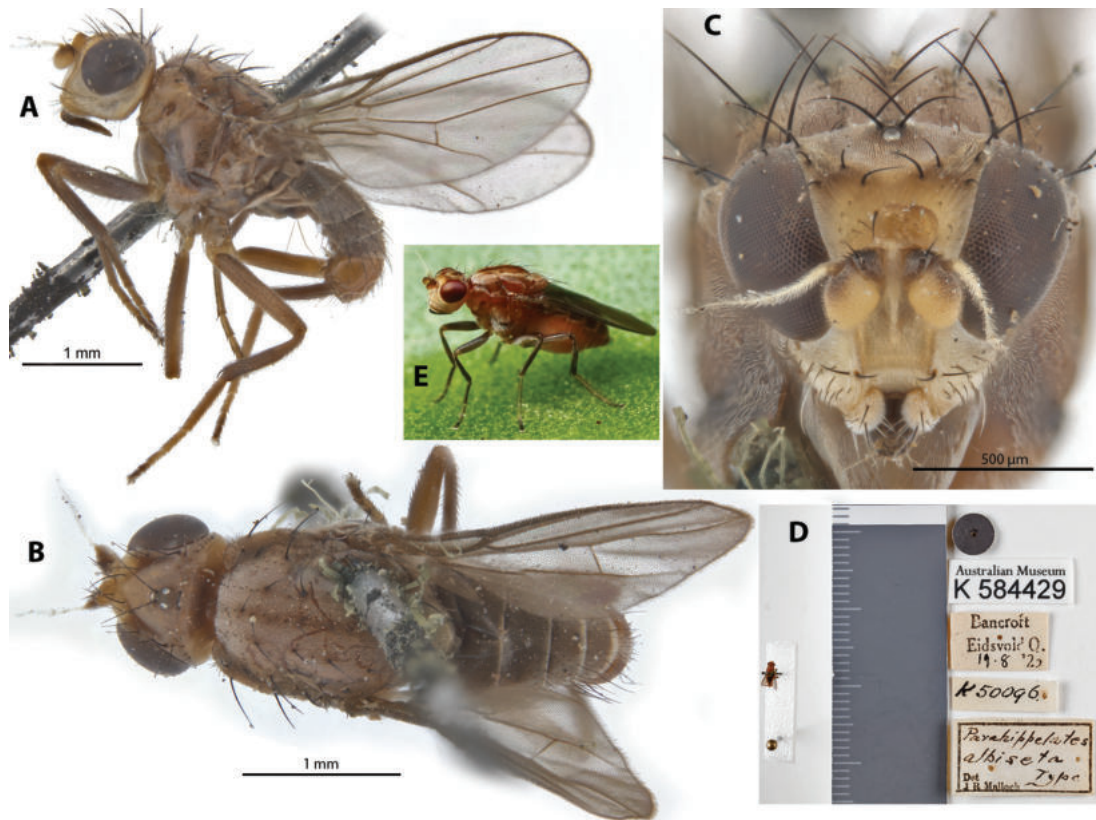


Figure 5. *Apotropina albisetata* (Malloch) holotype ♂ (K 584429) and live specimen ♀ **A** holotype ♂ habitus, lateral view **B** holotype ♂ habitus, dorsal view **C** holotype ♂ head, anterior view **D** holotype ♂ specimen labels **E** ♀ live specimen, iNaturalist observation (Sarna 2020).

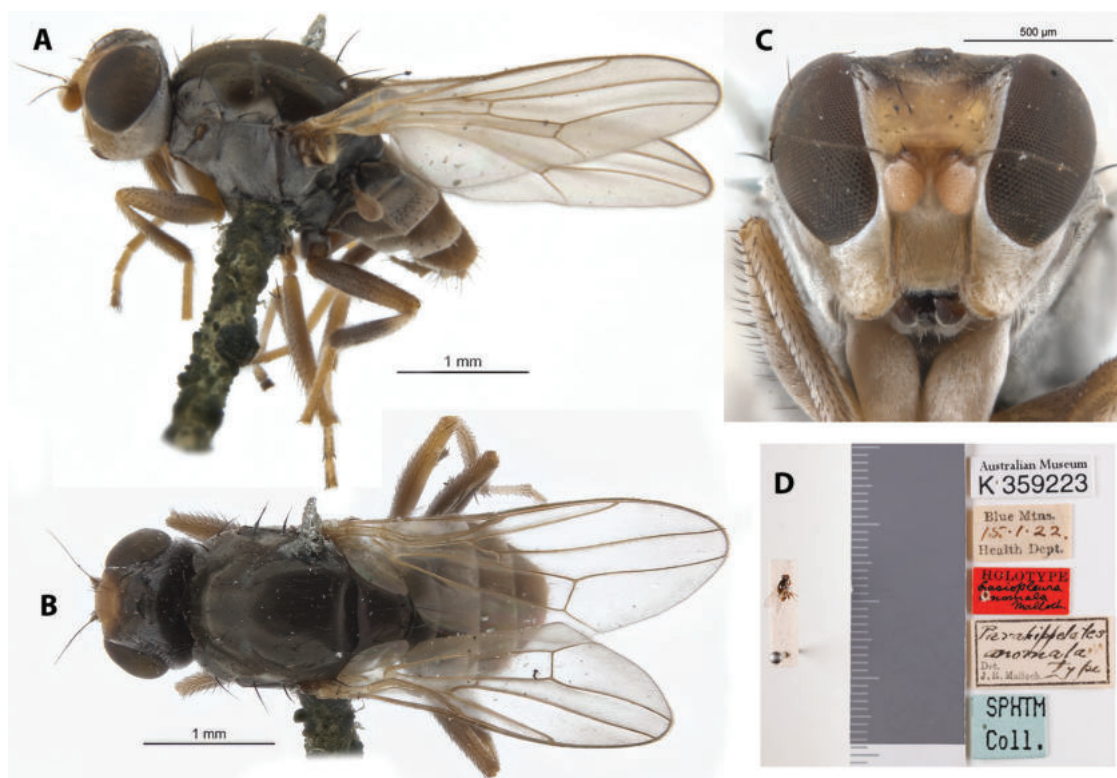


Figure 6. *Apotropina anomala* (Malloch) holotype ♀ (K 359223) **A** habitus, lateral view **B** habitus, dorsal view **C** head, anterior view **D** specimen labels.

Type locality. AUSTRALIA: New South Wales (Blue Mountains).

Distribution. AUSTRALIA: New South Wales (Blue Mountains), South Australia (Mt. Eba).

Examined material. Holotype ♀ Label transcription: "Australian Museum, K 359223; Blue Mtns., 15.1.22., Health Dept.; HOLOTYPE, *Lasiopleura anomala* Malloch; *Parahippelates anomala* Type, Det. J.R.Malloch; SPHTM Coll."; 33°39'55"S, 150°17'4"E. Deposited in the AMRI.

Taxonomic notes. This is a dark colored species with whitish tomentosity. It is noted for its sexually dimorphic wing venation. Initially described based on female specimens (Malloch 1925) with normal venation (Fig. 6B), male specimens were found to have R_{2+3} curved anteriorly and R_{4+5} curved posteriorly, creating a much wider r_{2+3} and narrower r_1 cells (Malloch 1940). Chaetotaxy as observed: 1 (white) vibrissa; 3 weak proclinate interfrontal setae; 2 postpronotal setae; at least 1 scapular seta; 1+1 notopleural setae; weak biseriate acrostichal row; 1+3 dorsocentral setae; postalar and intrapostalar setae present. Currently, the holotype and five paratypes are Deposited in the AMRI. Original description and subsequent taxonomic notes in Suppl. material 1.

***Apotropina australis* (Malloch, 1924)**

Fig. 7A–E

Ephydroscinis australis Malloch, 1924: 331.

Type locality and distribution. AUSTRALIA: New South Wales (Woy Woy).

Examined material. Holotype ♂ Label transcription: "Australian Museum, K 359224; WoyWoy, 2.Sept. '23, Mackerras; HOLOTYPE, *Ephydroscinis australis* Mall.; *Ephydroscinis australis* Type, Det. J R Malloch; SPHTM Coll."; 33°29'10"S, 151°19'24"E. Deposited in the AMRI.

Taxonomic notes. This distinctive species is dark colored with whitish tomentosity. It was described from a male (holotype; Fig. 7A–C) and female specimen from the type locality and is noted for the male's sexually dimorphic geniculate arista; female has normal bare arista (Fig. 7E). Chaetotaxy as observed: no vibrissae; 5 or 6 weak proclinate interfrontal setae; 2 postpronotal setae; 1+1 notopleural setae; weak biseriate acrostichal row; 1+3 dorsocentral setae; katepisternal seta missing/indistinct. Original description in Suppl. material 1.

***Apotropina brunneicosta* (Malloch, 1923)**

Fig. 8A–C

Parahippelates brunneicosta Malloch, 1923: 620.

Lasiopleura (*Lasiopleura*) *brunneicosta*: Malloch 1940: 272.

Type locality and distribution. AUSTRALIA: Northern Territory (Darwin).

Examined material. Holotype ♀ Label transcription: "TYPE; Darwin, G. F. Hill; *Parahippelates brunneicosta* Type, Det. J.R.Malloch"; deposited in the SAMA.

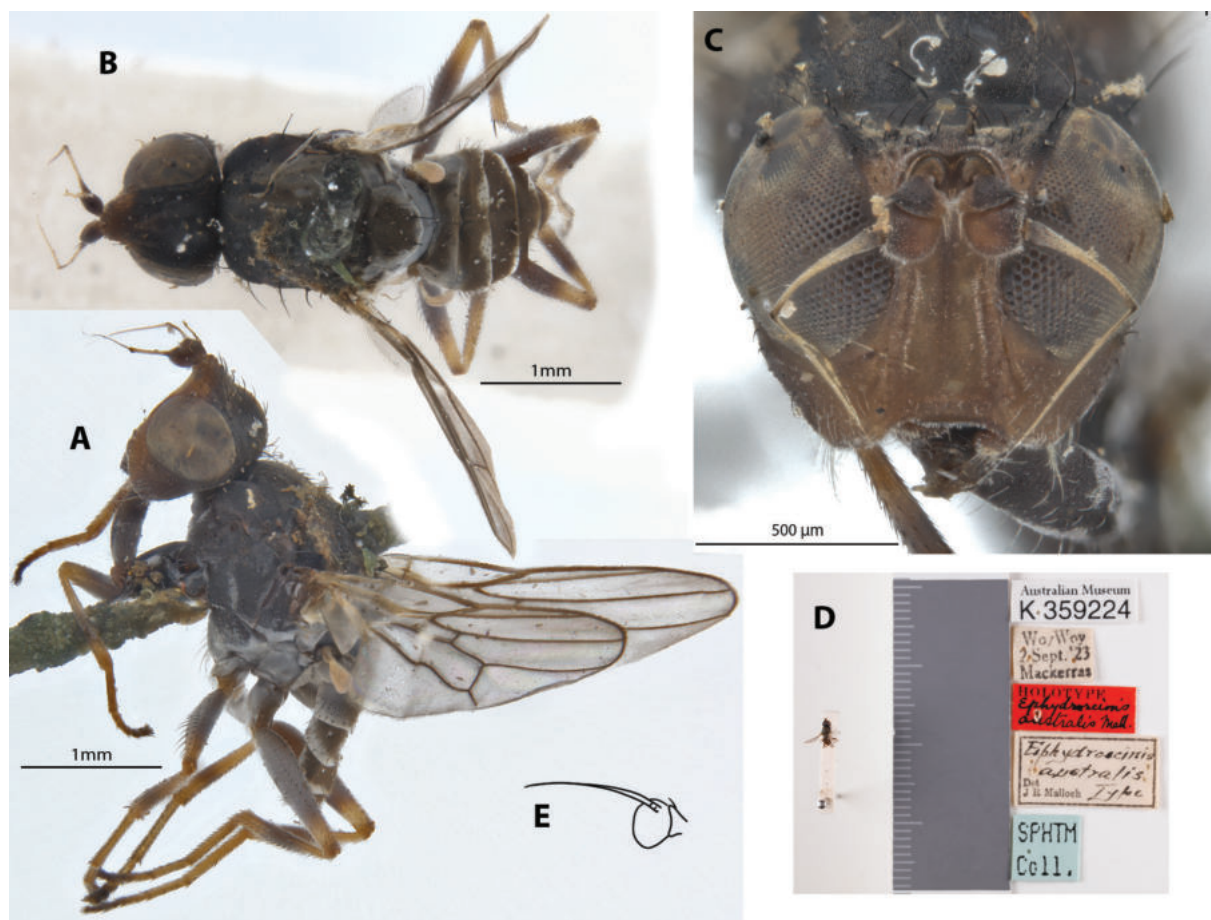


Figure 7. *Apotropina australis* (Malloch) holotype ♂ (K 359224) & female. **A** holotype ♂ habitus, lateral view **B** holotype ♂ habitus, dorsal view **C** holotype ♂ head, anterior view **D** holotype ♂ specimen labels **E** ♀ antennae, illustration adapted from Malloch, 1924: 332.

Taxonomic notes. This testaceous species is distinctive for having its costal regions of the wing browned from the apex of R_1 to M_1 (Fig. 8A). Chaetotaxy as observed: 1 to 2 vibrissae; at least 3 weak proclinate interfrontal setae; 2 postpronotal setae; 2 scapular setae; 1+1 notopleural setae; weak biseriate divergent acrostichal row; 1+3 discal setae; 1+1 supra-alar setae; postalar setae and intrapostalar setae present; scutellum with 1 dorsocentral setulae; katepisternal seta present but weak. It is described based on a single female; male morphology remains unknown. Original description in Suppl. material 1.

***Apotropina conopsea* (Duda, 1934)**

Fig. 9A–D

Parahippelates conopseus Duda, 1934: 45.

Lasiopleura (*Lasiopleura*) *conopsea*: Malloch 1936: 23; 1940: 273.

Type locality and distribution. AUSTRALIA: Queensland (Cairns).

Examined material. **Syntype** ♀ Label transcription: "Holotypus"; Typus; Cairns, N. Queensland., 1907; coll. Lichtwardt; *Parahippelates conopseus* D., ♀ d. Duda; <http://coll.mfn-berlin.de/u/5c8591>". Deposited in the MfN.

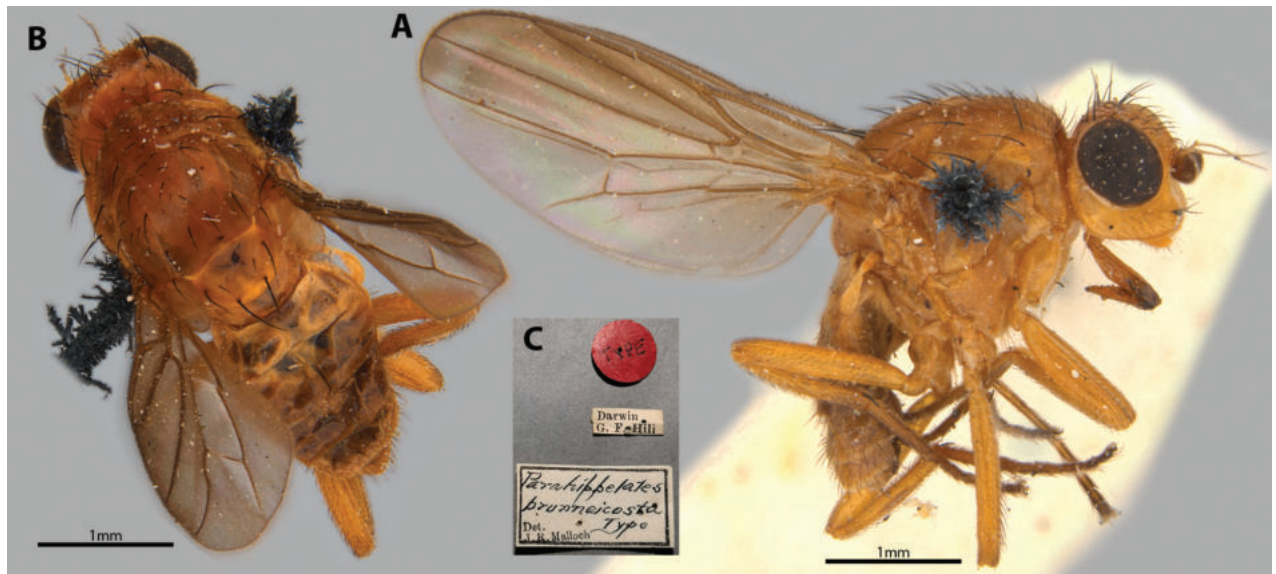


Figure 8. *Apotropina brunneicosta* (Malloch) holotype ♀ **A** habitus, lateral view **B** habitus, dorsal view **C** specimen labels.

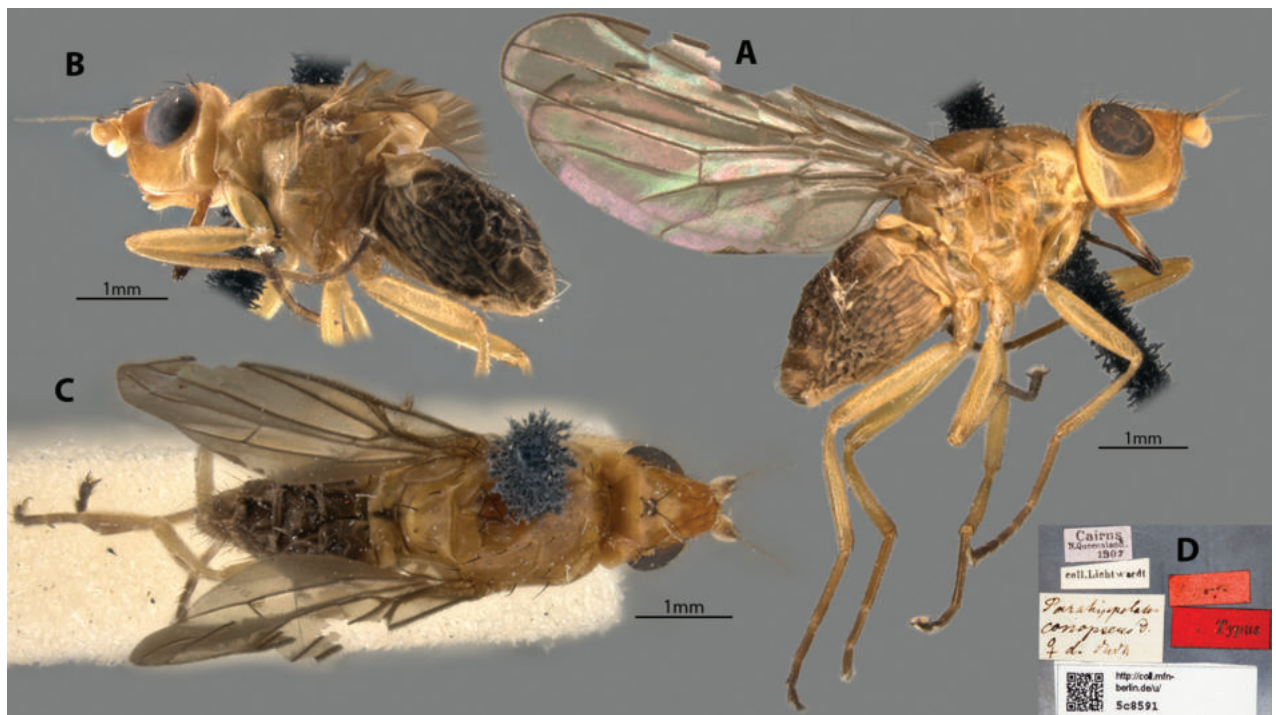


Figure 9. *Apotropina conopsea* (Duda) syntype ♀ (5c8591) **A** habitus, right lateral view **B** habitus, left lateral view **C** habitus, dorsal view **D** specimen labels.

Taxonomic notes. This testaceous species is distinctive for its deep gena, relatively small eyes, long dark geniculate proboscis (Fig. 9A, B) and strongly projected frons (Fig. 9C). Originally described in detail by Duda (1934) based on five specimens (2♂, 3♀), with Malloch (1936) adding more details. Chaetotaxy as observed: no vibrissae; 3 strong proclinate interfrontal setae; 2 postpronotal setae; 2 scapular setae; 1+1 notopleural setae; weak biseriate divergent acrostichal row; 1+3 dorsocentral setae; 1+1 supra-alar setae; postalar and intrapostalar setae present; scutellum with 1 discal setula; katepisternal seta missing/

indistinct. Note that Malloch (1940) stated the type locality (being N. Territory: Darwin) in error, which should be Queensland instead. Original description and subsequent taxonomic notes in Suppl. material 1.

***Apotropina costumaculata* (Malloch, 1924)**

Fig. 10A–D

Parahippelates costumaculata Malloch, 1924: 329.

Lasiopleura (*Lasiopleura*) *costumaculata*: Malloch 1940: 270.

Type locality and distribution. AUSTRALIA: New South Wales (Sydney).

Examined material. *Holotype* ♂ Label transcription: “Australian Museum, K 50094; Sydney, 31.12.22, Health Dept.; (red circle label); K50094; *Parahippelates costumaculata* Type, Det J R Malloch”; 33°52'S, 151°13'E. Deposited in the AMRI.

Taxonomic notes. This brownish species is similar to *A. maculigena* sp. nov. in that it has a genal macula and wing with an elongate macula on the costal region within cells r_1 and r_{2+3} (Fig. 10A) but can be reliably differentiated from the latter by its much smaller genal macula (never close to reaching the ventral margin: Fig. 10A), bearing both dark and whitish genal setae (all black in *A. maculigena* sp. nov.), lighter anterior gena and legs, and also a less projected frons (Fig. 10B). Three male specimens from the type locality are known thus far. Female morphology currently unknown but based on the sexual dimorphism exhibited in *A. maculigena* sp. nov., it is likely that females in *A. costumaculata* will also have completely hyaline wings. Chaetotaxy as observed: 3–4 vibrissae; 2 strong decussate interfrontal setae; 2 postpronotal setae; 2 scapular setae; 1+1 notopleural setae; weak biseriate divergent acrostichal row; 1+3 dorsocentral setae; 1+1 supra-alar setae; postalar and intrapostalar setae present; 1 strong prescutellar seta; scutellum with 1 discal setula; katepisternal seta missing/indistinct. Original description in Suppl. material 1.

***Apotropina dasypleura* (Malloch, 1928)**

Fig. 11A–D

Parahippelates (*Terraeregina*) *dasypleura* Malloch, 1928: 303.

Lasiopleura (*Terraeregina*) *dasypleura*: Malloch 1940: 270.

Type locality and distribution. AUSTRALIA: Queensland (Macknade).

Examined material. *Holotype* ♀ Label transcription: “Australian Museum, K 359225; Macknade, 1918., Q.; HOLOTYPE, *Lasiopleura* (*Terraeregina*) *dasypleura* Type, Det. J.R. Malloch”; 18°35'15"S, 146°15'38"E. Deposited in the AMRI.

Taxonomic notes. This is a dark colored species with whitish tomentosity and is distinct for its completely whitish pruinose pleura (including anepisternum: Fig. 11A), and two longitudinal strips on the scutum (Fig. 11B). Chaetotaxy as observed: no vibrissae; at least 2 weak proclinate interfrontal setae; 2 postpronotal setae; 2 scapular setae; 1+1 notopleural setae; weak biseriate divergent acrostichal row; 1+3 dorsocentral setae; 1+1 supra-alar setae; postalar

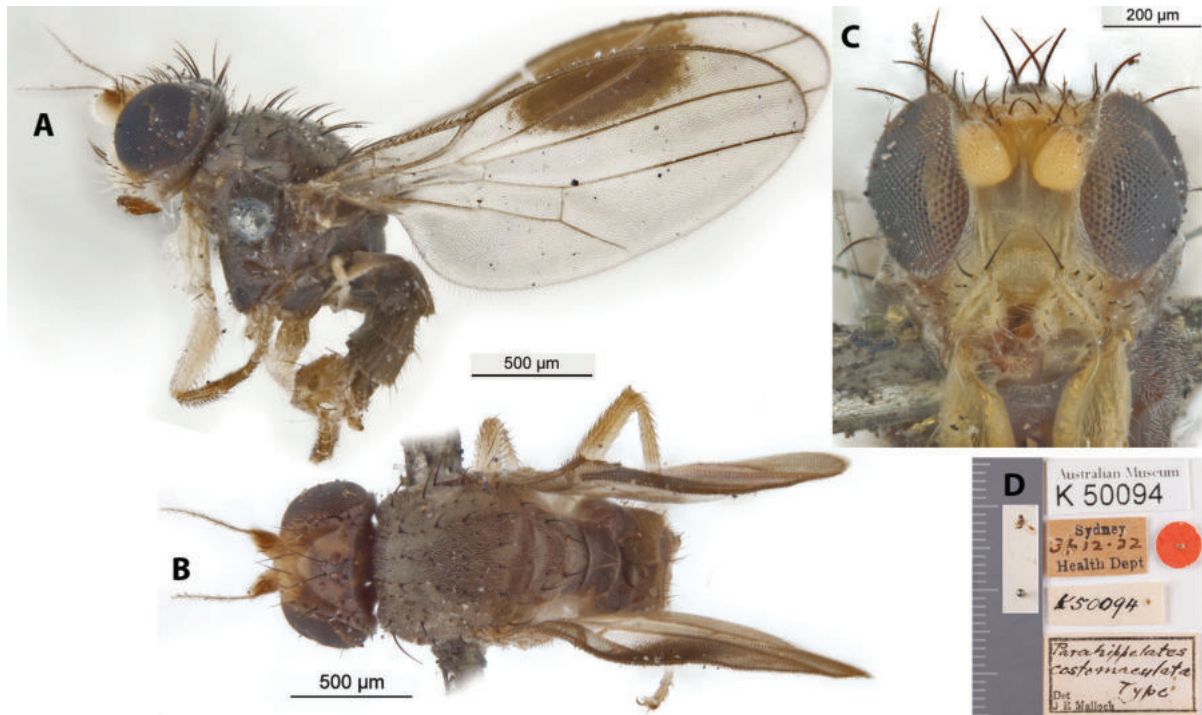


Figure 10. *Apotropina costomaculata* (Malloch) holotype ♂ (K 50094) A habitus, lateral view B habitus, dorsal view C head, anterior view D specimen labels.

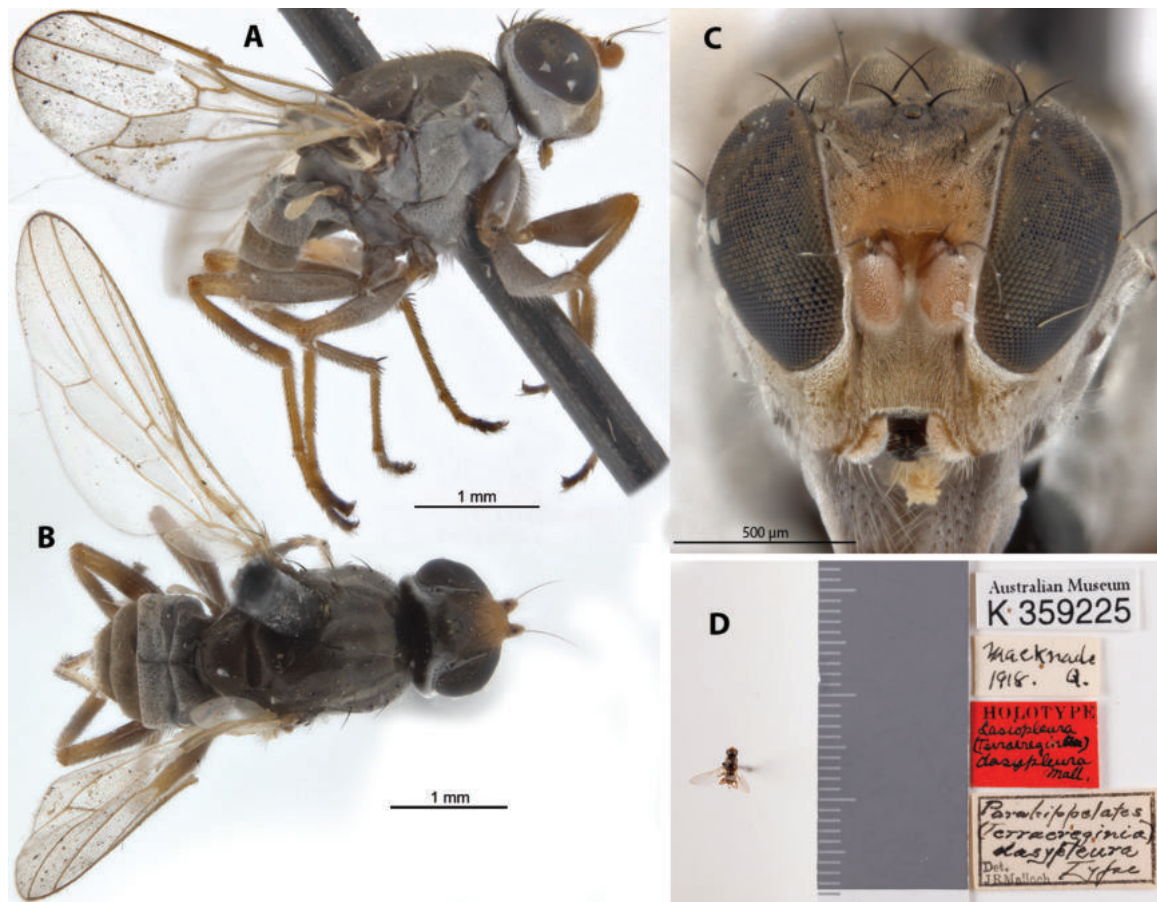


Figure 11. *Apotropina dasypleura* (Malloch) holotype ♀ (K 359225) A habitus, lateral view B habitus, dorsal view C head, anterior view D specimen labels.

and intrapostalar setae present; scutellum with 1 discal setula; katepisternal seta missing/indistinct. It is described from one female specimen and is only known from the type locality.

Original description in Suppl. material 1.

***Apotropina duplicata* (Malloch, 1928)**

Fig. 12A–C

Parahippelates duplicata Malloch, 1923: 621.

Lasiopleura (*Lasiopleura*) *duplicata*: Malloch 1940: 272.

Type locality and distribution. AUSTRALIA: Northern Territory (Melville Is.).

Examined material. Holotype ♂ Label transcription: “Melville Is., N.T., G. F. Hill; *Parahippelates duplicata* Type, Det. J.R.Malloch”. Deposited in the SAMA.

Taxonomic notes. This is a relatively testaceous species with darkened dorsum, glossy hypopygium and yellowish legs, largely covered in whitish tomentosity (Fig. 12A, B). It does not have any immediately distinctive diagnosable character sets based on existing descriptions but can be identified based on the provided key. Thus far only known from the male type specimen; female morphology unknown. Chaetotaxy as observed: 2 vibrissae; 3 strong inclinate/decussate interfrontal setae; 2 postpronotal setae; 2 scapular setae; 1+1 notopleural setae; weak biseriate divergent acrostichal row; 1+3 dorsocentral setae; 1+1 supra-alar setae; postalar and intrapostalar setae present; 1 strong prescutellar seta; scutellum with 1 discal setula; katepisternal seta missing/indistinct. Original description in Suppl. material 1.

***Apotropina exquisita* (Malloch, 1940)**

Fig. 13A–D

Lasiopleura (*Lasiopleura*) *exquisita* Malloch, 1940: 270.

Type locality and distribution. AUSTRALIA: Western Australia (Geraldton).

Examined material. Holotype ♂ Label transcription: “Australian Museum, K 359226; Geraldton, W.A., 5. Sept. 1926., E.W. Ferguson; HOLOTYPE, *Lasiopleura exquisita* Mall.; *Lasiopleura exquisita* Type, det. JRMALLOCH; SPHTM Coll.”; 28°46'S, 114°37'E. Deposited in the AMRI.

Taxonomic notes. *Apotropina exquisita* belongs to a group of described species (including *A. ornatipennis*, *A. proxima*, and *A. raymenti*) that have dark bodies with shiny tomentosity, wings with distinct dark patterning covering at least the medial region from costal margin to beyond R_{2+3} vein, and usually shiny-white alula. *Apotropina exquisita* can be distinguished from other species in this group with the following combination of characters: short capitate proboscis, with more than two distal tarsal segments dark, pleuron not completely whitish tomentose, wing with completely dark venation especially basally, and femora dark with extreme apices yellow (Fig. 13A–C). This species is only known from female specimens, male morphology unknown. However, there is evidence that species in this group may have sexually dimorphic color patterns (see Fig. 1)

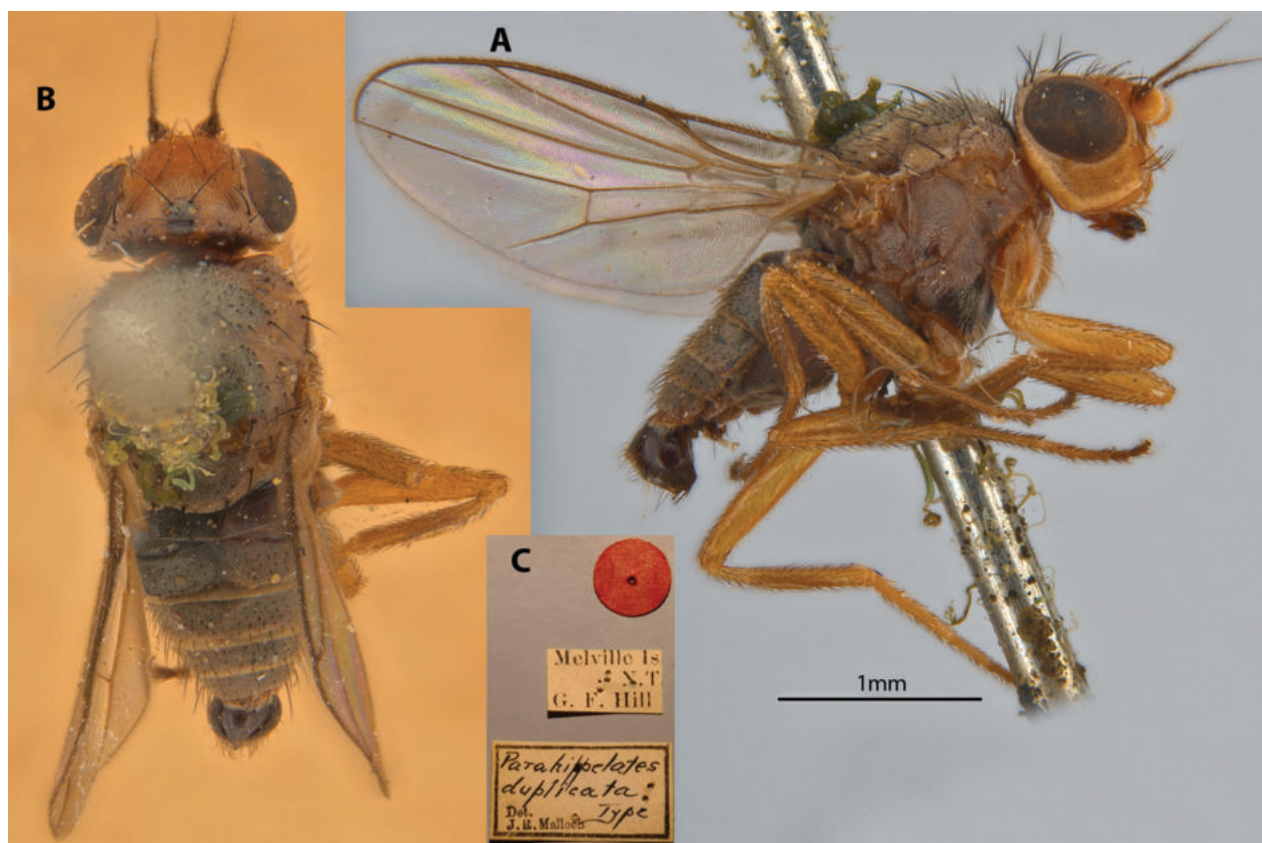


Figure 12. *Apotropina duplicata* (Malloch) holotype ♂ **A** habitus, lateral view **B** habitus, dorsal view **C** specimen labels.

where males may have more prominent patterns than females. Chaetotaxy as observed: 1 vibrissa; 2 weak proclinate interfrontal setae; 2 postpronotal setae; 2 scapular setae; 1+1 notopleural setae; short weak biseriate acrostichal row only in medial region of scutum; 1+3 dorsocentral setae; 1+1 supra-alar setae; postalar and intrapostalar setae present; scutellum with 1 discal setula; katepisternal seta missing/indistinct. Original description in Suppl. material 1.

***Apotropina griseovitta* (Malloch, 1936)**

Fig. 14A–C

Lasiopleura griseovitta Malloch, 1936: 25, 1940: 25.

Type locality and distribution. AUSTRALIA: Queensland (Mt Molloy).

Examined material. Holotype ♂ Label transcription: "Australian Museum, K 359227; Mt. Molloy, QUEENSLAND, F.H. Taylor; HOLOTYPE, *Lasiopleura "griseohirta"* [note: likely a misspelling] Mall.; *Lasiopleura griseovitta* Type, det. JRMALLOCH; SPHTM Coll."; 16°40'27"S, 145°19'50"E. Deposited in the AMRI.

Taxonomic notes. Malloch (1936) described this species based on a single male specimen, which has a predominantly tawny thorax, darker abdomen, yellowish legs, and the scutum has a broad central pruinose stripe along the dorso-centrals. Unfortunately, the male holotype specimen is currently damaged: head missing, pruinosity pattern on scutum likely abraded (Fig. 14A, B). Malloch (1940)

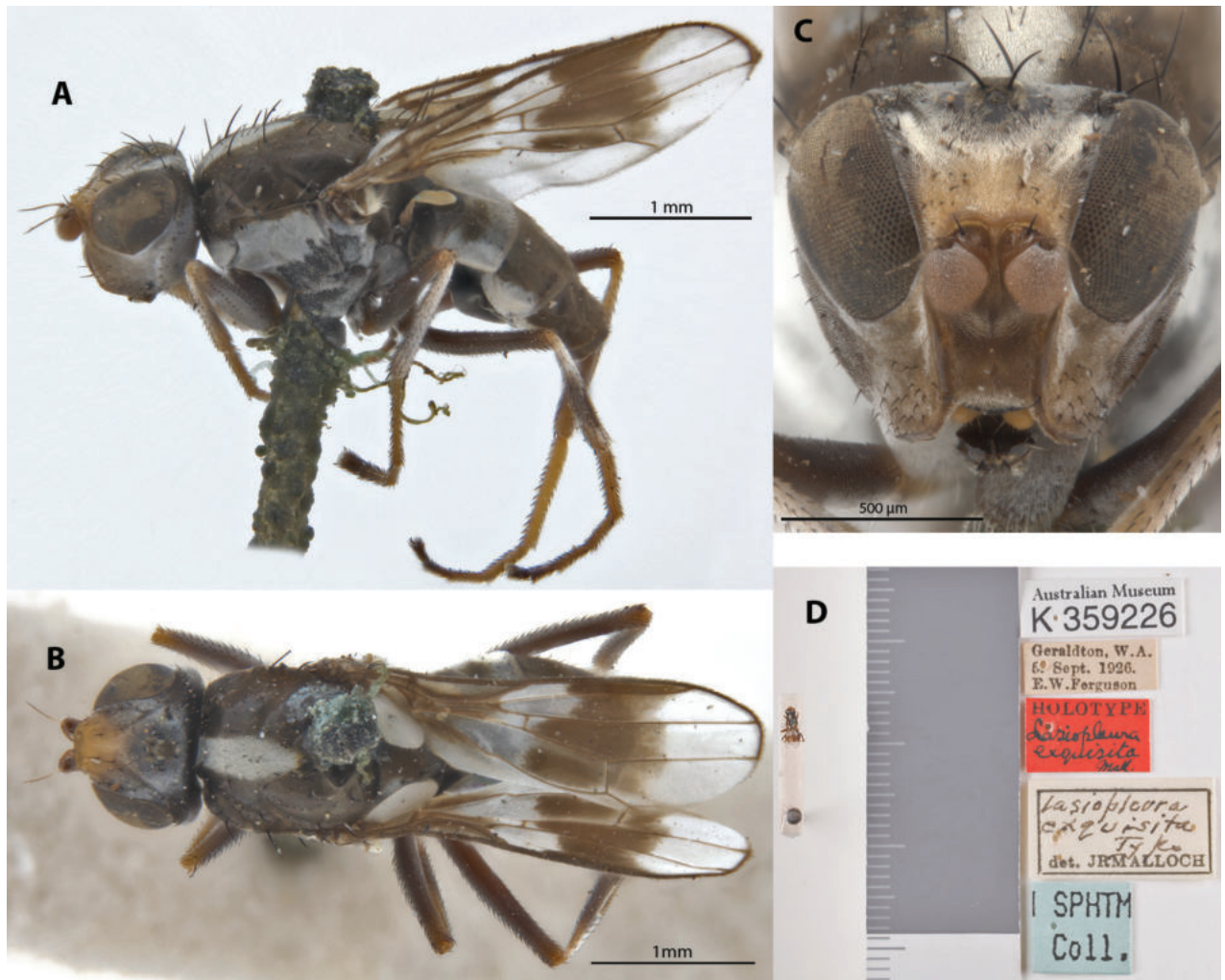


Figure 13. *Apotropina exquisita* (Malloch) holotype ♀ (K 359226) **A** habitus, lateral view **B** habitus, dorsal view **C** head, anterior view **D** specimen labels.

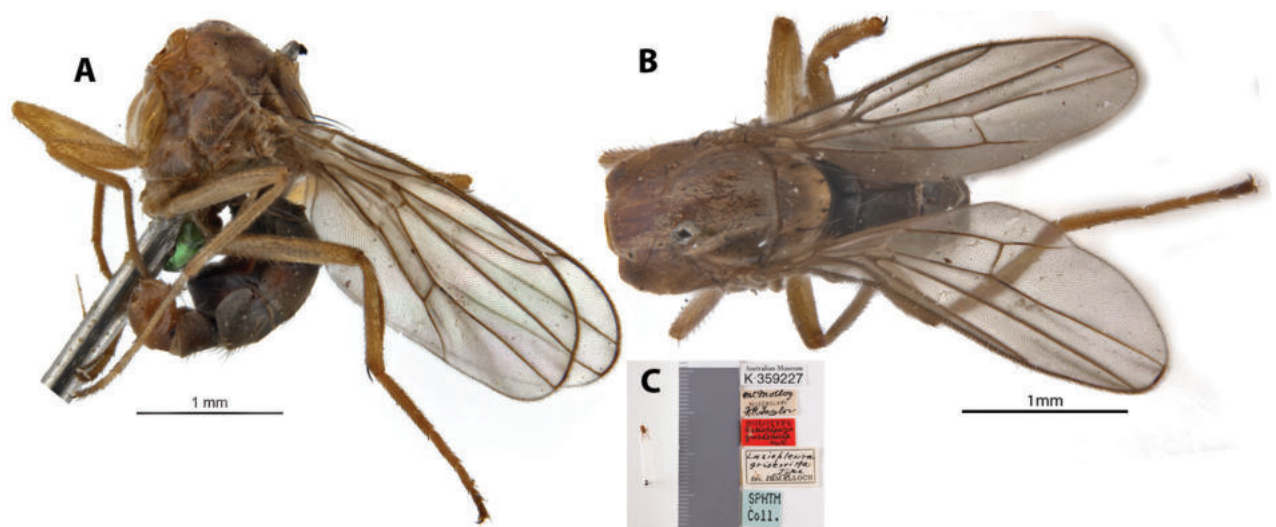


Figure 14. *Apotropina griseovitta* (Malloch) holotype ♂ (missing head; K 359227) **A** habitus, lateral view **B** habitus, dorsal view **C** specimen labels.

subsequently determined a female specimen from the type locality without providing his reasoning for assigning it to this species, and noted that the female has two narrow pruinose stripes on the scutum (as opposed to a single broad stripe in the male). We were unable to examine the female specimen for this study. Based on Malloch's (1936, 1940) descriptions, there are no autapomorphies to easily diagnose this species, and the set of characters used to delimit this species contains multiple interpretations (e.g., the basal pilosity on the arista is either twice as long [♂] or just as long as the basal width of arista [♂ & ♀], arista either pale-yellow [♂] or brownish [♀] and the aforementioned sexually dimorphic difference in scutal pruinosity pattern). Malloch (1940) acknowledges this multiplicity in the diagnosis of this species and makes three possible interpretations in his key; this is reflected in ours as well. In our opinion, the species limits for *A. griseovitta* are poorly defined and need to be further investigated with more character systems (e.g., genitalia, molecular data). Chaetotaxy as observed: 2 postpronotal setae; 1+1 notopleural setae; postalar and intrapostalar setae present; scutellum with 1 dorsocentral setula; katepisternal seta missing/indistinct. Original description and subsequent taxonomic notes in Suppl. material 1.

***Apotropina nigripila* (Duda, 1934)**

Fig. 15A–D

Parahippelates nigripilus Duda, 1934: 48.

Type locality and distribution. AUSTRALIA: Northern Territory (Darwin: Palmerston).

Examined material. Syntype ♂ Label transcription: "Palmerston, N. Australien, XI. 1908; coll. Lichtwardt; *Parahippelates nigripilus* Duda, ♂ d Duda; Typus; <http://coll.mfn-berlin.de/u/5c8585>". Deposited in the MfN.

Taxonomic notes. This is a testaceous species comparable to *A. rufescens* but with more distinct and stronger setation (Fig. 15A–C). It was described based on male specimens and is only known from the type locality. Female morphology unknown. This species does not have any immediately distinctive diagnosable character sets based on existing descriptions but can be identified based on the provided key. Chaetotaxy as observed: 2 vibrissae; at least 3 proclinate interfrontal setae; 2 postpronotal setae; 2 scapular setae; 1+1 notopleural setae; strong biseriate divergent acrostichal row; 1+3 dorsocentral setae; 1+1 supra-alar setae; postalar and intrapostalar setae present; scutellum with 1 discal setula; katepisternal seta missing/indistinct. Original description, translation, and subsequent taxonomic notes in Suppl. material 1.

***Apotropina nudiseta* (Becker, 1911)**

Fig. 25C, D

Parahippelates nudiseta Becker, 1911: 113.

Lasiopleura (*Lasiopleura*) *nudiseta*: Malloch 1940: 274.

Type locality and distribution. AUSTRALIA: New South Wales (Botany Bay, Sydney; Wahroonga, nr. Sydney).

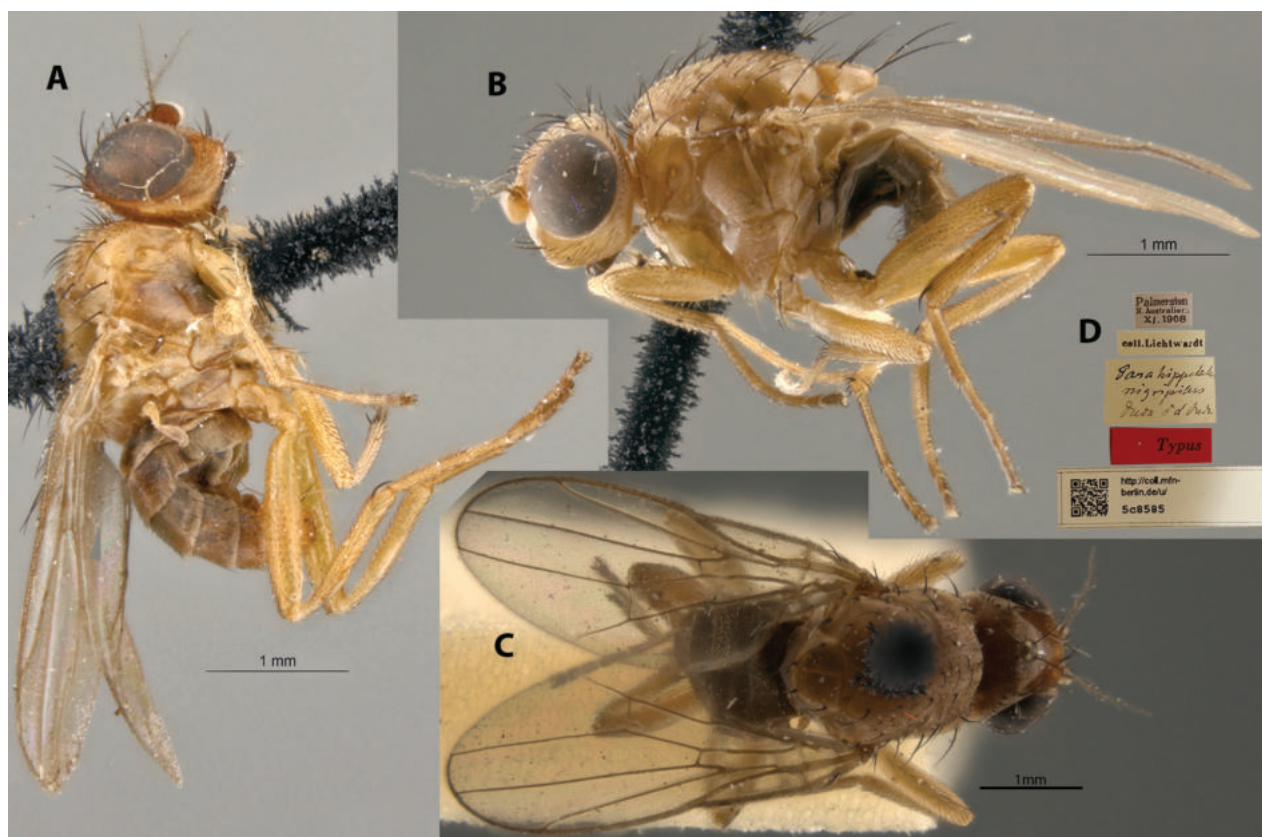


Figure 15. *Apotropina nigripila* (Duda) syntype ♂ (5c8585) **A** habitus, right lateral view **B** habitus, left lateral view **C** habitus, dorsal view **D** specimen labels.

Taxonomic notes. This species was described from the type locality (Sydney) and remains known only from the area. Type material is noted to be in the same collection as *A. aequalis* Becker, apparently deposited in the Hungarian Natural History Museum, Hungary; however, the authors were not able to examine the material for this study. Malloch (1940) provides illustrations of the arista and hind tibial spur (Fig. 25C, D). This species does not have any immediately distinctive diagnosable character sets based on existing descriptions but can be identified based on the provided key. The original description and subsequent taxonomic notes in Suppl. material 1, which indicate chaetotaxy as having four or more strong decussate acrostichals and “similarly arranged” dorsocentral setae.

***Apotropina ornatipennis* (Malloch, 1940)**

Fig. 16A–C

Parahippelates ornatipennis Malloch, 1923: 620.

Lasiopleura (*Lasiopleura*) *ornatipennis*: Malloch 1940: 270.

Type locality and distribution. AUSTRALIA: Victoria (Chelsea), New South Wales (Collaroy, nr. Sydney).

Examined material. *Holotype* ♀ Label transcription: “Chelsea, V., 28.9.19; *Parahippelates ornatipennis* Type, Det. J.R.Malloch”. Deposited in the SAMA.

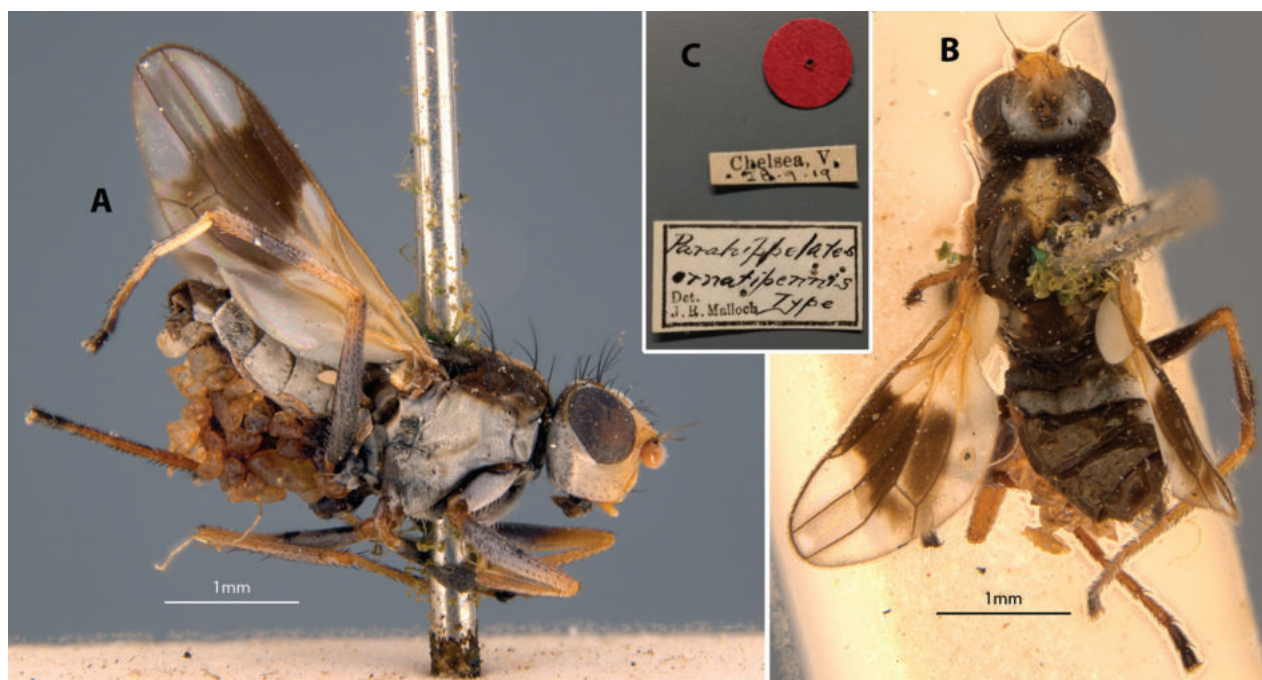


Figure 16. *Apotropina ornatipennis* (Malloch) holotype ♀ **A** habitus, lateral view **B** habitus, dorsal view **C** specimen labels.

Taxonomic notes. *Apotropina ornatipennis* belongs to a group of described species (including *A. exquisita*, *A. proxima* and *A. raymenti*) that have dark bodies with shiny tomentosity, wings with distinct dark patterning covering at least the medial region from costal margin to beyond R_{2+3} vein, and usually shiny-white alula. *Apotropina ornatipennis* can be distinguished from other species in this group with the following combination of characters: short capitate proboscis, with more than two distal tarsal segments dark, katepisternum completely whitish tomentose, wing veins lighter basally, darker brown near apex, femora dark but broadly yellow at least a quarter to the apices (Fig. 16A, B). This species is only known from female specimens, male morphology unknown. However, there is evidence that species in this group may have sexually dimorphic color patterns (see Fig. 1) where males may have more prominent patterns than females. Chaetotaxy as observed: 1 vibrissa; 2 moderately-strong proclinate interfrontal setae; 2 postpronotal setae; 1+1 notopleural setae; short weak biseriate acrostichal row only in medial region of scutum; katepisternal seta missing/indistinct. Original description in Suppl. material 1.

***Apotropina pallipes* (Malloch, 1940)**

Fig. 17A–D

Lasiopleura (*Lasiopleura*) *parva* var. *pallipes* Malloch, 1940: 273.

Type locality and distribution. AUSTRALIA: New South Wales (Narrabeen, Sydney).

Examined material. **Holotype** ♀ Label transcription: "Australian Museum, K 359228; Sydney, Narrabeen, 21.7.23, Health Dept.; HOLOTYPE, *L. parva pallipes* Mall.; Probable type of *pallipes*; in Mall. Colln. With paratype of *parva*.,

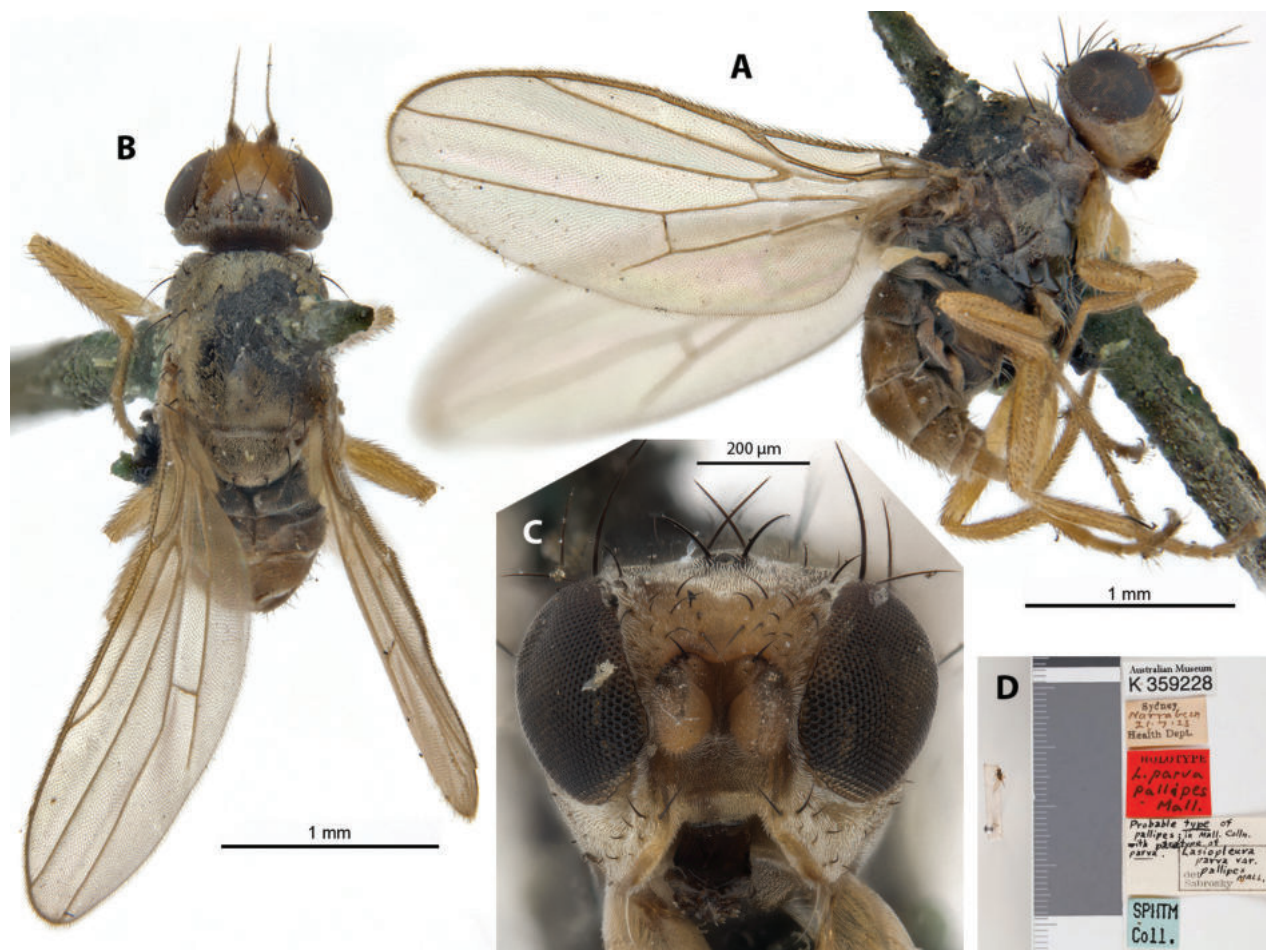


Figure 17. *Apotropina pallipes* (Malloch) holotype ♀ (K 359228) **A** habitus, lateral view **B** habitus, dorsal view **C** head, anterior view **D** specimen labels.

Lasiopleura parva var. *pallipes* MALL., det. Sabrosky; SPHTM Coll.”; 33°42'54"S, 151°17'4"E. Deposited in the AMRI.

Taxonomic notes. This dark brown species with yellowish legs was described as a variety of *A. parva*, based on a single female specimen from the type locality as the latter (Malloch, 1940), where he noted differences from *A. parva* in having legs entirely ‘honey-yellow’, the gena being more narrowed anteriorly (Fig. 17A, B), but “having only one specimen of each form available I do not care to go farther into details”. It was subsequently upgraded to species level (Sabrosky, 1989). The authors have also noted that *A. pallipes* additionally has M_4 ending well before wing margin (Fig. 17A), as opposed to *A. parva* where the vein ends at the wing margin (Fig. 18B). This species does not have any immediately distinctive diagnosable character sets based on existing descriptions but can be identified based on the provided key. Chaetotaxy as observed: 2 vibrissae; 3 moderately strong proclinate interfrontal setae; 2 postpronotal setae; 1+1 notopleural setae; short weak biseriate acrostichal row; 1+3 dorsocentral setae; 1+1 supra-alar setae; postalar and intrapostalar setae present; 1 weak acrostichal prescutellar setae; scutellum with 1 discal setulae; katapisternal seta missing/indistinct. Original taxonomic note in Suppl. material 1.

***Apotropina parva* (Malloch, 1928)**

Fig. 18A–D

Hippelates parva Malloch, 1928: 302.

Lasiopleura (Lasiopleura) parva: Malloch 1940: 273.

Type locality and distribution. AUSTRALIA: New South Wales (Sydney).

Examined material. *Holotype* ♀ Label transcription: “Australian Museum, K 359229; Sydney, 31.12.23, Health Dept.; HOLOTYPE, *Lasiopleura parva* Mall.; *Parahippelates parva* Type, det. JRMALLOCH; SPHTM Coll.”; 33°52'S, 151°13'E. Deposited in the AMRI.

Taxonomic notes. This dark-brown species has brown-banded yellowish legs and hyaline wings (Fig. 18A, B). It resembles *A. taylori* and *A. pallipes*, but can be distinguished from the former based on the longer, stronger hind tibial spur and presutural acrostichal setae, and from the latter based on characters described in the taxonomic notes for *A. pallipes*. This species does not have any immediately distinctive diagnosable character sets based on existing descriptions but can be identified based on the provided key. Chaetotaxy as observed: 2 vibrissae; 3 strong decussate interfrontal setae; 2 postpronotal setae; 2 scapular setae; 1+1 notopleural setae; short weak reclinate biseriata acrostichal row; 1+3 dorsocentral setae; 1+1 supra-alar setae; postalar and intrapostalar setae present; missing/indistinct prescutellar setae; scutellum with 1 discal setula; katepisternal seta missing/in-distinct. Original description and subsequent taxonomic note in Suppl. material 1.

***Apotropina proxima* (Rayment, 1959)**

Fig. 25E, F

Ephydroscinis proxima Rayment, 1959: 332.

Type locality and distribution. AUSTRALIA: Victoria (Mt. Richmond Reserve).

Taxonomic notes. *Apotropina proxima* likely belongs to a group of described species (including *A. exquisita*, *A. ornatipennis* and *A. raymenti*) that have dark bodies with shiny tomentosity, wings with distinct dark patterning covering at least the medial region from costal margin to beyond R_{2+3} vein. Based on the species description, *A. proxima* can be distinguished from other species in this group with its long geniculate proboscis, having only two distal tarsal segments dark and scutum with a silvery-green metallic pattern divided by three longitudinal black lines. The description did not indicate any deposited type material for examination, but did provide drawings which depict the fly with brown macula at the radial sector, a long, geniculate proboscis (Fig. 25E) and three longitudinal black strips along the scutum (Fig. 25F). However, the illustration does not reflect any “basally angulated fore tibiae” as indicated in the description, and as such the authors have opted to exclude this ambiguous character from the key. This species was described with life history information - as a likely hyperparasitoid associated with two other predatory/parasitoid species *Sericophorus chalybeus* (F. Smith, 1851) (syn. *S. victoriensis* Rayment) and *Acanthostethus portlandensis* (Rayment, 1953) (Rayment 1959). Original description in Suppl. material 1, which only reflects the only chaetotaxy as possessing four dorsocentral setae.

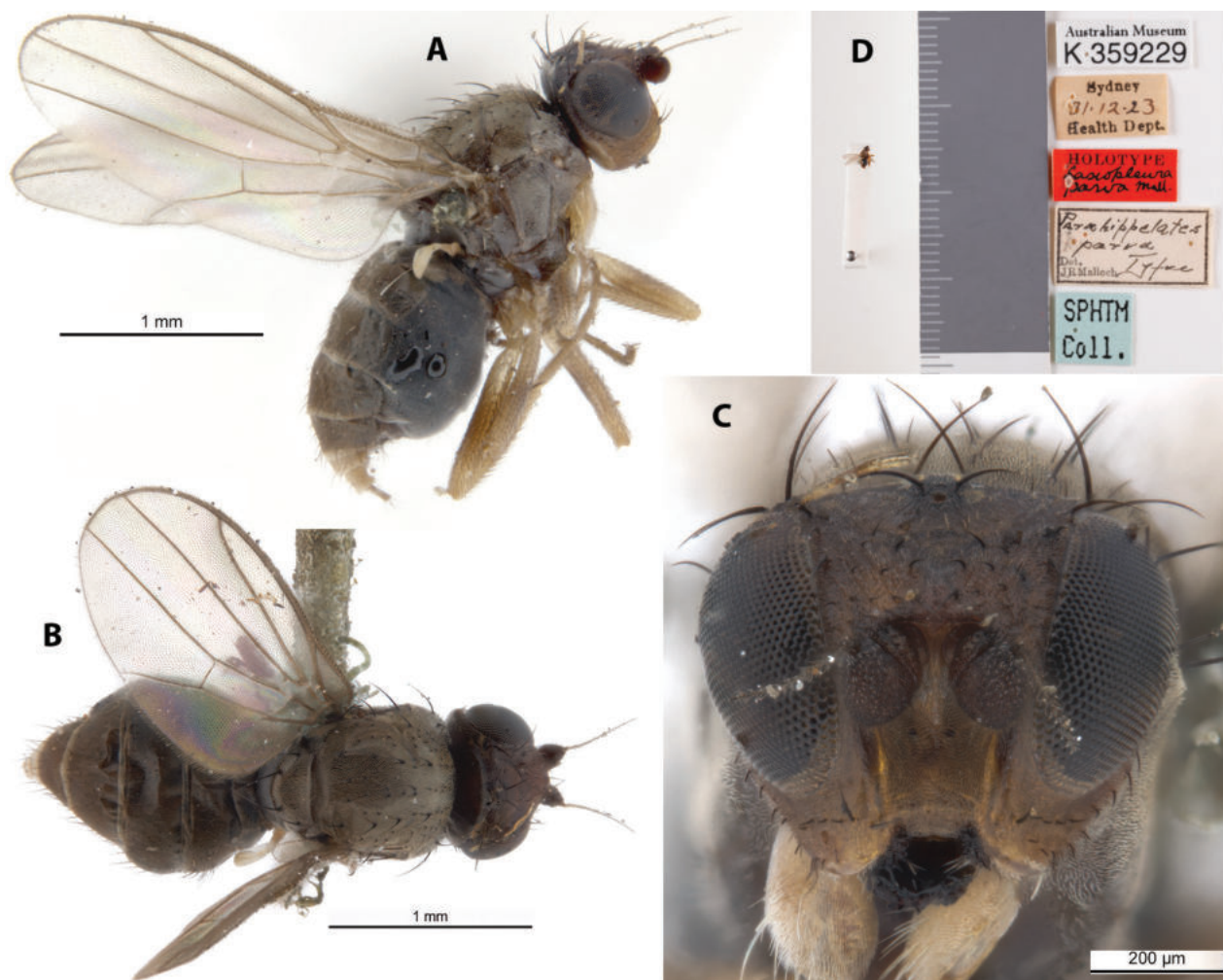


Figure 18. *Apotropina parva* (Malloch) holotype ♀ (K 359229) **A** habitus, lateral view **B** habitus, dorsal view **C** head, anterior view **D** specimen labels.

***Apotropina pruinosa* (Thomson, 1869)**

Fig. 19A–D

Oscinis pruinosa Thomson, 1869: 606.

Parahippelates seticauda Malloch 1928: 302 (nomenclatural changes: Sabrosky 1955: 188 [transferred to *Lasiopleura*]; Sabrosky 1989: 651 [synonymized under *A. pruinosa*]).

Type locality and distribution. AUSTRALIA: New South Wales (Sydney); Victoria (Warburton).

Examined material. **Holotype** *Parahippelates seticauda* Malloch, 1928 ♂ Label transcription: “Australian Museum, K 359230; Sydney, 25.1.25, Health Dept.; HOLOTYPE, *Lasiopleura seticauda* Mall.; *Parahippelates seticauda* Type Mall., Det J R Malloch; SPHTM Coll.”; 33°53'S, 151°13'E; Deposited in the AMRI.

Taxonomic notes. This species has a blackish thorax, brownish abdomen with white bands, as well as pale yellow legs, hypopygium and front portion of head. It is distinctive in having its body (including hypopygium) and posterior portion of head completely covered in dusty white pruinosity (Fig. 19A, B). It was originally described by Thomson (1869) under *Oscinis* Loew; Malloch

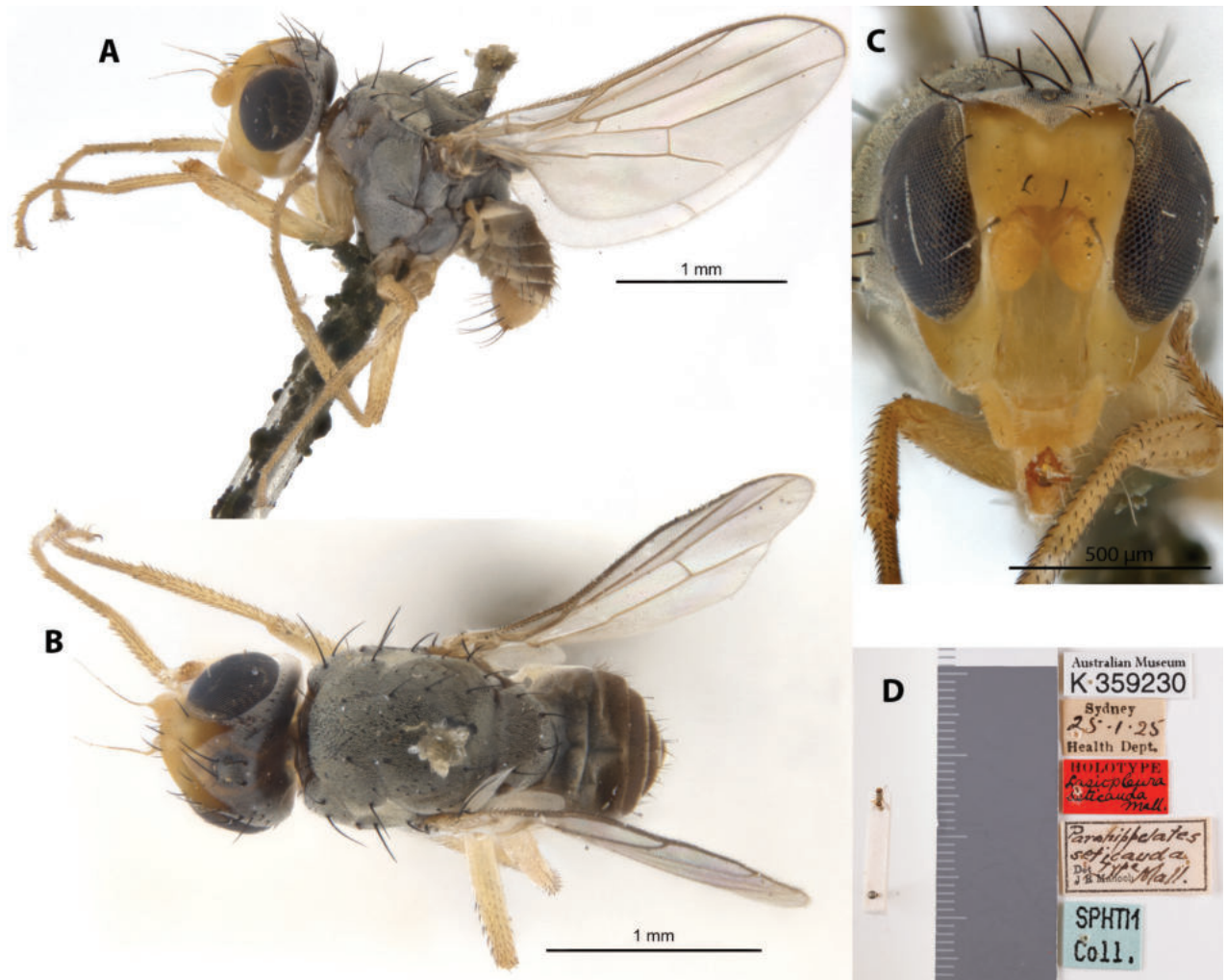


Figure 19. *Parahippelates seticauda* Malloch holotype ♂, (synonym of *Apotropina pruinosa*; K 359230) **A** habitus, lateral view **B** habitus, dorsal view **C** head, anterior view **D** specimen labels.

(1928) described another species *P. seticauda*, which was subsequently transferred to *Lasiopleura* (Sabrosky 1955) and further synonymized under *A. pruinosa* (Sabrosky 1989). Note that the images provided here are of the *P. seticauda* holotype specimen (Fig. 19A–D). Chaetotaxy as observed: 1 vibrissa; 1 strong proclinate interfrontal setae; 2 postpronotal setae; 2 scapular setae; 1+1 notopleural setae; short weak reclinate biseriate acrostichal row; 1+3 dorsocentral setae; 1+1 supraalar setae; postalar and intrapostalar setae present; missing/indistinct prescutellar setae; scutellum without discal setulae; katepisternal seta missing/indistinct. Original descriptions and subsequent taxonomic note in Suppl. material 1.

***Apotropina raymenti* (Curran, 1930)**

Fig. 20A–D

Ephydroscinis raymenti Curran, 1930: 1.

Neoborborus speculabundus: Rayment 1931: 191; Richards 1973: 396 (synonymization).

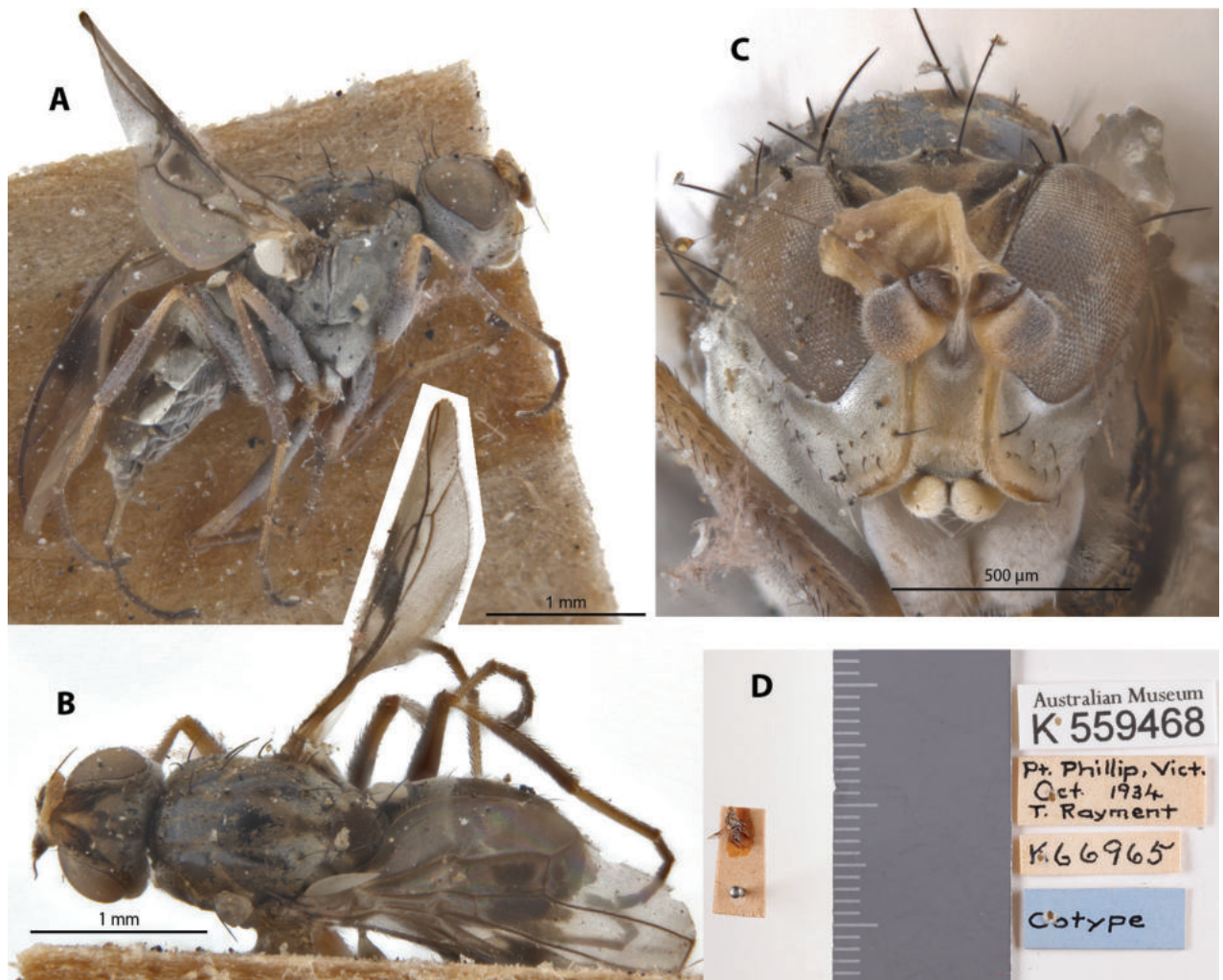


Figure 20. *Apotropina raymenti* (Curran) 'cotype' [=paratype] ♀ (K 559468) **A** habitus, lateral view **B** habitus, dorsal view **C** head, anterior view **D** specimen labels.

Type locality and distribution. AUSTRALIA: Victoria (Sandringham, Pt Phillip).

Examined material. **Cotype** [= paratype] series for *Ephydroscinis raymenti* Curran, 1930 ♀♀♀ K66965 (separated to three specimens individually: K 559467, K 559468, K 559469). Deposited in the AMRI. Label transcription of imaged specimen: "Australian Museum, K 559468; Pt. Phillip, Vict., OCT 1934, T. Rayment; K66965; Cotype".

Taxonomic notes. *Apotropina raymenti* belongs to a group of described species (including *A. exquisita*, *A. ornatipennis* and *A. proxima*) that have dark bodies with shiny tomentosity, wings with distinct dark patterning covering at least the medial region from costal margin to beyond R_{2+3} vein, and usually shiny-white alula. *Apotropina raymenti* can be distinguished from other species in this group with the following combination of characters: short capitate proboscis, arista completely brown; scutal color pattern with paired white lateral vittae on postscutum and none on prescutum; katepisternum completely whitish tomentose; wing veins lighter basally but darker near apex (Fig. 20A, B). This species is only known from female specimens, male morphology unknown. However, there is evidence that species in this group may have sexually dimorphic color patterns (see Fig. 1) where males may have more prominent patterns than

females. This species was described with life history information, as a likely parasitoid associated with the bee species *Lasioglossum (Homalictus) niveifrons* (Cockerell), where it visits the host's ground burrows near the coastline. Rayment (1931) further erected a new genus to describe a species, *Neoborborus speculabundus* Rayment under family Borboridae Newman [=Sphaeroceridae Macquart]; it was subsequently transferred to Chloropidae by Richards (1973: 396) and synonymized under *A. raymenti* (Sabrosky 1989). In AMRI are deposited a cotype [=paratype] series (K66965) of three female specimens (K 559467, K 559468 (imaged), K 559469). Chaetotaxy as observed: 1 vibrissa; 3 weak proclinate interfrontal setae; 2 postpronotal setae; 2 scapular setae; 1+1 notopleural setae; short weak reclinate biseriate acrostichal row only on the medial region; 1+3 dorsocentral setae; 1+1 supra-alar setae; postalar and intrapostalar setae present; missing/indistinct prescutellar setae; scutellum without discal setulae; katepisternal seta weak. Original descriptions provided in Suppl. material 1.

***Apotropina rufescens* (Duda, 1934)**

Fig. 21A–D

Parahippelates rufescens Duda, 1934: 49.

Lasiopleura (Lasiopleura) rufescens: Malloch 1936: 24; 1940: 272.

Type locality and distribution. AUSTRALIA: Northern Territory (Darwin: Palmerston).

Examined material. Syntype ♀ Label transcription: "Palmerston, N. Australien, XI. 1908; coll. Lichtwardt; *P. rufescens* D., ♀ d. Duda; Typus; <http://coll.mfn-berlin.de/u/5c8578>"; Deposited in the MfN.

Taxonomic notes. This species has a dark brown body and largely yellowish head and legs, superficially similar to *A. pruinosa*, but is distinctive for its plumose arista with the pilosity at its basal half almost the length of the postpedicel (Fig. 21A–C). Only known from the type locality. Chaetotaxy as observed: 2 vibrissae; 3 weak proclinate interfrontal setae; 2 postpronotal setae; 2 scapular setae; 1+1 notopleural setae; short weak reclinate biseriate acrostichal row; 1+3 dorsocentral setae; 1+1 supra-alar setae; scutellum with 1 discal setula; katepisternal seta missing/indistinct. Original description, translation, and subsequent taxonomic notes in Suppl. material 1.

***Apotropina taylori* (Malloch, 1940)**

Fig. 22A–D

Lasiopleura (Lasiopleura) taylori Malloch, 1940: 273.

Type locality and distribution. AUSTRALIA: New South Wales (Blue Mts; Hampton).

Examined material. Holotype ♂ Label transcription: "Australian Museum, K 359231; Blue Mtns., 13.4.22, Health Dept.; Presumed HOLOTYPE, *Lasiopleura taylori* MALL., (ex. MALL. Colln 1954), det Sabrosky; HOLOTYPE *Lasiopleura taylori*; SPHTM Coll."; Deposited in the AMRI.

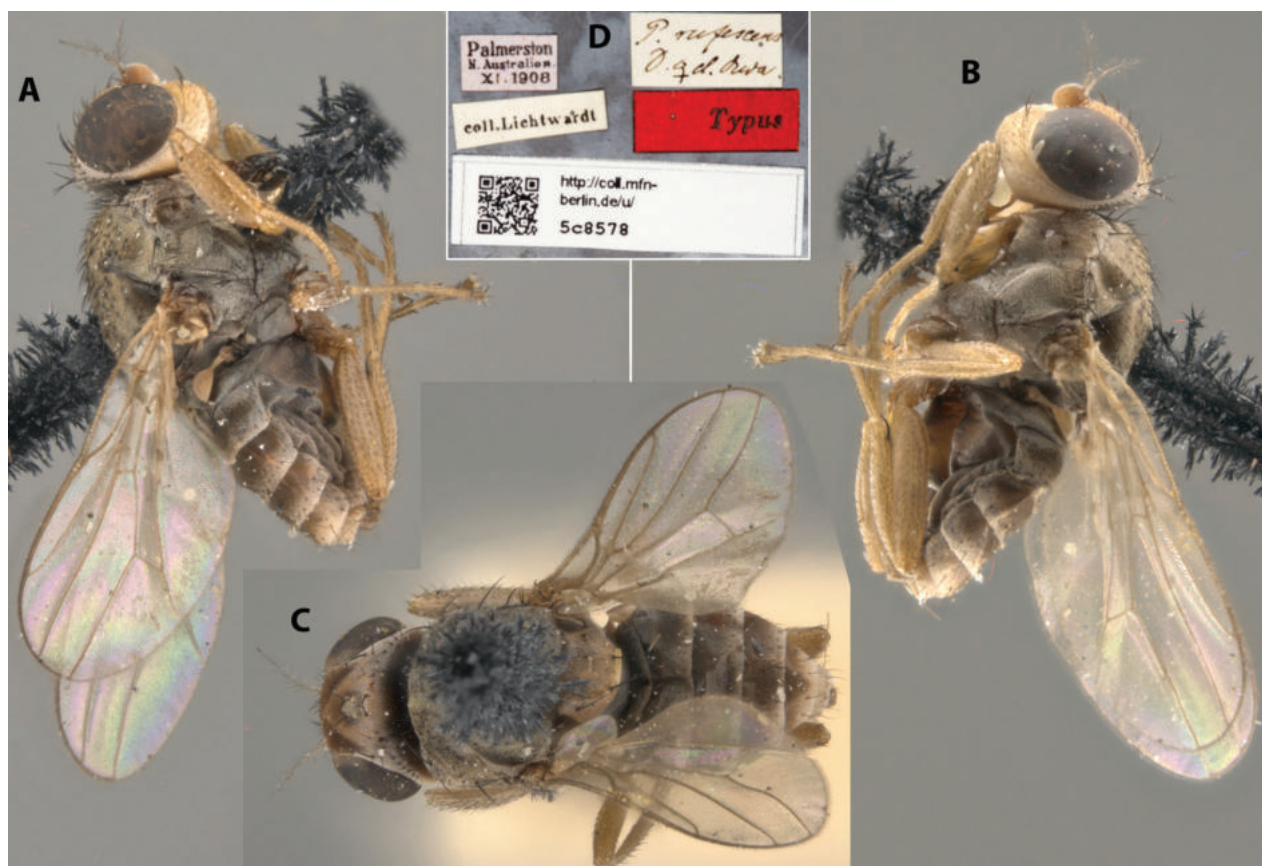


Figure 21. *Apotropina rufescens* (Duda) syntype ♀ (5c8578) **A** habitus, right lateral view **B** habitus, left lateral view **C** habitus, dorsal view **D** specimen labels.

Taxonomic notes. This species has a dark brown body and largely testaceous head and legs, largely covered in pruinosity, superficially similar to *A. pruinosa*, but can be distinguished from that species based on its brownish antennae (which is fully yellow in *A. pruinosa*; see Fig. 19A) and its overall darker color (Fig. 22A–C). It was described based on male specimen and is only known from the type locality. Female morphology unknown. This species does not have any immediately distinctive diagnosable character sets but can be identified based on the provided key. Chaetotaxy as observed: 2 vibrissae; 3 strong slightly inclinate interfrontal setae; 2 postpronotal setae; 2 scapular setae; 1+1 notopleural setae; short weak reclinate biseriate acrostichal row; 1+3 dorsocentral setae; katapisternal seta missing/indistinct. Original description in Suppl. material 1.

***Apotropina viduata* (Schiner, 1868)**

Fig. 23A–C

Ectropa viduata Schiner, 1868: 243.

Parahippelates fuscipes: Malloch, 1924: 330; Sabrosky 1980: 102 (synonymization).

Type locality and distribution. AUSTRALIA: New South Wales (Blue Mts; Hampton; Sydney, Collaroy).

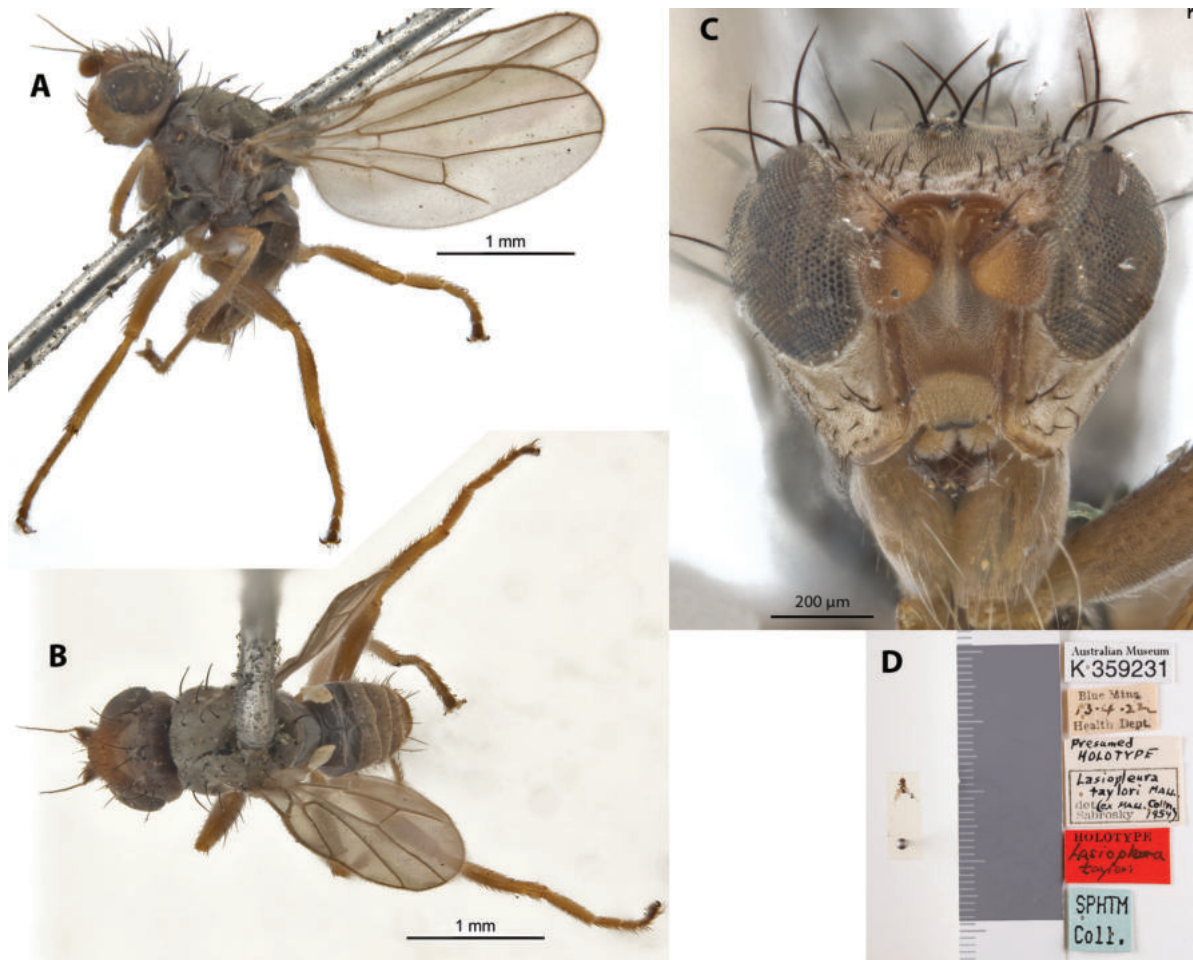


Figure 22. *Apotropina taylori* (Malloch) holotype ♂ (K 359231) A habitus, lateral view B habitus, dorsal view C head, anterior view D specimen labels.

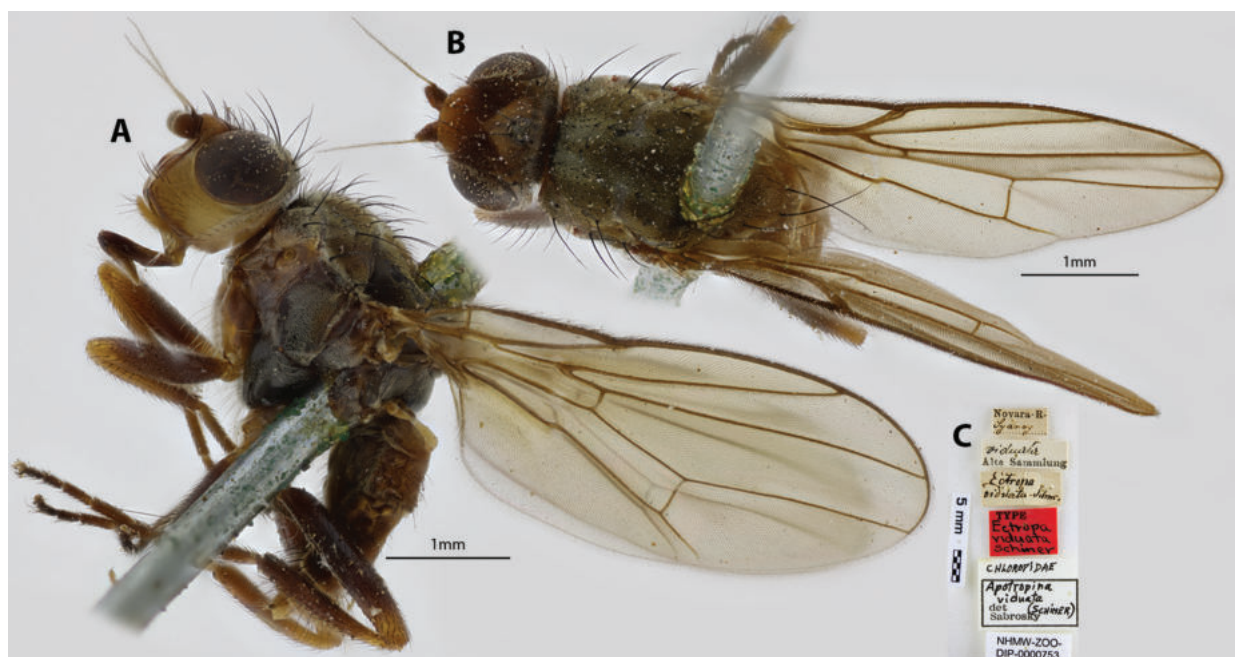


Figure 23. *Apotropina viduata* (Schiner) holotype ♀ NHMW-ZOO-DIP-0000753 A habitus, lateral view B habitus, dorsal view C specimen labels.

Examined material. Holotype ♀ Label transcription: “Novara. R., Sydney; *viduata*, Alte Sammlung; *Ectropa viduata* Schiner.; TYPE *Ectropa viduata* Schiner; CHLOROPIDAE, *Apotropina viduata* (SCHINER), det. Sabrosky; NHMW-ZOO-DIP-0000753”; Deposited in the AMRI.

Taxonomic notes. This is a dark-bodied species with tawny legs and lighter colored head (Fig. 23A, B). Chaetotaxy as observed: 3 vibrissae; 3 proclinate interfrontal setae; 2 postpronotal setae; 2 scapular setae; 1+1 notopleural setae; biseriate acrostichal row that gets strong in medial of scutum; 1+3 dorsocentral setae; 1+1 supra-alar setae; postalar setae and intrapostalar setae present; scutellum with 2 discal setulae; katepisternal seta whitish, indistinct. The taxonomic history for this species is already detailed in the introduction section (See Sabrosky, 1980 for details). Original descriptions provided in Suppl. material 1.

***Apotropina bispinosa* (Becker, 1911)**

Fig. 24A–C

Oscinella bispinosa Becker, 1911: 152.

Oscinelloides bispinosa: Malloch 1940: 268.

Type locality and distribution. AUSTRALIA: Queensland (Weipa). PAPUA NEW GUINEA: Huon (Sattleberg), New Britain (Rabaul).

Taxonomic notes. This species has a problematic type series assignment. It was originally described from, and limited to, Papua New Guinea based on six specimens (Becker 1911). Malloch (1940) identified an additional female of *Apotropina bispinosa* from Papua New Guinea and transferred this species to his newly erected genus *Oscinelloides* Malloch, providing further morphological description of the species. *Oscinelloides* was subsequently synonymized with *Apotropina* (Sabrosky 1989). Thereafter, specimens from Australia were identified to the *A. bispinosa* (Forster, 1992). We were able to examine two specimens in MfN marked as types (see Fig. 24 for one imaged specimen; label transcription: “Sattleberg, Huon-Golf.; 547474; Typus; N.-Guinea, Biró 1899.; Sammlung Dr. Th. Becker; *Rhodesiella* sp., det J.W. Ismay 2002; <http://coll.mfn-berlin.de/u/5c8582>”) and found that both specimens have no dorsocentral setae except for the posterior one and have completely dark brown femora and tibiae. These features do not correspond to descriptions provided by Becker (1911) and Malloch (1940), where both state that *A. bispinosa* has two strong pairs of dorsocentral setae, lighter-colored yellowish legs with darkened apices on mid and hind femora as well as fore tibiae. In fact, the morphology of the examined specimens matches that of genus *Rhodesiella* Adams. Given that the two MfN specimens [547474 (5c8582 and 5c85bb)] do not correspond to the original description (see Suppl. material 1) despite belonging to the same locality, a detailed assessment on *A. bispinosa*’s type series should be done. With that, the designation of a lectotype would clarify this species identity. Furthermore, as we could not examine Forster’s (1992) Australian specimens, we refrain from adding *A. bispinosa* to the key.



Figure 24. *Apotropina bispinosa* (Malloch) syntype ♀ 57474 (5C8582) **A** habitus, lateral view **B** habitus, dorsal view **C** specimen labels.

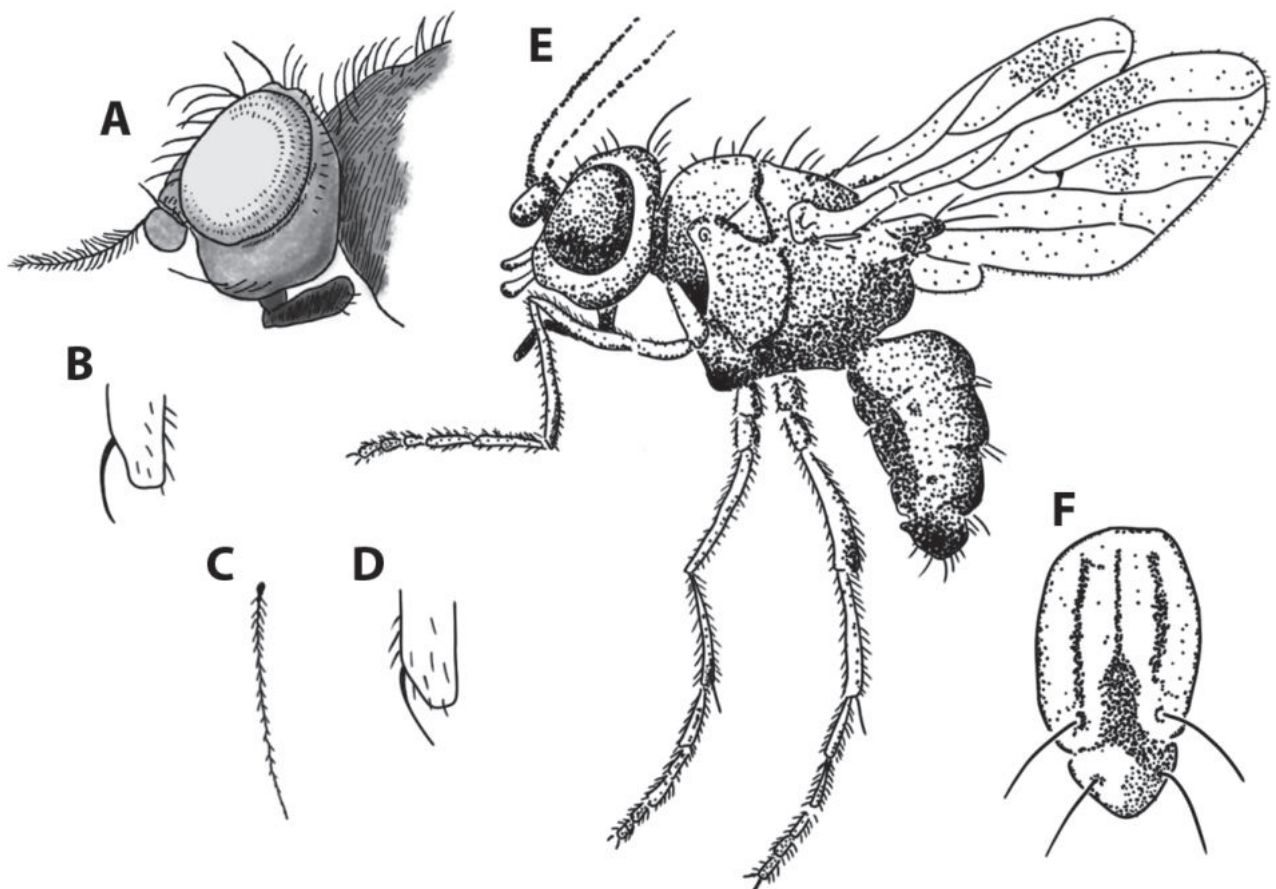


Figure 25. illustrations for various *Apotropina* spp. **A** *A. aequalis* head, lateral view (from Becker 1911: Tafel I, Fig. 15) **B** *A. aequalis* hind tibial spur (from Malloch 1940: 271, Fig. 15) **C** *A. nudiseta* antennal arista (from Malloch 1940: 271, Fig. 17) **D** *A. nudiseta* hind tibial spur (from Malloch 1940: 271, Fig. 18) **E** *A. proxima* habitus, lateral view (from Rayment 1959: plate XXXIX, Fig. 1) **F** *A. proxima* thorax, dorsal view (from Rayment 1959: plate XXXIX, Fig. 2).

Acknowledgements

The authors would like to thank Simon Grove (Tasmanian Museum and Art Gallery) and Julie Sarna for contributing their in situ photos of live *Apotropina*, Natalie Tees, Matthew Shaw, and Alessandro Camargo for photographing the images of the AMRI, SAMA and NHMW type specimens respectively, and Leshon Lee (National University of Singapore) for his help in sequencing the specimens.

Additional information

Conflict of interest

The authors have declared that no competing interests exist.

Ethical statement

No ethical statement was reported.

Funding

PRR benefits from the program CAPES-HUMBOLDT, grant no. 88881.512934/2020-01. AY benefits from the LKCNHM-RCC Research Fund.

Author contributions

Conceptualization: YA. Data curation: PRRR, JL, YA. Formal analysis: YA, PRRR. Funding acquisition: YA, PRRR. Investigation: PRRR, YA. Methodology: YA. Project administration: YA. Visualization: YA. Writing - original draft: PRRR. Writing - review and editing: PRRR, JL, YA.

Author ORCIDs

Yuchen Ang  <https://orcid.org/0000-0001-5889-018X>

James Lumbers  <https://orcid.org/0009-0007-4895-0936>

Paula R. Riccardi  <https://orcid.org/0000-0003-4850-7524>

Data availability

All of the data that support the findings of this study are available in the main text or Supplementary Information.

References

- Andersson H (1977) Taxonomic and phylogenetic studies on Chloropidae (Diptera) with special reference to Old World genera. *Entomologica Scandinavica (Supplementum 8)*: 1–200.
- Becker T (1911) Chloropidae. Eine monographische Studie. III. Teil. Die indo-australische Region. *Annales Historico-Naturales Musei Nationalis Hungarici* 9: 35–170. [Tab I–II.] <https://doi.org/10.5962/bhl.title.9555>
- Curran CH (1930) Four new Diptera from Australia. *American Museum Novitates* 442: 1–4.
- Duda O (1934) Weitere neue und wenig bekannte orientalische und australische Chloropiden (Diptera) des Deutschen Entomologischen Instituts in Berlin-Dahlem. *Arbeiten über morphologische und taxonomische Entomologie aus Berlin-Dahlem* 1: 39–60.

- Forster PI (1992) Insects associated with the flowers of *Marsdenia cymulosa* Benth. (Asclepiadaceae) and their possible role in pollination. *Australian Entomological Magazine* 19(1): 45–47.
- GroveS (2019) iNaturalist observation. <https://www.inaturalist.org/observations/19347756>; <https://www.inaturalist.org/photos/29751169> [Accessed 5 June 2023]
- Ismay B, Ang Y (2019) First records of *Pseudogaurax* Malloch 1915 (Diptera: Chloropidae) from Singapore, with the description of two new species discovered with NGS barcodes. *The Raffles Bulletin of Zoology* 67: 412–420. <https://doi.org/10.26107/RBZ-2019-0033>
- Ismay JW, Ismay B, Deeming JC (2021) 96. Chloropidae. In: Kirk-Spriggs AH, Sinclair BJ (Eds) *Manual of Afrotropical Diptera. Volume 3. Brachycera – Cyclorrhapha, Excluding Calypttratae – Higher Diptera. Suricata* 8(3). South African National Biodiversity Institute, Pretoria, 2035–2114.
- Malloch JR (1923) Notes on Australian Diptera with descriptions, I. *Proceedings of the Linnean Society of New South Wales* 48: 601–622.
- Malloch JR (1924) Notes on Australian Diptera, III. *Proceedings of the Linnean Society of New South Wales* 49(3): 329–338.
- Malloch JR (1925) Notes on Australian Diptera, VI. *Proceedings of the Linnean Society of New South Wales* 50(2): 80–97.
- Malloch JR (1928) Notes on Australian Diptera, XIV. *Proceedings of the Linnean Society of New South Wales* 53: 295–309.
- Malloch JR (1936) Notes on Australian Diptera, XXXV. *Proceedings of the Linnean Society of New South Wales* 61: 10–26.
- Malloch JR (1940) Notes on Australian Diptera, XXXVIII. Family Chloropidae, Part II. *Proceedings of the Linnean Society of New South Wales* 65(3–4): 261–288.
- Mortelmans J, Hussin M, Lee L, Ang Y (2022) First records of snail-killing flies (Diptera: Sciomyzidae) from Singapore with notes on morphology and DNA sequencing. *Nature in Singapore* 15: e2022014. <https://doi.org/10.26107/NIS-2022-0014>
- Rayment T (1931) The furrow-bees and a fly. *The Victorian Naturalist* 47: 184–191.
- Rayment T (1935) *A Cluster of Bees: Sixty Essays on the Life-histories of Australian Bees, with specific descriptions of over 100 new species, and an introduction by Professor E. F. Phillips. D.Ph., Cornell University, U.S.A.* Endeavour Press, Sydney, 752 pp. [+ frontispiece + colour plates 40 & 66]
- Rayment T (1959) Hyperparasitism by a minute fly and the specific description of a new species. *Australian Zoologist* 12: 330–333. [pl. XXXIX]
- Riccardi PR, Baziar Z, Lamas CE (2018) New genus of the subfamily Oscinellinae from Brazil (Diptera: Chloropidae). *Zootaxa* 4438(2): 394–400. <https://doi.org/10.11646/zootaxa.4438.2.13>
- Richards OW (1973) The Sphaeroceridae (= Borboridae or Cypselidae; Diptera Cyclorrhapha) of the Australian Region. *Australian Journal of Zoology, supplementary Series* 22: 297–401. <https://doi.org/10.1071/AJZS022>
- Sabrosky CW (1955) Notes and descriptions of Australian Chloropidae (Diptera). *Proceedings of the Linnean Society of New South Wales, Sydney* 79: 182–192.
- Sabrosky CW (1980) Unexpected synonymy in Chloropidae, from the Family Ephydriidae (Diptera). *Australian Entomological Magazine* 6(6): 101–102.
- Sabrosky CW (1989) 100. Family Chloropidae. In: Evenhuis N (Ed.) *Catalog of the Diptera of the Australasian and Oceanian Regions*. Bishop Museum Press, Honolulu & EJ Brill, Leiden, 650–665.

- Sarna J (2020) iNaturalist observation. <https://www.inaturalist.org/observations/48861099>; <https://www.inaturalist.org/photos/77545425> [Accessed 5 June 2023]
- Schiner IR (1868) 1. Diptera. Reise der österreichischen Fregatte Novara um die Erde in den Jahren 1857, 1858, 1859 unter den Befehlen des Commodore B. von Wüllerstorff-Urbair. Zoologischer Theil. Zweiter Band. 1. Abtheilung, B: VI + 388 pp. [Kaiserlich-Königliche Hof- und Staatsdruckerei (In Commission bei Karl Gerolds's Sohn), Wien]
- Thomson CG (1869) 6. Diptera. Species novas descripsit C.G. Thomson. Pp. 443–614, Taf. IX in: Kongliga svenska fregatten Eugénies resa omkring jorden under befäl af C.A. Virgin. Åren 1851–1853. Vetenskapliga iakttagelser på H.M. Konung OSCAR Den Förstes befallning utgifna af K. Svenska Vetenskaps Akademien. Andra Delen [= Vol. 2]. Zoologi. 1. Insecta: V + 617 pp. [Tafel. I–IX; P.A. Norstedt & Söner, Stockholm]

Supplementary material 1

Original descriptions and relevant subsequent taxonomic notes for Australian *Apotropina* fauna

Authors: Yuchen Ang, James Lumbers, Paula R. Riccardi

Data type: pdf

Copyright notice: This dataset is made available under the Open Database License (<http://opendatacommons.org/licenses/odbl/1.0/>). The Open Database License (ODbL) is a license agreement intended to allow users to freely share, modify, and use this Dataset while maintaining this same freedom for others, provided that the original source and author(s) are credited.

Link: <https://doi.org/10.3897/zookeys.1187.108497.suppl1>

Corrections and additions to the catalogue of the bees (Hymenoptera, Anthophila) of Russia

Maxim Yu. Proshchalykin¹, Alexander V. Fateryga², Yulia V. Astafurova³

1 Federal Scientific Center of the East Asia Terrestrial Biodiversity, Far East Branch of the Russian Academy of Sciences, Vladivostok 690022, Russia

2 T.I. Vyazemsky Karadag Scientific Station – Nature Reserve of RAS – Branch of A.O. Kovalevsky Institute of Biology of the Southern Seas of RAS, Nauki Str. 24, Kurortnoye, 298188 Feodosiya, Russia

3 Zoological Institute, Russian Academy of Sciences, Saint Petersburg 199034, Russia

Corresponding author: Maxim Yu. Proshchalykin (proshchalikin@biosoil.ru)

Abstract

The present study is an update to the first catalogue of Russian bees published in 2017. For the Russian fauna, five recently described species are reported, as well as 45 species newly recorded since the first catalogue (including one invasive species), nine species overlooked in this previous Russian checklist, and 17 published synonymies. Original records are provided for nine species previously unknown to Russia and, as a taxonomic act, one species, *Anthidium ovasi* Warncke, 1980, **syn. nov.**, is synonymised with *Icteranthidium floripetum* (Eversmann, 1852). Additionally, 14 species are excluded from the original catalogue and numerous other taxonomic changes and clarifications are included. The present work revises the total number of genera for Russia to 64 and the total number of species to 1,268.

Key words: Biodiversity, conservation, continental checklist, new record, new synonym, pollinators, taxonomy



Academic editor: Thorleif Dörfel

Received: 25 September 2023

Accepted: 11 December 2023

Published: 21 December 2023

ZooBank: <https://zoobank.org/2977D380-731F-4089-9A56-526BC4CB86CD>

Citation: Proshchalykin MYu, Fateryga AV, Astafurova YuV (2023) Corrections and additions to the catalogue of the bees (Hymenoptera, Anthophila) of Russia. ZooKeys 1187: 301–339. <https://doi.org/10.3897/zookeys.1187.113240>

Copyright: © Maxim Yu. Proshchalykin et al. This is an open access article distributed under terms of the Creative Commons Attribution License ([Attribution 4.0 International – CC BY 4.0](https://creativecommons.org/licenses/by/4.0/)).

Introduction

The ‘Annotated Catalogue of Russian bees’ (Astafurova and Proshchalykin 2017; Levchenko et al. 2017; Proshchalykin 2017a; Proshchalykin et al. 2017; Proshchalykin and Astafurova 2017; Proshchalykin and Fateryga 2017), is a major milestone in the study of this diverse group of hymenopteran insects in a vast territory such as that of Russia. Due to the intensive work of the team of authors, it was possible to include all the published data on bees from Russia known at that time in the catalogue. In total, the catalogue contained 1,215 species from 66 genera and six families (Colletidae – 100 species/2 genera; Andrenidae – 244/5; Halictidae – 263/13; Melittidae – 25/3; Megachilidae – 198/18; Apidae – 385/25).

For such works, it has become common practice to publish corrections and additions accumulated over time approximately once every five years. Similar updates have already been released twice for the European Bee Checklist (Rasmont et al. 2017; Ghisbain et al. 2023), first published in 2014 (Nieto et al. 2014). This first update of the catalogue of Russian bees allows for the correction of previous errors, the introduction of the latest nomenclatural and taxonomic changes, as well as the inclusion of taxa recorded for the first time and species newly described for science from this territory.

Materials and methods

Bringing together new literature records and taxonomic updates for this work was made possible by (i) an exhaustive review of the literature published since the first catalogue of Russian bees (Astafurova and Proshchalykin 2017; Levchenko et al. 2017; Proshchalykin 2017a; Proshchalykin et al. 2017; Proshchalykin and Astafurova 2017; Proshchalykin and Fateryga 2017), (ii) an in-depth revision of the literature not considered in the catalogue, and (iii) original information provided by the authors of the present work. This new list is mostly based on material directly examined by taxonomists and does not include data published online that has not otherwise been validated by experts (e.g., observations reported on iNaturalist, Discover Life, GBIF).

How to use the updated list

The species are ordered by family and listed alphabetically within the following sections:

- Species recently described as new to science (i.e., new species described after 2017);
- Published synonymies (i.e., synonymies published after 2017);
- Other taxonomic changes and clarifications (i.e., relevant changes published after 2017, such as new combinations, taxa upgraded to species rank or downgraded to subspecies rank, as well as clarifications of interesting cases that have led to changes in the updated checklist of the Russian bees);
- Species recorded in Russia after 2017 (i.e., published as new to Russia but not new to science);
- Species overlooked in the Russian catalogue (i.e., species recorded in Russia before 2017 but not included in the annotated catalogue of 2017);
- New species records for Russia (new entries presented in this article for the first time);
- Species to be excluded from the Russian checklist (discussions and explanations of the exclusion of certain species from this new checklist).

The systematics at family, subfamily and tribe levels are mainly based on Michener (2007) and Ascher and Pickering (2023). Generic and subgeneric classifications are generally consistent with those used by Ghisbain et al. (2023), except

in some cases noted in the text. In the dating of Morawitz's species, we follow Kerzhner (1984) and Ebmer (2021). The names "Radoszkowski", "Lepelletier de Saint-Fargeau", and "Audinet-Serville" are standardised here, since these authors' names were originally written variably in different articles. The acronyms for institutions that loaned specimens or provided photographs used in this study are as follows:

- CAFK** research collection of Alexander V. Fateryga, Feodosiya, Russia.
CMKH research collection of Max Kasperek, Heidelberg, Germany.
ETHZ Entomological Collection of ETH Zurich, Switzerland.
FSCV Federal Scientific Center of the East Asia Terrestrial Biodiversity, Far Eastern Branch of the Russian Academy of Sciences, Vladivostok, Russia.
ISZP Institute of Systematics and Evolution of Animals, Polish Academy of Sciences, Krakow, Poland.
OLBL Oberösterreichisches Landesmuseum, Biologiezentrum, Linz, Austria.
ZISP Zoological Institute of the Russian Academy of Sciences, Saint Petersburg, Russia.
ZMMU Zoological Museum of the Moscow State University, Russia.

Taxonomic updates of the wild bee fauna of Russia

Family Colletidae Lepelletier de Saint-Fargeau, 1841

Species recently described as new to science

Colletes ravuloides Kuhlmann & Proshchalykin, 2023

Colletes ravuloides Kuhlmann & Proshchalykin in Proshchalykin and Kuhlmann 2023: 37, ♂ (holotype: ♂, Russia, Tuva Republic, 11 km W of Ust'-Elegest, steppe, 27.VII.2018, S. Luzyanin, D. Sidorov, ZISP).

Distribution. Russia (Eastern Siberia: Tuva Republic).

Published synonymies

Hylaeus (Hylaeus) montivagus Dathe, 1986

Notes. Synonymised with *Hylaeus tsingtauensis* (Strand, 1915), which is the senior synonym according to Proshchalykin and Dathe (2018: 582).

Species recorded in Russia after 2017

Colletes asiaticus Kuhlmann, 1999

Distribution. First recorded for Russia (North Caucasus: Dagestan Republic) by Proshchalykin and Kuhlmann (2019: 162). Outside Russia known from Turkey, Azerbaijan, Iran, and Turkmenistan (Proshchalykin 2017b).

***Colletes cariniger* Pérez, 1903**

Distribution. First recorded for Russia (south of European part: Astrakhan Province) by Proshchalykin and Kuhlmann (2020: 22). Records from Crimea by Filatov (2006: 110) and Filatov et al. (2006: 258) need to be checked. Outside Russia known from Bulgaria, Greece, Turkey, Azerbaijan, Israel, Jordan, Lebanon, Syria, Libya, and Egypt (Proshchalykin 2017b).

***Colletes conradti* Noskiewicz, 1936**

Distribution. First recorded for Russia (south of European part: Astrakhan Province) by Proshchalykin and Kuhlmann (2020: 22). Outside Russia known from Uzbekistan, Kyrgyzstan, Tajikistan, Kazakhstan, and China (Qinghai, Xinjiang) (Proshchalykin 2017b).

***Colletes dorsalis* Morawitz, 1888**

Distribution. First recorded for Russia (North Caucasus: Dagestan Republic) by Proshchalykin and Kuhlmann (2019: 162). Outside Russia known from Turkey, Georgia, Armenia, Azerbaijan, Kazakhstan, Uzbekistan, Kyrgyzstan, Turkmenistan, Tajikistan, and Iran (Proshchalykin 2017b).

***Colletes edentulus* Noskiewicz, 1936**

Distribution. First recorded for Russia (North Caucasus: Dagestan Republic) by Proshchalykin and Kuhlmann (2019: 161). Outside Russia known from Georgia, Armenia, Azerbaijan, Turkey, Mongolia, and Turkmenistan (Proshchalykin and Kuhlmann 2018).

***Colletes hethiticus* Warncke, 1978**

Distribution. First recorded for Russia (North Caucasus: Dagestan Republic) by Proshchalykin and Kuhlmann (2019: 162). Outside Russia known from Romania, Bulgaria, Greece, Turkey, and Azerbaijan (Proshchalykin 2017b).

***Colletes uralensis* Noskiewicz, 1936**

Distribution. First recorded for Russia (North Caucasus: Dagestan Republic) by Proshchalykin and Kuhlmann (2019: 162). Records from Tuva Republic (Kuhlmann and Proshchalykin 2011: 8) belongs to *Colletes kaszabi* Kuhlmann, 2002 (see Proshchalykin and Kuhlmann 2015: 326). Outside Russia known from Kazakhstan, Tajikistan, and China (Inner Mongolia) (Proshchalykin 2017b).

***Colletes wollmani* Noskiewicz, 1936**

Distribution. First recorded for Russia (North Caucasus: Dagestan Republic) by Proshchalykin and Kuhlmann (2019: 161). Outside Russia known from Azerbaijan, Kazakhstan, Kyrgyzstan, Uzbekistan, Turkmenistan, Tajikistan, Iran, Pakistan, and China (Proshchalykin and Kuhlmann 2018).

***Hylaeus (Dentigera) breviceps* Morawitz, 1876**

Distribution. First recorded for Russia (North Caucasus: Dagestan Republic) by Proshchalykin and Dathe (2021: 174). Outside Russia known from the Caucasus, Central Asia, and China (Proshchalykin and Dathe 2021).

***Hylaeus (Dentigera) imparilis* Förster, 1871**

Distribution. First recorded for Russia (North Caucasus: Dagestan Republic) by Proshchalykin and Dathe (2021: 174). Outside Russia known from the West Palaearctic and Iran (Proshchalykin and Dathe 2021).

***Hylaeus (Dentigera) intermedius* Förster, 1871**

Distribution. First recorded for Russia (North Caucasus: Dagestan Republic) by Proshchalykin and Dathe (2021: 174). Outside Russia known from the West Palaearctic (Proshchalykin and Dathe 2021).

***Hylaeus (Hylaeus) kotschisus* (Warncke, 1981)**

Distribution. First recorded for Russia (North Caucasus: Dagestan Republic) by Proshchalykin and Dathe (2021: 176). Outside Russia known from the East Mediterranean, the Caucasus, and Turkey (Proshchalykin and Dathe 2021).

***Hylaeus (Spatulariella) iranicus* Dathe, 1980**

Distribution. First recorded for Russia (North Caucasus: Dagestan Republic) by Proshchalykin and Dathe (2021: 181). Outside Russia known from the Caucasus, Turkey, and Iran (Proshchalykin and Dathe 2021).

Species overlooked in the previous Russian checklist

***Colletes brevigena* Noskiewicz, 1936**

Distribution. First recorded for Russia (Crimea) by Proshchalykin and Kuhlmann (2012: 25). Outside Russia known from Portugal, Spain, France, Austria,

Hungary, Italy, Croatia, North Macedonia, Serbia, Bulgaria, Greece, Cyprus, Turkey, and Azerbaijan (Proshchalykin 2017b).

Family Andrenidae Latreille, 1802

Published synonymies

***Andrena (Campylogaster) nova* Popov, 1940**

Notes. Synonymised with *Andrena chengtehensis* Yasumatsu, 1935, which is the senior synonym according to Astafurova et al. (2023: 418).

***Andrena (Leimelissa) ispida* Warncke, 1965**

Notes. Following de Dalla Torre (1896: 121), both Warncke (1967: 269) and Gusenleitner and Schwarz (2002: 176) incorrectly considered *Andrena fallax* Eversmann, 1852 to be a junior synonym of *A. (Notandrena) chrysoseles* Kirby, 1802. However, the lectotype specimen of *Andrena fallax* is conspecific with another species, *A. ispida* Warncke, 1965. According to Article 23.9.1 of the ICZN (1999), the prevailing usage of “*Andrena ispida*” as a valid name must not be maintained since *A. fallax* Eversmann, 1852 was mentioned as a valid name after 1899 by Popov (1950) and *A. ispida* Warncke, 1965 has been mentioned in fewer than 25 publications (Astafurova et al. 2022a: 400).

***Andrena (Melandrena) gallica* Schmiedeknecht, 1883**

Notes. Synonymised with *Andrena assimilis* Radoszkowski, 1876, which is the senior synonym according to Wood and Monfared (2022: 60).

***Andrena (Taeniandrena) similis* Smith, 1849**

Notes. Synonymised with *Andrena russula* Lepeletier de Saint-Fargeau, 1841, which is the senior synonym according to Praz et al. (2022: 404).

***Andrena (Andrena) bulgariensis* Warncke, 1965**

Notes. Synonymised with *Andrena inconstans* Morawitz, 1877, which is the senior synonym according to Wood (2023: 58).

Other taxonomic changes and clarifications

Subgeneric classification of *Andrena* Fabricius, 1775

In the last few years, new subgenera have been described and new combinations have been proposed. These changes are included in the current updated list.

- Andrena (Campylogaster) incisa* Eversmann, 1852 = *A. (incertae sedis) incisa* Eversmann, 1852
- Andrena (Carandrena) semiflava* Lebedev, 1932 = *A. (Notandrena) semiflava* Lebedev, 1932
- Andrena (Didonia) stepposa* Osytshnjuk, 1977 = *A. (Hamandrena) stepposa* Osytshnjuk, 1977
- Andrena (Larandrena) sericata* Imhoff, 1868 = *A. (Leucandrena) sericata* Imhoff, 1868
- Andrena (Larandrena) ventralis* Imhoff, 1832 = *A. (Leucandrena) ventralis* Imhoff, 1832
- Andrena (Poliandrena) altaica* Lebedev, 1932 = *A. (Ulandrena) altaica* Lebedev, 1932
- Andrena (Poliandrena) florea* Fabricius, 1793 = *A. (Bryandrena) florea* Fabricius, 1793
- Andrena (Poliandrena) limbata* Eversmann, 1852 = *A. (Limbandrena) limbata* Eversmann, 1852
- Andrena (Poliandrena) ornata* Morawitz, 1866 = *A. (incertae sedis) ornata* Morawitz, 1866
- Andrena (Poliandrena) polita* Smith, 1847 = *A. (Ulandrena) polita* Smith, 1847
- Andrena (Poliandrena) tatjanae* Osytshnjuk, 1995 = *A. (incertae sedis) tatjanae* Osytshnjuk, 1995
- Andrena (Proxiandrena) alutacea* E. Stoeckhert, 1942 = *A. (Micrandrena) alutacea* Stöckhert, 1942
- Andrena (Proxiandrena) proxima* (Kirby, 1802) = *A. (Micrandrena) proxima* (Kirby, 1802)
- Andrena (Ptilandrena) vetula* Lepeletier de Saint-Fargeau, 1841 = *A. (Simandrena) vetula* Lepeletier de Saint-Fargeau, 1841
- Andrena (Thysandrena) hypopolia* Schmiedeknecht, 1884 = *A. (incertae sedis) hypopolia* Schmiedeknecht, 1884
- Andrena (Thysandrena) ranunculorum* Morawitz, 1877 = *A. (incertae sedis) ranunculorum* Morawitz, 1877
- Andrena (Zonandrena) chrysopyga* Schenck, 1853 = *A. (Melandrena) chrysopyga* Schenck, 1853
- Andrena (Zonandrena) flavipes* Panzer, 1799 = *A. (Melandrena) flavipes* Panzer, 1799
- Andrena (Zonandrena) sibirica* Morawitz, 1888 = *A. (Melandrena) sibirica* Morawitz, 1888

***Andrena (Hoplandrena) scotica* Perkins, 1916**

Notes. This name replaces the use of *Andrena carantonica* sensu auctorum; *A. carantonica* Pérez, 1902 is treated as a nomen dubium (Wood et al. 2022: 403).

Distribution. Europe, Russia (European part, Urals), Armenia, Azerbaijan, Iran (Gusenleitner and Schwarz 2002).

***Andrena (Plastandrena) aulica* Morawitz, 1876**

Notes. According to Warncke (1967: 179) and Gusenleitner and Schwarz (2002: 130) *A. aulica* Morawitz, 1876 is a junior synonym of *A. bimaculata* (Kirby, 1802). However, Popov (1949), Osytshnjuk et al. (1978) and Astafurova et al. (2021) regarded *A. aulica* as a valid species. Wood and Monfared (2022: 66) regarded *A. aulica* as a subspecies of *A. bimaculata* (Kirby, 1802). The taxonomic status of *A. bimaculata* sensu lato is problematic and requires a revision. Although Astafurova et al. (2021) reported *A. aulica* from the European part of Russia, the distribution of this species is unclear due to ongoing taxonomic confusion with *A. bimaculata*. In the present update, we do not treat *A. aulica* as a full species.

***Andrena (Taeniandrena) eversmanniana* Osytshnjuk, 1994**

Notes. Recognised as a valid species (not as a synonym of *Andrena marginata* Fabricius, 1776) according to Astafurova et al. (2022a: 404).

Distribution. Russia (Urals: Orenburg Province), Kazakhstan, and Uzbekistan (Astafurova et al. 2022a).

***Andrena (Taeniandrena) afzeliella* (Kirby, 1802)**

Notes. Recognised as a valid species (not as a synonym of *Andrena ovatula* Schenck, 1853) according to Praz et al. (2022: 383), *Andrena afzeliella* here replaces *A. ovatula* sensu auctorum from the 2017 checklist.

Distribution. Europe, Egypt, Russia, the Caucasus, Turkey, Israel, Syria, Iraq, Iran, Afghanistan, Central Asia (Praz et al. 2022).

***Andrena (Truncandrena) rufomaculata* Friese, 1921**

Notes. The reports of this species from Crimea (Proshchalykin et al. 2017: 275) actually referred to *Andrena optata* Warncke, 1975 (Wood et al. 2020: 30).

Distribution. Eastern Europe, the Balkans, and Turkey. *Andrena rufomaculata* is distributed in Turkey, Iran and the Levant (Wood et al. 2020; Wood and Monfared 2022).

Species recorded in Russia after 2017

***Andrena (Brachyandrena) pinguis* Ariana, Scheuchl, Tadauchi & Gusenleitner, 2009**

Distribution. First recorded for Russia (south of European part: Volgograd Province) by Wood and Monfared (2022: 105). Outside Russia known from Turkey and Iran (Wood and Monfared 2022).

Species overlooked in the previous Russian checklist

***Andrena (Andrena) fulva* (Müller, 1766)**

Distribution. First recorded for Russia (north-west of European part: Metgethen, now Kosmodem'yanskoe, Kaliningrad Province) by Möschler (1938: 273). Outside Russia known from Europe and eastern Turkey (Gusenleitner and Schwarz 2002; Wood 2023).

***Andrena (Euandrena) meripes* Friese, 1922**

Distribution. First recorded for Russia (Eastern Siberia: Irkutsk, as *Andrena nigripes* Friese, 1914, nec Provancher, 1895) by Friese (1914: 225). Outside Russia known from eastern Kazakhstan (Friese 1922).

Species to be excluded from the Russian checklist

***Andrena (incertae sedis) lateralis* Morawitz, 1876**

Distribution. It was reported from Russia by Astafurova et al. (2022b: 136) on the base of an erroneous record. The species occurs in Europe, the Caucasus, Turkey, Israel, Iran, Afghanistan, Central Asia (Astafurova et al. 2022b).

***Andrena (Truncandrena) albopicta* Radoszkowski, 1874**

Distribution. It was reported from Russia by Lykov (2008: 32) and Rasmont et al. (2017: 19) on the base of an erroneous record. The species occurs in Armenia, Azerbaijan, Turkey and Iran (Morawitz 1877; Wood and Monfared 2022).

Family Halictidae Thomson, 1869

Published synonymies

***Lasioglossum (Hemihalictus) sabulosum* (Warncke, 1986)**

Notes. Synonymised with *Lasioglossum monstificum* (Morawitz, 1891), which is the senior synonym according to Pauly and Belval (2017: 27).

***Sphecodes orientalis* Astafurova & Proshchalykin, 2014**

Notes. Synonymised with *Sphecodes pieli* Cockerell, 1931, which is the senior synonym according to Astafurova et al. (2018: 38).

Other taxonomic changes and clarifications

Generic and subgeneric classification of Halictini

The generic and subgeneric classification of Halictini has remained unclear and inconsistent depending on the author or authors. The subgeneric classification of *Halictus* follows Michener (2007). The genus *Seladonia* is not used here, and species included in *Seladonia* in Ghisbain et al. (2023) are placed here in the subgenera *Pachyceble* Moure, 1940, *Seladonia* Robertson, 1918, and *Vestitohalictus* Blüthgen, 1961. The subgeneric classification of *Lasioglossum* is based on the conclusions of Gibbs et al. (2013) and follows Ghisbain et al. (2023) and Ascher and Pickering (2023). Species included in the subgenus *Evythaeus* in the first catalogue of Russian bees (Astafurova and Proshchalykin 2017) are now split into the subgenera *Biennialaeus* Pesenko, 2007, *Dialictus* Robertson, 1902, *Hemihalictus* Cockerell, 1897, *Pygihalictus* Warncke, 1975, and *Sphecodogastra* Ashmead, 1899.

***Nomiapis monstrosa* (Costa, 1861)**

Notes. *Nomiapis armata* (Olivier, 1812) was synonymised with *N. monstrosa* by Baker (2002: 36). We now follow the position that *N. armata* (Olivier, 1812) is a nomen dubium (since was described from the deserts of Arabia, from which *N. monstrosa* has never been recorded).

Species recorded in Russia after 2017

***Lasioglossum (Hemihalictus) medinai* (Vachal, 1895)**

Distribution. First record for Russia (south of European part: Volgograd Province) by Pauly et al. (2019: 32). Outside Russia known from North Africa, Southern Europe, and Israel (Pauly et al. 2019).

***Lasioglossum (Hemihalictus) adabaschum* (Blüthgen, 1931)**

Distribution. First record for Russia (south of European part: Astrakhan Province, Kalmykia Republic) by Astafurova and Proshchalykin (2023a: 2). Outside Russia known from Turkmenistan (Astafurova and Proshchalykin 2023a).

New species records for Russia

***Pseudapis bytinski* (Warncke, 1976)**

Distribution. New record. RUSSIA, North Caucasus: 2 ♂♂, Dagestan Republic, Kamyshchay River valley, 41°54'29"N, 48°13'59"E, 29.VI.2018, Yu. Astafurova (ZISP). Outside Russia known from Egypt, Israel, Turkey, Armenia, and Azerbaijan (Astafurova 2014).

***Sphecodes kozlovi* Astafurova & Proshchalykin, 2015**

Distribution. **New record** RUSSIA, Far East: 4 ♀♀, Amurskaya Province, Tukuringra Ridge, Zeya Mts., 12.VI.1912, Kozhanchikov (ZMMU); 1 ♂, Primorskiy Territory, Lazo Nature Reserve, 23 km SE of Lazo, 4.IX.1981, Yu. Pesenko (ZISP); 1 ♂, Primorskiy Territory, Suputinka River, 4.VIII.1948, Gussakovskij (ZMMU). Outside Russia known from China (Inner Mongolia, Shanxi, Ningxia) and Mongolia (Dornod, Khentii) (Astafurova et al. 2018).

Species overlooked in the previous Russian checklist

***Lasioglossum (Leuchalictus) majus* (Nylander, 1852)**

Distribution. RUSSIA, centre of European part: 2 ♀♀, Kursk Province, near Kursk, 4.VI.1916, S. Malyshev (ZISP); 2 ♀♀, Kursk Province, Borisovka, 4.VI.1916, S. Malyshev (ZISP). Pesenko (1986: 113) recorded this species from “south of the European part of the USSR” without giving a precise locality for Russia. The record from Russia (Stavropol Territory) by Chenikalova (2005: 26) needs to be checked. Outside of Russia known from north-western Africa (Tunisia, Algeria), Europe (nearly throughout from Spain in the west as far as northern Germany, Poland), and through Turkey to northern Iran (Ebmer 1988; Pesenko et al. 2000).

Family Melittidae Schenck, 1860

Species overlooked in the previous Russian checklist

***Macropis frivaldszkyi* Mocsáry, 1878**

Distribution. First recorded for Russia (Crimea and Eastern Siberia: Krasnoyarsk Territory) by Popov (1958: 502). Outside Russia known from Balkans to Turkey, Syria, and Kazakhstan (Popov 1958; Michez and Patiny 2005).

Family Megachilidae Latreille, 1802

Species recently described as new to science

***Hoplitis (Hoplitis) astragali* Fateryga, Müller & Proshchalykin, 2023**

Hoplitis astragali Fateryga et al. 2023: 664, ♀, ♂ (holotype: ♂, Russia, Dagestan, Levashi district, Tsudakhar, 10.VI.2019, A. Fateryga, ZISP).

Distribution. Russia (North Caucasus: Dagestan Republic), Azerbaijan (Nakhchivan Autonomous Republic), and southernmost Turkmenistan.

***Hoplitis (Hoplitis) dagestanica* Fateryga, Müller & Proshchalykin, 2023**

Hoplitis dagestanica Fateryga et al. 2023: 647, ♀, ♂ (holotype: ♂, Russia, Dagestan, Levashi district, Tsudakhar, 11.VI.2019, A. Fateryga, ZISP).

Distribution. Russia (North Caucasus: Dagestan Republic).

Published synonymies

***Coelioxys (Allocoelioxys) conspersus* Morawitz, 1873**

Notes. Synonymised with *Coelioxys polycentris* Förster, 1853, which is the senior synonym according to Schwarz and Gusenleitner (2003: 1224). This synonymy was previously overlooked by Proshchalykin and Fateryga (2017) (see also Fateryga et al. 2019).

***Pseudoanthidium (Pseudoanthidium) eversmanni* (Radoszkowski, 1886)**

Notes. Synonymised with *Pseudoanthidium tenellum* (Mocsáry, 1880), which is the senior synonym according to Litman et al. (2021: 1313).

***Pseudoanthidium (Pseudoanthidium) reptans* (Eversmann, 1852)**

Notes. Synonymised with *Pseudoanthidium nanum* (Mocsáry, 1880), which is the subjective synonym according to Litman et al. (2021: 1296). *Pseudoanthidium reptans* is a nomen oblitum, while *P. nanum* is a nomen protectum.

Other taxonomic changes and clarifications

Subgeneric classification of *Coelioxys* Latreille, 1809

A comprehensive morphological revision of the *Coelioxys* subgenera by da Rocha Filho and Packer (2016) was not followed by Proshchalykin and Fateryga (2017). According to this revision, *Coelioxys alatus* Förster, 1853, *C. elongatus* Lepeletier de Saint-Fargeau, 1841, *C. inermis* (Kirby, 1802), and *C. mandibularis* Nylander, 1848 should be placed in the subgenus *Paracoelioxys* Gribodo, 1884, *C. aurolimbatus* Förster, 1853 and *C. rufescens* Lepeletier de Saint-Fargeau & Audinet-Serville, 1825 should be placed in the subgenus *Rozeniana* da Rocha Filho, 2016, and *C. conoideus* (Illiger, 1806) should be placed in the monotypic subgenus *Melissoctonia* da Rocha Filho, 2016. The subgeneric placement of four species from the Russian fauna was not mentioned by da Rocha Filho and Packer (2016). Based on the material examined from the Primorskiy Territory of Russia, we hereby place *C. pielianus* Friese, 1935 in the subgenus *Paracoelioxys* and *C. ruficinctus* Cockerell, 1931 in the subgenus *Rozeniana*. At the same time, the subgeneric placement of *C. lanceolatus* Nylander, 1852 and *C. obtusispina* Thomson, 1872 still remains uncertain (see also Ghisbain et al. 2023).

***Icteranthidium floripetum* (Eversmann, 1852)**

Fig. 1A–F

Anthidium floripetum Eversmann, 1852: 83, ♀, ♂ (lectotype: ♀, “Spask Aug” [Russia: Orenburg Province, Spasskoye], IZSP, designated by Litman et al. (2021: 1300)).

Anthidium ovasi Warncke, 1980: 176, ♀, ♂ (holotype: ♀, “Yesilhisar/Kayseri, Türkiye” [Turkey], 3.VIII.1979, K. Warncke, OLBL), syn. nov.

Notes. *Anthidium floripetum* was first placed in the genus *Icteranthidium* Michener, 1948 by Litman et al. (2021: 1300). Previously it was treated in the genus *Pseudoanthidium* Friese, 1898 (Proshchalykin and Fateryga 2017: 302) due to an incorrect synonymisation with *P. lituratum* (Panzer, 1801) by Warncke (1980: 161). Kasperek (2022: 168) first published high-quality illustrations of the female holotype of *Icteranthidium ovasi*, which allowed us to ascertain that it is surprisingly almost identical in morphology to the female lectotype of *I. floripetum* (Fig. 1A, C, F). Therefore, these species should be treated as conspecific with Eversmann’s name taking priority. It is also of note that the male paralectotype of *I. floripetum* has the same large reddish-brown maculation in upper gena behind the eye (Fig. 1B, D) as the female types of both *I. floripetum* and *I. ovasi*, while the male paratypes of *I. ovasi* do not have them, according to Kasperek (2022: 168).

Distribution. Russia (Urals: Orenburg Province), Turkey, Iran, and Kazakhstan (Atyrau Province) (Litman et al. 2021; Kasperek 2022).

***Megachile (Chalicodoma) albocristata* Smith, 1853**

Fig. 2A

Notes. This name replaces the use of *Megachile lefebvrei* sensu Proshchalykin and Fateryga (2017: 305) and references therein. In the narrow sense, *M. lefebvrei* (Lepelletier de Saint-Fargeau, 1841) is present in North Africa and the Iberian Peninsula, and possibly in southern France (Ghisbain et al. 2023). Specimens from Russia were re-identified as *M. albocristata* by Fateryga and Proshchalykin (2020: 228). These species differ in the colour of the vestiture and the nature of the tergal fasciae in the female sex: in *M. lefebvrei*, the vestiture is predominantly grey-white and the tergal fasciae are interrupted medially; in *M. albocristata*, the vestiture is predominantly black, sometimes with spots of white hairs laterally on the terga (Fateryga and Proshchalykin 2020: 228; Ghisbain et al. 2023: 63). The typical form of *M. albocristata* occurs in Crimea, while a form from Dagestan has some traits intermediate with *M. hungarica* Mocsáry, 1877 (Fateryga and Proshchalykin 2020: 228). The taxonomy of this species complex, known as the *lefebvrei* group (*M. lefebvrei*, *M. hungarica*, *M. albocristata*, as well as *M. lucidifrons* Ferton, 1905 and *M. roeweri* (Alfken, 1927)), requires further investigation (Ghisbain et al. 2023: 63).

Distribution. Russia (North Caucasus, Crimea), south-eastern Europe, Georgia, Azerbaijan, Turkey, and Iran (Fateryga and Proshchalykin 2020; Maharramov et al. 2021; Ghisbain et al. 2023).



Figure 1. *Icterantheidium floripetum* (Eversmann, 1852) **A, C, E** lectotype, female **B, D, F** paralectotype, male **A, B** habitus in dorsal view **C, D** head in dorsal view **E, F** metasoma in dorsal view. Scale bars: 1 mm.

***Megachile (Eutricharaea) argentata* (Fabricius, 1793)**

Notes. This species was confirmed as the senior synonym of the widespread species *Megachile pilidens* Alfken, 1924 (Praz and Bénon 2023: 167; Ghisbain et al. 2023: 64).

Distribution. Russia (European part, Urals, Western Siberia), Western, Southern, and Eastern Europe, North Africa, Georgia, Armenia, Azerbaijan, Turkey, Jordan, Israel, Iran, and Kazakhstan (Maharramov et al. 2021; Praz and Bénon 2023).



Figure 2. Some species of bees recently reported from Russia **A** female of *Megachile albocristata* Smith, 1853 at flower of *Teucrium chamaedrys* L. (Lamiaceae), Dagestan Republic, 13.VI.2021 **B** female of *Trachusa integra* (Eversmann, 1852) on inflorescence of *Lomelosia argentea* (L.) Greuter & Burdet (Caprifoliaceae), Crimea, 10.VII.2023 **C** female of *Megachile sculpturalis* Smith, 1853 at her nest, Crimea, 24.VII.2021 **D** male of *Pseudoanthidium stigmaticorne* (Dours, 1873) on inflorescence of *Anthemis ruthenica* M. Bieb. (Asteraceae), Crimea, 5.VI.2021. Photographs by A. Fateryga.

***Trachusa (Paraanthidium) integra* (Eversmann, 1852)**

Fig. 2B

Notes. Recognised as a valid species (not as a synonym of *Trachusa interrupta* (Fabricius, 1781)) according to Kasperek (2020: 22). In the narrow sense, *T. interrupta* is a mainly Mediterranean species distributed from southern Spain and France, southern Switzerland and Austria over the Balkans to Greece and western Turkey; in south-eastern and Eastern European countries, the distribution extends to Slovakia, Hungary, Romania, and Ukraine (Kasperek 2020, 2022).

Distribution. Russia (south of European part, North Caucasus, Crimea), France, Albania, North Macedonia, Greece, Bulgaria, and Turkey (Kasperek 2020, 2022).

Species recorded in Russia after 2017

***Anthidium (Anthidium) melanopygum* Friese, 1917**

Distribution. First recorded for Russia (North Caucasus: Dagestan Republic, as *Anthidium spiniventre melanopygum*) by Fateryga et al. (2019: 1167). *Anthidium melanopygum* is currently treated as a distinct species, not a subspecies of *A. spiniventre* Friese, 1899 (Kasperek and Fateryga 2023: 567). Outside Russia known from Greece, Bulgaria, Turkey, Armenia, Azerbaijan, Lebanon, Iran, and Turkmenistan (Kasperek 2022; Kasperek and Fateryga 2023).

***Coelioxys (Allocoelioxys) acanthura* (Illiger, 1806)**

Distribution. First recorded for Russia (North Caucasus: Dagestan Republic) by Fateryga et al. (2019: 1169). Outside Russia known from Europe, North Africa, Georgia, Turkey, Cyprus, Israel, Iran, Turkmenistan, Uzbekistan, Kyrgyzstan, Kazakhstan, and China (Fateryga et al. 2019; Ascher and Pickering 2023).

***Coelioxys (Allocoelioxys) mielbergi* Morawitz, 1880**

Distribution. First recorded for Russia (south of European part: Volgograd Province) by Fateryga and Proshchalykin (2020: 228). Outside Russia known from Uzbekistan, Turkmenistan, and Tajikistan (Fateryga and Proshchalykin 2020).

***Coelioxys (Liothyrapis) decipiens* (Spinola, 1838)**

Distribution. First recorded for Russia (North Caucasus: Dagestan Republic) by Fateryga et al. (2019: 1171). Outside Russia known from North Africa, Greece, Turkey, Israel, Yemen, Oman, Iran, Iraq, Turkmenistan, Tajikistan, Uzbekistan, Kyrgyzstan, Kazakhstan, China, India, Myanmar, and Thailand (Fateryga et al. 2019; Ascher and Pickering 2023).

***Hoplitis (Alcidamea) beijingensis* Wu, 1987**

Distribution. First recorded for Russia (Eastern Siberia: Buryatia Republic) by Proshchalykin and Müller (2019: 165). Outside Russia known from northern China (Proshchalykin and Müller 2019; Müller 2023).

***Hoplitis (Alcidamea) curvipes* (Morawitz, 1871)**

Distribution. First recorded for Russia (North Caucasus: Dagestan Republic) by Fateryga and Proshchalykin (2020: 226). Outside Russia known from Spain, France, Italy, Greece, Bulgaria, Turkey, Azerbaijan, and Syria (Fateryga and Proshchalykin 2020; Ivanov et al. 2023; Müller 2023).

***Hoplitis (Alcidamea) mollis* Tkalčů, 2000**

Distribution. First recorded for Russia (Crimea) by Fateryga and Ivanov (in press). Outside Russia known from Bulgaria, Azerbaijan, Turkey, Syria, Jordan, Uzbekistan, Kyrgyzstan, and Kazakhstan (Müller 2023).

***Hoplitis (Hoplitis) carinata* (Staneek, 1969)**

Distribution. First recorded for Russia (Crimea) by Fateryga et al. (2019: 1168). Outside Russia known from Greece, Croatia, North Macedonia, Bulgaria, Armenia, Azerbaijan, Turkey, Syria, Jordan, and Iran (Fateryga et al. 2019; Müller 2023).

***Hoplitis (Hoplitis) kaszabi* Tkalčů, 2000**

Distribution. First recorded for Russia (Siberia: Altai and Buryatia republics) by Proshchalykin and Müller (2019: 168). Outside Russia known from Tajikistan, Kazakhstan, Mongolia, and North China (Proshchalykin and Müller 2019; Müller 2023).

***Hoplitis (Platosmia) inconspicua* Tkalčů, 1995**

Distribution. First recorded for Russia (Siberia: Altai, Khakassia and Tuva republics) by Proshchalykin and Müller (2019: 169). Outside Russia known from Mongolia (Proshchalykin and Müller 2019; Müller 2023).

***Icteranthidium ferrugineum* (Fabricius, 1787)**

Distribution. First recorded for Russia (South of European part and North Caucasus: Astrakhan Province, Kalmykia and Dagestan republics) by Fateryga et al. (2019: 1167). Outside Russia known from Southern Europe, West and North Africa, Turkey, Cyprus, Syria, Israel, Saudi Arabia, Yemen, Oman, UAE, Afghanistan, Pakistan, Turkmenistan, Kazakhstan, and China (Fateryga et al. 2019; Ascher and Pickering 2023).

***Lithurgus tibialis* Morawitz, 1875**

Distribution. First recorded for Russia (North Caucasus: Dagestan Republic) by Fateryga et al. (2019: 1166). Outside Russia known from Southern Europe, North Africa, Azerbaijan, Turkey, Cyprus, Syria, Jordan, Israel, United Arab Emirates, Iraq, Iran, Afghanistan, Pakistan, Turkmenistan, Tajikistan, Uzbekistan, and India (Fateryga et al. 2019; Maharramov et al. 2023).

***Megachile (Callomegachile) sculpturalis* Smith, 1853**

Fig. 2C

Distribution. First recorded for Russia (Crimea) by Ivanov and Fateryga (2019: 10). Outside Russia known from China (including Taiwan), Korean Peninsula, and Japan; introduced into USA, Canada, Switzerland, Lichtenstein, Germany, Austria, Spain, France, Italy, Slovenia, Serbia, Croatia, Bosnia and Herzegovina, Hungary, Ukraine, and India (Ivanov and Fateryga 2019; Sardar et al. 2021; Laner et al. 2022; Mulencko et al. 2022).

***Megachile (Chalicodoma) albonotata* Radoszkowski, 1886**

Distribution. First recorded for Russia (North Caucasus: Dagestan Republic) by Fateryga et al. (2019: 1171). Outside Russia known from Southern Europe, Armenia, Azerbaijan Turkey, Israel, Iran, and Turkmenistan (Fateryga et al. 2019; Maharramov et al. 2021).

***Megachile (Chalicodoma) alborufa* Friese, 1911**

Distribution. First recorded for Russia (North Caucasus: Karachay-Cherkesia Republic, as *Megachile pyrenaica* (Lepeletier de Saint-Fargeau, 1841)) by Fateryga et al. (2019: 1171), but that report referred to *M. alborufa* (Fateryga and Proshchalykin 2020: 229); also reported as *M. alborufa* from Adygea and North Ossetia – Alania republics by Fateryga and Proshchalykin (2020: 229). These two species are closely related and differ in the colour of the legs, as well as the vestiture and the nature of the tergal fasciae in the female sex: *Megachile alborufa* has reddish legs from tibiae onwards and pale pubescence on terga 1 and 2; in *M. pyrenaica*, the legs are mostly black except reddish tarsi while pale pubescence is developed on terga 1–5. As there are no differences in structural morphology, *M. alborufa* may actually represent just a colour form or a subspecies of *M. pyrenaica* (Fateryga and Proshchalykin 2020). The taxonomy of this species complex requires further investigation. *Megachile alborufa* is known outside Russia from Georgia, Azerbaijan, and Turkey (Fateryga and Proshchalykin 2020). In the narrow sense, *M. pyrenaica* is known from Western and Southern Europe, North Africa, Armenia, Azerbaijan, Turkey, Israel, Tajikistan, and Kazakhstan (Maharramov et al. 2021).

***Megachile (Eutricharaea) burdigalensis* Benoist, 1940**

Distribution. First recorded for Russia (North Caucasus: Dagestan Republic) by Fateryga et al. (2019: 1171). Outside Russia known from Western and Southern Europe, Georgia, Armenia, Azerbaijan, and Kazakhstan (Fateryga et al. 2019; Maharramov et al. 2021).

***Megachile (Pseudomegachile) flavipes* Spinola, 1838**

Distribution. First recorded for Russia (North Caucasus: Dagestan Republic) by Fateryga et al. (2019: 1171). Outside Russia known from Greece, North Africa, Armenia, Azerbaijan, Turkey, Cyprus, Syria, Israel, Saudi Arabia, Oman, Iran, Iraq, Afghanistan, Pakistan, Turkmenistan, Tajikistan, Uzbekistan, Kyrgyzstan, and India (Fateryga et al. 2019; Maharramov et al. 2021).

***Megachile (Pseudomegachile) tecta* Radoszkowski, 1888**

Distribution. First recorded for Russia (south of European part and North Caucasus: Kalmykia and Dagestan republics) by Fateryga et al. (2019: 1173); also known from Western Siberia: Altai Territory from where it was earlier incorrectly reported as *Megachile farinosa* Smith, 1853 by Byvaltsev et al. (2018) (see below). Outside Russia known from Azerbaijan, Iran, Afghanistan, Turkmenistan, Uzbekistan, Tajikistan, Kyrgyzstan, Kazakhstan, and China (Fateryga et al. 2019; Maharramov et al. 2021).

***Osmia (Helicosmia) cinerea* Warncke, 1988**

Distribution. First recorded for Russia (North Caucasus: Dagestan Republic) by Fateryga and Proshchalykin (2020: 227). Outside Russia known from Azerbaijan, Turkey, Turkmenistan, and Kyrgyzstan (Fateryga and Proshchalykin 2020; Müller 2023).

***Osmia (Hoplosmia) ligurica* Morawitz, 1868**

Distribution. First recorded for Russia (North Caucasus: Dagestan Republic) by Fateryga and Proshchalykin (2020: 227). Outside Russia known from Western, Southern, and Eastern Europe, North Africa, Georgia, Armenia, Azerbaijan, Turkey, Cyprus, Syria, Jordan, Israel, Iran, and Turkmenistan (Fateryga and Proshchalykin 2020; Müller 2023).

***Osmia (Pyrosmia) cyanoxantha* Pérez, 1879**

Distribution. First recorded for Russia (North Caucasus: Dagestan Republic) by Fateryga and Proshchalykin (2020: 228); also known from Crimea (Fateryga and Ivanov in press). Outside Russia known from Western, Southern, and Eastern Europe, North Africa, Armenia, Azerbaijan, Turkey, Cyprus, Syria, Jordan, Israel, and Iran (Fateryga and Proshchalykin 2020; Müller 2023).

***Osmia (Pyrosmia) hellados* van der Zanden, 1984**

Distribution. First recorded for Russia (Crimea) by Fateryga and Ivanov (in press). Outside Russia known from Southern and Eastern Europe, Georgia, Azerbaijan, Turkey, Cyprus, Jordan, and Israel (Müller 2023).

***Protosmia (Protosmia) glutinosa* (Giraud, 1871)**

Distribution. First recorded for Russia (North Caucasus: Dagestan Republic) by Fateryga and Proshchalykin (2020: 228). Outside Russia known from Western, Southern, and Eastern Europe, North Africa, Azerbaijan, Turkey, Cyprus, Syria, Jordan, Lebanon, Israel, and Iran (Fateryga and Proshchalykin 2020; Müller 2023).

***Pseudoanthidium (Pseudoanthidium) stigmaticorne* (Dours, 1873)**

Fig. 2D

Distribution. First recorded for Russia (Crimea and North Caucasus: Dagestan Republic) by Litman et al. (2021: 1307). It was also reported earlier from Crimea as *Pseudoanthidium* sp. aff. *nanum* (Mocsáry, 1880) by Fateryga et al. (2018: 243). Outside Russia known from Western, Southern, and Eastern Europe, North Africa, Azerbaijan, Turkey, Cyprus, Syria, Jordan, Israel, Iran, and Turkmenistan (Litman et al. 2021).

Species overlooked in the previous Russian checklist

***Coelioxys (Allocoelioxys) argenteus* Lepeletier de Saint-Fargeau, 1841**

Distribution. First recorded for Russia (North Caucasus: Dagestan Republic, as *Coelioxys constrictus* Förster, 1853) by Morawitz (1873: 185) but this record was overlooked by Proshchalykin and Fateryga (2017) (see also Fateryga et al. 2019); also reported from the south of European part: Astrakhan Province (Fateryga et al. 2019: 1171). Outside Russia known from Western, Southern, and Eastern Europe, North Africa, the Caucasus, Turkey, Cyprus, Syria, Jordan, Israel, Iran, Turkmenistan, Tajikistan, Uzbekistan, Kyrgyzstan, Kazakhstan, and China (Fateryga et al. 2019; Ascher and Pickering 2023).

***Megachile (Megachile) pyrenaea* Pérez, 1890**

Distribution. First recorded for Russia (north-west and north of European part: Leningrad Province and Karelia Republic) by Elfving (1968: 37) but this record was overlooked by Proshchalykin and Fateryga (2017). Outside Russia known from Europe, Armenia, and Turkey (Ascher and Pickering 2023).

***Pseudoanthidium (Exanthidium) eximium* (Giraud, 1863)**

Distribution. First recorded for Russia (North Caucasus: Ingushetia Republic) by Mavromoustakis (1948: 175) but this record was overlooked by Proshchalykin and Fateryga (2017) (see also Kasperek 2021). Outside Russia known from Portugal in the west across the Mediterranean, Turkey and the Caucasus to the Iranian Elburz Mountains (Kasperek 2021).

New species records for Russia

***Anthidiellum (Anthidiellum) troodicum* Mavromoustakis, 1949**

Distribution. New record RUSSIA, North Caucasus: 1 ♀, 1 ♂, Dagestan Republic, vicinity of Talgi, 42°52'36"N, 47°26'42"E, on *Teucrium canum*, 18.VI.2021, A. Fateryga (CAFK). Outside Russia known from Croatia, Greece, Bulgaria, Azerbaijan, Turkey, Cyprus, Syria, Jordan, Lebanon, and Israel (Kasperek 2022; Kasperek et al. 2023).

***Anthidium (Anthidium) dalmaticum* Mocsáry, 1884**

Distribution. New record RUSSIA, North Caucasus: 6 ♂, Dagestan Republic, vicinity of Talgi, 42°52'36"N, 47°26'42"E, 13.VI.2021, A. Fateryga; 2 ♀, idem, on *Teucrium canum*, 13.VI.2021, A. Fateryga (1 ♀, 4 ♂ CAFK; 1 ♀, 2 ♂ CMKH). Outside Russia known from the eastern part of the Adriatic Sea (Croatia), Greece, Bulgaria, Turkey, and the Levant to the Caucasus and Iran; also reported from Afghanistan (Kasperek 2022). Specimens from Dagestan resemble the subspecies *A. dalmaticum syriacum* Pérez, 1912.

***Hoplitis (Alcidamea) ozbeki* Tkalců, 2000**

Distribution. New record RUSSIA, North Caucasus: 1 ♀, North Ossetia – Alania Republic, Tsey Gorge, 42°47'38"N, 43°54'54"E, on *Leontodon* sp., 30.VI.2021, A. Fateryga (CAFK); 1 ♀, 1 ♂, Dagestan Republic, 3 km NW Khotoch, 42°25'38"N, 46°55'44"E, on *Medicago glutinosa*, 17.VI.2023, A. Fateryga (CAFK). Outside Russia known from Georgia and Turkey (Müller 2023).

***Hoplitis (Hoplitis) linguaria* (Morawitz, 1875)**

Distribution. New record RUSSIA, North Caucasus: 1 ♀, Dagestan Republic, Tsudakhar, 42°19'40"N, 47°09'48"E, 11.VI.2019, A. Fateryga (CAFK); 2 ♀, 1 ♂, idem, 16.VI.2021, S. Ivanov (1 ♀ CAFK; 1 ♀, 1 ♂ ETHZ); 1 ♀, idem, on *Onosma caucasica*, 16.VI.2021, A. Fateryga (CAFK); 1 ♂, idem, 20.VI.2021, A. Fateryga (CAFK); 2 ♀, 1 ♂, idem, 20.VI.2021, S. Ivanov (CAFK); 1 ♀, idem, on *Onosma caucasica*, 28.VI.2021, A. Fateryga (CAFK); 1 ♂, idem, 29.V.2022, A. Fateryga (CAFK); 5 ♀, idem, on *Onosma caucasica*, 15.VI.2023, A. Fateryga (CAFK). Outside Russia known from Georgia and Turkey (Müller 2023).

***Megachile (Eutricharaea) anatolica* Rebmann, 1968**

Distribution. **New record** RUSSIA, south of European part: 2 ♂, Astrakhan Province, 13 km S Liman, 24–26.VII.2015, M. Proshchalykin, V. Loktionov, M. Mokrousov, S. Belokobylskij (FSCV); 1 ♂, 35 km NNW Astrakhan, 26.VII.2015, M. Proshchalykin, V. Loktionov, M. Mokrousov, S. Belokobylskij (FSCV); 2 ♂, Kalmykia Republic, 17 km SWW Artezian, Kuma River, 18–21.VII.2015, M. Proshchalykin, V. Loktionov, M. Mokrousov, S. Belokobylskij (CAFK; FSCV); 1 ♂, 22 km E Yashkul, 16–18.VII.2015, M. Proshchalykin, V. Loktionov, M. Mokrousov, S. Belokobylskij (FSCV). Outside Russia known from Italy, Greece, Croatia, Turkey, Cyprus, Jordan, Lebanon, Israel, and Iran (Ascher and Pickering 2023; Praz and Bénon 2023).

Species to be excluded from the Russian checklist

***Hoplitis (Alcidamea) laboriosa* (Smith, 1878)**

Distribution. Was reported on the base of an erroneous record (based on a locality misinterpretation). The species occurs in Kazakhstan, Mongolia, and China (Ghisbain et al. 2023; Müller 2023).

***Hoplitis (Alcidamea) turcestanica* (Dalla Torre, 1896)**

Distribution. This species was earlier reported from Russia as *Hoplitis caularis* (Morawitz, 1875) (Proshchalykin and Fateryga 2017; Fateryga et al. 2018), which was considered a senior synonym of *H. turcestanica* (Ungricht et al. 2008). Then, *H. turcestanica* was reinstated as a valid species by Fateryga and Proshchalykin (2020: 226), who provided an additional record from the south of European part: Astrakhan Province. Although, *H. turcestanica* and *H. caularis* are indeed two very different species, the material from Crimea, reported as *H. caularis*, belongs not to *H. turcestanica* but to *H. mollis* (Fateryga and Ivanov in press; see also above), while specimens from the Astrakhan Province belong to an apparently undescribed species (A. Müller, personal communication). *Hoplitis turcestanica* is confirmed to Turkmenistan, Tajikistan, Kyrgyzstan, and Kazakhstan, while *H. caularis* is known from Kazakhstan (Müller 2023). The records of both species from Turkey, Syria, Uzbekistan, and China require confirmation, as are the records of *H. turcestanica* from the North Caucasus and Urals mentioned by Proshchalykin and Fateryga (2017) and Fateryga and Proshchalykin (2020).

***Hoplitis (Anthocopa) taurica* (Radoszkowski, 1874)**

Notes. *Pseudosmia taurica* Radoszkowski, 1874 is considered to be a nomen dubium by Müller (2023) based on the poor description and the unavailability of the type material.

***Hoplitis (Hoplitis) ravouxi* (Pérez, 1902)**

Distribution. The reports of this species from Crimea (Proshchalykin and Fateryga 2017; Fateryga et al. 2018) actually referred to *Hoplitis carinata* (Stanek, 1969) (Fateryga et al. 2019) (see above). *Hoplitis ravouxi* is distributed in Western, Southern, and Eastern Europe (Müller 2023).

***Hoplitis (Pentadentoscopia) nitidula* (Morawitz, 1877)**

Distribution. Was reported on the base of an apparently erroneous record (based on a locality misinterpretation). The species occurs in Armenia, Iran, Pakistan, Turkmenistan, Uzbekistan, and Kazakhstan (Ghisbain et al. 2023; Müller 2023).

***Osmia (Helicosmia) cyanescens* Morawitz, 1875**

Distribution. Was reported on the base of an erroneous record (based on a locality misinterpretation). The species occurs in Tajikistan, Kyrgyzstan, and Kazakhstan (Ghisbain et al. 2023; Müller 2023).

***Osmia (Hemiosmia) difficilis* Morawitz, 1875**

Distribution. Was reported on the base of an erroneous record (based on a locality misinterpretation). The species occurs in Azerbaijan, Turkey, Syria, Lebanon, Israel, Iran, Tajikistan, Uzbekistan, Kyrgyzstan, and Kazakhstan (Müller 2020, 2023).

***Osmia (Osmia) melanocephala* Morawitz, 1875**

Distribution. Was reported on the base of an erroneous record (based on a locality misinterpretation). The species occurs in Turkmenistan, Tajikistan, Uzbekistan, Kyrgyzstan, Kazakhstan, Mongolia, and China (Müller 2023).

***Osmia (Pyrosmia) gallarum* Spinola, 1808**

Distribution. The reports of this species from Crimea (Proshchalykin and Fateryga 2017; Fateryga et al. 2018) actually referred to *Osmia hellados* van der Zanden, 1984 (Fateryga and Ivanov in press) (see above). *Osmia gallarum* is distributed in Western, Southern, and Eastern Europe, North Africa, and Turkey (Müller 2023).

***Megachile (Pseudomegachile) farinosa* Smith, 1853**

Distribution. First recorded for Russia (North Caucasus: Dagestan Republic, as *Megachile derasa* Gerstäcker, 1869) by Morawitz (1873: 149). This record

was overlooked by Proshchalykin and Fateryga (2017) (see also Fateryga et al. 2019). An additional report of this species was made by Byvaltsev et al. (2018) from Western Siberia: Altai Territory. All these records, however, referred to *M. tecta* (see above). *Megachile farinosa* is distributed in East Mediterranean (Greece, Turkey, Cyprus), Israel north of the Dead Sea, Middle East, and Iran (Dorchin and Praz 2018).

Family Apidae Latreille, 1802

Species recently described as new to science

***Epeolus asiaticus* Astafurova & Proshchalykin, 2022**

Epeolus asiaticus Astafurova and Proshchalykin 2022a: 309, ♀, ♂ (holotype: ♀, Mongolia, Terkhin-Gol, Chulut and Khoit Rivers, 30.VI.1975, E. Narchuk, ZISP). Paratypes from Russia (Altai Republic).

Distribution. Russia (Siberia: Altai Republic, Tuva Republic, Zabaikalskiy Territory), Mongolia (Arkhangai, Bayankhongor, Bayan-Ölgii, Dornod, Dornogovi, Govi-Altai, Khuvsgul, Omnogovi, Selenge, Sukhbaatar, Tuv, Ulaanbaatar, Uvs, Uvurkhangai, Zavkhan).

***Epeolus rasmonti* Astafurova & Proshchalykin, 2022**

Epeolus rasmonti Astafurova and Proshchalykin 2022b: 202, ♀, ♂ (holotype: ♀, Russia, Buryatia Republic, Gusinoe Lake, Baraty, 25.VII.2007, A. Lelej, M. Proshchalykin, V. Loktionov, ZISP).

Distribution. Russia (Eastern Siberia: Buryatia Republic), Mongolia (Bulgan, Dornod, Khentii, Sukhbaatar), China (Beijing).

Published synonymies

***Anthophora (Anthophora) salviae* (Panzer, 1805)**

Notes. Synonymised with *Anthophora crinipes* Smith, 1854, which is the valid name according to Maghni et al. (2017: 5). The latter authors considered the basionym *Lasius salviae* Panzer, 1805 a nomen dubium (Ghisban et al. 2023: 26).

***Anthophora (Paramegilla) prshewalskyi* Morawitz, 1880**

Notes. Synonymised with *Anthophora segnis* Eversmann, 1852 (not a synonym of *A. podagra* Lepeletier de Saint-Fargeau, 1841), which is the senior synonym according to Ghisban et al. (2023: 27).

***Eucera (Eucera) eucnemidea* Dours, 1873**

Notes. Synonymised with *Eucera grisea* Fabricius, 1793, which is the senior synonym according to Dorchin (2023: 12).

***Eucera (Pareucera) nigrita* Friese, 1895**

Notes. Synonymised with *Eucera albofasciata* Friese, 1895, which is the senior synonym according to Boustani et al. (2021: 123).

***Eucera (Synhalonia) alternans* (Brullé, 1832)**

Notes. *Eucera rufa* (Lepeletier de Saint-Fargeau, 1841), which is the junior synonym, is retained by Dorchin (2023: 23) as the valid name for this species under the principle of name stability. *Eucera rufa* replaces *E. alternans* from the 2017 checklist, and that *E. alternans* auctorum is referred to in present list by *E. ruficollis*.

***Nomada obscuriceps* Schwarz & Levchenko, 2017**

Notes. Synonymised with *Nomada mitaii* Proshchalykin, 2010, which is the senior synonym according to Proshchalykin et al. (2019: 26).

Other taxonomic changes and clarifications

The following nomenclatural changes were proposed by Dorchin (2023): *Tetralonia* Spinola, 1838 is reestablished as genus, including *Tetraloniella* Ashmead, 1899 (Dorchin et al. 2018); *Cubitalia* Friese, 1911 is treated as subgenus of *Eucera* Scopoli, 1770; and *Synhalonia* Patton, 1879 is retained as subgenus of *Eucera* as in Michener (2007). Therefore, the following three species previously included in the genus *Cubitalia* and 14 species previously included in the genus *Tetraloniella* (Levchenko et al. 2017) are now transferred to the genus *Eucera* and *Tetralonia* respectively: *Eucera (Cubitalia) morio* Friese, 1911, *E. (C.) parvicornis* Mocsáry, 1878, *E. (C.) tristis* Morawitz, 1876, *Tetralonia alticincta* (Lepeletier de Saint-Fargeau, 1841), *T. dentata* (Germar, 1839), *T. fulvescens* Giraud, 1863, *T. graja* (Eversmann, 1852), *T. inulae* Tkalců, 1979, *T. julliani* (Pérez, 1879), *T. lyncea* Mocsáry, 1879, *T. mitsukurii* Cockerell, 1911, *T. nana* Morawitz, 1873, *T. pollinosa* (Lepeletier de Saint-Fargeau, 1841), *T. salicariae* (Lepeletier de Saint-Fargeau, 1841), *T. scabiosae* (Mocsáry, 1881), *T. strigata* (Lepeletier de Saint-Fargeau, 1841), and *T. vicina* Morawitz, 1876.

***Anthophora (Pyganthophora) erschowi* Fedtschenko, 1875**

Notes. The type series was revised in ZISP by P. Rasmont (Ghisbain et al. 2023: 26). The specimens comprising the type series are only females, all belonging to the difficult group of *Anthophora aestivalis* (Panzer, 1801), in which generally only males can be reliably identified. Therefore, the name *Anthophora erschowi*

was considered to be a species inquirenda and removed from the European (including Russian) checklists.

***Apis cerana ussuriensis* Ilyasov, Takahashi, Proshchalykin, Lelej & Kwon, 2019**

Notes. Recognised as a separate subspecies according to Ilyasov et al. (2019: 310).

Distribution. Russia (Far East: Primorskiy and Khabarovsk territories) (Proshchalykin and Sergeev 2020).

***Eucera (Eucera) pollinosa* Smith, 1854**

Notes. This species was previously referred to as *Eucera chrysopyga* Pérez, 1879 (Levchenko et al. 2017: 320), as when *Eucera* and *Tetraloniella* were treated as a single genus, *Eucera pollinosa* Smith became a junior homonym of *E. pollinosa* (Lepeletier de Saint-Fargeau, 1841). Now that *Tetralonia* is restored as a genus (which also includes *Tetraloniella*), *E. pollinosa* (Lepeletier de Saint-Fargeau) is moved to *Tetralonia*, and *E. pollinosa* Smith is no longer a junior homonym and becomes the senior synonym of *E. chrysopyga* Pérez. *Eucera pollinosa* Smith was made a nomen protectum by Dorchin (2023).

***Bombus (Bombus) czerskianus* Vogt, 1911**

Notes. Recognised as a separate species (not as a subspecies of *Bombus sporadicus* Nylander, 1848) according to Williams (2021: 271).

Distribution. Russia (Eastern Siberia, Far East), North Korea, north-eastern China, and Mongolia (Williams 2021).

***Bombus (Melanobombus) alagesianus* Reinig, 1930**

Notes. Recognised as a valid species (not as a synonym of *Bombus keriensis* Morawitz, 1887) according to Williams et al. (2020: 81).

Distribution. Russia (North Caucasus), Turkey, Georgia, Armenia, and Iran (Williams et al. 2020).

***Bombus (Melanobombus) incertoides* Vogt, 1911**

Notes. Recognised as a valid species (not as a synonym of *Bombus keriensis* s. lat.) according to Williams et al. (2020: 87).

Distribution. Russia (Siberia: Tuva and Altai republics) and Mongolia (Williams et al. 2020).

***Bombus (Pyrobombus) koropokkrus* Sakagami & Ishikawa, 1972**

Notes. Recognised as a valid species (not as a synonym of *Bombus hypnorum* (Linnaeus, 1802)) according to Williams et al. (2022: 62).

Distribution. Russia (Far East: Sakhalin) and Japan (Hokkaido) (Williams et al. 2022).

***Bombus (Thoracobombus) mocsaryi* Kriechbaumer, 1877**

Notes. The taxon *mocsaryi* Kriechbaumer, 1877 was re-assessed as a subspecies of *Bombus laesus* Morawitz (1875) by Brasero et al. (2021) based on genetic and semio-chemical analyses.

Species recorded in Russia after 2017

***Anthophora (Lophanthophora) crysocnemis* Morawitz, 1877**

Distribution. First recorded for Russia (south of European part: Volgograd Province) by Ghisbain et al. (2023: 27). Outside Russia known from Armenia and Kazakhstan (Ghisbain et al. 2023).

***Epeolus mongolicus* Astafurova & Proshchalykin, 2021**

Distribution. First recorded for Russia (Eastern Siberia: Tuva Republic) by Astafurova and Proshchalykin (2022a: 324). Outside Russia known from Kyrgyzstan and Mongolia (Bulgan, Zavkhan) (Astafurova and Proshchalykin 2022a).

***Eucera (Synhalonia) distinguenda* (Morawitz, 1875)**

Distribution. First recorded for Russia (south of European part: Astrakhan Province) by Levchenko (2019: 20). Outside Russia known from Armenia, Iran, Turkmenistan, and Kazakhstan (Morawitz 1875, 1877, 1894; Popov 1967).

***Nomada minuscula* Noskiewicz, 1930**

Distribution. First recorded for Russia (European part) by Smit (2018: 188). Outside Russia known from Europe, Morocco, Algeria, and Tunisia (Smit 2018).

***Nomada subcornuta* (Kirby, 1802)**

Distribution. First recorded for Russia (European part) by Ghisbain et al. (2023: 45). Outside Russia known from United Kingdom, Belgium, Netherlands, Germany, Czech Republic, Hungary, Estonia, and Finland (Ghisbain et al. 2023).

Species overlooked in the previous Russian checklist

Epeolus nudiventris Bischoff, 1930

Distribution. Described from Russia (Siberia: Buryatia Republic) by Bischoff (1930: 14). Outside Russia known from Kazakhstan, Uzbekistan, Kyrgyzstan, Turkmenistan, Tajikistan, and Mongolia (Khovd) (Astafurova and Proshchalykin 2023b).

New species records for Russia

Epeolus ruficornis Morawitz, 1875

Distribution. New record RUSSIA, south of European part: 2 ♀♀, 2 ♂♂, Kalmykia Republic, 17 km SSW Artezian, Kuma River, 2–3.VII.2016, Yu. Astafurova; 1 ♂, Astrakhan Province, 35 km NNW Astrakhan, 26.VII.2015, M. Proshchalykin; 1 ♂, Astrakhan Province, Sedlistoye, 8.VI.1927, Plotnikov (ZISP). Outside Russia known from Azerbaijan, Kazakhstan, Uzbekistan, Kyrgyzstan, Turkmenistan, Tajikistan, Mongolia, and China (Xinjiang, Gansu) (Astafurova and Proshchalykin 2023b).

Tetralonia yoshihiro (Ikudome, 2022)

Distribution. New record RUSSIA, Far East: 1 ♂, Primorskiy Territory, Kamen-Rybolov, 28.VIII.1980, Romankov (FSCV); 1 ♂, Primorskiy Territory, Novokachalinsk, 4.VIII.2006, Belokobylskij (ZISP); 2 ♀♀, idem, 21.VIII.2009, A. Lelej, M. Proshchalykin, V. Loktionov (FSCV). Outside Russia known from Japan (Honshu, Kyushu, Tanegashima), South Korea, and China (Beijing, Zhejiang, Anhui) (Ikudome 2022).

Species to be excluded from the Russian checklist

Bombus (Melanobombus) keriensis Morawitz, 1887

Distribution. The Russian records of *Bombus keriensis* in Levchenko et al. (2017: 329) refer to *B. separandus* Vogt, 1909 (Siberia: Tuva and Altai republics) and *B. alagesianus* Reinig, 1930 (North Caucasus) (Williams et al. 2020).

Thyreus aberrans (Morawitz, 1875)

Notes. This taxon has been treated as a nomen dubium according to Ghisbain et al. (2023: 28). Records from the European part of Russia must therefore be considered to be unclear due to this taxonomic uncertainty.

Conclusions

Here we have presented an update on the knowledge of the species diversity and taxonomy of the bee fauna of Russia, considering all the advances made after the publication of the catalogue of Russian bees (Astafurova and Proshchalykin 2017; Levchenko et al. 2017; Proshchalykin 2017a; Proshchalykin et al. 2017;

Table 1. Updated species totals for Russian bees.

Family	Subfamily	Tribe	Genus	Number of species
Colletidae	Colletinae	Colletini	<i>Colletes</i>	53
	Hylaeinae	Hylaeini	<i>Hylaeus</i>	61
Andrenidae	Andreninae	Andrenini	<i>Andrena</i>	231
	Panurginae	Panurgini	<i>Camptopoeum</i>	2
			<i>Panurginus</i>	13
			<i>Panurgus</i>	1
Melliturgini	<i>Melitturga</i>	3		
Halictidae	Rophitinae	–	<i>Dufourea</i>	8
			<i>Flavodufourea</i>	1
			<i>Rhophitoides</i>	1
			<i>Rophites</i>	6
			<i>Systropha</i>	2
	Nomiinae	–	<i>Lipotriches</i>	1
			<i>Nomiapis</i>	6
			<i>Pseudapis</i>	3
	Nomioidinae	–	<i>Ceylalictus</i>	1
			<i>Nomioides</i>	2
	Halictinae	Halictini	<i>Halictus</i>	48
			<i>Lasioglossum</i>	150
			<i>Sphecodes</i>	38
Melittidae	Dasypodainae	Dasypodaini	<i>Dasypoda</i>	8
	Melittinae	–	<i>Macropis</i>	5
			<i>Melitta</i>	13
Megachilidae	Megachilinae	Lithurgini	<i>Lithurgus</i>	3
		Osmiini	<i>Chelostoma</i>	6
			<i>Heriades</i>	3
			<i>Hoplitis</i>	33
			<i>Osmia</i>	44
			<i>Protosmia</i>	3
			<i>Anthidiellum</i>	2
		Anthidiini	<i>Anthidium</i>	13
			<i>Bathanthidium</i>	2
			<i>Eoanthidium</i>	1
			<i>Icteranthidium</i>	5
			<i>Pseudoanthidium</i>	7
			<i>Stelis</i>	14
			<i>Trachusa</i>	3
		Dioxyini	<i>Aglaopis</i>	1
			<i>Dioxys</i>	1
		Megachilini	<i>Coelioxys</i>	26
			<i>Megachile</i>	53

Family	Subfamily	Tribe	Genus	Number of species	
Apidae	Xylocopinae	Xylocopini	<i>Xylocopa</i>	6	
		Ceratinini	<i>Ceratina</i>	14	
	Nomadinae	Nomadini	<i>Nomada</i>	117	
			Epeolini	<i>Epeolus</i>	17
			<i>Triepeolus</i>	2	
		Ammobatoidini	<i>Ammobatoides</i>	2	
		Biastini	<i>Biastes</i>	4	
		Ammobatini	<i>Ammobates</i>	4	
			<i>Parammobatodes</i>	1	
			<i>Pasites</i>	2	
	Apinae	Osirini	<i>Epeoloides</i>	1	
		Ancylaini	<i>Ancyla</i>	1	
		Ctenoplectrini	<i>Ctenoplectra</i>	1	
		Eucerini	<i>Eucera</i>	36	
			<i>Tetralonia</i>	16	
		Anthophorini	<i>Amegilla</i>	9	
			<i>Anthophora</i>	41	
			<i>Habropoda</i>	1	
		Melectini	<i>Melecta</i>	11	
			<i>Thyreomelecta</i>	2	
			<i>Thyreus</i>	9	
		Bombini	<i>Bombus</i>	92	
	Apini	<i>Apis</i>	2		
	Total:	14 subfamilies	27 tribes	64 genera	1,268 species

Proshchalykin and Astafurova 2017; Proshchalykin and Fateryga 2017) and considering material that was overlooked by that work. An updated total of 1,268 species belonging to 64 genera and six families are now recorded within Russia (Table 1, Suppl. material 1).

After the revision of the first checklist, we report five species recently described, 45 species newly recorded since the first catalogue (including one species non-native to Russia), nine species overlooked in the previous Russian checklist, and 17 published synonymies. We provide original records for nine species previously unknown to Russia and, as original taxonomic act, we synonymise one species and exclude 14 species from the previous checklist. Numerous other taxonomic changes and clarifications are also included. The final count of species per family, subfamily, tribe and genus is available in Table 1. An updated list of Russian bees is available as Suppl. material 1.

Acknowledgements

We are grateful to Thomas Wood (Mons, Belgium), Paolo Rosa (Mons, Belgium), Timofey Levchenko (Moscow, Russia), and Max Kasperek (Heidelberg, Germany) for their valuable comments, which helped to improve the quality of this paper, as well as to Andreas Müller (Zurich, Switzerland) for identification of some specimens of the tribe Osmiini.

Additional information

Conflict of interest

The authors have declared that no competing interests exist.

Ethical statement

No ethical statement was reported.

Funding

This investigation was supported by the Russian Funds for Basic Research (grant number 20-54-44014), and the state research projects 121031000151-3, 121032300023-7, and 122031100272-3.

Author contributions

All authors have contributed equally.

Author ORCIDs

Maxim Yu. Proshchalykin  <https://orcid.org/0000-0001-7870-8226>

Alexander V. Fateryga  <https://orcid.org/0000-0002-5346-3477>

Yulia V. Astafurova  <https://orcid.org/0000-0003-0557-7792>

Data availability

All of the data that support the findings of this study are available in the main text or Supplementary Information.

References

- Ascher JS, Pickering J (2023) Discover Life bee species guide and world checklist (Hymenoptera: Apoidea: Anthophila). http://www.discoverlife.org/mp/20q?guide=Apoidea_species [Accessed 09.09.2023]
- Astafurova YuV (2014) Bees of the subfamilies Rophitinae and Nomiinae (Hymenoptera, Halictidae) of Russia and adjacent territories. KMK Scientific Press Ltd., Moscow, 383 pp. [In Russian]
- Astafurova YuV, Proshchalykin MYu (2017) Family Halictidae. In: Lelej AS, Proshchalykin MYu, Loktionov VM (Eds) Annotated catalogue of the Hymenoptera of Russia (Vol. 1). Symphyta and Apocrita: Aculeata. Proceedings of the Zoological Institute RAS, Supplement 6: 277–292. <https://doi.org/10.31610/trudyzin/2017.supl.6.5>
- Astafurova YuV, Proshchalykin MYu (2022a) Review of the *Epeolus cruciger* species group (Hymenoptera: Apidae, *Epeolus* Latreille, 1802) of Asia, with the description of two new species. *Journal of Hymenoptera Research* 92: 305–328. <https://doi.org/10.3897/jhr.92.90098>
- Astafurova YuV, Proshchalykin MYu (2022b) Review of the *Epeolus julliani* species group (Hymenoptera, Apidae, *Epeolus* Latreille, 1802), with descriptions of two new species. *Journal of Hymenoptera Research* 94: 191–213. <https://doi.org/10.3897/jhr.94.96429>
- Astafurova YuV, Proshchalykin MYu (2023a) First record of *Lasioglossum adabaschum* (Blüthgen, 1931) (Hymenoptera: Halictidae) from Europe with description of hitherto unknown male. *Far Eastern Entomologist* 479: 1–6. <https://doi.org/10.25221/fee.479.1>

- Astafurova YuV, Proshchalykin MYu (2023b) The genus *Epeolus* Latreille, 1802 (Hymenoptera: Apidae) in Central Asia. *ZooKeys* 1181: 241–263. <https://doi.org/10.3897/zookeys.1181.110416>
- Astafurova YuV, Proshchalykin MYu, Niu Z, Zhu C (2018) New records of bees of the genus *Sphecodes* Latreille (Hymenoptera, Halictidae) in the Palearctic part of China. *ZooKeys* 792: 15–44. <https://doi.org/10.3897/zookeys.792.28042>
- Astafurova YuV, Proshchalykin MYu, Sidorov DA, Osytshnjuk AZ (2021) The type specimens of bees (Hymenoptera, Apoidea) deposited in the Zoological Institute of the Russian Academy of Sciences, St. Petersburg. Contribution IV. Family Andrenidae, genus *Andrena* Fabricius, 1775, species described by F. Morawitz. *Zootaxa* 5037(1): 1–78. <https://doi.org/10.11646/zootaxa.5037.1.1>
- Astafurova YuV, Proshchalykin MYu, Sidorov DA (2022a) The type specimens of bees (Hymenoptera, Apoidea) deposited in the Zoological Institute of the Russian Academy of Sciences, St. Petersburg. Contribution V. Family Andrenidae, genus *Andrena* Fabricius, 1775, species described by E. Eversmann. *Zootaxa* 5190(3): 393–418. <https://doi.org/10.11646/zootaxa.5190.3.4>
- Astafurova YuV, Proshchalykin MYu, Sidorov DA (2022b) The bees of the genus *Andrena* Fabricius, 1775 (Hymenoptera, Andrenidae) described by Ferdinand Morawitz from the collection of Aleksey Fedtschenko. *ZooKeys* 1120: 105–176. <https://doi.org/10.3897/zookeys.1120.90206>
- Astafurova YuV, Proshchalykin MYu, Sidorov DA (2023) The type specimens of bees (Hymenoptera: Apoidea) deposited in the Zoological Institute of the Russian Academy of Sciences, St. Petersburg. Contribution VI. Family Andrenidae, genus *Andrena* Fabricius, 1775, taxa described by V. Popov. *Zootaxa* 5301(4): 401–426. <https://doi.org/10.11646/zootaxa.5301.4.1>
- Baker DB (2002) On Palearctic and Oriental species of the genera *Pseudapis* W.F. Kirby, 1900, and *Nomiapis* Cockerell, 1919 (Hymenoptera, Halictidae, Nomiinae). *Beiträge zur Entomologie* 52(1): 1–83. <https://doi.org/10.21248/contrib.entomol.52.1.1-83>
- Bischoff H (1930) Beitrag zur Kenntnis palaarktischer Arten der Gattung *Epeolus*. *Deutsche Entomologische Zeitschrift* 1930: 1–15. <https://doi.org/10.1002/mmnd.193019300102>
- Boustani M, Rasmont P, Dathe HH, Ghisbain G, Kasperek M, Michez D, Müller A, Pauly A, Risch S, Straka J, Terzo M, Van Achter X, Wood TJ, Nemer N (2021) The bees of Lebanon (Hymenoptera: Apoidea: Anthophila). *Zootaxa* 4976(1): 1–146. <https://doi.org/10.11646/zootaxa.4976.1.1>
- Brasero N, Ghisbain G, Lecocq T, Michez D, Valterová I, Biella P, Monfared A, Williams PH, Rasmont P, Martinet B (2021) Resolving the species status of overlooked West-Palearctic bumblebees. *Zoologica Scripta* 50(5): 616–632. <https://doi.org/10.1111/zsc.12486>
- Byvaltsev AM, Belova KA, Danilov YuN, Molodtsov VV, Proshchalykin MYu (2018) Megachilid bees (Hymenoptera: Megachilidae) of the forest-steppe and steppe zones of the West Siberian Plain to the eastward of Irtysh River. *Far Eastern Entomologist* 364: 10–28. <https://doi.org/10.25221/fee.364.3>
- Chenikalova EV (2005) Wild bees of the Stavropol Kray, their efficiency and reservation in agrolandscapes. *Argus, Stavropol*, 112 pp. [In Russian]
- da Rocha Filho LC, Packer L (2016) Phylogeny of the cleptoparasitic Megachilini genera *Coelioxys* and *Radoszkowskiana*, with the description of six new subgenera in *Coelioxys* (Hymenoptera: Megachilidae). *Zoological Journal of the Linnean Society* 180(2): 354–413. <https://doi.org/10.1111/zoj.12484>

- de Dalla Torre CG (1896) *Catalogus Hymenopterorum hucusque descriptorum systematicus et synonymicus*. Vol. X. Apidae (Anthophila). Engelmann, Lipsiae, viii + 643 pp.
- Dorchin A (2023) Revision of the historical type collections of long-horn bees (Hymenoptera: Apidae: Eucerini) preserved in the Muséum national d'Histoire naturelle, Paris. *Annales de la Société Entomologique de France (N.S.)* 59(2): 115–149. <https://doi.org/10.1080/00379271.2023.2192693>
- Dorchin A, Praz CJ (2018) Taxonomic revision of the Western Palaearctic bees of the subgenus *Pseudomegachile* (Hymenoptera, Apiformes, Megachilidae, Megachile). *Zootaxa* 4524(3): 251–307. <https://doi.org/10.11646/zootaxa.4524.3.1>
- Dorchin A, López-Urbe MM, Praz CJ, Griswold T, Danforth BN (2018) Phylogeny, new generic-level classification, and historical biogeography of the *Eucera* complex (Hymenoptera: Apidae). *Molecular Phylogenetics and Evolution* 119: 81–92. <https://doi.org/10.1016/j.ympev.2017.10.007>
- Ebmer AW (1988) Kritische Liste der nicht-parasitischen Halictidae Österreichs mit Berücksichtigung aller mitteleuropäischen Arten (Insecta: Hymenoptera: Apoidea: Halictidae). *Linzer Biologische Beiträge* 20(2): 527–711.
- Ebmer AW (2021) Abweichende Datierungen der von Ferdinand Morawitz beschriebenen Bienenarten (Insecta: Hymenoptera: Apoidea) durch Vorausdrucke. *Annalen des Naturhistorischen Museums in Wien, Serie B* 123: 277–294.
- Elfving R (1968) Die Bienen Finnlands. *Fauna Flora Fennica* 21: 1–69.
- Eversmann E (1852) Fauna hymenopterologica volgo-uralensis (Continuatio). *Bulletin de la Société Impériale Naturalistes de Moscou* 25(3): 3–137.
- Fateryga AV, Ivanov SP (in press) Corrections and additions to the list of the megachilid bees (Hymenoptera: Megachilidae) of the Crimean Peninsula. *Ekosistemy*. [In press]
- Fateryga AV, Proshchalykin MYu (2020) New records of megachilid bees (Hymenoptera: Megachilidae) from the North Caucasus and the south of European Russia. *Caucasian Entomological Bulletin* 16(2): 225–231. <https://doi.org/10.23885/181433262020162-225331>
- Fateryga AV, Ivanov SP, Filatov MA (2018) Megachilid-bees (Hymenoptera: Megachilidae) of the Crimean Peninsula. *Entomofauna* 39: 235–283.
- Fateryga AV, Proshchalykin MYu, Astafurova YuV, Popov IB (2019 [“2018”]) New records of megachilid bees (Hymenoptera, Megachilidae) from the North Caucasus and neighboring regions of Russia. *Entomological Review* 98(9): 1165–1174. <https://doi.org/10.1134/S0013873818090026>
- Fateryga AV, Müller A, Proshchalykin MYu (2023) Two new *Hoplitis* species of the subgenus *Hoplitis* Klug, 1807 (Hymenoptera, Megachilidae) and the nesting biology of *H. astragali* sp. nov. in Dagestan. *Journal of Hymenoptera Research* 96: 641–656. <https://doi.org/10.3897/jhr.96.109255>
- Filatov MA (2006) To the bee fauna (Hymenoptera, Apoidea) of Opuk Nature Reserve. *Trudy Gosudarstvennogo Nikitskogo botanicheskogo sada* 126: 110–117. [In Russian]
- Filatov MA, Ivanov SP, Budashkin Yul (2006) The bees (Hymenoptera, Apoidea) of the Kazantip Nature Reserve. *Trudy Gosudarstvennogo Nikitskogo botanicheskogo sada* 126: 258–262. [In Russian]
- Friese H (1914) Neue Apiden der palaearktischen Region. *Stettiner Entomologische Zeitung* 75: 218–233. <https://doi.org/10.1002/mmnd.191419140311>
- Friese H (1922) Neue Formen der Bienengattung *Andrena* (Hym.). *Konowia* 1: 209–217.
- Ghisbain G, Rosa P, Bogusch P, Flaminio S, Le Divelec R, Dorchin A, Kasperek M, Kuhlmann M, Litman J, Mignot M, Müller A, Praz C, Radchenko VG, Rasmont P, Risch S,

- Roberts SPM, Smit J, Wood TJ, Michez D, Reverté S (2023) The new annotated checklist of the wild bees of Europe (Hymenoptera: Anthophila). *Zootaxa* 5327(1): 1–147. <https://doi.org/10.11646/zootaxa.5327.1.1>
- Gibbs J, Packer L, Dumesh S, Danforth BN (2013) Revision and reclassification of *Lasioglossum* (*Evylaeus*), *L. (Hemihalictus)* and *L. (Sphecodogastra)* in eastern North America (Hymenoptera: Apoidea: Halictidae). *Zootaxa* 3672(1): 1–117. <https://doi.org/10.11646/zootaxa.3672.1.1>
- Gusenleitner F, Schwarz M (2002) Weltweite checkliste der bienengattung *Andrena* mit bemerkungen und ergänzungen zu paläarktischen arten (Hymenoptera, Apidae, Andreninae, *Andrena*). *Entomofauna* (Supplement 12): 1–1280.
- ICZN [International Commission on Zoological Nomenclature] (1999) International Code of Zoological Nomenclature. 4th edition. The International Trust for Zoological Nomenclature, London, [XXX +] 306 pp.
- Ikudome S (2022) A new species of the bee genus *Eucera* Scopoli, 1770 (Hymenoptera: Apidae) from Japan. *Esakia* 55: 64–69. <https://doi.org/10.5109/6610223>
- Ilyasov RA, Youn HG, Lee M, Kim KW, Proshchalykin MYu, Lelej AS, Takahashi J-i, Kwon HW (2019) Phylogenetic relationships of Russian Far-East *Apis cerana* with other North Asian populations. *Journal of Apicultural Science* 63(2): 289–314. <https://doi.org/10.2478/jas-2019-0024>
- Ivanov SP, Fateryga AV (2019) First record of the invasive giant resin bee *Megachile (Callomegachile) sculpturalis* Smith, 1853 (Hymenoptera: Megachilidae) in the Crimea. *Far Eastern Entomologist* 395: 7–13. <https://doi.org/10.25221/fee.395.2>
- Ivanov SP, Fateryga AV, Müller A (2023) Brood cells like conifer cones: The peculiar nesting biology of the osmiine bee *Hoplitis (Alcidamea) curvipes* (Morawitz, 1871) (Hymenoptera, Megachilidae). *Journal of Hymenoptera Research* 96: 735–750. <https://doi.org/10.3897/jhr.96.109587>
- Kasperek M (2020) Revision of the Palaearctic *Trachusa interrupta* species complex (Apoidea: Anthidiini) with description of four new species. *Zootaxa* 4728(1): 1–48. <https://doi.org/10.11646/zootaxa.4728.1.1>
- Kasperek M (2021) The bee genus *Pseudoanthidium*: revision of the subgenus *Exanthidium* with the description of a new species (Apoidea: Megachilidae). *Fragmenta Entomologica* 53(2): 333–346. <https://doi.org/10.13133/2284-4880/525>
- Kasperek M (2022) The resin and wool carder bees (Anthidiini) of Europe and Western Turkey. Identification – distribution – biology. Chimaira, Frankfurt am Main, 290 pp.
- Kasperek M, Fateryga AV (2023) DNA barcoding confirms the validity of *Anthidium melanopygum* Friese, 1917 stat. nov. (Hymenoptera: Megachilidae) as a distinct species of Western Asia. *Zootaxa* 5346(5): 567–580. <https://doi.org/10.11646/zootaxa.5346.5.4>
- Kasperek M, Wood TJ, Ferreira S, Benarfa N (2023) ["2022"] Taxonomic status of the disjunct populations of the resin bee *Anthidiellum breviusculum* (Pérez, 1890) s. l. in the Mediterranean (Apoidea: Anthidiini). *Journal of Natural History* 56(45–48): 2047–2063. <https://doi.org/10.1080/00222933.2022.2152749>
- Kerzhner IM (1984) Dates of publication of "Trudy Russkogo Entomologicheskogo Obshchestva" and "Horae Societatis Entomologicae Rossicae", 1861–1932. *Entomologicheskoe Obozrenie* 63(4): 849–857. [In Russian]
- Kuhlmann M, Proshchalykin MYu (2011) Bees of the genus *Colletes* Latreille 1802 of the Asian part of Russia with a key to species (Hymenoptera, Apoidea: Colletidae). *Zootaxa* 3068: 1–48. <https://doi.org/10.11646/zootaxa.3068.1.1>

- Lanner J, Dubos N, Geslin B, Leroy B, Hernández-Castellano C, Bila Dubaić J, Bortolotti L, Diaz Calafat J, Četković A, Flaminio S, Le Féon V, Margalef-Marrase J, Orr M, Pachinger B, Ruzzier E, Smagghe G, Tuerlings T, Vereecken N, Meimberg H (2022) On the road: Anthropogenic factors drive the invasion risk of a wild solitary bee species. *The Science of the Total Environment* 827: 154246. <https://doi.org/10.1016/j.scitotenv.2022.154246>
- Levchenko TV (2019) Bees of the tribe Eucerini (Hymenoptera: Apidae) with three submarginal cells in the fauna of Russia. In: Proshchalykin MYu (Ed.) IV Euroasian Symposium on Hymenoptera (Vladivostok, 9–15 September 2019): Abstracts. FSC Biodiversity FEB RAS, Vladivostok, 19–20.
- Levchenko TV, Byvaltsev AM, Proshchalykin MYu (2017) Family Apidae. In: Lelej AS, Proshchalykin MYu, Loktionov VM (Eds) Annotated catalogue of the Hymenoptera of Russia (Vol. 1). Symphyta and Apocrita: Aculeata. Proceedings of the Zoological Institute RAS, Supplement 6: 309–332. <https://doi.org/10.31610/trudyzin/2017.supl.6.5>
- Litman JR, Fateryga AV, Griswold TL, Aubert M, Proshchalykin MYu, Le Divelec R, Burrows S, Praz CJ (2021) Paraphyly and low levels of genetic divergence in morphologically distinct taxa: Revision of the *Pseudoanthidium scapulare* (Latreille, 1809) complex of carder bees (Apoidea, Megachilidae, Anthidiini). *Zoological Journal of the Linnean Society* 195(4): 1287–1337. <https://doi.org/10.1093/zoolinnean/zlab062>
- Lykov VA (2008) The bees (Hymenoptera, Apoidea) of the insular Kungur forest-steppe. *Bulletin of the Perm University. Series. Biology (Basel)* 9: 32–36. [In Russian]
- Maghni N, Louadi K, Ortiz-Sánchez FJ, Rasmont P (2017) Les Anthophores de la région des Aurès (nord-est de l'Algérie) (Hymenoptera: Apidae: Anthophorini). *Annales de la Société Entomologique de France (N.S.)* 53(1): 55–73. <https://doi.org/10.1080/00379271.2017.1305916>
- Maharramov MM, Fateryga AV, Proshchalykin MYu (2021) Megachilid bees (Hymenoptera: Megachilidae) of the Nakhchivan Autonomous Republic of Azerbaijan: tribes Lithurgini, Dioxyini, and Megachilini. *Far Eastern Entomologist* 428: 12–24. <https://doi.org/10.25221/fee.428.3>
- Maharramov MM, Fateryga AV, Proshchalykin MYu (2023) New records of megachilid bees (Hymenoptera: Megachilidae) from the Nakhchivan Autonomous Republic of Azerbaijan. *Far Eastern Entomologist* 472: 18–24. <https://doi.org/10.25221/fee.472.2>
- Mavromoustakis GA (1948) New and little-known bees of the subfamily Anthidiinae (Apoidea). – Part III. *Annals & Magazine of Natural History* 1(3): 171–177. <https://doi.org/10.1080/00222934808653899>
- Michener CD (2007) *The bees of the world*. 2nd edition. Johns Hopkins University Press, Baltimore, [xvi + [i] +] 953 pp., 20 pls.]
- Michez D, Patiny S (2005) World revision of the oil-collecting bee genus *Macropis* Panzer 1809 (Hymenoptera, Apoidea, Melittidae) with a description of a new species from Laos. *Annales de la Société Entomologique de France (N.S.)* 41(1): 15–28. <https://doi.org/10.1080/00379271.2005.10697439>
- Morawitz F (1873 [“1874”]) *Die Bienen Daghestans*. *Horae Societatis Entomologicae Rossicae* 10(2–4): 129–189.
- Morawitz F (1875) A travel to Turkestan by the member-founder of the society A.P. Fedtschenko accomplished from the Imperial Society of Naturalists, Anthropologists, and Ethnographers on a Commission from the General-Governor of Turkestan K.P. von Kaufmann. Issue 9. Vol. 2. Zoogeographical investigations. Part 5. Division 7. Bees (Mellifera). In: Proceedings of the Imperial Society of Devotees of Natural His-

- tory, Anthropology and Ethnography (Vol. 19, issue 2). Typography of M. Stasyulevich, St Petersburg & Moscow, [i–ii +] 1–160. [In Russian]
- Morawitz F (1877) Nachtrag zur Bienenfauna Caucasiens. *Horae Societatis Entomologicae Rossicae* 14(1): 3–112.
- Morawitz F (1894 [“1895”]) Beitrag zur Bienenfauna Turkmeniens. *Horae Societatis Entomologicae Rossicae* 29(1–2): 1–76.
- Möschler A (1938) Ein Beitrag zur Bienenfauna in Östpreußen, insbesondere der Kurischen Nehrung. *Schriften der Physikalisch-Ökonomischen Gesellschaft zu Königsberg* 70(2): 243–288.
- Mulenko M, Gorenkov D, Burkovsky O, Pylypiuk K, Honchar H (2022) New records of the invasive species *Megachile sculpturalis* Smith, 1853 in Ukraine. *Studia Biologica* 16(3): 61–70. <https://doi.org/10.30970/sbi.1603.690>
- Müller A (2020) Palaearctic *Osmia* bees of the subgenera *Hemiosmia*, *Tergosmia* and *Erythrosmia* (Megachilidae, Osmiini): Biology, taxonomy and key to species. *Zootaxa* 4778(2): 201–236. <https://doi.org/10.11646/zootaxa.4778.2.1>
- Müller A (2023) Palaearctic Osmiine Bees. ETH Zürich. <http://blogs.ethz.ch/osmiini> [Accessed 09.09.2023]
- Nieto A, Roberts SPM, Kemp J, Rasmont P, Kuhlmann M, García Criado M, Biesmeijer JC, Bogusch P, Dathe HH, De la Rúa P, De Meulemeester T, Dehon M, Dewulf A, Ortiz-Sánchez FJ, Lhomme P, Pauly A, Potts SG, Praz C, Quaranta M, Radchenko VG, Scheuchl E, Smit J, Straka J, Terzo M, Tomozii B, Window J, Michez D (2014) European Red List of Bees. Publication Office of the European Union, Luxembourg, 84 pp. <https://doi.org/10.2779/77003>
- Osytsnjuk AZ, Panfilov DV, Ponomareva AA (1978) Superfamily Apoidea – Bees. In: Medvedev GS (Ed.) A Key to insects of the European part of the USSR. Vol. 3. Hymenoptera. Pt 1. Nauka, Leningrad, 279–519. [In Russian]
- Pauly A, Belval S (2017) Atlas des Halictidae de France (Hymenoptera: Apoidea). *Belgian Journal of Entomology* 53: 1–34.
- Pauly A, Noel G, Sonet G, Notton D, Boevé J (2019) Integrative taxonomy resuscitates two species in the *Lasioglossum villosulum* complex (Kirby, 1802) (Hymenoptera: Apoidea: Halictidae). *European Journal of Taxonomy* 541(541): 1–43. <https://doi.org/10.5852/ejt.2019.541>
- Pesenko YuA (1986) An annotated key to the Palaearctic species of bees of the genus *Lasioglossum* sensu stricto (Hymenoptera, Halictidae) for females, with descriptions of new subgenera and species. *Proceedings of the Zoological Institute of the Academy of Sciences of the USSR* 159: 113–151. [In Russian]
- Pesenko YuA, Banaszak J, Radchenko VG, Cierznik T (2000) Bees of the family Halictidae (excluding *Sphcodes*) of Poland: taxonomy, ecology, bionomics. Pedagogical University, Bydgoszcz, 348 pp.
- Popov VB (1949) The subgenus *Plastandrena* Hedicke and its new forms (Hymenoptera, Apoidea). *Entomologicheskoe Obozrenie* 30(3/4): 389–404. [In Russian]
- Popov VB (1950) Hymenoptera. In: Pavlovsky EN, Vinogradov BS (Eds) *Animal World of the USSR*. Vol. 3. The Steppe Zone. Zoological Institute of the Academy of Sciences of the USSR, Moscow, Leningrad, 214–268. [In Russian]
- Popov VB (1958) On the co-evolution of *Macropis*, *Epeoloides* (Hymenoptera, Apoidea) and *Lysimachia* (Primulaceae). *Entomologicheskoe Obozrenie* 37(3): 499–519. [In Russian]
- Popov VB (1967) The bees (Hymenoptera, Apoidea) of Iran. *Proceedings of the Zoological Institute of the Academy of Sciences of the USSR* 43: 184–216. [In Russian]

- Praz CJ, Bénon D (2023) Revision of the *leachella* group of *Megachile* subgenus *Eutricharaea* in the Western Palaearctic (Hymenoptera, Apoidea, Megachilidae): A renewed plea for DNA barcoding type material. *Journal of Hymenoptera Research* 95: 143–198. <https://doi.org/10.3897/jhr.95.96796>
- Praz C, Genoud D, Vaucher K, Bénon D, Monks J, Wood TJ (2022) Unexpected levels of cryptic diversity in European bees of the genus *Andrena* subgenus *Taeniandrena* (Hymenoptera: Andrenidae): implications for conservation. *Journal of Hymenoptera Research* 91: 375–428. <https://doi.org/10.3897/jhr.91.82761>
- Proshchalykin MYu (2017a) Family Colletidae. In: Lelej AS, Proshchalykin MYu, Loktionov VM (Eds) Annotated catalogue of the Hymenoptera of Russia (Vol. 1). Symphyta and Apocrita: Aculeata. Proceedings of the Zoological Institute RAS, Supplement 6: 257–262. <https://doi.org/10.31610/trudyzin/2017.supl.6.5>
- Proshchalykin MYu (2017b) The bees of the genus *Colletes* Latreille (Hymenoptera, Colletidae) of the Palaearctic Region: Taxonomic diversity and distribution patterns. Meetings in memory of N.A. Cholodkovsky 68(2): 1–81. [In Russian]
- Proshchalykin MYu, Astafurova YuV (2017) Family Melittidae. In: Lelej AS, Proshchalykin MYu, Loktionov VM (Eds) Annotated catalogue of the Hymenoptera of Russia (Vol. 1). Symphyta and Apocrita: Aculeata. Proceedings of the Zoological Institute RAS, Supplement 6: 293–294. <https://doi.org/10.31610/trudyzin/2017.supl.6.5>
- Proshchalykin MYu, Dathe HH (2018) In the footsteps of history: the bees of the genus *Hylaeus* Fabricius (Hymenoptera, Apoidea: Colletidae) collected by V.I. Roborovsky and P.K. Kozlov in Northwest China (1895–1926). *Zootaxa* 4434(3): 573–588. <https://doi.org/10.11646/zootaxa.4434.3.11>
- Proshchalykin MYu, Dathe HH (2021) New and little-known bees of the genus *Hylaeus* Fabricius, 1793 (Hymenoptera: Colletidae) from the Caucasus region. *Journal of Hymenoptera Research* 84: 169–185. <https://doi.org/10.3897/jhr.84.68250>
- Proshchalykin MYu, Fateryga AV (2017) Family Megachilidae. In: Lelej AS, Proshchalykin MYu, Loktionov VM (Eds) Annotated catalogue of the Hymenoptera of Russia (Vol. 1). Symphyta and Apocrita: Aculeata. Proceedings of the Zoological Institute RAS, Supplement 6: 295–308. <https://doi.org/10.31610/trudyzin/2017.supl.6.5>
- Proshchalykin MYu, Kuhlmann M (2012) The bees of the genus *Colletes* Latreille 1802 of the Ukraine, with a key to species (Hymenoptera: Apoidea: Colletidae). *Zootaxa* 3488(1): 1–40. <https://doi.org/10.11646/zootaxa.3488.1.1>
- Proshchalykin MYu, Kuhlmann M (2015) Additional records of the genus *Colletes* (Hymenoptera: Apoidea: Colletidae) from Siberia, with a checklist of Russian species. *Zootaxa* 3949(3): 323–344. <https://doi.org/10.11646/zootaxa.3949.3.2>
- Proshchalykin MYu, Kuhlmann M (2018) New records of rarely collected bees of the genus *Colletes* Latreille (Hymenoptera, Colletidae) from Asia and the Caucasus. *Far Eastern Entomologist* 355: 1–12. <https://doi.org/10.25221/fee.355.1>
- Proshchalykin MYu, Kuhlmann M (2019) To the knowledge of the bee genus *Colletes* Latreille, 1802 (Hymenoptera: Apoidea: Colletidae) of Dagestan, Russia. *Caucasian Entomological Bulletin* 15(1): 159–163. <https://doi.org/10.23885/181433262019151-159163>
- Proshchalykin MYu, Kuhlmann M (2020) New data on bees of the genus *Colletes* Latreille (Hymenoptera: Colletidae) from Russia. *Far Eastern Entomologist* 406: 21–26. <https://doi.org/10.25221/fee.406.3>
- Proshchalykin MYu, Kuhlmann M (2023) New and little-known bees of the genus *Colletes* Latreille, 1802 (Hymenoptera, Colletidae) from Siberia. *Journal of Hymenoptera Research* 96: 33–43. <https://doi.org/10.3897/jhr.96.101740>

- Proshchalykin MYu, Müller A (2019) Additional records of osmiine bees (Hymenoptera: Megachilidae: Osmiini) from Siberia. *Zootaxa* 4563(1): 163–174. <https://doi.org/10.11646/zootaxa.4563.1.9>
- Proshchalykin MYu, Sergeev ME (2020) New distribution data of *Apis cerana ussuriensis* (Hymenoptera, Apidae) from Primorsky krai, Russia. *Nature Conservation Research* 5(4): 111–112. [In Russian] <https://doi.org/10.24189/ncr.2020.049>
- Proshchalykin MYu, Astafurova YuV, Sidorov DA (2017) Family Andrenidae. In: Lelej AS, Proshchalykin MYu, Loktionov VM (Eds) Annotated catalogue of the Hymenoptera of Russia (Vol. 1). Symphyta and Apocrita: Aculeata. Proceedings of the Zoological Institute RAS, Supplement 6: 263–276. <https://doi.org/10.31610/trudyzin/2017.supl.6.5>
- Proshchalykin MYu, Astafurova YuV, Levchenko TV, Shlyakhtenok AS, Schwarz M (2019) The species-group names of bees (Hymenoptera: Apoidea, Apiformes) described from Crimea, North Caucasus, European part of Russia and Ural. Part III. Families Melittidae and Apidae (except *Bombus* Latreille and *Apis* Linnaeus). *Far Eastern Entomologist* 396: 17–44. <https://doi.org/10.25221/fee.396.3>
- Rasmont P, Devalez J, Pauly A, Michez D, Radchenko VG (2017) Addition to the checklist of IUCN European wild bees (Hymenoptera: Apoidea). *Annales de la Société Entomologique de France* (N. S.) 53(1): 17–32. <https://doi.org/10.1080/00379271.2017.1307696>
- Sardar S, Rameshkumar A, Kazmi SI (2021) First report of *Megachile* (*Callomegachile*) *sculpturalis* Smith, 1853 (Apoidea: Megachilidae) from India. *Journal of Insect Biodiversity* 23(2): 43–49. <https://doi.org/10.12976/jib/2021.23.2.2>
- Schwarz M, Gusenleitner F (2003) Ergebnisse der Untersuchung von F. Morawitz beschriebenen *Coelioxys*-Arten, so wie weiterer von Eversmann, Friese und Radoszkowski beschriebenen Arten, nebst einigen Bemerkungen (Hymenoptera: Apidae: Megachilidae). *Linzer Biologische Beiträge* 35(2): 1221–1239.
- Smit J (2018) Identification key to the European species of the bee genus *Nomada* Scopoli, 1770 (Hymenoptera: Apidae), including 23 new species. *Entomofauna. Monographie* 3: 1–253.
- Ungricht S, Müller A, Dorn S (2008) A taxonomic catalogue of the Palaearctic bees of the tribe Osmiini (Hymenoptera: Apoidea: Megachilidae). *Zootaxa* 1865(1): 1–253. <https://doi.org/10.11646/zootaxa.1865.1.1>
- Warncke K (1967) Beitrag zur Klärung paläarktischer *Andrena*-Arten. *Eos* (Revista Española de Entomología) 43(1/2): 171–318.
- Warncke K (1980) Die Bienengattung *Anthidium* Fabricius, 1804 in der Westpaläarktis und im turkestanischen Becken. *Entomofauna* 1: 119–210.
- Williams PH (2021) Not just cryptic, but a barcode bush: PTP re-analysis of global data for the bumblebee subgenus *Bombus* s. str. supports additional species (Apidae, genus *Bombus*). *Journal of Natural History* 55(5–6): 271–282. <https://doi.org/10.1080/00222933.2021.1900444>
- Williams PH, Altanchimeg D, Byvaltsev A, De Jonghe R, Jaffar S, Japoshvili G, Kahono S, Liang H, Mei M, Monfared A, Nidup T, Raina R, Ren Z, Thanosing C, Zhao Y, Orr MC (2020) Widespread polytypic species or complexes of local species? Revising bumblebees of the subgenus *Melanobombus* world-wide (Hymenoptera, Apidae, *Bombus*). *European Journal of Taxonomy* 719(1): 1–120. <https://doi.org/10.5852/ejt.2020.719.1107>
- Williams PH, Dorji P, Ren Z, Xie Z, Orr M (2022) Bumblebees of the *hypnorum*-complex world-wide including two new near-cryptic species (Hymenoptera: Apidae). *European Journal of Taxonomy* 847: 46–72. <https://doi.org/10.5852/ejt.2022.847.1981>

- Wood TJ (2023) New Old World *Andrena* species, with a focus on Turkey (Hymenoptera: Andrenidae). *Zootaxa* 5266(1): 1–72. <https://doi.org/10.11646/zootaxa.5266.1.1>
- Wood TJ, Monfared A (2022) A revision of the *Andrena* (Hymenoptera: Andrenidae) fauna of Iran, with the description of 16 new species. *European Journal of Taxonomy* 843(1): 1–136. <https://doi.org/10.5852/ejt.2022.843.1947>
- Wood TJ, Boustani M, Rasmont P (2020) A revision of the *Andrena* (Hymenoptera: Andrenidae) of Lebanon with the description of six new species. *Annales de la Société Entomologique de France (N.S.)* 56(4): 279–312. <https://doi.org/10.1080/00379271.2020.1794960>
- Wood TJ, Hogan J, Edwards M, Paxton RJ, Praz C, Seidel M, Schmid-Egger C (2022) *Andrena scotica* Perkins is the valid name for the widespread European taxon previously referred to as *Andrena carantonica* Pérez (Hymenoptera: Andrenidae). *British Journal of Entomology and Natural History* 35(4): 393–408.

Supplementary material 1

Updated checklist of the wild bee fauna of Russia

Authors: Maxim Yu. Proshchalykin, Alexander V. Fateryga, Yulia V. Astafurova

Data type: doc

Explanation note: Checklist of six families, 14 subfamilies, 27 tribes, 64 genera and 1,268 species of bees from Russia.

Copyright notice: This dataset is made available under the Open Database License (<http://opendatacommons.org/licenses/odbl/1.0/>). The Open Database License (ODbL) is a license agreement intended to allow users to freely share, modify, and use this Dataset while maintaining this same freedom for others, provided that the original source and author(s) are credited.

Link: <https://doi.org/10.3897/zookeys.1187.113240.suppl1>

A revision of the millipede family Paracortinidae (Diplopoda, Callipodida)

Nesrine Akkari¹, Oliver Macek¹, Pavel Stoev^{2,3}

¹ Naturhistorisches Museum Wien, Burgring 7, 1010 Wien, Austria

² National Museum of Natural History at the Bulgarian Academy of Sciences, Tsar Osvoboditel Blvd. 1, 1000 Sofia, Bulgaria

³ Pensoft Publishers, Prof. G. Zlatarski Str. 12, Sofia, Bulgaria

Corresponding author: Nesrine Akkari (nesrine.akkari@nhm-wien.ac.at)

Abstract

The taxonomy of the family Paracortinidae Wang & Zhang, 1993 is revised based on literature, old and recently collected material. A new genus *Crassipetalum* Akkari & Stoev, **gen. nov.** is described, to accommodate a new species *Crassipetalum magnum* Akkari & Stoev, **gen. nov. et sp. nov.** and a recently described species *Crassipetalum inflatum* (Chen, Zheng & Jian, 2023), **comb. nov.** The genus *Scotopetalum* Shear, 2000 hitherto described for the Vietnamese species *S. warreni* Shear, 2000 and subsequently synonymised with the genus *Paracortina* Wang & Zhang, 1993 is here resurrected and supplemented with another species, *S. chinensis* (Stoev & Geoffroy, 2004), **comb. nov.**, ex *Paracortina chinensis* Stoev & Geoffroy, 2004. The status of the fourth genus in the family, *Angulifemur* Zhang, 1997, is reconfirmed. Based on recently collected specimens from China, two new species of the genus *Paracortina* are described: *P. asciformis* Akkari & Stoev, **sp. nov.** (Sichuan Prov., Lixian County) and *P. kabaki* Akkari & Stoev, **sp. nov.** (Yunnan, Shangrila County). The Vietnamese species *Paracortina multisegmentata* Stoev & Geoffroy, 2004 and *Paracortina kyrang* Nguyen, Stoev, Nguyen & Vu, 2023 are considered of uncertain taxonomic position within Paracortinidae. Differential diagnoses for the proposed genera as well as for all the species are presented, and descriptions or descriptive notes for all the species are provided, using a standardised terminology, and when possible, accompanied by micrographs of the habitus and gonopod structures. An identification key based on gonopod structures is proposed for all the members of the family. A discussion on species affinities, secondary sexual characters, troglomorphic characters, geographical distribution, and habitat preferences are also provided together with a distribution map for all members of the family.

Key words: China, descriptions, gonopods, identification key, new genus, new species, taxonomy, Vietnam

Introduction

The South-East Asian family Paracortinidae Wang & Zhang, 1993 is known to comprise two genera, viz., *Paracortina* Wang & Zhang, 1993 (13 species) and *Angulifemur* Zhang, 1997 (two species). All species occur in China, except *Paracortina warreni* (Shear, 2000), *P. multisegmentata* Stoev & Geoffroy, 2004, and *P. kyrang* Nguyen, Stoev, Nguyen & Vu, 2023, which are known from north



This article is part of:

Global Taxon Reviews

Edited by M. Engel, F. Konstantinov

Academic editor: Dragan Antić

Received: 29 September 2023

Accepted: 14 November 2023

Published: 28 December 2023

ZooBank: <https://zoobank.org/2F796283-3187-447E-88C6-4B61C50B640C>

Citation: Akkari N, Macek O, Stoev P (2023) A revision of the millipede family Paracortinidae (Diplopoda, Callipodida). ZooKeys 1187: 341–399. <https://doi.org/10.3897/zookeys.1187.113473>

Copyright: © Nesrine Akkari et al.

This is an open access article distributed under terms of the Creative Commons Attribution License ([Attribution 4.0 International – CC BY 4.0](https://creativecommons.org/licenses/by/4.0/)).

Vietnam (Shear 2000; Stoev and Geoffroy 2004; Enghoff et al. 2015; Nguyen et al. 2023). Despite being the subject of a number of studies (Wang and Zhang 1993; Shear 2000; Stoev 2004; Stoev and Geoffroy 2004; Stoev et al. 2008; Enghoff et al. 2015; Liu and Tian 2015; Chen et al. 2023; Nguyen et al. 2023), the taxonomy of this family and its genera is still far from being settled. The original diagnosis of the family was based on a combination of a few habitual and gonopod characters, namely “the presence of 2–5 setae on pleurotergites 1–4, 6–7 setae on pleurotergite 5, all in the back of segments 6 to penultimate, females with reduced leg-pair 2 and divided cyphopods, males with gonopods presenting a large cone-shaped sternal process, and two large prefemoral processes” (Wang and Zhang 1993: 386). The family was originally described to enclose three genera, *Paracortina* Wang & Zhang, 1993, *Altum* Wang & Zhang, 1993, and *Relictus* Wang & Zhang, 1993, of which, latter two were later downgraded to a subgeneric rank by Wang (1996) (see also Wang and Mauriès 1996).

The preliminary “phylogenetic analysis” of the family (Wang 1996) is quite controversial and not in accordance with the taxonomy of the family. Shear (2000) questioned the validity of the family and described a new monospecific genus from Vietnam, namely *Scotopetalum* Shear, 2000, which is morphologically similar to the other paracortinids but that he assigned to the European-Asia Minor family Schizopetalidae. Shear (2000) commented on the variability of the setal distribution in Callipodida and discussed the origin of the processes as interpreted by Wang and Zhang (1993). The same author attempted to homologise the gonopodal structures, pointing to the similarities between the Schizopetalidae and Paracortinidae and criticising the use of setal pattern as a character to separate the different genera.

Stoev (2004), Stoev and Geoffroy (2004), and later Enghoff et al. (2015) presented a list of external characters that in their opinion could justify the validity of the family Paracortinidae. These are pleurotergal crests well developed, poriferous ones prominent; head in males convex; coxal pores on leg-pairs 3–23; gonosternum reduced or fused with coxae; gonocoxae freely connected through a medial membranous lamina; telopodite with one or two prefemoroidal processes, their apical parts usually covered with macrosetae; basal and proximal parts of femoroidal stem simple, unbranched; distal part usually broadened, with several processes; a parasolenomere always present; leg 2 in females reduced to two simple sclerites. Stoev (2004) described *Paracortina wangi* Stoev, 2004, which he later synonymised with *Angulifemur unidigitis* Zhang, 1997 (Stoev et al. 2008), considering a potential synonymy of *Angulifemur* with *Paracortina* (see also Liu and Tian 2015). However, in the latest taxonomic treatment of the family (Enghoff et al. 2015) *Angulifemur* and *Paracortina* are kept as separate genera. Stoev and Geoffroy (2004) synonymised the (sub)genera *Altum*, *Relictus*, and *Scotopetalum* with *Paracortina*, and refined the diagnosis of the family, presenting an identification key to all paracortinid species, based on external morphology and gonopod structures.

Recently, Liu and Tian (2015) described two morphologically similar species of genus *Paracortina* from caves in Guizhou and Guangxi provinces of China, viz., *P. zhangji* Liu & Tian, 2015 and *P. yinae* Liu & Tian, 2015. Nguyen et al. (2023) described *Paracortina kyrang* Nguyen, Stoev, Nguyen & Vu, 2023 from a cave in northern Vietnam, and Chen et al. (2023) described *Paracortina inflata* Chen, Zheng & Jiang, 2023 from Yintiaoling in China.

In addition to Paracortinidae, two other extant callipodidan families occur in Southeast Asia, namely the Caspiopetalidae Lohmander, 1931, which is mostly distributed in Central Asia (one genus, eight species), with a single outlying species *Bollmania beroni* Stoev & Enghoff, 2005 from a cave in Yunnan, China (Stoev and Enghoff 2005) and Sinocallipodidae Zhang, 1993 (one genus, six species), the latter being the only family of Callipodida restricted to the tropics (Stoev and Enghoff 2011).

In this work, we redefine and revise the taxonomy of the family Paracortinidae, describing one new species of a new genus *Crassipetalum* gen. nov., and two new species of the genus *Paracortina*. Moreover, we resurrect the genus *Scotopetalum* to accommodate *Scotopetalum warreni* and *S. chinensis* (Stoev & Geoffroy 2004), comb. nov. Due to their highly derived gonopod morphology, we question the exact position of the species *P. multisegmentata* and *P. kyrang* in the genus *Paracortina*.

Descriptive notes using a standard terminology for the gonopod structures and micrographs are provided for representatives of all genera and most species to help understanding the complex gonopod configuration. The family does in our understanding include 19 species in four genera that we delimit based on a number of apomorphies in the gonopod structures. We provide the most relevant citations for the species as an exhaustive list. The repositories of the respective types were provided in earlier publications (Stoev et al. 2008; Enghoff et al. 2015; Liu and Tian 2015; Chen et al. 2023; Nguyen et al. 2023).

A discussion addressing the taxonomic affinities of the different species is presented along with a review of the different secondary sexual characters and their potential importance in delimiting taxa. Additional notes on the troglomorphic features and the geographic distribution of the species are provided together with a distribution map for all members of the family.

Materials and methods

The material was obtained from different museums (see list of repositories), studied and photographed using a Nikon DS-Ri2 camera mounted on a Nikon SMZ25 stereomicroscope, using NIS-Elements Microscope Imaging Software with an Extended Depth of Focus (EDF). Obtained images were edited in Adobe Photoshop CS6 and assembled in Adobe InDesign CS6. The map is performed using QGIS 3.28.9 (Firenze) with Open Topography-DEM-Downloader 2.0 plugin and WGS 84.

Acronyms of the repositories:

- IZCAS** National Zoological Museum of China, Institute of Zoology, Chinese Academy of Sciences, Beijing, China.
NMNHS National Museum of Natural History, Bulgarian Academy of Sciences, Sofia, Bulgaria.
ZMUM Zoological Museum of Moscow University, Moscow, Russia.

List of abbreviations:

- a** lobe-like mesal process of coxa **b** (sub-)falcate mesal process of coxa

c	coxa	p	lateral process of the proximal part of telopodite
Ca	Coxal anterior lobe	pf1	prefemoroidal process 1
Cl	Coxal lateral lobe	pf2	prefemoroidal process 2
dl	distal lamella of telopodite	pr	prefemur
dp	distal process of telopodite	ps	parasolenomere
k	lateral process of the distal part of telopodite	PT	pleurotergites
M	mesal process of the distal part of telopodite	s	solenomere
n	notch on the distal part of the telopodite	T	telopodite
		tb	blunt tooth of telopodite
		Tp	telopodital projection
		tr	trochanter

Taxonomic account

Order Callipodida Pocock, 1894

Family Paracortinidae Wang & Zhang, 1993

Emended diagnosis. Middle-sized callipodidans with well-developed pleurotergal crests, poriferous ones prominent; male head either unmodified or with a prominent bulge. Pleurotergal setae apically pointed, usually in anterior position until PT4, on PT 5 some setae migrate posteriorly, and from PT6 all are in posterior position. Gonopods: parallel, diverging or converging. Sternum reduced or fused with coxae; coxae freely connected through a medial membranous lamina. Each gonopod with one or two prefemoroidal processes clavate and setose (**pf1**, **pf2**); one or two coxal lobes and a mesal coxal process varying in size; telopodite (**T**) long, unbranched in proximal parts, sometimes curved, twisted or forming a sharp angle at mid-length, distally complex with apical folds and lamellae and smaller projections, ending with solenomere (**s**) and parasolenomere (**ps**). Leg 2 in adult females reduced to two simple sclerites.

In most representatives of the family we examined, the chaetotaxy in the anterior pleurotergites is the same and follows this distribution (Table 1), except in the Vietnamese species *Paracortina multisegmentata* and *P. kyrang*. As already established by Wang and Zhang (1993), some paracortinids have a greater number of setae on each hemipleurite (6 or 7) from PT 6 onwards. However, the majority of the species show a 5+5 pattern.

Table 1. Chaetotaxy of anterior pleurotergites in species of the family Paracortinidae, except in the Vietnamese species *P. multisegmentata* Stoev & Geoffroy, 2004 and *P. kyrang* Nguyen, Stoev, Nguyen & Vu, 2023.

	Anterior setae	Posterior setae
Collum	a, b, c, d, e	–
PT 2	a, b, c, d, e	–
PT 3	a, b, c, d, e	–
PT 4	a, b, c, d, e	–
PT 5	a, d	b, c, e
PT 6	–	a, b, c, d, e

Included genera.

Angulifemur Zhang 1997 – two species.

Crassipetalum Akkari & Stoev, gen. nov. – two species.

Paracortina Wang & Zhang, 1993 – 13 species.

Scotopetalum Shear 2000, stat. rev. – two species.

Genus *Angulifemur* Zhang, 1997

Type species. *Angulifemur tridigitis* Zhang, 1997.

Included species. *Angulifemur tridigitis* Zhang, 1997; *Angulifemur unidigitis* Zhang, 1997.

Diagnosis. Head with no projection on vertex, leg-pair 7 with a long subfalcate mesal process and a broader triangular one on coxa. Gonopods diverging from the base. Each gonopod with two short, clavate, uniformly setose prefemoro-idal processes (**pf1** and **pf2**); reduced coxal processes: (**a**) an anterior lobe-like projection and (**b**) a generally reduced thin, hyaline subfalcate or cone-shaped process not reaching telopodite's mid-length. Telopodite (**T**) with a stout stem forming an angular projection at ~ 1/3 to mid-length, distal part twisting and sharply narrowing, tapering towards its apex. Telopodite distally twisted, with one (*A. unidigitis*) or more (*A. tridigitis*) spine-like or tooth-like processes. Differs from *Paracortina* and *Scotopetalum* by the diverging stems of telopodite and from the genus *Crassipetalum* gen. nov. by the much smaller prefemoro-idal process/es and a subfalcate coxal process (**b**) never surpassing the telopodite.

***Angulifemur tridigitis* Zhang, 1997**

Fig. 28

Angulifemur tridigitis Zhang, 1997: 2, figs 1–11.

Diagnosis. It can easily be distinguished from *A. unidigitis* by having larger fal-cate coxal process (**b**) nearly reaching mid-length of the telopodite, much less sinuous distal part of telopodite (**T**) and more angular projection (**Tp**). Distal part of the telopodite differing in the presence of two downturned spine-like processes (vs one in *A. unidigitis*).

Comments. Known only from the original description (Zhang 1997).

Distribution. Known only from Yang-fen and Niupeng-yanzi caves in Mengzi County, Yunnan, China (Fig. 28)

***Angulifemur unidigitis* Zhang, 1997**

Figs 1, 2, 26A, B, 28

Angulifemur unidigitis Zhang, 1997: 2, figs 12–15.

Paracortina wangi Stoev, 2004: 2, figs 1–11; Stoev et al. 2008: 17 (synonymisation).

Material examined. 1 female, CHINA, Yunnan, Menzi County, Wulichong Sinkhole Cave (No 3), 04.01.1989, P. Beron leg. (BG-NMNHS-INV-000000006259 NMNHS),

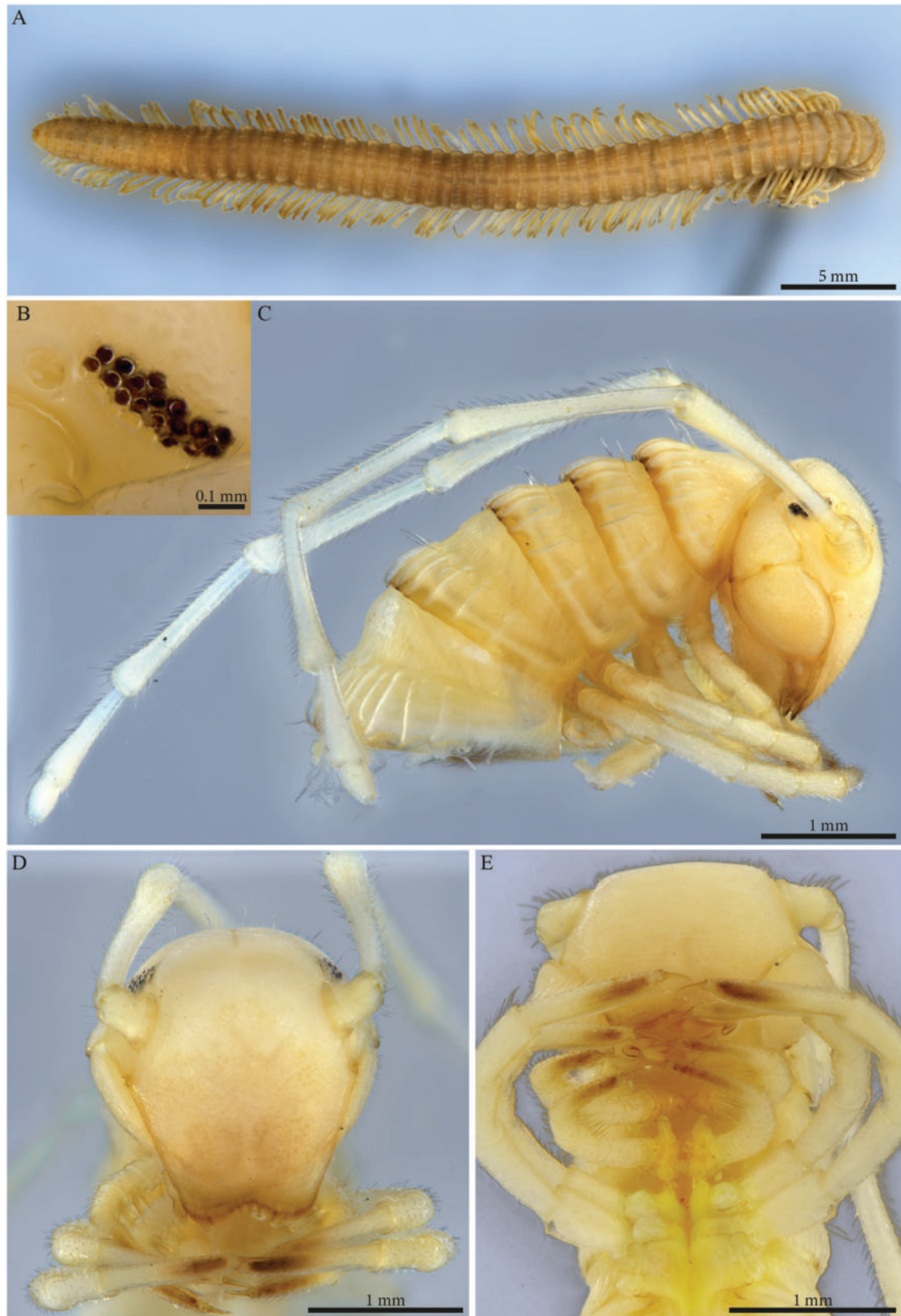


Figure 1. *Angulifemur unidigitis* Zhang, 1997, male (BG-NMNHS-INV-000000006260 NMNHS) **A** middle and posterior part of body, dorsal view **B** head: organ of Tömösváry and ommatidia **C–E** head and anterior pleurotergites **C** lateral view **D** frontal view **E** ventral view.

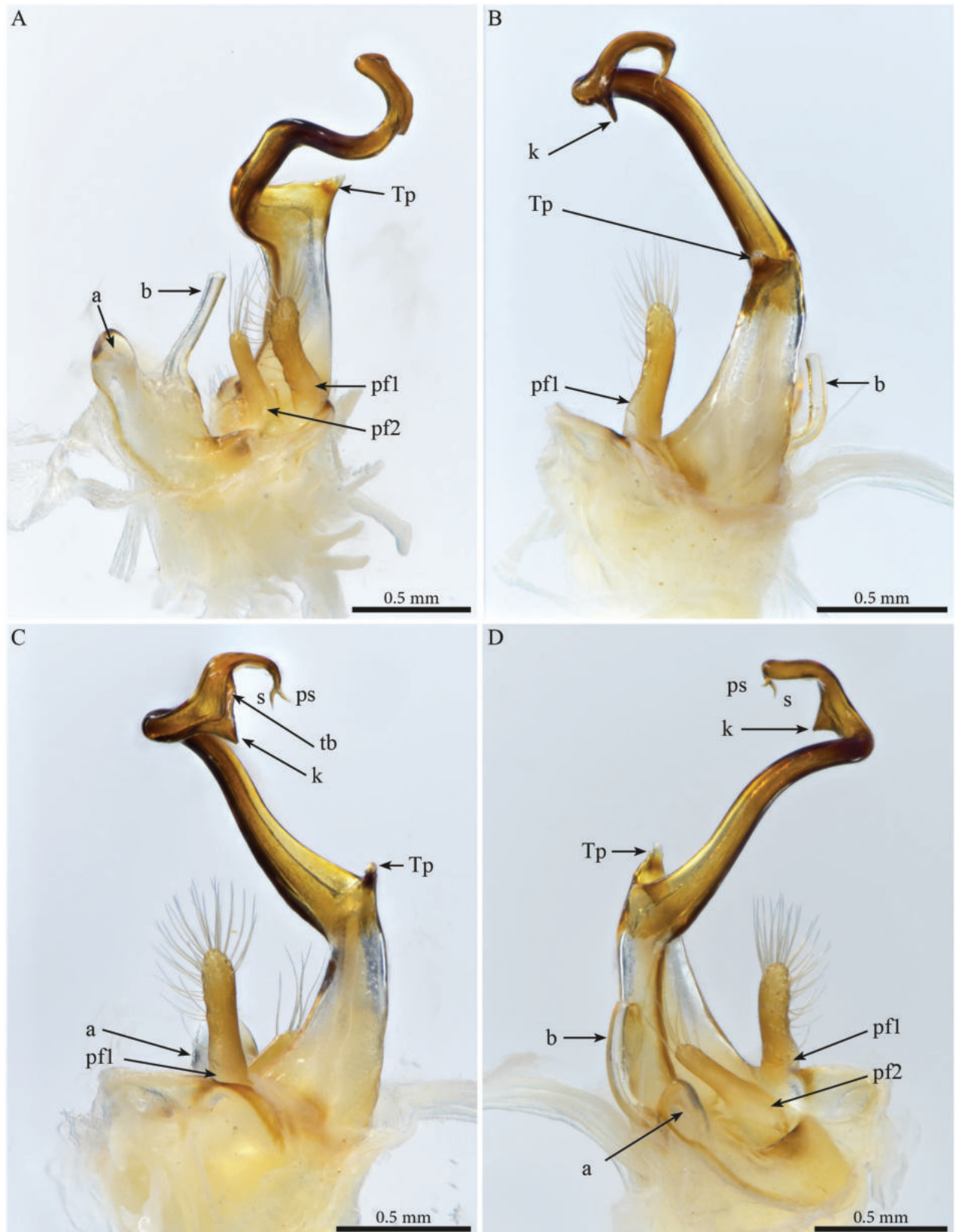


Figure 2. *Angulifemur unidigitis* Zhang, 1997, male (BG-NMNHS-INV-000000006260 NMNHS), right gonopod **A** anterior view **B** posterior view **C** lateral view **D** mesal view. Abbreviations: a = mesal process of coxa; b = falcate mesal process of coxa; pf1 = prefemoroidal process 1; pf2 = prefemoroidal process 2; k = lateral process of the distal part of telopodite; ps = parasolenomere; s = solenomere; tb = blunt tooth of telopodite; Tp = telopodital projection.

Stoev det. 25.07.2003, 1 male, CHINA, Yunnan, Menzi County, Long Bao Pao Dong (cave), 07.01.1989, P. Beron leg. (BG-NMNHS-INV-00000006260 NMNHS).

Diagnosis. It can easily be distinguished from *A. tridigitis* by the much shorter and upright coxal process, a distally more sinuous telopodite, bearing a pointed process at its mid length (**Tp**); distal part of telopodite with one tooth-shaped process (**k**).

Descriptive notes. Habitus matching the description of *Paracortina wangi* (Stoev 2004). The species is characterised by long walking legs and antennae, absence of projection on head vertex in adult males, reduced number of ommatidia and a strongly enlarged organ of Tömösváry (Fig. 1).

Male sexual characters. Leg-pairs 1 and 2 reduced and more setose than the rest, showing prefemoral and tarsal brushes (Fig. 1E), leg-pair 2 with a small anterior process and posterior gonopore, leg-pair 3 with a smaller triangular process on coxa (Fig. 1E), leg-pair 6 with one small hyaline triangular mesal process on coxa, prefemur showing proximally a constriction on the posterior margin (Fig. 26A), leg-pair 7 with two coxal processes (Fig. 26B), a long subfalcate mesal process and a shorter, larger, subtriangular one (corresponding to *f* and *t*, respectively in Stoev 2004: fig. 6), coxal sacs (Fig. 1E) present on leg-pair 3–23.

Gonopods (Fig. 2). Each gonopod with two short, clavate, setose prefemoral processes (**pf1** and **pf2**), with **pf1** slightly larger and more setose than **pf2** (Fig. 2A, C). Coxa with two reduced processes on the median margin: (**a**) a rounded lobe directed mesad (Fig. 2A, C, D), and (**b**) a reduced, cone-shaped one, pointing distad (Fig. 2A, B, D). Telopodital (**T**) stem proximally broad, with a pointed triangular projection (**Tp**) at the third to mid-length of its posterior margin, marking an abrupt twist and narrowing of the process (Fig. 2A–D). Distal half of **T** sinusoidal, gently narrowing distad, and bent laterad. Distal part of **T** darkly pigmented, with a sharp triangular tooth (**k**) and a much smaller blunt one (**tb**) on the lateral margin (Fig. 2B–D). **T** further narrowing distad, marking a complete loop, its apex projecting in a short curved downturned process, bifurcated into solenomere (**s**) and parasolenomere (**ps**).

Comments. The specimens studied here are part of the type series of the species *Paracortina (Altum) wangi* Stoev, 2004. Stoev (2004) described this millipede as a new species of the genus *Paracortina* and subgenus *Altum* based on the presence of five posterior setae on the sixth hemipleurite. While describing *P. wangi* Stoev (2004) was unaware of the publication of Zhang (1997). Being also described from the same type locality (Longbaopo-Wulichong cave system) in Mengzi County, Stoev et al. (2008) subsequently synonymised *P. wangi* with *Angulifemur unidigitis*.

Distribution. Until now, the species is known only from Long Bao Pao - Wulichong cave system and Laoxiao Cave, Mengzi County, China (Fig. 28).

***Crassipetalum* Akkari & Stoev, gen. nov.**

<https://zoobank.org/07C4E7B1-8D0C-407D-B932-F564546568A7>

Type species. *Crassipetalum magnum* Akkari & Stoev, sp. nov.

Included species. *Crassipetalum magnum* Akkari & Stoev, sp. nov.; *Crassipetalum inflatum* (Chen, Zheng & Jian, 2023), comb. nov.

Diagnosis. Head with no projection on vertex, leg-pairs 6 and 7 without noticeable modifications. Gonopods parallel, distal part of the telopodites crossing. Each gonopod with a large clavate prefemoroidal process (**pf1**) reaching the distal part of telopodite (and sometimes accompanied by a smaller one); coxa with a protruding rounded anterior projection and a large coxal process, latter almost of the same size as the telopodite. Telopodite (**T**) with a stout stem, distally expanding in three main folds including a horizontal mesal projection accommodating the solenomere (**s**) and parasolenomere (**ps**). Different from all the other genera of Paracortinidae by the enlarged mesal falcate coxal process and prefemoroidal process, and by the shape of the distal part of the telopodites.

Etymology. A combination of *crassus*, meaning fat/stout, referring to the large mesal coxal process and *petalum* a suffix used in many genera in the order Callipodida.

***Crassipetalum magnum* Akkari & Stoev, sp. nov.**

<https://zoobank.org/B9A36E4F-DAAF-4FD5-9670-551A38D3B62A>

Figs 3, 4, 28

Material examined. Holotype: adult male, CHINA, Gansu Province, Cha-gang Village, Zhou-qu County, alt. 1650 m., on 12.05.1998, leg. Chen De-niu, Zhang Guo-qia (TM_206979 IZCAS).

Etymology. Species epithet refers to the unusually large mesal coxal and prefemoroidal processes.

Diagnosis. Different from *Crassipetalum inflatum* by the larger and elongated shape of the prefemoroidal process, the absence of a second prefemoroidal process, and the different distal part of telopodite.

Description. Body cylindrical, length 37–38 mm, maximal width ca 2.2 mm at PT6; body narrowing anteriorly and posteriorly from PT6; 54 (52 + 2 apodous) pleurotergites (PTs) + telson. Live colour unknown. Preserved specimen with yellow to pale brownish metazona (Fig. 3A, B); prozona greyish white (Fig. 3B); no stripes or other particular colour patterns; legs yellowish (Fig. 3C). Head: same colour as the body, vertex slightly darker, antennae whitish yellow (Fig. 3A). Fields of ommatidia subtriangular, blackish, composed of ~ 65 transparent ommatidia in eight rows from dorsal to ventral. Organ of Tömösváry ~ 2–3 × larger than ommatidium, situated close to and touching anterior side of eye. Head convex, with no particular modifications (Fig. 3C), covered with minute setae. Antennae short, extending backwards to around mid-length of PT5 (Fig. 3A, C); length of antennomeres (mm): 1 = 0.2; 2 = 0.87; 3 = 0.7; 4 = 0.76; 5 = 0.32; 6 = 0.45; 7 = 0.19. PTs composed of smooth prozona and carinate metazona, latter being greater in diameter than prozona. Prozona without crests, anterior part of metazona with scale-like ornamentation followed by a sharply raising posterior part forming well-developed longitudinal narrow and subparallel crests (Fig. 3B), well-separated from one another and extending over whole-body ring; crests gradually reduced in size laterally and ventrally. Chaetotaxy: all setae in anterior position on PTs 1–4, setae *b*, *c*, *e* migrated posteriorly on PT5; all setae on posterior position from PT6 onwards. Crests well developed, also on collum, comprising primary and secondary series; collum with seven

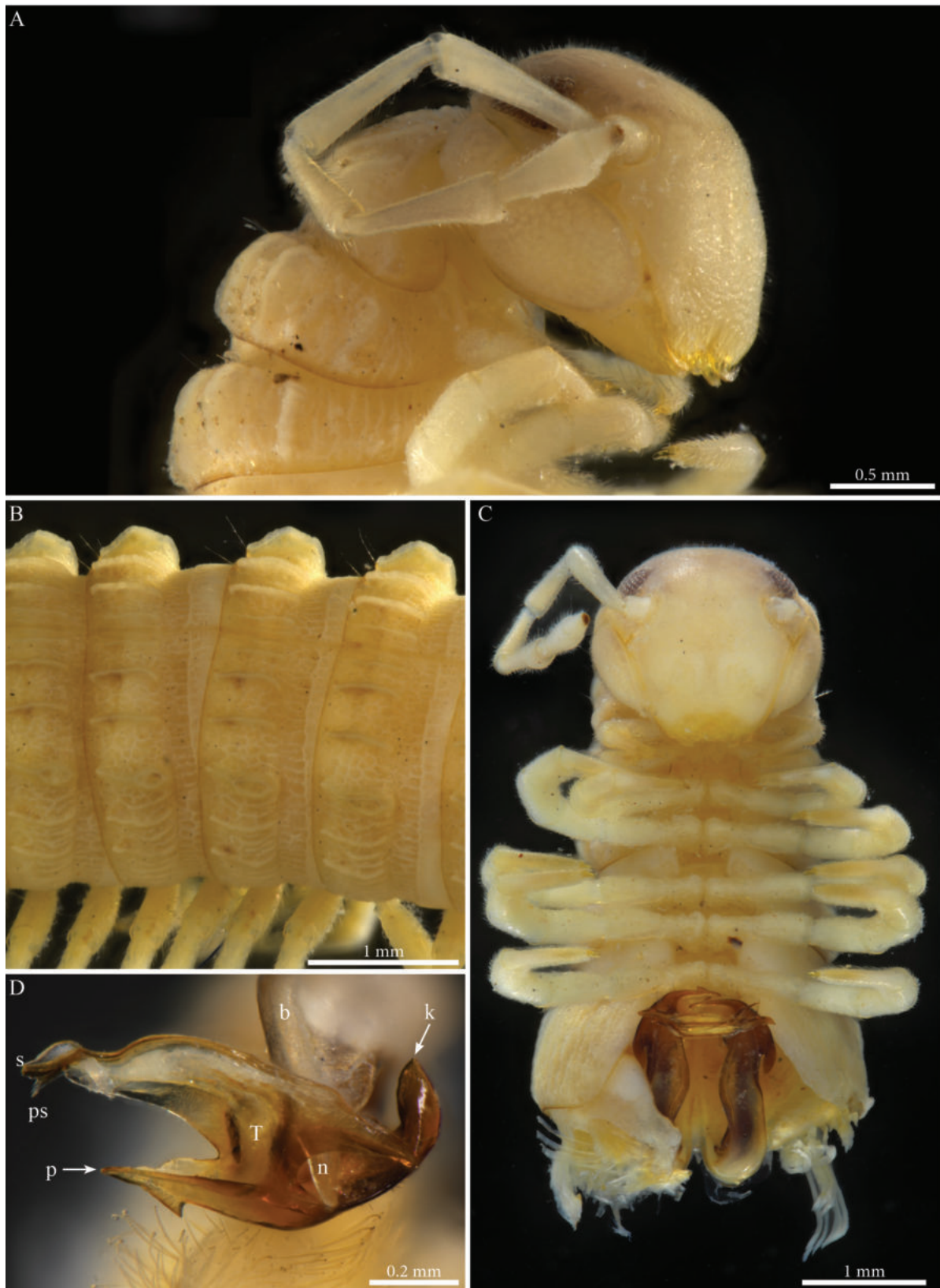


Figure 3. *Crassipetalum magnum* Akkari & Stoev, gen. nov., sp. nov., male holotype (No. TM_206979 IZCAS) **A** head and anterior pleurotergites, laterofrontal view **B** midbody pleurotergites, dorsolateral view **C** head and anterior pleurotergites with gonopods in situ, ventral view **D** right gonopod, distal part, anterior view. Abbreviations: b = falcate mesal process of coxa; k = lateral process of the distal part of telopodite; n = notch on the distal part of the telopodite; p = lateral process on the distal part of telopodite; ps = parasolenomere; s = solenomere; T = telopodite.

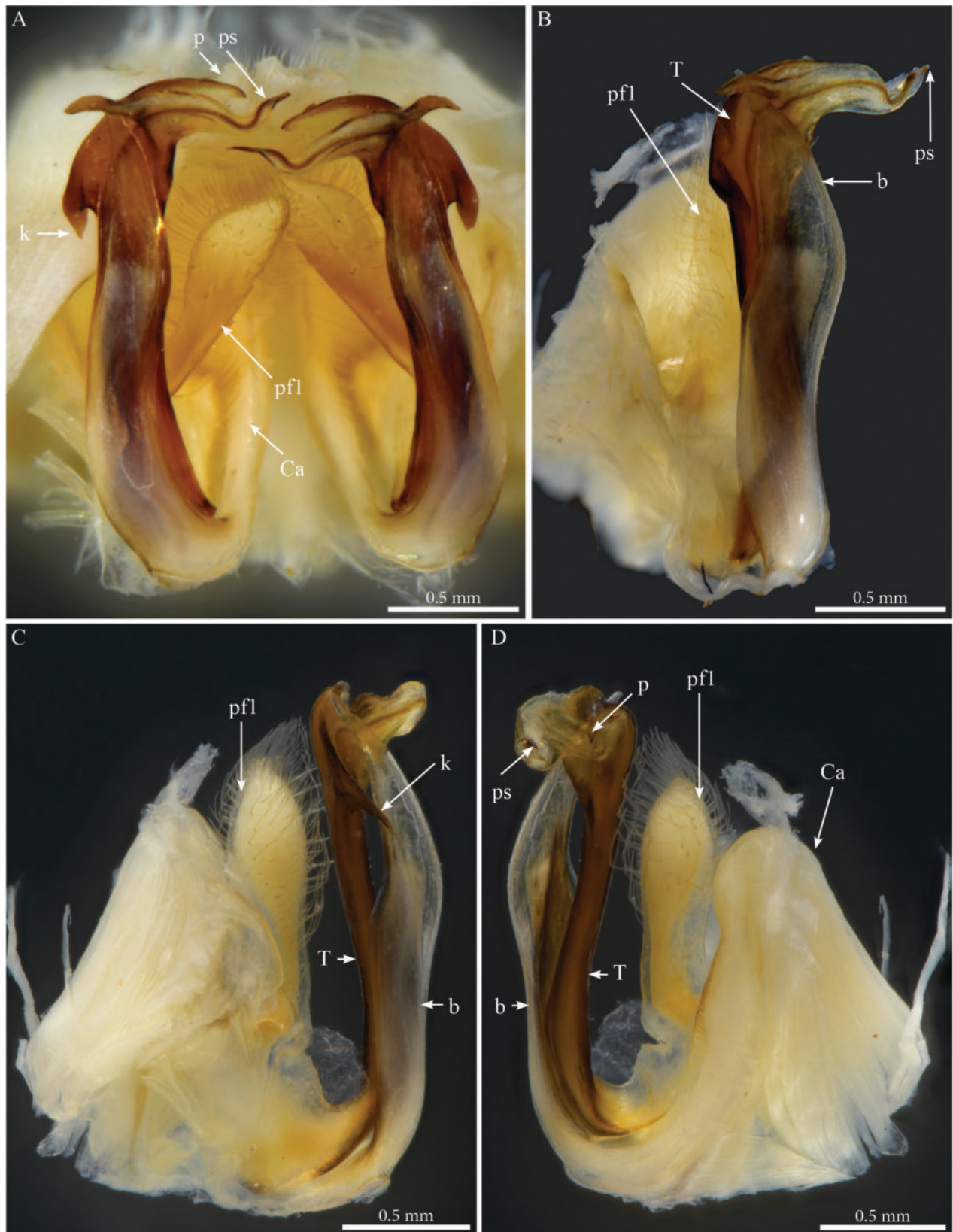


Figure 4. *Crassipetalum magnum* Akkari & Stoev, gen. nov., sp. nov. male holotype (No. TM_206979 IZCAS), gonopods **A** ventral view **B** right gonopod, posterolateral view **C** lateral view **D** anteromesal view. Abbreviations: b = falcate mesal process of coxa; Ca = coxal lobe; k = lateral process of the distal part of telopodite; p = lateral process of the proximal part of telopodite; ps = parasolenomere; s = solenomere; T = telopodite.

or eight crests on each hemipleurite. Ozopores visible from sixth to the 49th PT, located on fourth (largest) crest. Hypoproct tripartite, median sclerite largest, subrectangular, bearing a pair of basal macrosetae; lateral sclerites smaller, triangular, with one seta each. Paraprocts divided into large ventral and smaller dorsal sclerites, each paraproct with a pair of long macrosetae. Spinnerets long and slender, arising from the caudal edge of epiproct and extending well beyond the margins of paraprocts.

Male sexual characters. PTs 6 and 7 enlarged, leg-pairs 1 and 2 reduced and more setose than the rest, showing femoral and tarsal “brushes”, leg-pair 2 with posterior gonopore, legs 1–7 without noticeable modifications (Fig. 3C), coxal sacs present (visible) on leg-pairs 3–16.

Gonopods (Figs 3C, D, 4). Parallel, distally crossing. Each gonopod with one elongated, setose, clavate prefemoroidal process (**pf1**), reaching the distal part of telopodite (Fig. 4A, C, D). Setae of prefemoroidal process large and dense. Coxa with a protruding rounded anterior lobe (**Ca**) (Fig. 4D) and a large coxal process (**b**), almost of the same size as telopodite (Fig. 4), narrowing at mid-length and apically projecting in a pointed tip lodged in small lateral notch of the distal part of the telopodite (Fig. 3D). Telopodite (**T**) with a stout stem, distally with a large lateral triangular downturned projection (**k**), a large mesal notch (**n**) separating a mesal spur-like process (**p**) and a posterior plateau-like horizontal process with a bifurcated mesal projection accommodating the solenomere (**s**) and parasolenomere (**ps**).

Female unknown.

Distribution. Zhou-qu County, Cha-gang Village, China (Fig. 28).

***Crassipetalum inflatum* (Chen, Zheng & Jian, 2023), comb. nov.**

Paracortina inflata Chen, Zheng & Jian, 2023: 54–57, figs 7–10.

Diagnosis. Different from *Crassipetalum magnum* Akkari & Stoev, sp. nov. by the ovoid shape of the prefemoroidal process, the presence of a second, smaller prefemoroidal process, and by the differently shaped and more complex distal part of the telopodite (Chen et al. 2023).

Distribution. Hongqi Longtan Cave, Yintiaoling National Nature Reserve, Wuxi County, Chongqing, China (Fig. 28).

Genus *Paracortina* Wang & Zhang, 1993

= *Altum* Wang & Zhang, 1993: 381.

= *Relictus* Wang & Zhang, 1993: 378.

Type species. *Paracortina leptoclada* Wang & Zhang, 1993.

Included species.

P. asciformis Akkari & Stoev, sp. nov. – Lixian County, Sichuan, China.

P. carinata (Wang & Zhang, 1993) – Shangrila County (=Zhong Dian/ Zhongdian County), Yunnan, China.

P. kabaki Akkari & Stoev, sp. nov. – Shangrila County, Yunnan, China.

- P. kyrang* Nguyen, Stoev, Nguyen & Vu, 2023 – Ky Rang Cave, Quoc Toan Commune, Quang Hoa District, Cao Bang, Vietnam.
- P. leptoclada* Wang & Zhang, 1993 – Shangrila County, Yunnan, China.
- P. multisegmentata* Stoev & Geoffroy, 2004 – Ngọc Lặc County, Thanh Hoa District, Vietnam.
- P. serrata* (Wang & Zhang, 1993) – Deqin County, Yunnan, China.
- P. stimula* (Wang & Zhang, 1993) – Shangrila County, Yunnan, China.
- P. thallina* (Wang & Zhang, 1993) – Batang County, Sichuan, and Shangrila County, Yunnan, China.
- P. viriosa* (Wang & Zhang, 1993) – Shangrila County, Yunnan, and Mang kang County/Markam? County, Tibet Autonomous Region, China.
- P. voluta* Wang & Zhang, 1993 – Yajiang County and Yanyuan County (new record), Sichuan, China.
- P. yinae* Liu & Tian, 2015 – Cave in Yanchang Village, Guangxi, China.
- P. zhangji* Liu & Tian, 2015 – Cave Qiaoxia Dong, Guizhou, China.

Diagnosis. The type genus of the family Paracortinidae, which differs from *Angulifemur* by having parallel stems of telopodites; from *Scotopetalum* by the presence of large anteromedian subfalcate coxal process, and from the genus *Crassipetalum* gen. nov. by the much smaller prefemoroidal process/es and a subfalcate coxal process **b** (never surpassing the telopodite).

***Paracortina asciformis* Akkari & Stoev, sp. nov.**

<https://zoobank.org/73289E5B-1469-43C2-8573-6B3D812886AE>

Figs 5–7, 27E, 28

Material examined. Holotype: 1 adult male CHINA, Sichuan Prov., Lixian County, SW of Tonghua Village, 31°33'29"N, 103°19'36"E, 08.07.2012, alt. 1905 m, I. Belousov & G. Davidian leg. (Rd 5347 ZMUM); **paratype:** 1 adult female, 60 PTs + telson, same data as holotype (Rd 5348 ZMUM).

Etymology. The species epithet *ascia* + *formis*, referring to the distal shape of the telopodite having a shape of an axe in lateral view. Adjective.

Diagnosis. Different from all other species of the genus *Paracortina* by the distinctive shape of the distal part of telopodite resembling an axe.

Description. Length 39 mm, maximal width ca 2.3 mm at PT6; body narrowing anteriorly and posteriorly from PT6; 60 (59 + 1 apodous) pleurotergites + telson. Live colour unknown. Preserved specimen dark brown, metazona dorsally dark brown, especially on crests, laterally and ventrally paler; prozona greyish; legs yellowish (Figs 5A, 6A). Head: frontal part yellowish, vertex slightly dark brown, antennae yellow (Figs 5C, 6A).

Fields of ommatidia subtriangular, blackish, composed of ~ 56 transparent ommatidia in eight or nine rows (Fig. 5B). Organ of Tömösváry ~ 2 × an ommatidium situated close to and touching anterior side of eye. Antennae moderately long (Figs 5C, 6A). Length of antennomeres (mm): 1 = 0.12; 2 = 0.93; 3 = 0.86; 4 = 0.58; 5 = 0.65; 6 = 0.33; 7 = 0.11. PTs composed of smooth prozona and carinate metazona (Fig. 5D, E), latter being more pronounced and greater in diameter in the posterior part. Prozona void of crests, anterior part of metazona with low carinae followed by a sharply raising posterior part forming well-developed



Figure 5. *Paracortina asciformis* Akkari & Stoev, sp. nov. **A, B, D, E** Female paratype (Rd 5348 ZMUM) **A** anterior body lateral view **B** head left side, organ of Tömösváry, and ommatidia **C** male holotype (Rd 5347 ZMUM) head and anterior pleurotergites, lateral view **D, E** midbody pleurotergites, **D** lateral view **E** dorsal view.



Figure 6. *Paracortina asciformis* Akkari & Stoev, sp. nov., male holotype (Rd 5347 ZMUM) **A** head and anterior pleurotergites, frontal view **B** telson and posterior part of body, posterolateral view **C** right gonopod mesal coxal process and distal part of telopodite, posterior view. Abbreviations: b = falcate mesal process of coxa; M = mesal process of the distal part of telopodite; s = solenomere; T = telopodite.

longitudinal narrow and subparallel crests, well-separated from one another; crests gradually reduce in size laterally and ventrally (Fig. 5C–E). Chaetotaxy follows the pattern of all setae being in anterior position on PTs 1–4, setae *b*, *c*, *e* migrating posteriorly on PT5 and all setae posteriorly on PT6 onwards. Crests moderately developed, also on collum, comprising alternating primary and secondary series, primary slightly higher than secondary; collum with ca nine crests

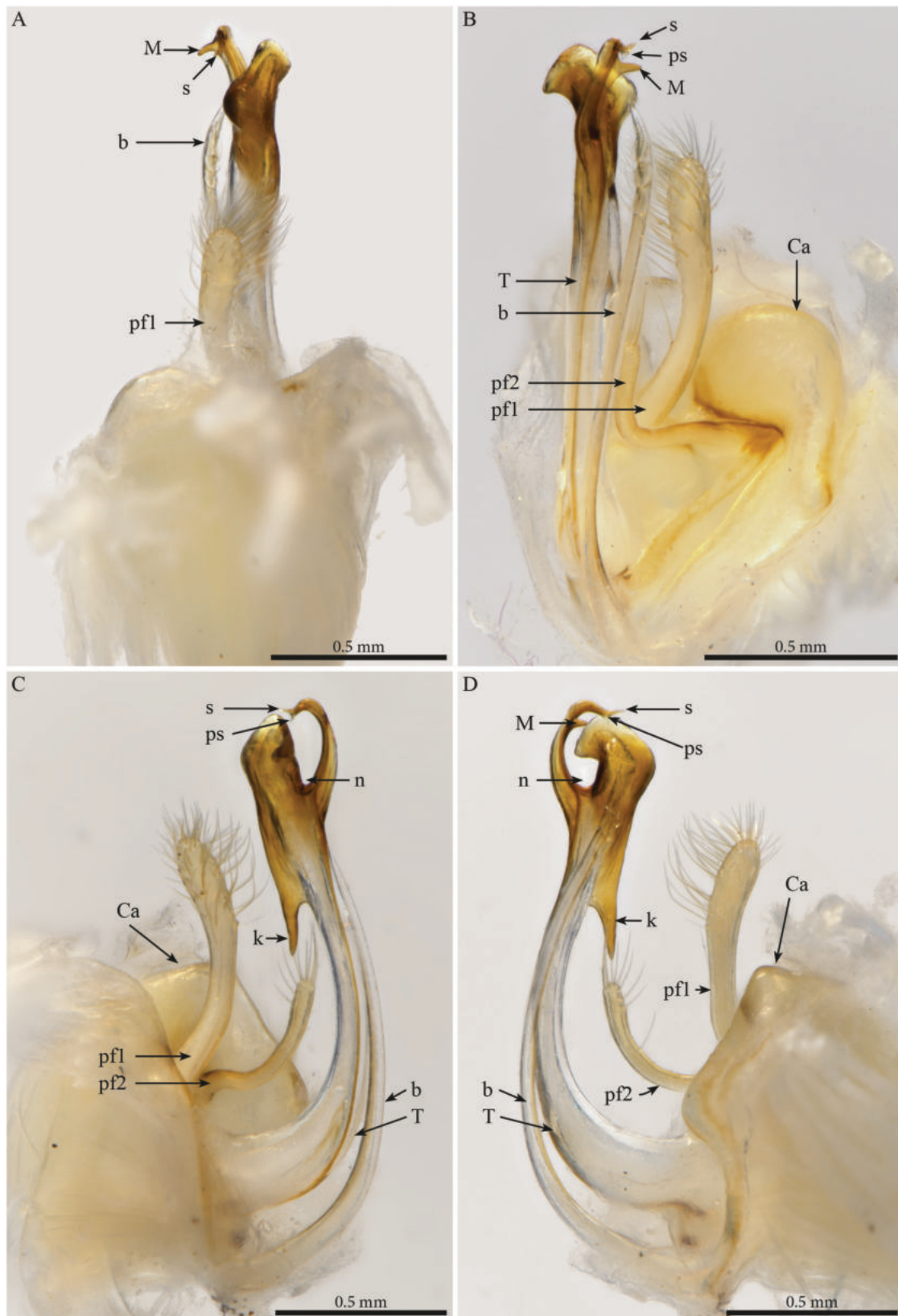


Figure 7. *Paracortina asciformis* Akkari & Stoev, sp. nov., 1 male holotype (Rd 5347 ZMUM), right gonopod **A** anterior view **B** posterior view **C** lateral view **D** mesal view. Abbreviations: b = falcate mesal process of coxa; Ca = anterior lobe of coxa; pfl = prefemoroid process 1; pf2 = prefemoroid process 2; k = lateral process of the distal part of telopodite; M = mesal process of the distal part of telopodite; n = notch on the distal part of the telopodite; ps = parasolenomere; s = solenomere; T = telopodite.

on each hemipleurite. Ozopores visible from 6th to 59th PT, located on 6th (largest) PT. Hypoproct tripartite, median sclerite largest, subrectangular, bearing a pair of basal macrosetae; lateral sclerites smaller, triangular, with one seta each. Paraprocts divided into large ventral and smaller dorsal sclerites, each pair with a pair of long macrosetae. Spinnerets long and slender, arising from the caudal edge of epiproct and extending well beyond the margins of paraprocts (Fig. 6B).

Male sexual characters. Head with a pronounced beak-shaped projection (Figs 6C, 7A), covered with minute setae. Leg-pairs 1 and 2 reduced and more setose than the rest, leg-pair 2 with a small anterior process and posterior opening of the gonopores, leg-pair 7 with a protruding curved mesal process pointing laterad and a shorter subtriangular one on coxa, trochanter with an anterior triangular projection covered with setae (Fig. 27E) Coxal sacs present (noticeable) on leg-pairs 3–13/16.

Gonopods. Parallel, each gonopod with two short, slender, clavate, asymmetrical, and apically setose prefemoroidal processes **pf1** and **pf2** (Fig. 7B–D); coxa with a low rounded lobe on the anterior margin (**Ca**), one long falcate mesal coxal process (**b**), reaching the distal part of the telopodite, its distal part showing ca four beaded structures (Fig. 6C). Telopodite (**T**) stout, with a broad stem proximally, gradually narrowing until its distal third before expanding in two main darkly pigmented parts separated by a rounded notch (**n**), the larger part axe-shaped (Fig. 7C, D), showing a round apical margin and a sharp triangular opposite end (**k**), second part as a slender curved stem, apically bifurcated in solenomere (**s**) and parasolenomere (**ps**) and bearing a smaller subapical triangular tooth (**M**) (Fig. 7).

Distribution. Known only from its type locality (Fig. 28).

***Paracortina carinata* (Wang & Zhang, 1993)**

Fig. 28

Altum carinatum Wang & Zhang, 1993: 385, figs 29–32.

Paracortina carinata: Stoev and Geoffroy 2004: 94.

Paracortina carinata: Liu and Tian 2015: 139, key.

Diagnosis. *P. carinata* appears most similar to *P. stimula* especially in the expanded distal part of the telopodite, of which the distal part is downturned and crossing with the curved process of the solenomere, differing in the shape of the distal process, showing as a subrectangular plate in *carinata* vs dome-shaped in *P. stimula*. Both species could be recognised also by the body colouration which is dark brown in *P. carinata* and yellow in *P. stimula*.

Descriptive notes. (based on Wang and Zhang 1993) Holotype 42 mm long, 2.5 mm wide, 60 podous + 2 apodous PTs, with a dark brown colour.

Gonopods. Each gonopod with two asymmetrical prefemoroidal processes (**pf1**, **pf2**), with **pf1** larger and more setose than **pf2**, a stout and falcate coxal process, reaching 2/3rd of the telopodite; telopodite (**T**) with a uniformly broad stem, distal part abruptly expanding antero-posteriad and showing in a lateral view (Wang and Zhang 1993, fig. 29) a subrectangular plate with an irregular apical margin, and a notch on the anteromesal side separating the main branch from a curved narrow process pointing distad, terminating in a slender branch bifurcated in solenomere (**s**) and parasolenomere (**ps**).

Distribution. Shangrila (= Zhong Dian) County, Yunnan, China (Fig. 28).

Comments. Known only from its original description (Wang and Zhang 1993).

***Paracortina kabaki* Akkari & Stoev, sp. nov.**

<https://zoobank.org/7F96C628-A9B7-49F3-804E-A993B9D4BAE2>

Figs 8–10, 27E, 28

Material examined. Holotype: CHINA, Yunnan, Shangrila County, Degen, 214 Ntn Road, NE slope of SE Baima Mt. Range, between Cukatongcun & Nali, alt. 2465 m, 28°2'23"N, 99°12'16"E, 8.06.2013, I. Belousov, I. Kabak & G. Davidian leg. (Rd 5349 ZMUM); **Paratype:** 1 male 54PTs, same data as holotype (Rd 5350 ZMUM).

Etymology. The species epithet is a patronym to honours of one of the collectors, Ilya Kabak from the Zoological Institute of the Russian Academy of Sciences St Petersburg. Noun in the genitive case.

Diagnosis. Different from all species of the genus *Paracortina* by the distinctive shape of the distal part of telopodite with the ruffle of distolateral lamella.

Description (Holotype). Body cylindrical, length 77.4 mm, maximal width ca 3.2 mm at PT5; body narrowing anteriorly and posteriorly from PT6; 60 (59 + 1 apodous) pleurotergites (PTs) + telson. Live colour unknown. Preserved specimen with a general dark brown to greyish aspect contrasted with pale legs and antennae (Fig. 8A, B), prozona greyish, sputtered with fine brown dots (Fig. 8A, D); metazona dorsally dark greyish brown especially on crests, anterior part greyish, finely sputtered with pale brown interrupted by larger irregular yellow alveolate spots, colour paler laterally below the ozopores and ventrally; legs yellowish (Fig. 8C, D). Head: frontal part pale brown to yellowish, vertex dark grey-brown, antennae yellow (Fig. 8A, B).

Fields of ommatidia subtriangular, black, composed of ~ 75 transparent ommatidia in nine or ten rows. Organ of Tömösváry large, ~ 1.2 mm, 3 × as large as an ommatidium, situated close to and touching anterior side of eye (Fig. 8A). Antennae long; length of antennomeres (mm): 1 = 0.18; 2 = 1.29; 3 = 1.27; 4 = 1.01; 5 = 1.08; 6 = 0.69; 7 = 0.23.

PTs composed of smooth prozona and carinate metazona, latter being more pronounced in the posterior part. Prozona with no crests, anterior part of metazona with low, fine carinae, posterior part sharply raising forming well-developed longitudinal narrow and subparallel crests, well-separated from one another; crests gradually reduce in size laterally and ventrally (Fig. 8C). Chaetotaxy follows the pattern of all setae being in anterior position on PTs 1–4, setae *b*, *c*, *e* migrating posteriorly on PT5 and all setae posteriorly on PT6 onwards. Crests moderately developed, also on collum, comprising alternating primary and secondary series, primary slightly higher than secondary; collum with ca nine crests on each hemipleurite. Ozopores visible from 6th to 59th PT, located on 6th (largest) PT. Hypoproct tripartite, median sclerite largest, subrectangular, bearing a pair of basal macrosetae; lateral sclerites smaller, triangular, with one seta each. Paraprocts divided into large ventral and smaller dorsal sclerites, each pair with a pair of long macrosetae. Spinnerets long and slender, arising from the caudal edge of epiproct and extending well beyond the margins of paraprocts.

Male sexual characters. Head with a pronounced beak-shaped projection covered with minute setae (Fig. 8A, B). Leg-pairs 1 and 2 reduced and more se-



Figure 8. *Paracortina kabaki* Akkari & Stoev, sp. nov., male holotype (Rd 5349 ZMUM) **A, B** head and anterior pleurotergites **A** lateral view **B** frontal view **C, D** midbody pleurotergites **C** lateral view **D** dorsal view.

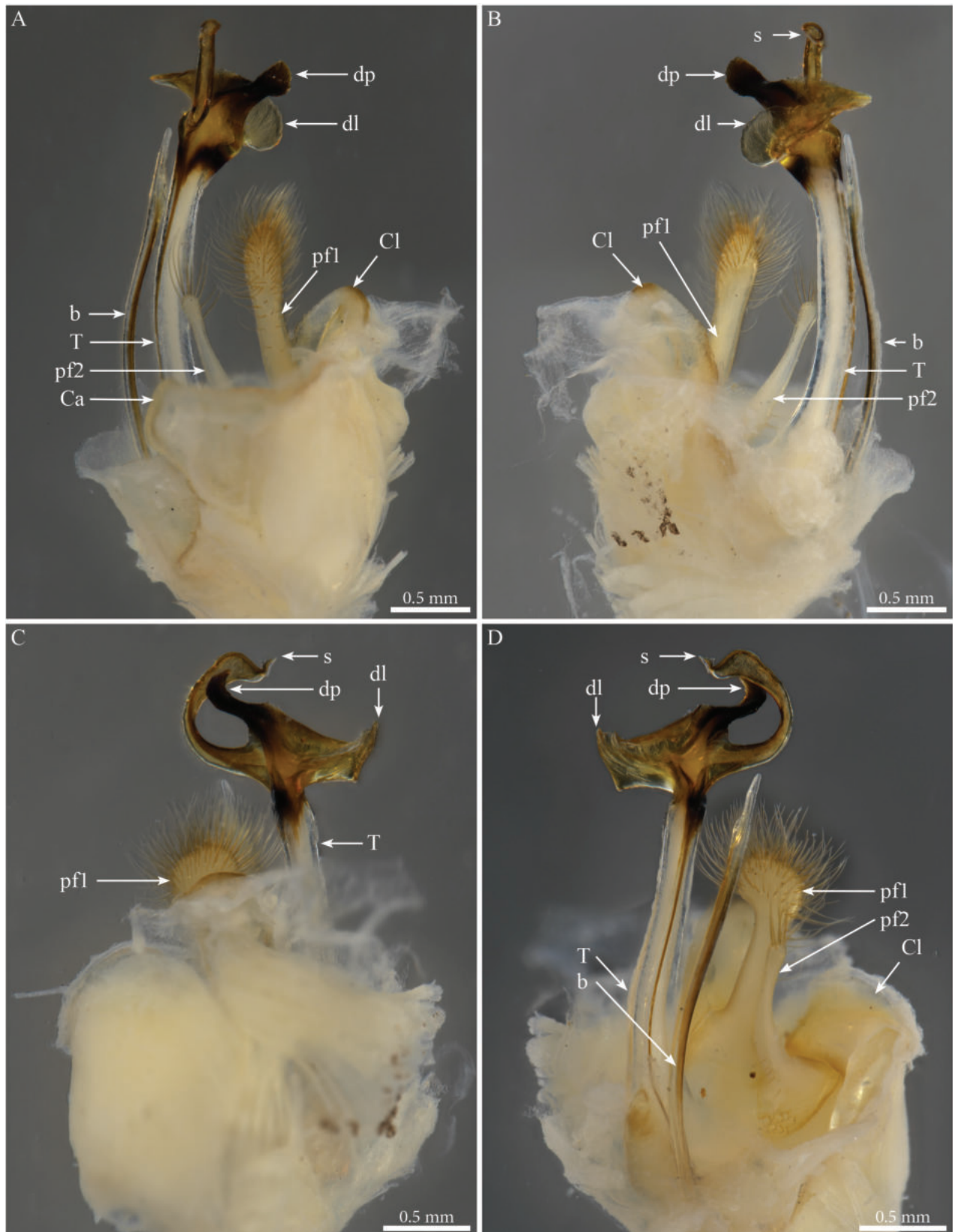


Figure 9. *Paracortina kabaki* Akkari & Stoev, sp. nov., male holotype (Rd 5349 ZMUM), right gonopod **A** anterior view **B** posterior view **C** lateral view **D** mesal view. Abbreviations: b = mesal process of coxa; Ca = anterior lobe of coxa; Cl = lateral lobe of coxa; dl = distal lamella of telopodite; dp = a median projection of the distal part of telopodite; pf1 = prefemoro-oidal process 1; pf2 = prefemoro-oidal process 2; s = solenomere; T = telopodite.

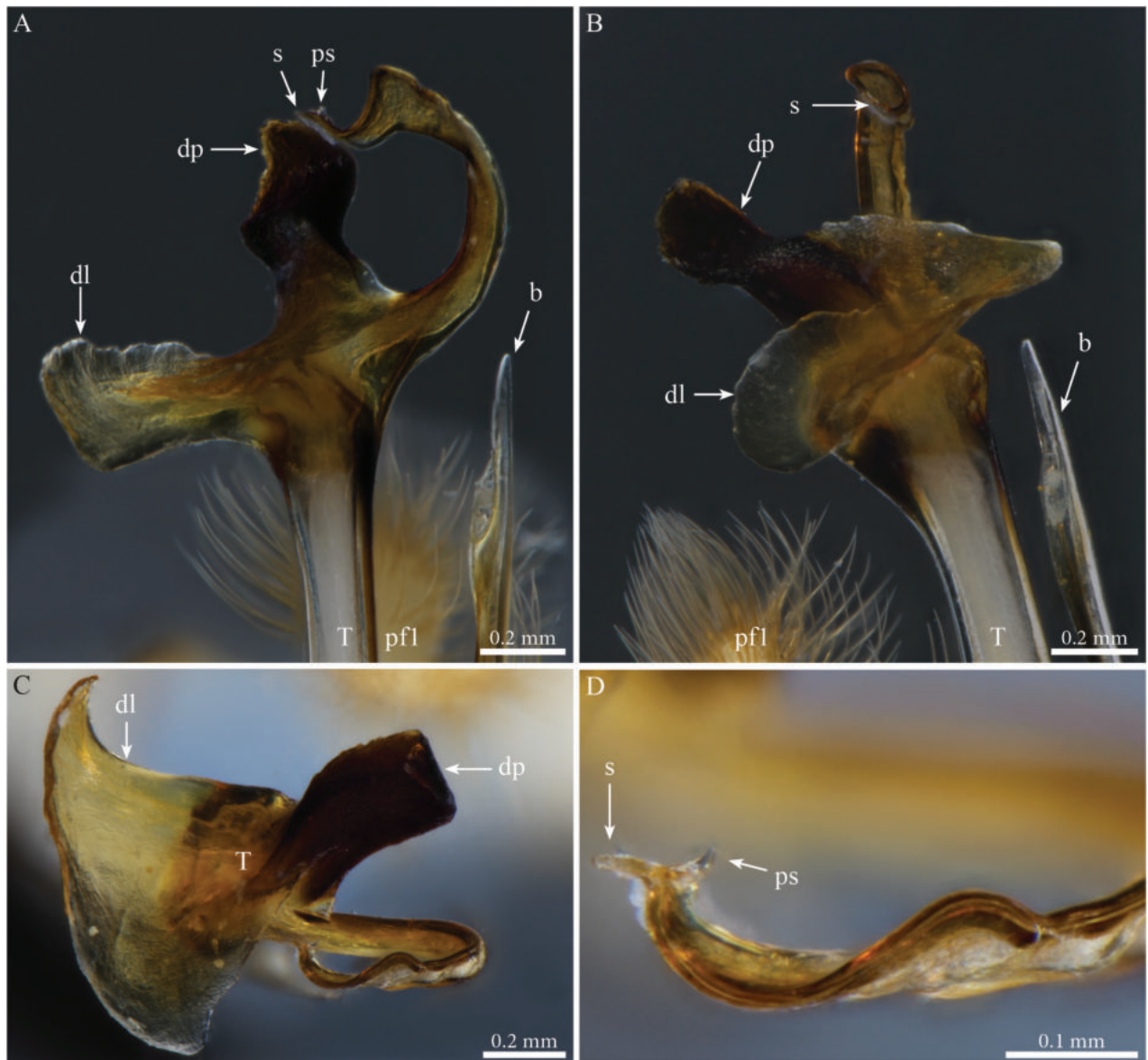


Figure 10. *Paracortina kabaki* Akkari & Stoev, sp. nov., male holotype (Rd 5349 ZMUM) **A–C** right gonopod telopodite, distal part, **A** mesoventral view **B** posteromesal view **C** ventral view **D** detail of solenomere, ventral view. Abbreviations: b = mesal process of coxa 2; dl = distal lamella of telopodite; dp = a median projection of the distal part of telopodite; pf1 = prefemoroidal process 1; ps = parasolenomere; s = solenomere; T = telopodite.

tose than the rest, leg-pair 2 with a small anterior process and posterior opening of the gonopores. Leg-pair 7 with a large cone-shaped and apically rounded mesal process on coxa, a lateral angular margin separated by a notch, an apical tuft of setae on trochanter, prefemur with a strong constriction proximally on the anterior margin, then strongly swollen distally (Fig. 27F). Coxal sacs present (noticeable) on leg-pairs 3–13/16.

Gonopods (Figs 9, 10). Parallel, each gonopod with asymmetrical, clavate prefemoroidal processes: a thin, short (**pf1**) process bearing a few apical setae, and a much larger densely setose (**pf2**) one (Fig. 9A, B); coxa with rounded lobes on the anterior side (**Ca**) and the lateral side (**Cl**) respectively, engulfing the prefemoroidal processes (Fig. 9 A), and a long falcate mesal coxal process (**b**), reaching the distal part of the telopodite (Fig. 9A, B, D). Telopodite (**T**) stout and straight,

with a uniformly broad stem expanding distally in a complex apex comprising a large hyaline lamella (**dl**) with a serrated margin extending anterolaterally in a double horizontal ruffle (Fig. 9B), and a darkly pigmented median projection (**dp**) apically folded and pointing distolaterad (Figs 9, 10); a slender mesal process, curved 180 degrees and pointing anteriorly, slightly swollen apically (Figs 9C, D, 10A) before further narrowing and bifurcating in solenomere (**s**) and parasolenomere (**ps**).

***Paracortina kyrang* Nguyen, Stoev, Nguyen & Vu, 2023**

Fig. 28

Paracortina kyrang Nguyen, Stoev, Nguyen & Vu, 2023: 183, figs 1–7.

Diagnosis. The gonopods of this species differ from those of the other congeners in the sinuous aspect of the telopodite, distally narrowing, reminding more of the genus *Angulifemur*, from which this species differs by the absence of (**Tp**) process and the presence of a long coxal process (**b**) reaching the distal part of telopodite.

Descriptive notes. (based on Nguyen et al. 2023) Species with 68–74 PTs + telson, general colour pale, living specimens greenish-white, head strongly modified in males with a well-protruding projection, 19–20 ommatidia in two or three rows.

Male sexual characters. PTs 6 and 7 strongly enlarged, leg-pairs 1 and 2 smaller and more setose than the rest, showing femoral and tarsal “brushes”, leg-pair 2 with a small anterior process and posterior gonopore, leg-pair 7 with a round mesal projection and a small spine (Nguyen et al. 2023: fig. 6a, b), coxal sacs present on leg-pairs 3–26.

Gonopods. Each gonopod with two clavate, slender, and setose prefemoroid processes (**pf1**, **pf2**), coxa low with anterior and lateral rounded lobes and a long falcate mesal process, reaching the distal part of the telopodital stem. Telopodite (**T**) sinuous bearing a distomesal triangular tooth, further twisted and expanding mesolaterad, then strongly constricted and apically narrowed, terminating in a slender branch bifurcated into solenomere (**s**) and parasolenomere (**ps**).

Distribution. Ky Rang Cave, Quoc Toan commune, Quang Hoa District, Cao Bang Province, Vietnam (Fig. 28).

Comments. Nguyen et al. (2023) described a slightly different chaetotaxy for *Paracortina kyrang* with two pairs of setae distributed posteriorly on the collum (usually all setae are positioned anteriorly) and five pairs of posterior setae on PT5 (instead of three pairs).

***Paracortina leptoclada* Wang & Zhang, 1993**

Fig. 28

Paracortina leptoclada Wang & Zhang, 1993: 376–377, figs 1–5; Stoev and Geoffroy 2004: 99, 103, key; Liu and Tian 2015: 139, key.

Diagnosis. Most similar to *P. thallina*, with an expanded distal part of the telopodite bearing a large rounded lateral lamella and a hook-shaped process pointing

anterodistad. Different in the shape and orientation of the distal lamella, laterally positioned and folded 180 degrees and a shorter mesal coxal process.

Descriptive notes. Male holotype 55 mm long, 2.3 mm wide, general colour brown, 55 podous +2 apodous PTs, coxa of leg pairs 1 and 7 with two processes (Wang and Zhang 1993; Wang 1996), head with a large projection on the vertex (Wang 1996).

Male sexual characters. (based on Wang and Zhang 1993: fig. 19) Leg-pair 7 with two processes on coxa.

Gonopods. Parallel and slightly diverging. Each gonopod with two uniformly setose, clavate prefemoroid processes (**pf1** and **pf2**), one large falcate coxal process narrowing at mid-length and apically projecting in a pointed tip, reaching the distal part of the telopodite. Telopodite (**T**) with a stout stem, distally expanding in a larger process projecting in a broad lateral folded lamella and a thin curved mesal process pointing anterodistad, apically bifurcated to accommodate the solenomere (**s**) and parasolenomere (**ps**).

Distribution. Shangrila County, Yunnan, China (Fig. 28).

Comments. Species known only from its original description.

***Paracortina multisegmentata* Stoev & Geoffroy, 2004**

Figs 11–13, 26C, 28

Paracortina multisegmentata Stoev & Geoffroy, 2004: 97, figs 9–17; Liu and Tian 2015: 139, key.

Material examined. 1 male paratype, VIETNAM, Thanh Hoa Province, Ngọc Lặc, Moc-Trach Cave, alt. 15 m, 8–10.12.1929, Colani leg. (BG-NMNHS-INV-00000006261 NMNHS). Stoev det. April 2004.

Diagnosis. Unique in having the highest number (81–85) of pleurotergites and gonopods with proximally crossing telopodites, distally bent at 90 degrees.

Descriptive notes. Species with 81–85 PTs + telson, general colour of conserved specimens pale brownish (Fig. 11A, B), head convex, unmodified (Figs 11A, 12A), ~ 40 ommatidia in five or six rows (Fig. 11A).

Male sexual characters. PTs 6 and 7 strongly enlarged, leg-pairs 1 and 2 reduced and more setose than the rest, showing prefemoral and tarsal brushes, leg-pair 2 with the posterior gonopore (Fig. 12A, B), leg-pair 7 with a small mesal spine on coxa and a tuft of setae on trochanter (Fig. 26C), coxal sacs present on leg-pairs 3–23.

Gonopods (Figs 12B, 13). Converging, proximally crossing (Fig. 12B). Each gonopod with one slender and distally uniformly setose prefemoroid process (**pf1**), reaching to overpassing the mid-length of telopodite (Fig. 13); coxa with a mesal rounded lobe (**a**) connected to a slender falcate mesal process (**b**), latter reaching mid-length of the telopodite. Telopodite (**T**) with uniformly slender stem, distally 90 degrees bent laterad (Fig. 12A, B), distal part expanding and terminating in two asymmetrical branches (Fig. 13): a shorter horizontally leaf-like subapical process, surmounted by a triangular tooth (**k**) pointing distolaterad, second branch longer, extending laterad before curving distad, with the apical part terminating in two asymmetrical bulges, the largest accommodating the bifurcated branch with the opening of the solenomere (**s**) and parasolenomere (**ps**).



Figure 11. *Paracortina multisegmentata* Stoev & Geoffroy, 2004, male paratype (BG-NMNHS-INV-00000006261 NMNHS) **A** head and anterior pleurotergites, lateral view **B, C** midbody pleurotergites **B** lateral view **C** dorsal view.

Distribution. Ngoc-Lac and Loc Thinh, Thanh Hoa, Vietnam (Fig. 28).

Comments. This species possesses unique characters within the family, not only by having the highest number of pleurotergites but also in being the only species of Paracortinidae with telopodites proximally crossing and their distal part being bent to 90 degrees. This combination of characters could justify the description of a new genus to accommodate the species. However, similar to



Figure 12. *Paracortina multisegmentata* Stoev & Geoffroy, 2004, male paratype (BG-NMNHS-INV-00000006261 NMNHS) **A** head, anterior pleurotergites and legs, frontal view **B** gonopods in situ, posterior view.

P. kyrang, until more material becomes available, we refrain from erecting new genera for these two species and leave them in the genus *Paracortina* until further analyses are available.



Figure 13. *Paracortina multisegmentata* Stoev & Geoffroy, 2004, male paratype (BG-NMNHS-INV-00000006261 NMNHS), right gonopod **A** anterior view **B** posterior view **C** lateral view **D** mesal view. Abbreviations: a = mesal coxal lobe; b = coxal falcate process; pfl = prefemoroïdal process 1; k = lateral process of the distal part of telopodite; ps = parasolenomere; s = solenomere; T = telopodite.

***Paracortina serrata* (Wang & Zhang, 1993)**

Fig. 28

Altum serratum Wang & Zhang, 1993: 383–385, figs 24–28.

Paracortina serrata: Stoev and Geoffroy 2004: 102, key; Liu and Tian 2015: 139, key.

Diagnosis. Most similar to the new species *P. kabaki* sp. nov., especially in the distal part of the telopodite with a large, serrated lamella, differing by the short trapezoid lamella (vs larger rectangular one).

Descriptive notes. Holotype 45 mm long, 2.9 mm wide, 52 podous + apodous PTs, general colour brown.

Male sexual characters. Leg-pair 7 with two coxal processes (Wang and Zhang 1993; Wang 1996). **Gonopods** (based on Wang and Zhang 1993: figs 24–26). Parallel, each gonopod with two asymmetrical, clavate prefemoroidal processes, with (**pf1**) larger and more setose than (**pf2**), the latter distally folded; one large broad and long coxal process (**b**), reaching the distal part of the telopodite and apically projecting in a pointed tip. Telopodite (**T**) with a stout stem, distally expanding into a lateral lamella with a serrated margin, separated by a deep notch from a median branch. Latter presenting a blunt subapical projection, and a longer twisted process, curved and bifurcating at the tip, with the opening of the solenomere (**s**) and parasolenomere (**ps**).

Distribution. Deqin County, Yunnan, China (Fig. 28).

Comments. Species known only from its original description.

***Paracortina stimula* (Wang & Zhang, 1993)**

Fig. 28

Relictus stimulus Wang & Zhang, 1993: 379–380, figs 10–13.

Paracortina stimula: Stoev and Geoffroy 2004: 102, key; Liu and Tian 2015: 139, key.

Diagnosis. Most similar to *P. carinata*, differing in the distal process, being dome-shaped (vs sub rectangular in *P. carinata*). Both species could be recognised also by the body colouration which is dark brown in *P. carinata* and yellow in *P. stimula*.

Descriptive notes. Holotype 35.5 mm long, 1.9 mm wide, number of PTs in holotype not specified, in female allotype 53 podous + 3 apodous; general colour light yellow (Wang and Zhang 1993).

Gonopods (based on Wang and Zhang 1993: figs 10, 11). Each gonopod with two asymmetrical clavate prefemoroidal processes with (**pf1**) large and setose, (**pf2**) small with only a pair of large setae; one large falcate coxal processes (**b**) reaching the distal part of the telopodite, apically projecting in a pointed tip. Telopodite (**T**) with a stout stem, distally expanding into dome-like plate, with a notch on the mesal margin separating two oppositely directed crossing projections of more or less similar length: a downturned projection and upturned process pointing distomesad, bifurcated at tip with the opening of the solenomere (**s**) and parasolenomere (**ps**).

Distribution. Shangrila (= Zhong Dian) County, Yunnan, China (Fig. 28).

Comments. Species known only from its original description.

***Paracortina thallina* (Wang & Zhang, 1993)**

Figs 14–16, 26D, E, 28

Relictus thallinus Wang & Zhang, 1993: 380, figs 14–18.

Paracortina thallina: Stoev and Geoffroy 2004: 103, key; Liu and Tian 2015: 139, key.

Material examined. 1 male, CHINA, Yunnan, Shangrila, Degen, SW of Benziban-zhen, 214 Nm Road, NE slope of SE Baima Mt. Range, 28°6'50"N, 99°12'24"E, alt. 3260, 07.06.2013, I. Belousov, I. Kabak & G. Davidian leg. (Rd 5344 ZMUM), Stoev & Akkari det. 2023.

Diagnosis. Most similar to *P. leptoclada* in the expanded distal part of the telopodite bearing a large rounded lateral lamella and a hook-shaped process pointing anterodistad. Different in the shape and orientation of the distal lamella, (vs laterally expanded and folded lamella and a shorter mesal coxal process in *P. leptoclada*).

Descriptive notes. Male with 55 PTs + Telson. Length ca 39.7 mm. Live colour unknown. Preserved specimen with a general dark brown to greyish colour, legs and antennae yellowish with a dark sputter (Figs 14, 15A), prozona greyish with fine brown sputter (Figs 14A, 15B); metazona dark greyish brown dorsally especially on crests, anterior part greyish with a fine pale brown sputter interrupted by larger irregular yellow alveolate spots, colour gradually fading below the ozopores and ventrally. Head with dark pigmentation on the vertex and frons, mandibular stipes and gnathochilarium yellowish (Fig. 14B, C). Fields of ommatidia subtriangular, composed of ~ 62 ommatidia in ten rows. Organ of Tömösváry very large, ~ 0.8 mm, situated close to and touching the anterior side of eye (Fig. 14B).

Male sexual characters. Head with a triangular protruding projection on vertex (Figs 14B, C, 15A). Leg-pairs 1 and 2 reduced and setose (Fig. 14C), showing prefemoral and tarsal brushes, leg-pair 2 with a dome-shaped anterior process on coxa and posterior gonopore, leg-pair 4 with an anterior triangular process on coxa (Fig. 15A), leg-pair 6 with a small mesal tooth on coxa (Fig. 26D), leg-pair 7 with one mesal and one lateral slender hyaline pointed processes on coxa (Fig. 26E), coxal sacs (Fig. 15C) noticeable from leg-pair 3–23.

Gonopods (Figs 15D, E, 16). Diverging. Each gonopod with two large, setose, clavate prefemoroid processes (**pf1**, **pf2**) with **pf1** slightly larger than **pf2** (Fig. 15D); coxa with a large lobe laterally (**Cl**) and a low projection (**Ca**) anteriorly (Figs 15D, 16), a mesal anterior triangular process (**a**) and a long falcate coxal processes (**b**) reaching the distal part of the telopodite (both broken in the studied specimen). Telopodite (**T**) with a long slightly curved stem, distally abruptly expanding in a sub-rectangular posterior process with rounded margins (Fig. 16C, D) connected to a transparent jagged lamella (**dl**) projecting anteriorly (Fig. 15D), apically folded (Fig. 16C, D), and a curved hook-shaped process pointing meso-anteriorly (Fig. 16), narrowing towards its apex and bifurcating into the opening of the solenomere (**s**) and parasolenomere (**ps**).

Distribution. Batang County, Sichuan, and Shangrila County, Yunnan, China (Fig. 28).

Comments. This is the second record of the species since its original description. Here we provide the first micrographs illustrating the habitus of the species (Figs 14, 15).



Figure 14. *Paracortina thallina* (Wang & Zhang, 1993), male (Rd 5344 ZMUM) **A** habitus (head missing), dorsal view **B, C** head and anterior pleurotergites **B** lateral view **C** frontal view.

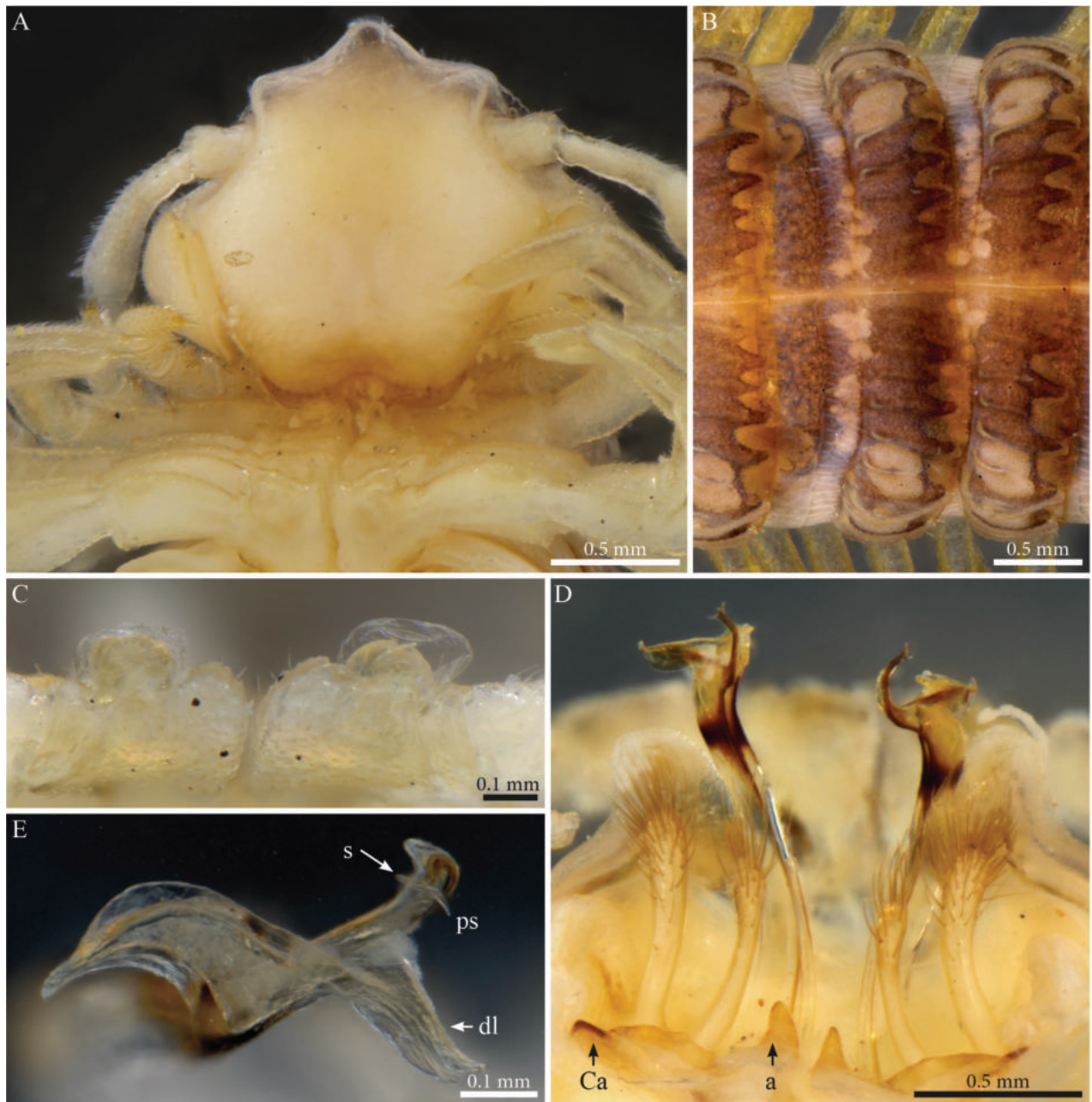


Figure 15. *Paracortina thallina* (Wang & Zhang, 1993) male (Rd 5344 ZMUM) **A** head and anterior pleurotergites and legs, frontal view **B** midbody pleurotergites, dorsal view **C** 9th leg pair coxal sacs, posterior view **D** gonopods, anterior view **E** right telopodite, apical section, ventral view. Abbreviations: a = mesal anterior triangular process of coxa; Ca = anterior lobe of coxa; dl = distal lamella of telopodite; ps = parasolenomere; s = solenomere.

***Paracortina viriosa* (Wang & Zhang, 1993)**

Figs 17–19, 27A, B, 28

Altum viriosum Wang & Zhang, 1993: 381, figs 19–23.

Paracortina viriosa: Stoev and Geoffroy 2004: 103, key; Liu and Tian 2015: 139, key.

Studied material. 1 male, CHINA, W Lijiang, W Yangtze, W Xinhucun, 0.7 km NW Daqingtou, 26°56'23"N, 99°52'16"E, 2720m, 01.06.2018, I. Belousov & I.

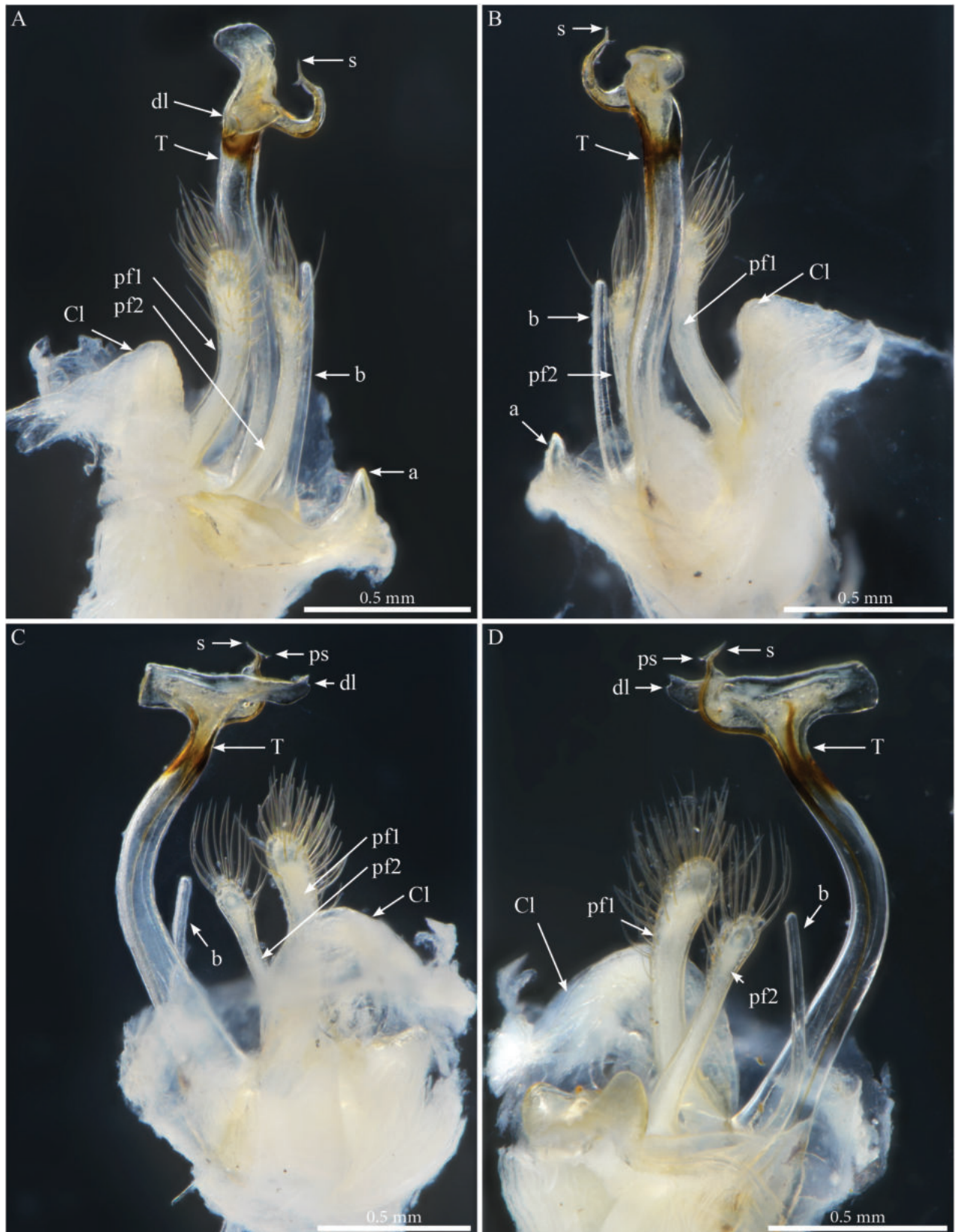


Figure 16. *Paracortina thallina* (Wang & Zhang, 1993), male (Rd 5344 ZMUM), right gonopod **A** anterior view **B** posterior view **C** lateral view **D** mesal view. Abbreviations: a = mesal anterior triangular process of coxa; b = falcate mesal process of coxa; Cl = lateral lobe of coxa; dl = distal lamella of telopodite; pf1 = prefemoroidal process 1; pf2 = prefemoroidal process 2; ps = parasolenomere; s = solenomere; T = telopodite.

Kabak leg. (Rd 5354 ZMUM), Akkari det. 2023, 2 males, CHINA, NW Lijiang, W Chang J. NW Jinzhuang, 2.5 km N Tuozhi Vill, 27°09'32"N, 99°41'47"E, 2315 m, 17.05.2017, I. Belousov & I. Kabak leg. (Rd 5345 ZMUM), Akkari det. 2023.

Diagnosis. Most similar to *P. voluta* especially in the distal part of the telopodite with two main folds and a strong hook-shaped median processes, but differs from the latter by the shape of the distal process, in posterior view subquadrate with a shallow notch (vs earlobe-shaped), the shape and position of the anterior lamella (at the basis of the distal part, rounded and serrated on the lower margin vs more distal and smaller).

Descriptive notes. Male with 68 PTs + telson. Length ca 60.5 mm. Live colour unknown. Preserved specimen with a general tawny dark brown, legs and antennae with a slightly fading colour but showing hints of dark sputter (Fig 17A), prozona dark brown with paler alveolate spots (Fig. 17C, E); metazona dorsally dark brown, especially on crests, interrupted by larger irregular yellow alveolate spots on the lateral crests; colour gradually fading below the ozopores and ventrally. Head with dark pigmentation on the vertex and frons, mandibular stipes and gnathochilarium with yellowish spots, labral area paler (Fig. 17A, B). Fields of ommatidia subtriangular, composed of ~ 60 ommatidia in eight rows. Organ of Tömösváry large, situated close to and touching, anterior side of eye (Fig. 17A).

Male sexual characters. Head with a small projection on vertex (Fig. 17B). Leg-pairs 1 and 2 reduced and more setose than the rest, showing prefemoral and tarsal brushes (Fig. 17B), leg-pair 2 with a large dome-shaped anterior process on coxa and posterior gonopore (Fig. 17D), leg-pairs 3 and 4 with anterior triangular projections on coxa (Fig. 17D), leg-pair 6 with a small rounded mesal projection on coxa and a slight constriction of prefemur proximally on the posterior margin (Fig. 27A), leg-pair 7 with strongly modified coxa, anteriorly projecting in a large mesal slightly curved horn (Fig. 27B), trochanter with strong setae.

Gonopods. Parallel, distal solenomeral processes of telopodites crossing (Fig. 18A, B, D, E). Each gonopod with two asymmetrical clavate prefemoroid processes, with **pf1** broader and more setose than **pf2** (Figs 18A, B, 19); coxa with a large rounded anterior lobe (**Ca**) and a smaller lateral one (**Cl**) (Fig. 19A); long and falcate mesal coxal process (**b**), reaching the distal part of the telopodite and distally projecting in a pointed tip (broken in the studied specimen). Telopodite (**T**) with a long and uniformly broad stem, distally abruptly expanding in an apically folded subquadrate plate, with, in posterior view, a slightly oblique and indented lateral margins (Fig. 18A), in anterior view (Fig. 18B) showing a darkly pigmented jagged lamella (**dl**) projecting antero-laterad (Fig. 18C–E), and a strong hook-shaped curved process pointing distad, gently narrowing towards its apex (Figs 18, 19) and bifurcating into the opening of the solenomere (**s**) and parasolenomere (**ps**).

Distribution. Shangrila and Lijiang County, Yunnan, and Mangkang/Markam? County, Tibet Autonomous Region, China (Fig. 28).

Comments. The structures on the tip of the falcate mesal coxal process of the gonopod were also illustrated in the original description of *P. viriosa* by Wang and Zhang (1993) although never mentioned in the description of the species (Wang and Zhang 1993: 382, fig. 21).



Figure 17. *Paracortina viriosa* (Wang & Zhang, 1993), male (Rd 5345 ZMUM) **A, B** head and anterior pleurotergites **A** lateral view **B** frontal view **C, E** midbody pleurotergites **C** lateral view **D** leg-pairs 1-5 posterior view **E** dorsal view.

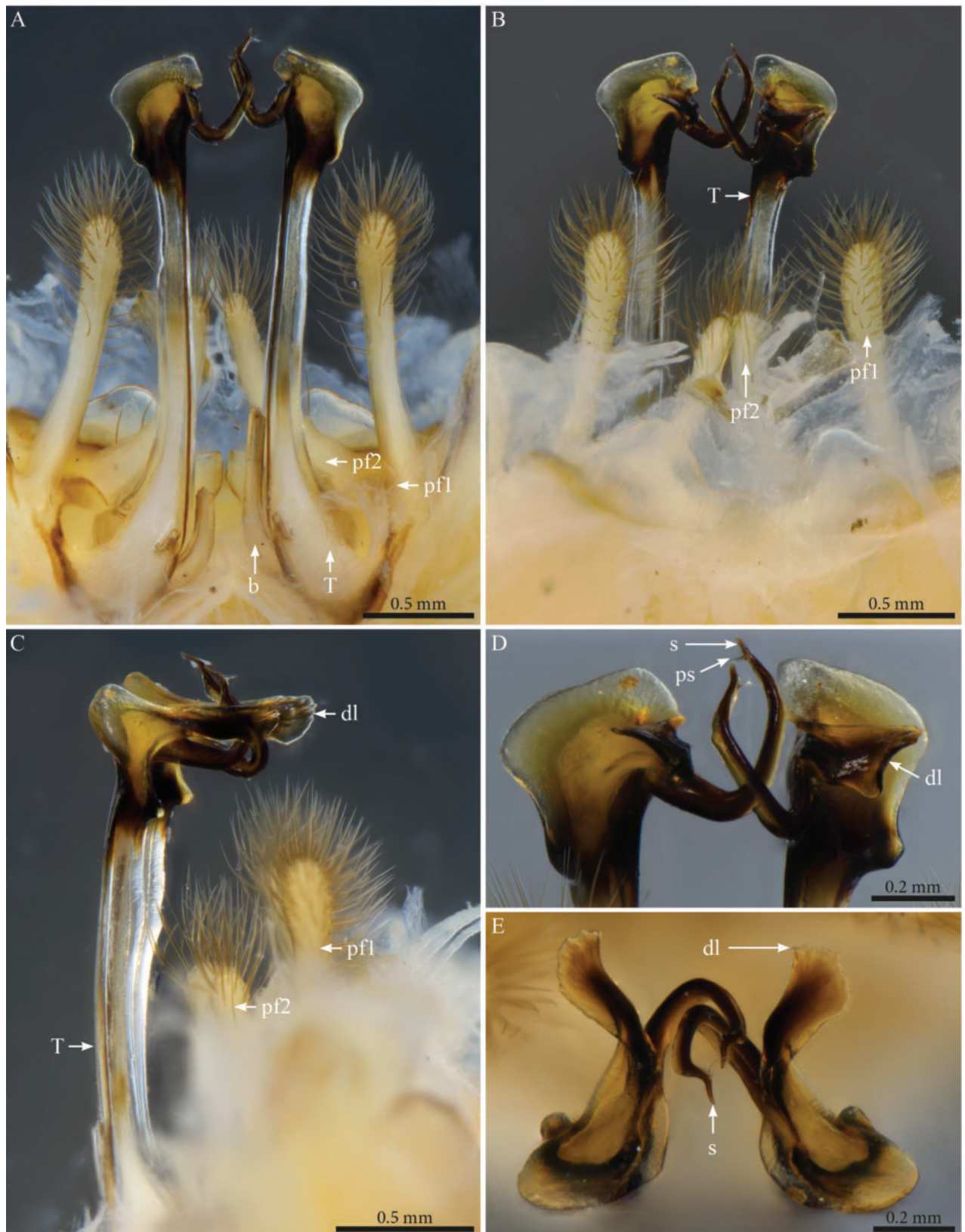


Figure 18. *Paracortina viriosa* (Wang & Zhang, 1993), male (Rd 5345 ZMUM), gonopods **A** posterior view **B** anterior view **C** lateral view **D, E** telopodites distal part, **D** anterior view **E** ventral view. Abbreviations: b = falcate mesal process of coxa; dl = distal lamella of telopodite; pf1 = prefemoroidal process 1; pf2 = prefemoroidal process 2; ps = parasolenomere; s = solenomere; T = telopodite.

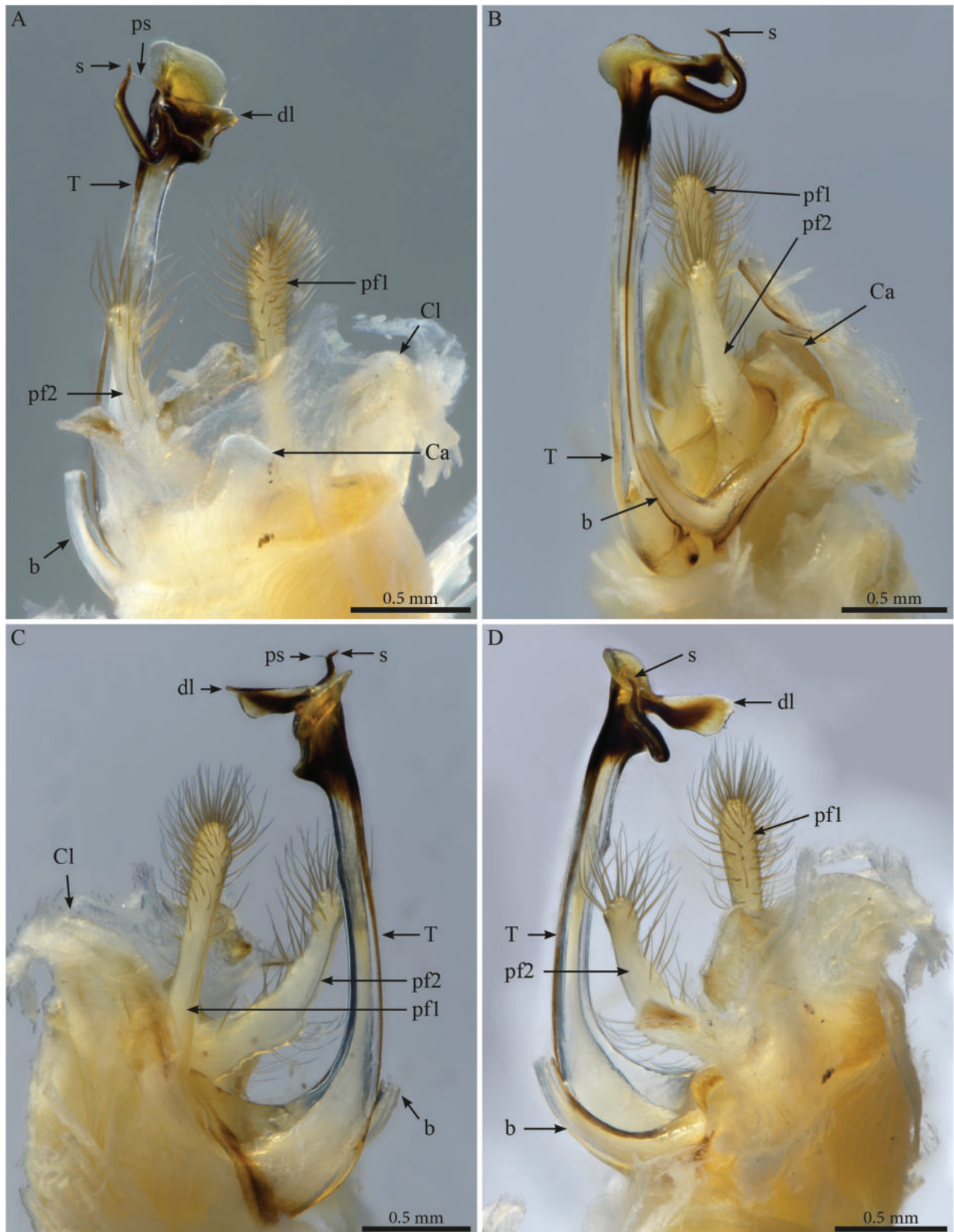


Figure 19. *Paracortina viriosa* (Wang & Zhang, 1993), male (Rd 5345 ZMUM), right gonopod **A** anterior view **B** posteromesal view **C** lateral view **D** mesal view. Abbreviations: b = falcate mesal process of coxa (broken); Ca = anterior lobe of coxa; Cl = lateral lobe of coxa; dl = distal lamella of telopodite; pf1 = prefemoroidal process 1; pf2 = prefemoroidal process 2; ps = parasolenomere; s = solenomere; T = telopodite.

***Paracortina voluta* Wang & Zhang, 1993**

Figs 20–22, 27C, D, 28

Paracortina voluta Wang & Zhang, 1993: 377, figs 6–9; Stoev and Geoffroy 2004: 103, key; Liu and Tian 2015: 139, key.

Studied material. 2 males, 1 female, CHINA, Sichuan Province, NW Pingchuan, 27°40'07"N, 101°44'04"E, 18.07.2011, I. Belousov & I. Kabak leg. (Rd 5346 ZMUM), Akkari det. 2023.

Diagnosis. Most similar to *P. viriosa* in the shape of the distal part of the telopodite with two main folds and a strong hook-shaped median processes, differing in the earlobe-shaped distal process and the smaller and more distally located anterior lamella.

Descriptive notes. Male with 56PTs+Telson. Length ca 49.5 mm. Live colour unknown. Preserved specimen with a brownish general colour, legs and antennae dark brown (Figs 20, 21A), Head with dark pigmentation on the vertex and frons (Fig. 20B, C), mandibular stipes and gnathochilarium with yellowish spots. Fields of ommatidia subtriangular, composed of ~ 47 ommatidia in ten rows (Fig. 20B, C). Organ of Tömösváry very large, ~ 1.2 mm, situated close to and touching anterior side of eye (Fig. 20B). Prozona brownish sputtered with a paler colour; metazona dorsally dark tawny-brown, especially on crests, anterior part pale with brown alveolate spots (Fig. 20A, B).

Male sexual characters. Head with a protruding triangular projection on vertex (Fig. 20B, C, 21A). Leg-pairs 1 and 2 reduced and more setose than the rest, showing prefemoral and tarsal brushes, leg-pair 2 with a large anterior process on coxa and posterior gonopore (Fig. 21A), leg-pair 4 with anterior triangular projection on coxa (Fig. 21A), leg-pair 6 with one short triangular mesal process and a smaller lateral one on coxa, prefemur proximally slightly constricted on the posterior margin (Fig. 27C), leg-pair 7 with one mesal hyaline pointed process and a rounded projection surmounted by a similar but slightly smaller one, trochanter with a tuft of strong setae (Fig. 27D).

Gonopods. Parallel, slightly converging with the distal solenomeral processes of telopodites crossing (Fig. 21B–D). Each gonopod with two asymmetrical, short, clavate prefemoroid processes with (**pf1**) broader and more setose than (**pf2**) (Figs 21B, C, 22); coxal anterior lobe lower than the lateral lobes low (Fig. 21C), long and falcate coxal process (**b**) reaching the distal part of the telopodite and apically pointed (Figs 21C, 22A, B, D). Telopodite (**T**) with a long stem, distally expanding in an earlobe shape with rounded lateral margin seen in posterior view (Fig. 21C, D), in anterior view as an oblique subtrapezoidal plate (Fig. 21B), with a transparent lamella (**dl**) attached on the lower part, marking and S-shape and serrated on the lower margin (Fig. 21B), mesal process curved upward, twisted and narrowing towards its apex (Figs 21B–D, 22A, B), bifurcating into the opening of the solenomere (**s**) and parasolenomere (**ps**).

Distribution. This species was originally described from Ya Jang (= Jajiang) County, Sichuan, China. Here we add a new record from Yanyuan County which is ~ 250 km away in a straight line from the type locality (Fig. 28).



Figure 20. *Paracortina voluta* Wang & Zhang, 1993 (Rd 5346 ZMUM) **A** female habitus, lateral view **B, C** male head and anterior pleurotergites **B** lateral view **C** frontal view.



Figure 21. *Paracortina voluta* Wang & Zhang, 1993, male (Rd 5346 ZMUM) **A** head, anterior pleurotergites and legs, frontal view **B–D** gonopods **B** anterior view **C** posterior view **D** telopodite distal part. Abbreviations: b = falcate mesal process of coxa 2; pf1 = prefemoroidal process 1; pf2 = prefemoroidal process 2; ps = parasolenomere; s = solenomere; T = telopodite.

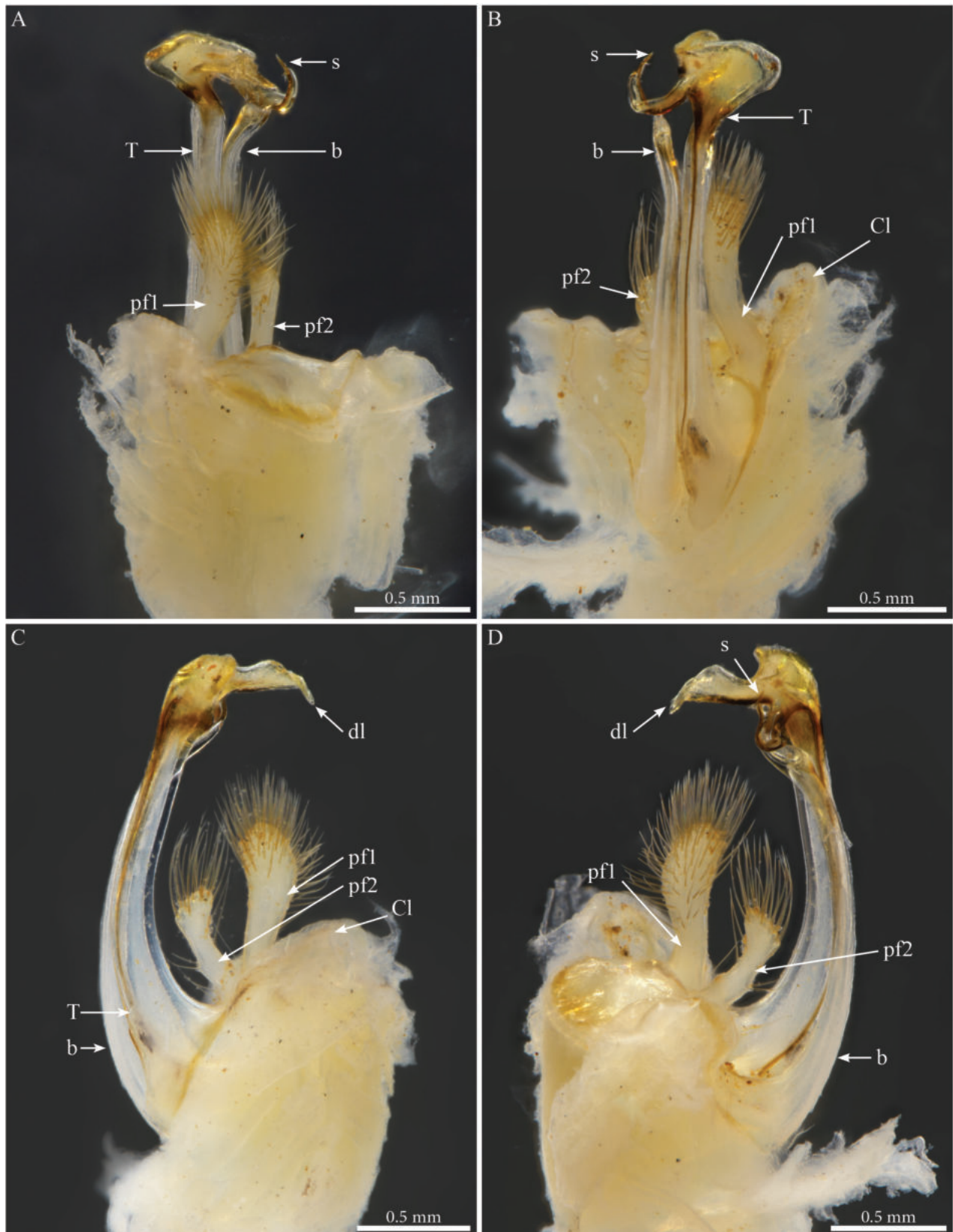


Figure 22. *Paracortina voluta* Wang & Zhang, 1993, male (Rd 5346 ZMUM), left gonopod **A** anterior view **B** posterior view **C** lateral view **D** mesal view. Abbreviations: b = falcate mesal process of coxa; Cl = lateral lobe of coxa; dl = distal lamella of telopodite; pf1 = prefemoroidal process 1; pf2 = prefemoroidal process 2; s = solenomere; T = telopodite.

Comments. Although we have no doubt about the identity of the studied specimens, when comparing the gonopod of the new material in mesal view (Fig. 20D) with the drawing provided in the original description of *P. voluta* (Wang & Zhang, 1993: fig. 6), we noticed a few differences in the shape of the distal process of the telopodite, with the mesal process more twisted and curved, the anterior lamella more serrated and turned downwards, and the “s-twist” more obvious in our specimen (visualised with a rounded notch in mesal view).

Both available identification keys for the family Paracortinidae (Stoev and Geoffroy 2004; Liu and Tian 2015) mention eight or nine “macrosetae” on the small prefemoroidal process and use this character to separate the species from its congener *P. leptoclada*. However, in the specimens we examined, this number greatly exceeds that (see Figs 21, 22), proving that this character is not reliable for species discrimination.

***Paracortina yinae* Liu & Tian, 2015**

Fig. 28

Paracortina yinae Liu & Tian, 2015: 131, figs 23–45.

Diagnosis. Gonopods very similar to those in *Paracortina zhangii*. The species, can, however, be recognised by the presence of a spiniform mesal process on coxa 6, and a different shape of the coxa of leg 7 (Liu and Tian 2015).

Descriptive notes. (after Liu and Tian 2015) Species with 53–61 PTs + telson, general colour pale brownish yellow, head with a well protruding beak-shaped projection, ommatidia 21–32 in four irregular rows.

Male sexual characters. Head with a small beak-shaped projection on vertex (Liu and Tian 2015: fig. 23), PT6 strongly enlarged, leg-pairs 1 and 2 reduced and more setose than the rest, leg-pair 2 with a small anterior process and posterior opening of the gonopores, leg-pair 6 with a small pointed mesal process on coxa, leg-pair 7 with a mesal slender and pointed triangular process and a large rounded projection on coxa (Liu and Tian 2015: figs 30, 31), coxal sacs noticeable on leg-pairs 3–25.

Gonopods. Parallel, with a general slender aspect. Each gonopod with one prefemoroidal process that is clavate, slender, and setose (**pf1**), coxa with an anterior lobe and a short falcate mesal process (**b**) not reaching mid-length of the telopodite. Telopodite (**T**) broad at the base, gently narrowing distad, distal part dark with a lamella extending in a subtriangular fold, apically blunt and almost rounded, subapically more acuminate and the base slightly uneven, and a short slender bifurcated process, terminating in solenomere (**s**) and parasolenomere (**ps**).

Distribution. Cave 1, 24.875732°N, 105.150143°E, Yanchang Village, Tianshengqiao Town, Longlin County, Guangxi, South China (Fig. 28).

Comments. Very similar to *P. zhangii* (see below), differing mostly in the presence of small, pointed, mesal processes on coxae 6 in males and different shape of the coxa on leg-pair 7 (Liu and Tian 2015). The gonopods of the two species are strikingly similar but an accurate comparison is virtually impossible as the authors did not illustrate the gonopods in the exact same view.

***Paracortina zhangii* Liu & Tian, 2015**

Fig. 28

Paracortina zhangii Liu & Tian, 2015: 125, figs 1–22.

Diagnosis. Most similar to *Paracortina yinae*, from which it differs only in the absence of the spiniform process on the mesal side of coxa 6, different shape of coxa 7 (Liu and Tian 2015).

Descriptive notes. (based on Liu and Tian 2015) Species with 55–58 PTs +telson, general colour pale brownish yellow, head with a well protruding beak-shaped projection, ommatidia: 16–23 in four irregular rows.

Male sexual characters. Head with a large beak-shaped projection on vertex (Liu and Tian 2015: figs 1, 2), PT6 strongly enlarged, leg-pair 1 and 2 reduced and more setose than the rest, leg-pair 2 with a small anterior process and posterior opening of the gonopores, leg-pair 6 with no modifications on coxa, leg-pair 7 with a protruding mesal triangular process and a very large subtriangular-rounded projection on coxa (Liu and Tian 2015: fig. 8), coxal sacs noticeable from leg-pairs 3–23.

Gonopods. Parallel, with a general slender aspect. Each gonopod with one clavate, slender, setose prefemoroidal process (**pf1**), coxa with an anterior lobe and a short falcate mesal process (**b**), not reaching mid-length of the telopodite (**T**). Telopodite broad at the base and gently narrowing distad, distal part dark with a transparent lamella (seen in lateral view; Liu and Tian 2015: fig. 9) extending in an apical fold, and laterally in a second one circling in part of the thin bifurcated branch terminating in solenomere (**s**) and parasolenomere (**ps**).

Distribution. Cave Qiaoxia Dong 24°03.008'N, Rongdu Village, Qianxinan Zizhizhou, Ceheng County, Guizhou, southern China. The coordinates in Liu and Tian (2015) include a typo (24°03.008'N instead of 25°03.008'N), rendering the type locality appearing 100 km south of their locality description and map. In the distribution map (Fig. 28), we used the corrected coordinates.

Comments. The interpretation of the distal part of the telopodite remains tentative and rendered difficult as it is entirely based on the original description of the leg-pair 7 and gonopods (Liu and Tian 2015: figs 8–10, 15–18).

Genus *Scotopetalum* Shear, 2000, stat. rev.

Scotopetalum Shear, 2000: 96, fig. 1; Stoev and Geoffroy 2004: 94, figs 1–8 (proposed synonymy with genus *Paracortina*).

Type species. *Scotopetalum warreni* Shear, 2000.

Included species. *Scotopetalum chinensis* (Stoev & Geoffroy, 2004), comb. nov.; *Scotopetalum warreni* Shear, 2000.

Diagnosis. Differs from *Angulifemur* by having parallel stems of telopodites; from *Paracortina* by the absence of large anteromedian subfalcate coxal process, and from the genus *Crassipetalum* gen. nov. by the much smaller prefemoroidal process/es and the very reduced subfalcate coxal process (**b**).

Comments. Shear (2000) described the genus *Scotopetalum* in the family Schizopetalidae, with the following diagnosis: “distinct from other genera of Schizopetalidae in lacking any indication of a sternum or coxal process in the gonopod, and in having no crest transition (full number of primary crests present on all segments). Each hemipleurite bears a series of five setae; all are in anterior position on segments 1–4, setae *b*, *d*, and *e* migrating posteriorly on segment 5, and all setae are posterior on segment 6.” The author doubted the validity of family Paracortinidae, which he believed could only have a status of subfamily within Schizopetalidae. He also interpreted the long falcate process typical for the family to be of a sternal origin.

In their review of the family, Stoev and Geoffroy (2004) described two new species of Paracortinidae from China and Vietnam, with the Chinese species (*Paracortina chinensis*) being quite similar to the species previously described by Shear (2000). The authors correctly noted this fact and compared the two species, highlighting the characters that distinguish them. They also synonymised *Scotopetalum* with *Paracortina*, considering the absence of a falcate coxal process and a second prefemoroidal process to be variable characters in the family. However, Stoev and Geoffroy (2004) failed to compare the structure of the telopodite in detail, which is quite specific in these two species. After a careful analysis, and now having much more material for comparison (including some of the *Paracortina* species described by Wang and Zhang 1993), we believe that *Scotopetalum* is a clearly defined morphological group and here we revive its original status.

***Scotopetalum chinensis* (Stoev & Geoffroy, 2004), comb. nov.**

Figs 23–25, 27G, 28

Paracortina chinensis Stoev & Geoffroy, 2004: 94, figs 1–8.

Studied material. Paratypes: 1 male, 2 subadult females, China, Yunnan Region, Zheng Xiong County, Liao Jun Don Cave (Touristic cave), millipedes collected close to rat corpse, 17.08.1999, J. & B Lips leg. (BG-NMNHS-INV-00000006262), Stoev det. April 2004.

Diagnosis. Different from *Scotopetalum warreni* in the presence of a reduced mesal coxal process (vs absent in *S. warreni*), as well as the distal part of the telopodite. Also, in the number of ommatidia 30 ommatidia in five or six rows (vs 15 ommatidia in 6 rows), and by having 2+2 dorsal crests between poriferous crests (vs 6+6).

Descriptive notes. Corresponds to the description of the species as provided by Stoev and Geoffroy (2004); see also Figs 23, 24A, B.

Male sexual characters. Leg-pairs 1 and 2 reduced and more setose than the rest (Fig. 23B), leg-pair 2 with a small anterior process and posterior opening of the gonopores. Leg-pair 7 with a short mesal triangular process and a large, rounded projection on coxa, trochanter with a smaller, rounded projection covered with setae (Fig. 27G).

Gonopods. Parallel (Figs 24C, D, 25). One reduced, slender, and distally uniformly setose prefemoroidal process (less than half telopodite length)



Figure 23. *Scotopetalum chinensis* (Stoev & Geoffroy, 2004), comb. nov., male paratype (BG-NMNHS-INV-000000006262 NMNHS) **A, B** head and anterior pleurotergites **A** lateral view **B** frontal view **C** close-up of ommatidia and organ of Tömösváry.

(**pf1**). Coxa with a very reduced anterior lobe (**Ca**) (Fig. 25A), mesally with a triangular lobe (**a**) and a rudimentary posterior tooth (**b**) (Fig. 24D, 25B, C). Telopodite (**T**) with a uniformly slender stem, gently curved, distally with a broad notch (**n**) separating a downturned bifurcated process (Fig. 24C, D, 25) bearing the solenomere (**s**) and parasolenomere (**ps**), overpassing a shorter anteriorly directed process (**M**), and a third flattened and acuminate process (**k**) emerging laterally.

Distribution. Known from the caves Ke Ma Dong (Grotte du Brouillard Matinal), Liao Jun Dong (Tourist cave) and Da Hei Dong (Grande Grotte Noire) in Zhen Xiong County, Yunnan, China.

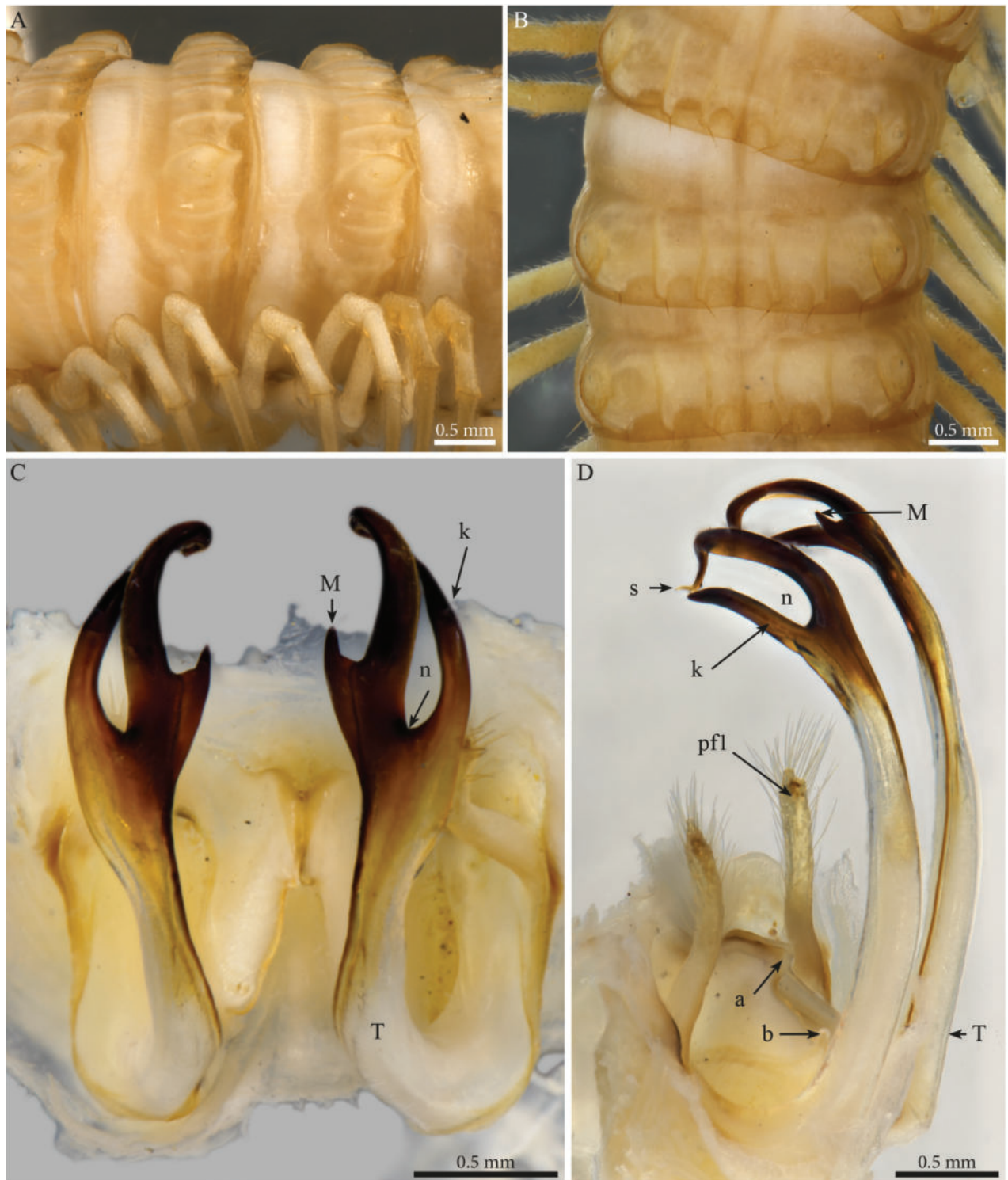


Figure 24. *Scotopetalum chinensis* (Stoev & Geoffroy, 2004), comb. nov., male paratype (BG-NMNHS-INV-00000006262 NMNHS) **A, B** midbody pleurotergites **A** dorsolateral view **B** dorsal view **C, D** gonopods **C** postero-ventral view **D** postero-lateral view. Abbreviations: a = mesal process of coxa; b = falcate mesal process of coxa; k = lateral process of the distal part of telopodite; M = mesal process of the distal part of telopodite; n = notch; pf = prefemoroidal process; s = solenomere; T = telopodite.



Figure 25. *Scotopetalum chinensis* (Stoev & Geoffroy, 2004), comb. nov., male paratype (BG-NMNHS-INV-00000006262 NMNHS) gonopods **A** left gonopod, anterior view **B** both gonopods lateral view **C** left gonopod, lateral view **D** both gonopods posterior view. Abbreviations: a = mesal process of coxa; b = falcate mesal process of coxa; Ca = anterior lobe of coxa; k = lateral process of the distal part of telopodite; M = mesal process of the distal part of telopodite; n = notch; pf = prefemoroidal process; ps = parasolenomere; s = solenomere; T = telopodite.

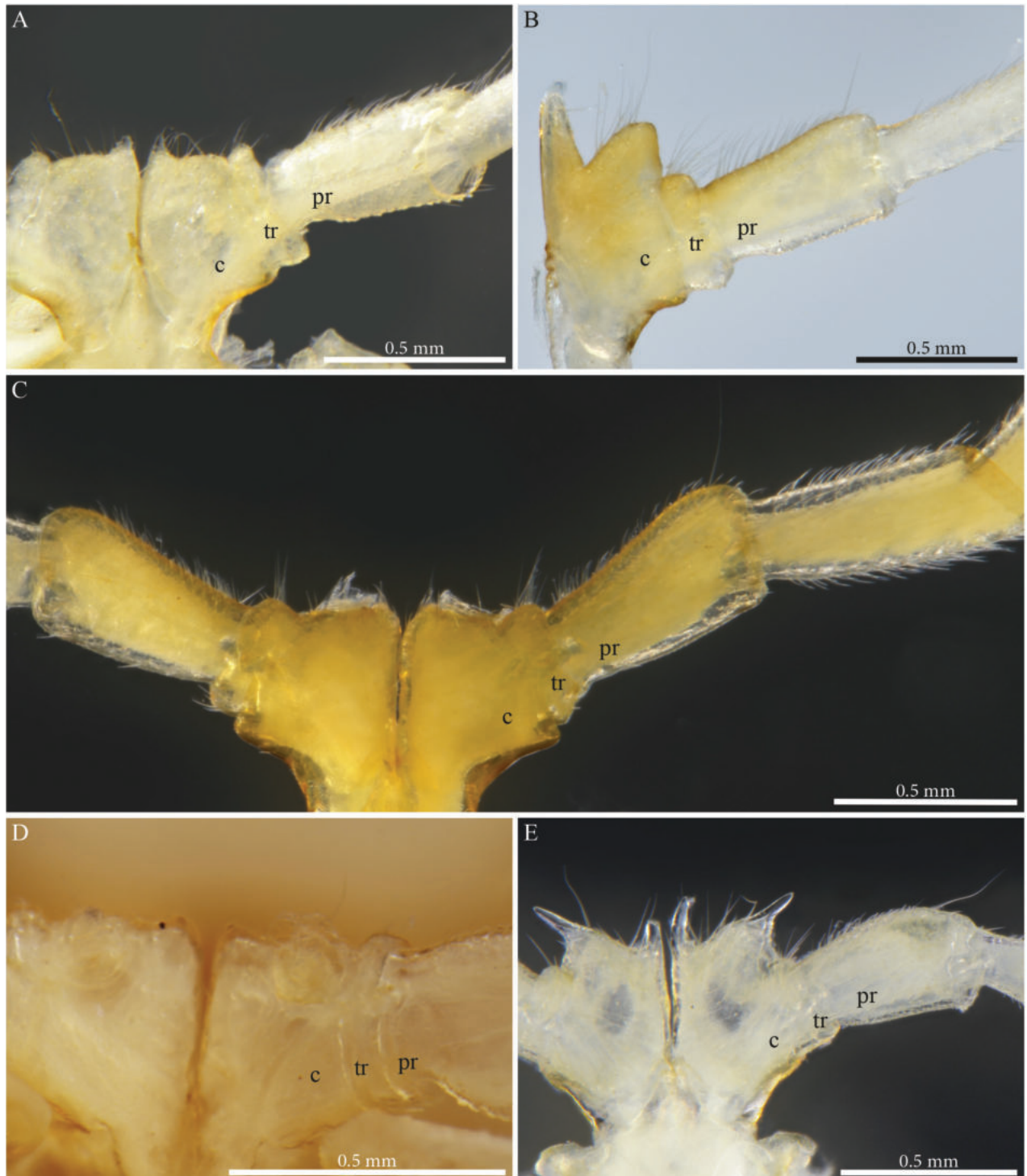


Figure 26. Modifications on leg-pair 6 and leg-pair 7 in adult males of species of Paracortinidae **A, B** *Angulifemur unidigitis* Zhang, 1997, male **A** leg pair **B** leg 7 **C** *Paracortina multisegmentata* Stoev & Geoffroy, 2004, male paratype leg pair 7 **D, E** *Paracortina thallina* (Wang & Zhang, 1993), male **D** leg pair 6 **E** leg pair 7. Abbreviations: c = coxa; pr = prefemur; tr = trochanter.

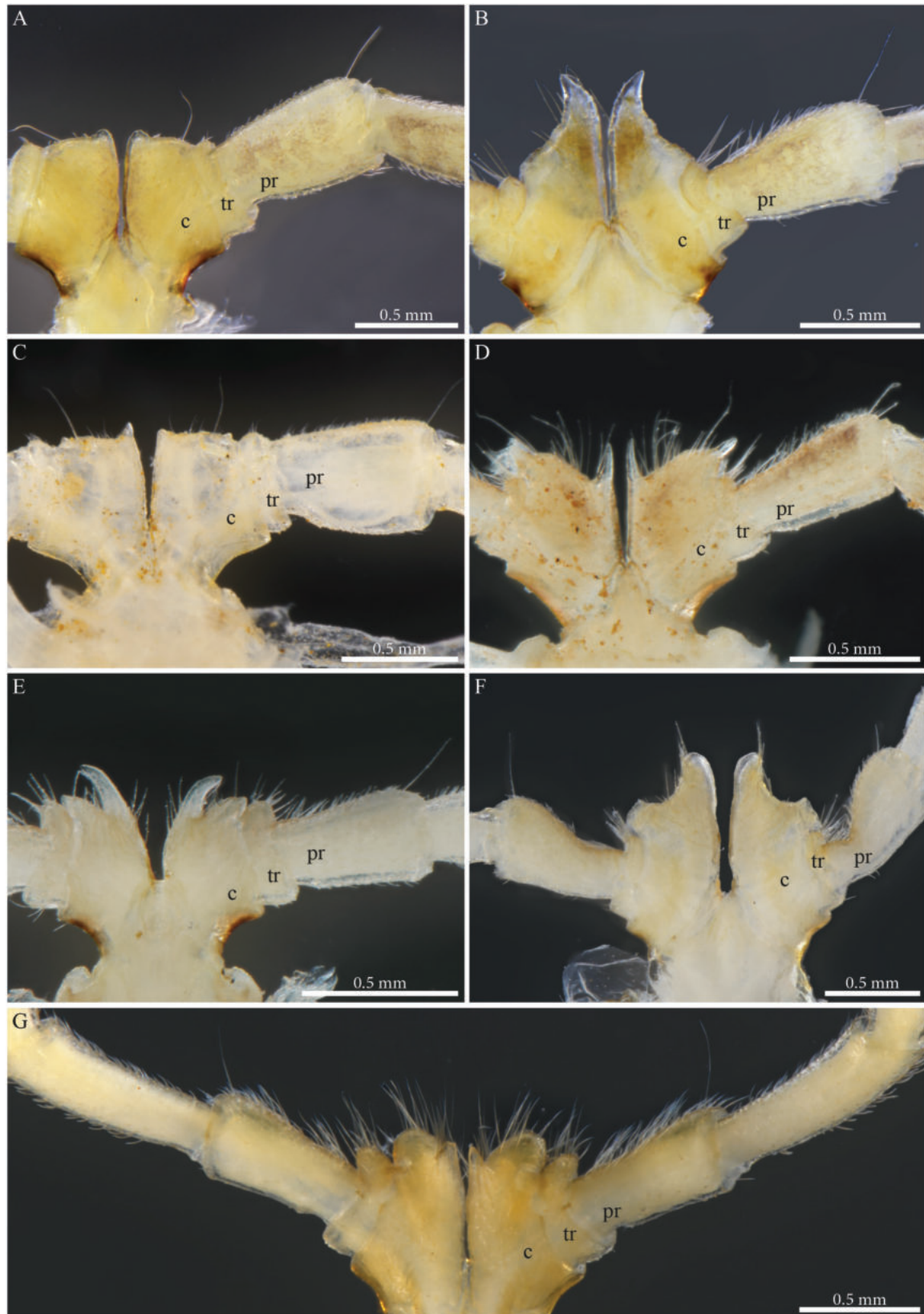


Figure 27. Modifications on leg-pair 6 and leg-pair 7 in adult males of species of Paracortinidae **A, B** *Paracortina viriosa* (Wang & Zhang, 1993), male **A** leg pair 6 **B** leg pair 7 **C, D** *Paracortina voluta* Wang & Zhang, 1993, male **C** leg pair 6 **D** leg pair 7 **E** *Paracortina asciformis* Akkari & Stoev, sp. nov., male holotype, leg pair 7 **F** *Paracortina kabaki* Akkari & Stoev, sp. nov., male holotype, leg pair 7 **G** *Scotopetalum chinensis* (Stoev & Geoffroy, 2004) comb. nov., male paratype, leg pair 7. Abbreviations: c = coxa; pr = prefemur; tr = trochanter.

Scotopetalum warreni Shear, 2000

Fig. 28

Paracortina warreni Shear, 2000: 87, fig. 1 Stoev and Geoffroy 2004: 93.

Diagnosis. Different from *Scotopetalum chinensis* in the complete absence of the mesal coxal process (vs a reduced tooth-shaped process in *S. chinensis*), as well as the distal part of the telopodite. Also, the presence of 15 ommatidia in three rows and 6+6 dorsal crests between poriferous crests.

Descriptive notes. Species with 53 PTs +telson, general colour yellowish-tan, head without modifications, 6+6 dorsal crests between poriferous crests, 15 ommatidia in three rows, pleurotergal setae 5+5, coxal sacs on legpairs 3–19, coxa 7 unmodified (meso-ventral thorns). Gonopods: parallel (based on Shear 2000: fig. 1). One reduced slender and distally uniformly setose prefemoral process (< ½ telopodite length) (**pf1**). Coxa with an anterior triangular coxal lobe (**a**). Telopodite (**T**) with a uniformly slender and gently curved stem, distally with a broad notch (**n**) separating an apical curved process pointing anteriorly and a second downturned bifurcated process into solenomere (**s**) and parasolenomere (**ps**), overhanging a third flattened and acuminate process (**k**). At the level of the notch, a small hook-like process is inserted on the mesal side (Shear 2000: fig. 1, process **ttp**).

Comments. The species is only known from its original description thus not much can be said about its morphology nor the configuration of the gonopods in other views besides the lateral one (Shear 2000: fig. 1). Therefore, it remains unclear if the “hook-like basal process (**ttp**)” described for this species could actually be homologues with process (**k**) of *Paracortina chinensis*.

Distribution. Caves at Hong Mat, Hoa Binh, Vietnam. In the distribution map (Fig. 28), we used the original coordinates as stated by Shear (2000).

Identification key to the species of the family Paracortinidae (based on gonopods)

- 1 Telopodites proximally crossing **Paracortina multisegmentata**
- Telopodites parallel, distally crossing, or diverging **2**
- 2 Telopodite sinuous, broad at base, with a sharp angle at mid-length, distally twisting and narrowing *Angulifemur*..... **3**
- Telopodites parallel, sometimes distally crossing **4**
- 3 Coxal process falcate, almost reaching mid-length of the telopodital stem, distal part of telopodite with two spine-like processes surrounding the solenomere **A. tridigitis**
- Coxal process reduced, cone-shaped, distal part of telopodite with one well-developed tooth-shaped process **A. unidigitis**
- 4 One slender prefemoral process, coxa with an expanded rounded anterior lobe; coxal process absent; telopodite distally forked *Scotopetalum* ... **5**
- One or two prefemoral processes of different sizes, coxa with a long mesal process **6**
- 5 Distal part of telopodite with a short process **k**; 15 ommatidia in 3 rows; 6+6 dorsal crests between poriferous crests..... **S. warreni**
- Distal part of telopodite with a longer process **k**; 30 ommatidia in 5 or 6 rows; 2+2 dorsal crests between poriferous crests..... **S. chinensis**

- 6 Large prefemoroidal process, coxa with very large mesal process *Crassipetalum* gen. nov. 7
- One or 2 significantly smaller and thinner prefemoroidal process/es, coxa with smaller lobes and a shorter falcate process 8
- 7 Two prefemoroidal processes, one large ovoid process and a smaller one; distal part of telopodite complex, with 10 apices ***C. inflatum***
- One large and elongated prefemoroidal process, telopodite less complex ***C. magnum***
- 8 Telopodite with a thin stem, its distal part generally simple, curved or sinuous..... 9
- Telopodite with a broad stem, its distal part complex, greatly expanding, with lamellae and a hook-shaped bifurcated mesal process 10
- 9 One slender prefemoroidal process, coxal process short and slender (less than half the length of the telopodite); telopodite distally gently curved, with a small, reduced lamella ***P. zhangi* and *P. yinae****
- Two slender prefemoroidal processes, coxal process larger and longer, reaching the distal part of the telopodite; telopodite sinuous, strongly narrowed towards the apex..... ***P. kyrang***
- 10 Two subequal prefemoroidal processes 11
- One large and one smaller prefemoroidal processes 12
- 11 Distal part of telopodite with a broad lateral folded lamella ***P. leptoclada***
- Distal part of the telopodite with a sinuous, differently oriented lamella ***P. thallina***
- 12 Distal part of the telopodite expanded proximo-distad in an axe-shaped process ***P. asciformis***
- Distal part of the telopodite different..... 13
- 13 Distal part of the telopodite with a broad subrectangular or dome-shaped lobe (lateral view), of which the apical part downturned, crossing with the curved process of the solenomere..... 14
- Distal part of the telopodite with a subquadrate/earlobe-shaped process and a broad serrated lamella 15
- 14 Distal part of the telopodite as a subrectangular plate with a horizontal apical irregular margin (lateral view)..... ***P. carinata***
- Distal part of the telopodite as a dome-like process with a rounded apical margin and an anterior narrow downturned process..... ***P. stimula***
- 15 Distal part of the telopodite with two main processes 16
- Distal part of the telopodite with three main processes..... 17
- 16 Distal part of the telopodite earlobe-shaped with a rounded lateral margin in posterior view, anterior lamella rounded and transparent, located on the lower margin part of the distal process ***P. voluta***
- Distal part of the telopodite sub-quadrate with a slightly notched lateral margin in posterior view, anterior lamella subrectangular and darkly pigmented, located on the upper margin part of the distal process, the hook-shaped process with the solenomere longer and stouter ***P. viriosa***

* Species separated by the absence vs presence of a spiniform coxal process on leg-pair 6 and the processes on coxa 7 in adult males (Liu and Tian 2015)

- 17 Telopodite distal part with a subtrapezoidal serrated process and a short solenomere ***P. serrata***
- Telopodite (T) distal part with a large subrectangular lamella with serrated margin extending anterolaterally in a double horizontal ruffle, solenomere long, slender and curved, marking an almost 180 degrees fold ... ***P. kabaki***

Discussion

On the taxonomy of the family Paracortinidae and species affinities

The Asian millipede family Paracortinidae still represents a challenge for taxonomists although it has been the subject of several treatments and reviews, including new species descriptions. Initially, this family was described to include seven species placed in three genera (Wang and Zhang 1993), viz., *Paracortina* (*P. leptoclada*, *P. voluta*), *Relictus* (*P. stimula*, *P. thallina*) and *Altum* (*P. viriosa*, *P. serrata*, *P. carinata*), all from south China. The latter two were subsequently downgraded to a subgeneric level of *Paracortina* (Wang 1996; Wang and Mauriès 1996), later formally synonymised with *Paracortina* by Stoev and Geoffroy (2004). A second genus, *Angulifemur* Zhang, 1997 containing two species, both found in caves in Yunnan, was added to the family by Zhang (1997). That article, being among the last ones of Prof. Chong-zhou Zhang and published in an obscure outlet 'Contributions from Tianjin Natural History Museum' remained largely unknown to the myriapodologists for nearly a decade (Stoev et al. 2014). A few years later, Shear (2000) described another monospecific calipodidan genus, *Scotopetalum*, from caves in north Vietnam which he placed in the family Schizopetalidae. Stoev (2004) doubted this placement and suggested that the genus described by Shear (2000) belonged to the family Paracortinidae. Later, Stoev and Geoffroy (2004) reviewed the family and added two new species from Vietnam and China. Here, we erect a new genus, presenting a gonopod morphology that significantly differs from the other genera of the family. viz., *Crassipetalum* gen. nov., to accommodate *C. inflatum* and the new species *Crassipetalum magnum* sp. nov.

With the present paper, the number of species in the family Paracortinidae reaches 19 in four genera, which without doubt does not reflect the real diversity of the family given how poorly studied the group is in China, Vietnam, and neighbouring countries. Perhaps what rendered the taxonomy of the family controversial as well as determining the different species and/or assigning them to genera was the fact that the original descriptions of these taxa (Wang and Zhang 1993) posed a language impediment for most taxonomists who worked on the group despite the brief species accounts given in English. The illustrations, however, proved to be useful even though one to two views were provided at most, which is often not sufficient to properly understand the morphology of the complex gonopods and most species have remained known only from their original descriptions. Here, we rediscover and document three species of the genus *Paracortina* described by Wang and Zhang (1993), viz., *P. voluta*, *P. thallina*, and *P. viriosa*; we restudy one species of the genus *Angulifemur*, *A. unidigitis* based on the type series of its junior synonym *Paracortina wangi*, and we further provide micrographs of the species *Paracortina multisegmentata* and *Scotopetalum chinensis* comb. nov. based on their respective type materials.

In parallel to the shortcomings mentioned above, the taxonomy of this family did suffer from a choice of characters that mostly relied on variable habitual features in addition to discrepancies in the terminologies used to describe the gonopods, with no attempts to properly understand the structures and homologise them. Shear (2000) had already pointed out this issue more than twenty years ago, although he himself failed to properly understand at that time the taxonomic affinities of the genus he described, and he assigned it to the family Schizopetalidae. Wang (1996) made an isolated attempt to understand the relationships of the different species of *Paracortina*, using “cladistic analyses” but the results are not very coherent due to the poor choice of morphological characters. Here, we mostly follow the terminology proposed by Wang and Zhang (1993) and later by Stoev (2004), Stoev and Geoffroy (2004), and Enghoff et al. (2015). When possible, we tried to homologise the different structures, using the same abbreviations for those processes we think homologous or at least having a comparable placement and orientation in the gonopods. What we do not attempt at this stage is to hypothesise on the origins of the processes and we follow the already established terminology for the order. Although the gonopods in this family appear morphologically diverse, all the species assigned to Paracortinidae agree in having the following four characteristics:

1. anterior and lateral projections (lobes) of the coxa. These can be variable in shape, number but also size. Not much attention has previously been given to these structures unless for example when the anterior lobe is large and prominent;
2. coxal process, originating mesally and usually projecting mesoanteriad, that can be reduced (*Scotopetalum chinensis* comb. nov.) to very large, where it lies posterior to the telopodite (*Crassipetalum magnum* gen. nov., sp. nov.). However, in most species of the genus *Paracortina*, for example, this process is usually falcate, narrowing towards the tip and its size varies from mid-length of the telopodite to reaching its distal part;
3. one or two setose, clavate prefemoroidal process/es that appear on the anterolateral side of the gonopods in symmetrical or asymmetrical pairs or as one process, with a variable size that usually never exceeds the mid-length of the telopodite except in the genus *Crassipetalum*;
4. an elongate telopodite with a sometimes sinuous (*Angulifemur*, *Paracortina kyrang*) or curved (*Scotopetalum chinensis* comb. nov.) stem that is often expanded and complex distally (ex. *Paracortina serrata*, *P. kabaki* sp. nov.). In all species, a median curved process detaches from the apical part and points mesoanteriad, with a bifurcation at the tip bearing the solenomere and parasolenomere. This process has a characteristic hook-shape and the left and right often intersect in the genera *Paracortina* as well as *Crassipetalum* gen. nov.

Two species of *Paracortina* are quite different from their congeners, namely *P. multisegmentata* and *P. kyrang*: both are described from Vietnam and are geographically distant from the other species found in the Chinese provinces of Guangxi, Guizhou, Sichuan, Yunnan, and Tibet Autonomous Region (Fig. 28). *Paracortina multisegmentata* is the only representative of the family with proximally crossing telopodites and *P. kyrang* with strongly twisted telopodites. Both

species are also similar in having a low coxa with rounded lobes and shorter (than most species of *Paracortina*) subfalcate processes; additionally, the shape of the coxa on leg-pair 7 has a round projection surmounted by a small spine. However, the placement of these two species in the genus *Paracortina* remains tentative until more morphological and genetic evidence is available to elucidate their taxonomic position in the family.

Secondary sexual characters in the family Paracortinidae

In addition to their genitalia (gonopods, vulvae), adult males and females of the family Paracortinidae present a number of secondary sexual structures that affect various parts of their external morphology (Table 2). Adult females were occasionally described in previous taxonomic treatments, and they presented enlarged pleurotergites 1 and 2, a special setal arrangement on leg-pairs 1–3 (“brushes”), with leg-pair 2 strongly reduced anterior to female genitalia or cyphopods. Prefemora of leg-pairs 3 and 4 were also described as enlarged in *P. zhangii* (Liu and Tian 2015).

Adult males present secondary sexual characters on the head vertex, pleurotergites, and legs. While males of the genera *Crassipetalum*, *Scotopetalum*, and *Angulifemur* show an unmodified head vertex, all species of the genus *Paracortina* display a distally curved triangular projection on the vertex (unknown in *P. carinata* and *P. serrata*) or a beak-shaped projection (as in *P. zhangii* and *P. yinae*). These structures are in fact not uncommon in adult male millipedes and modifications on head vertex have also been observed in the callipodidan genus *Cyphocallipus* Verhoeff, 1909 from the Pyrenees (Mauriès 1978) and a few African species of the family Trichopolydesmidae (Polydesmida) from Cameroon (Golovatch et al. 2018). A “boletiform epicranial protuberance” was described and documented for several species of the African genus *Hemisphaeroparia* (Golovatch et al. 2018, 2019) and considered diagnostic for several species of the genus (ca 15 species). This “knob-like” structure could be different sizes, placed in a depression (e.g., *H. mouanko* Golovatch, Nzoko Fiemapong, Tamesse, Mauriès & VandenSpiegel, 2018), or have a shape as a “bundle of filaments” (e.g., *H. falcata* Golovatch, Nzoko Fiemapong, Tamesse, Mauriès & VandenSpiegel, 2018). The genus *Mabocus* Chamberlin, 1951 belonging to the same family is also characterised by the presence of such a head structure (Golovatch et al. 2019). The pyrgodesmid genus *Cryptocorypha* (Polydesmida, Pyrgodesmidae) also presents modified heads in adult males (Golovatch 2019). Secondary sexual structures on the head of adult males in millipedes have also been observed in Chordeumatida, and a remarkable example is perhaps that of *Adshardicus strasseri* Golovatch, 1981 (Antić and Makarov 2016: 20, fig. 10B, C), where the structure resembles to a certain extent those recorded in Callipodida. Other examples of Chordeumatida include the species *Bulgarosoma bureschi* Verhoeff, 1926 and *B. ocellatum* (Tabacaru, 1967) (see Strasser 1962: 450, fig. 17; Tabacaru 1967).

The leg-pairs 1–7 in most cases present secondary sexual characters in adult males. In fact, leg-pairs 1 and 2 are significantly smaller in all species, and just like in the adult females they are setose, showing prefemoral and tarsal brushes. Leg-pair 2 bears the gonopores posteriorly and in some species also an anterior process on coxa (Table 2). Leg-pair 3 is in most species unmodified, except in *P. viriosa* where it presents an anterior triangular mesal projection on the coxa (Fig. 11D).

Table 2. Secondary sexual characters in adult males of the family Paracortinidae (excluding the gonopods). modif. = modification, empty cells = no information.

Species/ male sexual chars except gonopods	leg-pair 1-2	leg-pair 3	leg-pair 4	leg-pair 5	leg-pair 6	leg-pair 7	head vertex	PT6 and 7	Coxal sacs	Tarsal pads
<i>A. tridigitis</i>	"comb-like tarsal spines" (Zhang 1997) reduced and setose, with prefemoral and tarsal combs		a small triangular anterior process	no modif	a small triangular hyaline mesal process on coxa	2 processes on coxa (Zhang 1997) a long subfalcate mesal process and a shorter larger triangular projection on coxa	no projection no projection		3-23	tarsal pads 3-10
<i>C. magnum</i>	reduced and setose	no modif	no modif	no modif	no modif	no modif	no projection	enlarged		
<i>C. infiatum</i>	reduced and setose	no modif	no modif	no modif	no modif	no modif	no projection	enlarged		
<i>P. ascaformis</i> sp. nov.	reduced and more setose than the rest, leg-pair 2 with a small anterior process	no modif	no modif	no modif	no modif	a protruding curved mesal process pointing laterad (Fig. 18B) and a shorter subtriangular one on coxa, trochanter with an anterior triangular projection covered with setae	a large beak-shaped projection			
<i>P. carinata</i>	no modif	no modif	no modif	no modif	no modif	no modif (Wang 1996)	no projection (Wang 1996)			
<i>P. kabaki</i> sp. nov.	reduced and more setose than the rest, leg-pair 2 with a small anterior process	no modif	no modif	no modif	no modif	a large cone-shaped and apically rounded mesal process on coxa, and an angular lateral margin separated by a notch; trochanter with an apical tuft of setae, prefemur with a strong constriction proximally on the anterior margin, then strongly swollen distally	a large beak-shaped projection			
<i>P. kyang</i>	reduced and setose, with prefemoral and tarsal combs; legpair 2 with an anterior process on coxa (Nguyen et al. 2023)					a round mesal projection and a small spine	A large projection (Nguyen et al. 2023)	strongly enlarged	3-26	tarsal pads until 126
<i>P. leptoclada</i>										
<i>P. multisegmentata</i>	reduced and more setose than the rest, showing prefemoral and tarsal combs	no modif	no modif	no modif	no modif	2 processes on coxa (Zhang 1997)	a large projection (Wang 1996)		3-18	3-10
<i>P. serrata</i>		no modif	no modif	no modif	no modif	a small mesal spine on coxa and a tuft of setae on trochanter	no projection	23)		
<i>P. stimula</i>						2 processes on coxa (Zhang 1997)	no projection (Wang 1996)			
<i>P. thallina</i>	reduced and setose, showing prefemoral and tarsal combs; leg-pair 2 with an anterior process on coxa	no modif	anterior triangular process on coxa	no modif	a small mesal tooth on coxa	one mesal and one lateral slender hyaline pointed process on coxa	a triangular protruding projection on vertex			
<i>P. viriosa</i>	reduced and setose, showing prefemoral and tarsal combs; leg-pair 2 with a large anterior process on coxa	anterior triangular projection	anterior triangular projection on coxa	no modif	a small rounded mesal projection on coxa and a slight constriction of prefemur proximally on the posterior margin	strongly modified coxa, anteriorly projecting in a large mesal slightly curved horn (Fig. 27B), trochanter with strong setae	a small projection on vertex			
<i>P. voluta</i>	reduced and setose, showing prefemoral and tarsal combs; leg-pair 2 with a large anterior process on coxa	no modif	anterior triangular projection on coxa	no modif	a short mesal triangular process and a smaller lateral process on coxa; prefemur slightly constricted proximally on the posterior margin	one pointed mesal hyaline process and a rounded projection surmounted by a similar but slightly smaller one, trochanter with a tuft of strong setae	a protruding triangular projection on vertex			
<i>P. yinae</i>	reduced and more setose than the rest, leg-pair 2 with a small anterior process				a small pointed mesal process on coxa	a slender mesal and pointed triangular process and a large rounded projection on coxa	a small beak-shaped projection on vertex		3-25	3-15
<i>P. zhangji</i>	reduced and more setose than the rest, leg-pair 2 with a small anterior process				no modif	a protruding mesal triangular process and a very large subtriangular-rounded projection on coxa	a large beak-shaped projection		3-23	3-15
<i>S. chinensis</i>	reduced and more setose than the rest, leg-pair 2 with a small anterior process	no modif	no modif	no modif	no modif	a short mesal triangular process and a large rounded projection on coxa, trochanter with a smaller rounded projection covered with setae.	no projection		3-9/10	3-18
<i>S. warreni</i>	"dense brushes of dark setae". Shear 2000					"with small mesoventral thorns" Shear 2000	no projection		3-19	3-19

In *Paracortina thallina*, *P. viriosa*, and *P. voluta*, the coxa of the same leg-pair presents an anterior mesal projection. Leg-pair 5 is unmodified in all species, while leg-pair 6 and, especially leg-pair 7, bear the most noticeable structures. When modified, leg-pair 6 displays one to two small anterior small processes on the coxa and enlarged prefemora. On the other hand, leg-pair 7 will display a more pronounced sexual dimorphism, with what appears so far to be species-specific shapes of the coxa (Table 2; Figs 26, 27). Whether these structures represent taxonomically or phylogenetically informative characters remains to be explored although their location, for instance, on the coxa of leg-pair 7 seem to be fixed for each species. It is noteworthy that the two species we considered to have an uncertain taxonomic position within the family Paracortinidae (*P. multisegmentata* and *P. kyrang*) do present more or less similar patterns of modification on coxa 7 (Fig. 26C; Nguyen et al. 2023), very different from the remaining species of *Paracortina* (typically with one or two sets of barely conspicuous to very prominent projections). Wang (1996) recorded no modifications on coxa 7 for the species *P. carinata* and *P. stimula* but this needs to be verified with the rediscovery of these species as he, in the same paper, recorded modifications in the species *P. serrata* and *P. leptoclada*, which in both cases has been revealed as erroneous (see Table 2). On the other hand, *S. chinensis* (Fig. 27G) displays a rather unique morphology of the coxa 7 that does not seem to match the description for its congener *S. warreni* (Shear 2000).

Just like the modifications of the head vertex, secondary sexual modifications on legs 1–7 in Callipodida and Chordeumatida are common and regularly appear in species descriptions. The modification of male leg-pair 7 has been considered as a good taxonomic character for the genera *Balkanopetalum* Verhoeff, 1926 (Schizopetalidae), *Dorypetalum* Verhoeff, 1900 (Dorypetalidae), *Apfelbeckia* Verhoeff, 1896 (see Stoev and Enghoff 2003, 2006, 2008), and *Hepetium* Loomis, 1937 (see Loomis 1937).

The distribution of coxal sacs on leg-pairs 3–23 was proposed by Stoev and Geoffroy (2004) and Enghoff et al. (2015) as a possible character that defines the family. However, this number does not appear to be stable since different authors provided different accounts (see Table 2). In many instances, it is simply not possible to see these with certainty beyond the leg-pair 16, so whether the coxal sacs distribution represents an apomorphy for the family remains to be assessed. Many of these structures appear in the Callipodida's sister group Chordeumatida but they have never been the subject of a close morphological or anatomical study; thus any interpretation of their putative function remains tentative though it is almost certain that they play a role during mating and copulation as they are completely absent in juveniles and immature specimens. The coxal sacs are known to serve for sperm storage in Chordeumatida (Koch 2015).

Troglomorphic species and convergent characters

Nine species of the family Paracortinidae were described from caves, including all members of the genera *Crassipetalum*, *Scotopetalum*, and *Angulifemur*, and four species of the genus *Paracortina* (*P. multisegmentata*, *P. kyrang*, *P. yinae*, and *P. zhangii*). These species exhibit (to a different extent in each species) classical troglomorphic characters, such as depigmentation of the cuticle, reduction in the number of ommatidia, elongation of legs and antennae, and, in

extreme cases, even an increase in the number of pleurotergites, reaching 85 in *P. multisegmentata*. The highest degree of troglomorphy is observed in *Angulifemur unidigitis*, *S. warreni*, and especially *P. kyrang*. Completely blind species are, however, lacking, also the case of Sinocallipodidae, the most speciose family in the area (Stoev and Enghoff 2011).

Geographical distribution

The family Paracortinidae is the most diverse family of the order Callipodida in Southeast Asia. The highest species diversity was found in the Chinese provinces of Yunnan (3 genera, 10 species) and Sichuan (1 genus, 3 species). Representatives of the family are also found in the provinces of Gansu, Guizhou, and Guangxi, as well as in the Tibet Autonomous Region. Outside China, the family is also found in North Vietnam in Thanh Hóa and Cao Bang provinces.

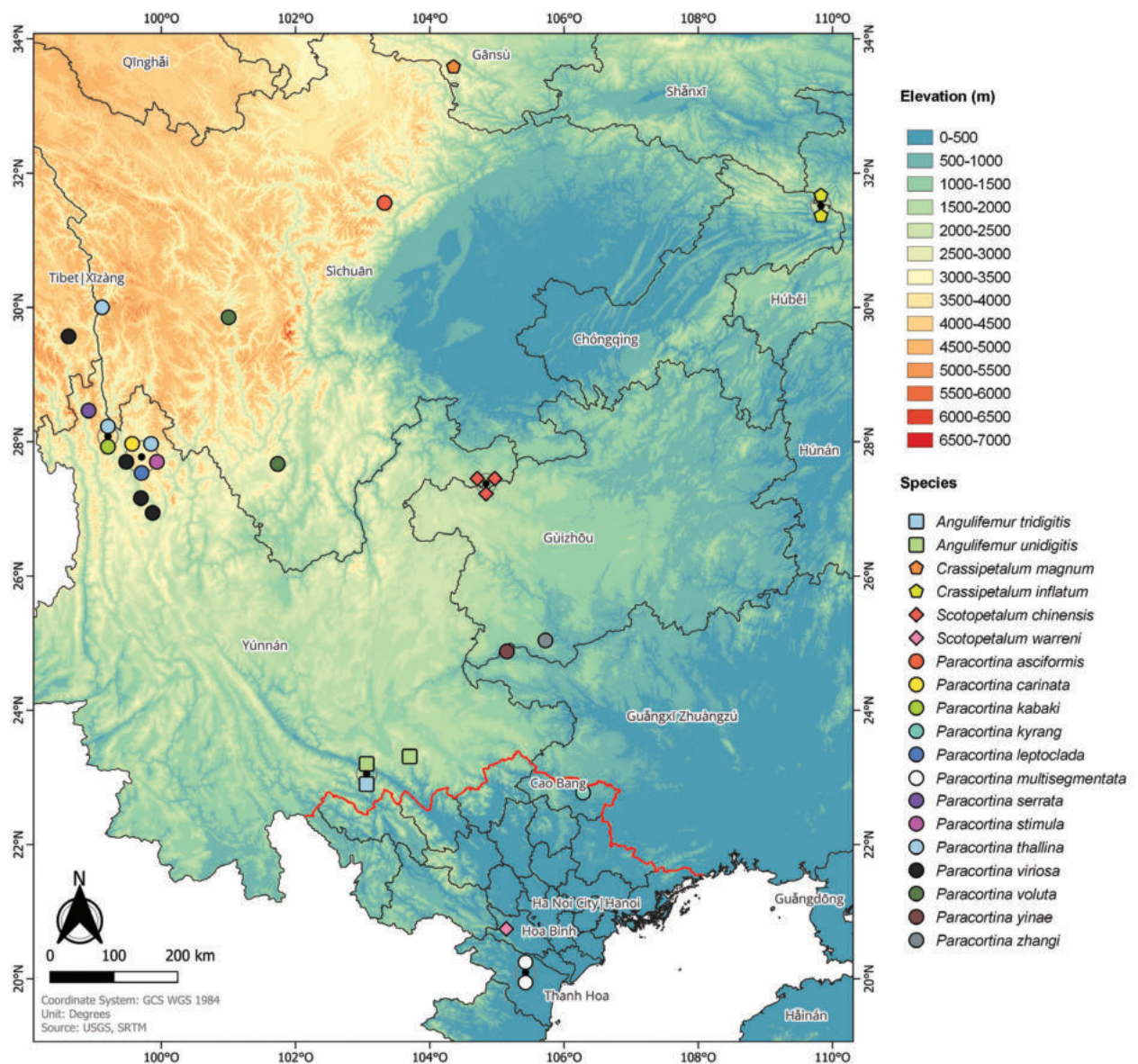


Figure 28. Distribution map of Paracortinidae in China and Vietnam.

The northern distribution limit of the family runs through the middle of Sichuan, ca the 32nd North parallel, the only exception being *Crassipetalum magnum* sp. nov., with an even more northerly locality in the Zhou-qu area of Gansu Province (Fig. 28). It is possible that the family reaches further northeast, as female calpodidans from Cisian-shan, 25 km south of Nanjing (Jiangsu Province) were reported as *Bollmania* sp. by Golovatch (1981), 12 years before the description of the family Paracortinidae. This find was later commented upon by Shear et al. (2003) as likely belonging to an undescribed genus and species of the family Paracortinidae (see also Stoev and Enghoff 2005). In the south, the family reaches ~ 20 N parallel in the province Thanh Hóa in Vietnam, where the species *S. warreni* and *P. multisegmentata* have been reported. From west to east, the family extends from eastern Tibet and western parts of Sichuan and Yunnan to northeastern Vietnam, with the easternmost locality being *Crassipetalum inflatum* from Chongqing in China. Thus, until now, members of the family are known from ~ 97th to 106th Eastern meridian. If the Nanjing area record turns out to be truly representative of the family, it will be the easternmost of all. It is likely that the distribution of the family Paracortinidae also cover northern Myanmar and eastern Laos, and possibly northern Sichuan Province, central and western Yunnan, northwestern Guizhou, and Guangxi. In Vietnam, the family is probably also distributed in the northwestern parts, in the provinces of Hà Giang, Lao Cai, for example.

Acknowledgements

Many thanks are due to Dragan Antić (University of Belgrade, Serbia) for the insightful discussions and comments on an earlier version of the manuscript, to Henrik Enghoff (The Natural History Museum of Denmark), and to Willam Shear (Virginia, USA) for their useful comments and corrections. The ZooKeys copy editor Nathalie Yonow carefully edited the final version of the manuscript. We are also obliged to Sergei Golovatch (Institute for Problems of Ecology and Evolution, Russian Academy of Sciences) for providing a large part of the research material. Our thanks are extended to Nathalie Fial (University of Vienna, Austria) for producing the distribution map of the species. PS is grateful to Shuqiang Li and Kaibaryer Meng for hosting him at the Institute of Zoology, Chinese Academy of Sciences in November 2013. The visit of PS was part of the project "Speciation and conservation of cave invertebrate animals", financially supported by the bilateral exchange program of the Chinese and Bulgarian academies of sciences.

Additional information

Conflict of interest

The authors have declared that no competing interests exist.

Ethical statement

No ethical statement was reported.

Funding

No funding was reported.

Author contributions

NA and PS contributed to conceptualization, species identification and description and writing the original draft. NA further contributed study of specimens, imaging, analyses of the data and writing the manuscript. OM contributed imaging and producing the figure plates. All authors edited the original draft and further contributed corrections during the reviewing process and the proofs.

Author ORCIDs

Nesrine Akkari  <https://orcid.org/0000-0001-5019-4833>

Oliver Macek  <https://orcid.org/0000-0002-8146-5373>

Pavel Stoev  <https://orcid.org/0000-0002-5702-5677>

Data availability

All of the data that support the findings of this study are available in the main text.

References

- Antić D, Makarov SE (2016) The Caucasus as a major hotspot of biodiversity: Evidence from the millipede family Anthroleucosomatidae (Diplopoda, Chordeumatida). *Zootaxa* 4211(1): 001–205. <https://doi.org/10.11646/zootaxa.4211.1.1>
- Chen H-M, Zheng C-B, Jiang X-K (2023) The millipedes (Diplopoda) in Yintiaoling National Natural Reserve, Southwest China. *Zootaxa* 5257(1): 049–081. <https://doi.org/10.11646/zootaxa.5257.1.1>
- Enghoff H, Golovatch SI, Short M, Stoev P, Wesener T (2015) Diplopoda – taxonomic overview. In: Minelli A (Ed.) *Treatise on Zoology – Anatomy, Taxonomy, Biology. The Myriapoda* 2(16): 363–453. https://doi.org/10.1163/9789004188273_017
- Golovatch SI (1981) Some East-Asiatic millipeds (Diplopoda) in the collection of the Institute of Zoology of the Polish Academy of Sciences. *Annales Zoologici* 36(8): 161–168.
- Golovatch SI (2019) The millipede genus *Cryptocorypha* Attems, 1907 revisited with descriptions of two new Oriental species (Diplopoda: Polydesmida: Pyrogodesmidae). *Arthropoda Selecta* 28(1): 179–190. <https://doi.org/10.15298/arthsel.28.2.01>
- Golovatch SI, Nzoko Fiemapong AR, Tamesse JL, Mauriès JP, VandenSpiegel D (2018) Trichopolydesmidae from Cameroon, 1: The genus *Hemisphaeroparia* Schubart, 1955. With a genus-level reclassification of Afrotropical genera of the family (Diplopoda, Polydesmida). *ZooKeys* 785: 49–98. <https://doi.org/10.3897/zookeys.785.27422>
- Golovatch SI, Fiemapong ARN, VandenSpiegel D (2019) Trichopolydesmidae from Cameroon, 2: A species-level reclassification of Afrotropical trichopolydesmids (Diplopoda, Polydesmida), with two new species and two new records from Cameroon, and two new species from the Nimba Mountains, Guinea. *ZooKeys* 891: 31–59. <https://doi.org/10.3897/zookeys.891.46986>
- Koch M (2015) Diplopoda – General morphology. In: Minelli (Ed.) *The treatise on zoology – Anatomy, Taxonomy, Biology. The Myriapoda* 2(2): 7–67. https://doi.org/10.1163/9789004188273_003
- Liu WX, Tian MY (2015) Two new cave-dwelling species of the millipede genus *Paracortina* Wang & Zhang, 1993 from southern China (Diplopoda, Callipodida, Paracortinidae). *ZooKeys* 517: 123–140. <https://doi.org/10.3897/zookeys.517.9949>
- Loomis HF (1937) Crested millipeds of the family Lysiopetalidae in North America, with Descriptions of new genera and species. *Proceedings of the United States National Museum* 84(3006): 97–135. <https://doi.org/10.5479/si.00963801.84-3006.97>

- Mauriès J-P (1978) Myriapods – Diplopodes du sud de l'Espagne. Description d'une espèce nouvelle, d'espèces mal connues et revision des types du Muséum de Vienne. *Annalen des Naturhistorischen Museen in Wien* 81: 575–588.
- Nguyen AD, Stoev P, Nguyen LTP, Vu TT (2023) A new species of *Paracortina* from a Vietnamese cave, with remarkable secondary sexual characters in males (Callipodida, Paracortinidae). *ZooKeys* 1149: 181–195. <https://doi.org/10.3897/zookeys.1149.99651>
- Shear WA (2000) A new genus and species of callipodidan millipede from Vietnam (Callipodida, Schizopetalidae). *Myriapodologica* 6(11): 95–100.
- Shear W, Shelley R, Heatwole H (2003) Occurrence of the milliped *Sinocallipus simplipodicus* Zhang, 1993 in Laos, with reviews of the Southeast Asian and global callipodidan faunas, and remarks on the phylogenetic position of the order (Callipodida: Sinocallipodidea: Sinocallipodidae). *Zootaxa* 365(1): 1–20. <https://doi.org/10.11646/zootaxa.365.1.1>
- Stoev P (2004) The first troglomorphic species of the millipede genus *Paracortina* Wang & Zhang, 1993 from south Yunnan, China (Diplopoda: Callipodida: Paracortinidae). *Zootaxa* 441: 1–8. <https://doi.org/10.11646/zootaxa.441.1.1>
- Stoev P, Enghoff H (2003) Systematics, phylogeny and biogeography of genus *Balkanopetalum* Verhoeff, 1926 (Diplopoda: Callipodida: Schizopetalidae). *Zootaxa* 272(1): 1–26. <https://doi.org/10.11646/zootaxa.272.1.1>
- Stoev P, Enghoff H (2005) A new cave-dwelling millipede of the genus *Bollmania* Silvestri, 1896 from Yunnan, China, with remarks on the reduction of the second female leg-pair (Diplopoda: Callipodida: Caspiopetalidae). *Journal of Natural History* 39(21): 1875–1891. <https://doi.org/10.1080/00222930400025896>
- Stoev P, Enghoff H (2006) A review of the millipede genus *Dorypetalum* Verhoeff, 1900 (Diplopoda: Callipodida: Dorypetalidae). *Zootaxa* 1254(1): 29–43. <https://doi.org/10.11646/zootaxa.1254.1.2>
- Stoev P, Enghoff H (2008) A revision of the millipede tribe Apfelbeckiini Verhoeff, 1900 (Diplopoda: Callipodida: Schizopetalidae). *Steenstrupia* (Copenhagen) 30(1): 47–66.
- Stoev P, Enghoff H (2011) A review of the millipede genus *Sinocallipus* Zhang, 1993 (Diplopoda: Callipodida: Sinocallipodidae), with notes on gonopods monotony vs. peripheral diversity in millipedes. *ZooKeys* 90: 13–34. <https://doi.org/10.3897/zookeys.90.1291>
- Stoev P, Geoffroy JJ (2004) Review of the millipede family Paracortinidae Wang & Zhang, 1993 (Diplopoda: Callipodida). *Acta Arachnologica* 53(2): 93–103. <https://doi.org/10.2476/asjaa.53.93>
- Stoev P, Sierwald P, Billey A (2008) An annotated world catalogue of the millipede order Callipodida (Arthropoda: Diplopoda). *Zootaxa* 1706(1): 1–50. <https://doi.org/10.11646/zootaxa.1706.1.1>
- Stoev P, Li S, Meng K (2014) Chong-zhou Zhang. In memoriam (1930–2014). *Bulletin du Centre International de Myriapodologie* 47: 25–29.
- Strasser K (1962) Diplopoden aus Bulgarien und Jugoslawien. *Senckenbergiana Biologica* 43(6): 437–470.
- Tabacaru I (1967) Beiträge zu Kenntnis der cavernicolen Antroleucosomatiden (Diplopoda, Ascospemphora). *International Journal of Speleology* 3: 1–31. <https://doi.org/10.5038/1827-806X.3.1.1>
- Wang D (1996) A preliminary study on the phylogeny and biogeography of the family Paracortinidae (Myriapoda: Callipodida): a cladistic analysis. In: Geoffroy JJ, Mauriès J-P, Nguyen Duy-Jacquemin M (Eds) *Acta Myriapodologica. Mémoires du Muséum national d'Histoire naturelle* 169: 307–311.

- Wang D, Mauriès JP (1996) Review and perspective of study on myriapodology of China. In: Geoffroy JJ, Mauriès J-P, Nguyen Duy-Jacquemin M (Eds) *Acta Myriapodologica*. Mémoires du Muséum national d'Histoire naturelle 169: 81–99.
- Wang D, Zhang C (1993) A new family of millipeds (Diplopoda: Callipodida) from south-western China. *Peking National History Museum Memoirs* 53: 375–390.
- Zhang CZ (1997) Diplopoda from Yunnan Caves III. A new genus *Angulifemur*, including two new species of the cave-dwelling callipodid millipedes (Diplopoda, Callipodida, Paracortinidae). *Thesis Compilation of Tianjin Natural History Museum* 14: 1–5.

Two new genera (*Vittiblatta* gen. nov. and *Planiblatta* gen. nov.) of Blattinae (Blattodea, Blattidae) from Southwest China and the discovery of chirally dimorphic male genitalia in *Vittiblatta punctata* sp. nov.

Xin-Xing Luo^{1,2}, Wen-Bo Deng^{1,2}, Yan-Li Che^{1,2}, Zong-Qing Wang^{1,2}

¹ College of Plant Protection, Southwest University, Beibei, Chongqing 400715, China

² Key Laboratory of Agricultural Biosafety and Green Production of Upper Yangtze River (Ministry of Education), Southwest University, Chongqing 400715, China

Corresponding author: Zong-Qing Wang (zqwang2006@126.com)

Abstract

This study examines Blattinae samples from Southwest China collected in recent years. Based on morphological characters, we establish two genera, *Vittiblatta* gen. nov. and *Planiblatta* gen. nov., and describe four new species, *Vittiblatta punctata* Luo & Wang, sp. nov., *Vittiblatta ferruginea* Luo & Wang, sp. nov., *Vittiblatta undulata* Luo & Wang, sp. nov., and *Planiblatta crassispina* Luo & Wang, sp. nov. These two new genera resemble *Periplaneta* s.s., but are easily distinguished from it and other genera of Blattinae by morphological characters (genital sclerite L4C). Our results indicate that sclerites L4C and R1G of male genitalia might be important in species delimitation of Blattinae. In addition, chiral dimorphism is found in male genitalia of *Vittiblatta punctata* sp. nov.

Key words: Chiral dimorphism, male genitalia, new species



Academic editor: Fred Legendre

Received: 28 September 2023

Accepted: 1 December 2023

Published: 28 December 2023

ZooBank: <https://zoobank.org/91B4F76C-D389-4BE5-8AD0-7E3C82B75052>

Citation: Luo X-X, Deng W-B, Che Y-L, Wang Z-Q (2023) Two new genera (*Vittiblatta* gen. nov. and *Planiblatta* gen. nov.) of Blattinae (Blattodea, Blattidae) from Southwest China and the discovery of chirally dimorphic male genitalia in *Vittiblatta punctata* sp. nov. ZooKeys 1187: 401–421. <https://doi.org/10.3897/zookeys.1187.113403>

Copyright: © Xin-Xing Luo et al.

This is an open access article distributed under terms of the Creative Commons Attribution License (Attribution 4.0 International – CC BY 4.0).

Introduction

Blattinae Latreille, 1810, the nominotypical subfamily of Blattidae Latreille, 1810, presently includes 25 genera and about 262 species worldwide (Beccaloni 2023). They are mainly distributed in the Oriental, Australian, and Afrotropical realms. In recent years, molecular studies have revealed that Blattinae is non-monophyletic and the subfamily has been revised accordingly (Wang et al. 2017; Evangelista et al. 2018; Liao et al. 2021; Djernæs and Muriene 2022; Deng et al. 2023), resulting in the rediagnosis of Blattinae (Deng et al. 2023).

Periplaneta Burmeister, 1838 (*sensu lato*) is the most species-rich genus of Blattinae in China. This genus has been shown to be largely polyphyletic in recent studies (Legendre et al. 2015; Bourguignon et al. 2018; Liao et al. 2021; Djernæs and Muriene 2022; Li et al. 2022; Deng et al. 2023; Malem et al. 2023), and it should be divided into at least four separate taxa (Deng et al. 2023). This genus and most related genera were distinguished by a few external morphological characters (e.g. Asahina 1980; Bohn 1985), but with the increasing number of species, genital features should be given more consideration. Lucañas

(2023) started to revise *Periplaneta* and established two genera, *Hobbitoblatta* and *Nazgulatare*, based on male genitalia. Luo et al. (2023) then proposed synapomorphies of *Periplaneta* s.s. by comparative morphology, based on the type species, *P. americana* (Linnaeus, 1758), and two species that were previously placed under *Shelfordella* Adelung, 1910.

In this study, we examine Blattinae samples from Southwest China and find four new species by morpho-anatomic characters. The external morphology of these four species is similar to *Periplaneta* s.s., but they can be clearly distinguished by male genitalia. We also compare their morphology with that of other genera of Blattinae and conclude that these four species should be grouped into two new genera, which we establish here. In addition, we found chirally dimorphic male genitalia in one of the new species.

Materials and methods

Specimen source and treatment

Blattinae specimens from Southwest China were stored in anhydrous ethanol at -20°C . Male and female genitalia were placed in 10% NaOH at 70°C for 10 min to dissolve soft tissue, they were observed under a CNOPTEC SZ780 stereomicroscope, then stored in glycerol. Images were taken with a Canon M5 camera with a Laowa 65 mm F2.8 CA-Dreamer Macro 2× macro lens or a Leica M205A stereomicroscope with a Leica DFC 550 camera, and edited with Adobe Photoshop CC2019. All materials examined are deposited in the College of Plant Protection, Southwest University, Chongqing, China (SWU).

Morphological terminology

In this paper, the terminology mainly follows Roth (2003), Li et al. (2018) (veins), Klass (1997) (male genitalia), and McKittrick (1964) (female genitalia). The abbreviations used are as follows: cubitus (**Cu**), cubitus anterior (**CuA**), cubitus posterior (**CuP**), media (**M**), postcubitus (**Pcu**), radius (**R**), radius anterior (**RA**), radius posterior, (**RP**), subcostal posterior (**ScP**), vannal veins (**V**); sclerites of left phallomere (**L1**, **L2**, **L3**, **L4C**, **L4D**, **L4E**, **L4G**), sclerites of right phallomere (**R1G**, **R1H**, **R1F**, **R2**, **R3**); tergum X (**TX**), first valve (**v.I.**), first valvifer (**vlf.I.**), second valve (**v.II.**), posterior lobes of valvifer II (**p.I.**), laterosternite IX (**ltst.IX**), anterior arch (**a.a.**), spermathecal plate (**sp.pl.**), spermathecal opening (**sp.o.**), basivalvulae (**bsv.**), laterosternal shelf (**ltst.sh.**).

Taxonomy

Vittiblatta Luo & Wang, gen. nov.

<https://zoobank.org/89FF89FE-72B0-4D24-A2E4-A63B67CB2AFD>

Type species. *Vittiblatta punctata* Luo & Wang, sp. nov.

Diagnosis. Some typical characteristics indicate that *Vittiblatta* gen. nov. belongs to the subfamily Blattinae (front femur of type A_2 , tarsi long and slender, cerci long and distinctly segmented, subgenital plate symmetrical). The new genus differs from the other genera of Blattinae as follows:

- 1) This sexually dimorphic genus can be distinguished from sexually monomorphic genera. **Apterous:** *Apterisca* Princis, 1963; *Brinckella* Princis, 1963; *Macrostylopyga* Anisyutkin, Anichkin & Thinh, 2013; *Miostylopyga* Princis, 1966. **Micropterous:** *Afrostylopyga* Anisyutkin, 2014; *Henicotyle* Rehn & Hebard, 1927; *Neostylopyga* Shelford, 1911. **Macropterous:** *Dorylaea* Stål, 1877; *Eroblatta* Shelford, 1910a; *Hobbitoblatta* Lucañas, 2023; *Homalosilpha* Stål, 1874; *Mimosilpha* Bey-Bienko, 1957; *Nazgultaure* Lucañas, 2023; *Thyrsochera* Burmeister, 1838.
- 2) This genus (tegmina and wings of male developed, tegmina of female only reaching the first tergite of abdomen) can be distinguished from the genera in which the female are apterous (*Archiblatta* Snellen van Vollenhoven, 1862, *Catara* Walker, 1868, *Deropeltis* Burmeister, 1838) and micropterous (*Pseudoderopeltis* Krauss, 1890; *Blatta* Linnaeus, 1758; *Planiblatta* Luo & Wang, gen. nov.).
- 3) Hind metatarsus of this genus is longer than or equal to the remaining tarsal segments combined and therefore different from *Eumethana* Princis, 1951 and *Scabinopsis* Bey-Bienko, 1969.
- 4) This genus has visible tergal gland and can be distinguished from *Cartoblatta* Shelford, 1910b, *Periplaneta* s.s., and *Blatta*.
- 5) In male genitalia, sclerites L4C and R1G can be used for distinguishing genera in Blattinae. L4C of this new genus is thin, ribbon-like and its basal part has densely spiny process; R1G of this genus has a curved spine. These characters are readily different from that of *Archiblatta*, *Blatta*, *Bundoksia* Lucañas, 2021, *Catara*, *Hobbitoblatta*, *Homalosilpha*, *Mimosilpha*, *Nazgultaure*, and *Protagonista* Shelford, 1908 (Wang et al. 2016; Liao et al. 2021; Lucañas 2021; Li et al. 2022; Deng et al. 2023; Lucañas 2023; Luo et al. 2023). These two sclerites are similar between this genus and *Periplaneta* s.s., but the distal part of L4C of *Periplaneta* s.s. is expanded and the hind margin of L4C is nearly truncated.

Generic description. Sexual dimorphism. **Male.** Interocular space wider than interocellar space, shorter than the distance between antennal sockets. Antennae longer than the body. Pronotum subelliptical. Tegmina and wings well developed, surpassing the tip of abdomen. Front femur of type A₂; pulvilli present on 1–4 or 2–4 tarsal segments, claws symmetrical and unspecialized, arolium slightly smaller than other genera. The posterior-lateral angles of metanotum without or with small projections. First tergite of male abdomen with visible gland. Posterolateral corners of abdominal tergites V–VII not produced. The hind margin of supra-anal plate slightly concave. L1 of genitalia weakly sclerotized with pubescence; L3 unciform and the distal part bifurcated; L4C thin ribbon-like, with densely spiny process near basal inner margin. The basal part of R1H flat, inner margin with one or two small spines; the distal part of R1G with a curved spine inward. **Female.** Tegmina and wings reduced. Tegmina squamiform, only reaching the first tergite of abdomen; lateral margins of tegmina beveled, the outer corner rounded. Hind wings small and lobe-like. Pulvilli present on 1–4 or 2–4 tarsal segments, claws symmetrical and unspecialized, arolium small. Spermatheca with two branches, the leading duct short, the branching duct relatively long, and the end capsule rod-shaped.

Etymology. The generic epithet is from two Latin words “*vitta*” and “*blatta*”, meaning that L4C is thin and ribbon-like. The gender of *Vittiblatta* is feminine.

Distribution. China (Sichuan, Yunnan).

Key to species of *Vittiblatta* Luo & Wang, gen. nov. (males)

- 1 Pronotum with punctures ***V. punctata* Luo & Wang, sp. nov.**
- Pronotum smooth, without punctures **2**
- 2 The hind margin of subgenital plate convex
..... ***V. ferruginea* Luo & Wang, sp. nov.**
- The hind margin of subgenital plate wave-like
..... ***V. undulata* Luo & Wang, sp. nov.**

***Vittiblatta punctata* Luo & Wang, sp. nov.**

<https://zoobank.org/337CEA3C-952C-4AEC-A463-15C46682CEB0>

Figs 1–3, 7 (in part)

Type materials. Holotype: CHINA • ♂; Sichuan, Miyi County, Panzhihua City; 20.VII.2021; Lu Qiu leg.; SWU-B-BL-083301. **Paratypes:** CHINA • 1♂; Sichuan, Mt Lushan, Xichang City, Liangshan Autonomous Prefecture; 21.VII.2022; Bianlun Li & Lin Guo leg.; SWU-B-BL-083302 • 1♂; Sichuan, Mt Lushan, Xichang City, Liangshan Autonomous Prefecture; 1800 m alt.; 30.VI.2015; Chao Zhou leg.; SWU-B-BL-083303 • 1♀; Sichuan, Mt Lushan, Xichang City, Liangshan Autonomous Prefecture; 21.VII.2022; Wei Han & Xinxing Luo leg.; SWU-B-BL-083304 • 2♂♂; Sichuan, Mt Daheishan, Panzhihua City; 20–21.V.2011; Keliang Wu leg.; SWU-B-BL-083305 to 083306 • 5♂♂; Yunnan, Mt Ailaoshan, Xiping County; 1988 m alt.; 24.V.2018; Lu Qiu, Wenbo Deng & Zhiwei Dong leg.; SWU-B-BL-083307 to 083311 • 1♂, 2♀; Yunnan, Mt Ailaoshan, Xiping County; 1988 m alt.; 11–13.V.2016; Lu Qiu & Zhiwei Qiu leg.; SWU-B-BL-083312 to 083314 • 4♀♀; Yunnan, Xishan Scenic Area, Kunming City; 2240 m alt.; 27.VI.2021; Jiawei Zhang & Jinlin Liu leg.; SWU-B-BL-083315 to 083318 • 1♂; Yunnan, Wenquan Street, Kunming City; 1900 m alt.; 3–4.VI.1974; Yao Zhou & Feng Yuan leg.; SWU-B-BL-083319 • 1♂; Qiongzhu Temple, Kunming City; 2166 m alt.; 14.VI.1980; collector unknown; SWU-B-BL-083320 • 2♂♂; Yunnan, Mengxima Town, Yingjiang County, Dehong Autonomous Prefecture; 1470 m alt.; 9.VI.2008; Weiwei Zhang leg.; SWU-B-BL-083321 to 083322 • 1♂; Yunnan, Menghai County, Xishuangbanna Autonomous Prefecture; 1160 m alt.; 27–31.VI.1974; Yao Zhou & Feng Yuan leg.; SWU-B-BL-083323 • 1♂; Yunnan, Baihualing, Mt Gaoligong, Baoshan City; 1523 m alt.; 19.IV.2014; Yunkong Jiang & Tian Lu leg.; SWU-B-BL-083324 • 2♂; Yunnan, Hanlongzhai, Baihualing, Mt Gaoligong, Baoshan City; 1508 m alt.; 11.VI.2023; Xinran Li & Yifeng Liu leg.; SWU-B-BL-083325 to 083326 • 1♂; Yunnan, Yuxi City; 13.V.1980; Jingrong Zhao leg.; SWU-B-BL-083327.

Diagnosis. Combining the following characteristics, this species is easily distinguished from other species of this genus: 1) pronotum with dense punctures; 2) the middle and hind femora with sparse spines; 3) body brown and cerci yellowish brown; 4) L4C with densely spiny process; 5) the end of L2 with one long spine; 6) the distal part of R1G with a thick spine; 7) the surface of the

basivalvulae with furrows and microtrichia; 8) the end capsule of the spermatheca rod-shaped.

Description. Sexual dimorphism present. **Coloration.** Male body brown to dark brown and female body black; ocelli white; cerci and styli yellowish brown (Fig. 1A–D).

Male (Fig. 1A, B). Body length including tegmen: 30.6–39.5 mm; body length: 20.7–29.8 mm; pronotum length × width: 4.3–6.8 mm × 6.6–9.2 mm; tegmina length × width: 26.0–32.9 mm × 7.4–10.2 mm. **Head and thorax.** Vertex slightly exposed. Interocular space slightly wider than the interocellar space, shorter than the distance between antennal sockets (Fig. 1E). Antennae longer than the body. Pronotum subelliptical, with the lateral edges not curved downward; anterior margin nearly concave, the median of hind margin convex; the widest point after the midpoint, the surface thin with dense punctures (Fig. 1F). The posterior-lateral angles of metanotum without projections (Fig. 1H). Tegmina and wings well developed, surpassing the tip of abdomen (Fig. 1A, B, I, J). Tegmina with ScP strong, posterior branch of R not reaching the end of tegmina (Fig. 1I). Legs slender. Front femur of type A₂ (Fig. 1G). Mid- and hind legs with sparsely spines on ventral margin. Hind metatarsus approximately equal to the remaining segments combined. Pulvilli present on 1–4 tarsal segments, claws symmetrical and unspecialized, arolium small (Fig. 7A). **Abdomen.** First tergite of male abdomen with visible gland, setose gland sparse and not obscured by metanotum (Fig. 1H). Supra-anal plate short, lateral margin shrunken inward; the middle part of hind margin concave at an obtuse angle. Paraprocts (pp.) long, strip-shaped. Cerci robust (Fig. 1K). Subgenital plate nearly square; the hind margin arcuate, and the middle slightly concave. Styli symmetrical and apically rounded (Fig. 1L). **Genitalia** (Fig. 1M). L1 composed of one elongate sclerite and membrane bearing pubescence. L4C thin ribbon-like, with a densely spiny process near basal inner margin. L2 irregular, the end with one long spine inward. L3 unciform and well sclerotized, the basal part bifurcated. The distal part of R1H broad, the inner margin bifurcated with two small spines. The distal part of R1G with a slightly curved and thick spine inward.

Female (Fig. 1C, D). Body length: 21.6–24.7 mm; pronotum length × width: 6.4–8.2 mm × 8.5–10.5 mm; tegmina length × width: 6.3–7.5 mm × 5.1–6.4 mm. **Head and thorax.** Interocular space slightly wider than the interocellar space and the distance between antennal sockets (Fig. 1D). Pronotum subelliptical, the widest point near hind margin; anterior margin and hind margin straight (Fig. 1C). Tegmina and hind wings reduced. Tegmina squamiform, reaching the first tergite of abdomen; the outer margin oblique (Fig. 1C). Hind wings small lobe-like. Hind metatarsus approximately equal to the remaining segments combined. Pulvilli present on 1–4 tarsal segments, claws symmetrical and unspecialized, arolium smaller than male (Fig. 7A). **Abdomen.** Hind margin of tergum X (TX) with median invagination, and with a membranous line inside; cerci thick and upturned (easily broken) (Fig. 2A, D). **Genitalia** (Fig. 1N). First valve (v.I.) well sclerotized. First valvifer (vlf.I) small. Second valve (v.II) with strip-like sclerite. Posterior lobes of valvifer II (p.I.) irregular, the outer margin slightly connected with laterosternite IX (ltst.IX). Laterosternite IX broad and irregular. The base of anterior arch (a.a.) extended downward, surface densely covered with microtrichia. Spermathecal plate (sp.pl.) small, connected to basivalvulae (bsv.) by membrane. Spermathecal opening (sp.o.) located at the base of

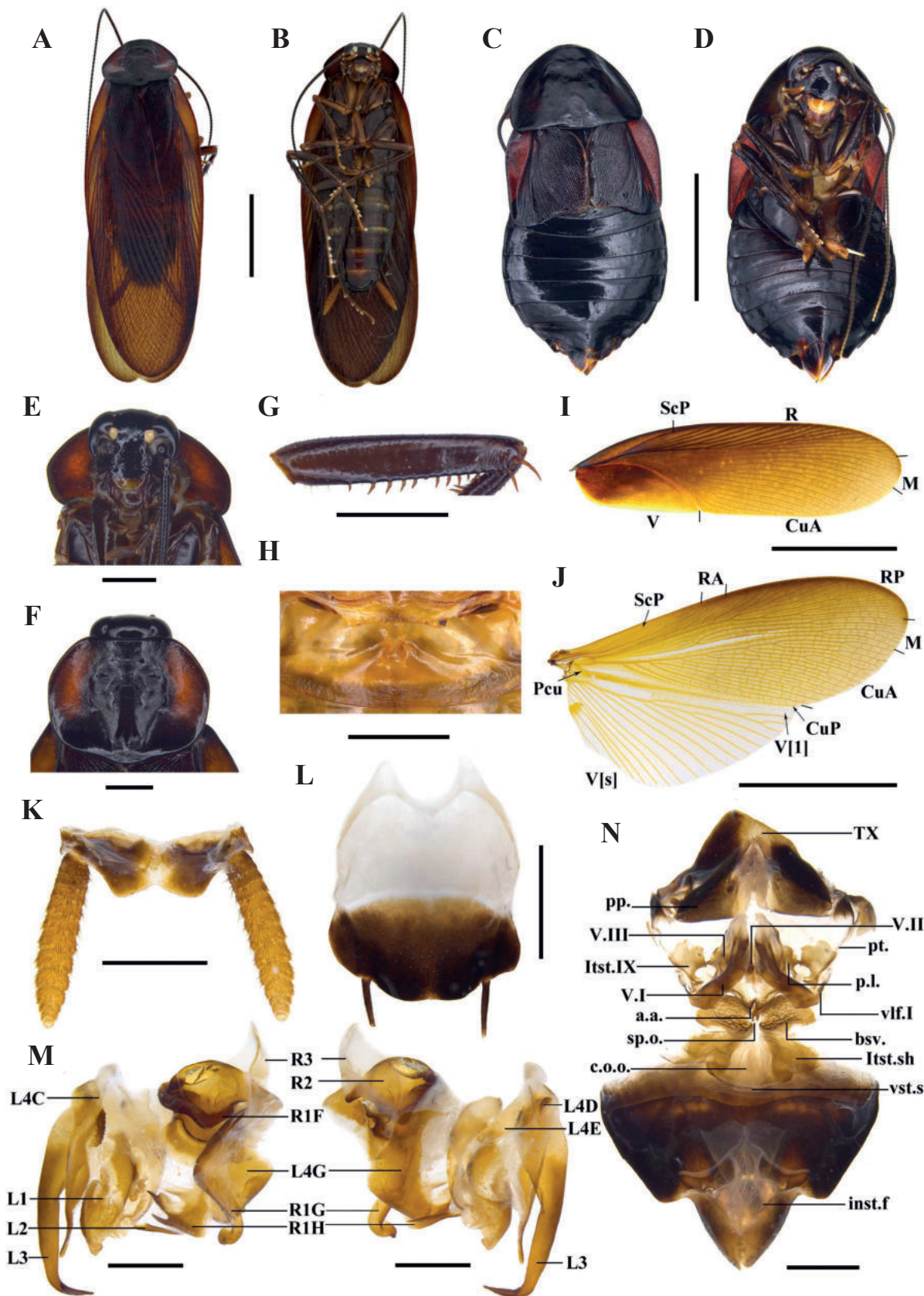


Figure 1. *Vittiblatta punctata* Luo & Wang, sp. nov. **A, B, E–M** male holotype **C, D, N** female paratypes **A, C** habitus, dorsal view **B, D** habitus, ventral view **E** head **F** pronotum **G** front femur **H** hind margin of metanotum and tergal gland **I** tegmen **J** hind wing **K** supra-anal plate, ventral view **L** subgenital plate, dorsal view **M** male genitalia, dorsal (left) and ventral view (right) **N** female genitalia, dorsal view. Scale bars: 10.0 mm (**A–D, I, J**); 2.0 mm (**E–H, K, L, N**); 1.0 mm (**M**).

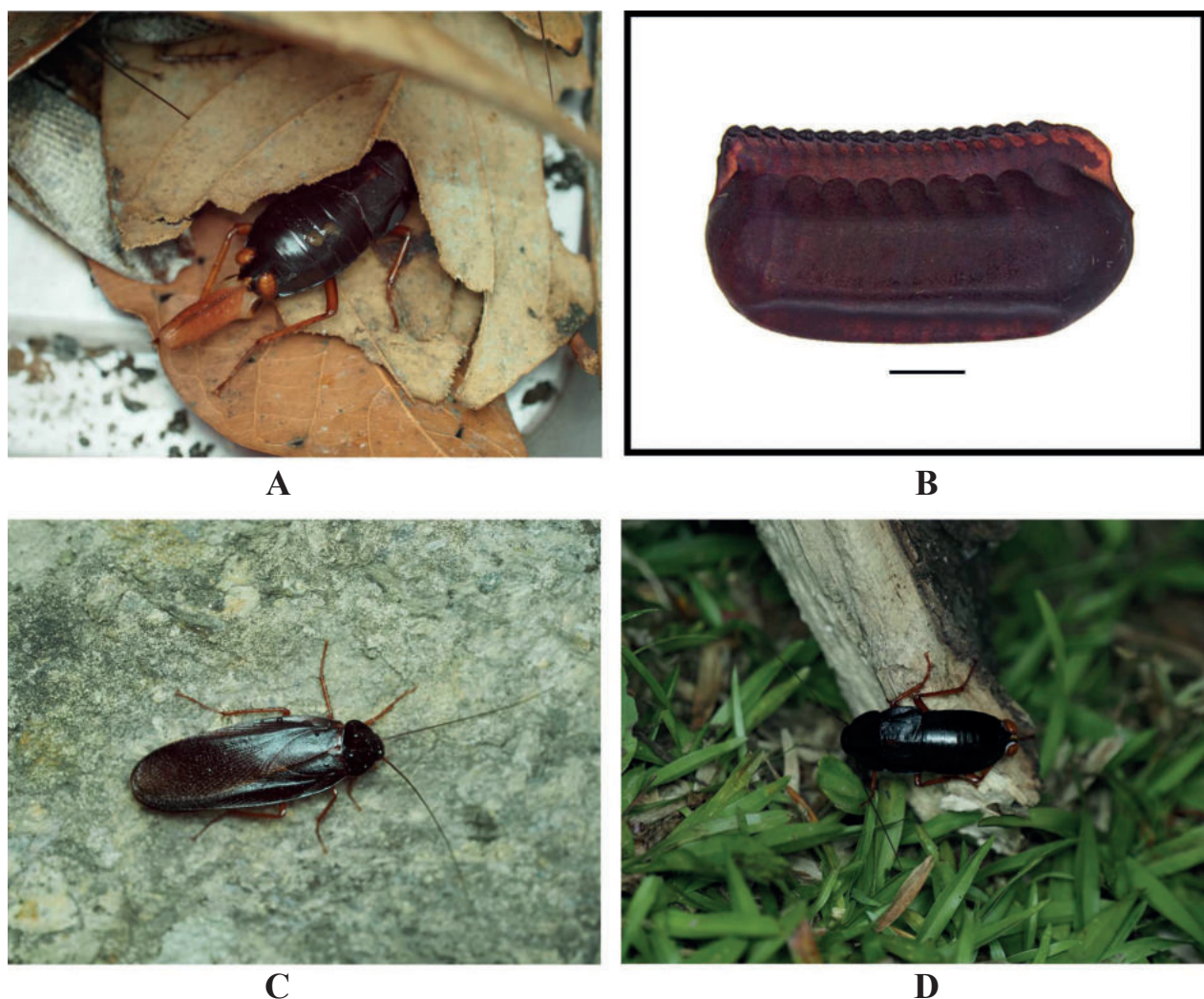


Figure 2. *Vittiblatta punctata* Luo & Wang, sp. nov. **A** ootheca-carrying female **B** ootheca **C** male on rocks **D** female in the grass. Scale bars: 2.0 mm (**B**). **A**, **C**, **D** photographed by Xinran Li.

basivalvulae. Spermatheca branched, the leading duct short, the branching duct relatively long, and the end capsule rod-shaped (Fig. 7E). Basivalvulae bulbous and flared, surface with furrows and microtrichia. Laterosternal shelf (ltst. sh.) symmetrical, the base with furrows.

Ootheca. 11.4 mm long, 5.6 mm wide, reddish brown. Overall long, ridge slightly broad with serrations (Fig. 2A, B).

Etymology. The species epithet is from the Latin word “*punctatus*”, which is in reference to the dense punctures on the pronotum.

Natural history. This species has been found in the wild not far from human habitats, on roadsides or in grassy areas (Fig. 2C, D).

Distribution. China (Sichuan, Yunnan).

Remarks. Stochastic chiral dimorphism was found in male genitalia of this species. The genitalia of some male samples are left–right mirrored in comparison with common arrangement of Blattinae (Fig. 3A–C). We carefully examined all male specimens, and this phenotype was found in samples from three localities: Mt Ailaoshan (normal genitalia in two samples and mirrored genitalia in three samples), Baihualing (normal genitalia in one sample and mirrored gen-

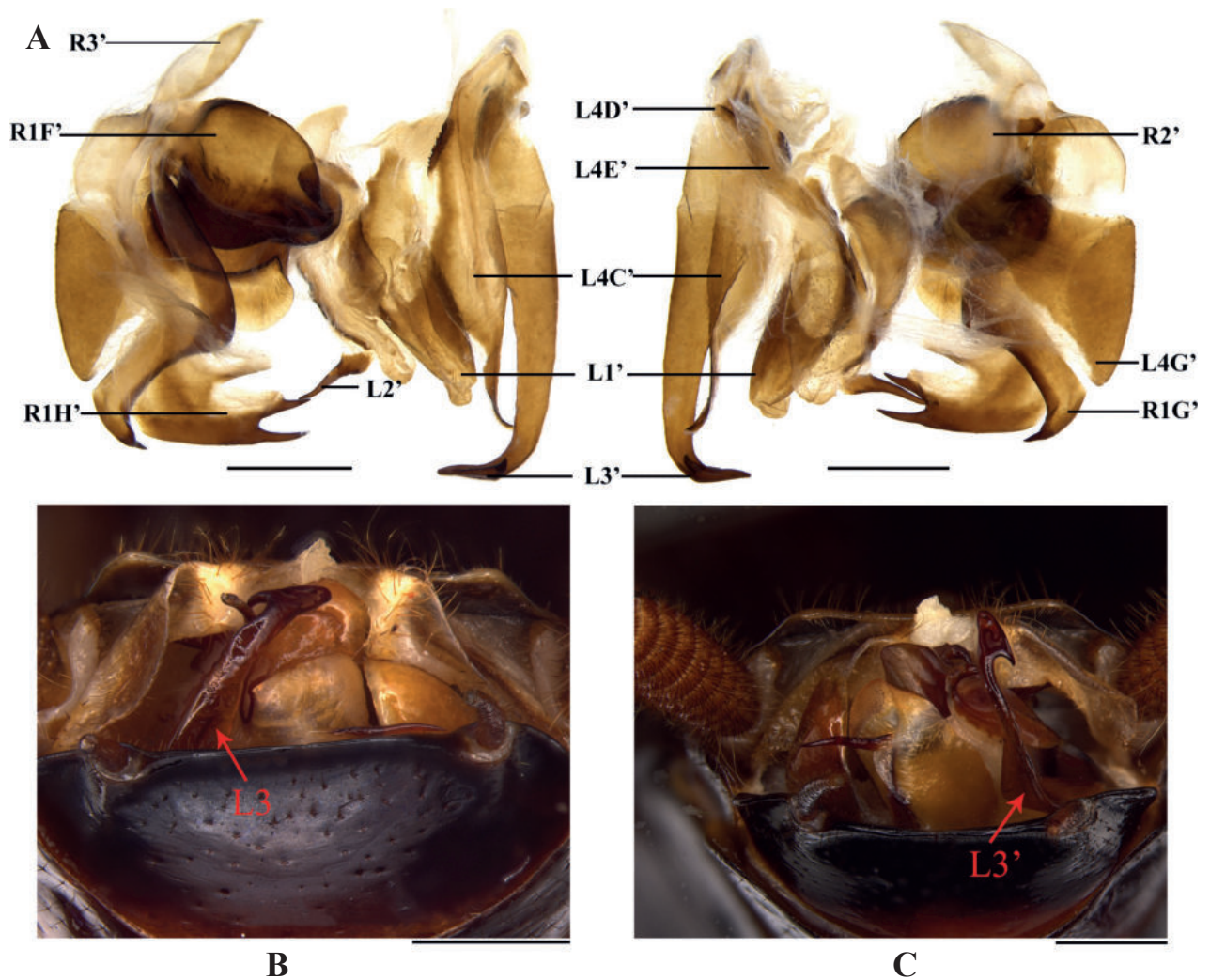


Figure 3. Chiral dimorphism in male genitalia of *Vittiblatta punctata* Luo & Wang, sp. nov. **A–C** male paratypes, the samples from Mt Ailaoshan **A** mirrored genitalia, dorsal and ventral views **B** normal genitalia, ventro-caudal view (L3 on the left) **C** mirrored genitalia, ventro-caudal view (L3 on the right). Scale bars: 1.0 mm.

italia in one sample) and Mt Daheishan (normal genitalia in one sample and reversed genitalia in one sample). In addition, there are no significant differences between the two kinds of genitalia, so they should be the same species. This is the first discovery of intraspecific genitalic chirality in Blattodea.

***Vittiblatta ferruginea* Luo & Wang, sp. nov.**

<https://zoobank.org/450A2E05-DDC9-4601-9B07-6129BF4C8C79>

Figs 4, 7 (in part)

Type materials. Holotype: CHINA • ♂; Yunnan, Tongbiguan Township, Yingjiang County, Dehong Dai and Jingpo Autonomous Prefecture; 1345 m alt.; 1.VI.2018; Lu Qiu & Wenbo Deng leg.; SWU-B-BL-082401. **Paratypes:** CHINA • 6♂♂; Yunnan, Tongbiguan Township, Yingjiang County, Dehong Dai and Jingpo Autonomous Prefecture; 1345 m alt.; 1–5.VI.2018; Lu Qiu & Wenbo Deng leg.; SWU-B-BL-082402 to 082407 • 6♂♂, 1♀; Yunnan, Meizihu Reservoir Highway, Pu'er

City; 20–21.V.2016; Lu Qiu & Zhiwei Qiu leg.; SWU-B-BL-082408 to 082414 • 1♂; Xishuangbanna Tropical Botanical Garden, Chinese Academy of Sciences, Menglun Town, Mengla County, Xishuangbanna Prefecture; 27. V. 2016; Lu Qiu & Zhiwei Qiu leg.; SWU-B-BL-082415 • 1♂; Yunnan, Xiniu (Rhino) Plains Scenic Area, Pu'er National Park, Pu'er City, Pu'er National Park; 1602 m alt.; 2.VII.2021; Jiawei Zhang & Jinlin Liu leg.; SWU-B-BL-082416.

Diagnosis. Combining the following characteristics, this species is easily distinguished from other species of this genus: 1) body dark reddish brown; 2) pronotum smooth without punctures; 3) the hind margin of subgenital plate arcuate; 4) the inner margin of L4C with serrate auriculate projection; 5) the distal part of R1G with a slender spine; 6) anterior arch with furrow; 7) the surface of basivalvulae flat.

Description. Sexual dimorphism present. **Coloration.** Body reddish brown to dark reddish brown; ocelli white; cerci and styli brown to black (Fig. 4A–D).

Male (Fig. 4A, B). Body length including tegmen: 25.4–30.9 mm; body length: 18.2–21.9 mm; pronotum length × width: 4.6–5.9 mm × 5.8–7.0 mm; tegmina length × width: 22.5–26.9 mm × 6.3–8.2 mm. **Head and thorax.** Vertex slightly exposed. Interocular space slightly wider than the interocellar space, shorter than the distance between antennal sockets. Antennae longer than the body (Fig. 4E). Pronotum subelliptical; anterior margin slightly concave, hind margin slightly convex; the widest point near the midpoint (Fig. 4F). The posterior-lateral angles of metanotum with symmetrical and small projections (Fig. 4J). Tegmina and wings well developed, surpassing the tip of abdomen (Fig. 4A, B, G, H). Tegmina with ScP strong, posterior branch of R not reaching the end of tegmina (Fig. 4G). Front femur of type A₂ (Fig. 4I). Mid- and hind legs with strong spines. Hind metatarsus longer than the remaining segments combined. Pulvilli present on 2–4 tarsal segments, claws symmetrical and unspecialized, arolium small (Fig. 7B). **Abdomen.** First tergite of male abdomen with visible gland, setose gland curved and downward (Fig. 4J). Supra-anal plate rectangular, lateral margin not shrunken inward; middle part of hind margin slightly concave. Paraprocts (pp.) long, strip-shaped. Cerci robust (Fig. 4L). Subgenital plate nearly square; the hind margin arcuate. Styli symmetrical and apically rounded (Fig. 4K). **Genitalia** (Fig. 4M). L1 composed of a elongate sclerite and membrane bearing pubescence. L4C thin, ribbon-like, the inner margin with serrate auriculate projection. L2 irregular, near distal part with two small spines and the end with one long spine inward. L3 unciform and well sclerotized, the basal part bifurcated. The distal part of R1H broad, the inner margin bifurcated with two small spines. The distal part of R1G with a curved, long spine inward.

Female (Fig. 4C, D). Body length: 22.2 mm; pronotum length × width: 6.1 mm × 7.4 mm; tegmina length × width: 5.8 mm × 5.2 mm. **Head and thorax.** Interocular space slightly wider than interocellar space and the distance between antennal sockets (Fig. 4D). Pronotum subelliptical, the widest point near hind margin; anterior margin and hind margin straight (Fig. 4C). Tegmina and hind wings reduced. Tegmina squamiform, reaching the first tergite of abdomen; the outer margin oblique (Fig. 4C). Hind wings small, lobe-like. Hind metatarsus approximately equal to the remaining segments combined. Pulvilli present on 2–4 tarsal segments, claws symmetrical and unspecialized, arolium smaller than male. **Abdomen.** Hind margin of tergum X (TX) with median invagination, and with a membranous line inside; cerci thick and not upturned (Fig. 4N). **Genitalia**

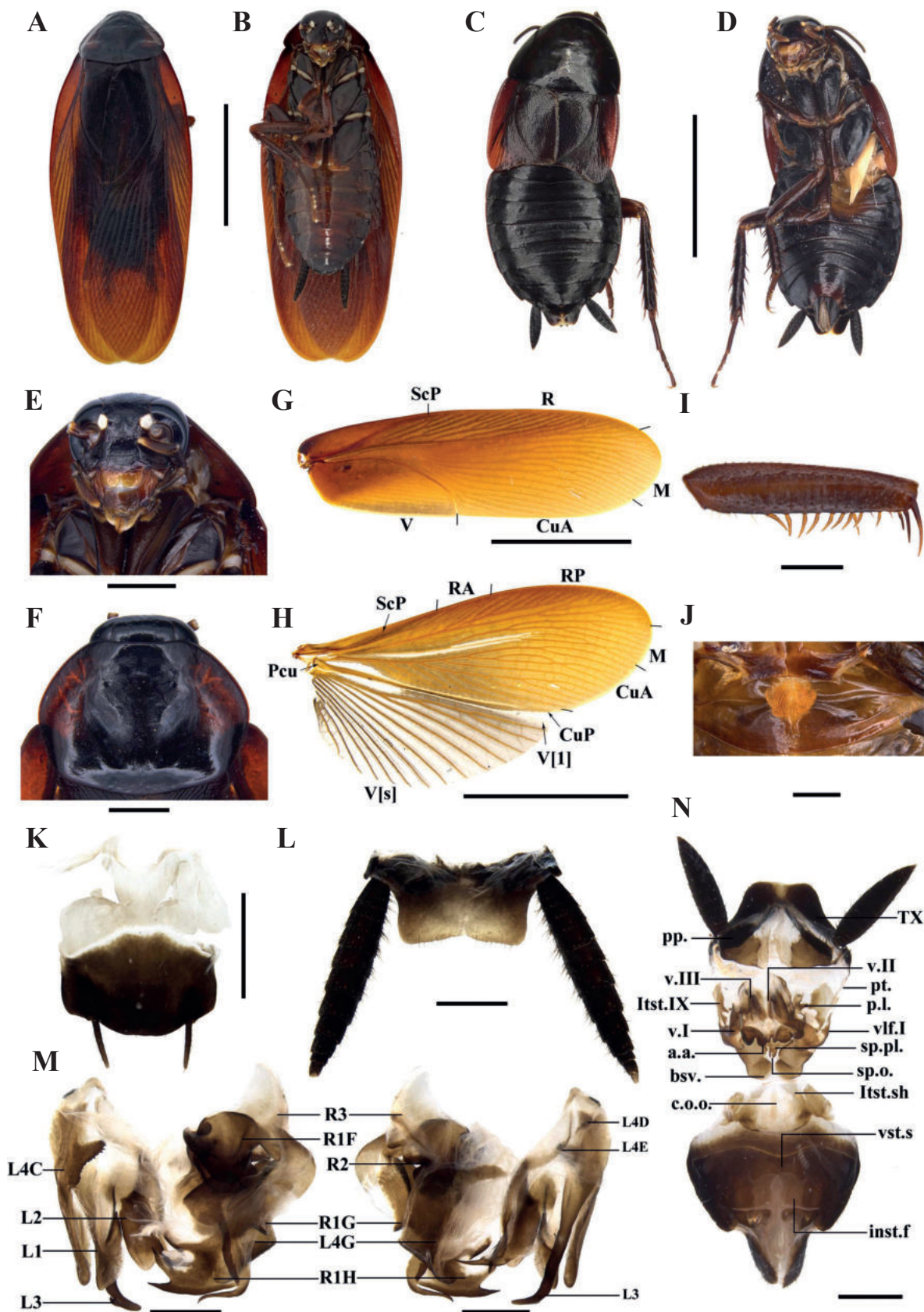


Figure 4. *Vittiblatta ferruginea* Luo & Wang, sp. nov. A, B, E–M male holotype C, D, N female paratypes A, C habitus, dorsal view B, D habitus, ventral view E head F pronotum G tegmen H hind wing I front femur J hind margin of metanotum and tergal gland K subgenital plate, dorsal view L supra-anal plate, ventral view M male genitalia, dorsal (left) and ventral (right) view N female genitalia, dorsal view. Scale bars: 10.0 mm (A–D, G, H); 2.0 mm (E, F, K, L, N); 1.0 mm (I, J, M).

(Fig. 4N). The base of first valve (v.I.) with dense microtrichia. First valvifer (vlf.I) thin. Second valve (v.II) with strip-like sclerite. Posterior lobes of valvifer II (p.I.) irregular, the outer margin disconnected with laterosternite IX (ltst. IX). Laterosternite IX broad and irregular. Anterior arch (a.a.) with furrow, and two symmetrical projections near outer margin, inner margin with microtrichia. Spermathecal plate (sp.pl.) broad, connected to basivalvulae (bsv.) by membrane. Spermathecal opening (sp.o.) located at the base of basivalvulae. Spermatheca branched, the leading duct short, the branching duct relatively long, and the end capsule unknown (Fig. 7E). Basivalvulae reniform, surface flat and margin with sparsely microtrichia. Laterosternal shelf (ltst.sh.) symmetrical.

Etymology. The species epithet is from the Latin word “*ferrugineus*”, in reference to the reddish brown or dark reddish brown body.

Distribution. China (Yunnan).

***Vittiblatta undulata* Luo & Wang, sp. nov.**

<https://zoobank.org/965CF6AF-9985-49EC-ADD6-15AFFB166498>

Figs 5, 7 (in part)

Type materials. Holotype: CHINA • ♂; Yunnan, Nabang Town, Yingjiang County, Dehong Dai and Jingpo Autonomous Prefecture; 282 m alt.; 11–13.VII.2012; collector unknown; SWU-B-BL-081901. **Paratype:** CHINA • 1 ♂; Yunnan, Nabang Town, Yingjiang County, Dehong Dai and Jingpo Autonomous Prefecture; 252 m alt.; 4.VI.2018; Lu Qiu & Wenbo Deng leg.; SWU-B-BL-081902.

Diagnosis. Combining the following characteristics, this species is easily distinguished from other species of this genus: 1) body yellowish brown; 2) hind margin of subgenital plate wavy; 3) male genitalia L2 without spine at end, only a small protuberance; 4) the distal part of R1H broad, slightly sclerotized and hyaline, the end with an elongate and curved spine inward.

Description. Coloration. Body yellowish brown; ocelli white; hind margin of subgenital plate nearly brown (Fig. 5A, B).

Male (Fig. 5A, B). Body length including tegmen: 30.5–32.7 mm; body length: 27.1 mm; pronotum length × width: 6.2–6.6 mm × 7.7–8.2 mm; tegmina length × width: 24.9–25.4 mm × 8.0–8.2 mm. **Head and thorax.** Vertex unexposed. Interocular space slightly wider than the interocellar space, shorter than the distance between antennal sockets (Fig. 5C). Antennae longer than the body. Pronotum subelliptical; anterior margin straight, hind margin slightly convex; the widest point near the midpoint (Fig. 5D). The posterior-lateral angles of metanotum with symmetrical and small projections (Fig. 5E). Tegmina and wings well developed, surpassing the tip of abdomen (Fig. 5A, B, G, H). Tegmina with ScP strong, posterior branch of R not reaching the end of tegmina (Fig. 5G). Front femur of type A₂ (Fig. 5F). Mid- and hind legs with strong spines. Hind metatarsus longer than the remaining segments combined. Pulvilli present on 1–4 tarsal segments, claws symmetrical and unspecialized, arolium small (Fig. 7C). **Abdomen.** First tergite of male abdomen with visible gland, setose gland curved, and directed toward left, right, and down (Fig. 5E). Supra-anal plate rectangular, lateral margin slightly shrunken inward; middle part of hind margin concave. Paraprocts (pp.) long, strip-shaped. Cerci robust (Fig. 5I). Subgenital plate nearly square; the hind margin wavy. Styli symmetrical and

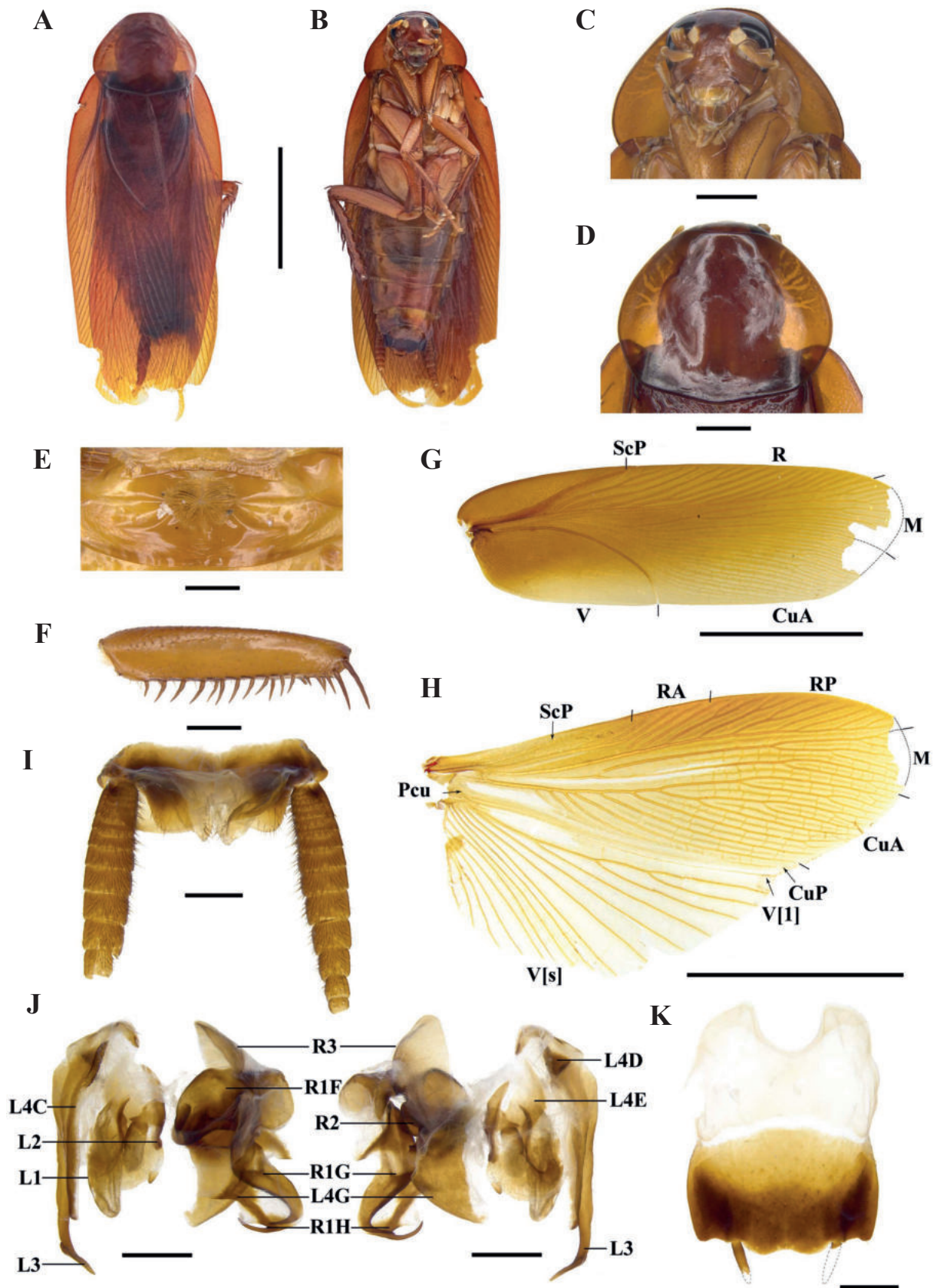


Figure 5. *Vittiblatta undulata* Luo & Wang, sp. nov. A–K male holotype A habitus, dorsal view B habitus, ventral view C head D pronotum E hind margin of metanotum and tergal gland F front femur G tegmen H hind wing I supra-anal plate, ventral view J male genitalia, dorsal (left) and ventral view (right) K subgenital plate, dorsal view. Scale bars: 10.0 mm (A, B, G, H); 2.0 mm (C, D); 1.0 mm (E, F, I–K).

apically rounded (Fig. 5K). **Genitalia** (Fig. 5J). L1 membranous with pubescence. L4C thin and ribbon-like, the inner margin with a long projection of densely microtrichia. L2 irregular, the distal part with a small projection. L3 unciform and well sclerotized, the basal part bifurcated. The distal part of R1H broad, slightly sclerotized and hyaline, the end with an elongate and curved spine inward. The distal part of R1G with a curved, strong spine inward.

Female. Unknown, possibly brachypterous.

Etymology. The species epithet is from the Latin word “*undulata*”, in reference to the way hind margin of subgenital plate.

Distribution. China (Yunnan).

***Planiblatta* Luo & Wang, gen. nov.**

<https://zoobank.org/35B1FFC2-904E-4A07-831B-637D0D94C776>

Type species. *Planiblatta crassispina* Luo & Wang, sp. nov.

Diagnosis. This genus belongs to subfamily Blattinae (front femur of type A₂, tarsi long and slender, cerci long and distinctly segmented, subgenital plate symmetrical) and can be distinguished from other genera of Blattinae by the following characters: 1) this sexually dimorphic genus can be distinguished from sexually monomorphic genera (see the diagnosis of *Vittiblatta* gen. nov.); 2) the genus (male macropterous, female micropterous) can be distinguished from the genera that female are apterous (see the diagnosis of *Vittiblatta* gen. nov.) and brachypterous (*Vittiblatta* gen. nov., *Cartoblatta*, *Scabinopsis*, *Bundokisia*); 3) hind metatarsus of this genus is longer than or equal to the remaining segments combined, distinguished from *Eumethana* and *Scabinopsis*; 4) visible tergal gland could be used to differ from *Cartoblatta*, *Periplaneta* s.s., and *Blatta*; 5) mesonotum and metanotum of this genus without finger-like projections can be distinguished from *Pseudoderopeltis*; 6) as mentioned in the diagnosis of *Vittiblatta* gen. nov., the difference of sclerite L4C and R1G within a genus is stable, this new genus (L4C curved and subhyaline, R1G with two curved, strong spines) can be distinguished from 10 genera of Blattinae (see the diagnosis of *Vittiblatta* gen. nov.).

Generic description. Sexual dimorphism present. **Male.** Body flat. Antennae longer than the body. Pronotum subelliptical. The posterior-lateral angles of metanotum without finger-like projections. Tegmina and wings well developed, surpassing the tip of abdomen. Front femur of type A₂; hind metatarsus equal to the remaining segments combined; pulvilli present, pulvilli of front metatarsus developed; claws symmetrical and unspecialized, arolium moderate. First tergite of the male abdomen with visible gland, setose gland not obscured by metanotum. Posterolateral corners of abdominal tergite V–VII produced. Supra-anal plate short, the hind margin slightly concave. The hind margin of subgenital plate straight. L2 folded, the dorsal sclerite broad, the distal part with one long spine. L3 unciform and the distal part bifurcated, longer than other sclerites. L4C less sclerotized, curved and subhyaline. The inner margin of R1H with two strong spines. The distal part of R1G with two curved and strong spines. **Female.** Tegmina and wings reduced. Tegmina small lobes. Hind wings absent. Spermatheca branched, the leading duct longer than the branching duct, the end capsule oval.

Etymology. The generic epithet is from two Latin words “*plan*” and “*blatta*”, in reference to the flat male body. The gender of *Planiblatta* is feminine.

Distribution. China (Yunnan).

***Planiblatta crassispina* Luo & Wang, sp. nov.**

<https://zoobank.org/A47F1B88-7E4B-46D6-B9D4-FB3C9E6BE744>

Figs 6, 7 (in part)

Type materials. Holotype: CHINA • ♂; Yunnan, Yaonan Village, Mt Ailaoshan, Xinping County, Yuxi City; 12.V.2016; Lu Qiu & Zhiwei Qiu leg.; SWU-B-BL-082901. **Paratypes:** CHINA • 3♂♂, 2♀♀; Yunnan; Yaonan Village, Mt Ailaoshan, Xinping County, Yuxi City; 11–12.V.2016; Lu Qiu & Zhiwei Qiu leg.; SWU-B-BL-082902 to 082906.

Diagnosis. Combining the following characteristics, this species is easily distinguished from other Blattinae species: 1) pulvilli developed, pulvilli of front metatarsus occupy nearly 1/3 of ventral surface; 2) supra-anal plate short; 3) L4C curved and subhyaline, the base irregular; 4) the distal part of R1G with two curved and strong spines; 5) female tegmina small, lobe-like, and hind wings absent.

Description. Sexual dimorphism present. **Coloration.** Body dark brown to black; vertex black; ocelli white; tegmina dark yellowish brown (Fig. 6A–D).

Male (Fig. 6A, B). Body length including tegmen: 28.5–30.1 mm; body length: 19.6–21.4 mm; pronotum length × width: 4.2–4.7 mm × 5.7–6.7 mm; tegmina length × width: 24–26.6 mm × 6.4–7.8 mm. **Head and thorax.** Vertex slightly exposed. Interocular space slightly wider than the interocellar space, slightly shorter than the distance between antennal sockets (Fig. 6E). Antennae longer than the body. Pronotum subelliptical; anterior margin straight, hind margin slightly convex; the widest point near the midpoint (Fig. 6F). The posterior-lateral angles of metanotum without finger-like projections (Fig. 6K). Tegmina and wings well developed, surpassing the tip of abdomen (Fig. 6 A, B, G, H). Tegmina with ScP strong, posterior branch of R not reaching the end of tegmina (Fig. 6G). Front femur of type A₂ (Fig. 6I). Hind metatarsus equal to the remaining segments combined (Fig. 7D). Pulvilli present, pulvilli of front metatarsus developed, pulvilli of front metatarsus occupy nearly 1/3 of ventral surface (Fig. 6J). Claws symmetrical and unspecialized, arolium moderate (Fig. 7D). **Abdomen.** First tergite of male abdomen with visible gland, setose gland not obscured by metanotum and grown upward and downward (Fig. 6K). Postero-lateral corners of abdominal tergite V–VII produced. Supra-anal plate short, lateral margin slightly shrunken inward; middle part of hind margin concave at an obtuse angle. Paraprocts (pp.) long, strip-shaped, the end curved downward. Cerci long and robust (Fig. 6L). Subgenital plate nearly square; the hind margin straight. Styli symmetrical and apically rounded (Fig. 6M). **Genitalia** (Fig. 6N). L1 membranous and irregular, margin thick. L4C curved and subhyaline, the base irregular. L2 irregular and folded, the dorsal sclerite broad, the distal part with a long spine. L3 unciform and well sclerotized, the basal part bifurcated. L4G strip-like. R1H slightly broad, inner margin of the distal part with two strong spines. The distal part of R1G with two curved, strong spines inward.

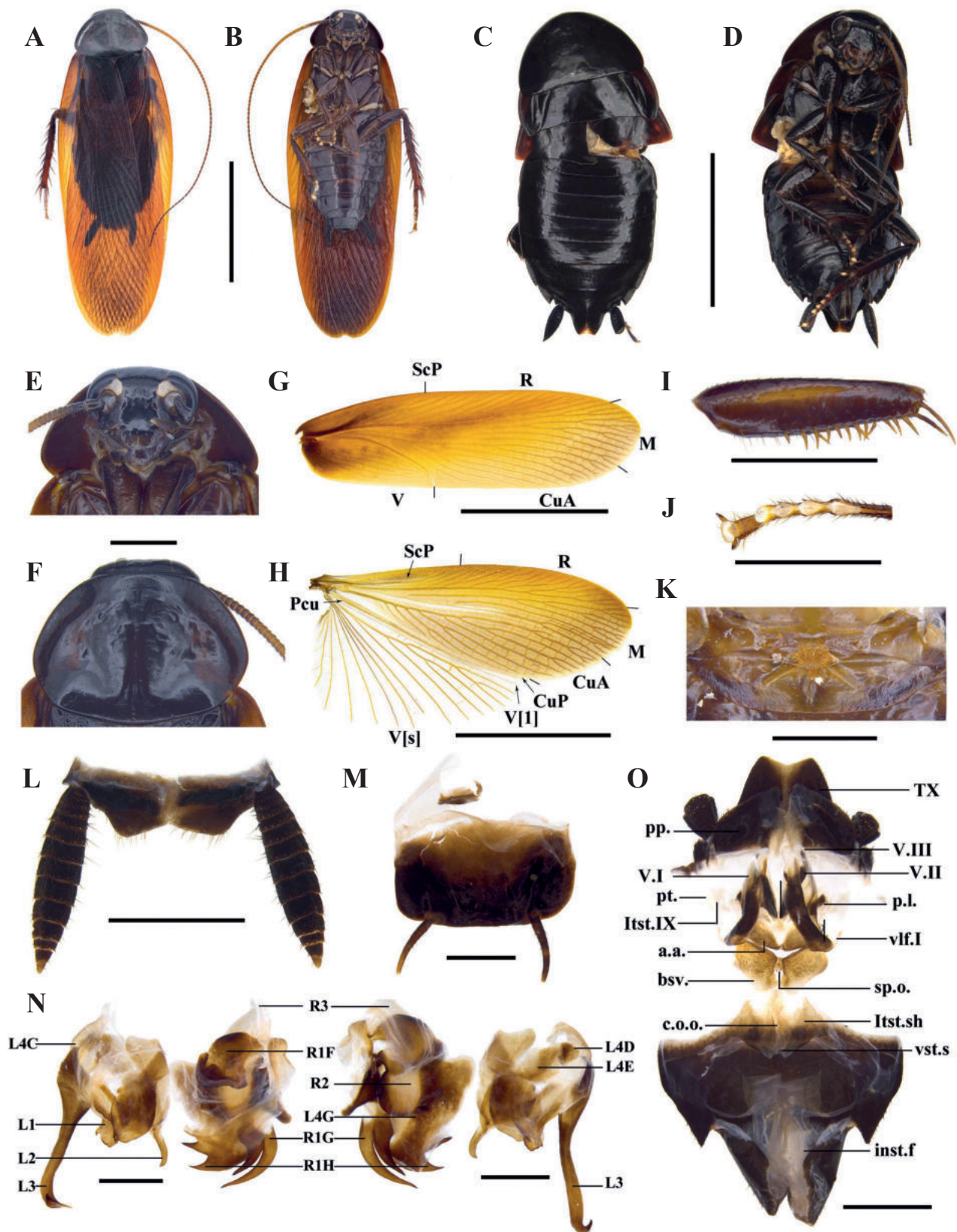


Figure 6. *Planiblatta crassispina* Luo & Wang, sp. nov. A, B, E–K male holotype C, D, O female paratypes A, C habitus, dorsal view B, D habitus, ventral view E head F pronotum G tegmen H hind wing I front femur J front tarsi K hind margin of metanotum and tergal gland L supra-anal plate, ventral view M subgenital plate, dorsal view N male genitalia, dorsal (left) and ventral (right) view O female genitalia, dorsal view. Scale bars: 10.0 mm (A–D, G, H); 2.0 mm (E, F, I–L, O); 1.0 mm (M, N).

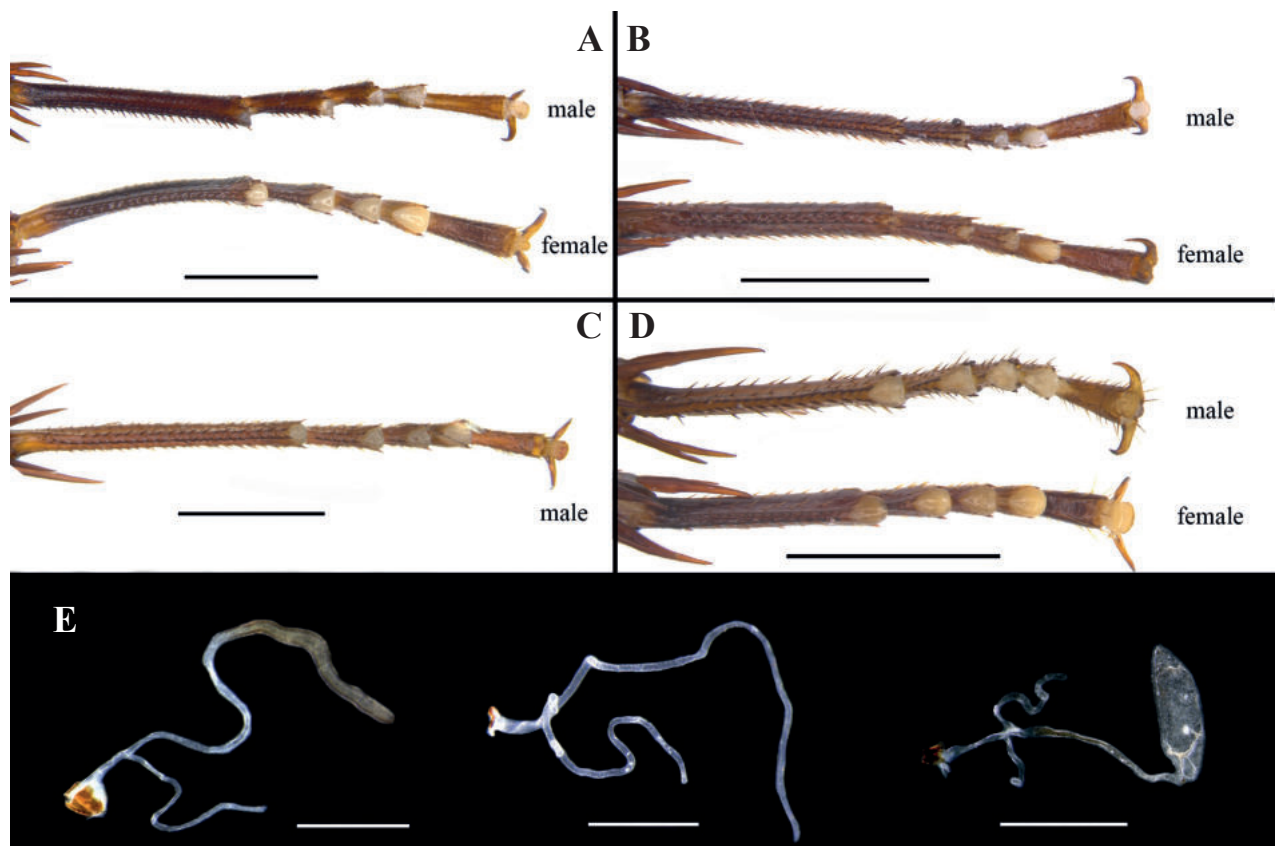


Figure 7. A–D hind tarsi **A** *Vittiblatta punctata* Luo & Wang, sp. nov. **B** *V. ferruginea* Luo & Wang, sp. nov. **C** *V. undulata* Luo & Wang, sp. nov. **D** *Planiblatta crassispina* Luo & Wang, sp. nov. **E** spermatheca, in order from left to right: *V. punctata* Luo & Wang, sp. nov., *V. ferruginea* Luo & Wang, sp. nov., *P. crassispina* Luo & Wang, sp. nov. Scale bars: 2.0 mm (A–D); 0.5 mm (E).

Female (Fig. 5C, D). Body length: 17.9; pronotum length × width: 5.4–5.6 mm × 7.9–8.0 mm; tegmina length × width: 3.5–3.7 mm × 2.3 mm. **Head and thorax.** Pronotum subelliptical, the widest point near hind margin; anterior margin curved, hind margin nearly straight (Fig. 6C). Tegmina and wings reduced. Tegmina small, lobe-like (Fig. 6C). Pulvilli present, pulvilli of front metatarsus developed, pulvilli of front metatarsus occupy nearly 1/3 of ventral surface (Fig. 6J). Claws symmetrical and unspecialized, arolium moderate (Fig. 7D). **Abdomen.** Hind margin of tergum X (TX) with median invagination, and with a membranous line inside (Fig. 6O). **Genitalia** (Fig. 6O). The surface of first valve (v.l.) with small punctures. First valvifer (vlf.I) slightly sclerotized and hyaline. Posterior lobes of valvifer II (p.l.) irregular, the outer margin unclear. Laterosternite IX (ltst.IX) slightly sclerotized and hyaline. Anterior arch (a.a.) with microtrichia near basal surface. Spermathecal plate (sp.pl.) nearly triangle. Spermathecal opening (sp.o.) located at the base of basivalvulae (bsv.). Spermatheca branched, the leading duct longer than the branching duct, and the branching duct also branched, the end capsule oval (Fig. 7E). Basivalvulae broad, surface with microtrichia; the left and right basivalvulae connected. Laterosternal shelf (ltst.sh.) symmetrical.

Etymology. The species epithet is from the Latin word “*crassispinus*”, in reference to the two strong spines on the distal part of R1G.

Distribution. China (Yunnan).

Discussion

Deng et al. (2023) suggested that sclerite L4C has a high diversity in Blattinae, but we find this character, along with R1G, conservative in two new genera, and so in *Periplaneta* s.s. (Luo et al. 2023). We find that these two sclerites together can clearly distinguish *Vittiblatta* gen. nov. and *Planiblatta* gen. nov. from morphologically similar relatives, at least those examined in this study. Combined with external morphological characters, these two new genera are well supported. However, it needs to be confirmed whether L4C and R1G can be used to identify the genera not examined in this study, *Afrostylopyga*, *Apterisca*, *Cartoblatta*, *Brinckella*, *Deropeltis*, *Dorylaea*, *Eroblatta*, *Eumethana*, *Henicotyle*, *Macrostylopyga*, *Miostylopyga*, *Pseudoderopeltis*, *Scabinopsis*, and *Thyrsocera*.

Genital reversal within species is common in Blattodea, such as Blaberidae, most Pseudophyllodromiidae, and some Ectobiidae species (Brown 1975; Nieves and Bohn 1987; Klass 1997). However, our study is the first report of chiral dimorphism of male genitalia within a single species. Chiral dimorphism of male genitalia occurs rarely within an insect species, e.g. Coleoptera: Ahrens and Lago 2008, Hemiptera: Guglielmino et al. 2016, Lepidoptera: Nupponen 2009, Mantodea: Holwell and Herberstein 2010, Phasmatodea: Heleodoro 2022, Trichoptera: Botosaneanu and Hyslop 1998. Schilthuizen (2007, 2013) suggested that this phenomenon might be related to sexual selection. In *Drosophila melanogaster*, this phenomenon is a result from mutations in the allele of Myo31DF (Hozumi et al. 2006; Spéder et al. 2006; Inaki et al. 2018), but whether it is the same in Blattodea needs to be investigated.

Acknowledgements

We extend our sincere thanks to the specimen collectors involved in this paper. We are also grateful to Dr. Xinran Li for providing us with ecological photographs of *V. punctata*. We sincerely thank him for his comments on our manuscript. We also sincerely thank two anonymous reviewers for their valuable suggestions on our manuscript.

Additional information

Conflict of interest

The authors have declared that no competing interests exist.

Ethical statement

No ethical statement was reported.

Funding

This study is supported by a Program of the Ministry of Science and Technology of the People's Republic of China (2022FY202100) and the National Natural Sciences Foundation of China (no. 32170458).

Author contributions

Funding acquisition: ZW. Methodology: XL. Project administration: YC. Visualization: XL, WD. Writing – original draft: XL. Writing – review and editing: XL, WD, ZW.

Author ORCIDs

Xin-Xing Luo  <https://orcid.org/0009-0000-6838-1696>

Wen-Bo Deng  <https://orcid.org/0000-0001-5796-241X>

Yan-Li Che  <https://orcid.org/0000-0003-3214-9494>

Zong-Qing Wang  <https://orcid.org/0000-0001-9413-1105>

Data availability

All of the data that support the findings of this study are available in the main text.

References

- Adelung Nv (1910) Ueber einige bemerkenswerte Orthopteren aus dem palacarktischen Asien. *Horae Societatis Entomologicae Rossicae* 39: 328–358.
- Ahrens D, Lago PK (2008) Directional asymmetry reversal of male copulatory organs in chafer beetles (Coleoptera: Scarabaeidae): implications on left–right polarity determination in insect terminalia. *Journal of Zoological Systematics and Evolutionary Research* 46(2): 110–117. <https://doi.org/10.1111/j.1439-0469.2007.00449.x>
- Anisyutkin LN (2014) New and little known Blattidae (Dictyoptera) from the collection of the Muséum d'histoire naturelle de Genève. *Revue Suisse de Zoologie* 121(1): 33–50.
- Anisyutkin LN, Anichkin AE, Thinh NV (2013) *Macrostylopyga* gen. nov., a new genus of cockroaches (Dictyoptera: Blattidae), with descriptions of two new species. *Zootaxa* 3635(5): 520–532. <https://doi.org/10.11646/zootaxa.3635.5.2>
- Asahina S (1980) Taxonomic notes on non-domiciliary *Periplaneta* species from the Ryukyus, Taiwan, Hong Kong and Thailand. *Japanese Journal of Sanitary Zoology* 31(2): 103–115. <https://doi.org/10.7601/mez.31.103>
- Beccaloni GW (2023) Cockroach Species File. [Accessed 26 September 2023]. <https://cockroach.speciesfile.org>
- Bey-Bienko GY (1957) Blattoidea of Szechwan and Yunnan. I. The results of the Joint Soviet-Chinese Zoological and Botanical Expedition to SE China in 1955–1956. *Entomologicheskoe Obozrenie* 36(4): 895–915.
- Bey-Bienko GY (1969) New genera and species of cockroaches (Blattoptera) from tropical and subtropical Asia. *Entomologicheskoe Obozrenie* 48(4): 831–862.
- Bohn H (1985) *Blatta furcata* (Karny), the nearest relative of the Oriental cockroach (*Blatta orientalis* L.) (Insecta: Blattodea: Blattidae). *Israel Journal of Zoology* 33: 39–50.
- Botosaneanu L, Hyslop EJ (1998) A systematic and biogeographic study of the caddisfly fauna of Jamaica (Insecta: Trichoptera). *Bulletin de l'Institut Royal des Sciences Naturelles de Belgique. Entomologie* 68: 5–28.
- Bourguignon T, Tang Q, Ho SYW, Juna F, Wang ZQ, Arab DA, Cameron SL, Walker J, Rentz D, Evans TA, Lo N (2018) Transoceanic dispersal and plate tectonics shaped global cockroach distributions: Evidence from mitochondrial phylogenomics. *Molecular Biology and Evolution* 35(4): 970–983. <https://doi.org/10.1093/molbev/msy013>
- Brown VK (1975) Development of the male genitalia in *Ectobius* spp. Stephens (Dictyoptera: Blattidae). *International Journal of Insect Morphology & Embryology* 4(1): 49–59. [https://doi.org/10.1016/0020-7322\(75\)90005-7](https://doi.org/10.1016/0020-7322(75)90005-7)
- Burmeister H (1838) Kakerlaken, Schaben. *Blattina. Handbuch der Entomologie* 2(2): 469–517.
- Deng WB, Luo XX, Ho SYW, Liao SR, Wang ZQ, Che YL (2023) Inclusion of rare taxa from Blattidae and Anaplectidae improves phylogenetic resolution in the cockroach su-

- perfamily Blattoidea. *Systematic Entomology* 48(1): 23–39. <https://doi.org/10.1111/syen.12560>
- Djernæs M, Muriene J (2022) Phylogeny of Blattoidea (Dictyoptera: Blattodea) with a revised classification of Blattidae. *Arthropod Systematics & Phylogeny* 80: 209–228. <https://doi.org/10.3897/asp.80.e75819>
- Evangelista D, Thouzé F, Kohli MK, Lopez P, Legendre F (2018) Topological support and data quality can only be assessed through multiple tests in reviewing Blattoidea phylogeny. *Molecular Phylogenetics and Evolution* 128: 112–122. <https://doi.org/10.1016/j.ympev.2018.05.007>
- Guglielmino A, D'Urso V, Bückle C (2016) Revision of the *Dicranotropis hamata* group (Auchenorrhyncha, Delphacidae) and remarks on the implication of chiral dimorphism in its history. *Deutsche Entomologische Zeitschrift* 63(1): 89–108. <https://doi.org/10.3897/dez.63.6625>
- Heleodoro RA (2022) The first two cases of antisymmetry in the male genitalia of Phasmatodea reveal a new species of *Isagoras* Stål, 1875 (Phasmatodea: Pseudophasmatidae: Xerosomatinae) from the Brazilian Atlantic Forest. *Zoologischer Anzeiger* 296: 161–178. <https://doi.org/10.1016/j.jcz.2021.12.006>
- Holwell GI, Herberstein ME (2010) Chirally dimorphic male genitalia in praying mantids (Ciulfina: Liturgusidae). *Journal of Morphology* 271(10): 1176–1184. <https://doi.org/10.1002/jmor.10861>
- Hozumi S, Maeda R, Taniguchi K, Kanai M, Shirakabe S, Sasamura T, Spéder P, Noselli S, Aigaki T, Murakami R, Matsuno K (2006) An unconventional myosin in *Drosophila* reverses the default handedness in visceral organs. *Nature* 440(7085): 798–802. <https://doi.org/10.1038/nature04625>
- Inaki M, Sasamura T, Matsuno K (2018) Cell chirality drives left-right asymmetric morphogenesis. *Frontiers in Cell and Developmental Biology* 6: 1–34. <https://doi.org/10.3389/fcell.2018.00034>
- Klass KD (1997) The external male genitalia and the phylogeny of Blattaria and Mantodea. *Bonner Zoologische Monographien* 42: 1–341.
- Krauss HA (1890) Beitrag zur Kenntnis westafrikanischer Orthopteren. 2. Orthopteren der Guinea-Inseln São Thomé und Rolas, gesammelt von Prof. Dr. Richard Greeff. *Zoologische Jahrbucher. Abteilung für Systematik, Ökologie und Geographie der Tiere* 5: 647–668.
- Latreille PA (1810) *Considérations Générales sur l'ordre Naturel des Animaux Composant les Classes des Crustacés, des Arachnides, et des Insectes; Avec un Tableau Méthodique de Leurs Genres, Disposés en Familles*. F. Schoell, Paris, 444 pp. <https://doi.org/10.5962/bhl.title.39620>
- Legendre F, Nel A, Svenson GJ, Robillard T, Pellens R, Grandcolas P (2015) Phylogeny of Dictyoptera: Dating the origin of cockroaches, praying mantises and termites with molecular data and controlled fossil evidence. *PLoS ONE* 10(7): e0130127. <https://doi.org/10.1371/journal.pone.0130127>
- Li XR, Zheng YH, Wang CC, Wang ZQ (2018) Old method not old-fashioned: Parallelism between wing venation and wing-pad tracheation of cockroaches and a revision of terminology. *Zoomorphology* 137(4): 519–533. <https://doi.org/10.1007/s00435-018-0419-6>
- Li Y, Luo XX, Zhang JW, Wang ZQ, Che YL (2022) A new species of *Bundoksia* Lucañas, 2021 with comments on its subfamilial placement, based on morphological and molecular data. *ZooKeys* 1085: 145–163. <https://doi.org/10.3897/zookeys.1085.72927>

- Liao SR, Wang YS, Jin DT, Chen R, Wang ZQ, Che YL (2021) Exploring the relationship of *Homalophilpha* and *Mimosilpha* (Blattodea, Blattidae, Blattinae) from a morphological and molecular perspective, including a description of four new species. *PeerJ* 9: e10618. <https://doi.org/10.7717/peerj.10618>
- Linnaeus C (1758) *Systema naturæ* 1, Editio Decima. Holmiæ, Sweden, 824 pp.
- Lucañas CC (2021) *Bundoksia* gen. nov. (Dictyoptera: Blattodea: Blattidae), a new sexually dimorphic cockroach from the Philippines. *Journal of Natural History* 55(15–16): 1009–1020. <https://doi.org/10.1080/00222933.2021.1928317>
- Lucañas CC (2023) Revisions on the genus *Periplaneta* Burmeister, 1838 (Blattodea: Blattidae: Blattinae) part 1: two new genera from the Philippines and Borneo. *Oriental Insects* 57(3): 1–16. <https://doi.org/10.1080/00305316.2022.2164804>
- Luo XX, Li QQ, Zamani A, Che YL, Wang ZQ (2023) Redescription of *Periplaneta arabica* (Bey-Bienko, 1938) (Blattodea, Blattidae), with a comparative analysis of three species of *Periplaneta* Burmeister, 1838 (*sensu stricto*). *ZooKeys* 1146: 165–183. <https://doi.org/10.3897/zookeys.1146.90817>
- Malem J, Robillard T, Cluzel D, Bellier L, Nattier R, Grandcolas P, Legendre F (2023) Origins of old lineages in New Caledonia: A geologically informed test of the island-hopping hypothesis. *Journal of Biogeography* 50(9): 1587–1601. <https://doi.org/10.1111/jbi.14673>
- McKittrick FA (1964) Evolutionary studies of cockroaches. *Cornell University Agricultural Experiment Station* 389: 1–197.
- Nieves JL, Bohn RA (1987) Reversal of the right-left asymmetry in male genitalia of some Ectobiinae (Blattaria: Blattellidae) and its implications on sclerite homologization and classification. *Insect Systematics & Evolution* 18(4): 293–359. <https://doi.org/10.1163/187631287X00160>
- Nupponen K (2009) *Scythris antisymmetrica* Nupponen, sp. n. from Central Spain, an example of antisymmetric male genitalia in the order Lepidoptera (Lepidoptera: Scythrididae). *SHILAP Revista de Lepidopterologia* 37(148): 439–444.
- Princis K (1951) Neue und wenig bekannte Blattarien aus dem Zoologischen Museum, Kopenhagen. *Spolia Zoologica Musei Hauniensis* 12: 5–72.
- Princis K (1963) Blattariae. Revision der südafrikanischen Blattarienfauna. In: Hanström P, Brinck P, Rudebeck G (Eds) *South African Animal Life. Results of the Lund University Expedition in 1950–1951*. Swedish Natural Science Resource Council, Stockholm 9: 9–318.
- Princis K (1966) Kleine Beiträge zur Kenntnis der Blattarien und ihrer Verbreitung. IX. *Opuscula Entomologica*. Editio Societas Entomologica Lundensis 31(1–2): 43–60.
- Rehn JAG, Hebard M (1927) The Orthoptera of West Indies. Number 1. Blattidae. *Bulletin of the American Museum of Natural History* 54(1): 1–320.
- Roth LM (2003) Systematics and phylogeny of cockroaches (Dictyoptera: Blattaria). *Oriental Insects* 37(1): 1–186. <https://doi.org/10.1080/00305316.2003.10417344>
- Schilthuizen M (2007) The evolution of chirally dimorphic insect genitalia. *Tijdschrift voor Entomologie* 150(2): 347–354. <https://doi.org/10.1163/22119434-900000234>
- Schilthuizen M (2013) Something gone awry: Unsolved mysteries in the evolution of asymmetric animal genitalia. *Animal Biology* 63(1): 1–20. <https://doi.org/10.1163/15707563-00002398>
- Shelford R (1908) Some new genera and species of Blattidae, with notes on the form of the pronotum in the subfamily Perisphaeriinae. *Annals & Magazine of Natural History* 8(1): 157–177. <https://doi.org/10.1080/00222930808692379>

- Shelford R (1910a) Orthoptera fam. Blattidae subfam. Blattinae (= Periplanetinae). In: Wytzman P (Ed.). *Genera Insectorum*. Belgique, 1–27.
- Shelford R (1910b) Blattodea. In *Wissenschaftliche Ergebnisse der Schwedischen Zoologischen Expedition nach dem umgebenden Masaisteppe Deutsch-Ostafrika, 1905–1906, unter Leitung von Y. Sjöstedt*. 3 (17. Orthoptera). Stockholm: 13–48.
- Shelford R (1911) The latest in nomenclature. *Entomologist's Record and Journal of Variation* 23(9): 241–242. <https://doi.org/10.5962/bhl.part.14315>
- Snellen van Vollenhoven SC (1862) Beschrijving eenre nieuwe soort van Kakkeriak uit Sumatra, *Archiblatta hoevenii*. *Tijdschrift voor Entomologie* 5: 106–110.
- Spéder P, Ádám G, Noselli S (2006) Type ID unconventional myosin controls left–right asymmetry in *Drosophila*. *Nature* 440(7085): 803–807. <https://doi.org/10.1038/nature04623>
- Stål C (1874) Recherches sur le système des Blattaires. Bihang Till K. Svensk. Vet-Akad Handlingar 2(13): 3–18.
- Stål C (1877) Orthoptera nova ex Insulis Philippinis descripsit. Öfversigt af Kongliga Vetenskaps-Akademiens Förhandlingar 34(10): 33–58.
- Walker F (1868) In *Catalogue of the Specimens of Blattariae in the Collection of the British Museum*. British Museum (Natural History), E. Newman, Printer, London, 239 pp. <https://doi.org/10.5962/bhl.title.118688>
- Wang CC, Wang ZQ, Che YL (2016) *Protagonista lugubris*, a cockroach species new to China and its contribution to the revision of genus *Protagonista*, with notes on the taxonomy of Archiblattinae (Blattodea, Blattidae). *ZooKeys* 574: 57–73. <https://doi.org/10.3897/zookeys.574.7111>
- Wang ZQ, Shi Y, Qiu ZW, Che YL, Lo N (2017) Reconstructing the phylogeny of Blattodea: Robust support for interfamilial relationships and major clades. *Scientific Reports* 7(1): e3903. <https://doi.org/10.1038/s41598-017-04243-1>

